BIMETALLIC OLEFIN POLYMERIZATION CATALYSIS: MECHANISMS AND APPLICATIONS OF PROXIMAL EFFECTS

Thesis by
Madalyn Rachel Radlauer

In Partial Fulfillment of the Requirements
for the Degree of Doctor of Philosophy

CALIFORNIA INSTITUTE OF TECHNOLOGY
Division of Chemistry and Chemical Engineering
Pasadena, California
2014
(Defended on January 16, 2014)

To my parents, Julie and David,
my brother, Jeffrey,
and my fiancé, Aaron

ACKNOWLEDGEMENTS

Looking back on the past 5.3 years, I appreciate that graduate school, like many worthwhile endeavors, cannot be completed successfully alone. There are so many people who have helped, advised, and mentored me, as well as many whose friendship and patience I have relied on almost constantly. I know that I could not have made it to this point without you all.

My PI, Prof. Theo Agapie, must be first in my acknowledgements. When I arrived at Caltech for my visit weekend, I was thrilled by Theo's enthusiasm for chemistry. He convinced me that Caltech would be the best place to get a PhD – a sentiment heartily seconded by my undergraduate advisor – and to Caltech I came. I intended from the time of my visit to work with Theo, who I knew would be an involved mentor with a hands-on style, someone from whom I could learn a lot. Indeed, all those things have borne out in my years here. Because I had done research on polymerization catalysis in Bob Waymouth's group as an undergraduate, I though I was ready to branch out, but Theo's proposal on palladium complexes with pendant Lewis acids for polar monomer polymerizations intrigued me. I appreciate now that I didn't know very much about polymerization catalysis when I got here, and I'm glad to have stuck with it, as I have found a real passion for the complexities of bimetallic catalysts and for polymerization chemistry in general. I am extremely grateful to have worked on such an exciting project. Though the initial ideas did not pan out in the long run, I take great pride in the systems that we have developed and their interesting properties. As part of Theo's first class, I had the unique opportunity to help set up the lab, an experience whose lessons I hope to apply in the future. With only 5 people in the starting class and no senior students, I got/had to take on a variety of group jobs. Organizing group outreach efforts, being the group safety officer, and mentoring undergraduates are responsibilities that I have learned from and enjoyed (most of the time). Theo has pushed hard and made sure that I learned from my mistakes; he's taught me to be extremely thorough in my research and given me ample occasion to present my research so that I feel confident of my results and the way I share them. I wouldn't be the researcher and scientist I am without his mentorship and feedback.

One of the amazing things about CCE at Caltech is how many amazing professors are here. I am lucky to have three phenomenal scientists on my committee from whom I have learned a lot. Much thanks goes to Profs. Bob Grubbs, Julie Kornfield and John Bercaw for leading me through my PhD at meetings and for helping me decide what next steps to take in my career after Caltech. Bob, thank you for your invaluable advice on my props, for coming to every meeting, for advising me on my choice of postdoc, and even going so far as to mention possible job opportunities for my fiancé near UMN. Julie, you always have a smile and an anecdote to share and I really appreciate your earnest advice both scientific and professional and your engineer's perspective on my chemistry. John, even before you became my fourth committee member, thank you for taking an interest in my research and for always finding time to meet with me.

A few other professors have made an impact on my time at Caltech. Prof. Brian Stoltz, thank you for your advice. Prof. Sarah Reisman, I had never really taken an advanced synthesis class and while I hope that I never have occasion for a 10 hour exam again, I learned so much in 242a and have even applied a good deal of it in ligand synthesis. I must also thank you for recommending MOM-group directed lithiation to replace bromination and lithium-halogen exchange; my ligand synthesis became a lot more reliable with that change. Prof. Tom Miller, thank you for our very frank conversations about science and safety, I have enjoyed hearing your perspective. Prof. Harry Gray, I am inspired by your love of chemistry and your ability to connect with so many people, an ability that has done much to shape my experience with the broader inorganic group at Caltech. Thank you also for taking the time to chat with me about my career.

Dr. Jay Winkler, Dr. Jay Labinger, and Dr. Scott Virgil are amazing resources to Caltech chemistry. Jay Winkler, I have a great time TAing for you and talking about Stanford. Go Card! Jay Labinger, you taught me so much about organometallic chemistry in 154 and in our occasional meetings. Scott, when my ligand syntheses were getting to be overwhelming, you really helped me out. Thank you all for sharing your expertise with me.

The Agapie group started at Caltech with my year of graduate students and has since then picked up a great bunch of people. Huge thanks go to all of you for everything from talking chemistry, to letting me put show tunes on the group radio every once in a while, to helping me edit my papers, to being lots of fun. The Agapie group is wonderful, and I really appreciate having had the opportunity to work with you all. Emily Tsui, Sibo Lin, Paul Kelley, and Stephen Chao, starting out together as the first class was a challenge, but I know that part of how I made it through that first year was that you all were there too. Stephen, though you left early, I really enjoyed sharing room 303 with you. Paul, I know we've had our ups and downs, especially regarding the organization of our glovebox, but I am really grateful to have worked next to someone so steadfast and funny. Siboster, you constantly amaze me with your abilities to put away a two-liter of soda in a single sitting, to fall asleep literally anywhere, and to work straight through >24 hours. Thanks also for co-hosting IOS with me our third year. Emily, you are one of the most hardworking and intelligent people I know and you really inspire me. On top of that, thank you for teaching me to love so many types of Asian cuisine (with help from Sandy) and for being a great friend. Davide Lionetti, Sandy Suseno, and Kyle Horak – my Chicken Milanese buddies – thank you all for great conversations. Davide, Med Café Mondays geared me up at the start of my work week. Thank you for being a great friend and confidant. Sandy and Kyle, thanks for lending a helping hand with everything: from telling me to go home when I was sick to driving me home when my bike's front wheel was stolen. You really have taken care of me. Dr. Dave Herbert, Dr. Po Heng Lin, Dr. David Abrect, Jacob Kanady, Guy Edouard, Justin Henthorn, Josh Wiensch, and Josh Buss y'all are a lively group that have made graduate school that much better by your company. A special acknowledgement must go to Guy for taking over as safety officer and introducing Aaron to the Buckets. I have also enjoyed the short time I've had getting to know first years Jess Sampson, Marcus Low, and HB Lee. Jess, I'm so excited that you're taking over the polymer project. There's so much to be excited about, and I know you're going to do an amazing job. To every graduate student and postdoc in the group, I am so glad you were part of my graduate school experience, you all have taught me so much about life, the universe, and everything. Thanks and good luck!

15 undergraduates have worked in the Agapie group so far. They are an enthusiastic and interesting bunch and I wish them all the best. I would like to give a special acknowledge the three that I co-mentored. Andreas Wierschen, when you joined the lab my first summer, I was still getting my bearings, but you came in with such amazing joie de chemistry that I felt immediately ready to have a great time working with you. Thank you for keeping in touch and visiting, and especially for telling me that you like how tidy I keep my workspace. Nadia Lara, when Stephen left the group, getting to work with you was the silver lining. Your energy, curiosity, and drive to learn and to teach make you a pleasure to be around. I was also glad to have a friend with whom I could share my love of Disney music. Aya Buckley, you powered through your summer here and really caught on fast. While I'd love to congratulate me for being such a great mentor, I am pretty sure most of the credit for your success lies squarely on your shoulders. Andreas, Nadia, and Aya, working with you led to great chemistry and conversation; it was so much fun. I know you will all succeed in your chemistry endeavors and I hope to be kept in the loop. Best of luck to you guys!

Outside of the group I need to thank my past roommate, Renee Thomas. In the little time off that we had, we managed to go on a number of adventures. It was always a treat to come home and watch *Murder She Wrote* before bed or share in some good food like my quesadillas and your green bean casserole. We had quite a time.

Many members of other groups played a significant role in my time at Caltech. The Bercaw group has been the big brother to the Agapie group, sharing advice, experience, and equipment. As we didn't have any senior students in the Agapie group, it was invaluable to have them downstairs, particularly for things such as the logistics and formatting of our candidacy report or thesis outlines. When I first started, Dr. Ned West, and (now Drs.) Alex Miller and Ian Tonks sat together in the Bercaw office. I went down there for council and advice more times than I can remember, yet they always seemed happy to help. We even made some HBArF together on the high vac line. Ian, Alex, and Steve Baldwin were among the students who convinced me at visiting week to come to Caltech. Ian also introduced me to my roommate Renee at lunch my first week here. These and other Bercaw group members, have listened to practice talks, helped me edit materials for candidacy and props, and have been great

resources for organometallic chemistry know-how. Dr. Taylor Lenton, who was my year, was a great person to talk to about polymerizations and wine. Taylor (and Justin Chartron), I am so glad that Aaron and I had the pleasure of hanging out with you. Drs. Dave Leitch, Aaron Sattler, and Tom Teets now hold up the Bercaw fort and what they lack in numbers they certainly make up for in awesomeness. Indeed, I still find myself dropping by the Bercaw group office on a fairly regular basis for advice and chemistry conversations.

Members of the Gray and Grubbs groups have also been a big help to me, but I will only name a few. Dr. Jillian Dempsey worked down the hall for my first few years here and was always a help. She bandaged up my left index finger the time I sliced it with some broken glass so that I didn't have to find a doctor and took me for celebratory Fosselman's ice cream after my candidacy exam. Dr. Maraia Ener was one of the first people I met of my year. She gets special thanks as that person who smiles at you and looks actively engaged at all your talks. When Maraia is in the audience, you can't help but feel like you're doing a great job, which I think is a self-fulfilling type of feeling. Dr. Chris Daeffler was the GLA on Daytona before me, taught me everything I know about tuning NMRs manually, and ran a great fantasy football league. Dr. Keith Keitz, Dr. Garrett Miyake and Ben Sveinbjornsson trained me on the Grubbs group GPC and helped me with instrument issues and data workup and analysis.

The Stoltz and Reisman groups also deserve mention. I spent hours in the Stoltz and Riesman group offices discussing synthesis, both for class and for practical use. They taught me how to dry load columns and provided me with tricks that ultimately improved my ligand syntheses. The Reisman group started the same year as the Agapie group and the shared experiences of starting with an untenured professor here was something about which I bonded with many of the first crop of students.

Additional thanks go to Kyle Horak, Sibo Lin, Davide Lionetti, Aaron Sattler, Tom Teets, Ian Tonks, Emily Tsui, and Aaron Rosekind for reading and editing portions of this dissertation.

Practically all of this work was made possible by the expert assistance of the CCE staff. Thanks to Dr. Dave VanderVelde for running the NMR facility, being a great leader of the NMR GLAs, giving many talks on NMR topics, and always being

available to help with any and all things NMR related. Dave, you are an immeasurable resource and in addition to very much enjoying our discussions, I have learned a great deal from you. Thanks to Larry Henling, the late Dr. Mike Day, and Dr. Mike Takase for teaching me about crystallography, running my crystals even when they didn't look promising, and training me to work up my own data, a skill which I am very glad to possess. Thanks to Dr. Jens Kaiser for running a few samples for me on the synchrotron. Thanks to Dr. Mona Shahgholi and Naseem Torian for mass spectrometry assistance and for always being so friendly. Thanks to Rick Gerhart for being a master of glassware and building every piece of specialty glassware in the lab; to Mike Roy and Steve Olsen for machining perfectly sized shelves for the gloveboxes and helping me put together several iterations of high pressure polymerization setups; to Tom Dunn and Jeff Groseth for fixing all things electronic and always having that adapter I needed, to Steve Gould for deftly handling all sorts of orders so that I never had to; to Cora and Carlos for always having a smile and the solvents I needed. Thanks to Agnes Tong and Anne Penney in the front office for helping me keep all the needed paperwork in order. Thanks to Margarita Davis, Pat Anderson, Linda Syme, Andrea Acosta, and Marcy Fowler for making sure that scheduling everything that involved my committee was as painless as possible. Thanks to Paul Carroad and Joe Drew for being the safety liaisons between safety officers and EHS; to the safety committee for trying out the safety day idea; to Prof. John Bercaw and Prof. Linda Hsieh-Wilson for adding a section on sleep to their safety presentation; and to my fellow safety officers for working with me on safety day projects and discussing safety topics. Thanks to Jerzy Klosin at DOW for an industry perspective on my chemistry and for running a number of high temperature GPC samples. Thanks to James Maloney, and the CCC for arranging outreach opportunities and for connecting Theo with Ms. Seo at Marshall High School. Thanks to Ms. Seo for inviting us into her classroom.

I would be remiss not to take this opportunity to acknowledge my pre-graduate school mentors. Two of my high school teachers, Ms. Denise Ekberg, my first chemistry teacher, and Dr. Mary Gubala, my AP biology teacher, recognized my passion for science and inspired me to pursue it further. They are both brilliant women and fantastic teachers. I learned a lot from them, including the joy of experimentation from

the laboratory units. Prof. Zeev Rosenzweig was my first PI. In two summers in his group I was introduced to research and academia. Prof. Bob Waymouth at Stanford taught me to be excited about polymer chemistry. As an undergraduate who had just declared herself a chemistry major, I ran into Bob at the San Francisco airport. Upon hearing that I had declared chemistry he congratulated me and told me to come by and talk to him if I was interested in working in his lab. I did so, and he showed me samples of polymers and explained how tacticity changes the mechanical properties of a polymer. I was hooked! For the two years I spent doing research in his group I was mentored by Dr. Liz Kiesewetter (then Tanzini) who taught me how to make molecules. I also had the benefit of working closely with a number of other graduate students who confirmed my path to graduate school including Liz's now husband, Dr. Matt Kiesewetter. I still talk with Liz and Matt about chemistry and they have given me tons of support. Bob also played a major role in my coming to Caltech by telling me that it was the right choice and recommended that I take advantage of the opportunity to work for a new professor.

I would like to also thank a number of people outside of the chemistry community. Thanks to all my friends and family who have stuck by me despite my all-but-neglecting them for the past 5 years. Thanks to my soon-to-be parents-, sister-, and dog-in-law, Mark Rosekind, Deb Babcock, Eve Rosekind, and Meg who have welcomed me into their family and supported and encouraged me. Humongous thanks to my parents, David Radlauer and Julie Schwartz, my brother, Jeffrey Radlauer, and my dogs, Huey and Rocket, whose love and support have carried me though my life. Mom and Dad, you instilled in me a love for learning and education and have always told me that I could do anything I put my mind to. The confidence that inspired in me makes me who I am. And lastly, I would like to thank my fiancé, Aaron Rosekind. Aaron, there are too many things to say, so I will put it simply, thank you for joining me for my graduate school adventure and for all the adventures to come. I love you.

ABSTRACT

This dissertation covers progress with bimetallic polymerization catalysts. The complexes we have designed were aimed at expanding the capabilities of homogeneous polymerization catalysts by taking advantage of multimetallic effects. Such effects were examined in group 4 and group 10 bimetallic complexes; proximity and steric repulsion were determined to be major factors in the effects observed.

Chapters 2 and 3 introduce the rigid *p*-terphenyl dinucleating framework utilized in most of this thesis. The permethylation of the central arene allows for the separation of syn and anti atropisomers of the terphenyl compounds. Kinetic studies were carried out to examine the isomerization of the dinucleating bis(salicylaldimine) ligand precursors. Metallation of the syn and anti bis(salicylaldimine)s using $Ni(Me)_2(tmeda)$ and excess pyridine afforded dinickel bisphenoxyiminato complexes with a methyl and a pyridyl ligand on each nickel. The syn and anti atropisomers of the dinickel complexes were structurally characterized and utilized in ethylene and ethylene/α-olefin polymerizations. Monometallic analogues were also synthesized and tested for polymerization activity. Ethylene polymerizations were performed in the presence of primary, secondary, and tertiary amines – additives that generally deactivate nickel polymerization catalysts. Inhibition of this deactivation was observed with the syn atropisomer of the bimetallic species, but not with the anti or monometallic analogues. A mechanism was proposed wherein steric repulsion of the substituents on proximal nickel centers disfavors simultaneous ligation of base to both of the metal centers. The bimetallic effect has been explored with respect to size and binding ability of the added base.

Chapter 4 presents the optimization of the bisphenoxyimine ligand synthesis and synthesis of syn and anti *m*-terphenyl analogues. Metallation with $NiClMe(PMe_3)_2$ yielded phosphine-ligated dinickel complexes, which have been structurally characterized. Ethylene/1-hexene copolymerizations in the presence of amines using $Ni(COD)_2$ as a phosphine scavenger showed significantly improved activity relative to the pyridine-ligated analogues. Incorporation of amino olefins in copolymerizations with ethylene was accomplished, and a mechanism was proposed based on proximal effects. Copolymerization trials with a variety of amino olefins and ethylene/1-hexene/amino olefin terpolymerizations were completed.

Early transition metal complexes based on the rigid *p*-terphenyl framework were designed with a variety of donor sets (Chapter 5 and Appendix B). Chapter 5 details the use of syn dizirconium di[amine bis(phenolate)] complexes for isoselective 1-hexene and propylene homopolymerizations. Ligand variation and monometallic complexes were studied to determine the origin of tacticity control. A mechanistic proposal was presented based on the symmetry at zirconium and the steric effects of the proximal metal center. Appendix B covers additional studies of bimetallic early transition metal complexes based on the *p*-terphenyl. Dititanium, dizirconium, and asymmetric complexes with bisphenoxyiminato ligands and derivatives thereof were targeted. Progress toward the synthesis of these complexes is described along with preliminary polymerization data. 1-hexene/diene copolymerizations and attempted polymerizations in the presence of ethers and esters with the syn dizirconium di[amine bis(phenolate)] complexes demonstrate the potential for further applications of this system in catalysis.

Appendix A includes work toward palladium catalysts for insertion polymerization of polar monomers. These complexes were based on dioxime and

diimine frameworks with the intent of binding Lewis acidic metals at the oxime oxygens, at pendant phenolic donors, or at pendant aminediol moieties. The synthesis and structural characterization of a number of palladium and Lewis acid complexes is presented. Due to the instability of the desired species, efforts toward isolation of the desired complexes proved unsuccessful, though preliminary ethylene/methyl acrylate copolymerizations using *in situ* activation of the palladium species were attempted.

Table of Contents

List of Figures and Charts

List of Schemes

APPENDIX B

List of Tables

CHAPTER 1

General Introduction

This dissertation is focused on the study of multimetallic effects in polymerization catalysis and the potential applications of those effects. The majority of species presented herein are bimetallic complexes with group 4 and group 10 transition metals based on a terphenyl backbone. This framework affords rigidity, and permethylation of the central arene allows for the isolation of syn and anti atropisomers of the complexes. A variety of multimetallic polymerization catalysts have been reported in recent literature, but understanding of the origin of bimetallic effects is limited. Comparisons of the syn and anti atropisomers of complexes presented herein provide the ability to deconvolute electronic and steric effects on polymerization activity, while the rigidity of the backbone offers the possibility for specific variation of the metal–metal distances. Background information and the associated references are presented at the start of each chapter; this introduction will serve to put the work of this dissertation in the broader context, explain the motivations behind the research, and outline development of the projects.

Olefin polymerization chemistry by homogeneous catalyst systems has been widely researched and represents an important industrial application of organometallic chemistry. High volumes of polymeric materials are synthesized each year for a variety of applications from packaging to construction materials to specialized medical devices. Continued research in polymerization chemistry promises the development of new polymers and new applications. Novel catalytic systems can be designed to access desirable material properties. These systems are aimed at producing polymers at higher activities, with greater control of the polymer microstructure including molecular weight, tacticity, and incorporation of comonomers.

Coordination insertion polymerization of polar monomers remains a significant challenge in polymerization chemistry. Early transition metal catalysts used for non-functionalized olefin polymerization are inhibited by the presence of polar moieties due to the oxophilicity of the complexes. While many late transition metal catalysts have been developed to incorporate a variety of polar comonomers, none of these effectively pairs high incorporation with high activity at an industrially relevant level. Mechanistic studies on palladium diimine catalysts by Brookhart, Jordan, and others suggested that the formation of 5- and 6-membered chelates wherein the polar group of a polar monomer coordinates to the active palladium after incorporation severely impedes polymerization and often will only be opened by the competition of excess non-polar olefin. Inspired by these findings, we targeted palladium-diimine-derived systems with pendant Lewis acids (Appendix A). The Lewis acidic metals would compete with palladium for the coordination of the polar moiety, shifting the equilibria subsequent to polar olefin insertion towards olefin coordination. These heterometallic complexes would take advantage of the ability of palladium diimine systems to generate high molecular weight polymers with relatively high activity and engender increased tolerance and incorporation of polar monomers. In the course of the palladium research, a very enthusiastic MURF student from the University of North Carolina, Andreas Wierchen joined the project. Progress was made toward dioximine and diimine frameworks, but complexes bearing Lewis acidic metals were generally unstable as the reactive Lewis acids would bind to multiple ligand sets to satisfy their oxophilicity.

Aiming to simplify the synthesis of the complexes and avoid the instability presented by the Lewis acidic moieties, late transition metal homobimetallic complexes

were targeted. The *p*-terphenyl framework with a permethylated central arene was designed as a modular backbone that could support a variety of bimetallic complexes. Bimetallic cooperation with these complexes would presumably function under a different mechanism than the palladium/Lewis acid systems, though depending on the polar comonomer and the propensity of the systems for β-hydride elimination and reinsertion, the second metal center may serve to compete for polar moiety coordination and help disfavor chelation. Polymerization studies from Grubbs, Mecking and others on nickel phenoxyiminato complexes indicated high activity and the added benefit of some heteroatom tolerance including the capability for emulsion polymerization in water. We successfully synthesized dinickel bisphenoxyiminato complexes with pyridine ligands and studied their polymerization activity (Chapter 2). In general, the syn atropisomer was less active than the anti atropisomer, and no incorporation was observed with a variety of polar monomers. The attempted copolymerization of dimethylallyl amine with ethylene generated polymer with no amino olefin incorporation, but the syn and the anti complexes functioned at the same level of activity. This led us to study the relative amine tolerance of the syn and anti dinickel complexes (Chapter 3).

The enhanced tolerance of amines by the syn atropisomer was attributed to steric effects of the proximal metal center, but applications of these findings were limited by the relatively low activity of the pyridine-ligated complexes. We therefore aimed to improve the activity by altering the ligands on nickel. Using PMe_3-ligated species and $Ni(COD)_2$ as a phosphine scavenger, the activity of the dinickel bisphenoxyiminato complexes improved by orders of magnitude, especially in

ethylene/1-hexene copolymerizations (Chapter 4). Aya Buckley, a SURF student from Columbia University, joined the project and synthesized the meta analogues, allowing us to study the effects of altering the metal–metal distance and orientation. With these more active dinickel *p*- and *m*-terphenyl complexes, we were able to incorporate 1-hexene in the presence of amines. We accomplished the objective of polar monomer incorporation in ethylene/amino olefin copolymerizations with the dinickel bisphenoxyiminato complexes, but at low turnover and incorporation. Nonetheless, we aimed to apply the bimetallic strategy demonstrated by the successes of the dinickel complexes, to systems with inherently higher activity and comonomer incorporation ability, namely, early transition metal systems.

Fujita and many others have built a significant body of work on titanium and zirconium phenoxyiminato complexes for polymerization catalysis. We therefore set out to metallate our dinucleating bisphenoxyiminato complexes with titanium and zirconium precursors (Appendix B). The monometallic monophenoxyiminato complexes were not reported to be highly active or capable of notable amounts of α-olefin incorporation in copolymerizations with ethylene, and experiments with our bimetallic bisphenoxyiminato complexes bore out those results. Monometallic species with two phenoxyiminato ligands or a tridentate phenoxyiminato ligand were reported to display high activity and α-olefin incorporation. Appending supplementary donors, either via addition of a separate phenoxyiminato ligand or through modification of the imine aryl to provide a covalently linked third donor for each metal center, was attempted. The tetraphenoxyimnato complexes could not be synthesized and only limited success in pursuit of the bis(tridentate) complexes has been achieved thus far.

Concurrent with the research on dititanium and dizirconium bisphenoxyiminato complexes, dititanium and dizirconium di[amine bis(phenolate)] complexes were pursued (Appendix B). Kol and coworkers reported highly active α-olefin polymerization systems based on C_S-symmetric monozirconium amine bisphenolate complexes. We synthesized analogous syn dizirconium complexes on our *p*-terphenyl framework (Chapter 5). Unlike the monometallic catalysts, which make stereoirregular polymers, our bimetallic systems generate isoregular polymers with similar activity to the monometallic species. Pairing high activity and stereospecificity is a major goal for post-metallocene polymerization catalysis and these results represent a bimetallic strategy for achieving this aim. The potential applications of the dizirconium di[amine bis(phenolates)] extend beyond simple α-olefin polymerization (Appendix B). α-Olefin/diene copolymerizations targeting of ladder polymers via formation of the "rungs" by insertions of one of the olefinic moieties of a single diene at each zirconium center, would constitute a more controlled method for polymer chain cross-linking. Polymerizations in the presence of ester or ether additives have been unproductive, but further experimentation varying conditions and polar moiety is needed. Additionally, alkoxide-ligated analogues of the bimetallic complexes could be accessed by ligand exchange and studied for ring opening polymerizations.

As the mechanisms that we have proposed for the bimetallic effects observed with our dinickel and our dizirconium complexes rely primarily on the steric effects of the proximal metal centers, similar effects may be accomplished without the second active metal center, as long as sufficient steric bulk exists in the system. Thus, another direction of research has focused on the synthesis of asymmetric bimetallic complexes

wherein only one metal center is active for polymerization and the other provides steric bulk to the system (Appendix B). Monometallated intermediates have been synthesized, but appending the second metal has been unsuccessful so far.

Various bimetallic complexes have been presented in this work. Short metal–metal distances (< 8 Å) were achieved for the syn atropisomers of these complexes by employing a rigid terphenyl backbone with substitution of the central arene hindering rotation around the aryl–aryl bonds. Tolerance and incorporation of amines were accomplished with syn dinickel complexes. Enhanced stereoselectivity was accomplished with syn dizirconium complexes. Comparisons with the anti atropisomers or monometallic complexes have led to improved understanding of the origin of these proximal effects. The findings with bimetallic complexes demonstrate only a few of the potential applications of these systems. Indeed, the reported complexes hold promise for a diverse array of applications in polymer catalysis.

CHAPTER 2

DINICKEL BISPHENOXYIMINATO COMPLEXES FOR THE POLYMERIZATION OF ETHYLENE AND α-OLEFINS

Published in part as:
Radlauer, M. R., Day, M. W., and Agapie, T. *Organometallics* **2012**, *31*, 2231-2243.

ABSTRACT

Dinuclear nickelphenoxyiminato olefin polymerization catalysts based on rigid *p*-terphenyl frameworks are reported. Permethylation of the central arene of the terphenyl unit and oxygen substitution on the peripheral rings ortho to the aryl–aryl bonds blocks rotation around these linkages, allowing atropisomers of the ligand to be isolated. The corresponding syn and anti dinickel complexes (**25-s** and **25-a**) were synthesized and characterized by single crystal X-ray diffraction. These frameworks limit the movement of each metal center, thereby restricting the possible range of metal–metal distances. Kinetics studies of isomerization of a ligand precursor (**7-a**) allowed the calculation of the activation parameters for the isomerization process ($\Delta H^{\ddagger}$ = 28.0 ± 0.4 kcal mol^{-1} and $\Delta S^{\ddagger}$ = –12.3 ± 0.4 cal mol^{-1} K^{-1}). The reported nickel complexes are active for ethylene polymerization [TOF up to 3700 (mol C_2H_4) (mol Ni)$^{-1}$ h^{-1}] and ethylene/α-olefin copolymerization. Only methyl branches are observed in the polymerization of ethylene indicative of β-H elimination and reinsertion events, while α-olefins are incorporated without apparent chain walking. These catalysts are active in the presence of polar additives and in neat tetrahydrofuran. The syn and anti isomers differ in polymerization activity, polymer branching and molecular weight. For comparison, a series of mononuclear nickel complexes (**26**, **27-s**, **27-a**, **28**, **30**) was prepared and studied. The effects of structure and catalyst nuclearity on reactivity are discussed.

INTRODUCTION

In recent years, a variety of multinuclear polymerization catalysts have been developed.[1] These systems are conceptually inspired by enzyme active sites, which often contain a multimetallic core. For example, in hydrolases and lyases, Lewis acidic metal centers cooperatively activate substrates to facilitate catalysis.[2-4] In search of catalysts with enhanced olefin polymerization abilities, complexes incorporating two potential polymerization sites have been synthesized and investigated. In comparison to monometallic analogues, many of these bimetallic systems have been reported to incorporate higher levels of bulky olefins in copolymerizations with ethylene.[5-10] For dinuclear catalysts based on late metals, increased incorporation of polar monomers has been observed.[1] However, these favorable properties are not general and some systems are reported to have decreased polymerization activities. Further studies are necessary to gain a detailed understanding of how bimetallic cooperativity can be achieved and controlled to generate desirable polymers.

Multinucleating ligands are commonly used to preorganize metal centers in close proximity. Cyclopentadienyl, phenoxide, amide, imine, pyridine, and other neutral and anionic donors have been utilized as part of such multinucleating ligand architectures.[1] Typically, two identical moieties known to support olefin polymerization catalysis are connected via a linker that controls the relative orientation of the metals and the dynamics of the catalyst. The nature of the linker ranges from flexible, saturated alkyl chains to unsaturated olefins, arenes, biphenyls, and rigid ring systems.

The nickel phenoxyiminato system represents a well-studied catalyst family.[11] These catalysts are highly active for ethylene polymerization, and the incorporation of

other monomers has been reported. Notably, polymerizations can be performed in the presence of polar additives such as ethers and amines, which typically poison classical early metal catalysts.[12] Examples of ethylene polymerizations performed in aqueous emulsions are common with nickel phenoxyiminato catalysts.[13-16]

Due to their catalytic versatility and ease of synthesis, bimetallic versions of nickel phenoxyiminato systems have been developed (Chart 2.1).[10,16-23] In these systems, the two nickel centers are chelated via either the imine donor (**a**, **b**, **e**, **f,** **g**), the phenoxide donor (**d**, **h**), or both (**c**). The measured or proposed Ni–Ni distance varies from 3.1 Å (**h**) to between 7.5-8.5 Å (**c**, **d**, **e**, and **f**).[18-23] Analysis of the solid-state structures highlights the challenge in orienting the metal centers such that they would react cooperatively with substrates. For some of the reported systems the metals are found in geometries that make intramolecular cooperativity unlikely. For example, in system **c**, the nickel coordination planes are almost parallel which may be a favorable orientation for cooperative binding of substrate, but the two sites involved face in opposite directions.[20] In **d**, the coordination planes of the nickel centers are oriented at dihedral angles slightly higher than 90°, and the polymerization sites of each metal are directed away from the other metal.[18,19] In system **f**, the metal centers are placed anti with respect to the aromatic linker.[22]

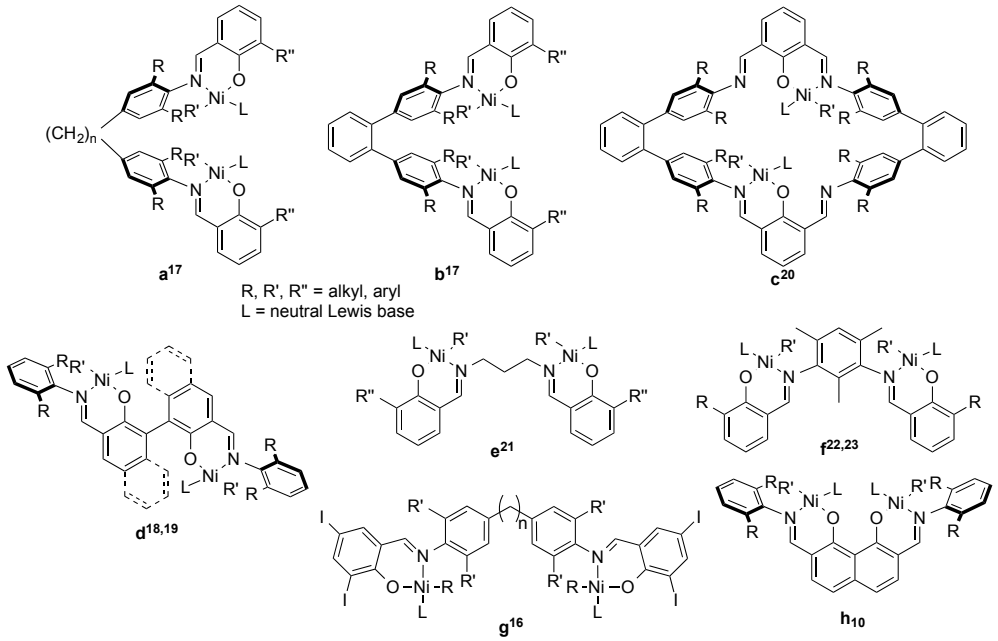

Chart 2.1. Previously reported dinuclear nickel phenoxyiminato complexes.

The dinuclear complexes in Chart 2.1 differ from their mononuclear counterparts in some aspects of catalytic behavior.[10,16-23] With systems **a** and **b**, ethylene polymerization activities are similar to mononuclear controls, but enhanced comonomer incorporation and activity occur in the copolymerization of ethylene with functionalized norbornene derivatives.[17,20] Increased incorporation of comonomers and increased methyl branching occur with system **h** relative to mononuclear analogues.[10] The bimetallic effects in systems **a**, **b** and **h** were proposed to involve coordination of the same monomer to both metal centers due to their spatial proximity.[17] When activated with MAO, system **e** produces polymer with higher M_w than some previously reported mononuclear systems.[21] Complex **f** (R = Ph) shows increased ethylene polymerization activity compared to a mononuclear system studied under the same conditions and produces polymers with higher M_w, but broader molecular weight distributions.[22] Observed differences in polymerization behavior between the mono and dinuclear

systems were attributed to potential electronic communication of the nickel centers through the ligand bridge in the bimetallic complex.[22] Further investigation of variants of **f** indicates similar functional group tolerance as compared to mononuclear counterparts. System **g** displays higher ethylene polymerization activity and produces polymers with increased M_w relative to the mononuclear systems studied.[16]

The ligand frameworks above highlight a strategy for synthesizing complexes with a fixed metal-metal distance – the linker must be rigid and the coordination sites involved in polymerization accessible from the same direction for both metals. To access a family of dinickel complexes that would allow for studies of the effect of the Ni–Ni distance and orientation of the metal coordination plane, we developed a ligand framework based on a terphenyl moiety, with blocked rotation around aryl-aryl bonds due to ring substitution. The synthesis of dinickel and mononickel complexes supported by this ligand architecture is reported herein along with polymerization and copolymerization studies with a variety of olefins.

RESULTS AND DISCUSSION

Synthesis of binucleating salcylaldimine ligands

The synthesis of the binucleating ligands is based on well-documented procedures (Scheme 2.1). 2-Bromo-4-*tert*-butyl-anisole (**1**) and 1,4-dibromo-2,3,5,6-tetramethylbenzene (**2**) starting materials were synthesized according to literature procedures.[24-26] Lithium-halogen exchange of **1**, followed by treatment with $ZnCl_2$ afforded an aryl-zinc reagent suitable for a double Negishi cross-coupling with **2**. The palladium-catalyzed coupling reaction led to a 1-to-2 mixture of two atropisomers, syn (**3-s**) and anti (**3-a**). Bromination of **3** with Br_2 ortho to the methoxy groups generated **4**. Column chromatography was used to separate the two atropisomers, which were then carried forward to the final ligand precursors, **7-s** and **7-a**, by the same synthetic procedures. Lithium–halogen exchange on **4** followed by addition of excess *N,N*-dimethylformamide (DMF) provided the diformyl species **5** upon aqueous work-up. Removal of the methyl protecting groups was accomplished with excess BBr_3 to afford compounds **6**. Condensation with aniline generated the binucleating ligand precursors **7**. The syntheses were high yielding overall: approximately 40% yield for the anti analogue (**7-a**) and 25% yield for the syn analogue (**7-s**). This synthesis was revised and optimized to eliminate the bromination step, as the specificity of this transformation was unreliable and bromination at the benzyl positions on the central arene was often observed (see Chapter 4; Scheme 4.1).

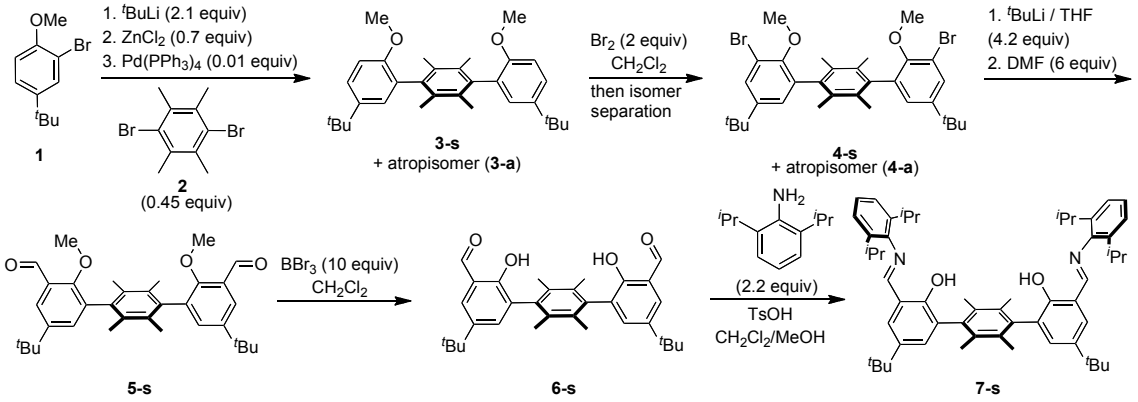

Scheme 2.1. Synthesis of bis-salcylaldimine framework.

Synthesis of mononucleating salcylaldimine ligands based on biphenyl and terphenyl frameworks

For comparison with the dinuclear systems, mononucleating ligands were also prepared. Several aspects of the terphenyl framework were investigated. The steric effect close to the metal center was tested by targeting catalysts based on a salcylaldimine substituted with pentamethylphenyl ortho to the oxygen (**13**). A previously reported variant (**29**)[27] of this ligand includes a phenyl group instead of pentamethylphenyl and was studied as a more sterically open version of **13**.

Dinucleating ligand precursors **7-s** and **7-a** bear steric bulk on both peripheral rings of the terphenyl unit. Three mononucleating terphenyl ligands were prepared to mimic the remote steric environment of **7-s** and **7-a**. All are fully substituted on the central ring. Two have oxygen substitution on both peripheral aryls in the position ortho to the central ring. This substitution pattern blocks the aryl-aryl rotation and leads to syn and anti isomers (**19-s** and **19-a**, respectively). The third mononucleating terphenyl ligand (**24**) has 3,5-di-*tert*-butyl substitution on the second peripheral ring.

The synthesis of salcylaldimine **13** was accomplished in five steps (Scheme 2.2). Negishi cross-coupling of **1** and pentamethylbromobenzene[28] afforded biphenyl species **9**. Subsequent steps are similar to the synthesis of ligands **7-s** and **7-a**. Bromination, followed by lithium–halogen exchange and DMF treatment installed the formyl moiety to give **11**. Deprotection of the ether group and condensation with 2,6-diisopropyl aniline provided **13** in 14% overall yield.

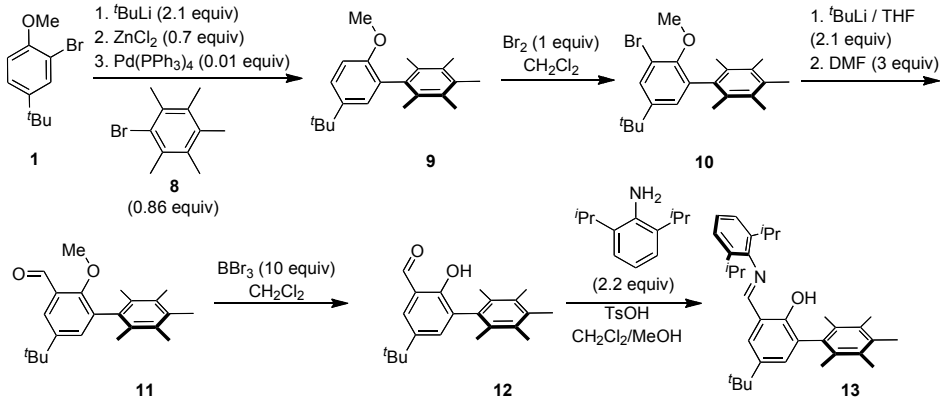

Scheme 2.2. Synthesis of mononucleating biphenyl-based salcylaldimine framework.

The synthesis of the mononucleating terphenyl ligand analogues was accomplished via a modification of the procedure in Scheme 1. Negishi cross-coupling of **2** with 2.2 equivalents of zinc reagent stemming from methoxymethyl (MOM)-protected 2-bromo-4-*tert*-butylphenol afforded both the expected terphenyl species as well as a bromo-substituted biphenyl species **15** (Scheme 2.3). The isolation of the mono-cross-coupled product (**15**) was instrumental to the preparation of asymmetric terphenyl ligands. A second cross-coupling, with orthogonally protected 2-bromo-4-*tert*-butylanisole (**1**), afforded the syn and anti atropisomers of terphenyl species **16** in a ratio of 1:1. Deprotonation directed by the MOM-protected ether using *n*-butyllithium and *N,N,N',N'*-tetramethylethylenediamine (tmeda) led, upon reaction with DMF and

aqueous workup, to the installation of a single formyl group. Acid-catalyzed removal of the MOM group followed by condensation with 2,6-diisopropylaniline afforded **19-a** and **19-s** in 35 and 37% yield, respectively, starting from compounds **16**. Separation of the two atropisomers was accomplished by column chromatography after the second Negishi cross-coupling (compounds **16**). The third mononucleating terphenyl ligand was synthesized starting from the Negishi cross-coupling of **15** with the aryl-zinc reagent derived from 3,5-di-*tert*-butylbromobenzene to yield asymmetric terphenyl **21** (Scheme 2.4). On adaptation of the protocols from the synthesis of **19**, **21** was converted to monophenol **24** in 34% overall yield from **15**. A single isomer is expected because of the lack of substitution ortho to the central ring and due to the symmetrical substitution pattern on the peripheral aryl.

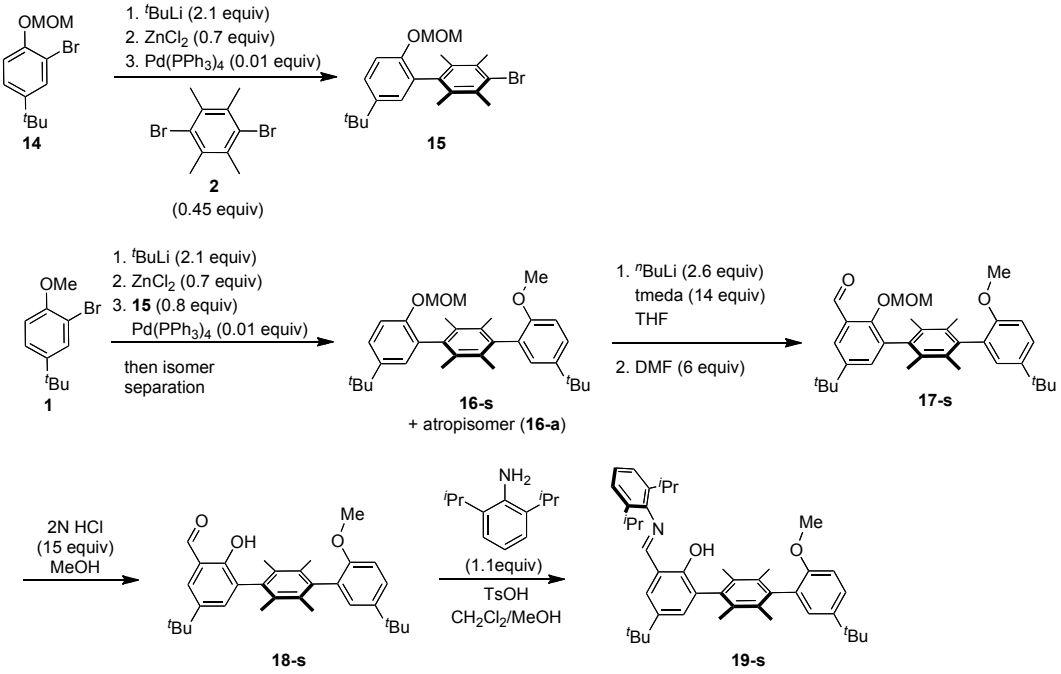

Scheme 2.3. Synthesis of mononucleating terphenyl-based salcylaldimine framework with methoxy substitution.

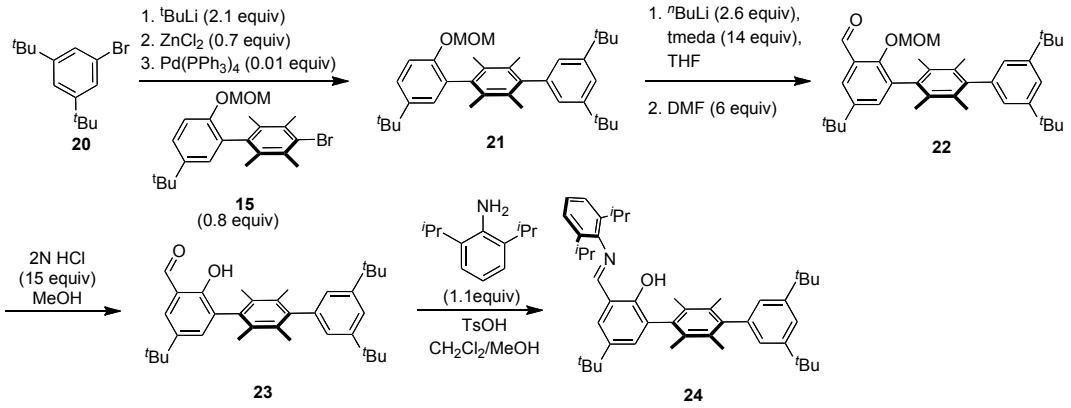

Scheme 2.4. Synthesis of mononucleating terphenyl-based salcylaldimine framework without methoxy substitution.

Studies of the interconversion of atropisomers

In the context of preserving the steric environment and the metal–metal separation in complexes supported by ligands with restricted rotation around aryl–aryl bonds, it is of interest to determine the kinetic and thermodynamic behavior of the atropisomers. Kinetics studies of the interconversion of ligand precursor **7-a** to **7-s** were performed in [D_0]-1-bromonaphthalene at 140, 150, 160 and 170 °C and were monitored by ^{1}H NMR spectroscopy. With either **7-s** or **7-a** as the starting material, equilibrium was reached over 20 h at 140 °C, 8 h at 150 °C, 3.5 h at 160 °C, and 1.75 h at 170 °C. At these temperatures, the equilibrium constant is K_{eq} = [**7-s**]/[**7-a**] = 0.61 (eq 2.1). The studied processes fit the integrated rate expression for approach to equilibrium of first-order kinetics (eq 2.2; X_e = concentration at equilibrium; X = concentration at time t) (see the experimental section at the end of the present chapter).[29] An Eyring plot using the determined rate constants provided activation energy parameters: $\Delta H^{\ddagger}$ = 28.0 ± 0.4 kcal mol^{-1} and $\Delta S^{\ddagger}$ = –12.3 ± 0.4 cal mol^{-1} K^{-1} (Figure 2.1). As expected, the calculated free energy barrier to rotation for **7-a** ($\Delta G^{\ddagger}$ =

32 kcal mol^{-1} at 298 K) is significantly higher than for a recently reported terphenyl system without permethylation of the central arene (14.6 kcal mol^{-1}).[30] Although the entropy of activation for conformational dynamic processes is typically close to 0, the larger absolute value determined here is still in the range reported for related fluxional processes: for example, rotation around the C–NMe_2 bond of a *N,N*-dimethylthiourethane ($\Delta S^{\ddagger} = -8 \pm 2$ cal mol^{-1} K^{-1}).[31] The significantly negative value suggests a relatively ordered transition state likely corresponding to the geometry with two aryl rings coplanar. This geometry may require significant distortions of the ring substituents. The barrier for isomerization for **7-a** is comparable to the reported value for the restricted rotation in hexaarylbenzenes ($\Delta G^{\ddagger} \approx 33$ kcal mol^{-1} at 419 K).[32] Extrapolating to 25 °C (the temperature at which most of the polymerizations discussed herein were run), the rate constant for the interconversion of **7-a** and **7-s** is approximately 10^{-11} s^{-1} indicating that virtually no isomerization takes place over the course of the polymerization experiment.

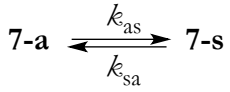

(2.1)

$$\ln(X_e - X) = -(k_{as} + k_{sa})t \quad (2.2)$$

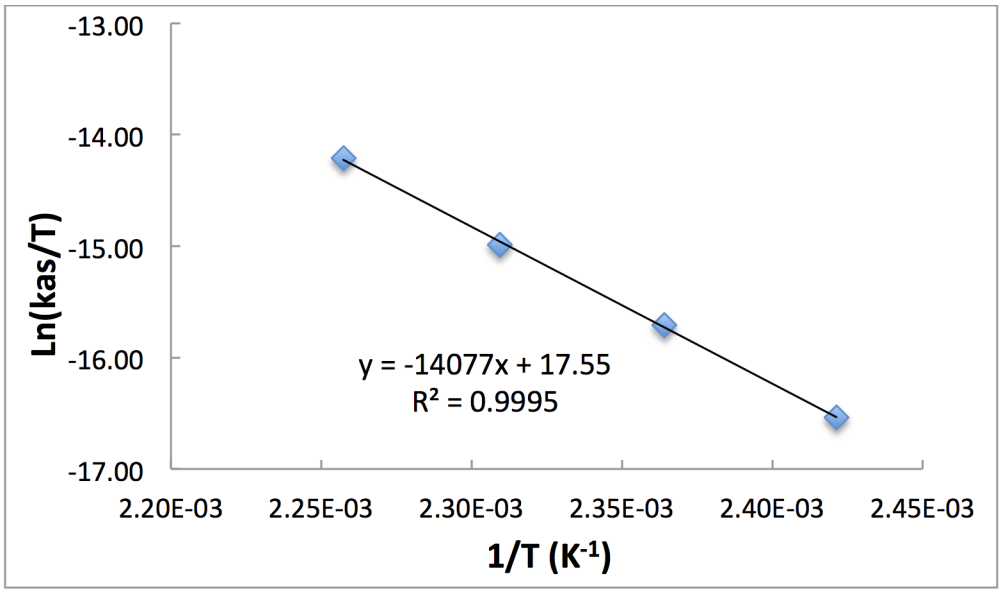

Figure 2.1. Eyring plot for the isomerization of **7-a** to **7-s**.

Synthesis of nickel complexes

Nickel complexes were prepared via alkane elimination. Reaction of phenols with a 10% excess of $NiMe_2$(tmeda) in diethyl ether in the presence of excess pyridine allowed for the isolation of the nickel–methyl species supported by the corresponding phenoxyiminato ligands with a bound pyridine (Scheme 2.5). When acetonitrile or tertiary amine (*N,N*-dimethylbutylamine or *N,N*-dimethylethylamine) were utilized instead of pyridine or if no additional labile ligand was added, the desired nickel complexes were not isolated cleanly. The ^{1}H NMR spectra of the isolated nickel complexes each display a single peak around –0.5 ppm, diagnostic of the Ni–CH_3 moiety. The atropisomers were assigned by ^{1}H-^{1}H NOESY and ROESY NMR studies. Through-space cross peaks are observed between the meta proton of the Ni-bound pyridine and the proton ortho to the aryl–aryl linkage for only one of the isomers (see the experimental section at the end of the present chapter). This isomer was assigned as the anti atropisomer (**25-a** and **27-a**).

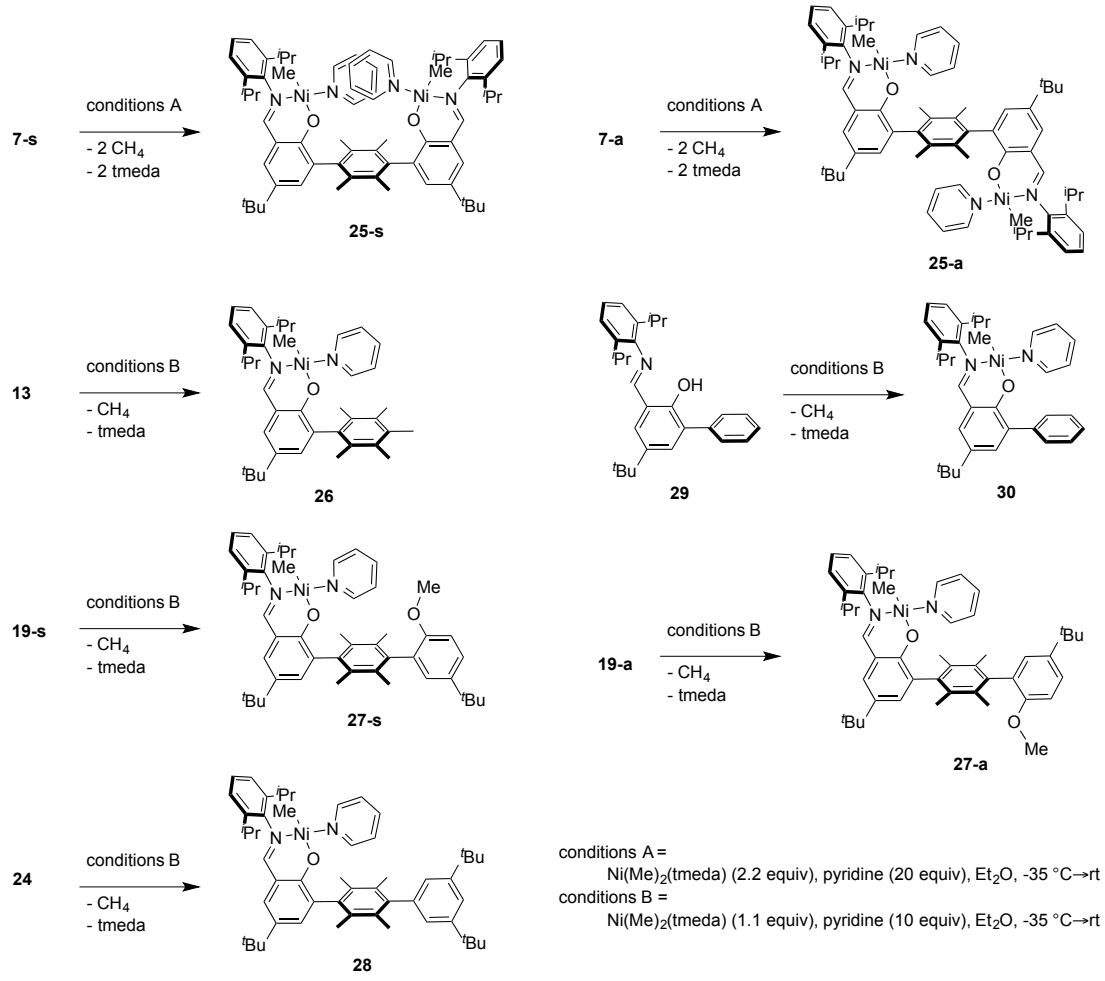

Scheme 2.5. Synthesis of nickel complexes.

NMR spectra of the nickel complexes are each indicative of a single ligand environment, suggesting that, for complexes with atropisomers, no isomerization occurs during synthesis. Heating solutions of **25-s** and **25-a** in benzene at 50 ºC for 13 h did not cause isomerization of **25-s** to **25-a** or **25-a** to **25-s**, respectively (^{1}H NMR spectroscopy). No decomposition was observed for **25-a**, though 70% decomposition of **25-s** was observed, on the basis of the disappearance of the Ni–CH_3 peak in the ^{1}H NMR spectrum. Heating of **25-s** and **25-a** at 70 ºC for 8 h led to 100% and 10% decomposition, respectively, but no isomerization. Further heating of **25-a** at 90 ºC for

12 h caused significant decomposition, but no isomerization to **25-s**. Analogous results were seen when heating **27-a** and **27-s** to 90 °C for 6 h resulting in about 60% decomposition of **27-s** and 80% decomposition of **27-a**. These studies indicate that the energetic barrier is too high for isomerization to occur at any appreciable rate at 25 °C, consistent with the kinetics studies completed with the bis-salcylaldimines **7-a** and **7-s** (vide supra).

Structure of dinickel complexes

X-ray quality single crystals were obtained from a concentrated pentane solution cooled at –35 °C for **25-s** and by vapor diffusion of hexanes into tetrahydrofuran at room temperature for **25-a**. X-ray diffraction studies provided structural confirmation of the identity of the isomers (Figure 2.2), as assigned by NMR spectroscopy above. The methyl groups are located trans to the phenoxide and the pyridine trans to the imine, as reported for similar coordination environments.[33] The Ni–Ni distance is 7.1 Å (average for the two molecules in the asymmetric unit) for the syn isomer (**25-s**). A slight distortion from square-planar geometry is observed, probably due to the pyridine ligands that extend toward each other and must tilt to avoid steric interaction. The planes of the two pyridines are about 3.86 Å apart, possibly indicative of a weak π interaction.[34] The direction of binding of the pyridine ligands indicates that appropriate substrates may reach both metal centers for cooperative interaction. Conversely, for the anti atropisomer (**25-a**) intramolecular cooperativity is not possible because of the large metal–metal distance (11.1 Å), and because the nickel centers are on opposite faces of the central arene ring. The N(1)–Ni(1)–N(2) and N(3)–Ni(2)–N(4) angles in the syn isomer of 173° and 166°, respectively (average for the two molecules in the asymmetric

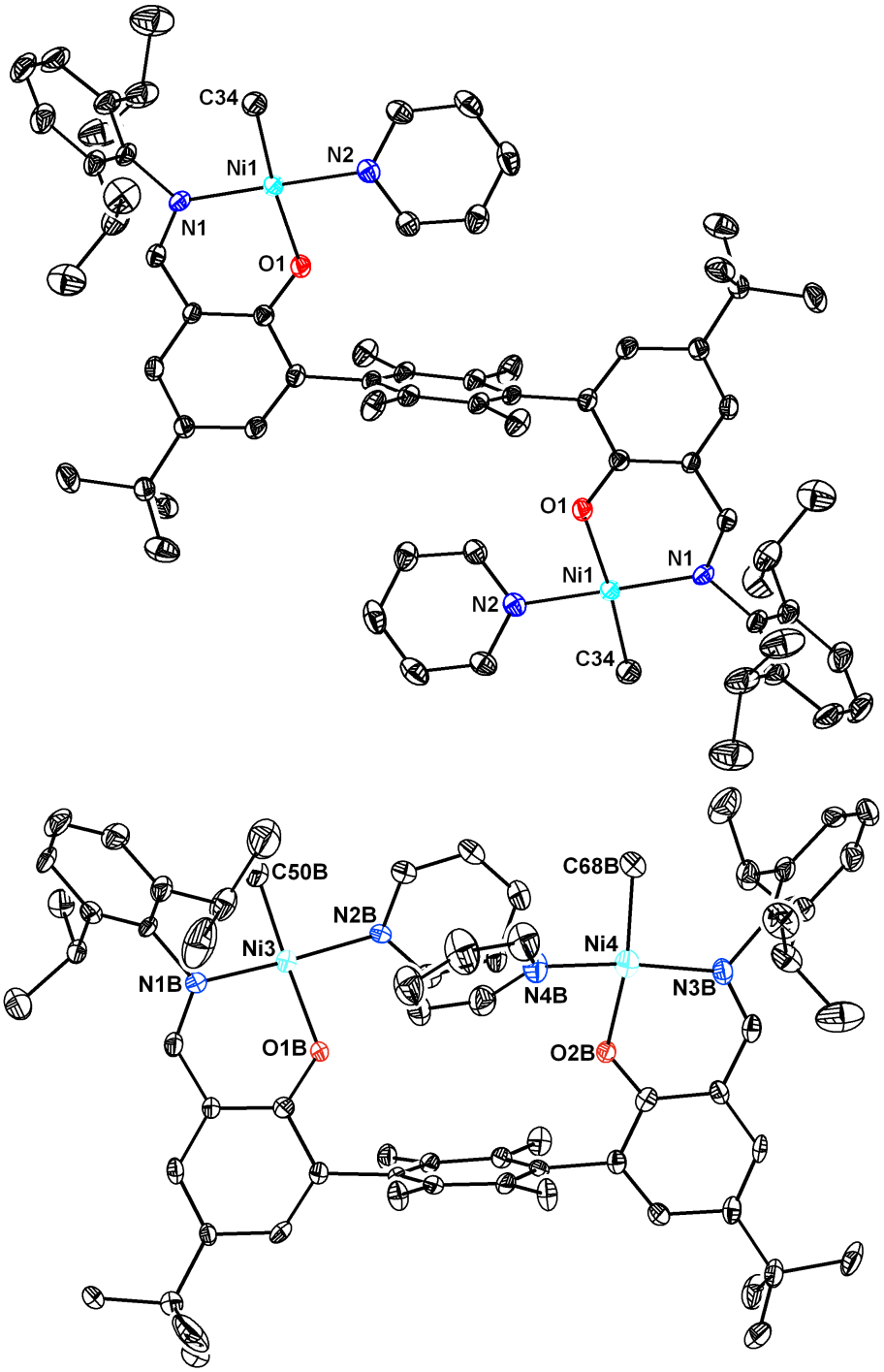

Figure 2.2. Solid-state structures of **25-a** (top) and **25-s** (bottom) with thermal ellipsoids at the 50 % probability level. For clarity, hydrogen atoms and solvent molecules are omitted.

unit), and the N(1)–Ni(1)–N(2) angle of 177° in the anti isomer are nearly linear. Ni–N, Ni–O, and Ni–Me distances are similar to known complexes.[20,22,27,33,35-36]

Ethylene polymerization

Ethylene homopolymerization trials were performed to determine the effect of reaction scale, reaction time, catalyst loading, and solvent (Table 2.1). Duplicate polymerization trials show changes in turnover frequencies (TOF) of less than 50 % in the majority of cases. Longer reaction time led to increased polymer yield indicating that the catalyst remains active over extended periods (e.g., entries 3–5, Table 2.1). Ethylene polymerizations in 25 mL of toluene with **25-a** and mononuclear counterparts **26**, **27-a**, **28**, and **30** resulted in similar catalytic activities (TOFs 1200–3700 (mol C_2H_4) (mol Ni)$^{-1}$ h^{-1}) (e.g., entries 3, 18, 23, 33, and 37, Table 2.1). This level of activity is similar or lower than seen with nickel phenoxyimines that have a phosphine or nitrile ligand in place of the pyridine, which may be due in part to the stability of the pyridine-bound complex.[12] The highest TOFs were observed using **25-a** and **26** (entries 3 and 18, Table 2.1). **25-s** exhibits catalytic activity an order of magnitude less than **25-a** (entries 10–13, Table 2.1), and is generally less active than the other investigated catalysts. Similarly, **27-s** has activity 3-fold lower than **27-a** (entries 28 and 29, Table 2.1). The observed difference in TOFs between **25-s** and **25-a** may be due to the effect of crowding of the catalytic pocket by the second nickel center. Similarly, steric bulk on the remote aryl of the terphenyl unit may be responsible for the difference between **27-s** and **27-a**.

Decreasing the scale of the polymerization reaction by five times (5 mL toluene) caused a significant drop in activity (e.g., entry 4 versus entry 7, Table 2.1). The

concentration of nickel complex was doubled in order to collect enough polymer for analysis when running polymerizations at this scale. These changes in scale and concentration resulted in a reduction of TOF by 2–10-fold (entries 4, 7; 12–15; 18–20; 23–25; 28–30; 33, 34; 37, 38, 40; Table 2.1). This effect is not well understood, but may be caused by changes in mixing of the solution and mass transfer problems, which could lower the effective concentration of ethylene in solution. To test the effect of mixing, a polymerization with **25-a** was run with stirring at one-third the rate used for all other polymerizations (entry 6, Table 2.1). The TOF in this polymerization was reduced by 2-fold from an identical trial with the higher stirring rate (entries 4 and 6, Table 2.1), supporting the hypothesis that insufficient mixing in the smaller scale polymerizations could contribute to the drop in activity. Changing the solvent from toluene to tetrahydrofuran (THF), did not significantly affect the activity of **25**–**28**, but decreased the activity of **30** by 4-fold (entries 7–9; 14–17; 20, 21; 30–32; 34–36; 40–42; Table 2.1). This drop in activity for **30** is similar to the 3–5-fold drop in TOF reported for polymerizations with phosphine-ligated nickel phenoxyimine complexes in the presence of excess ethers.[12,23] The notable lack of inhibition by THF of catalysts **25**–**28** may be due to the steric bulk of the fully substituted aryl group ortho to oxygen disfavoring ether coordination.

Polymer characterization by ^{1}H and ^{13}C NMR spectroscopy showed only methyl branch formation with peaks in the d_2-tetrachloroethane ^{13}C NMR spectrum at δ 20.1, 27.5, 30.4, 33.4 and 37.6 ppm assigned to the methyl branch carbon, the β carbon, the γ carbon, the methine carbon and the α carbon, respectively.[37] The variation in polymer branching level (determined by ^{1}H NMR spectroscopy) was less than 35% for repeated

Table 2.1. Ethylene homopolymerization trials.[a]

entry	complex	amt of Ni (mmol)	solvent	vol (mL)	time (h)	yield (g)	TOF[b]	branching[c]
1	**25-a**	0.0126	toluene	25	1	0.680	1924	3.4
2	**25-a**	0.0126	toluene	25	1	0.940	2660	
3	**25-a**	0.0200	toluene	25	1	2.079	3705	
4	**25-a**	0.0200	toluene	25	3	3.415	2029	7.5
5	**25-a**	0.0200	toluene	25	1.5	1.893	2250	6.0
6[d]	**25-a**	0.0200	toluene	25	3	1.875	1114	
7	**25-a**	0.0080	toluene	5	3	0.118	280	
8	**25-a**	0.0080	THF	5	3	0.101	150	18.8
9	**25-a**	0.0080	THF	5	3	0.224	333	17.3
10	**25-s**	0.0126	toluene	25	1	0.150	424	25.5
11	**25-s**	0.0126	toluene	25	1	0.110	311	27.0
12	**25-s**	0.0200	toluene	25	3	0.574	341	19.6
13	**25-s**	0.0200	toluene	25	3	0.894	531	16.5
14	**25-s**	0.0080	toluene	5	3	0.047	69	
15	**25-s**	0.0080	toluene	5	3	0.036	53	
16	**25-s**	0.0080	THF	5	3	0.041	60	70.3
17	**25-s**	0.0080	THF	5	3	0.043	64	67.5
18	**26**	0.0200	toluene	25	3	5.532	3287	
19	**26**	0.0200	toluene	25	3	4.791	2846	
20	**26**	0.0080	toluene	5	3	0.549	815	
21	**26**	0.0080	THF	5	3	0.675	1003	7.2
22	**26**	0.0080	THF	5	1	0.172	766	8.4
23	**27-a**	0.0200	toluene	25	3	3.113	1850	3.8
24	**27-a**	0.0200	toluene	25	3	2.901	1724	5.1
25	**27-a**	0.0080	toluene	5	3	0.083	123	12.0
26	**27-a**	0.0080	THF	5	3	0.122	182	20.8
27	**27-a**	0.0080	THF	5	3	0.170	253	15.7
28	**27-s**	0.0200	toluene	25	3	1.205	716	3.8
29	**27-s**	0.0200	toluene	25	3	1.301	773	4.3
30	**27-s**	0.0080	toluene	5	3	0.047	70	9.6
31	**27-s**	0.0080	THF	5	3	0.037	54	26.8
32	**27-s**	0.0080	THF	5	3	0.041	61	27.2
33	**28**	0.0200	toluene	25	3	3.107	1846	
34	**28**	0.0080	toluene	5	3	0.100	148	10.8
35	**28**	0.0080	THF	5	3	0.099	147	19.6
36	**28**	0.0080	THF	5	3	0.081	121	19.6
37	**30**	0.0200	toluene	25	3	1.975	1174	
38	**30**	0.0200	toluene	25	3	2.879	1710	
39	**30**	0.0200	toluene	25	1	0.720	1284	
40	**30**	0.0080	toluene	5	3	0.416	618	
41	**30**	0.0080	THF	5	3	0.152	225	37.8
42	**30**	0.0080	THF	5	3	0.076	113	40.5

[a]All polymerizations were run in a glass reactor under 100 psig of ethylene at 25 °C. [b]TOF = turnover frequency in (mol C_2H_4) (mol Ni)$^{-1}$ h^{-1}. [c]Branching was determined from ^{1}H NMR spectroscopy and is reported as the number of branches per 1000 carbons. [d]In this polymerization, the stirring was reduced to one-third of the rate used for all other polymerizations.

trials, indicating good reproducibility.[38-39] Polymers resulting from **25-s** have the highest level of branching by at least 2-fold compared to products from other catalysts under the same catalytic conditions (up to 70 branches/1000 C, entry 16, Table 2.1). An increase in polymer branching was also observed upon the combination of scale reduction, catalyst concentration increase, and the solvent change to THF (e.g. compare entries 12 and 16, Table 2.1). Polymer branching is caused by chain walking processes that are dependent on relative rates of olefin insertion and β-H elimination/isomerization.[39-42] Increased ethylene concentration allows for faster olefin insertion compared to isomerization and leads to lower levels of branching. Higher branch density in the small-scale experiments is consistent with lower concentration of monomer due to inefficient mixing (as proposed for the decreased yield) and with the lower solubility of ethylene in THF.

The selectivity for methyl branches is notable. Previously reported dinuclear nickel polymerization catalysts based on system **h** (Chart 2.1) also generate polyethylene with only methyl branches and there are a few additional accounts of dinuclear nickel systems producing polyethylene with predominantly methyl branches.[10] This contrasts with previously reported mononickel systems that show longer branches as well.[18,20-23] Catalysts **25–28** and **30** generate polyethylene with only methyl branches (path **A**, Scheme 2.6) suggesting that the proximal ligand environments hinder the formation of ethyl (or longer) branches regardless of the contributions from a second metal center. Bulky ligands can disfavor path **B** in Scheme 2.6, which involves species with nickel bound to a secondary carbon substituted with an ethyl group and the polymeryl chain. Similar to system **h**, the dinuclear syn isomer **25-s** generates increased branch density

compared to the mononuclear analogues. One explanation invokes slower propagation kinetics for **25-s** compared to **25-a** and the mononuclear systems, allowing for more extensive chain walking with **25-s**. In THF, compound **27-s** produced polymers with lower branching despite similar TOFs compared with **25-s** (entries 16, 17, 31, and 32, Table 2.1); this behavior suggests that the simple ligand sterics explanation is not fully satisfactory. However, a direct bimetallic interaction of pendant C–H bonds in the chain walking intermediates, as proposed for **h**, seems unlikely given the significant metal–metal distance.

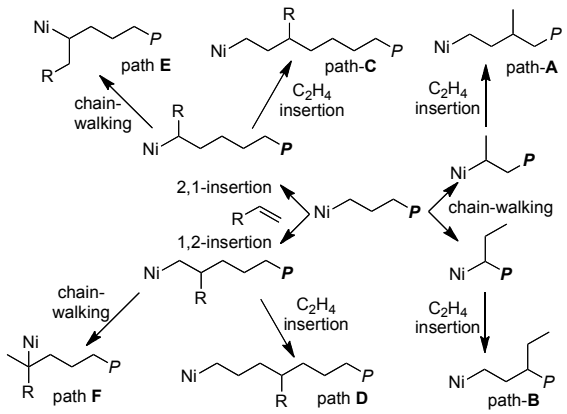

Scheme 2.6. Insertion and chain walking processes during polymerization.

Ethylene/1-hexene copolymerization

Ethylene/1-hexene copolymerization trials were also performed to determine the effects of reaction scale, comonomer concentration, reaction time, reaction temperature and solvent on the resultant copolymers (Table 2.2). As with the ethylene homopolymerizations, polymerizations with **25-s** and **27-s** produced the least polymer, and polymers synthesized using **25-s** display the largest amount of branching (e.g. entries 6, 16, 18, 21, 24, 27, and 29, Table 2.2). The change in activity from homopolymerizations of ethylene observed in experiments performed on a 25 mL scale

Table 2.2. Ethylene/1-hexene copolymerization trials.[a]

entry	complex	amt of Ni (mmol)	amt of 1-hexene (equiv)	solvent	vol (mL)	temp (°C)	time (h)	yield (g)	TOF[b]	branching[c]
1	**25-a**	0.0200	8000	toluene	25	25	1	0.107	191	36.3
2	**25-a**	0.0040	8000	toluene	5	25	3	0.030	89	49.1
3	**25-a**	0.0080	4000	toluene	5	25	3	0.043	64	33.0
4	**25-a**	0.0080	4000	THF	5	25	3	0.051	76	34.7
5	**25-a**	0.0080	3200	THF	5	25	3	0.112	167	31.1
6	**25-a**	0.0080	3200	THF	5	25	3	0.080	118	31.6
7	**25-s**	0.0040	8000	toluene	5	25	1	--[d]	-- [d]	92.2
8	**25-s**	0.0040	8000	toluene	5	25	3	0.020	59	76.6
9	**25-s**	0.0040	8000	toluene	5	25	12	0.016	12	65.2
10	**25-s**	0.0040	8000	toluene	5	25	12	0.040	30	78.4
11	**25-s**	0.0040	8000	toluene	5	40	3	0.012	36	
12	**25-s**	0.0040	8000	toluene	5	40	12	0.044	32	
13	**25-s**	0.0080	4000	toluene	5	25	3	0.023	34	54.0
14	**25-s**	0.0080	4000	toluene	5	25	3	0.017	25	
15	**25-s**	0.0080	3200	THF	5	25	3	0.018	26	63.7
16	**25-s**	0.0080	3200	THF	5	25	3	0.016	23	62.9
17	**26**	0.0080	3200	THF	5	25	3	0.193	287	32.8
18	**26**	0.0080	3200	THF	5	25	3	0.078	116	33.1
19	**27-a**	0.0080	3200	toluene	5	25	3	0.132	195	31.4
20	**27-a**	0.0080	3200	THF	5	25	3	0.092	136	34.8
21	**27-a**	0.0080	3200	THF	5	25	3	0.066	99	33.9
22	**27-s**	0.0080	3200	toluene	5	25	3	0.017	26	33.3
23	**27-s**	0.0080	3200	THF	5	25	3	0.028	42	38.9
24	**27-s**	0.0080	3200	THF	5	25	3	0.028	42	39.3
25	**28**	0.0080	3200	toluene	5	25	3	0.030	44	53.4
26	**28**	0.0080	3200	THF	5	25	3	0.063	94	38.5
27	**28**	0.0080	3200	THF	5	25	3	0.108	160	38.8
28	**30**	0.0080	3200	THF	5	25	3	0.094	140	44.6
29	**30**	0.0080	3200	THF	5	25	3	0.047	70	48.4

[a]All polymerizations were run in a glass reactor under 100 psig of ethylene. [b]TOF = turnover frequency in (mol C_2H_4) (mol Ni)$^{-1}$ h^{-1}. This value is not adjusted for the amount of 1-hexene incorporated. [c]Branching was determined from ^{1}H NMR spectroscopy and is reported as the number of branches per 1000 carbons. The type of branching was also determined (from ^{13}C NMR spectroscopy) and peaks for only methyl and butyl branches were observed. [d]Too little polymer to accurately determine.

(entry 1, Table 2.1 versus entry 1, Table 2.2) was one order of magnitude, matching previous reports on the decrease in activity from ethylene homopolymerization upon addition of an α-olefin comonomer in large excess.[35] The drop observed on a 5 mL scale, however, was not as significant (only up to 4.4 times). The decrease in activity was previously explained by a slower insertion rate of the α-olefins.[15,35] As expected, lower comonomer concentration led to higher TOF (entries 4 and 5, Table 2.2). Extension of the reaction time from 3 to 12 h resulted in a lowered TOF, presumably due to catalyst decomposition over time. Increasing the temperature resulted in a less than 2-fold decrease in activity in 3 h polymerization reactions and approximately no change in activity in 12 h polymerization runs (entries 8 and 11 and entries 10 and 12, Table 2.2). A change of solvent also had negligible effect on either the yield or the branching of the resultant polymers. Overall, the behavior of catalysts **25–28** and **30** is comparable to that of previously reported monometallic systems.[15,35] A noteworthy trend is the higher branching with the syn catalysts **25-s** and **27-s**; this may also be a consequence of the bulkier environment, which slows propagation in comparison to chain walking. Additionally, all of the polymers characterized by ^{13}C NMR spectroscopy displayed only methyl and butyl branches, which is a unique microstructure. Further study of this phenomenon was accomplished by polymerization trials with other α-olefins.

Ethylene/α-olefin copolymerization

Ethylene/α-olefin copolymerization trials were performed in duplicate with **25-a** and **25-s** and 1-pentene, 1-hexene, 1-heptene, and 1-octene to evaluate the effects of nickel-nickel proximity on branching, comonomer incorporation, TOF, molecular

weight and molecular weight distribution (Table 2.3). Again, significantly more branching was observed in polymers produced with **25-s** than in polymers produced with **25-a**, but the percent incorporations of 1-pentene and 1-hexene were similar. This behavior suggests that the difference in the extent of branching was due to the presence of additional methyl branches from chain walking rather than to the incorporation of additional comonomer. With the longer α-olefins, 1-heptene and 1-octene, a greater degree of comonomer incorporation was seen in polymers generated by **25-a** than by **25-s**, likely due to increased steric hindrance in **25-s**.

In all of the ethylene/α-olefin copolymers examined by ^{13}C NMR spectroscopy (Tables 2.2 and 2.3), only isolated methyl branches and branches the length of the comonomer chain were present. These data suggest that chain walking along the polyethylene chain to methyl branches occurs, but that after the insertion of a comonomer, no chain isomerization takes place before the coordination and insertion of the next ethylene monomer (paths **C** and **D**, Schemes 2.6 and 2.7). To the best of our knowledge, this type of polymer microstructure has not been previously reported for ethylene-α-olefin copolymerization; it formally corresponds to an ethylene-propylene-α-olefin copolymer, without chain walking.[15,35] Mecking et al. specifically report a variety of branch lengths including methyl, ethyl and butyl branches in the copolymerization of ethylene and 1-butene, which are attributed to various modes of insertion and subsequent chain walking.[15] Assuming 1,2-insertions are favored (paths **D** and **F**, Scheme 2.6), the difference in polymer microstructure achieved in polymerizations with the current systems may arise from the steric hindrance caused by

Table 2.3. Ethylene/α-olefin copolymerization trials with **25-a** and **25-s**.[a]

entry	com-plex	co-monomer	yield (g)	branch-ing[b]	branch type[c]	branch ratio[c]	inc (%)[d]	TOF e[e]	TOF co[e]	M_w[f]	M_n[f]	PDI[f]
1	**25-a**	none	0.101	17.3	m			150				
2	**25-a**	none	0.224	18.8	m			333		47591	6309	7.54
3	**25-s**	none	0.041	70.3	m			60				
4	**25-s**	none	0.043	67.5	m			64		8114	2697	3.01
5	**25-a**	1-pentene	0.087	33.4	m+p	1:1.2	3.9	124	2.0	15238	4271	3.57
6	**25-a**	1-pentene	0.086	31.3	m+p	1:1.3	3.7	123	1.9			
7	**25-s**	1-pentene	0.044	70.2	m+p	1:0.3	3.4	64	0.9	7707	2583	2.98
8	**25-s**	1-pentene	0.028	76.1	m+p	1:0.3	3.7	39	0.6			
9	**25-a**	1-hexene	0.112	31.1	m+b	1:2.1	4.6	159	2.6	14088	3712	3.80
10	**25-a**	1-hexene	0.080	31.6	m+b	1:2.3	4.8	112	1.9			
11	**25-s**	1-hexene	0.018	63.7	m+b	1:0.4	3.9	25	0.3			
12	**25-s**	1-hexene	0.016	62.9	m+b	1:0.3	3.1	22	0.2	2759	893	3.09
13	**25-a**	1-heptene	0.053	36.0	m+pn	1:2.7	6.0	74	1.4	9097	3037	3.00
14	**25-a**	1-heptene	0.045	40.7	m+pn	1:3.2	7.3	61	1.4			
15	**25-s**	1-heptene	0.022	68.0	m+pn	1:0.5	5.1	31	0.5	3619	1196	3.03
16	**25-s**	1-heptene	0.006	61.3								
17	**25-a**	1-octene	0.017	49.4	m+h	1:4.1	10.4	22	0.7	4472	1068	4.19
18	**25-a**	1-octene	0.017	49.5	m+h	1:6.2	11.5	22	0.7			
19	**25-s**	1-octene	0.012	61.0	m+h	1:0.6	5.3	17	0.2	2030	559	3.63
20	**25-s**	1-octene	0.009	51.1								
21	**25-a**	$C_{13}H_{24}O_2$[g]	0.037				2.7	45	1.3			
22	**25-s**	$C_{13}H_{24}O_2$[g]	0.002				1.6	1.7	0.03			

[a]All polymerizations were run for 3 h in a glass reactor with 0.0080 mmol of nickel in THF under 100 psig of ethylene with 3200 equivalents of comonomer at 25 °C. The total reaction volume was 5 mL. [b]Branching was determined from ^{1}H NMR spectroscopy and is reported as the number of branches per 1000 carbons. [c]Determined from ^{13}C NMR spectroscopy: m = methyl, p = propyl, b = butyl, pn = pentyl, h = hexyl. [d]Percent incorporation was calculated from the overall branching and the branch ratio. [e]TOF = turnover frequency in (mol monomer) (mol Ni)$^{-1}$ h^{-1}. "e" = ethylene, "co" = comonomer. Calculated from the yield and the % incoporation of comonomer. [f]Calculated from GPC results. [g]Ethyl undecylenate; used 2500 equivalents (4.8 mL) with 0.2 mL THF for a total volume of 5 mL.

the supporting ligand, disfavoring path **F**, in which nickel migration to a tertiary carbon from a primary carbon.[14,43-44]

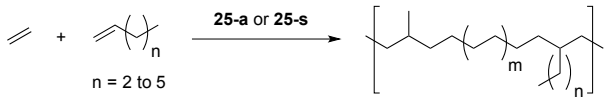

Scheme 2.7. Copolymerizations of ethylene and α-olefins leads to only two types of branches.

GPC analysis was performed on several of the ethylene/α-olefin copolymers (Table 2.3). In all cases, the molecular weights of polymers produced with **25-a** were higher than of polymers produced with **25-s**. The molecular weights for polymers produced with both **25-a** and **25-s** generally decreased with increasing comonomer size. The PDI values were between 3 and 4 except for the homopolymerization of ethylene with **25-a** (PDI = 7.5). Generally, lower PDI values were observed for **25-s** compared to **25-a**. The observed molecular weights and PDIs are in the range previously reported for mono- and dinickel catalysts.[10,12,17,20,33] Notably, high PDIs (5–8) were reported previously for bimetallic catalysts (**c** and **f**, Chart 2.1).[20,22] The difference in polymer molecular weight is indicative of the relative rates of propagation versus chain termination, which depend on the rates of olefin insertion and β-H elimination, respectively.[45] The lower molecular weights for **25-s** versus those for **25-a** contrast with previous reports of a bimetallic catalsyt leading to an increase in M_w versus the monometallic version,[22] but are consistent with the trends in TOF and branching level. In comparison to **25-a**, complex **25-s** displays lower TOF and higher branching consistent with lower olefin insertion rates and higher β-H elimination rates, which is in agreement with the observed lower molecular weight polymers. Similar agreement

between trends of M_w versus TOF and polymer branching (for **25-a**) were observed upon variation of the comonomer. The larger comonomers may lead to lower insertion rates due to steric reasons and result in lower M_w polymers.[15,35]

Copolymerizations of ethylene and polar monomers were also attempted. Using a large excess of a comonomer with a distal polar moiety, ethyl undecylenate (entries 21 and 22, Table 2.3; 2500 equivalents per nickel), led to a modest yield of polymer and incorporation within the range of previous reports for related catalysts.[35] Copolymerization attempts with 225 equivalents of *N,N*-dimethylallylamine per nickel resulted in polyethylene with no polar comonomer incorporation observed by ^{1}H or ^{13}C NMR spectroscopy, but larger inhibitory effects for **25-a** compared to **25-s**.[46] In contrast, copolymerization attempts with 225 equivalents of methyl acrylate per nickel resulted in no observable polymer. These data indicate that **25-a** and **25-s** tolerate some polar monomers. Additional investigations of the copolymerization of ethylene and polar monomers with these complexes will be discussed in Chapters 3 and 4.

CONCLUSIONS

The syn and anti atropisomers of a dinuclear neutral nickel bisphenoxyiminato complex (**25**) were synthesized and characterized. Kinetic studies of the bis-salcylaldimine precursors (**7**) indicate that virtually no isomerization between the syn and anti atropisomers occurs at 25 °C, making these terphenyl complexes suitable for the systematic study of the effects of metal–metal cooperativity. The terphenyl dinuclear complexes polymerize ethylene similarly to previously reported mononickel phenoxyimine complexes such as **30**. Ethylene polymerization leads to polyethylene with only methyl branches. Copolymerizations of ethylene and α-olefins with complexes **25**–**28** and **30** produce polyethylene with methyl branches and branches the length of the comonomer side-chain (three to six carbons depending on the comonomer). This polymer microstructure has not been previously reported, to our knowledge, for the copolymerization of ethylene and α-olefins with nickel phenoxyiminato catalysts. Complexes **25**–**28** retain polymerization activity in the presence of an excess of polar additives such as THF, in contrast to the decreased activity of complex **30**. Because no nickel–nickel cooperativity is expected in **25-a** or the mononuclear complexes, this tolerance is attributed to the steric environment of the permethylated arene that is not present in **30**. While no polymer was produced in attempted copolymerizations of ethylene with methyl acrylate, copolymerizations of ethylene with an olefin possessing a distal polar moiety is observed, indicating some functional monomer tolerance for **25-s** and **25-a**. Generally, the syn catalysts were found to be less active and to generate lower M_w polymers than the anti analogues. More branching is observed for the syn catalysts. These effects are explained in terms of

increased steric bulk. This steric effect will be discussed futher in the following chapters. The present systems provide a robust framework amenable for further studies of dinuclear catalysts for olefin polymerization. Future investigations include changing the relative position of the two metal centers on the terphenyl moiety, the nature of the metals, and the donor sets, all of which will be communicated in the following chapters.

EXPERIMENTAL SECTION

General considerations and instrumentation

All air- and/or water-sensitive compounds were manipulated using standard vacuum or Schlenk line techniques or in an inert atmosphere glovebox. The solvents for air- and moisture-sensitive reactions were dried over sodium/benzophenone ketyl or calcium hydride or by the method of Grubbs.[47] All NMR solvents were purchased from Cambridge Isotopes Laboratories, Inc. C_6D_6 was dried over sodium/benzophenone ketyl and vacuum-transferred prior to use. 1-Bromonaphthalene, pyridine, 1-pentene, 1-hexene, 1-heptene, 1-octene, ethyl undecylenoate, *N*,*N*-dimethylallylamine, and methyl acrylate were dried over calcium hydride and vacuum-transferred prior to use. Ethylene was purchased from Matheson and equipped with a PUR-Gas in-line trap to remove oxygen and moisture before use. All ^{1}H, ^{13}C, and 2D NMR spectra of small organic and organometallic compounds were recorded on Varian Mercury 300 MHz, Varian 400 MHz, or Varian INOVA-500 or 600 MHz spectrometers at room temperature. All ^{1}H and ^{13}C NMR spectra of polymers were recorded on the Varian INOVA-500 MHz spectrometer at 130 °C. Chemical shifts are reported with respect to residual internal deuterated solvent. J coupling are reported in Hz. 2-bromo-4-*tert*-butylphenol,[26] **2**,[25] **8**,[28] chloromethyl methyl ether,[48] $Ni(acac)_2(tmeda)$,[49] $NiMe_2(tmeda)$,[50] and 3-phenyl salicylaldehyde[51] were synthesized according to literature procedures.

Synthetic protocols

Compound 1. 2-Bromo-4-*tert*-butylmethoxybenzene was synthesized from 2-bromo-4-*tert*-butylphenol according to an analogous synthesis.[24] The ^{1}H NMR spectrum

matched literature assignments.[52] HRMS (EI+) Calcd for $C_{11}H_{15}OBr$: 242.0306. Found: 242.0305.

Compounds 3. Synthesis of these terphenyl compounds was accomplished via the Negishi coupling of 1,4-dibromo-2,3,5,6-tetramethylbenzene (**2**) with two equivalents of 2-bromo-4-*tert*-butylmethoxybenzene (**1**).[53] In the glovebox, **1** (25.44 g, 104 mmol, 1 equiv) and 250 mL of THF were combined in a large Schlenk tube and frozen in the cold well. ^{t}BuLi (1.7 M solution in pentane, 129 mL, 219 mmol, 2.1 equiv) was added to the thawing solution and stirred for 1 h while it was warmed to room temperature. The resultant yellow orange solution was refrozen in the cold well. Concurrently, a suspension of $ZnCl_2$ (9.98 g, 73 mmol, 0.7 equiv) in THF (100 mL) was frozen in the cold well. The thawing $ZnCl_2$ suspension was added to the thawing reaction mixture and stirred for 1 h resulting in a cloudy white solution. **2** (13.75 g, 47 mmol, 0.45 equiv), $Pd(PPh_3)_4$ (1.21 g, 1.1 mmol, 0.01 equiv) and THF (100 mL) were added to the reaction mixture at room temperature. The sealed Schlenk tube was brought out of the glovebox and heated to 75 °C for 5 days. Water was added to quench the reaction. The solution was filtered over silica gel, and the silica gel was washed with dichloromethane (DCM). The two atropisomers of the terphenyl compound were coprecipitated from methanol as a colorless solid (15.4 g, 71% yield). ^{1}H NMR (300 MHz, $CDCl_3$) δ = 7.36 (2dd, 2H, Ar*H*), 7.19 (2d, 2H, Ar*H*), 6.95 (2d, 2H, Ar*H*), 3.78 (2s, 6H, OC*H*$_3$), 1.99 (2s, 12H, ArC*H*$_3$), 1.34 (2s, 18H, C(C*H*$_3$)$_3$) ppm. ^{13}C NMR (75 MHz, $CDCl_3$) δ = 154.70 (Ar), 143.25 (Ar), 137.83 (Ar), 137.57 (Ar), 132.22 (Ar), 132.10 (Ar), 130.75 (Ar), 129.31 (Ar), 128.97 (Ar), 124.29 (Ar), 124.21 (Ar), 110.19 (Ar), 110.09 (Ar), 55.81 (O*C*H$_3$), 55.59 (O*C*H$_3$), 34.29 (Ar*C*(CH$_3$)$_3$), 31.75 (ArC(*C*H$_3$)$_3$),

18.07 (Ar*C*H_3), 18.00 (Ar*C*H_3) ppm. HRMS (EI+) Calcd. for $C_{32}H_{42}O_2$: 458.3185. Found: 458.3184.

Compounds 4. Compounds **3** (10.00 g, 21.8 mmol, 1 equiv), iron powder (0.079 g, 1.41 mmol, 0.06 equiv), and 35 mL DCM were combined in a 100 mL round bottom flask equipped with an addition funnel. The flask was covered with foil. Bromine (2.3 mL, 44.7 mmol, 2.05 equiv) and 5 mL of DCM were added to the addition funnel and dripped into the flask over 5 minutes. The reaction mixture was stirred for an additional 3 h at room temperature. The reaction was quenched with aqueous sodium hydrosulfite and sodium carbonate. The desired product was extracted into DCM. The organics were washed with water, dried with $MgSO_4$, filtered and volatiles were removed under vacuum. The two atropisomers were separated by column chromatography (2/1 hexanes/DCM). An 8.49 g amount of white solid was collected of the anti isomer and 4.73 g of white solid was collected of the syn isomer (overall yield of 98%). Data for **4-a** are as follows. ^{1}H NMR (300 MHz, $CDCl_3$) δ = 7.56 (d, *J*=2.4, 2H, Ar*H*), 7.03 (d, *J*=2.4, 2H, Ar*H*), 3.49 (s, 6H, OC*H*$_3$), 1.97 (s, 12H, ArC*H*$_3$), 1.33 (s, 18H, C(C*H*$_3$)$_3$) ppm. ^{13}C NMR (75 MHz, $CDCl_3$) δ = 152.09 (Ar), 148.45 (Ar), 137.61 (Ar), 136.84 (Ar), 131.96 (Ar), 129.12 (Ar), 128.40 (Ar), 117.22 (Ar), 60.35 (O*C*H_3), 34.66 (Ar*C*(CH$_3$)$_3$), 31.54 (ArC(*C*H$_3$)$_3$), 18.31 (Ar*C*H_3) ppm. HRMS (EI+) Calcd. for $C_{32}H_{40}O_2Br^{81}Br$: 616.1374. Found: 616.1376. Data for **4-s** are as follows. ^{1}H NMR (300 MHz, $CDCl_3$) δ = 7.56 (d, *J*=2.4, 2H, Ar*H*), 7.12 (d, *J*=2.4, 2H, Ar*H*), 3.38 (s, 6H, OC*H*$_3$), 2.00 (s, 12H, ArC*H*$_3$), 1.32 (s, 18H, C(C*H*$_3$)$_3$) ppm. ^{13}C NMR (75 MHz, $CDCl_3$) δ = 151.98 (Ar), 148.49 (Ar), 137.66 (Ar), 136.45 (Ar), 132.41 (Ar), 129.09 (Ar), 128.18 (Ar), 117.33 (Ar), 59.74

(O*C*H_3), 34.69 (Ar*C*(CH_3)$_3$), 31.50 (ArC(*C*H_3)$_3$), 18.22 (Ar*C*H_3) ppm. HRMS (EI+) Calcd. for $C_{32}H_{40}O_2Br^{81}Br$: 616.1374. Found: 616.1402.

Compound 5-a. Compound **4-a** (5.10 g, 8.28 mmol, 1 equiv) was dissolved in 200 mL of THF in a 500 mL Schlenk flask in the glovebox and the solution was frozen in the cold well. ^{t}BuLi (1.7 M in pentane, 20.44 mL, 34.8 mmol, 4.2 equiv) was added in four portions to the cold solution of **4-a**. The reaction turned yellow upon addition of ^{t}BuLi and was warmed to room temperature as it was stirred for 1 h. The reaction mixture was refrozen in the cold well. A solution of DMF (3.84 mL, 49.6 mmol, 6 equiv) in 10 mL of THF was also frozen in the cold well before it was added to the reaction mixture while thawing. The resulting colorless solution was warmed to room temperature and stirred for 2 h. The flask was brought out of the box, and the reaction was quenched with 100 mL of water. Volatiles were removed under vacuum and the desired product was extracted into DCM and washed with brine and water. The organic phase was dried over $MgSO_4$, filtered, and volatile materials were removed under vacuum to give an orange solid. Precipitation from methanol yielded 4.2 g (99% yield) of pale yellow solid. ^{1}H NMR (400 MHz, $CDCl_3$) δ = 10.45 (s, 2H, C*H*O), 7.87 (d, *J*=2.6, 2H, Ar*H*), 7.35 (d, *J*=2.6, 2H, Ar*H*), 3.51 (s, 6H, OC*H*$_3$), 2.00 (s, 12H, ArC*H*$_3$), 1.34 (s, 18H, C(C*H*$_3$)$_3$) ppm. ^{13}C NMR (101 MHz, $CDCl_3$) δ = 191.17 (Ar*C*HO), 158.82 (Ar), 147.23 (Ar), 137.22 (Ar), 136.06 (Ar), 135.75 (Ar), 132.34 (Ar), 128.56 (Ar), 123.84 (Ar), 62.16 (O*C*H_3), 34.72 (Ar*C*(CH_3)$_3$), 31.41 (ArC(*C*H_3)$_3$), 18.30 (Ar*C*H_3) ppm. HRMS (EI+) Calcd. for $C_{34}H_{42}O_4$: 514.3083. Found: 514.3084.

Compound 5-s. The lithium–halogen exchange and formylation of **4-s** were accomplished via the same procedures as for the anti isomer. The desired product was

isolated as a colorless solid in 85% yield (3.4 g). ^{1}H NMR (400 MHz, $CDCl_3$) δ = 10.46 (s, 2H, C*H*O), 7.89 (d, *J*=2.6, 2H, Ar*H*), 7.45 (d, *J*=2.6, 2H, Ar*H*), 3.45 (s, 6H, OCH_3), 2.05 (s, 12H, ArCH_3), 1.35 (s, 18H, C(CH_3)$_3$) ppm. ^{13}C NMR (101 MHz, $CDCl_3$) δ = 190.99 (Ar*C*HO), 158.71 (Ar), 147.32 (Ar), 137.34 (Ar), 135.88 (Ar), 135.49 (Ar), 132.78 (Ar), 128.73 (Ar), 123.76 (Ar), 61.40 (O*C*H$_3$), 34.79 (Ar*C*(CH$_3$)$_3$), 31.43 (ArC(*C*H$_3$)$_3$), 18.29 (Ar*C*H$_3$) ppm. HRMS (EI+) Calcd. for $C_{34}H_{42}O_4$: 514.3083. Found: 514.3089.

Compound 6-a. BBr_3 (7.74 mL, 81.6 mmol, 10 equiv) was syringed into a Schlenk flask containing a solution of **5-a** (4.20 g, 8.16 mmol, 1 equiv) in 200 mL of DCM under a nitrogen atmosphere. The solution turned from yellow to dark red and was stirred for 1.5 h before the reaction was stopped by the gradual addition of water and a color change to dark greenish brown was observed. The desired product was extracted into DCM. The organic phase was dried over $MgSO_4$, filtered, and volatile materials were removed under vacuum to give a greenish brown solid. Trituration with methanol followed by filtration yielded 2.55 g (64% yield) of **6-a** as an olive green solid. ^{1}H NMR (400 MHz, $CDCl_3$) δ = 11.12 (s, 2H, O*H*), 9.98 (s, 2H, C*H*O), 7.54 (2s, 4H, Ar*H*), 3.48 (s, 6H, OCH_3), 1.97 (s, 12H, ArCH_3), 1.35 (s, 18H, C(CH_3)$_3$) ppm. ^{13}C NMR (101 MHz, $CDCl_3$) δ = 197.20 (Ar*C*HO), 156.69 (Ar), 143.04 (Ar), 137.15 (Ar), 135.92 (Ar), 132.59 (Ar), 131.01 (Ar), 128.78 (Ar), 120.10 (Ar), 34.41 (Ar*C*(CH$_3$)$_3$), 31.44 (ArC(*C*H$_3$)$_3$), 17.93 (Ar*C*H$_3$) ppm. HRMS (EI+) Calcd. for $C_{32}H_{38}O_4$: 486.2770. Found: 486.2784.

Compound 6-s. The deprotection of **5-s** was accomplished via the same procedure as for the anti isomer. The desired product was isolated as a greenish solid in 93% yield (2.95 g). ^{1}H NMR (300 MHz, $CDCl_3$) δ = 10.91 (bs, 2H, O*H*), 9.98 (s, 2H,

C*H*O), 7.55 (d, *J*=2.5, 2H, Ar*H*), 7.45 (d, *J*=2.5, 2H, Ar*H*), 3.50 (s, 6H, OCH_3), 1.98 (s, 12H, ArCH_3), 1.35 (s, 18H, C(CH_3)$_3$) ppm. ^{13}C NMR (101 MHz, $CDCl_3$) δ = 196.96 (Ar*C*HO), 142.65 (Ar), 136.80 (Ar), 136.22 (Ar), 132.69 (Ar), 130.95 (Ar), 128.79 (Ar), 120.22 (Ar), 34.39 (Ar*C*(CH$_3$)$_3$), 31.47 (ArC(*C*H$_3$)$_3$), 17.95 (Ar*C*H$_3$) ppm. HRMS (EI+) Calcd. for $C_{32}H_{38}O_4$: 486.2770. Found: 486.2785.

Compound 7-a. The *anti*-bis-salcylaldimine compound was synthesized by mixing **6-a** (1.5 g, 3.08 mmol, 1 equiv), *p*-toluenesulfonic acid (0.059 g, 0.31 mmol, 0.1 equiv), 2,6-diisopropylamine (1.28 g, 6.78 mmol, 2.2 equiv), and methanol (150 mL) in a round-bottom flask equipped with a reflux condenser. A color change from green to orange was observed with the addition of aniline. The mixture was stirred at reflux for 4 h and then cooled to room temperature. A pale orange solid was collected from the red solution via filtration. The precipitate was further purified by column chromatography (7/1 hexanes/DCM) and 1.7 g (68% yield) of pale yellow solid was obtained. ^{1}H NMR (400 MHz, C_6D_6) δ = 13.45 (s, 2H, O*H*), 8.05 (s, 2H, NC*H*), 7.42 (d, 2H, Ar*H*), 7.28 (d, 2H, Ar*H*), 7.11 (bs, 6H, N-Ar*H*), 3.06 (sept, *J*=6.8, 4H, C*H*(CH$_3$)$_2$), 2.24 (s, 12H, ArCH_3), 1.29 (s,18H, C(CH_3)$_3$), 1.06 (d, *J*=6.8, 24H, CH(CH_3)$_2$) ppm. ^{13}C NMR (101 MHz, C_6D_6) δ = 168.05 (Ar*C*HN), 157.53 (Ar), 147.32 (Ar), 141.85 (Ar), 138.96 (Ar), 137.61 (Ar), 133.75 (Ar), 132.81 (Ar), 131.98 (Ar), 125.75 (Ar), 123.54 (Ar), 118.49 (Ar), 34.26 (Ar*C*(CH$_3$)$_3$), 31.60 (ArC(*C*H$_3$)$_3$), 28.63 (Ar*C*H(CH$_3$)$_2$), 23.42 (ArCH(*C*H$_3$)$_2$), 18.44 (Ar*C*H$_3$) ppm. HRMS (FAB+) Calcd. for $C_{56}H_{73}O_2N_2$: 805.5672. Found: 805.5693.

Compound 7-s. The imine condensation to form the *syn*-bis-salcylaldimine compound from **6-s** was accomplished via the same procedure as for the anti isomer. The desired product was isolated as a pale yellow solid in 43% yield (1.06 g). ^{1}H NMR

(400 MHz, C_6D_6) δ = 13.45 (s, 2H, O*H*), 8.06 (s, 2H, NC*H*), 7.45 (d, 2H, Ar*H*), 7.29 (d, 2H, Ar*H*), 7.13 (bs, 6H, N-Ar*H*), 3.12 (sept, *J*=6.8, 4H, C*H*$(CH_3)_2$), 2.22 (s, 12H, ArC*H*$_3$), 1.27 (s, 18H, C(C*H*$_3)_3$), 1.11 (d, *J*=6.8, 24H, CH(C*H*$_3)_2$) ppm. ^{13}C NMR (101 MHz, C_6D_6) δ = 168.04 (Ar*C*HN), 157.58 (Ar), 147.39 (Ar), 141.68 (Ar), 138.95 (Ar), 137.76 (Ar), 133.43 (Ar), 132.92 (Ar), 131.98 (Ar), 127.65 (Ar), 125.77 (Ar), 123.54 (Ar), 118.62 (Ar), 34.19 (Ar*C*$(CH_3)_3$), 31.57 (ArC(*C*$H_3)_3$), 28.67 (Ar*C*H$(CH_3)_2$), 23.46 (ArCH(*C*$H_3)_2$), 18.47 (Ar*C*H_3) ppm. HRMS (FAB+) Calcd. for $C_{56}H_{73}O_2N_2$: 805.5672. Found: 805.5688.

Compound 9. Synthesis of this biphenyl compound was accomplished via the Negishi coupling of **8** with one equivalent of **1** using a procedure analogous to the synthesis of **3**. The product was precipitated from methanol as a colorless solid (0.57 g, 50 % yield). ^{1}H NMR (300 MHz, $CDCl_3$) δ = 7.34 (dd, *J*=8.6, 2.6, 1H, Ar*H*), 7.06 (d, *J*=2.5, 1H, Ar*H*), 6.91 (d, *J*=8.6, 1H, Ar*H*), 3.74 (s, 3H, OC*H*$_3$), 2.31 (s, 3H, ArC*H*$_3$), 2.28 (s, 6H, ArC*H*$_3$), 1.96 (s, 6H, ArC*H*$_3$), 1.31 (s, 9H, C(C*H*$_3)_3$) ppm. ^{13}C NMR (75 MHz, $CDCl_3$) δ = 154.69 (Ar), 143.29 (Ar), 136.52 (Ar), 134.14 (Ar), 132.29 (Ar), 130.75 (Ar), 128.95 (Ar), 124.27 (Ar), 110.01 (Ar), 55.61 (O*C*H_3), 34.25 (Ar*C*$(CH_3)_3$), 31.70 (ArC(*C*$H_3)_3$), 18.19 (Ar*C*H_3), 17.08 (Ar*C*H_3), 16.85 (Ar*C*H_3) ppm. HRMS (EI+) Calcd. for $C_{22}H_{30}O$: 310.2297. Found: 310.2297.

Compound 10. Compound **9** (0.57 g, 1.83 mmol, 1 equiv), iron powder (0.0066 g, 0.12 mmol, 0.06 equiv), and 5 mL DCM were combined in a 20 mL scintillation vial equipped with a stirbar. The vial was covered with aluminum foil. Bromine (0.10 mL, 1.92 mmol, 1.05 equiv) and 1 mL of DCM were dripped into the vial over 5 minutes via syringe. The reaction mixture was stirred for an additional 2.5 h at room temperature.

The reaction was quenched with water. The desired product was extracted into DCM. The organic fractions were washed with water, dried with $MgSO_4$, filtered and volatiles were removed under vacuum. 0.71 g (99% yield) of colorless solid was collected. ^{1}H NMR (400 MHz, C_6D_6) δ = 7.57 (d, *J*=2.4, 1H, Ar*H*), 7.03 (d, *J*=2.5, 1H, Ar*H*), 3.45 (s, 3H, OC*H*$_3$), 2.34 (s, 3H, ArC*H*$_3$), 2.29 (s, 6H, ArC*H*$_3$), 2.00 (s, 6H, ArC*H*$_3$), 1.32 (s, 9H, C(C*H*$_3$)$_3$) ppm. ^{13}C NMR (101 MHz, C_6D_6) δ = 152.06 (Ar), 148.39 (Ar), 137.08 (Ar), 135.87 (Ar), 134.42 (Ar), 132.41 (Ar), 131.83 (Ar), 128.94 (Ar), 128.54 (Ar), 117.16 (Ar), 60.10 (O*C*H$_3$), 34.60 (Ar*C*(CH$_3$)$_3$), 31.47 (ArC(*C*H$_3$)$_3$), 18.52 (Ar*C*H$_3$), 16.99 (Ar*C*H$_3$), 16.79 (Ar*C*H$_3$) ppm. HRMS (EI+) Calcd. for $C_{22}H_{29}{}^{81}BrO$: 390.1381. Found: 390.1399.

Compound 11. Compound **10** (0.644 g, 1.65 mmol, 1 equiv) was dissolved in 40 mL of THF in a 100 mL Schlenk flask in the glovebox and the solution was frozen in the cold well. ^{t}BuLi (1.7 M in pentane, 2.04 mL, 3.47 mmol, 2.1 equiv) was added dropwise to the thawing solution of the bromide. The reaction turned yellow upon addition of ^{t}BuLi and was warmed to room temperature as it was stirred for 1 h over which time the reaction mixture turned red orange. The reaction mixture was refrozen in the cold well. DMF (0.38 mL, 4.96 mmol, 3 equiv) was added dropwise to the thawing reaction mixture. The color of the solution faded significantly as the reaction was warmed to room temperature and stirred for 2 h. The flask was brought out of the box, and the reaction was quenched with 20 mL of water. Volatiles were removed under vacuum and the desired product was extracted into DCM and washed with water. The organic phase was dried over $MgSO_4$, filtered, and volatile materials were removed under vacuum. Recrystallization from methanol yielded 0.481 g (86% yield) of pale orange crystals. ^{1}H NMR (400 MHz, $CDCl_3$) δ = 10.46 (s, 1H, C*H*O), 7.87 (d, *J*=2.6,

1H, Ar*H*), 7.35 (d, *J*=2.6, 1H, Ar*H*), 3.46 (s, 3H, OCH_3), 2.33 (s, 3H, ArCH_3), 2.29 (s, 6H, ArCH_3), 2.01 (s, 6H, ArCH_3), 1.33 (s, 9H, C(CH_3)$_3$) ppm. ^{13}C NMR (101 MHz, $CDCl_3$) δ = 191.10 (Ar*C*HO), 158.83 (Ar), 147.07 (Ar), 136.32 (Ar), 136.08 (Ar), 135.14 (Ar), 134.73 (Ar), 132.67 (Ar), 131.92 (Ar), 128.50 (Ar), 123.49 (Ar), 61.84 (O*C*H$_3$), 34.69 (Ar*C*(CH$_3$)$_3$), 31.39 (ArC(*C*H$_3$)$_3$), 18.52 (Ar*C*H$_3$), 17.02 (Ar*C*H$_3$), 16.84 (Ar*C*H$_3$) ppm. HRMS (EI+) Calcd. for $C_{23}H_{30}O_2$: 339.2324. Found: 339.2309.

Compound 12. BBr_3 (1 M solution in hexanes, 14.2 mL, 14.2 mmol, 10 equiv) was syringed into a Schlenk flask containing a solution of **11** (0.481 g, 1.42 mmol, 1 equiv) in 50 mL of DCM under a nitrogen atmosphere. The solution turned from light orange to dark brownish red and was stirred for 1.5 h before the reaction was stopped by the gradual addition of water and a color change to dark olive green was observed. The desired product was extracted into DCM. The organic phase was dried over $MgSO_4$, filtered, and volatile materials were removed under vacuum to give 0.46 g (99% yield) of an olive green solid. ^{1}H NMR (400 MHz, $CDCl_3$) δ = 10.99 (s, 1H, O*H*), 9.99 (s, 1H, C*H*O), 7.57 (d, *J*=2.5, 1H, Ar*H*), 7.44 (d, *J*=2.5, 1H, Ar*H*), 2.33 (s, 3H, ArCH_3), 2.30 (s, 6H, ArCH_3), 2.00 (s, 6H, ArCH_3), 1.38 (s, 9H, C(CH_3)$_3$) ppm. ^{13}C NMR (101 MHz, $CDCl_3$) δ = 197.02 (Ar*C*HO), 156.83 (Ar), 142.79 (Ar), 136.82 (Ar), 134.97 (Ar), 133.89 (Ar), 132.65 (Ar), 132.13 (Ar), 131.32 (Ar), 128.63 (Ar), 120.06 (Ar), 34.30 (Ar*C*(CH$_3$)$_3$), 31.39 (ArC(*C*H$_3$)$_3$), 18.07 (Ar*C*H$_3$), 17.01 (Ar*C*H$_3$), 16.81 (Ar*C*H$_3$) ppm. HRMS (EI+) Calcd. for $C_{23}H_{30}O_2$: 325.2168. Found: 325.2167.

Compound 13. The salcylaldimine compound was synthesized by mixing **12** (0.41 g, 1.26 mmol, 1 equiv), *p*-toluenesulfonic acid (0.024 g, 0.13 mmol, 0.1 equiv), 2,6-diisopropylamine (0.49 g, 2.78 mmol, 2.2 equiv), and methanol (40 mL) in a round

bottom flask equipped with a reflux condenser. A color change from olive green to rust red was observed with the addition of aniline. The mixture was stirred at reflux for 3 h and then cooled to room temperature and volatile materials were removed under vacuum. The orange residue was purified by column chromatography (4/1 hexanes/ethyl acetate) and 0.28 g (45% yield) of yellow orange solid was obtained. ^{1}H NMR (400 MHz, C_6D_6) δ = 13.35 (s, 1H, O*H*), 8.08 (s, 1H, NC*H*), 7.37 (d, *J*=2.1, 1H, Ar*H*), 7.27 (d, *J*=2.1, 1H, Ar*H*), 7.11 (s, 3H, N-Ar*H*), 3.12 – 3.01 (sept, *J*=6.8, 2H, C*H*$(CH_3)_2$), 2.19 (bs, 9H, ArC*H*$_3$), 2.15 (s, 6H, ArC*H*$_3$), 1.27 (s, 9H, C(C*H*$_3)_3$), 1.08 (d, *J*=6.8, 12H, CH(C*H*$_3)_2$) ppm. ^{13}C NMR (101 MHz, C_6D_6) δ = 167.99 (Ar*C*HN), 157.51 (Ar), 147.28 (Ar), 141.70 (Ar), 138.95 (Ar), 135.82 (Ar), 133.92 (Ar), 133.57 (Ar), 132.31 (Ar), 132.27 (Ar), 132.22 (Ar), 127.50 (Ar), 125.80 (Ar), 123.55 (Ar), 118.52 (Ar), 34.19 (Ar*C*$(CH_3)_3$), 31.59 (ArC(*C*$H_3)_3$), 28.64 (Ar*C*H$(CH_3)_2$), 23.50 (ArCH(*C*$H_3)_2$), 18.57 (Ar*C*H_3), 16.90 (Ar*C*H_3), 16.83 (Ar*C*H_3) ppm. HRMS (EI+) Calcd. for $C_{23}H_{30}O_2$: 484.3579. Found: 484.3568.

Compound 14. 2-bromo-4-*tert*-butylmethoxymethylphenol was synthesized from 2-bromo-4-*tert*-butylphenol according an analogous literature synthesis.[54] ^{1}H NMR (400 MHz, $CDCl_3$) δ = 7.30 (d, *J*=2.4 Hz, 1H, Ar*H*), 7.00 (dd, *J*=8.7, 2.4 Hz, 1H, Ar*H*), 6.83 (d, *J*=8.6 Hz, 1H, Ar*H*), 4.97 (s, 2H, OC*H*$_2$OCH$_3$), 3.27 (s, 3H, OCH$_2$OC*H*$_3$), 1.04 (s, 9H, C(C*H*$_3)_3$) ppm. ^{13}C NMR (101 MHz, $CDCl_3$) δ = 151.49 (Ar), 146.47 (Ar), 130.45 (Ar), 125.41 (Ar), 115.95 (Ar), 112.63 (Ar), 95.27 (O*C*H$_2$OCH$_3$), 56.37 (OCH$_2$O*C*H$_3$), 34.30 (Ar*C*$(CH_3)_3$), 31.42 (ArC(*C*$H_3)_3$) ppm. HRMS (FAB+) Calcd. for $C_{12}H_{17}BrO_2$: 272.0412. Found: 272.0411.

Compound 15. Synthesis of the biphenyl compounds was accomplished via the Negishi coupling of 1,4-dibromo-2,3,5,6-tetramethybenzene (**2**) with two equivalents of 2-bromo-4-tertbutylmethoxymethylphenol (**14**) using a procedure analogous to the synthesis of **3**.[53] In the glovebox, **14** (25.00 g, 91.5 mmol, 1 equiv) and 250 mL of THF were combined in a large Schlenk tube and frozen in the cold well. ^{t}BuLi (113.05 mL, 192 mmol, 2.1 equiv) was added to the thawing solution and stirred for 1 h while warming to room temperature. The resultant yellow orange solution was refrozen in the cold well. Concurrently, a suspension of $ZnCl_2$ (8.73 g, 64.1 mmol, 0.7 equiv) in THF (90 mL) was frozen in the cold well. The thawing $ZnCl_2$ suspension was added to the thawing reaction mixture and stirred for 1 h resulting in a colorless cloudy solution. **2** (12.03 g, 41.2 mmol, 0.45 equiv), $Pd(PPh_3)_4$ (1.06 g, 0.92 mmol, 0.01 equiv) and THF (90 mL) were added to the reaction mixture at room temperature. The sealed Schlenk tube was brought out of the glovebox and heated to 65 °C for 10 days. Water was added to quench the reaction. The solution was filtered over silica gel and the silica gel was washed with DCM. The filtrate was extracted between DCM and water. The organics were dried with $MgSO_4$, filtered, and volatiles were removed under vacuum. The monocoupled product was separated from the dicoupled products and other impurities by column chromatography (2/1 hexanes/DCM). 6.03 g of the monocoupled product were collected as a white solid. ^{1}H NMR (400 MHz, $CDCl_3$) δ = 7.32 (dd, *J*=8.6, 2.5 Hz, 1H, Ar*H*), 7.14 (d, *J*=8.7 Hz, 1H, Ar*H*), 6.99 (d, *J*=2.5 Hz, 1H, Ar*H*), 5.04 (s, 2H, OCH_2OCH_3), 3.32 (s, 3H, OCH_2OCH_3), 2.47 (s, 6H, $ArCH_3$), 1.99 (s, 6H, $ArCH_3$), 1.30 (s, 9H, $C(CH_3)_3$) ppm. ^{13}C NMR (101 MHz, $CDCl_3$) δ = 152.05 (Ar), 144.98 (Ar), 138.30 (Ar), 134.10 (Ar), 133.68 (Ar), 130.85 (Ar), 128.57 (Ar), 128.31 (Ar), 125.03 (Ar), 114.44

(Ar), 94.56 (OCH_2OCH_3), 55.88 (OCH_2OCH_3), 34.34 ($ArC(CH_3)_3$), 31.66 ($ArC(CH_3)_3$), 21.36 ($ArCH_3$), 19.00 ($ArCH_3$) ppm. HRMS (FAB+) Calcd. for $C_{22}H_{29}BrO_2$: 405.1429. Found: 405.1445.

Compounds 16. The two atropisomers of the terphenyl compound were synthesized together via a Negishi coupling using the same general procedure as for the synthesis of **3**. In the glovebox, **1** (1.50 g, 6.17 mmol, 1 equiv) and 25 mL of THF were combined in a Schlenk tube and frozen in the cold well. ^{t}BuLi (8.64 mL, 12.0 mmol, 2.1 equiv) was added to the thawing solution and stirred for 1 h while warming to room temperature. The resultant bright yellow solution was refrozen in the cold well. Concurrently, a suspension of $ZnCl_2$ (0.59 g, 4.32 mmol, 0.7 equiv) in THF (6 mL) was frozen in the cold well. The thawing $ZnCl_2$ suspension was added to the thawing reaction mixture and stirred for 2 h resulting in a colorless cloudy solution. **6** (2.00 g, 4.94 mmol, 0.8 equiv), $Pd(PPh_3)_4$ (0.07 g, 0.062 mmol, 0.01 equiv), and THF (6 mL) were added to the reaction mixture at room temperature. The sealed Schlenk tube was brought out of the glovebox and heated to 65 °C for 10 days. Water was added to quench the reaction. The solution was filtered over silica gel and the silica gel was washed with DCM. The filtrate was extracted between DCM and water. The organics were dried with $MgSO_4$, filtered, and volatiles were removed under vacuum. The anti atropisomer was isolated by precipitation of 0.82 g of the white solid from hexanes. The hexanes soluble material was pumped down to a yellow oil and the syn atropisomer was isolated by column chromatography (1/1 hexanes/DCM) as 0.82 g of white solid (70% overall yield). Data for **16-a** are as follows. ^{1}H NMR (400 MHz, $CDCl_3$) δ = 7.32 (m, 2H, Ar*H*), 7.14 (m, 3H, Ar*H*), 6.93 (d, *J*=8.5, 1H, Ar*H*), 5.08 (s, 2H, OCH_2OCH_3), 3.78

(s, 3H, OCH_3), 3.38 (s, 3H, OCH_2OCH_3), 1.96 (2s, 12H, ArCH_3), 1.32 (2s, 18H, C(CH_3)$_3$) ppm. ^{13}C NMR (101 MHz, $CDCl_3$) δ = 154.74 (Ar), 152.33 (Ar), 144.79 (Ar), 143.25 (Ar), 137.79 (Ar), 137.62 (Ar), 132.07 (Ar), 132.00 (Ar), 131.98 (Ar), 130.72 (Ar), 129.21 (Ar), 129.15 (Ar), 124.48 (Ar), 124.33 (Ar), 114.67 (Ar), 110.20 (Ar), 94.84 (OCH_2OCH_3), 55.89 (OCH_3), 55.82 (OCH_2OCH_3), 34.39 (ArC(CH$_3$)$_3$), 34.28 (ArC(CH$_3$)$_3$), 31.76 (ArC(CH$_3$)$_3$), 31.73 (ArC(CH$_3$)$_3$), 18.16 (ArCH$_3$), 18.02 (ArCH$_3$) ppm. HRMS (FAB+) Calcd. for $C_{33}H_{44}O_3$: 488.3290. Found: 488.3299. Data for **16-s** are as follows. ^{1}H NMR (400 MHz, $CDCl_3$) δ = 7.34 (m, 2H, ArH), 7.17 (m, 3H, ArH), 6.93 (d, J=8.6, 1H, ArH), 5.02 (s, 2H, OCH_2OCH_3), 3.73 (s, 3H, OCH_3), 3.28 (s, 3H, OCH_2OCH_3), 1.98 (2s, 12H, ArCH_3), 1.34 (2s, 18H, C(CH_3)$_3$) ppm. ^{13}C NMR (101 MHz, $CDCl_3$) δ = 154.67 (Ar), 152.41 (Ar), 145.10 (Ar), 143.41 (Ar), 137.90 (Ar), 137.87 (Ar), 132.44 (Ar), 132.26 (Ar), 132.20 (Ar), 130.79 (Ar), 128.93 (Ar), 128.88 (Ar), 128.47 (Ar), 124.64 (Ar), 124.35 (Ar), 115.65 (Ar), 110.36 (Ar), 95.43 (OCH_2OCH_3), 55.89 (OCH_3), 55.71 (OCH_2OCH_3), 34.42 (ArC(CH$_3$)$_3$), 34.32 (ArC(CH$_3$)$_3$), 31.75 (ArC(CH$_3$)$_3$), 31.72 (ArC(CH$_3$)$_3$), 18.09 (ArCH$_3$), 17.95 (ArCH$_3$) ppm. HRMS (FAB+) Calcd. for $C_{33}H_{44}O_3$: 488.3290. Found: 488.3276.

Compounds 19-a and 19-s. The same procedures were used for the synthesis of the syn and anti atropisomers of **19** starting from the Negishi coupled precursors (**16**). **16** (0.82 g, 1.68 mmol, 1 equiv), *N,N,N',N'*-tetramethylethylenediamine (3.5 mL, 23.5 mmol, 14 equiv) and THF (15 mL) were added to a Schlenk tube in the glovebox and frozen in the cold well. ^{n}BuLi (1.76 mL, 4.40 mmol, 2.6 equiv) was added to the thawing solution and stirred for 2 h. The resultant orange red solution was refrozen in the cold well. A solution of DMF (0.78 mL, 10.1 mmol, 6 equiv) in THF (5 mL) was also frozen

in the cold well. The thawing DMF solution was added to the thawing reaction mixture resulting in a pale amber solution, which was stirred for 5 h before the Schlenk tube was brought out of the glovebox and about 2 mL of water were added to quench the reaction. The desired product was extracted into DCM and the organic fraction was washed with water, dried with $MgSO_4$, filtered, and the volatiles were removed under vacuum to yield the orthoformylated products (**17-a** and **17-s**) with greater than 90% purity. These compounds were carried forward without further purification and 100% conversion was assumed for stoichiometry. Data for **17-a** are as follows. ^{1}H NMR (400 MHz, $CDCl_3$) δ = 10.50 (s, 1H, C*H*O), 7.88 (d, *J*=2.7, 1H, Ar*H*), 7.51 (d, *J*=2.6, 1H, Ar*H*), 7.35 (dd, *J*=8.6, 2.5, 1H, Ar*H*), 6.94 (m, 2H, Ar*H*), 4.67 (s, 2H, OC*H*$_2$OCH$_3$), 3.78 (s, 3H, OC*H*$_3$), 3.23 (s, 3H, OCH$_2$OC*H*$_3$), 1.99 (s, 6H, ArC*H*$_3$), 1.95 (s, 6H, ArC*H*$_3$), 1.35 (s, 9H, C(C*H*$_3$)$_3$), 1.32 (s, 9H, C(C*H*$_3$)$_3$) ppm. ^{13}C NMR (101 MHz, $CDCl_3$) δ = 191.37 (Ar*C*HO), 155.52 (Ar), 154.59 (Ar), 147.50 (Ar), 143.44 (Ar), 138.79 (Ar), 136.32 (Ar), 136.27 (Ar), 136.26 (Ar), 132.60 (Ar), 132.10 (Ar), 130.31 (Ar), 129.32 (Ar), 128.61 (Ar), 124.65 (Ar), 123.65 (Ar), 110.34 (Ar), 99.47 (O*C*H$_2$OCH$_3$), 57.33 (O*C*H$_3$), 55.84 (OCH$_2$O*C*H$_3$), 34.79 (Ar*C*(CH$_3$)$_3$), 34.21 (Ar*C*(CH$_3$)$_3$), 31.71 (ArC(*C*H$_3$)$_3$), 31.44 (ArC(*C*H$_3$)$_3$), 18.25 (Ar*C*H$_3$), 17.97 (Ar*C*H$_3$) ppm. HRMS (FAB+) Calcd. for Calcd. for $C_{34}H_{44}O_4$: 516.3240. Found: 516.3259. Data for **17-s** are as follows. ^{1}H NMR (400 MHz, $CDCl_3$) δ = 10.46 (s, 1H, C*H*O), 7.90 (d, *J*=2.6, 1H, Ar*H*), 7.52 (d, *J*=2.6, 1H, Ar*H*), 7.34 (dd, *J*=8.6, 2.5, 1H, Ar*H*), 7.14 (d, *J*=2.5, 1H, Ar*H*), 6.90 (d, *J*=8.6, 1H, Ar*H*), 4.70 (s, 2H, OC*H*$_2$OCH$_3$), 3.66 (s, 3H, OC*H*$_3$), 3.04 (s, 3H, OCH$_2$OC*H*$_3$), 2.02 (s, 6H, ArC*H*$_3$), 1.95 (s, 6H, ArC*H*$_3$), 1.35 (s, 9H, C(C*H*$_3$)$_3$), 1.31 (s, 9H, C(C*H*$_3$)$_3$) ppm. ^{13}C NMR (101 MHz, $CDCl_3$) δ = 191.17 (Ar*C*HO), 155.43 (Ar), 154.50 (Ar), 147.70 (Ar),

143.54 (Ar), 138.90 (Ar), 136.77 (Ar), 136.31 (Ar), 135.93 (Ar), 132.83 (Ar), 132.25 (Ar), 130.48 (Ar), 129.37 (Ar), 128.43 (Ar), 124.56 (Ar), 124.04 (Ar), 110.40 (Ar), 99.96 (OCH_2OCH_3), 57.07 (OCH_3), 55.61 (OCH_2OCH_3), 34.81 ($ArC(CH_3)_3$), 34.31 ($ArC(CH_3)_3$), 31.73 ($ArC(CH_3)_3$), 31.43 ($ArC(CH_3)_3$), 18.20 ($ArCH_3$), 17.90 ($ArCH_3$) ppm. HRMS (FAB+) Calcd. for $C_{34}H_{44}O_4$: 516.3240. Found: 516.3260.

The MOM moiety was cleaved from compounds **17** by refluxing with HCl. **17** (0.87 g, 1.68 mmol, 1 equiv), 2N HCl (13 mL, 25.2 mmol, 15 equiv), and methanol (84 mL) were added to a round bottom flask equipped with a reflux condenser and the reaction was refluxed for 12 h. Then the reaction was cooled to room temperature and the desired material was extracted into ethyl acetate (water and hexanes were added to aid in the separation of the methanol and ethyl acetate layers). The organic fractions were dried with $MgSO_4$, filtered, and the volatiles were removed under vacuum to yield the deprotected products (**18-a** and **18-s**) with greater than 90% purity. These compounds were carried forward without further purification and 100% conversion was assumed for stoichiometry. Data for **18-a** are as follows. ^{1}H NMR (400 MHz, $CDCl_3$) δ = 11.10 (s, 1H, O*H*), 9.99 (s, 1H, C*H*O), 7.55 (d, *J*=2.3, 1H, Ar*H*), 7.52 (d, *J*=2.4, 1H, Ar*H*), 7.34 (dd, *J*=8.5, 2.6, 1H, Ar*H*), 7.17 (d, *J*=2.7, 1H, Ar*H*), 6.93 (d, *J*=8.7, 1H, Ar*H*), 3.78 (s, 3H, OCH_3), 1.97 (2s, 12H, $ArCH_3$), 1.37 (s, 9H, $C(CH_3)_3$), 1.32 (s, 9H, $C(CH_3)_3$) ppm. ^{13}C NMR (101 MHz, $CDCl_3$) δ = 197.15 (Ar*C*HO), 156.84 (Ar), 154.57 (Ar), 143.47 (Ar), 142.83 (Ar), 138.45 (Ar), 137.25 (Ar), 135.05 (Ar), 132.57 (Ar), 132.12 (Ar), 131.30 (Ar), 130.49 (Ar), 129.24 (Ar), 128.66 (Ar), 124.35 (Ar), 120.09 (Ar), 110.13 (Ar), 55.86 (OCH_3), 34.39 ($ArC(CH_3)_3$), 34.32 ($ArC(CH_3)_3$), 31.74 $ArC(CH_3)_3$), 31.47 $ArC(CH_3)_3$), 18.04 ($ArCH_3$), 17.97 ($ArCH_3$) ppm. HRMS (FAB+) Calcd. for $C_{32}H_{40}O_3$:

472.2978. Found: 472.2963. Data for **18-s** are as follows. ^{1}H NMR (400 MHz, $CDCl_3$) δ = 10.99 (s, 1H, O*H*), 9.99 (s, 1H, C*H*O), 7.56 (d, *J*=2.5, 1H, Ar*H*), 7.49 (d, *J*=2.4, 1H, Ar*H*), 7.34 (dd, *J*=8.5, 2.5, 1H, Ar*H*), 7.12 (d, *J*=2.5, 1H, Ar*H*), 6.92 (d, *J*=8.5, 1H, Ar*H*), 3.73 (s, 3H, OCH_3), 1.99 (s, 6H, ArCH_3), 1.97 (s, 6H, ArCH_3), 1.37 (s, 9H, C(CH_3)$_3$), 1.33 (s, 9H, C(CH_3)$_3$) ppm. ^{13}C NMR (101 MHz, $CDCl_3$) δ = 197.03 (Ar*C*HO), 156.98 (Ar), 154.76 (Ar), 143.22 (Ar), 142.70 (Ar), 138.80 (Ar), 137.10 (Ar), 135.26 (Ar), 132.68 (Ar), 132.17 (Ar), 131.22 (Ar), 130.58 (Ar), 128.72 (Ar), 128.67 (Ar), 124.43 (Ar), 120.16 (Ar), 110.31 (Ar), 55.55 (O*C*H$_3$), 34.38 (Ar*C*(CH$_3$)$_3$), 34.30 (Ar*C*(CH$_3$)$_3$), 31.75 (ArC(*C*H$_3$)$_3$), 31.46 (ArC(*C*H$_3$)$_3$), 17.98 (Ar*C*H$_3$), 17.94 (Ar*C*H$_3$) ppm. HRMS (FAB+) Calcd. for $C_{32}H_{40}O_3$: 472.2978. Found: 472.2962.

Compounds **19** were synthesized via imine condensation. **18** (0.79 g, 1.68 mmol, 1 equiv), methanol (79 mL), *p*-toluenesulfonic acid (0.032 g, 0.17 mmol, 0.1 equiv), and 2,6-diisopropylaniline (0.35 mL, 1.85 mmol, 1.1 equiv) were added to a round bottom flask equipped with a reflux condenser and refluxed for about 5 h over which time the solution became deep red and some pale precipitate crashed out of solution. The reaction mixture was cooled to room temperature and then left to cool in a -20 °C freezer for more than 24 h. The desired product was collected via filtration and washed with cold methanol. 0.38 g (35% yield over 3 steps starting with **16-a**) was collected of the anti atropisomer and 0.40 g (37% yield over 3 steps starting with **16-s**) was collected of the syn atropisomer. Data for **19-a** are as follows. ^{1}H NMR (400 MHz, $CDCl_3$) δ = 13.43 (s, 1H, O*H*), 8.06 (s, 1H, NC*H*), 7.29 (m, 4H, Ar*H*), 7.11 (bs, 3H, Ar*H*), 6.72 (d, *J*=8.5, 1H, Ar*H*), 3.31 (s, 3H, OCH_3), 3.07 (sept, 2H, C*H*(CH$_3$)$_2$), 2.23 (s, 6H, ArCH_3), 2.16 (s, 6H, ArCH_3), 1.33 (s, 9H, C(CH_3)$_3$), 1.26 (s, 9H, C(CH_3)$_3$), 1.07 (d, *J*=6.6, 12H,

CH(CH_3)$_2$) ppm. ^{13}C NMR (101 MHz, $CDCl_3$) δ = 168.02 (Ar*C*HN), 157.54 (Ar), 155.22 (Ar), 147.32 (Ar), 143.51 (Ar), 141.74 (Ar), 138.95 (Ar), 138.90 (Ar), 137.22 (Ar), 133.71 (Ar), 132.58 (Ar), 132.54 (Ar), 132.00 (Ar), 131.78 (Ar), 128.96 (Ar), 127.44 (Ar), 125.76 (Ar), 124.64 (Ar), 123.54 (Ar), 118.46 (Ar), 110.54 (Ar), 55.03 (O*C*H_3), 34.29 (Ar*C*(CH$_3$)$_3$), 34.21 (Ar*C*(CH$_3$)$_3$), 31.84 (ArC(*C*H$_3$)$_3$), 31.57 (ArC(*C*H$_3$)$_3$), 28.64 (Ar*C*H(CH$_3$)$_2$), 23.44 (ArCH(*C*H$_3$)$_2$), 18.39 (Ar*C*H$_3$), 18.30 (Ar*C*H$_3$) ppm. HRMS (FAB+) Calcd. for $C_{44}H_{57}NO_2$: 632.4467. Found: 632.4481. Data for **19-s** are as follows. ^{1}H NMR (400 MHz, $CDCl_3$) δ = 13.40 (s, 1H, O*H*), 8.05 (s, 1H, NC*H*), 7.45 (d, *J*=2.4, 1H, Ar*H*), 7.31 (m, 2H, Ar*H*), 7.28 (d, *J*=2.5, 1H, Ar*H*), 7.13 (s, 3H, Ar*H*), 6.77 (d, *J*=9.3, 1H, Ar*H*), 3.35 (s, 3H, OC*H*$_3$), 3.10 (sept, *J*=6.8, 2H, C*H*(CH$_3$)$_2$), 2.22 (s, 6H, ArC*H*$_3$), 2.16 (s, 6H, ArC*H*$_3$), 1.30 (s, 9H, C(C*H*$_3$)$_3$), 1.27 (s, 9H, C(C*H*$_3$)$_3$), 1.10 (d, *J*=6.9, 12H, CH(C*H*$_3$)$_2$) ppm. ^{13}C NMR (101 MHz, $CDCl_3$) δ = 168.07 (Ar*C*HN), 157.55 (Ar), 155.36 (Ar), 147.39 (Ar), 143.36 (Ar), 141.71 (Ar), 139.05 (Ar), 138.96 (Ar), 137.30 (Ar), 133.55 (Ar), 132.64 (Ar), 132.62 (Ar), 131.99 (Ar), 131.79 (Ar), 128.73 (Ar), 127.59 (Ar), 125.77 (Ar), 124.75 (Ar), 123.53 (Ar), 118.57 (Ar), 110.87 (Ar), 55.16 (O*C*H$_3$), 34.22 (Ar*C*(CH$_3$)$_3$), 34.19 (Ar*C*(CH$_3$)$_3$), 31.80 (ArC(*C*H$_3$)$_3$), 31.56 (ArC(*C*H$_3$)$_3$), 28.65 (Ar*C*H(CH$_3$)$_2$), 23.45 (ArCH(*C*H$_3$)$_2$), 18.40 (Ar*C*H$_3$), 18.37 (Ar*C*H$_3$) ppm. HRMS (FAB+) Calcd. for $C_{44}H_{57}NO_2$: 632.4467. Found: 632.4451.

Compound 21. The terphenyl compound was synthesized via a Negishi coupling using the same general procedure as for the synthesis of **3**. In the glovebox, 3,5-di-*tert*-butylbromobenzene (**20**) (0.70 g, 2.60 mmol, 1 equiv) and 10 mL of THF were combined in a Schlenk tube and frozen in the cold well. ^{t}BuLi (3.64 mL, 5.46 mmol, 2.1 equiv) was added to the thawing solution and stirred for 1 h while warming

to room temperature. The resultant bright yellow solution was refrozen in the cold well. Concurrently, a suspension of $ZnCl_2$ (0.25 g, 1.82 mmol, 0.7 equiv) in THF (3 mL) was frozen in the cold well. The thawing $ZnCl_2$ suspension was added to the thawing reaction mixture and stirred for 2 h resulting in a colorless cloudy solution. **15** (0.84 g, 2.08 mmol, 0.8 equiv) and $Pd(PPh_3)_4$ (0.03 g, 0.026 mmol, 0.01 equiv) and THF (3 mL) were added to the reaction mixture at room temperature. The sealed Schlenk tube was brought out of the glovebox and heated to 65 °C for 3 days. Water was added to quench the reaction. The solution was filtered over silica gel and the silica gel was washed with DCM. Volatiles were removed under vacuum and the desired product was collected by precipitation from methanol as 0.77 g of white solid (72% yield). ^{1}H NMR (400 MHz, $CDCl_3$) δ = 7.35 (s, 1H, Ar*H*), 7.32 (d, *J*=8.6, 1H, Ar*H*), 7.17 (d, *J*=8.6, 1H, Ar*H*), 7.13 (s, 1H, Ar*H*), 7.04 (d, *J*=8.5, 2H, Ar*H*), 5.08 (s, 2H, OCH_2OCH_3), 3.38 (s, 3H, OCH_2OCH_3), 1.98 (s, 12H, $ArCH_3$), 1.36 (s, 9H, $C(CH_3)_3$), 1.35 (s, 9H, $C(CH_3)_3$), 1.32 (s, 9H, $C(CH_3)_3$) ppm. ^{13}C NMR (101 MHz, $CDCl_3$) δ = 152.14 (Ar), 150.24 (Ar), 150.19 (Ar), 144.66 (Ar), 142.13 (Ar), 141.61 (Ar), 137.60 (Ar), 132.14 (Ar), 131.60 (Ar), 131.52 (Ar), 128.82 (Ar), 124.45 (Ar), 124.04 (Ar), 123.98 (Ar), 119.40 (Ar), 114.40 (Ar), 94.56 (OCH_2OCH_3), 55.75 (OCH_2OCH_3), 34.87 ($ArC(CH_3)_3$), 34.22 ($ArC(CH_3)_3$), 31.57 ($ArC(CH_3)_3$), 31.54 ($ArC(CH_3)_3$), 18.22 ($ArCH_3$), 17.93 ($ArCH_3$) ppm. HRMS (FAB+) Calcd. for $C_{36}H_{50}O_2$: 514.3811. Found: 514.3828.

Compound 24. Compound 24 was synthesized from the Negishi coupled precursor (**21**) via analogous procedures to those used for the synthesis of compounds **19** starting from **16**. Compound **21** (0.77 g, 1.50 mmol, 1 equiv), *N,N,N',N'*-tetramethylethylenediamine (3.12 mL, 20.94 mmol, 14 equiv) and THF (13 mL) were

added to a Schlenk tube in the glovebox and frozen in the cold well. ^{n}BuLi (1.57 mL, 3.92 mmol, 2.6 equiv) was added to the thawing solution and stirred for 2 h. The resultant orange red solution was refrozen in the cold well. A solution of DMF (0.69 mL, 8.97 mmol, 6 equiv) in THF (4 mL) was also frozen in the cold well. The thawing DMF solution was added to the thawing reaction mixture resulting in a colorless solution, which was stirred for 6 h before the Schlenk tube was brought out of the box and about 2 mL of water were added to quench the reaction. The desired product was extracted into DCM and the organic fraction was washed with water, dried with $MgSO_4$, filtered, and the volatiles were removed under vacuum to yield the orthoformylated product (**22**) with greater than 90% purity. These compounds were carried forward without further purification and 100% conversion was assumed for stoichiometry. ^{1}H NMR (400 MHz, $CDCl_3$) δ = 10.51 (s, 1H, C*H*O), 7.90 (d, *J*=2.6, 1H, Ar*H*), 7.48 (d, *J*=2.7, 1H, Ar*H*), 7.37 (t, *J*=1.8, 1H, Ar*H*), 7.03 (t, *J*=1.8, 1H, Ar*H*), 6.89 (t, *J*=1.6, 1H, Ar*H*), 4.67 (s, 2H, OCH_2OCH$_3$), 3.25 (s, 3H, OCH$_2$OCH_3), 2.01 (s, 6H, ArCH_3), 1.97 (s, 6H, ArCH_3), 1.36 (s, 9H, C(CH_3)$_3$), 1.35 (s, 18H, C(CH_3)$_3$) ppm. ^{13}C NMR (101 MHz, $CDCl_3$) δ = 191.39 (Ar*C*HO), 155.58 (Ar), 150.68 (Ar), 150.64 (Ar), 147.60 (Ar), 143.33 (Ar), 141.45 (Ar), 136.28 (Ar), 136.12 (Ar), 132.38 (Ar), 132.31 (Ar), 129.38 (Ar), 123.88 (Ar), 123.79(Ar), 123.68 (Ar), 119.88 (Ar), 99.51 (O*C*H$_2$OCH$_3$), 57.41 (OCH$_2$O*C*H$_3$), 35.05 (Ar*C*(CH$_3$)$_3$), 34.80 (Ar*C*(CH$_3$)$_3$), 31.72 (ArC(*C*H$_3$)$_3$), 31.43 (ArC(*C*H$_3$)$_3$), 18.37 (Ar*C*H$_3$), 18.24 (Ar*C*H$_3$) ppm. HRMS (FAB+) Calcd. for $C_{37}H_{50}O_3$: 542.3760. Found: 542.3783.

The MOM group was cleaved from compound **22** by refluxing with HCl. **22** (0.81 g, 1.50 mmol, 1 equiv), 2N HCl (11 mL, 22.4 mmol, 15 equiv), and methanol (75

mL) were added to a round bottom flask equipped with a reflux condenser and the reaction was refluxed for 13 h. Then the reaction was cooled to room temperature and the desired material was extracted into ethyl acetate (water and hexanes were added to aid in the separation of the methanol and ethyl acetate layers). The organic fractions were dried with $MgSO_4$, filtered, and the volatiles were removed under vacuum to yield the deprotected product (**23**) with greater than 90% purity. These compounds were carried forward without further purification and 100% conversion was assumed for stoichiometry. ^{1}H NMR (400 MHz, $CDCl_3$) δ = 11.10 (s, 1H, O*H*), 9.99 (s, 1H, C*H*O), 7.56 (d, *J*=1.6, 1H, Ar*H*), 7.50 (d, *J*=1.6, 1H, Ar*H*), 7.35 (s, 1H, Ar*H*), 7.06 (d, *J*=14.9, 2H, Ar*H*), 1.98 (s, 6H, ArCH_3), 1.98 (s, 6H, ArCH_3), 1.36 (s, 9H, C(CH_3)$_3$), 1.35 (s, 18H, C(CH_3)$_3$) ppm. ^{13}C NMR (101 MHz, $CDCl_3$) δ = 196.98 (Ar*C*HO), 156.66 (Ar), 150.39 (Ar), 150.24 (Ar), 142.97 (Ar), 142.72 (Ar), 141.40 (Ar), 136.80 (Ar), 132.22 (Ar), 132.19 (Ar), 130.91 (Ar), 128.62 (Ar), 124.07 (Ar), 123.68 (Ar), 119.96 (Ar), 119.47 (Ar), 34.88 (Ar*C*(CH$_3$)$_3$), 34.24 (Ar*C*(CH$_3$)$_3$), 31.56 (ArC(*C*H$_3$)$_3$), 31.29 (ArC(*C*H$_3$)$_3$), 18.24 (Ar*C*H$_3$), 17.75 (Ar*C*H$_3$) ppm. HRMS (FAB+) Calcd. for $C_{35}H_{46}O_2$: 498.3498. Found: 498.3488.

Compound **24** was synthesized via imine condensation. **23** (0.75 g, 1.50 mmol, 1 equiv), methanol (75 mL), *p*-toluenesulfonic acid (0.029 g, 0.15 mmol, 0.1 equiv), and 2,6-diisopropylaniline (0.31 mL, 1.65 mmol, 1.1 equiv) were added to a round bottom flask equipped with a reflux condenser and refluxed for about 4 h over which time the solution became deep red and some pale precipitate crashed out of solution. The reaction mixture was cooled to room temperature and the desired product was collected via filtration and washed with cold methanol. 0.47 g (48% yield over 3 steps from **21**) was collected. ^{1}H NMR (400 MHz, C_6D_6) δ = 13.50 (s, 1H, O*H*), 8.07 (s, 1H, NC*H*),

7.57 (t, *J*=1.5, 1H, Ar*H*), 7.49 (d, *J*=2.4, 1H, Ar*H*), 7.31 (d, *J*=2.5, 1H, Ar*H*), 7.25 (m, 2H, Ar*H*), 7.12 (s, 3H, Ar*H*), 3.08 (sept, *J*=6.8, 2H, C*H*(CH_3)$_2$), 2.26 (s, 6H, ArC*H*$_3$), 2.12 (s, 6H, ArC*H*$_3$), 1.38 (s, 9H, C(C*H*$_3$)$_3$), 1.35 (s, 9H, C(C*H*$_3$)$_3$), 1.30 (s, 9H, C(C*H*$_3$)$_3$), 1.08 (d, *J*=6.8, 12H, CH(C*H*$_3$)$_2$) ppm. ^{13}C NMR (101 MHz, C_6D_6) δ = 167.69 (Ar*C*HN), 157.23 (Ar), 150.68 (Ar), 150.53 (Ar), 146.93 (Ar), 142.72 (Ar), 142.66 (Ar), 141.50 (Ar), 138.60 (Ar), 136.97 (Ar), 133.09 (Ar), 132.50 (Ar), 131.82 (Ar), 131.59 (Ar), 125.47 (Ar), 124.29 (Ar), 123.99 (Ar), 123.23 (Ar), 119.57 (Ar), 118.30 (Ar), 34.77 (Ar*C*(CH_3)$_3$), 34.69 (Ar*C*(CH_3)$_3$), 33.89 (Ar*C*(CH_3)$_3$), 31.47 (ArC(*C*H$_3$)$_3$), 31.43 (ArC(*C*H$_3$)$_3$), 31.25 (ArC(*C*H$_3$)$_3$), 28.32 (Ar*C*H(CH_3)$_2$), 23.11 (ArCH(*C*H$_3$)$_2$), 18.28 (Ar*C*H$_3$), 18.08 (Ar*C*H$_3$) ppm. HRMS (FAB+) Calcd. for $C_{47}H_{63}NO$: 657.4910. Found: 657.4902.

Complex 25-a. Synthesis of the *anti*-dinickelphenoxyiminato complex was achieved by a method similar to that of Mecking, et al.[33] A solution of **7-a** (0.20 g, 0.2484 mmol, 1 equiv) in 5 mL of diethyl ether and a solution of $NiMe_2$(tmeda) (0.11 g, 0.55 mmol, 2.2 equiv) in 3 mL of diethyl ether were cooled in the glovebox freezer to about –35 °C. The solution of the ligand precursor was added to the solution of nickel precursor. Pyridine (0.40 mL, 4.97 mmol, 20 equiv) was syringed into the mixture causing a color change to reddish orange. The reaction became gradually cloudier over 5 h of stirring at room temperature, at which point volatiles were removed under vacuum. Hexanes were added to the orange brown solid and the resulting suspension was washed over Celite with hexanes. The desired product was collected by flushing it through the Celite with THF. Black precipitate was left on the Celite indicating some decomposition of the nickel precursor. The solution of the product was placed under vacuum to remove volatiles leaving 0.21 g (76% yield) of bright orange solid. X-ray

quality crystals were grown from a room temperature vapor diffusion of hexanes into THF. ^{1}H NMR (400 MHz, C_6D_6) δ = 8.35 (d, 4H, Py*H*), 7.72 (s, 2H, Ar*H*), 7.41 (s, 2H, Ar*H*), 7.16 (bs, 6H, N-Ar*H*), 7.14 (s, 2H, Ar*H*), 6.87 (m, 2H, Py*H*), 6.27 (m, 4H, Py*H*), 4.32 (sept, *J*=6.6, 4H, C*H*(CH_3)$_2$), 1.97 (s, 12H, ArC*H*$_3$), 1.53 (d, *J*=6.6, 12H, CH(C*H*$_3$)$_2$), 1.43 (s, 18H, C(C*H*$_3$)$_3$), 1.13 (d, *J*=6.6, 12H, CH(C*H*$_3$)$_2$), -0.69 (s, 6H, NiC*H*$_3$) ppm. ^{13}C NMR (shifts determined from gHSQCAD and gHMBC experiments due to low solubility of **25-a**, C_6D_6) δ = 166.0 (Ar*C*HN), 163.5 (Ar), 151.6 (Py), 150.1 (Ar), 140.9 (Ar), 138.6 (Ar), 134.7 (Py), 132.6 (Ar), 131.6 (Ar), 127.0 (Ar), 123.2 (Ar), 122.1 (Py), 118.7 (Ar), 33.4 (Ar*C*(CH_3)$_3$), 31.3 (ArC(*C*H$_3$)$_3$), 28.2 (Ar*C*H(CH_3)$_2$), 24.6 (ArCH(*C*H$_3$)$_2$), 22.8 (ArCH(*C*H$_3$)$_2$), 18.0 (Ar*C*H$_3$), -7.9 (Ni*C*H$_3$) ppm. Anal. Calcd. for $C_{68}H_{86}N_4Ni_2O_2$: C, 73.66; H, 7.82; N, 5.05. Found: C, 72.76; H, 7.72; N, 4.96.

Complex 25-s. Metallation of **7-s** with $NiMe_2$(tmeda) was accomplished with the same procedure as for the metallation of the anti analogue, though due to differences in solubility, the purification methodology was changed. After the reaction, volatiles were removed under vacuum and the resulting oily solid was dissolved in pentane and filtered over Celite to remove nickel(0). Precipitation from cold pentane yielded 0.20 g (73% yield) of ca. 92% pure desired complex. The remaining impurity was the mono-nickel complex. Subsequent precipitations yielded only minimal increase in purity. Analytically pure **25-s** was obtained by treating the nearly pure complex with half an equivalent of $NiMe_2$(tmeda) and 5 equivalents of pyridine using the same conditions as the initial reaction. Volatiles were removed under vacuum and the resulting oily solid was dissolved in pentane and filtered over Celite to remove nickel(0). Precipitation from cold pentane yielded 0.084 g (30% yield) of pure desired complex. X-ray quality crystals

were grown from a cold pentane solution. ^{1}H NMR (400 MHz, C_6D_6) δ = 8.00 (d, 4H, Py*H*), 7.66 (s, 2H, Ar*H*), 7.54 (m, 2H, Py*H*), 7.48 (s, 2H, Ar*H*), 7.16 (bs, 6H, N-Ar*H*), 7.10 (s, 2H, Ar*H*), 6.60 (m, 4H, Py*H*), 4.27 (sept, 4H, C*H*$(CH_3)_2$), 1.98 (s, 12H, ArC*H*$_3$), 1.53 (d, 12H, CH(C*H*$_3)_2$), 1.33 (s, 18H, C(C*H*$_3)_3$), 1.09 (d, 12H, CH(C*H*$_3)_2$), -0.75 (s, 6H, NiC*H*$_3$) ppm. ^{13}C NMR (101 MHz, C_6D_6) δ = 166.62 (Ar*C*HN), 163.71 (Ar), 151.80 (Ar), 150.52 (Ar), 141.23 (Ar), 138.92 (Ar), 136.07 (Ar), 135.76 (Ar), 135.01 (Ar), 134.11 (Ar), 132.31 (Ar), 127.52 (Ar), 126.48 (Ar), 123.69 (Ar), 119.28 (Ar), 33.94 (Ar*C*$(CH_3)_3$), 31.66 (ArC(*C*$H_3)_3$), 28.65 (Ar*C*H$(CH_3)_2$), 25.05 (ArCH(*C*$H_3)_2$), 23.34 (ArCH(*C*$H_3)_2$), 18.70 (Ar*C*H_3), -7.33 (Ni*C*H_3) ppm. Anal. Calcd. for $C_{68}H_{86}N_4Ni_2O_2$: C, 73.66; H, 7.82; N, 5.05. Found: C, 73.44; H, 7.66; N, 5.03.

Complex 26. Metallation of **13** was achieved by a method analogous to that used for the dinuclear nickel complexes. A solution of **13** (0.10 g, 0.21 mmol, 1 equivalent) in 3 mL of diethyl ether and a solution of $NiMe_2$(tmeda) (0.047 g, 0.23 mmol, 1.1 equiv) in 4 mL of diethyl ether were cooled in the glovebox freezer to about –35 °C. The solution of the ligand precursor was added to the solution of nickel precursor. Pyridine (0.18 mL, 2.27 mmol, 11 equiv) was syringed into the mixture causing a color change to reddish orange. The reaction became gradually cloudier over 5 h of stirring at room temperature, at which point volatiles were removed under vacuum. The red brown solid was washed over Celite with pentane and the desired product was collected by flushing it through the Celite with Et_2O. Black precipitate was left on the Celite. The solution of the product was placed under vacuum to remove volatiles leaving 0.054 g (41% yield) of orange solid. ^{1}H NMR (400 MHz, C_6D_6) δ = 8.31 (dd, *J*=7.5, *J*=6.9, 2H, Py*H*), 7.67 (s, 1H, Ar*H*), 7.36 (d, *J*=2.6, 1H, Ar*H*), 7.16 (s, 3H, Ar*H*),

7.09 (d, *J*=2.6, 1H, Ar*H*), 6.60 (t, *J*=7.5, 1H, Py*H*), 6.08 (t, *J*=6.9, 2H, Py*H*), 4.27 (sept, *J*=6.4, *J*=6.9, 2H, C*H*(CH_3)$_2$), 2.21 (s, 3H, OCH_3), 2.06 (s, 6H, ArCH_3), 2.06 (s, 6H, ArCH_3), 1.49 (d, *J*=6.9, 6H, CH(CH_3)$_2$), 1.29 (s, 9H, C(CH_3)$_3$), 1.09 (d, *J*=6.4, 6H, CH(CH_3)$_2$), -0.71 (s, 3H, NiCH_3) ppm. ^{13}C NMR (101MHz, C_6D_6) δ = 166.55 (Ar*C*HN), 163.85 (Ar), 152.03 (Ar), 150.53 (Ar), 141.37 (Ar), 138.70 (Ar), 135.63 (Ar), 135.39 (Ar), 135.29 (Ar), 133.79 (Ar), 132.74 (Ar), 132.04 (Ar), 131.24 (Ar), 127.41 (Ar), 126.41 (Ar), 123.64 (Ar), 122.48 (Ar), 119.01 (Ar), 33.92 (Ar*C*(CH_3)$_3$), 31.64 (ArC(*C*H_3)$_3$), 28.60 (Ar*C*H(CH_3)$_2$), 25.10 (ArCH(*C*H_3)$_2$), 23.30 (ArCH(*C*H_3)$_2$), 18.78 (Ar*C*H_3), 16.80 (Ar*C*H_3), 15.62 (Ar*C*H_3), -7.37 (Ni*C*H_3) ppm. Anal. Calcd. for $C_{40}H_{52}N_2NiO$: C, 75.59; H, 8.25; N, 4.41. Found: C, 75.54; H, 8.16; N, 4.38.

Complex 27-a. Metallation of **19-a** was achieved by a method analogous to that used for the dinuclear nickel complexes. A solution of **19-a** (0.10 g, 0.16 mmol, 1 equiv) in 5 mL of diethyl ether and a solution of $NiMe_2$(tmeda) (0.036 g, 0.17 mmol, 1.1 equiv) in 3 mL of diethyl ether were cooled in the glovebox freezer to about –35 °C. The solution of the ligand precursor was added to the solution of nickel precursor. Pyridine (0.14 mL, 1.74 mmol, 11 equiv) was syringed into the mixture causing a color change to red orange. The reaction became gradually darker over 6 h of stirring at room temperature, at which point volatiles were removed under vacuum. The orange brown suspension was washed over Celite with hexanes. Black precipitate was left on the Celite. The solution of the product was placed under vacuum to remove volatiles and the desired product was reprecipitated from pentane and toluene. Filtration yielded 0.054 g of pure product as an orange solid in the first crop of precipitate (44% yield). ^{1}H NMR (400 MHz, C_6D_6) δ = 8.42 (d, *J*=5.2, 2H, Py*H*), 7.70 (s, 1H, Ar*H*), 7.34 (dd,

J=8.6, 2.5, 1H, Ar*H*), 7.26 (m, 2H, Ar*H*), 7.16 (s, 3H, N-Ar*H*), 7.11 (d, *J*=2.6, 1H, Ar*H*), 6.94 (t, *J*=8.1, 1H, Py*H*), 6.75 (d, *J*=8.6, 1H, Ar*H*), 6.33 (t, *J*=6.5, 2H, Py*H*), 4.36 (sept, *J*=13.7, 6.7, 2H, C*H*(CH_3)$_2$), 3.31 (s, 3H, OCH_3), 2.09 (s, 6H, ArCH_3), 2.04 (s, 6H, ArCH_3), 1.54 (d, *J*=6.9, 6H, CH(CH_3)$_2$), 1.43 (s, 9H, C(CH_3)$_3$), 1.30 (s, 9H, C(CH_3)$_3$), 1.13 (d, *J*=6.8, 6H, CH(CH_3)$_2$), -0.68 (s, 3H, NiCH_3) ppm. ^{13}C NMR (101MHz, C_6D_6) δ = 166.63 (Ar*C*HN), 163.88 (Ar), 155.55 (Ar), 152.29 (Ar), 150.60 (Ar), 142.99 (Ar), 141.41 (Ar), 140.07 (Ar), 137.51 (Ar), 135.72 (Ar), 135.15 (Ar), 135.12 (Ar), 133.98 (Ar), 132.89 (Ar), 132.27 (Ar), 131.45 (Ar), 126.43 (Ar), 124.65 (Ar), 123.67 (Ar), 122.58 (Ar), 119.03 (Ar), 110.91 (Ar), 55.10 (O*C*H$_3$), 34.28 (Ar*C*(CH_3)$_3$), 33.96 (Ar*C*(CH_3)$_3$), 31.94 (ArC(*C*H$_3$)$_3$), 31.64 (ArC(*C*H$_3$)$_3$), 28.66 (Ar*C*H(CH_3)$_2$), 25.12 (ArCH(*C*H$_3$)$_2$), 23.37 (ArCH(*C*H$_3$)$_2$), 18.60 (Ar*C*H$_3$), 18.25 (Ar*C*H$_3$), -7.18 (Ni*C*H$_3$) ppm. Anal. Calcd. for $C_{50}H_{64}N_2NiO_2$: C, 76.62; H, 8.23; N, 3.57. Found: C, 76.59; H, 8.36; N, 3.68.

Complex 27-s. Metallation of **19-s** $NiMe_2$(tmeda) was accomplished with the same procedure as the metallation of the anti analogue, though due to differences in solubility, the purification methodology was changed. After the reaction, volatiles were removed under vacuum and the resulting solid was dissolved in hexanes and left in the glovebox freezer at –35 °C for about 16 h. The solution was then filtered over Celite and washed with cold hexanes. The desired complex was flushed through the Celite with diethyl ether. Black precipitate was left on the Celite. Removal of the volatile materials from the ether wash yielded 0.07 g (59% yield) of red orange solid. ^{1}H NMR (400 MHz, C_6D_6) δ = 8.47 (d, *J*=5.5, 2H, Py*H*), 7.70 (s, 1H, Ar*H*), 7.43 (d, *J*=2.4, 1H, Ar*H*), 7.35 (dd, *J*=8.5, 2.3, 1H, Ar*H*), 7.27 (d, *J*=2.3, 1H, Ar*H*), 7.12 (d, *J*=2.4, 1H, Ar*H*), 6.80 (d, *J*=8.6, 1H, Ar*H*), 6.76 (t, *J*=7.4, 1H, Py*H*), 6.45 (t, *J*=6.7, 2H, Py*H*), 4.33

(sept, *J*=6.9, 2H, C*H*(CH_3)$_2$), 3.39 (s, 3H, OC*H*$_3$), 2.07 (s, 6H, ArC*H*$_3$), 2.01 (s, 6H, ArC*H*$_3$), 1.54 (d, *J*=6.8, 6H, CH(C*H*$_3$)$_2$), 1.31 (s, 9H, C(C*H*$_3$)$_3$), 1.29 (s, 9H, C(C*H*$_3$)$_3$), 1.11 (d, *J*=6.8, 6H, CH(C*H*$_3$)$_2$), -0.63 (s, 3H, NiC*H*$_3$) ppm. ^{13}C NMR (101MHz, C_6D_6) δ = 166.58 (Ar*C*HN), 163.88 (Ar), 155.03 (Ar), 152.17 (Ar), 150.55 (Ar), 143.86 (Ar), 141.40 (Ar), 140.13 (Ar), 137.65 (Ar), 135.69 (Ar), 135.51 (Ar), 135.06 (Ar), 133.83 (Ar), 133.04 (Ar), 132.06 (Ar), 131.66 (Ar), 129.25 (Ar), 127.51 (Ar), 126.43 (Ar), 124.59 (Ar), 123.66 (Ar), 122.95 (Ar), 119.19 (Ar), 110.74 (Ar), 55.04 (O*C*H$_3$), 34.25 (Ar*C*(CH_3)$_3$), 33.96 (Ar*C*(CH_3)$_3$), 31.77 (ArC(*C*H$_3$)$_3$), 31.67 (ArC(*C*H$_3$)$_3$), 28.65 (Ar*C*H(CH_3)$_2$), 25.14 (ArCH(*C*H$_3$)$_2$), 23.36 (ArCH(*C*H$_3$)$_2$), 18.57 (Ar*C*H$_3$), 18.28 (Ar*C*H$_3$), -7.56 (Ni*C*H$_3$) ppm. Anal. Calcd. for $C_{50}H_{64}N_2NiO_2$: C, 76.62; H, 8.23; N, 3.57. Found: C, 76.71; H, 8.30; N, 3.65.

Complex 28. Metallation of **24** was achieved by a method analogous to that used for the dinuclear nickel complexes. A solution of **24** (0.09 g, 0.14 mmol, 1 equiv) in 4 mL of diethyl ether and a solution of $NiMe_2$(tmeda) (0.031 g, 0.15 mmol, 1.1 equiv) in 3 mL of diethyl ether were cooled in the glovebox freezer to about –35 °C. The solution of the ligand precursor was added to the solution of nickel precursor resulting in a red orange suspension, which homogenized after about 5 minutes. Pyridine (0.12 mL, 1.52 mmol, 11 equiv) was syringed into the mixture causing a color change to red. The reaction became gradually darker over 6 h of stirring at room temperature, at which point volatiles were removed under vacuum. The red brown suspension was washed over Celite with hexanes. Black precipitate was left on the Celite. Volatiles were removed from the filtrate under vacuum and the desired product was precipitated from pentane. Filtration yielded 0.045 g of pure product as an orange solid in the first crop of

precipitate (40% yield). ^{1}H NMR (400 MHz, C_6D_6) δ = 8.42 (dd, *J*=6.5, 1.5, 2H, Py*H*), 7.72 (s, 1H, Ar*H*), 7.60 (t, *J*=1.8, 1H, Ar*H*), 7.47 (d, *J*=2.7, 1H, Ar*H*), 7.27 (m, 1H, Ar*H*), 7.21 (m, 1H, Ar*H*), 7.14 (d, *J*=2.6, 1H, Ar*H*), 6.90 (tt, *J*=7.6, 1.6, 1H, Py*H*), 6.32 (m, 2H, Py*H*), 4.35 (sept, *J*=6.9, 2H, C*H*$(CH_3)_2$), 2.12 (s, 6H, ArC*H*$_3$), 2.01 (s, 6H, ArC*H*$_3$), 1.54 (d, *J*=6.9, 6H, CH(C*H*$_3)_2$), 1.46 (s, 9H, C(C*H*$_3)_3$), 1.36 (s, 9H, C(C*H*$_3)_3$), 1.34 (s, 9H, C(C*H*$_3)_3$), 1.13 (d, *J*=6.8, 6H, CH(C*H*$_3)_2$), -0.67 (s, 3H, NiC*H*$_3$) ppm. ^{13}C NMR (101MHz, C_6D_6) δ = 166.66 (Ar*C*HN), 163.87 (Ar), 152.22 (Ar), 151.23 (Ar), 150.60 (Ar), 150.57 (Ar), 143.47 (Ar), 141.57 (Ar), 141.39 (Ar), 140.15 (Ar), 135.75 (Ar), 135.21 (Ar), 135.07 (Ar), 133.68 (Ar), 133.14 (Ar), 131.05 (Ar), 126.47 (Ar), 124.76 (Ar), 124.10 (Ar), 123.68 (Ar), 122.62 (Ar), 119.86 (Ar), 119.20 (Ar), 35.06 (Ar*C*$(CH_3)_3$), 33.97 (Ar*C*$(CH_3)_3$), 31.87 (ArC(*C*$H_3)_3$), 31.75 (ArC(*C*$H_3)_3$), 31.68 (ArC(*C*$H_3)_3$), 28.67 (Ar*C*H$(CH_3)_2$), 25.11 (ArCH(*C*$H_3)_2$), 23.37 (ArCH(*C*$H_3)_2$), 18.60 (Ar*C*H_3), 18.55 (Ar*C*H_3), -7.22 (Ni*C*H_3) ppm. Anal. Calcd. for $C_{53}H_{70}N_2NiO$: C, 78.61; H, 8.71; N, 3.46. Found: C, 78.43; H, 8.57; N, 3.18.

Compound 29. 3-phenyl salcylaldimine was synthesized by combining 3-phenyl salicylaldehyde (1.00 g, 5.04 mmol, 1 equiv), *p*-toluenesulfonic acid (0.096 g, 0.50 mmol, 0.1 equiv), 2,6-diisopropylamine (1.97 g, 11.10 mmol, 2.2 equiv), and methanol (100 mL) in a round bottom flask equipped with a reflux condenser. The mixture was stirred at reflux for 3 h and then cooled to room temperature. A color change from orange to orange-brown was observed during heating. 0.83 g (46% yield) of yellow crystals was collected via filtration. The ^{1}H NMR spectrum matched literature assignments.[27]

Complex 30. Metallation of 3-phenyl salcylaldimine was achieved by a method analogous to that used for the dinuclear nickel complexes. A solution of **29** (0.10 g, 0.28

mmol, 1 equivalent) in 4 mL of diethyl ether and a solution of $NiMe_2$(tmeda) (0.063 g, 0.31 mmol, 1.1 equiv) in 4 mL of diethyl ether were cooled in the glovebox freezer to about –35 °C. The solution of the ligand precursor was added to the solution of nickel precursor. Pyridine (0.25 mL, 3.08 mmol, 11 equiv) was syringed into the mixture causing a color change to reddish orange. The reaction became gradually cloudier over 5 h of stirring at room temperature, at which point volatiles were removed under vacuum. The red brown solid was washed over Celite with pentane and the desired product was collected by flushing it through the Celite with Et_2O. Black precipitate was left on the Celite. The solution of the product was placed under vacuum to remove volatiles leaving 0.13 g (88% yield) of orange solid. ^{1}H NMR (400 MHz, C_6D_6) δ = 8.49 (dd, *J*=6.4, 1.4, 2H, Py*H*), 7.61 (s, 1H, Ar*H*), 7.50 – 7.39 (td, 3H, Ar*H*), 7.12 (dd, *J*=9.2, 4.0, 2H, Ar*H*), 7.06 (t, *J*=7.3, 1H, Ar*H*), 6.98 (t, *J*=7.4, 3H, N-Ar*H*), 6.94 (dd, *J*=7.9, 1.7, 1H, Ar*H*), 6.62 (t, *J*=7.6, 1H, Ar*H*), 6.55 (t, *J*=7.5, 1H, Py*H*), 6.18 (dd, *J*=7.4, 6.6, 2H, Py*H*), 4.24 (sept, 2H, C*H*$(CH_3)_2$), 1.54 (d, *J*=6.9, 6H, CH(C*H*$_3)_2$), 1.11 (d, *J*=6.8, 6H, CH(C*H*$_3)_2$), -0.67 (s, 3H, NiC*H*$_3$) ppm. ^{13}C NMR (101MHz, C_6D_6) δ = 166.58 (Ar*C*HN), 165.33 (Ar), 151.97 (Ar), 150.28 (Ar), 140.81 (Ar), 135.51 (Ar), 134.63 (Ar), 133.92 (Ar), 129.97 (Ar), 128.59 (Ar), 127.51 (Ar), 126.59 (Ar), 125.79 (Ar), 123.65(Ar), 123.00 (Ar), 120.73 (Ar), 114.13 (Ar), 110.43 (Ar), 28.62 (Ar*C*H$(CH_3)_2$), 24.98 (ArCH(*C*H$_3)_2$), 23.25 (ArCH(*C*H$_3)_2$), -7.26 (Ni*C*H$_3$) ppm. Anal. Calcd. for $C_{31}H_{34}N_2NiO$: C, 73.11; H, 6.73; N, 5.50. Found: C, 73.04; H, 6.74; N, 5.40.

General polymerization procedures

A 3 oz. Andrews glass pressure reaction vessel equipped with Swagelok valves and a gauge was used for all high pressure polymerizations. All polymerizations

involving ethylene were carried out under the same conditions. The high-pressure setup was brought into the glovebox with a magnetic stirbar and charged with the desired amounts of solvent and comonomer. A syringe was loaded with a solution of nickel complex, and the needle was sealed with a rubber septum. The syringe and setup were brought out of the box, and the setup was clamped firmly over a hot plate with a mineral oil bath previously regulated to 25 °C (or the desired temperature). The solution was stirred vigorously (1200 rpm). A nylon core hose equipped with quick connect adaptors was purged with ethylene for 1 minute, and the pressure was set to 15 psi. The hose was connected to the setup and the setup was filled with ethylene. A bleed needle was inserted into a Teflon septum at the top of the high-pressure setup and flushed with ethylene. The solution of nickel complex was added via syringe, and the top of the setup was closed. The pressure was increased to 100 psig. After the desired time (generally 1 or 3 h), the ethylene hose was disconnected, the setup was vented, and the reaction mixture was quenched with acidified methanol (3 times the reaction volume) to precipitate the polymer, which was collected as a white or pale yellow solid by filtration over a fine frit. If only a small amount of polymer was precipitated, the entire mixture was collected and volatile materials were removed under vacuum. Sample ^{1}H and ^{13}C NMR spectra are included in Appendix C.

Kinetic studies of 7-a isomerization

The four samples were prepared in the glovebox by dissolving 0.044 g of **7-a** in 3.2 mL of 1-bromonaphthalene. 0.8 mL of the solution was transferred to each of four J. Young tubes and sealed. These samples were brought out of the box and placed in preheated silicone oil baths at 140, 150, 160, and 170 °C. The samples at 140 and 150

°C were monitored at 30 minute intervals and the samples at 160 and 170 °C were monitored at 15 minute intervals by removing the sample from the bath, cooling to room temperature, and recording the d_0 ^{1}H NMR spectrum. The isomerization process was observed by comparing integration of the phenol peak, the isopropyl methine peak and the isopropyl methyl peaks of the two isomers, which were distinguishable in the ^{1}H NMR spectrum (see below for sample spectra). The three values were averaged to determine the concentration for that time point. Time points were recorded until the reactions reached equilibrium. K_{eq} did not change between the four samples, so that the final ratio of **7-s** and **7-a** was 0.61. The four plots of ln(X_e-X) versus time are below.

Additional kinetics data

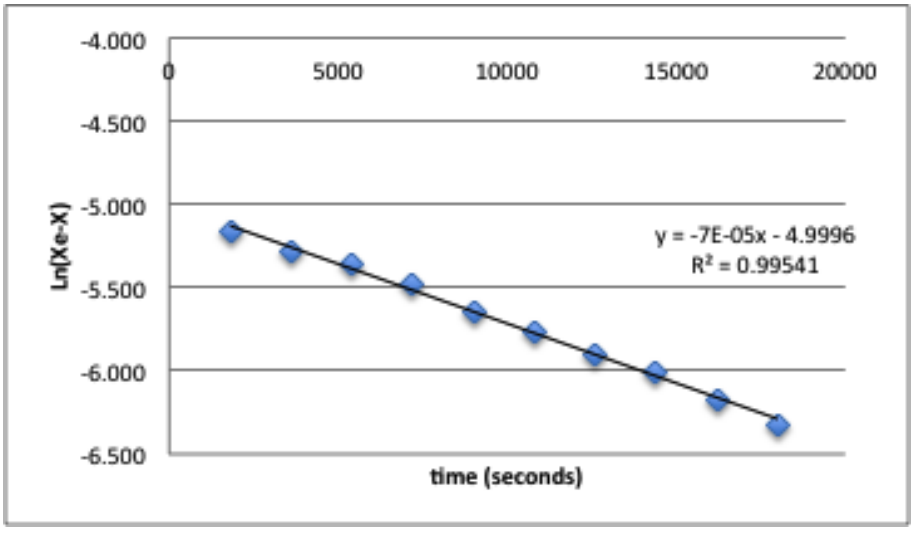

Figure 2.3. Ln(X_e-X) versus time for the 140 °C sample.

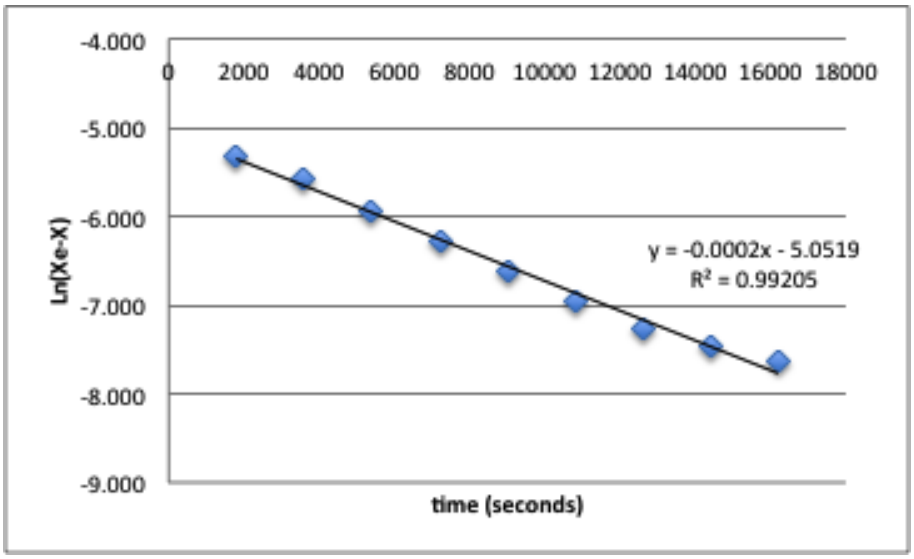

Figure 2.4. Ln(X_e-X) versus time for the 150 °C sample.

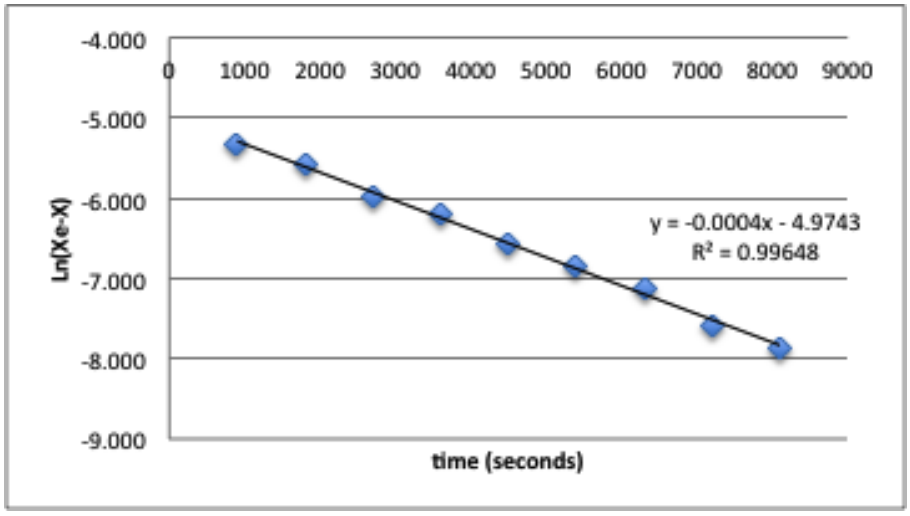

Figure 2.5. Ln(X_e-X) versus time for the 160 °C sample.

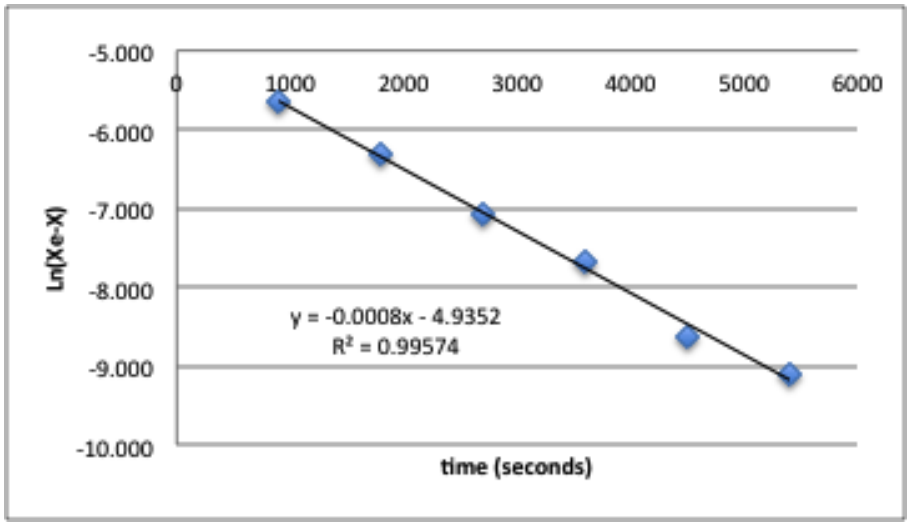

Figure 2.6. Ln(X_e-X) versus time for the 170 °C sample.

Table 2.4. Rate constants of the isomerization of **7-a** to **7-s**.

T (K)	k_{as} (x 10^4 s^{-1})	k_{sa} (x 10^4 s^{-1})
413	0.27	0.44
423	0.76	1.24
433	1.52	2.48
443	3.79	6.21

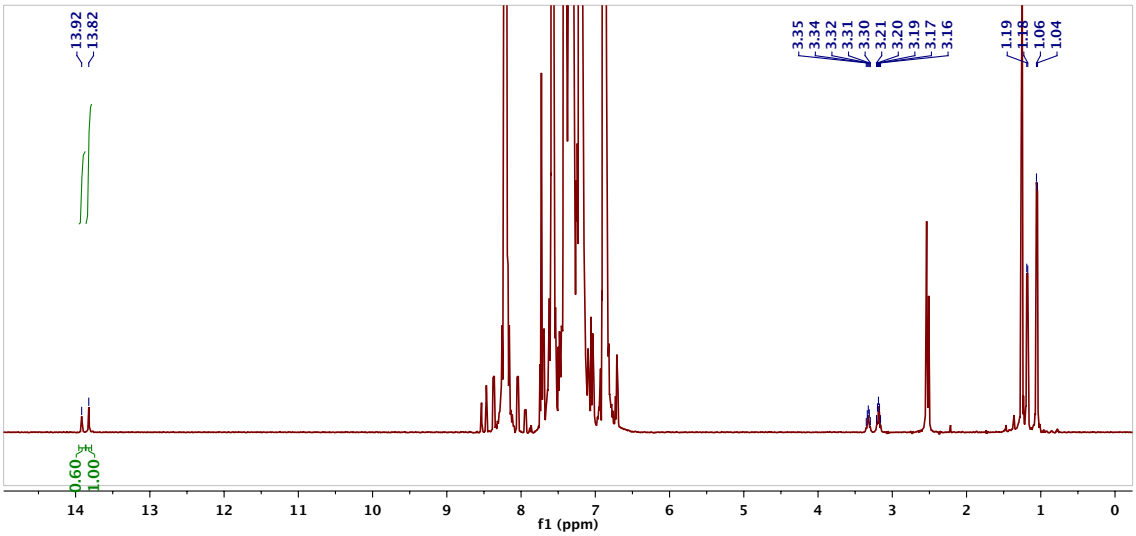

Figure 2.7. Sample [D_0]-1-bromonaphthalene ^{1}H NMR spectrum from kinetics studies of the isomerization of **7-a** to **7-s.** The phenol, isopropyl methine and isopropyl methyl peaks were used to follow the isomerization and are selected below.

NOESY and ROESY spectra with assignments

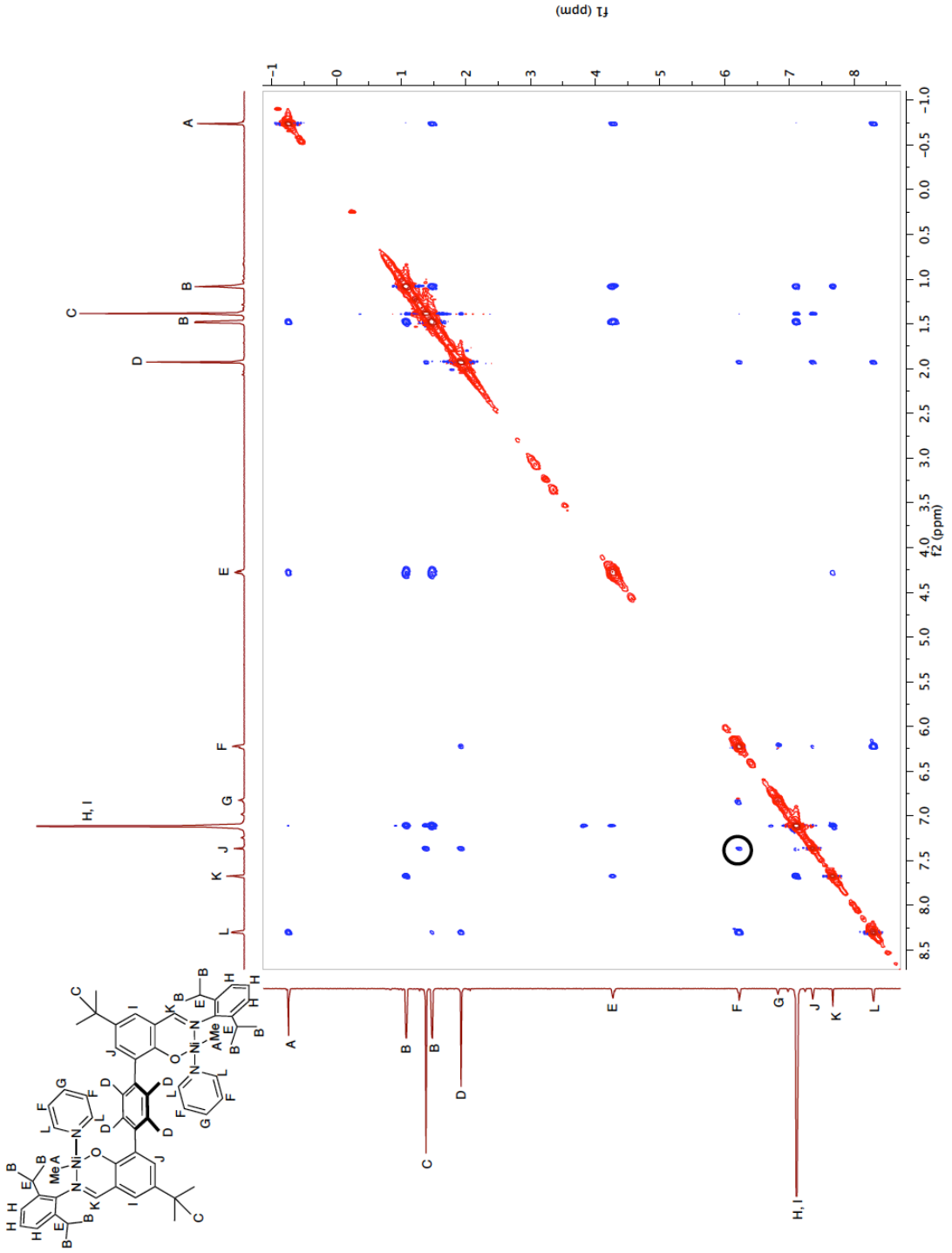

Figure 2.8. ^{1}H-^{1}H ROESY NMR spectrum of **25-a** in C_6D_6. The circled cross peak indicates that this is the anti atropisomer.

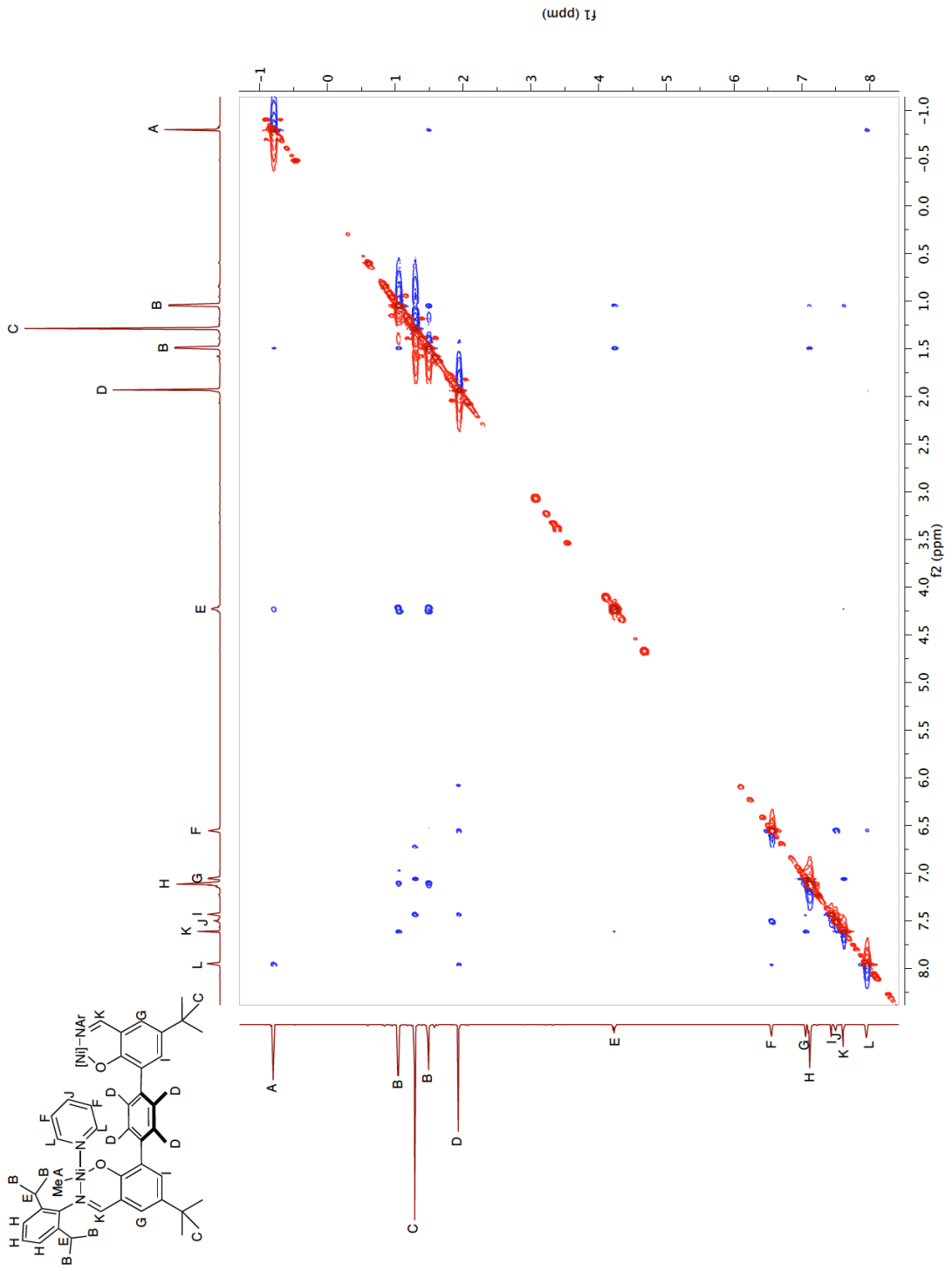

Figure 2.9. ^{1}H-^{1}H NOESY NMR spectrum of **25-s** in C_6D_6.

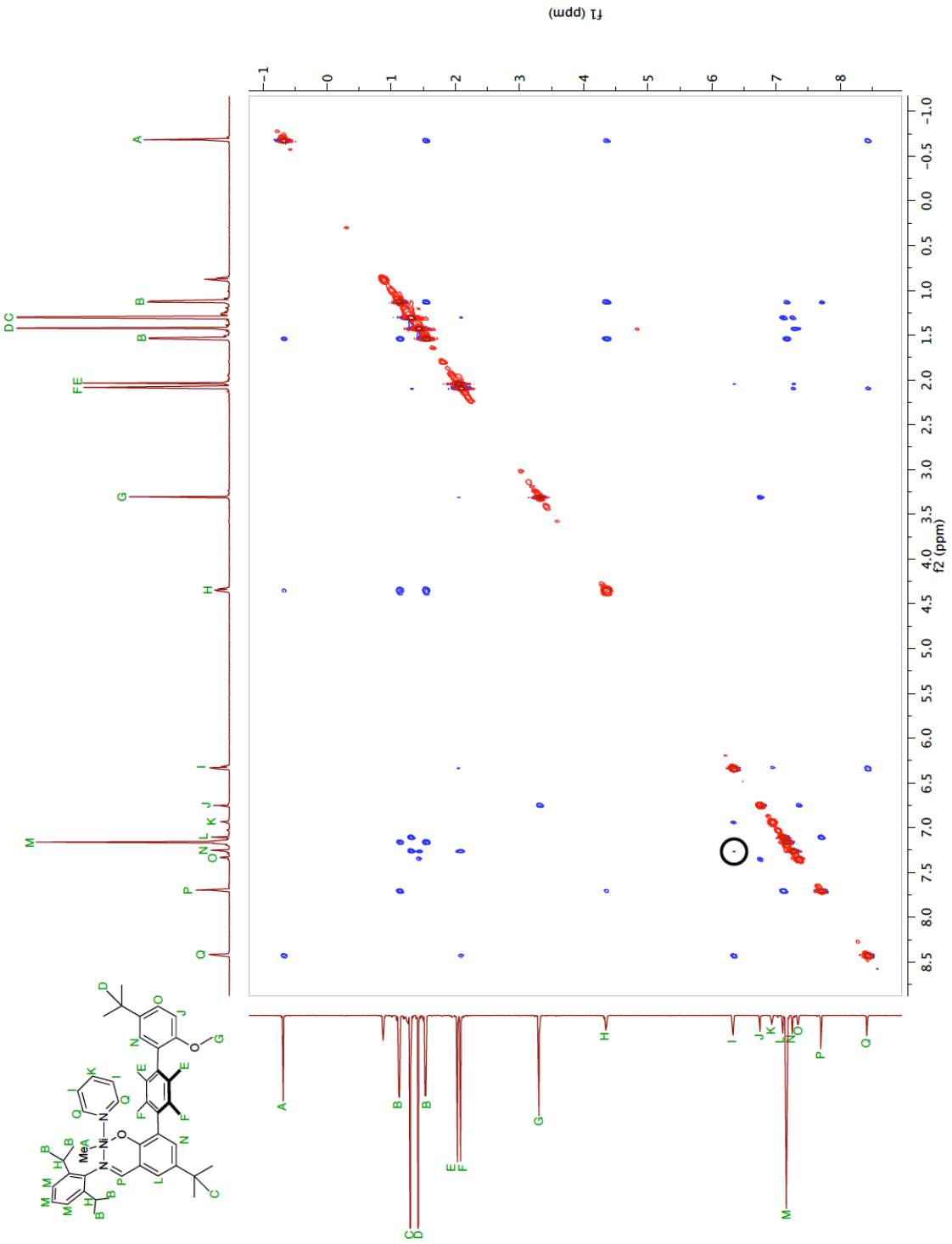

Figure 2.10. ^{1}H-^{1}H NOESY NMR spectrum of **27-a** in C_6D_6. The circled cross peak indicates that this is the anti atropisomer.

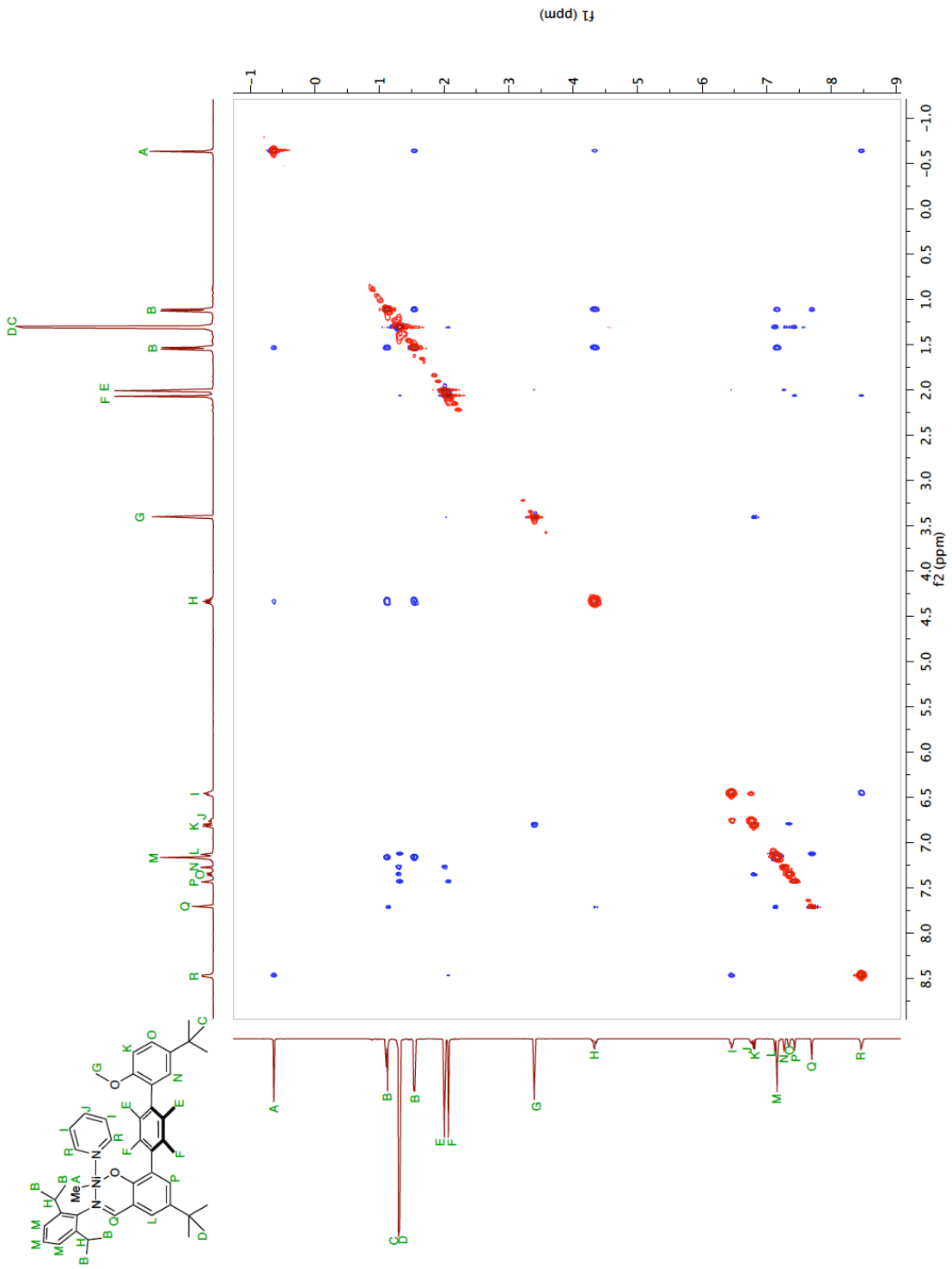

Figure 2.11. ^{1}H-^{1}H NOESY NMR spectrum of **27-s** in C_6D_6.

Crystallographic Information

Table 2.5. Crystal and refinement data for complexes **25-a** and **25-s**.

	25-a	**25-s**
CCDC Number	825810	825811
Empirical formula	$C_{68}H_{86}N_4O_2Ni_2 \bullet 2(C_7H_8)$	$2(C_{68}H_{86}N_4O_2Ni_2) \bullet C_5H_{12}$
Formula weight	1293.10	1144.90
T (K)	100(2)	100(2)
a, Å	10.8420(4)	17.1455(10)
b, Å	22.6464(7)	18.0109(10)
c, Å	14.5229(5)	23.4009(13)
a, deg	90	70.258(3)
b, deg	98.322(2)	72.094(3)
g, deg	90	84.191(3)
Volume, Å^3	3528.3(2)	6472.1(6)
Z	4	4
Crystal system	Monoclinic	Triclinic
Space group	P $2_1/c$	P-1
d_{calc}, g/cm^3	1.217	1.175
q range, deg	1.90 to 39.23	1.73 to 28.89
μ, mm^{-1}	0.583	0.627
Abs. Correction	none	none
GOF	3.870	1.277
R_1,[a] wR_2 [b] [I>2s(I)]	0.0628, 0.0754	0.0558, 0.0618

[a] $R_1 = \sum||F_o| - |F_c||/\sum|F_o|$. [b] $wR_2 = [\sum[w(F_o^2-F_c^2)^2]/\sum[w(F_o^2)^2]]^{1/2}$.

Special refinement details

Compound **25-a**

Crystals were mounted on a glass fiber using Paratone oil then placed on the diffractometer under a nitrogen stream at 100K.

Refinement of F^2 against ALL reflections. The weighted R-factor (*w*R) and goodness of fit (S) are based on F^2, conventional R-factors (R) are based on F, with F set to zero for negative F^2. The threshold expression of $F^2 > 2s(F^2)$ is used only for calculating R-factors(gt) etc. and is not relevant to the choice of reflections for refinement. R-factors based on F^2 are statistically about twice as large as those based on F, and R-factors based on ALL data will be even larger.

All esds (except the esd in the dihedral angle between two l.s. planes) are estimated using the full covariance matrix. The cell esds are taken into account individually in the estimation of esds in distances, angles and torsion angles; correlations between esds in cell parameters are only used when they are defined by crystal symmetry. An approximate (isotropic) treatment of cell esds is used for estimating esds involving l.s. planes.

Compound **25-s**

Crystals were mounted on a glass fiber using Paratone oil then placed on the diffractometer under a nitrogen stream at 100K.

Refinement of F^2 against ALL reflections. The weighted R-factor (*w*R) and goodness of fit (S) are based on F^2, conventional R-factors (R) are based on F, with F set to zero for negative F^2. The threshold expression of $F^2 > 2s(F^2)$ is used only for calculating R-factors(gt) etc. and is not relevant to the choice of reflections for refinement. R-factors based on F^2 are statistically about twice as large as those based on F, and R-factors based on ALL data will be even larger.

All esds (except the esd in the dihedral angle between two l.s. planes) are estimated using the full covariance matrix. The cell esds are taken into account individually in the estimation of esds in distances, angles and torsion angles; correlations between esds in cell parameters are only used when they are defined by crystal symmetry. An approximate (isotropic) treatment of cell esds is used for estimating esds involving l.s. planes.

REFERENCES

1. Delferro, M.; Marks, T. J. *Chem. Rev.* **2011**, *111*, 2450-2485.
2. Wilcox, D. E. *Chem. Rev.* **1996**, *96*, 2435-2458.
3. Lipscomb, W. N.; Sträter, N. *Chem. Rev.* **1996**, *96*, 2375-2434.
4. Cowan, J. A. *Chem. Rev.* **1998**, *98*, 1067-1088.
5. Guo, N.; Li, L.; Marks, T. J. *J. Am. Chem. Soc.* **2004**, *126*, 6542-6543.
6. Li, H. B.; Li, L. T.; Schwartz, D. J.; Metz, M. V.; Marks, T. J.; Liable-Sands, L.; Rheingold, A. L. *J. Am. Chem. Soc.* **2005**, *127*, 14756-14768.
7. Li, H. B.; Marks, T. J. *Proc. Natl. Acad. Sci. U.S.A.* **2006**, *103*, 15295-15302.
8. Salata, M. R.; Marks, T. J. *J. Am. Chem. Soc.* **2007**, *130*, 12-13.
9. Guo, N.; Stern, C. L.; Marks, T. J. *J. Am. Chem. Soc.* **2008**, *130*, 2246-2261.
10. Rodriguez, B. A.; Delferro, M.; Marks, T. J. *Organometallics* **2008**, *27*, 2166-2168.
11. Makio, H.; Terao, H.; Iwashita, A.; Fujita, T. *Chem. Rev.* **2011**, *111*, 2363-2449.
12. Younkin, T. R.; Conner, E. F.; Henderson, J. I.; Friedrich, S. K.; Grubbs, R. H.; Bansleben, D. A. *Science* **2000**, *287*, 460-462.
13. Bauers, F. M.; Mecking, S. *Macromolecules* **2001**, *34*, 1165-1171.
14. Wehrmann, P.; Mecking, S. *Macromolecules* **2006**, *39*, 5963-5964.
15. Wehrmann, P.; Zuideveld, M.; Thomann, R.; Mecking, S. *Macromolecules* **2006**, *39*, 5995-6002.
16. Wehrmann, P.; Mecking, S. *Organometallics* **2008**, *27*, 1399-1408.
17. Sujith, S.; Joe, D. J.; Na, S. J.; Park, Y. W.; Chow, C. H.; Lee, B. Y. *Macromolecules* **2005**, *38*, 10027-10033.
18. Hu, T.; Tang, L.-M.; Li, X.-F.; Li, Y.-S.; Hu, N.-H. *Organometallics* **2005**, *24*, 2628-2632.
19. Hu, T.; Li, Y. G.; Li, Y. S.; Hu, N. H. *J. Mol. Catal. A: Chem.* **2006**, *253*, 155-164.
20. Na, S. J.; Joe, D. J.; Sujith, S.; Han, W. S.; Kang, S. O.; Lee, B. Y. *J. Organomet. Chem.* **2006**, *691*, 611-620.
21. Wang, W. H.; Jin, G. X. *Inorg. Chem. Commun.* **2006**, *9*, 548-550.
22. Zhang, D.; Jin, G. X. *Inorg. Chem. Commun.* **2006**, *9*, 1322-1325.
23. Chen, Q.; Yu, J.; Huang, J. *Organometallics* **2007**, *26*, 617-625.
24. Yan, Y.; Qin, B.; Shu, Y. L.; Chen, X. Y.; Yip, Y. K.; Zhang, D. W.; Su, H. B.; Zeng, H. Q. *Org. Lett.* **2009**, *11*, 1201-1204.
25. Kaur, I.; Jazdzyk, M.; Stein, N. N.; Prusevich, P.; Miller, G. P. *J. Am. Chem. Soc.* **2010**, *132*, 1261-1263.

26. Kiesewetter, E. T.; Randoll, S.; Radlauer, M.; Waymouth, R. M. *J. Am. Chem. Soc.* **2010**, *132*, 5566-5567.

27. Wang, C. M.; Friedrich, S.; Younkin, T. R.; Li, R. T.; Grubbs, R. H.; Bansleben, D. A.; Day, M. W. *Organometallics* **1998**, *17*, 3149-3151.

28. Zysman-Colman, E.; Arias, K.; Siegel, J. S. *Can. J. Chem. Rev. Can. Chem.* **2009**, *87*, 440-447.

29. Moore, J. W.; Pearson, R. G. *Kinetics and Mechanism*; 3rd ed.; John Wiley & Sons: New York, 1981.

30. Lunazzi, L.; Mazzanti, A.; Minzoni, M.; Anderson, J. E. *Org. Lett.* **2005**, *7*, 1291-1294.

31. Hoogasian, S.; Bushweller, C. H.; Anderson, W. G.; Kingsley, G. *The Journal of Physical Chemistry* **1976**, *80*, 643-648.

32. Gust, D. *J. Am. Chem. Soc.* **1977**, *99*, 6980-6982.

33. Zuideveld, M. A.; Wehrmann, P.; Rohr, C.; Mecking, S. *Angew. Chem. Int. Ed.* **2004**, *43*, 869-873.

34. Janiak, C. *J. Chem. Soc., Dalton Trans.* **2000**, 3885-3896.

35. Connor, E. F.; Younkin, T. R.; Henderson, J. I.; Hwang, S. J.; Grubbs, R. H.; Roberts, W. P.; Litzau, J. J. *J. Polym. Sci., Part A: Polym. Chem.* **2002**, *40*, 2842-2854.

36. Göttker-Schnetmann, I.; Wehrmann, P.; Röhr, C.; Mecking, S. *Organometallics* **2007**, *26*, 2348-2362.

37. Crompton, T. R. *Analysis of Polymers: An Intoduction*; Pargamon Press, 1989.

38. The extent of polymer branching was determined by 1H NMR spectroscopy.

39. Gates, D. P.; Svejda, S. K.; Onate, E.; Killian, C. M.; Johnson, L. K.; White, P. S.; Brookhart, M. *Macromolecules* **2000**, *33*, 2320-2334.

40. Johnson, L. K.; Killian, C. M.; Brookhart, M. *J. Am. Chem. Soc.* **1995**, *117*, 6414-6415.

41. Mecking, S.; Johnson, L. K.; Wang, L.; Brookhart, M. *J. Am. Chem. Soc.* **1998**, *120*, 888-899.

42. Jenkins, J. C.; Brookhart, M. *J. Am. Chem. Soc.* **2004**, *126*, 5827-5842.

43. Schubbe, R.; Angermund, K.; Fink, G.; Goddard, R. *Macromol. Chem. Phys.* **1995**, *196*, 467-478.

44. Mecking reports both 1,2- and 2,1-insertions in α-olefin homopolymerizations, but indicates that this is in contrast with a report by Fink et al., wherein they report only 1,2-insertions for a non-phenoxyiminato nickel system. Mecking suggests that the reason for this difference is steric crowding of the Ni center disfavoring 2,1-insertions.

45. Klabunde, U.; Mulhaupt, R.; Herskovitz, T.; Janowicz, A. H.; Calabrese, J.; Ittel, S. D. *J. Polym. Sci., Part A: Polym. Chem.* **1987**, *25*, 1989-2003.

46. Radlauer, M. R.; Day, M. W.; Agapie, T. *J. Am. Chem. Soc.* **2012**, *134*, 1478-1481.

47. Pangborn, A. B.; Giardello, M. A.; Grubbs, R. H.; Rosen, R. K.; Timmers, F. J. *Organometallics* **1996**, *15*, 1518-1520.

48. Berliner, M. A.; Belecki, K. *J. Org. Chem.* **2005**, *70*, 9618-9621.

49. Kaschube, W.; Porschke, K. R.; Wilke, G. *J. Organomet. Chem.* **1988**, *355*, 525-532.

50. Connor, E. F.; Younkin, T. R.; Henderson, J. I.; Waltman, A. W.; Grubbs, R. H. *Chem. Commun.* **2003**, 2272-2273.

51. Gorl, C.; Alt, H. G. *J. Organomet. Chem.* **2007**, *692*, 5727-5753.

52. Lodeiro, S.; Xiong, Q. B.; Wilson, W. K.; Ivanova, Y.; Smith, M. L.; May, G. S.; Matsuda, S. P. T. *Org. Lett.* **2009**, *11*, 1241-1244.

53. Agapie, T.; Bercaw, J. E. *Organometallics* **2007**, *26*, 2957-2959.

54. Akama, T.; Ishida, H.; Shida, Y.; Kimura, U.; Gomi, K.; Saito, H.; Fuse, E.; Kobayashi, S.; Yoda, N.; Kasai, M. *J. Med. Chem.* **1997**, *40*, 1894-1900.

CHAPTER 3

BIMETALLIC EFFECTS ON ETHYLENE POLYMERIZATION IN THE PRESENCE OF AMINES: INHIBITION OF THE DEACTIVATION BY LEWIS BASES

Published in part as:
Radlauer, M. R., Day, M. W., and Agapie, T. *J. Am. Chem. Soc.* **2012**, *134*, 1478-1481.

ABSTRACT

Dinickel complexes supported by terphenyl ligands appended with phenoxy and imine donors were synthesized. Full substitution of the central arene blocks rotation around the aryl–aryl bond and allows for the isolation of atropisomers. The reported complexes perform ethylene polymerization in the presence of amines. The inhibiting effect of polar additives is up to 250 times lower for the syn atropisomer than for the anti atropisomer. ^{1}H NMR spectroscopy studies of the pyridine-ligated catalysts with a variety of amines revealed that the inhibition trends are consistent with the binding ability of the polar additive to the nickel centers. Comparisons with mononuclear systems indicate that the proximity of the metal centers leads to the observed attenuation of catalyst deactivation due to steric repulsion of the coordinated amines when bound to both metal centers of the syn atropisomer.

INTRODUCTION

In recent years, a bioinspired strategy has been used for the design of multimetallic olefin polymerization catalysts in which the proximity of the active nuclei is intended to facilitate catalysis in a manner similar to that observed in many metalloproteins.[1,2] A wide variety of multimetallic olefin polymerization catalysts have been reported, with a broad range of distances between the metal centers and varying degrees of flexibility of the ancillary ligand.[3-9] In comparison with their monometallic counterparts, some bimetallic early transition metal catalysts have been reported to incorporate more comonomer and bulkier olefins in copolymerizations with ethylene.[9-14] Enhanced stability and activity have been reported as well.[1,2] Although the nature of monomer interactions with bimetallic catalysts has been investigated in a few cases, studies of the effect of ligand rigidity and metal–metal distance on the polymerization outcome have been hindered by the scarcity of architectures in which these parameters can be controlled. Furthermore, the development of olefin polymerization catalysts that are not significantly affected by the presence of polar groups or that can incorporate polar monomers is of interest.

This chapter describes the use of bimetallic nickel complexes featuring a rigid terphenyl backbone and restricted intermetal distances for the polymerization of ethylene in the presence of polar additives. The synthesis and characterization of these compounds was described in detail in Chapter 2, along with the ethylene and α-olefin polymerization activity of these complexes. Mononickel catalysts were also synthesized and studied. Herein the polymerization activity of dinickel polymerization catalysts **25**

and mononickel polymerization catalysts **27** in the presence of polar additives is reported.

RESULTS AND DISCUSSION

Dinickel and mononickel complexes

In the design of a ligand for bimetallic catalysts, a 1,4-terphenyl moiety bearing four methyl substitutents on the central ring and one ortho oxygen substituent on each peripheral aryl ring was chosen as a suitably rigid backbone with restricted rotation around the aryl–aryl bonds. For comparison, both bimetallic (**25-s** and **25-a**) and monometallic (**27-s** and **27-a**) species were prepared and characterized as detailed in Chapter 2 (Chart 3.1).[15]

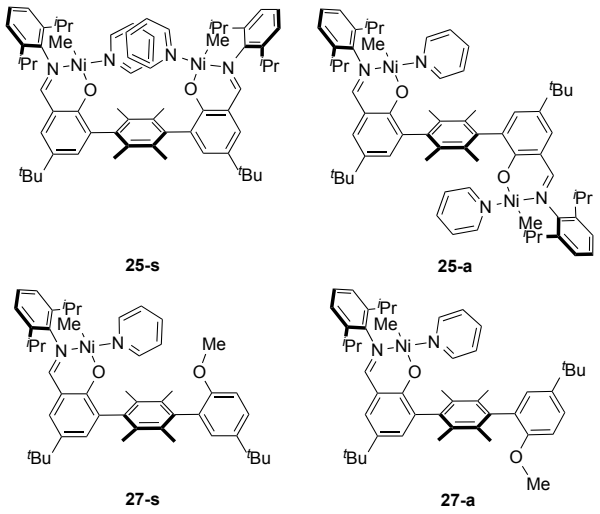

Chart 3.1. Mono- and dinickel complexes.

The solid-state structures of **25-s** and **25-a** revealed that the distance between the two metal centers is 7.1 Å in the syn isomer (average of the two molecules in the asymmetric unit) and 11.1 Å in the anti isomer (Chapter 2, Figure 2.2). A slight distortion of the square planar geometry is notable in **25-s**; the pyridine ligands extend toward the second metal center and bend away due to steric repulsion. The structure of the **25-a** forbids cooperative reactivity because the two nickel centers are on opposite faces of the central arene. The monometallic analogues **27-s** and **27-a** emulate the steric

effect of the terphenyl backbone without the presence of a second metal center. No interconversion of the syn and anti isomers of either the di- or mononickel complexes was observed over 13 hours at 50 °C (Chapter 2).

Ethylene polymerizations

Ethylene polymerization trials were performed with the isolated nickel complexes in toluene at 25 °C (Table 3.1). The present catalysts perform ethylene polymerization with activities similar to previously reported pyridine-ligated nickel phenoxyiminato systems.[16,17] These experiments generate polyethylene with methyl branches (4–20 branches per 1000 carbon atoms).[18] Of the studied complexes, catalysis with **25-s** was the slowest by a factor of 5, likely because of the increased steric bulk at the active site in comparison to the other systems. The neutral ligands coordinated to the nickel centers in **25-s** reach toward the other metal and hinder coordination of olefin. This proposal is supported by the distortion observed in the solid-state structure of **25-s**. Although the methoxy substituent is located syn with respect to nickel, the steric crowding in **27-s** is likely not as significant as that caused by the pyridine ligand bound to the second metal in **25-s**.

Ethylene polymerization trials in the presence of excess primary, secondary, and tertiary amines showed distinct inhibition trends (Tables 3.1 and 3.2). Complexes **25-a**, **27-a**, and **27-s** were inhibited by 2 orders of magnitude upon the addition of *N,N*-dimethylbutylamine (Table 3.2). This deactivation effect in the presence of added amines is similar to that reported previously for related mononickel systems.[19] In contrast, **25-s** was inhibited by only one order of magnitude. Consequently, in some cases (Table 3.1, entries 7, 8, and 11–17), addition of a tertiary amine afforded a syn

Table 3.1. Ethylene polymerization trials with **25-s** and **25-a** and polar additives.[a]

entry	additive	equiv	yield (g)		TOF[b]		R^c
			25-s	**25-a**	**25-s**	**25-a**	
1	none	n/a	0.574	3.415	341	2029	--
2	none	n/a	0.894	1.893[d]	531	2250[d]	--
3	NMe_2Et	500	0.150	1.440	89	856	0.5
4	NMe_2Et	500	0.148	1.032	88	613	0.7
5	NMe_2Et	5000	0.068	0.103	41	61	3.3
6	$NMeEt_2$	500	0.128	0.181	76	108	3.5
7	NEt_3	500	0.039	0.016	23	9	12.2
8	NEt_3	500	0.010[d]	0.006[d]	12[d]	7[d]	8.0
9	$NMe_2R^{1e,f}$	225	0.058	0.071	103	126	4.0
10	NMe_2R^{1e}	500	0.062	0.111	36	66	2.7
11	$NMe_2{}^nPr$	500	0.036	0.025	21	15	7.2
12	NMe^nPr_2	500	0.070	0.019	41	11	18.4
13	N^nPr_3	500	0.055	0.001	33	1	269
14	$NMe_2{}^nBu$	500	0.047	0.019	25	10	12.1
15	$NMe_2{}^nBu$	500	0.066	0.028	39	17	11.6
16	NMe^nBu_2	500	0.012	0.009	7	5	6.3
17	N^nBu_3	500	0.003	--[i]	2	--[i]	--
18	NMe_2Ph	500	0.619	2.867	367	1703	1.1
19	NMe_2Bz	500	0.252	1.330	150	790	0.9
20	HN^nPr_2	20	--[i]	--[i]	--[i]	--[i]	--
21	$HNMe^nBu$	20	--[i]	--[i]	--[i]	--[i]	--
22	HN^nBu_2	20	--[i]	--[i]	--[i]	--[i]	--
23	HN^iPr_2	20	0.299	0.149	178	88	9.9
24	H_2N^nBu	5	--[i]	--[i]	--[i]	--[i]	--
25	H_2NR^{2g}	50	0.011	--[i]	7	--[i]	--
26	H_2NR^{2g}	20	0.022	--[i]	13	--[i]	--
27	H_2NR^{2g}	5	0.080	0.003	48	2	136
28	H_2NR^{3h}	5	0.086	0.006	51	4	69.4
29	pyridine	10	--[i]	--[i]	--[i]	--[i]	--

[a]All polymerizations were run for 3 hours at 25°C under 100 psig of ethylene in 25 ml of toluene with 10 μmol of dinickel complex. The number of equivalents of base listed is the number of equivalents per nickel. [b]TOF = turnover frequency = (mol C_2H_4) (mol Ni)$^{-1}$ h^{-1}. [c]R = ([TOF for **25-a** with no additive]/[TOF for **25-a** with additive])/([TOF for **25-s** with no additive]/[TOF for **25-s** with additive]). [d]Polymerization was run for 1.5 hours. [e]R^1 = allyl. [f]Polymerization was run for 1 hour. [g]R^2 = 1,1-dimethylpropyl. [h]R^3 = 1,1,3,3-tetramethylbutyl. [i]Insufficient product to accurately determine (<1 mg).

catalyst that was more productive than the anti analogue. The inhibition of the deactivation by amines observed only with **25-s** is hereafter termed the bimetallic effect. The ratio of the deactivations for **25-a** versus **25-s** (*R*, Table 3.1) provides a quantitative measure of this effect. Relative to **25-s**, catalyst **25-a** was inhibited 10–25 times more by triethylamine, *N*-methyldipropylamine, and *N,N*-dimethylbutylamine and up to 270 times more by tripropylamine. Differential inhibition by triethylamine was also observed at a shorter polymerization time that resulted in lower polymer yields for both **25-s** and **25-a**, indicating that the calculated *R* is not due to different decomposition of the catalysts (Table 3.1, entries 7 and 8). The use of secondary or primary amines resulted in greater inhibition than for tertiary amines and, in all cases that yielded polymer, also displayed greater inhibition of **25-a** than of **25-s** (Table 1, entries 23, and 25–28). Relative to **25-s**, catalyst **25-a** is inhibited ca. 10 times more with diisopropylamine and 70–100 times more with 1,1-dimethylpropylamine and 1,1,3,3-tetramethylbutylamine (Table 3.1, entries 23, and 25–28).

Table 3.2. Ethylene polymerization trials with 500 equivalents of *N,N*-dimethylbutylamine per nickel.[a]

entry	complex	yield (g)	TOF[b]	*R*[d]
1	**25-s**	0.047	28	15
2	**25-s**	0.066	39	11
3	**25-a**	0.019	11	190
4	**25-a**	0.028	17	130
5	**27-s**	0.012	7	105
6	**27-s**	0.010	6	121
7	**27-a**	0.053	31	57
8	**27-a**	0.048	29	62

[a]All polymerizations were run for 3 hours at 25°C under 100 psig of ethylene in 25 ml of toluene with 20 μmol of nickel. [b]TOF = turnover frequency = (mol C_2H_4) (mol Ni)$^{-1}$ h^{-1}. [d]R = (TOF with no additive)/(TOF with additive).

Ligand exchange studies

The effect of amines on **25-s** and **25-a** was studied by ^{1}H NMR spectroscopy. New Ni–CH_3 peaks were observed in the ^{1}H NMR spectra upon addition of the amines to **25-a** or **25-s**, indicating competitive substitution of pyridine, and allowing for the qualitative measurement of the ligand exchange. All investigated amines displaced more pyridine from **25-a** than from **25-s**.

With the tertiary amines, a large excess of amine (greater than 50 equivalents per nickel) was required to detect new nickel species. Specifically, with *N,N*-dimethylethylamine, the addition of 170 equivalents to the anti analogue resulted in a new Ni–CH_3 peak that integrated to about one fifth relative to the Ni–CH_3 peak of the bis-pyridine complex. The addition of 130 equivalents of *N,N*-dimethylethylamine to the syn analogue resulted in a couple of new Ni–CH_3 peaks, but none of the peaks integrated to more than one fiftieth relative to the Ni–CH_3 peak of the bis-pyridine complex. With *N,N*-dimethylbutylamine, the addition of 80 equivalents to the anti analogue resulted in a new Ni–CH_3 peak that integrated to about two-thirds relative to the Ni–CH_3 peak of the bis-pyridine complex. The addition of 75 equivalents of *N,N*-dimethylethylamine to the syn analogue resulted in a couple of new Ni–CH_3 peaks, the largest of which integrated to one tenth relative to the Ni–CH_3 peak of the bis-pyridine complex. With *N,N*-dimethylbenzylamine, the addition of 200 equivalents to the anti or 60 equivalents to the syn analogue results in several new Ni–CH_3 peaks, but none of them integrate to more than one fiftieth relative to the Ni–CH_3 peak of the bis-pyridine complex.

In contrast, the addition of a single equivalent of 1,1-dimethylpropylamine per nickel resulted in a number of new peaks (Figure 3.1). The peaks marked with a diamond correspond to the bis-pyridine complex. The peaks marked with a dot correspond to the bis-amine complex. The peaks correspond to the mono-pyridine mono-amine complex. These assignments were made based on the spectra of the isolated bis-pyridine complexes and the number and relative integration of the remaining peaks. For **25-a**, the ratio of these peaks from the most downfield to the most upfield is 2:1:5:2. For **25-s**, the ratio of these peaks from the most downfield to the most upfield is 0.3:1:0.1:0.3. This is consistent with the data from the experiments with the tertiary amines, which also show more displacement of pyridine in the anti analogue.

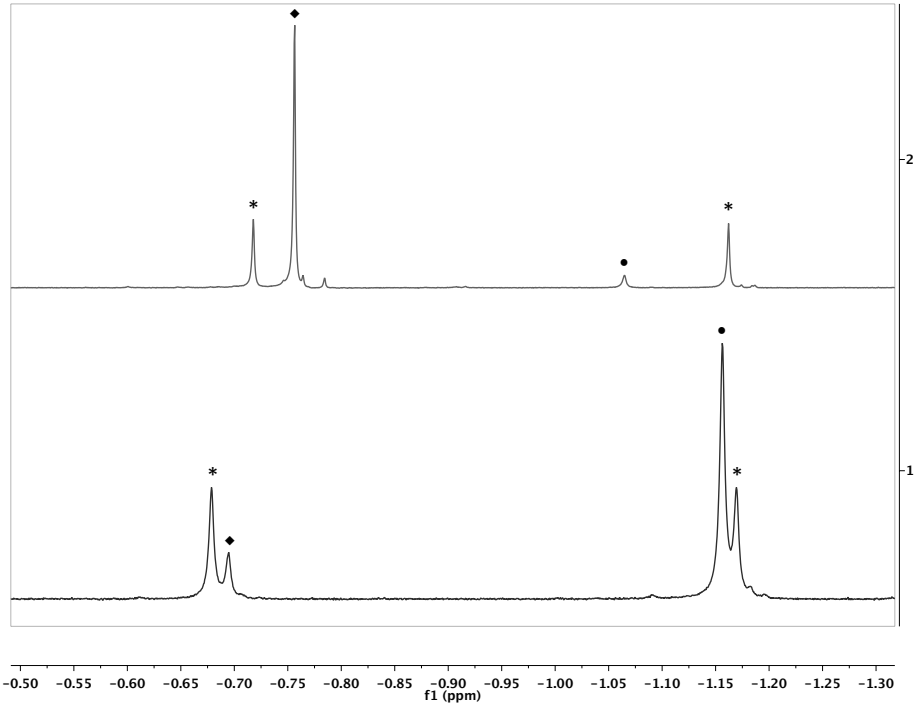

Figure 3.1. ^{1}H NMR spectra of the **25-s** (top) and **25-a** (bottom) dinickel complexes with 2 equivalents of 1,1-dimethylpropylamine (◆ = bis-pyridine, • = bis-amine, * = mono-pyridine mono-amine).

Qualitatively, the binding ability was found to vary in the following order: pyridine ≈ 1,1-dimethylpropylamine >> *N,N*-dimethylbutylamine > *N,N*-dimethylethylamine >> *N,N*-dimethylbenzylamine (additional analysis included at the end of this chapter). This trend mirrors the degree of inhibition recorded in ethylene polymerizations (Table 3.1, entries 4, 14, 19, 27, and 29). The correlation suggests that stronger amine binding to nickel increases the bimetallic effect.

Mechanistic proposal

The observed catalytic behavior suggests a bimetallic effect on inhibition by added base. Polymer formation is dependent on coordination of olefin and turnover-limiting olefin insertion into the metal–polymeryl bond.[20-21] Lewis bases compete with olefin for coordination to the metal and decrease the overall polymerization rate and polymer yield. [22-25] While steric bulk from the ligand framework could cause a decrease in deactivation by hindering the binding of amine, the studied complexes show similar inhibition profiles for **25-a**, **27-a**, and **27-s** in contrast to **25-s**. The proximal arrangement of the two metal centers in compound **25-s** is proposed to cause the difference in deactivation relative to **25-a**, **27-a**, or **27-s** (Scheme 3.1). Simultaneous binding of a bulky base to each nickel center of **25-s** is expected to be sterically disfavored compared to binding bases to all metal centers of **25-a**, **27-a**, or **27-s**. Hence, for **25-s**, ethylene may compete successfully with the amine for coordination to nickel. This has the net effect of inhibiting deactivation by the base for **25-s** compared to **25-a**, **27-a**, or **27-s**. Intriguingly, the proposed mechanism might also be relevant to the polymerization of olefins with binuclear cationic early transition metal catalysts, with the couteranions acting as inhibiting bases instead of amines.[10-12,14]

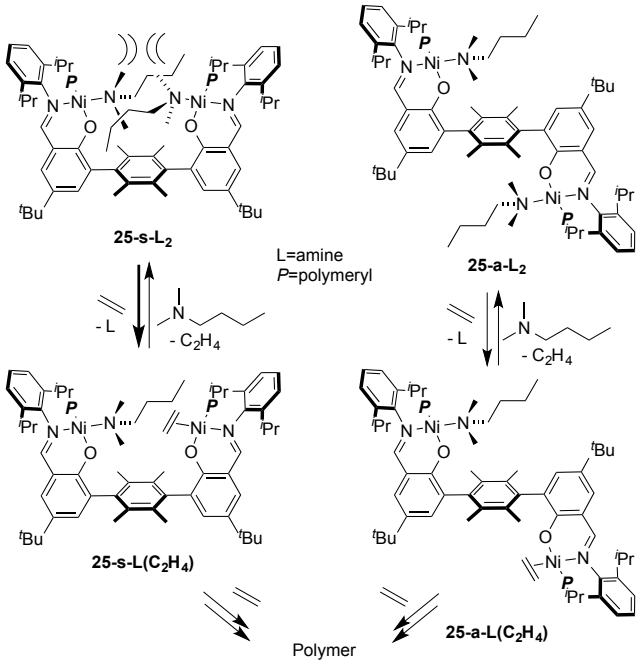

Scheme 3.1. Competition between ethylene and amine for binding to nickel in bimetallic complexes.

In agreement with the above mechanistic proposal, the extent of inhibition was found to be dependent on the nature of the amine. The smallest amines induced a smaller difference between **25-s** and **25-a**. Binding of a smaller amine to one of the nickel centers of **25-s** leaves space to bind a second amine to the other nickel center, thereby causing inhibition similar to that seen for **25-a**. For several of the secondary and primary amines (dipropylamine, *N*-methylbutylamine, dibutylamine, and butylamine), tight coordination and insufficient bulk resulted in no polymerization (Table 3.1, entries 20–22 and 24). With intermediate-size tertiary amines, as the size increased, the inhibition of **25-s** decreased relative to **25-a** ($NMeEt_2$ vs. NEt_3 and $NMe_2{}^n Bu$ vs. $NMe_2{}^n Pr$ vs. $NMe^n Pr_2$ vs. $N^n Pr_3$). This is consistent with the first coordinated amine hindering the binding of the second. Although X-ray quality crystals of the corresponding syn isomer could not been obtained, the solid-state structure of the 1,1-

dimethylpropylamine adduct of the bimetallic anti isomer (**31-a**) highlights how the alkyl substituent of the primary amine extends toward the opposite aryl group, likely blocking the binding of a second amine in **25-s** (Figure 3.2). With larger amines (NMe^{n}Bu$_2$ and N^{n}Bu$_3$), it is proposed that binding of an amine at one nickel prevents the binding of ethylene at the second nickel of **25-s**; hence, the bimetallic effect is not apparent. Bulky and less basic *N,N*-dimethylbenzylamine and *N,N*-dimethylaniline likely show low inhibition because of weak binding to either isomer.

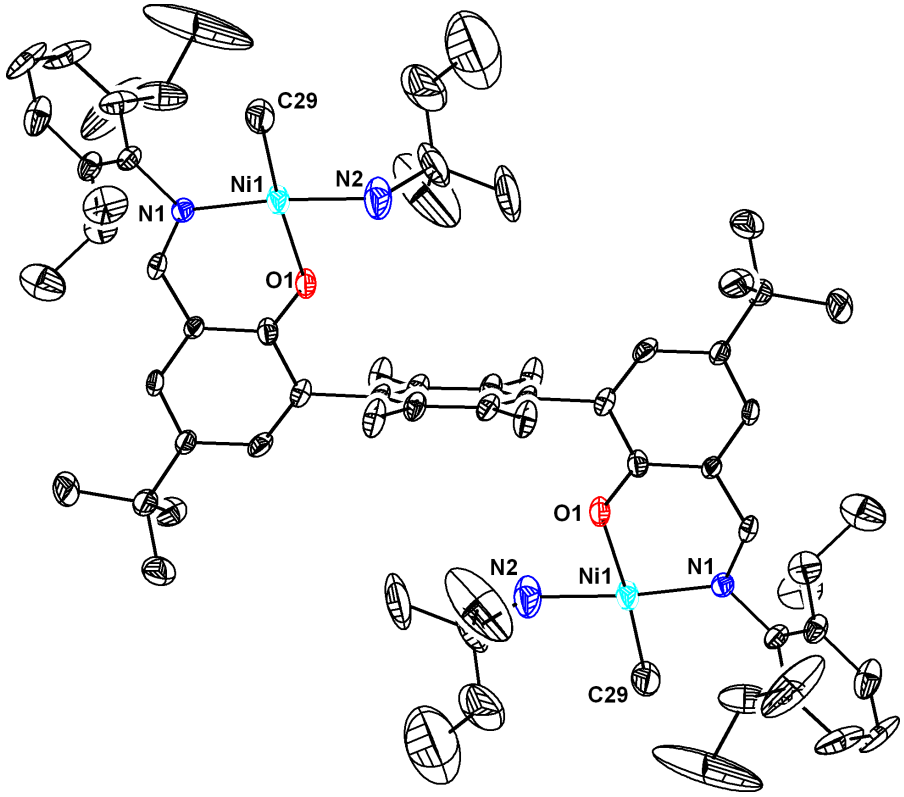

Figure 3.2. Solid-state structure of **31-a** with thermal ellipsoids at the 50 % probability level. Solvent molecules and hydrogen atoms were omitted for clarity.

CONCLUSIONS

The syn and anti atropisomers of mono- and dinickel phenoxyiminato complexes were studied for ethylene polymerization in the presence of Lewis bases. The syn bimetallic catalyst (**25-s**) showed less inhibition by added amines relative to the anti bimetallic (**25-a**) and the monometallic catalysts (**27-s** and **27-a**). The bimetallic effect observed with **25-s** is proposed to arise from the close proximity of the nickels, which disfavors simultaneous ligation of base to both of the metal centers. The bimetallic effect generally increased with the size and the binding ability of the added base. The effect was observed with tertiary, secondary and primary amines, as long as the amine had sufficient bulk to sterically interact with the labile ligands on the other nickel center. This behavior has applications in the design of olefin polymerization catalysts with increased functional group tolerance and with potential for copolymerization of polar olefins by sterically favoring catalyst interactions with the olefin rather than the polar moiety. One such system is detailed in Chapter 4. Extension of the terphenyl motif with restricted rotation to other multimetallic catalyst systems is discussed in Chapter 5 and Appendix B.

EXPERIMENTAL SECTION

General considerations and instrumentation

All air- and/or water-sensitive compounds were manipulated using standard vacuum or Schlenk line techniques or in an inert atmosphere glovebox. The solvents for air- and moisture-sensitive reactions were dried over sodium/benzophenone ketyl, calcium hydride, or by the method of Grubbs.[26] All NMR solvents were purchased from Cambridge Isotopes Laboratories, Inc. and dried over sodium/benzophenone ketyl or calcium hydride. Pyridine and amines were dried over calcium hydride and distilled prior to use. All ^{1}H, ^{13}C, and 2D NMR spectra were recorded on Varian Mercury 300 MHz, or Varian INOVA-500 or 600 MHz spectrometers at room temperature. Chemical shifts are reported with respect to residual internal deuterated solvent. J coupling are reported in Hz. The syntheses of the ligand frameworks were communicated in reference 15 and are detailed in Chapter 2.[15]

General polymerization procedure

A 3 oz. Andrews glass pressure reaction vessel equipped with Swagelok valves and a gauge was used for all high pressure polymerizations. For all polymerizations, the high-pressure setup was brought into the glovebox with a magnetic stirbar and charged with the desired amounts of toluene and amine. Concurrently, a syringe was loaded with the nickel complex dissolved in toluene and the needle was sealed with a rubber septum. The syringe and setup were brought out of the glovebox and the setup was clamped firmly over a hot plate. The temperature was regulated to 25 °C, and the solution was stirred vigorously (1200 rpm). A nylon core hose equipped with quick connect adaptors was purged with ethylene for 1 minute and the pressure was set to 15 psig. The hose

was connected to the setup and the setup was filled with ethylene. A bleed needle was inserted into a Teflon septum at the top of the high-pressure setup and flushed with ethylene. The solution of nickel complex was added via syringe and the top of the setup was closed. The pressure was increased to 100 psig. After the desired time (generally 3 hours), the ethylene hose was disconnected, the setup was vented and the reaction mixture was quenched with acidified methanol (3 times the reaction volume, 75 mL) to precipitate the polymer, which was collected as a white solid by filtration over a fine frit. If less than 10 mg of polymer was precipitated, the quenched reaction mixture was pumped down from about 100 mL to about 20 mL and the precipitate was collected from the more concentrated suspension. All of the precipitates were air-dried for at least 24 hours and transferred to scintillation vials, which were placed under vacuum on the Schlenk line for at least one hour before the polymer masses were recorded. In cases where less than 100 mg of polymer was collected, ^{1}H NMR spectra were recorded in tetrachloroethane-D_2 at 130 °C on the Varian INOVA-500 MHz NMR spectrometer to confirm that the collected precipitate was polyethylene.

^{1}H NMR spectroscopy ligand exchange experiments

^{1}H NMR spectroscopy was used to examine the exchange of pyridine for a number of amines with complexes **25-s** and **25-a**. The amines studied were 1,1-dimethylpropylamine, *N,N*-dimethylethylamine, N,N-dimethylbutylamine, and N,N-dimethylbenzylamine. In all of the experiments, a known quantity of **25-s** or **25-a** was added to a J. Young tube with about 0.7 mL of d_6-benzene in the glovebox. The tube was sealed and brought out of the glovebox, and a ^{1}H NMR spectrum was acquired. In all cases, **25-a** was not fully soluble so that orange precipitate was seen at the bottom of

the tube. The J Young tube was brought back into the glovebox and a set number of equivalents of amine were syringed into the open tube, which was again sealed, inverted several times, and brought out of the glovebox. Another ^{1}H NMR spectrum was acquired. These steps were repeated to add more amine until a significant change had occurred or at least 50 equivalents of amine per nickel had been added. There was no additional change from the time the amine was added for over 12 hours after addition, so that all spectra, regardless of the amount of time passed between addition and the acquisition of the spectrum were considered equally relevant for comparison. The Ni–CH_3 peak in the ^{1}H NMR spectrum is diagnostic of the dinickel complexes and appears between -0.5 and -1.5 ppm depending on the other ligand on nickel. The new Ni–CH_3 peaks that were observed were confirmed to be from an amine-bound species that could be converted back to the pyridine-bound species and not from a decomposition product. An experiment wherein 100 equivalents of amine were added followed by 25 equivalents of pyridine or 25 equivalents of pyridine were added followed by 100 equivalents of amine yielded the same spectrum. With **25-s** only pyridine-bound complex remained at the end of this experiment, whereas with **25-a** the ratio of the pyridine-bound Ni–CH_3 peak and the amine-bound Ni–CH_3 peak was about 20:1.

Crystallographic Information

Table 3.3. Crystal and refinement data for complex **31-a**.

	31-a
CCDC Number	846768
Empirical formula	$C_{68}H_{102}N_4O_2Ni_2$
Formula weight	1124.96
T (K)	100(2)
a, Å	9.7952(5)
b, Å	22.8485(13)
c, Å	14.6159(7)
a, deg	90
b, deg	96.415(3)
g, deg	90
Volume, Å^3	3250.6(3)
Z	2
Crystal system	Monoclinic
Space group	P $2_1/c$
d_{calc}, g/cm^3	1.149
q range, deg	1.66 to 30.53
μ, mm^{-1}	0.623
Abs. Correction	none
GOF	2.064
R_1 ,[a] wR_2 [b] [I>2s(I)]	0.0705, 0.1550

[a] $R_1 = \sum||F_o| - |F_c||/\sum|F_o|$. [b] $wR_2 = [\sum[w(F_o^2-F_c^2)^2]/\sum[w(F_o^2)^2]]^{1/2}$.

Special refinement details

Compound **31-a**

Crystals were mounted on a glass fiber using Paratone oil then placed on the diffractometer under a nitrogen stream at 100K.

Refinement of F^2 against ALL reflections. The weighted R-factor (*w*R) and goodness of fit (S) are based on F^2, conventional R-factors (R) are based on F, with F set to zero for negative F^2. The threshold expression of $F^2 > 2s(F^2)$ is used only for calculating R-factors(gt) etc. and is not relevant to the choice of reflections for refinement. R-factors based on F^2 are statistically about twice as large as those based on F, and R-factors based on ALL data will be even larger.

All esds (except the esd in the dihedral angle between two l.s. planes) are estimated using the full covariance matrix. The cell esds are taken into account individually in the estimation of esds in distances, angles and torsion angles; correlations between esds in cell parameters are only used when they are defined by crystal symmetry. An approximate (isotropic) treatment of cell esds is used for estimating esds involving l.s. planes.

REFERENCES

1. Delferro, M.; Marks, T. J. *Chem. Rev.* **2011**, *111*, 2450-2485.
2. Makio, H.; Terao, H.; Iwashita, A.; Fujita, T. *Chem. Rev.* **2011**, *111*, 2363-2449.
3. Sujith, S.; Joe, D. J.; Na, S. J.; Park, Y. W.; Chow, C. H.; Lee, B. Y. *Macromolecules* **2005**, *38*, 10027-10033.
4. Hu, T.; Li, Y. G.; Li, Y. S.; Hu, N. H. *J. Mol. Catal. A: Chem.* **2006**, *253*, 155-164.
5. Na, S. J.; Joe, D. J.; Sujith, S.; Han, W. S.; Kang, S. O.; Lee, B. Y. *J. Organomet. Chem.* **2006**, *691*, 611-620.
6. Wang, W. H.; Jin, G. X. *Inorg. Chem. Commun.* **2006**, *9*, 548-550.
7. Zhang, D.; Jin, G. X. *Inorg. Chem. Commun.* **2006**, *9*, 1322-1325.
8. Chen, Q.; Yu, J.; Huang, J. *Organometallics* **2007**, *26*, 617-625.
9. Rodriguez, B. A.; Delferro, M.; Marks, T. J. *Organometallics* **2008**, *27*, 2166-2168.
10. Guo, N.; Li, L.; Marks, T. J. *J. Am. Chem. Soc.* **2004**, *126*, 6542-6543.
11. Li, H. B.; Li, L. T.; Schwartz, D. J.; Metz, M. V.; Marks, T. J.; Liable-Sands, L.; Rheingold, A. L. *J. Am. Chem. Soc.* **2005**, *127*, 14756-14768.
12. Li, H. B.; Marks, T. J. *Proc. Natl. Acad. Sci. U.S.A.* **2006**, *103*, 15295-15302.
13. Salata, M. R.; Marks, T. J. *J. Am. Chem. Soc.* **2008**, *130*, 12-13.
14. Guo, N.; Stern, C. L.; Marks, T. J. *J. Am. Chem. Soc.* **2008**, *130*, 2246-2261.
15. Radlauer, M. R.; Day, M. W.; Agapie, T. *Organometallics* **2012**, *31*, 2231-2243.
16. Zuideveld, M. A.; Wehrmann, P.; Rohr, C.; Mecking, S. *Angew. Chem. Int. Ed.* **2004**, *43*, 869-873.
17. Wehrmann, P.; Zuideveld, M.; Thomann, R.; Mecking, S. *Macromolecules* **2006**, *39*, 5995-6002.
18. Crompton, T. R. *Analysis of Polymers: An Intoduction*; Pargamon Press, 1989.
19. Younkin, T. R.; Conner, E. F.; Henderson, J. I.; Friedrich, S. K.; Grubbs, R. H.; Bansleben, D. A. *Science* **2000**, *287*, 460-462.
20. Johnson, L. K.; Killian, C. M.; Brookhart, M. *J. Am. Chem. Soc.* **1995**, *117*, 6414-6415.
21. Ittel, S. D.; Johnson, L. K.; Brookhart, M. *Chem. Rev.* **2000**, *100*, 1169-1204.
22. Mecking, S.; Johnson, L. K.; Wang, L.; Brookhart, M. *J. Am. Chem. Soc.* **1998**, *120*, 888-899.
23. Jenkins, J. C.; Brookhart, M. *J. Am. Chem. Soc.* **2004**, *126*, 5827-5842.
24. Wu, F.; Foley, S. R.; Burns, C. T.; Jordan, R. F. *J. Am. Chem. Soc.* **2005**, *127*, 1841-1853.

25. Berkefeld, A.; Drexler, M.; Moller, H. M.; Mecking, S. *J. Am. Chem. Soc.* **2009**, *131*, 12613-12622.

26. Pangborn, A. B.; Giardello, M. A.; Grubbs, R. H.; Rosen, R. K.; Timmers, F. J. *Organometallics* **1996**, *15*, 1518-1520.

CHAPTER 4

Bimetallic Coordination-Insertion Polymerization of Unprotected Polar Monomers: Copolymerization of Amino Olefins and Ethylene by Dinickel Bisphenoxyiminato Catalysts

Published in part as:
Radlauer, M. R., Buckley, A. K., Henling, L. M., and Agapie, T. *J. Am. Chem. Soc.* **2013**, *135*, 3784-3787.

ABSTRACT

Dinickel bisphenoxyiminato complexes based on highly substituted *p*- and *m*-terphenyl backbones were synthesized, and the corresponding atropisomers were isolated. In the presence of a phosphine scavenger, $Ni(COD)_2$, the phosphine-ligated syn-dinickel complexes copolymerized α-olefins and ethylene in the presence of amines to afford 0.2–1.3 % α-olefin incorporation. These complexes also copolymerized amino olefins and ethylene with a similar range of incorporation (0.1–0.8 %). The present rigid catalysts provide a bimetallic strategy for insertion polymerization of polar monomers without masking of the heteroatom group. Functionalized olefins with bipyridine, diamine, aminediol, or secondary amine moieties were also investigated, though no successful copolymerization with these comonomers has been achieved to date. The effects of the catalyst structure on the reactivity were studied by comparisons of the syn and anti atropisomers, and the *p*- and *m*-terphenyl systems. A mechanism for incorporation was proposed wherein coordintion of the amine moiety to one nickel center sterically hinders binding of an amine to the second nickel center for the syn complexes. Instead, ethylene or the olefin moiety of the polar monomer, which have lower steric profiles than the amine, can coordinate to the second nickel and afford chain growth.

INTRODUCTION

Functionalized polyolefins have desirable physical properties, including improved adhesion to substrates, response to stimuli, and increased compatibility with other materials for use in polymer blends and composites.[1-8] While numerous functionalized polymers have been synthesized, even on industrial scales, their synthesis is primarily achieved through radical polymerization or post-polymerization modification, which often provide only limited control over the polymer microstructure (e.g., tacticity, branching, functionality incorporation).[4,6,9-15] Polymers generated by metathesis[16] or coordination polymerization with polar groups including ester,[17-25] amine,[16-17,19,25-39] alcohol,[13,19,22,25-27,29,37,40,41] and acid[19,22] functionalities have been reported. For insertion polymerization of amino olefins, protection of the amine or masking with a Lewis acid is common.[19,25,37,42] Insertion polymerization of α-olefins functionalized with tertiary amines catalyzed by zirconocene complexes favors bulky substituents on the amine to discourage base coordination to Zr and afford olefin coordination.[29,31-33] Herein we present a strategy for amino olefin copolymerization employing an alternate mechanism in which inhibitory binding of base to the metal is disfavored by the proximity of two catalytic sites.

Mono- and multinuclear late transition metal catalysts have been employed for the incorporation of olefins with polar moieties by coordination insertion polymerization.[18,20,43-45] Such catalysts are generally more tolerant of polar groups because of their reduced oxophilicity.[18,22-24,46-48] With dinickel systems, increased incorporation of comonomers has been observed.[44,49] In the copolymerizations of ethylene and functionalized norbornene derivatives, coordination of the polar moiety at

one nickel center and subsequent coordination of the olefinic moiety at the other nickel center has been proposed to account for higher activity and higher incorporation of the polar comonomer relative to monometallic analogues.[44,49]

We have recently investigated dinickel bisphenoxyiminato catalysts with pyridine auxiliary ligands for the copolymerization of ethylene and α-olefins (Chapter 2).[50] Permethylation of the central arene of the *p*-terphenyl backbone allowed for the isolation of syn and anti atropisomers of the complex.[50] The syn atropisomer (25-s, Figure 4.1) successfully polymerized ethylene in the presence of up to 500 equivalents of tertiary amine per nickel center (Chapter 3).[51] This is notable in view of reports that related neutral nickel catalysts are more inhibited by tertiary amines than by water, alcohols, and ethers.[43,52] We attribute the increased tolerance to a steric effect wherein the binding of an amine to one nickel center of the syn atropisomer disfavors the binding of an amine to the other nickel, allowing polymerization to continue (Chapter 3).[51] We expected this effect to allow for the incorporation of polar monomers, but the inherently low turnover and low levels of α-olefin incorporation of these catalysts precluded amino olefin polymerization. This chapter presents the synthesis of phosphine-ligated dinickel bisphenoxyiminato complexes, their polymerization activity, specifically copolymerizations of ethylene and amino olefins, and a mechanistic proposal for the copolymerizations.

RESULTS AND DISCUSSION

Synthesis of binucleating salcylaldimine ligands

The synthesis of the binucleating ligands (**7**) with a *p*-terphenyl backbone was presented in Chapter 2 (Scheme 2.1). This synthesis was altered (Scheme 4.1) due to issues with selectivity in the ortho-bromination step: **3** was often also brominated at the benzyl positions of the central arene, yielding a product that was difficult to separate from the desired dibromide **4**. To remove the need for the problematic ortho-bromination, the starting phenol was protected with a methoxymethyl (MOM) moiety (**14**) before the Negishi coupling with **2**. After Negishi coupling to yield both atropisomers of compound **32**, the MOM group was utilized to direct lithiation at the ortho position, which produced the dilithiated compound, and the addition of excess N,N-dimethylformamide (DMF) provided the diformyl species **33**. Removal of the MOM groups was accomplished with excess HCl to afford compounds **6**. Column chromatography was used to separate the two atropisomers, which were then carried forward to **7** via imine condensation with 2,6-diisopropyl aniline.

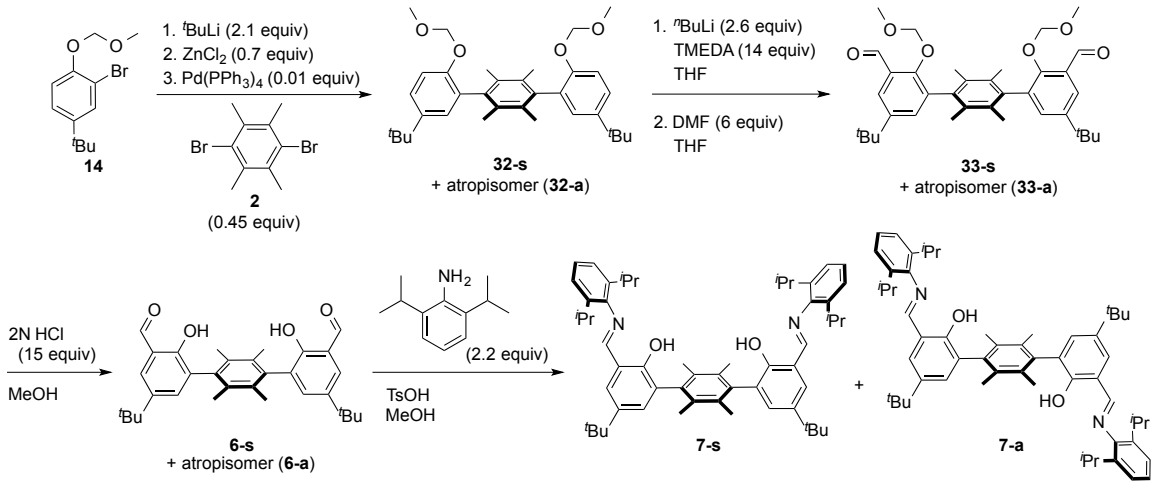

Scheme 4.1. Synthesis of *p*-bis-salcylaldimine compounds (alternative to previously reported route).[50]

For comparison to the para systems, the binucleating ligands based on *m*-terphenyl frameworks were also synthesized. The synthesis of the *m*-bis-salicylaldimine compounds, **42-a**, **42-s**, and **43-s**, was accomplished via an analogous route to that in Scheme 4.1. Negishi cross-coupling of **14** with 0.45 equivalents of dibromide **34** or **35** afforded both atropisomers of the desired terphenyl compounds (**36** and **37**). Column chromatography was used to separate the two atropisomers of each, and **36-a**, **36-s**, and **37-s** were carried forward to the binucleating ligand precursors by the same synthetic procedures in 10, 6, and 5 % overall yield, respectively.

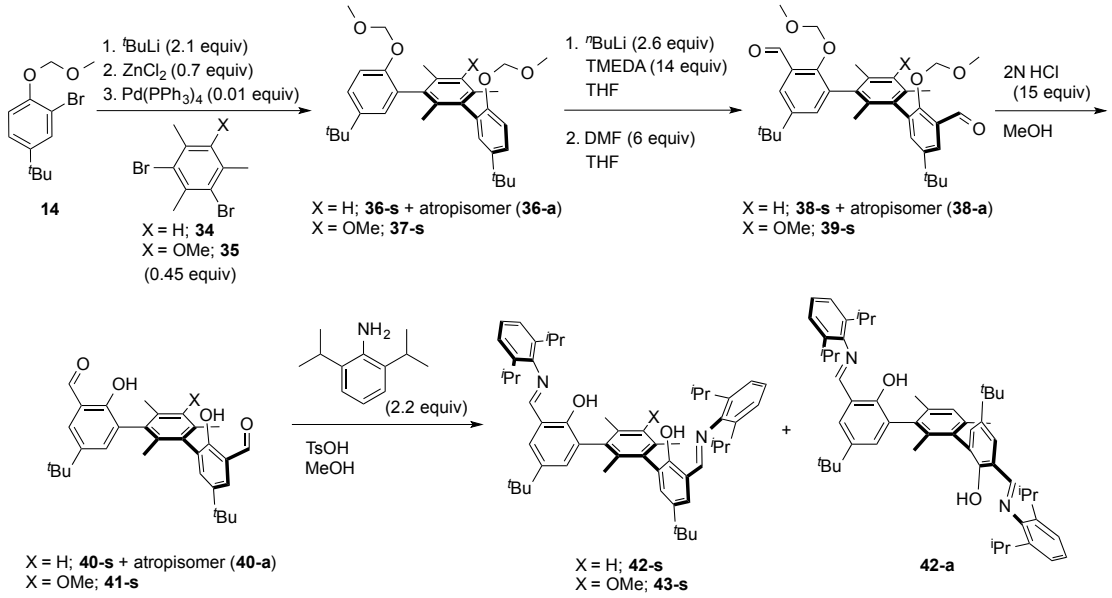

Scheme 4.2. Synthesis of *m*-bis-salicylaldimine compounds.

Synthesis of nickel complexes

A variant of our pyridine-ligated bimetallic complexes (**25**) with a different auxiliary ligand was targeted because the stability of the pyridine-ligated complexes causes lower activity.[53] A variety of mono- and dinickel alkyl phenoxyiminato complexes with pyridine, amine, nitrile, and phosphine auxiliary ligands have been employed as

catalyst precursors.[43,49,53] No activator or scavenger is needed for pyridine, amine, or nitrile ligated complexes, and the precursor behaves as a single component catalyst.[43,50,53-55] Alternatively, for phosphine-ligated complexes, $Ni(COD)_2$ and $B(C_6F_5)_4$ were utilized as phosphine scavengers.[43-44,49,56] The PMe_3-ligated complexes **44-s** and **44-a** (Figure 4.2) were synthesized by deprotonation of the syn and anti *p*-terphenyl bis-salicylaldimines and subsequent metallation with $NiClMe(PMe_3)_2$ (Scheme 4.4 in the experimental section of this chapter). The desired complexes, **44-a** (anti isomer) and **44-s** (syn isomer), were isolated as orange solids by filtration over Celite to remove salt byproducts followed by precipitation from hexanes. In ethylene/1-hexene copolymerization studies, **44-s** displayed a significant increase in activity (> 2 orders of magnitude) relative to **25-s** (Table 4.1, entries 1–3).

Complexes **45** and **46** (Figure 4.2), the *m*-terphenyl analogues of **44**, were synthesized to examine the effects of changing Ni–Ni distance and relative orientation of the nickel coordination planes. The orientation of **46-s** was verified by nuclear Overhauser effect spectroscopy (Figure 4.6). The solid-state structures of **44-s** and **45-s** confirmed the syn orientation relative to the central ring and the coordination of the PMe_3 groups trans to the imines (Figure 4.1).[57] The Ni–Ni distances are larger than 8 Å, and the terphenyl backbones are bowed (the average bend of the terphenyl for **44-s** is 171° vs. 177° for **25-s**).[51] The Ni–Ni distances is significantly longer in **44-s** (8.9 Å) than in **25-s** (7.1 Å).[51] This likely occurs because the PMe_3 ligands have a relatively conical steric profile, whereas the planar pyridine ligands of **25-s** can avoid steric repulsion. The structural distortion of the ligand framework supports our proposal that the decreased

inhibition by amines with the syn isomer vs. the anti isomer is due to steric repulsion that hinders binding of amines at both nickel centers.

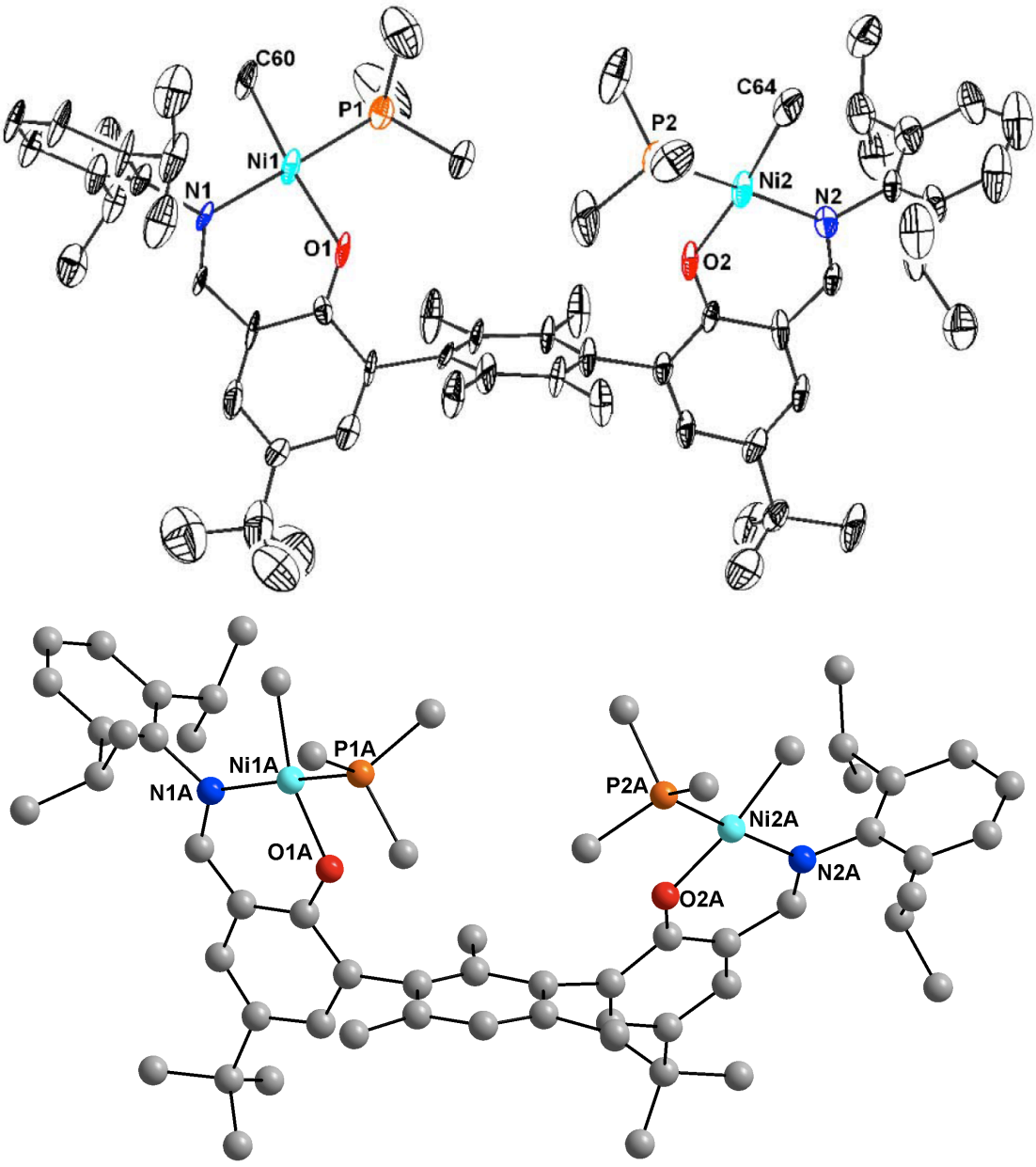

Figure 4.1. Solid-state structures of **44-s** (top) and **45-s** (bottom). Ni–Ni distances: 8.9 and 8.5 Å, respectively. Hydrogen atoms and solvent molecules were omitted for clarity. The quality of the data set for **45-s** precluded determination of anisotropic structural parameters.

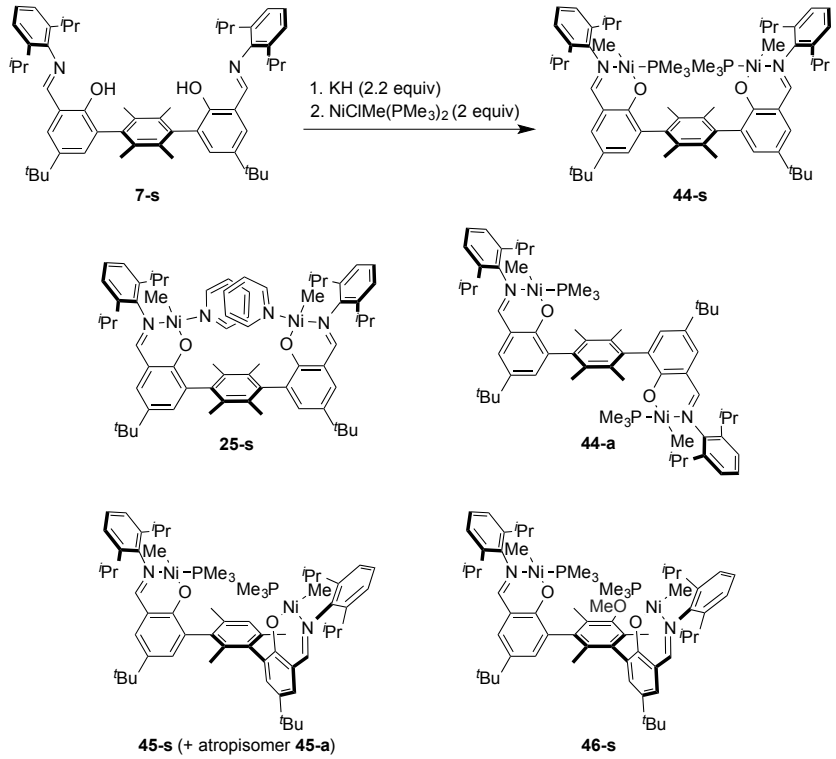

Figure 4.2. Dinickel bisphenoxyiminato complexes employed in this chapter.

Ethylene/1-hexene copolymerizations

The five PMe_3-ligated dinickel complexes displayed similar activities and 1-hexene incorporation in ethylene/1-hexene copolymerizations (Table 4.1, entries 3–7). The generated polymer contains primarily methyl and butyl branches, similar to the pyridine-ligated analogues, and up to 1.2 % incorporation of 1-hexene (as calculated from ^{1}H and ^{13}C NMR data).[50] Polymerizations run over different time periods indicated that the catalysts continued to produce polymer over the one hour trial (Table 4.2). Ethylene/1-hexene copolymerizations in the presence of tertiary amines revealed distinct inhibition trends. As expected from our previous studies of the pyridine-ligated catalysts,[51] the anti atropisomers were much more inhibited than the syn isomers, but their incorporation of 1-hexene was not significantly affected (Table 4.1, e.g., entries

Table 4.1. Ethylene/1-hexene copolymerizations.[a]

entry	complex	additive	yield (g)	activity[b]	*R*[c]	% incorp[d]	TON ethylene	TON 1-hexene
1	**25-s**	none[e]	0.003	1		--	--	--
2	**25-s**	none[f]	0.033	1		1.0	48	0.5
3	**44-s**	none[e]	1.266	317		1.2	10900	135
4	**44-a**	none[e]	1.590	397		1.1	13700	161
5	**45-s**	none[e]	1.444	361		1.1	12400	148
6	**45-a**	none[e]	1.469	367		1.0	12700	136
7	**46-s**	none[e]	1.095	274		0.9	9490	88
8	**44-s**	$NMeEt_2$	0.187	23	13	0.8	815	6.6
9	**44-a**	$NMeEt_2$	0.106	13	30	0.5	465	2.3
10	**45-s**	$NMeEt_2$	0.199	25	15	0.3	878	3.0
11	**45-a**	$NMeEt_2$	0.087	11	34	0.9	378	3.4
12	**46-s**	$NMeEt_2$	0.142	18	17	0.7	618	4.4
13	**44-s**	NEt_3	0.073	9	33	1.0	315	3.0
14	**44-a**	NEt_3	0.011	1	290	1.3	46	0.6
15	**45-s**	NEt_3	0.447	56	7	0.3	1980	5.3
16	**45-a**	NEt_3	0.006	1	515	--	--	--
17	**46-s**	NEt_3	0.457	57	5	0.7	1990	15
18	**44-s**	NMe^nPr_2	0.094	12	26	0.9	407	3.7
19	**44-a**	NMe^nPr_2	0.005	1	639	1.2	21	0.3
20	**45-s**	NMe^nPr_2	0.783	98	4	0.2	3460	8.2
21	**45-a**	NMe^nPr_2	--[g]	--	--	--	--	--
22	**46-s**	NMe^nPr_2	0.165	21	14	0.7	718	5.1
23	**44-s**	N^nPr_3	--[g]	--	--	--	--	--
24	**44-a**	N^nPr_3	--[g]	--	--	--	--	--
25	**45-s**	N^nPr_3	0.447	56	6	0.2	1980	3.4
26	**45-a**	N^nPr_3	--[g]	--	--	--	--	--
27	**46-s**	N^nPr_3	0.390	49	6	0.5	1720	7.9

[a]All polymerizations were run for 1 h at 25 °C under 100 psig of ethylene in toluene with 4 μmol of dinickel complex, 4 equivalents of $Ni(COD)_2$ and 500 equivalents of 1-hexene and additive per Ni. Solution volume = 5 mL. [b]Activity, defined in mass of polymer (in g) per mmol Ni per hour. [c]R = [activity with no additive]/[activity with additive]. [d]Mole percent incorporation of 1-hexene as determined from ^1H and ^{13}C NMR spectroscopy. [e]Polymerization run for 0.5 h. For entries 3-7, high viscosity limited mass transfer by that time. [f]Polymerization run for 3 h to get enough polymer for ^1H and ^{13}C NMR spectra. [g]Insufficient product for accurate mass determination (<1 mg).

14–16). **45-s** and **46-s**, which experienced the least inhibition of activity, produced polymers with the lowest levels of 1-hexene incorporation (Table 4.1, e.g., entries 15 and 17). The relative activities can be rationalized by the mechanistic proposal that steric interactions disfavor the binding of amines to both Ni centers in the syn complex.[51] Thus, a shorter Ni–Ni distance should disfavor the binding of a second amine, as observed for 45-s.

Table 4.2. Ethylene/1-hexene copolymerizations run for different lengths of time.[a]

entry	complex	additive	time (minutes)	yield (g)	activity[b]
1	**44-s**	none	30	1.266	317
2	**44-s**	none	30	1.156	289
3	**44-a**	none	30	1.590	397
4	**44-a**	none	30	1.540	385
5	**45-s**	none	30	1.444	361
6	**45-s**	none	30	1.461	366
7	**45-a**	none	30	1.469	367
8	**45-a**	none	30	1.464	366
9	**46-s**	none	30	1.095	274
10	**46-s**	none	30	1.262	315
11	**44-s**	NMe^nPr_2	60	0.094	12
12	**44-s**	NMe^nPr_2	60	0.064	8
13	**44-s**	NMe^nPr_2	30	0.023	6
14	**44-s**	NMe^nPr_2	30	0.044	11
15	**44-s**	NMe^nPr_2	5	0.002	3
16	**44-s**	NMe^nPr_2	5	0.002	3
17	**45-s**	NMe^nPr_2	60	0.783	98
18	**45-s**	NMe^nPr_2	30	0.335	84
19	**44-a**	NEt_3	60	0.011	1
20	**44-a**	NEt_3	30	0.002	1
21	**45-a**	NEt_3	60	0.006	1
22	**45-a**	NEt_3	30	--[c]	--

[a]All polymerizations were run at 25°C under 100 psig of ethylene in toluene with 4 μmol of dinickel complex, 4 equivalents of Ni(COD)2 and 500 equivalents of 1-hexene and additive per nickel. Reaction total volume = 5 mL. [b]Activity, defined in mass of polymer (in g) per mmol Ni per hour. [c]Insufficient product for accurate mass determination (<1 mg).

For **45-s**, where the metal centers are closest, the presence of amines caused the greatest decrease in 1-hexene incorporation (from 1.1 to 0.2–0.3 %; Table 4.1, entries 5,

10, 15, 20, and 25). For **44-s**, the 1-hexene incorporation dropped only from 1.2 to 0.8–1.0 % (Table 1, entries 3, 8, 13, and 18), but there was a greater activity decrease than for **45-s**. The steric considerations for simultaneous binding of two amines also apply to the relative binding of ethylene and 1-hexene when one amine is coordinated. For the closely spaced metal centers in **45-s**, amine coordination more strongly affects binding at the second metal site, resulting in less favorable 1-hexene coordination than for **44-s**. Variation in 1-hexene incorporation is expected to affect the catalyst activity, as previous reports indicated that the overall activity of the catalyst decreased significantly when an α-olefin was copolymerized with ethylene relative to the homopolymerization of ethylene.[50,54,58] Ethylene/1-hexene copolymerizations with **45-s** and **46-s** in the presence of amines resulted in different levels of incorporation of 1-hexene and a divergent trend in the activity (**46-s** produced more polymer in the presence of $N^{n}Pr_3$ than in the presence of $NMe^{n}Pr_2$, opposite to what was seen with **45-s**; Table 4.1, entries 20, 22, 25 and 27). These dissimilarities between the two syn complexes with *m*-terphenyl backbones suggest that subtle differences in the sterics affect the polymerization behavior and that tuning of the ligand framework may allow for optimization of the polymerization.

GPC analysis was performed on several of the ethylene/1-hexene copolymers (Table 4.3). In all cases, the molecular weights of polymers produced with the anti atropisomers were higher than of polymers produced with the syn atropisomers, consistent with what was observed for complexes **25** (Chapter 2). The molecular weights for polymers produced with **44-s** were lower than those calculated for **45-s**. The PDI values were between 1.9 and 3.4 except for the homopolymerization of ethylene

with **44-s** (PDI = 5.9). A significant drop in PDI was observed for **44-s** when amine was added to the polymerization (5.9 to 1.9), but almost no change was seen for **45-s** (2.5 to 2.6). In comparison to the anti analogues, the syn complexes display higher branching consistent with higher β-H elimination rates, which is in agreement with the observed lower molecular weight polymers.

Table 4.3. GPC data for ethylene/1-hexene copolymerizations.[a]

entry	complex	additive	yield (g)	activity[b]	*R*[c]	I[d]	branching[e]	M_w[f]	PDI[f]
1	**44-s**	none[e]	1.266	317		1.2	56	9697	5.9
2	**44-a**	none[e]	1.590	397		1.1	23	68349	3.1
3	**45-s**	none[e]	1.444	361		1.1	47	18676	2.5
4	**45-a**	none[e]	1.469	367		1.0	15	92110	3.4
5	**46-s**	none[e]	1.095	274		0.9	44	17453	2.6
6	**44-s**	NMe^nPr_2	0.094	12	26	0.9		2930	1.9
7	**45-s**	NMe^nPr_2	0.783	98	4	0.2		63578	2.6

[a]All polymerizations were run for 1 h at 25 °C under 100 psig of ethylene in toluene with 4 μmol of dinickel complex, 4 equivalents of $Ni(COD)_2$ and 500 equivalents of 1-hexene and additive per Ni. Solution volume = 5 mL. [b]Activity, defined in mass of polymer (in g) per mmol Ni per hour. [c]R = [activity with no additive]/[activity with additive]. [d]Mole percent incorporation of 1-hexene as determined from ^1H and ^{13}C NMR spectroscopy. [e]Branching was determined from ^1H NMR spectroscopy and is reported as the number of branches per 1000 carbons [f]Calculated from GPC results.

Ethylene/amino olefin copolymerizations

The ability of the reported complexes to incorporate 1-hexene in the presence of amines suggested that these complexes might be effective for the polymerization of amino olefins. Amino olefin substrates were selected to have ethyl or propyl substituents on the basis of the ability of the syn catalysts to perform ethylene/1-hexene copolymerizations in the presence of such tertiary amines (Table 4.1). Indeed, the use of a variety of tertiary amino olefins (500 equivalents) in copolymerizations with ethylene resulted in incorporation levels similar to those for 1-hexene (0.4–0.8 and 0.3–0.4 % with **44-s** and **45-s**, respectively; Table 4.4, entries 3–14). Incorporation of $N(allyl)^nPr_2$ was not successful with **44-s**, but 0.1 % incorporation was achieved using **45-s** (Table

4.4, entries 1 and 2). The proximity of the large N^{n}Pr$_2$ moiety at the allylic position likely hinders binding of olefin to the metal and insertion. All of the longer chain olefins were incorporated by both **44-s** and **45-s**. The number of methylene units between the olefin and amine moieties (beyond allyl amine) did not significantly affect the level of polar monomer incorporation. Copolymerizations of ethylene and N(pentenyl)^{n}Pr$_2$ performed with **44-a**, **45-a**, and **46-s** yielded no polymer, 6 times less polymer than with **45-s** with 0.7 % incorporation, and results similar to those for **45-s**, respectively (Table 4.4, entries 15–17). As with ethylene/1-hexene copolymerizations, ethylene/amino olefin copolymerizations run over different time periods indicated that the catalysts continued to produce polymer over the course of the trial (Table 4.5). The one exception to this behavior was ethylene/amino olefin copolymerizations with **44-s**, for reasons that are unclear at this time.

Diffusion ordered NMR spectroscopy (DOSY) confirmed that the amines were incorporated in the polymers (Figure 4.3). The diffusion constant for the CH_2 resonances of the polymer chain (at 1.4 ppm in $C_2Cl_4D_2$) matched the diffusion constant for the NCH_2 resonances (at 3.0 ppm). As expected, DOSY spectra of the analogously prepared ethylene/1-hexene polymers have no peaks around 3 ppm, indicating that no NCH_2 protons are present (Figure 4.4). Amino olefin incorporation levels were lower and activities higher with **45-s** than **44-s** for all of the polar monomers investigated, mirroring the copolymerizations with 1-hexene in the presence of amines (vide supra). The levels of amino olefin incorporation were in the same range as 1-hexene. The possibility that the incorporation of amines could lead to the formation of chelates that would inhibit polymerization or lead to termination was considered. The amino olefin

Table 4.4. Ethylene/amino olefin copolymerizations.[a]

entry	complex	comonomer	yield (g)	A[b]	I[c]	TON ethylene	TON amino olefin	M_w[d]	PDI[d]	amines /chain[d]
1	**44-s**	N(allyl)^{n}Pr$_2$	0.034	8	0.0	150	0.0			
2	**45-s**	N(allyl)^{n}Pr$_2$	0.083	21	0.1	366	0.3			
3	**44-s**	N(butenyl)^{n}Pr$_2$	0.019	5	0.4	84	0.4			
4	**45-s**	N(butenyl)^{n}Pr$_2$	0.044	11	0.4	192	0.7			
5	**44-s**	N(pentenyl)^{n}Pr$_2$	0.064	16	0.5	273	1.4	2793	2.1	0.8
6	**45-s**	N(pentenyl)^{n}Pr$_2$	0.178	45	0.3	780	2.5	67647	5.4	8.7
7	**44-s**	N(hexenyl)^{n}Pr$_2$	0.063	16	0.7	270	1.8	2552	2.4	0.8
8	**45-s**	N(hexenyl)^{n}Pr$_2$	0.217	54	0.3	945	3.3	95644	6.6	9.8
9	**44-s**	N(heptenyl)^{n}Pr$_2$	0.059	15	0.8	250	2.0	2731	2.4	1.0
10	**45-s**	N(heptenyl)^{n}Pr$_2$	0.310	78	0.3	1360	3.8	103813	5.6	9.3
11	**44-s**	N(octenyl)^{n}Pr$_2$	0.050	13	0.7	213	1.5	3210	3.1	0.8
12	**45-s**	N(octenyl)^{n}Pr$_2$	0.398	100	0.3	1740	4.7	126352	7.1	9.0
13	**44-s**	N(pentenyl)Et$_2$	0.034	8	0.5	146	0.7	2407	1.9	0.8
14	**45-s**	N(pentenyl)Et$_2$	0.151	38	0.3	665	1.7	55276	3.8	18
15	**44-a**	N(pentenyl)^{n}Pr$_2$	--[d]	--	--	--	--			
16	**45-a**	N(pentenyl)^{n}Pr$_2$	0.032	8	0.7	137	0.9	31457	4.7	9.0
17	**46-s**	N(pentenyl)^{n}Pr$_2$	0.176	44	0.3	769	2.5			

[a]All polymerizations were run for 0.5 h at 25 °C under 100 psig of ethylene in toluene with 4 μmol of dinickel complex, 4 equivalents of Ni(COD)$_2$ and 500 equivalents of comonomer per Ni. Solution volume = 5 mL. [b]Activity, defined in mass of polymer (in g) per mmol Ni per hour. [c]Mole percent incorporation of comonomer as determined from ^{1}H NMR spectroscopy. [d]Calculated from GPC results. [e]Insufficient product for accurate mass determination (<1 mg).

Table 4.5. Ethylene/N(pentenyl)^{n}Pr$_2$ copolymerizations run for different lengths of time.[a]

entry	complex	time (minutes)	yield (g)	activity[b]	% incorp[c]	TON ethylene	TON amino olefin
1	**44-s**	240	0.063	2	n.d.	n.d.	n.d.
2	**44-s**	60	0.067	8	0.54	286	1.6
3	**44-s**	30	0.064	16	0.5	273	1.4
4	**44-s**	5	0.054	81	0.82	231	1.9
5	**45-s**	30	0.178	45	0.3	780	2.5
6	**45-s**	30	0.240	60	0.3	1050	2.8
7	**45-s**	5	0.085	128	0.3	370	1.3
8	**45-a**	30	0.032	8	0.7	137	0.9
9	**45-a**	30	0.034	8	0.7	143	1.0
10	**45-a**	5	0.004	7	0.6	17	0.1

[a]All polymerizations were run at 25 °C under 100 psig of ethylene in toluene with 4 μmol of dinickel complex, 4 equivalents of Ni(COD)$_2$ and 500 equivalents of N(pentenyl)^{n}Pr$_2$ per Ni. Solution volume = 5 mL. [b]Activity, defined in mass of polymer (in g) per mmol Ni per hour. [c]Mole percent incorporation of comonomer as determined from ^{1}H NMR spectroscopy. [d]Insufficient product for accurate mass determination (<1 mg).

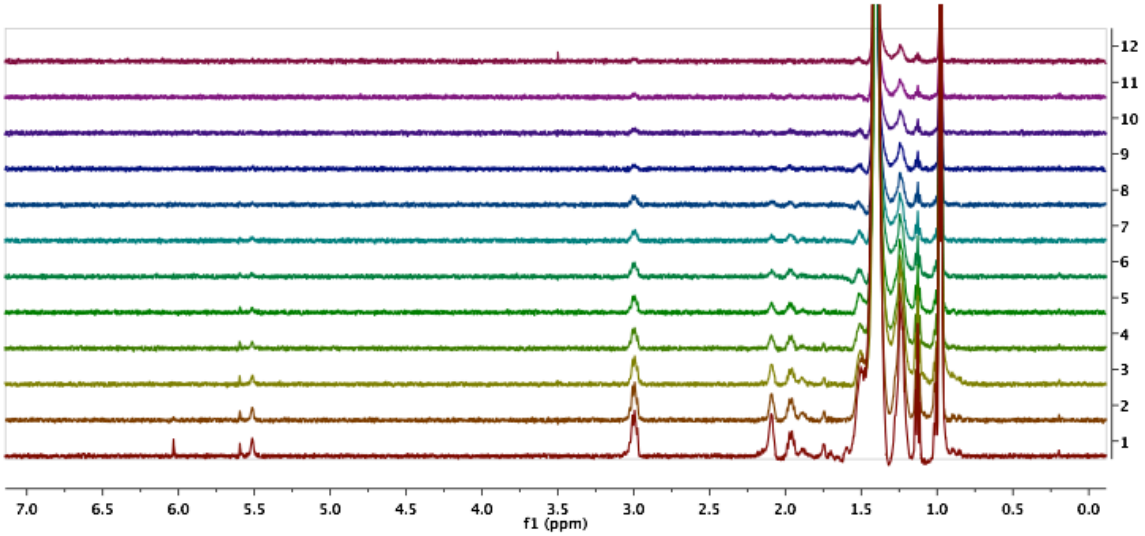

Figure 4.3. DOSY spectra in tetrachloroethane-D_2 at 130 °C of the ethylene/N(pentenyl)(^{n}Pr)$_2$ copolymer made with **44-s**. The peaks at 3 ppm are attenuated at the same rate at the other polymer peaks indicating that the NCH_2 peaks are part of the polymer.

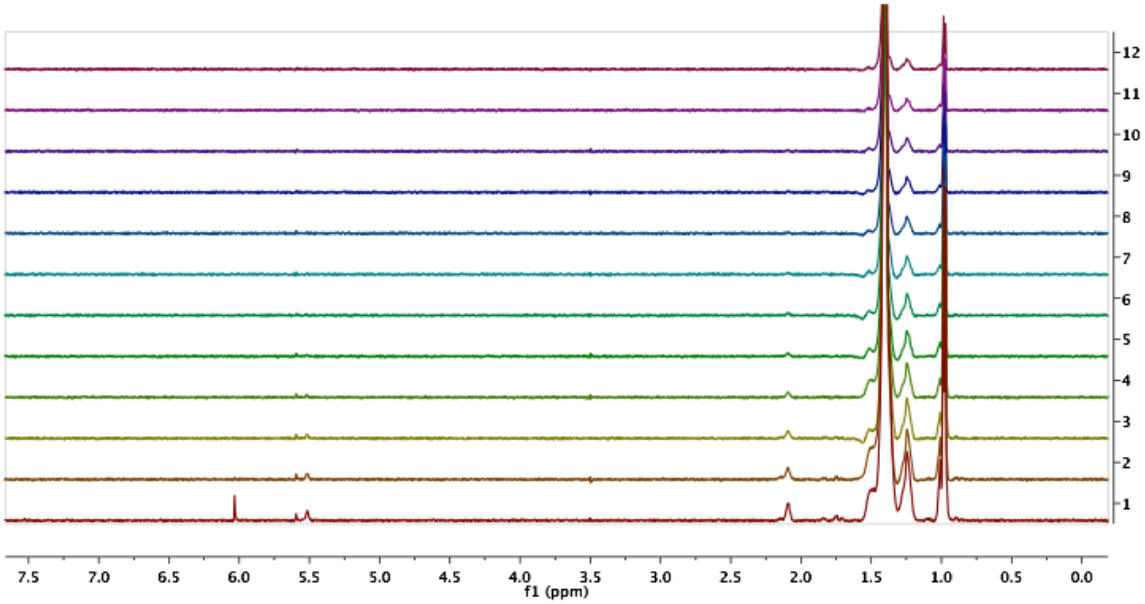

Figure 4.4. DOSY spectra in tetrachloroethane-D_2 at 130 °C of the ethylene/1-hexene copolymer made with **44-s**. There are no peaks around 3 ppm indicating that no NCH_2 protons are present.

monomers were examined by 1D total correlation NMR spectroscopy (TOCSY) and compared with the polymers (Figure 4.5). The TOCSY of the amino olefin precursors showed correlations between the NCH_2 peak and the olefinic peaks that was not observed for the polymer samples, indicating that the polymers were not terminated by the amine monomers.

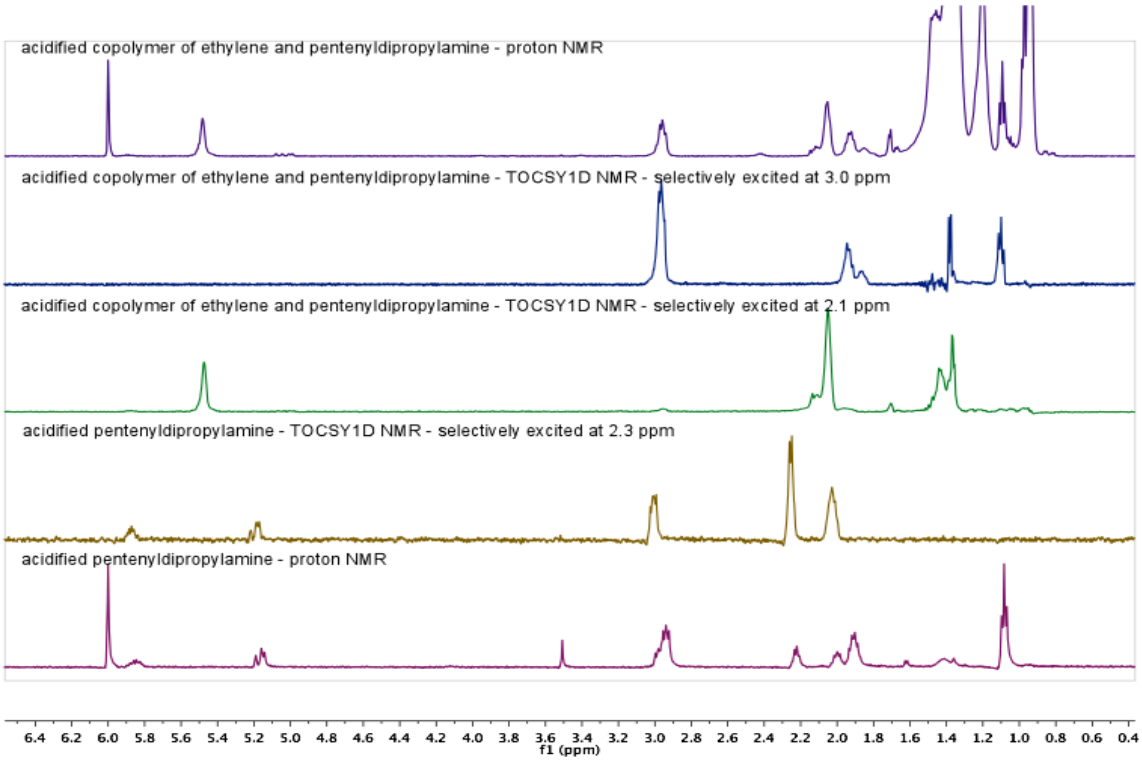

Figure 4.5. TOCSY and ^{1}H NMR spectra in tetrachloroethane-D_2 at 130 °C of the ethylene/N(pentenyl)(^{n}Pr)$_2$ copolymer made with **44-s** and acidified N(pentenyl)(^{n}Pr)$_2$.

Again, GPC analysis was performed on several of the ethylene/amino olefin copolymers (Table 4.3). The molecular weights of polymers produced with **45-s** were an order of magnitude higher than of polymers produced with **44-s**, a greater difference than was observed for the ethylene/1-hexene copolymer. The PDI values were between 1.9 and 3.1 for the polymerizations with **44-s**, while the PDI values were much higher for the polymerizations with **45-s**, between 3.8 and 7.1. From the mole percent

incorporation of the amines and the M_w of the resultant polymers, the average number of amines per chain could be calculated. For **44-s**, less than one amine per chain was incorporated, while the polymers synthesized with **45-s** were calculated to include between 8.7 and 18 amines per chain on average. These results indicate that, at least for **45-s**, the incorporation of an amine monomer did not automatically lead to chain termination, consistent with the TOCSY data. If monomer insertion leads to a change in the rate of the subsequent insertions, perhaps due to chelation, the PDI may increase with increasing disparity of the number of amines in a single chain, consistent with the higher PDIs seen for polymers produced by **45-s**.

Terpolymerizations of ethylene, 1-hexene, and N(pentenyl)Et_2 were performed to examine competition of the comonomers for insertion (Table 4.6). The observed incorporation levels of both 1-hexene and N(pentenyl)Et_2 are very similar to those without the other comonomer present (Table 4.1, entries 18 and 20; Table 4.4, entries 13 and 14). The activities and the GPC data match the results for the ethylene/N(pentenyl)Et_2 copolymerization without 1-hexene (Table 4.4, entries 13 and 14). Lower incorporation of N(pentenyl)Et_2 relative to 1-hexene can be explained by the larger monomer having a higher barrier for coordination, despite the distal nature of the steric bulk, though this effect is small. Overall the terpolymerizations are comparable to the copolymerization of ethylene and 1-hexene in the presence of amines and to the copolymerization of ethylene and N(pentenyl)Et_2, suggesting that there is not a substantial preference for one monomer over the other.

The similar levels of incorporation of amino olefin and 1-hexene (in the presence of tertiary amines), and the activity profiles in copolymerizations with various catalysts, support a related mechanism of polymerization for the two cases (Scheme

4.3). Coordination of the amine moiety to nickel sterically hinders binding of an amine to the second nickel center for the syn complexes. Ethylene or the olefin moiety of the polar monomer have a lower steric profile than the amine and hence can coordinate to the second nickel and afford chain growth.

Table 4.6. Ethylene/1-hexene/amino olefin terpolymerizations.[a]

entry	complex	amino olefin	yield (g)	A[b]	I[c] 1-hexene	I[c] amino olefin	M_w[d]	PDI[d]	amines /chain[d]
1	**44-s**	N(pentenyl)Et_2	0.035	9	1.0	0.5	3332	2.6	0.7
2	**45-s**	N(pentenyl)Et_2	0.131	33	0.5	0.2	50998	4.6	10.3

[a]All polymerizations were run for 0.5 h at 25 °C under 100 psig of ethylene in toluene with 4 μmol of dinickel complex, 4 equivalents of $Ni(COD)_2$, 500 equivalents of 1-hexene and 500 equivalents of amino olefin per Ni. Solution volume = 5 mL. [b]Activity, defined in mass of polymer (in g) per mmol Ni per hour. [c]Mole percent incorporation of comonomer as determined from ^1H NMR spectroscopy. [d]Calculated from GPC results.

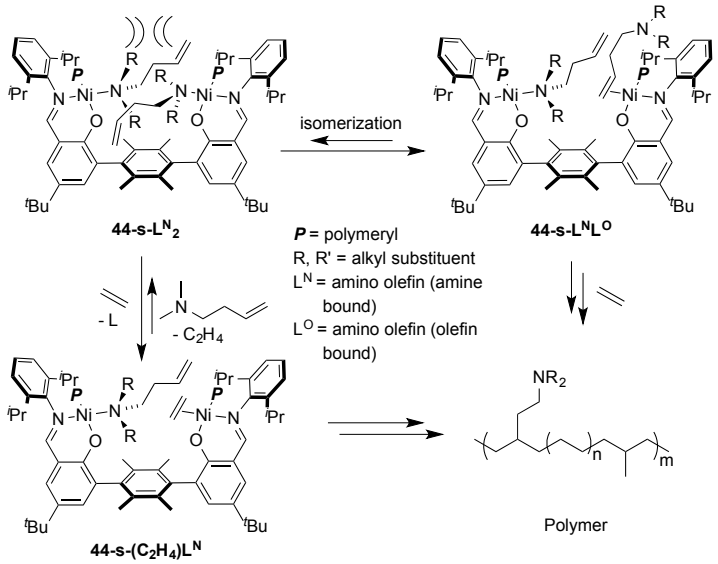

Scheme 4.3. Proposed mechanism for ethylene/amino olefin copolymerization.

The incorporation of amino olefins with the present catalysts is notable for several reasons. Monometallic neutral nickel catalysts are greatly inhibited by amines, as previously reported[43] and also observed for **25-a** (Chapter 3),[51] **44-a**, and **45-a** relative to the syn analogues. The proposed mechanism for polymerization and polar olefin incorporation relies on two metal centers, but is distinct from previous proposals.[45]

Greater incorporation of various monomers was explained by concomitant coordination of a CH bond or polar group to one nickel center and of an olefin to the other, thus favoring comonomer coordination and insertion.[44,49] The mechanism at work with the present catalysts is not consistent with those proposals because the metal centers are likely too distant for a single monomer to coordinate to both. Moreover, varying the number of methylene groups between the amine and olefin functionality would be expected to significantly affect the degree of polar monomer incorporation, which was not observed (Table 4.4). The ability of **45-a** to copolymerize ethylene and N(pentenyl)^{n}Pr$_2$, albeit at a reduced rate relative to the syn analogue, implies that a proximal metal center is not required for the copolymerization to take place. This provides further evidence that the copolymerization does not rely on the concurrent interaction of the monomer or polymer chain with both nickel centers.

The proposed mechanism (Scheme 4.3) is expected to extend to other classes of polar monomers. Binding of polar olefins through the heteroatom instead of the olefin typically leads to different steric profiles around the metal center. In the present design, binding of the olefin orients the substituents in the plane perpendicular to the metal–olefin interaction, and away from the second metal center. Conversely, coordination of the amine (or other polar) moiety would be expected to direct the steric bulk toward the second metal center. Hence, judicious design of metal−metal distance and ligand steric properties could be employed for the copolymerization of other polar olefins.

Attempted copolymerizations with other polar olefins

A number of polar olefins were targeted to test the range of functionality that could be tolerated and incorporated by the dinickel systems. Amino acid based

monomers were targeted using methods analogous to the synthesis of the tertiary amines, but the desired compounds could not be isolated cleanly (Chart 4.1). Successful synthesis of monomers with bipyridine, diamine, aminediol, and secondary amine moieties was accomplished via literature procedures for 4-(3-butenyl)-4'-methyl-2,2'-bipyridine[59] and via methods analogous to the synthesis of the tertiary amines for the other monomers (Chart 4.2). Copolymerizations with ethylene and 500 equivalents of these monomers resulted in no polymer. To investigate the conditions further, 4 equivalents of each comonomer were added to $Ni(COD)_2$ and to **44-s** (separately) and the ensuing reactions were monitored by ^1H NMR spectroscopy. The bipyridine containing monomer reacted immediately with $Ni(COD)_2$, precluding the necessary phosphine scavenging by the $Ni(COD)_2$ in polymerizations. The remaining comonomers did not appear to react with $Ni(COD)_2$ or with **44-s**. The chelation of the bulky diamine or aminediol moieties may have led to stronger binding of the polar moiety that would disfavor the isomerization and decoordination pathways that would allow for polymerization. Similarly, the secondary amine would be expected to bind much more strongly to the nickel. In the cases of these latter three comonomers, polymerization activity may be recovered by the use of fewer equivalents of the comonomer, just as bulky secondary and even primary amines were tolerated by **25-s** as long as only 20 equivalents were added.

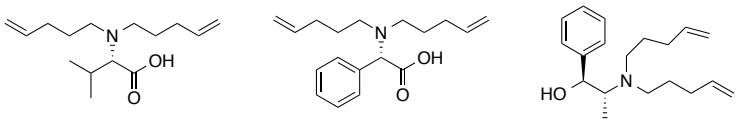

Chart 4.1. Target amino acid based monomers.

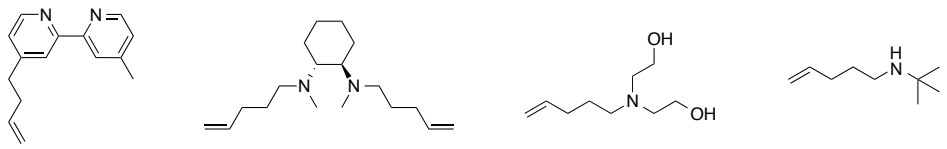

Chart 4.2. Monomers with bipyridine, diamine, aminediol, and secondary amine moieties.

Recent interest in aliphatic polymers incorporating ammonium and phosphonium moieties for fuel cell applications,[60-63] inspired us to target olefins functionalized with ammonium and phosphonium groups for copolymerization with ethylene (Chart 4.3). Pentenyl-di-*n*-propyl-methylammonium iodide was synthesized from N(pentenyl)^{n}Pr$_2$ and methyl iodide. Ni(COD)$_2$ was not stable in the presence of the ammonium monomer and thus the copolymerization with ethylene would not be successful, as was the case with 4-(3-butenyl)-4'-methyl-2,2'-bipyridine. Tetrakis[cyclohexyl(methyl)amino]phosphonium tetrafluoroborate was synthesized via literature conditions[64] and showed no appreciable reaction with Ni(COD)$_2$. Ethylene and ethylene/1-hexene polymerizations with the phosphonium additive will be performed to determine if the dinickel systems can tolerate the presence of the phosphonium. If successful, copolymerizations with a phosphonium monomer and ethylene will be attempted.

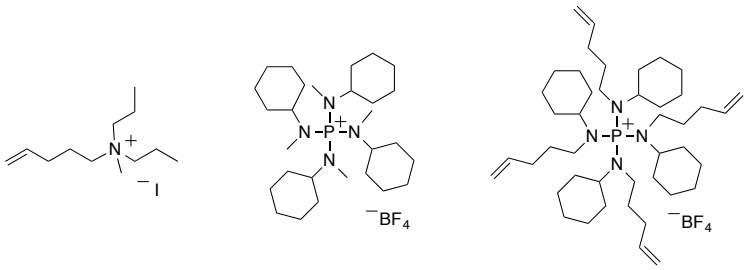

Chart 4.3. Ammonium monomer, phosphonium additive and proposed phosphonium monomer.

CONCLUSIONS

In summary, we have synthesized a series of rigid terphenyl dinickel bisphenoxyiminato complexes with phosphine auxiliary ligands that exhibit activity for copolymerization of ethylene and amino olefins. The syn complexes are more active than the anti analogues because of a bimetallic effect arising from the proximity of the nickel centers. The polar monomers and 1-hexene are incorporated at similar levels. Comparisons between the *m*- and *p*-terphenyl catalyst systems support a mechanism in which inhibitory coordination of amines at both nickel centers is disfavored because of steric repulsion. Thus, coordination of olefin moieties with smaller steric profiles is favored, allowing for polymer formation and polar monomer incorporation. Future efforts will focus on extending the present concept for polar olefin polymerization to other monomers and catalyst types, toward increasing the level of functional group incorporation, catalyst activity, and tolerance of other polar groups.

EXPERIMENTAL SECTION

General considerations and instrumentation

All air- and/or water-sensitive compounds were manipulated using standard vacuum or Schlenk line techniques or in an inert atmosphere glovebox. The solvents for air- and moisture-sensitive reactions were dried over sodium/benzophenone ketyl, calcium hydride, or by the method of Grubbs.[65] All NMR solvents were purchased from Cambridge Isotopes Laboratories, Inc. C_6D_6 was dried over sodium/benzophenone ketyl and vacuum transferred prior to use. Pyridine and all monomers and amines were dried over calcium hydride and vacuum transferred prior to use. Trimethylphosphine was dried over 4 Å molecular sieves prior to use. Ethylene was purchased from Matheson and equipped with a PUR-Gas in-line trap to remove oxygen and moisture before use. All ^{1}H, ^{13}C, ^{31}P, and 2D NMR spectra of small organic and organometallic compounds were recorded on Varian Mercury 300 MHz, Varian 400 MHz, or Varian INOVA-500 or 600 MHz spectrometers at room temperature. All ^{1}H and ^{13}C NMR spectra of polymers were recorded on the Varian INOVA-500 MHz spectrometer at 130 °C in tetrachloroethane-D_2. For ^{1}H and ^{13}C NMR spectra, chemical shifts are reported with respect to residual internal deuterated solvent: 7.16 and 128.06 (t) ppm (C_6D_6); 7.26 and 77.16 (t) ppm ($CDCl_3$); 5.32 and 53.84 (q) ppm (CD_2Cl_2); for ^{1}H and ^{13}C data. All ^{31}P NMR spectra were externally referenced to H_3PO_4 (0 ppm). J coupling are reported in Hz. Combustion analyses (C, H, and N) were performed by Complete Analysis Laboratories, Inc., Parsippany, NJ.

2-bromo-4-tert-butylphenol,[66] 2-bromo-4-tert-butylmethoxymethylphenol (**14**),[50] 1,4-dibromo-2,3,5,6-tetramethylbenzene (**2**)[67] 1,3-dibromomesitylene (**34**),[68] $Ni(PMe_3)_2MeCl$,[69,70] **25-s**,[50] 4-(3-butenyl)-4'-methyl-2,2'-bipyridine,[59] (*R*,*R*)-*N*,*N*'-

dimethylcyclohexane-1,2-diamine[71] and tetrakis[cyclohexyl(methyl)amino]phosphonium tetrafluoroborate[64] were synthesized according to literature procedures.

Initial synthesis and metallation of the meta analogues **44-a** and **44-s** were completed by undergraduate researcher Aya Buckley.

Preparation of ligands

Compounds 32. Synthesis of the terphenyl compounds **32** was accomplished via the Negishi coupling of **2** with two equivalents of **14** using literature conditions.[72] In the glovebox, **14** (10.46 g, 38.3 mmol) and 150 mL of THF were combined in a large Schlenk tube and frozen in the cold well. ^{t}BuLi (47.32 mL, 80.44 mmol, 2.1 equiv) was added to the thawing solution and stirred for 1 h while warming to room temperature. The resultant yellow orange solution was refrozen in the cold well. Concurrently, a suspension of $ZnCl_2$ (3.66 g, 26.8 mmol, 0.7 equiv) in THF (40 mL) was frozen in the cold well. The thawing $ZnCl_2$ suspension was added to the thawing reaction mixture and stirred for 1 h resulting in a colorless cloudy solution. **2** (5.03 g, 17.24 mmol, 0.45 equiv), $Pd(PPh_3)_4$ (0.44 g, 0.38 mmol, 0.01 equiv) and THF (40 mL) were added to the reaction mixture at room temperature. The sealed Schlenk tube was brought out of the glovebox and heated to 70 °C for 4 days. Water was added to quench the reaction. The solution was filtered over silica gel and the silica gel was washed with dichloromethane. The filtrate was extracted between DCM and water. The organics were dried with $MgSO_4$, filtered, and volatiles were removed under vacuum. The dicoupled products were coprecipitated from MeOH in a ratio of 1:0.73 anti/syn (4.75 g of white powder, 53 % yield) and used without further purification. ^{1}H NMR (300 MHz, $CDCl_3$) δ = 7.33-7.29 (2dd, *J*=8.6 Hz, 2.5, 2H per atropisomer, Ar*H*), 7.17-7.10 (4d, *J*=8.6 Hz, 2.5,

4H per atropisomer, Ar*H*), 5.07 (s, 4H, OCH_2OCH$_3$, anti), 4.97 (s, 4H, OCH_2OCH$_3$, syn), 3.37 (s, 6H, OCH$_2$OCH_3, anti), 3.24 (s, 6H, OCH$_2$OCH_3, syn), 1.97 (s, 12H, Ar-CH_3, syn), 1.95 (s, 12H, Ar-CH_3, anti), 1.32 (s, 18H per atropisomer, ArC(CH_3)$_3$) ppm.

Compounds 33. **32** (4.75 g, 9.16 mmol, 1 equiv), *N*,*N*,*N'*,*N'*-tetramethylethylenediamine (19.1 mL, 128.2 mmol, 14 equiv) and THF (80 mL) were added to a Schlenk tube in the glovebox and frozen in the cold well. ″BuLi (9.6 mL, 24.0 mmol, 2.6 equiv) was added to the thawing solution and stirred for 4 h. The resultant orange red solution was refrozen in the cold well. A solution of DMF (4.3 mL, 54.9 mmol, 6 equiv) in THF (30 mL) was also frozen in the cold well. The thawing DMF solution was added to the thawing reaction mixture resulting in a pale amber solution, which was stirred for 10 h before the Schlenk tube was brought out of the box and about 5 mL of water were added to quench the reaction. The desired product was extracted into DCM and the organic fraction was washed with water, dried with $MgSO_4$, filtered, and the volatiles were removed under vacuum to yield the doubly orthoformylated products, **33**, with greater than 90% purity. These compounds were carried forward without further purification and 100% conversion was assumed for stoichiometry. ^{1}H NMR (300 MHz, $CDCl_3$) δ = 10.49 (2s, 2H per atropisomer, OC*H*), 7.90 (2d, J=2.7 Hz, 2H per atropisomer, Ar*H*), 7.43 (d, J=2.7 Hz, 2H, Ar*H*, syn), 7.31 (d, J=2.6 Hz, 2H, Ar*H*, anti), 4.67 (s, 4H, OCH_2OCH$_3$, anti), 4.61 (s, 4H, OCH_2OCH$_3$, syn), 3.29 (s, 6H, OCH$_2$OCH_3, syn), 3.24 (s, 6H, OCH$_2$OCH_3, anti), 2.03 (s, 12H, Ar-CH_3, syn), 2.00 (s, 12H, Ar-CH_3, anti), 1.35 (2s, 18H per atropisomer, ArC(CH_3)$_3$) ppm.

Compounds 6. **33** (5.26 g, 9.2 mmol, 1 equiv), 2N HCl (69 mL, 137.4 mmol, 15 equiv), and methanol (275 mL) were added to a round bottom flask equipped with a

reflux condenser and the reaction was refluxed for 2 h. Then the reaction was cooled to room temperature and filtered to collect precipitate. The precipitate was dissolved in DCM and washed with water. Additional product was collected from the filtrate by extraction into DCM. The organic fractions were dried with $MgSO_4$, filtered, and the volatiles were removed under vacuum to yield the deprotected products, **6**. The atropisomers were separated via column chromatography (3/1 DCM/hexanes). 1.3 g of **6-a** and 0.7 g of **6-s** were isolated as white solids in 95 % purity (45 % overall yield). The ^1H and ^{13}C NMR spectra matched literature assignments.[50]

Compounds 7. The bisphenoxyimines were synthesized as we described previously from the bisaldehydes from **6-a** and **6-s** (Chapter 2).[50]

3,5-dibromomesitol was synthesized by the dropwise addition of a solution of Br_2 (1.48 mL, 28.76 mmol, 2.61 equiv) in DCM (6 mL) through an addition funnel to a solution of mesitol (1.5 g, 11.01 mmol, 1 equiv) and iron powder (0.04 g, 0.71 mmol, 0.06 equiv) in DCM (11 ml) in a covered round bottom flask with a stirbar over 30 minutes. The resulting red solution was stirred an additional 2.5 h before the reaction was quenched with aqueous sodium hydrosulfite ($Na_2S_2O_4$). The mixture was extracted between DCM and water. The organics were dried with $MgSO_4$, filtered, and volatiles were removed under vacuum. The desired product was obtained as a pale yellow solid in quantitative yield. The ^1H NMR spectrum matched literature assignments.[73]

3,5-dibromo-2,4,6-trimethyl-methoxybenzene (**35**) was synthesized from 3,5-dibromomesitol according to an analogous synthesis.[74] ^1H NMR (500 MHz, $CDCl_3$) δ = 3.67 (s, 3H, OCH_3), 2.61 (s, 3H, $ArCH_3$), 2.36 (s, 6H $ArCH_3$) ppm. ^{13}C NMR (126 MHz, $CDCl_3$) δ = 155.28 (Ar), 133.59 (Ar), 130.98 (Ar), 125.56 (Ar), 60.68 ($ArOCH_3$), 25.29

(Ar*C*H$_3$), 17.61 (Ar*C*H$_3$) ppm. HRMS (EI+) Calcd. for $C_{10}H_{12}OBr^{81}Br$: 307.9234. Found: 307.9246.

Compounds 36. Synthesis of the terphenyl compounds **36** was accomplished via the Negishi coupling of **34** with two equivalents of **14** using conditions analogous to the synthesis of compounds **32**. Precipitation from methanol yielded **36-a** as a white solid (2.5 g). **36-s** was collected in greater than 80 % purity via column chromatography (30/1 hexanes/ethyl acetate). **36-s** was then isolated as a colorless oil (2.3 g) via column chromatography of the 3/2 hexanes/ethyl acetate flush of the previous column (6.25/1 hexanes/ethyl acetate) (58 % total yield of both atropisomers). Data for **36-a** are as follows. ^{1}H NMR (500 MHz, $CDCl_3$) δ = 7.31 (dd, *J*=8.6, 2.6 Hz, 2H, Ar*H*), 7.16 (d, *J*=8.6 Hz, 2H, Ar*H*), 7.11 (d, *J*=2.5 Hz, 2H, Ar*H*), 7.09 (s, 1H, Ar*H*), 5.13 (d, *J*=6.8 Hz, 2H, OC*H*$_2$OCH$_3$), 5.08 (d, *J*=6.8 Hz, 2H, OC*H*$_2$OCH$_3$), 3.36 (s, 6H, OCH$_2$OC*H*$_3$), 2.08 (s, 6H, ArC*H*$_3$), 1.72 (s, 3H, ArC*H*$_3$), 1.30 (s, 18H, ArC(C*H*$_3$)$_3$) ppm. ^{13}C NMR (126 MHz, $CDCl_3$) δ = 152.29 (Ar), 144.76 (Ar), 136.50 (Ar), 135.51 (Ar), 135.50 (Ar), 130.41 (Ar), 128.67 (Ar), 128.42 (Ar), 124.77 (Ar), 114.31 (Ar), 94.63 (O*C*H$_2$OCH$_3$), 55.90 (OCH$_2$O*C*H$_3$), 34.34 (Ar*C*(CH$_3$)$_3$), 31.66 (ArC(*C*H$_3$)$_3$), 20.82 (Ar*C*H$_3$), 18.49 (Ar*C*H$_3$) ppm. HRMS (EI+) Calcd. for $C_{33}H_{44}O_4$: 504.3240. Found: 504.3251. Data for **36-s** are as follows. ^{1}H NMR (500 MHz, $CDCl_3$) δ = 7.32 (dd, *J*=8.6, 2.6 Hz, 2H, Ar*H*), 7.19 (d, *J*=2.6 Hz, 2H, Ar*H*), 7.15 (d, *J*=8.6 Hz, 2H, Ar*H*), 7.11 (s, 1H, Ar*H*), 5.05 (d, *J*=6.6 Hz, 2H, OC*H*$_2$OCH$_3$), 5.01 (d, *J*=6.6 Hz, 2H, OC*H*$_2$OCH$_3$), 3.32 (s, 6H, OCH$_2$OC*H*$_3$), 2.09 (s, 6H, ArC*H*$_3$), 1.75 (s, 3H, ArC*H*$_3$), 1.33 (s, 18H, ArC(C*H*$_3$)$_3$) ppm. ^{13}C NMR (126 MHz, $CDCl_3$) δ = 152.12 (Ar), 145.09 (Ar), 136.51 (Ar), 135.62 (Ar), 135.56 (Ar), 130.74 (Ar), 128.60 (Ar), 128.46 (Ar), 124.81 (Ar), 115.03 (Ar), 94.92 (O*C*H$_2$OCH$_3$), 55.82

(OCH_2OCH_3), 34.40 (Ar*C*(CH_3)$_3$), 31.68 (ArC(*C*H_3)$_3$), 20.83 (Ar*C*H_3), 18.52 (Ar*C*H_3) ppm. HRMS (EI+) Calcd. for $C_{33}H_{44}O_4$: 504.3240. Found: 504.3228.

Compound 37-s. Synthesis of the terphenyl compound **37-s** was accomplished via the Negishi coupling of **35** with two equivalents of **14** using conditions analogous to the synthesis of compounds **32**. **37-s** was collected in greater than 90 % purity via column chromatography (5/1/0.5 hexanes/ethyl acetate/DCM). **37-s** was then isolated as a colorless solid via precipitation from MeOH (4.0 g, 16 % yield). ^{1}H NMR (300 MHz, $CDCl_3$) δ = 7.31 (dd, *J*=8.6, 2.5 Hz, 2H, Ar*H*), 7.17 (d, *J*=2.5 Hz, 2H, Ar*H*), 7.11 (d, *J*=8.6 Hz, 2H, Ar*H*), 5.00 (d, *J*=6.5 Hz, 2H, OC*H*$_2$OCH$_3$), 4.97 (d, *J*=6.5 Hz, 2H, OC*H*$_2$OCH$_3$), 3.78 (s, 3H, ArOC*H*$_3$), 3.28 (s, 6H, OCH$_2$OC*H*$_3$), 2.04 (s, 6H, ArC*H*$_3$), 1.68 (s, 3H, ArC*H*$_3$), 1.31 (s, 18H, ArC(C*H*$_3$)$_3$) ppm. ^{13}C NMR (75 MHz, C_6D_6) δ = 155.53 (Ar), 152.84 (Ar), 145.11 (Ar), 138.51 (Ar), 131.65 (Ar), 131.07 (Ar), 128.84 (Ar), 128.56 (Ar), 125.33 (Ar), 115.84 (Ar), 95.02 (O*C*H$_2$OCH$_3$), 59.60 (O*C*H$_3$), 55.55 (O*C*H$_3$), 34.27 (Ar*C*(CH_3)$_3$), 31.66 (ArC(*C*H$_3$)$_3$), 18.94 (Ar*C*H$_3$), 14.47 (Ar*C*H$_3$) ppm. HRMS (EI+) Calcd. for $C_{34}H_{46}O_5$: 534.3345. Found: 534.3346.

Compound 38-a. Formylation of **36-a** was accomplished via the same procedure as for **33**. 0.53 g of doubly orthoformylated compound was collected as a pale yellow solid after extraction and moved forward without further purification (53 % yield). ^{1}H NMR (500 MHz, $CDCl_3$) δ = 10.44 (s, 2H, C*H*O), 7.88 (d, *J*=2.6 Hz, 2H, Ar*H*), 7.33 (d, *J*=2.6 Hz, 2H, Ar*H*), 7.09 (s, 1H, Ar*H*), 4.73 (d, *J*=6.0 Hz, 2H, OC*H*$_2$OCH$_3$), 4.70 (d, *J*=6.0 Hz, 2H, OC*H*$_2$OCH$_3$), 3.21 (s, 6H, OCH$_2$OC*H*$_3$), 2.09 (s, 6H, ArC*H*$_3$), 1.81 (s, 3H, ArC*H*$_3$), 1.34 (s, 18H, ArC(C*H*$_3$)$_3$) ppm. ^{13}C NMR (126 MHz, $CDCl_3$) δ = 191.05 (*C*HO), 155.38 (Ar), 147.78 (Ar), 136.22 (Ar), 135.45 (Ar), 135.41

(Ar), 135.39 (Ar), 134.89 (Ar), 129.47 (Ar), 129.30 (Ar), 124.62 (Ar), 99.84 (OCH_2OCH_3), 57.30 (OCH_2OCH_3), 34.71 ($ArC(CH_3)_3$), 31.38 ($ArC(CH_3)_3$), 20.91 ($ArCH_3$), 18.85 ($ArCH_3$) ppm. HRMS (EI+) Calcd. for $C_{35}H_{44}O_6$: 560.3138. Found: 560.3150.

Compound 38-s. Formylation of **36-s** was accomplished via the same procedure as for the anti, but a mixture of species resulted. Column chromatography was used to isolate the desired product as a pale yellow solid (0.30 g, 51 % yield). ^{1}H NMR (500 MHz, $CDCl_3$) δ = 10.49 (s, 2H, C*H*O), 7.89 (d, *J*=2.6 Hz, 2H, Ar*H*), 7.45 (d, *J*=2.6 Hz, 2H, Ar*H*), 7.15 (s, 1H, Ar*H*), 4.65 (s, 4H, OCH_2OCH_3), 3.36 (s, 6H, OCH2OCH_3), 2.12 (s, 6H, $ArCH_3$), 1.80 (s, 3H, $ArCH_3$), 1.34 (s, 18H, $ArC(CH_3)_3$) ppm. ^{13}C NMR (126 MHz, $CDCl_3$) δ = 191.19 (*C*HO), 155.40 (Ar), 147.87 (Ar), 136.50 (Ar), 135.63 (Ar), 135.58 (Ar), 134.32 (Ar), 129.61 (Ar), 129.58 (Ar), 124.21 (Ar), 99.34 (OCH_2OCH_3), 57.76 (OCH_2OCH_3), 34.81 ($ArC(CH_3)_3$), 31.40 ($ArC(CH_3)_3$), 20.93 ($ArCH_3$), 18.72 ($ArCH_3$) ppm. HRMS (EI+) Calcd. for $C_{35}H_{44}O_6$: 560.3138. Found: 560.3151.

Compound 39-s. Formylation of **37-s** was accomplished using a procedure analogous to the synthesis of **33**. 4.48 g of about 80% pure doubly orthoformylated compound was collected as a pale yellow solid after extraction and running through a silica plug to remove brown color with 3/1 hexanes/ethyl acetate. This material was moved forward without further purification. ^{1}H NMR (300 MHz, $CDCl_3$) δ = 10.48 (s, 2H, C*H*O), 7.90 (d, *J*=2.6 Hz, 2H, Ar*H*), 7.44 (d, *J*=2.6 Hz, 2H, Ar*H*), 4.64 (s, 2H, OCH_2OCH_3), 3.78 (s, 3H, $ArOCH_3$), 3.35 (s, 3H, OCH_2OCH_3), 2.09 (s, 6H, $ArCH_3$), 1.75 (s, 3H, $ArCH_3$), 1.34 (s, 18H, $ArC(CH_3)_3$) ppm.

Compound 40-a. Deprotection of **38-a** was accomplished using a procedure analogous to the synthesis of **6**. The desired product was isolated as an olive green solid in 95 % yield (0.86 g) after extraction. ^{1}H NMR (500 MHz, $CDCl_3$) δ = 11.06 (d, *J*=0.5 Hz, 2H, ArO*H*), 9.96 (s, 2H, C*H*O), 7.54 (d, *J*=2.5 Hz, 2H, Ar*H*), 7.52 (dd, *J*=2.5, 0.5 Hz, 2H, Ar*H*), 7.14 (s, 1H, Ar*H*), 2.07 (s, 6H, ArCH_3), 1.75 (s, 3H, ArCH_3), 1.34 (s, 18H, ArC(CH_3)$_3$) ppm. ^{13}C NMR (126 MHz, $CDCl_3$) δ = 197.12 (*C*HO), 156.79 (Ar), 143.01 (Ar), 137.00 (Ar), 136.46 (Ar), 135.52 (Ar), 134.02 (Ar), 129.69 (Ar), 129.22 (Ar), 128.99 (Ar), 120.17 (Ar), 34.40 (Ar*C*(CH$_3$)$_3$), 31.42 (ArC(*C*H$_3$)$_3$), 20.69 (Ar*C*H$_3$), 18.28 (Ar*C*H$_3$) ppm. HRMS (EI+) Calcd. for $C_{31}H_{36}O_4$: 472.2614. Found: 472.2593.

Compound 40-s. Deprotection of **38-s** was accomplished via the same procedure as for the anti. The desired product was isolated as a brown solid in quantitative yield (0.69 g) after extraction. ^{1}H NMR (500 MHz, $CDCl_3$) δ = 10.94 (s, 2H, ArO*H*), 9.96 (s, 2H, C*H*O), 7.54 (d, *J*=2.5 Hz, 2H, Ar*H*), 7.48 (d, *J*=2.5 Hz, 2H, Ar*H*), 7.15 (s, 1H, Ar*H*), 2.08 (s, 6H, ArCH_3), 1.75 (s, 3H, ArCH_3), 1.35 (s, 18H, ArC(CH_3)$_3$) ppm. ^{13}C NMR (126 MHz, $CDCl_3$) δ = 196.89 (*C*HO), 156.96 (Ar), 142.71 (Ar), 136.50 (Ar), 136.47 (Ar), 135.92 (Ar), 134.26 (Ar), 129.64 (Ar), 129.13 (Ar), 128.97 (Ar), 120.27 (Ar), 34.37 (Ar*C*(CH$_3$)$_3$), 31.44 (ArC(*C*H$_3$)$_3$), 20.74 (Ar*C*H$_3$), 18.21 (Ar*C*H$_3$) ppm. HRMS (FAB+) Calcd. for $C_{31}H_{37}O_4$: 473.2692. Found: 473.2675.

Compound 41-s. Deprotection of **39-s** was accomplished using a procedure analogous to the synthesis of **6**. The desired product was isolated as beige solid in 70 % yield (2.66 g) after extraction and column chromatography (10/1 hexanes/ethyl acetate). ^{1}H NMR (500 MHz, $CDCl_3$) δ = 10.96 (s, 2H, ArO*H*), 9.96 (s, 2H, C*H*O), 7.55 (d, *J*=2.5 Hz, 2H, Ar*H*), 7.47 (d, *J*=2.5 Hz, 2H, Ar*H*), 3.79 (s, 3H, ArOCH_3), 2.05 (s, 6H,

ArCH_3), 1.70 (s, 3H, ArCH_3), 1.36 (s, 18H, ArC(CH_3)$_3$) ppm. ^{13}C NMR (126 MHz, $CDCl_3$) δ = 196.89 (*C*HO), 156.93 (Ar), 154.92 (Ar), 142.72 (Ar), 136.51 (Ar), 135.59 (Ar), 131.42 (Ar), 129.70 (Ar), 129.62 (Ar), 129.03 (Ar), 120.28 (Ar), 60.17 (ArO*C*H$_3$) 34.37 (Ar*C*(CH$_3$)$_3$), 31.44 (ArC(*C*H$_3$)$_3$), 18.13 (Ar*C*H$_3$), 14.08 (Ar*C*H$_3$) ppm. HRMS (EI+) Calcd. for $C_{32}H_{38}O_5$: 502.2719. Found: 502.2718.

Compound 42-a. The imine condensation with 2,6-diisopropylaniline and **40-a** was accomplished using a procedure analogous to the synthesis of **7**. The desired product was isolated as a pale yellow solid in 66 % yield (0.26 g). ^{1}H NMR (500 MHz, $CDCl_3$) δ = 13.13 (s, 2H, ArO*H*), 8.38 (s, 2H, NC*H*) 7.45 (d, *J*=2.4 Hz, 2H, Ar*H*), 7.32 (d, *J*=2.4 Hz, 2H, Ar*H*), 7.20 (m, 7H, Ar*H*), 3.07 (sept, *J*=6.8 Hz, 4H, ArC*H*(CH$_3$)$_2$), 2.18 (s, 6H, ArCH_3), 1.97 (s, 3H, ArCH_3), 1.36 (s, 18H, ArC(CH_3)$_3$), 1.20 (d, *J*=6.8 Hz, 12H, ArCH(CH_3)$_2$), 1.18 (d, *J*=6.8 Hz, 12H, ArCH(CH_3)$_2$) ppm. ^{13}C NMR (126 MHz, $CDCl_3$) δ = 167.16 (N*C*H), 156.41 (Ar), 146.55 (Ar), 141.65 (Ar), 138.92 (Ar), 136.15 (Ar), 135.69 (Ar), 135.04 (Ar), 133.31 (Ar), 129.52 (Ar), 129.22 (Ar), 127.32 (Ar), 125.37 (Ar), 123.34 (Ar), 117.86 (Ar), 34.32 (Ar*C*(CH$_3$)$_3$), 31.58 (ArC(*C*H$_3$)$_3$), 28.21 (Ar*C*H(CH$_3$)$_2$), 23.67 (ArCH(*C*H$_3$)$_2$), 23.63 (ArCH(*C*H$_3$)$_2$), 20.91 (Ar*C*H$_3$), 18.55 (Ar*C*H$_3$) ppm. HRMS (ES+) Calcd. for $C_{55}H_{71}N_2O_2$: 791.5516. Found: 791.5518.

Compound 42-s. The imine condensation with 2,6-diisopropylaniline and **40-s** was accomplished via the same procedure as for the anti. The desired product was isolated as a pale yellow solid in 42 % yield (0.17 g). ^{1}H NMR (500 MHz, $CDCl_3$) δ = 12.93 (s, 2H, ArO*H*), 8.36 (s, 2H, C*H*N), 7.42 (d, *J*=2.5 Hz, 2H, Ar*H*), 7.31 (d, *J*=2.5 Hz, 2H, Ar*H*), 7.18 (m, 7H, Ar*H*), 3.04 (sept, *J*=6.9 Hz, 4H, ArC*H*(CH$_3$)$_2$), 2.19 (s, 6H, ArCH_3), 1.99 (s, 3H, ArCH_3), 1.39 (s, 18H, ArC(CH_3)$_3$), 1.19 (d, *J*=6.9 Hz, 12H,

ArCH(CH_3)$_2$), 1.17 (d, *J*=6.9 Hz, 12H, ArCH(CH_3)$_2$) ppm. ^{13}C NMR (126 MHz, $CDCl_3$) δ = 166.99 (N*C*H), 156.61 (Ar), 146.61 (Ar), 141.37 (Ar), 138.91 (Ar), 136.25 (Ar), 136.09 (Ar), 135.41 (Ar), 132.87 (Ar), 129.43 (Ar), 129.03 (Ar), 127.38 (Ar), 125.30 (Ar), 123.30 (Ar), 117.98 (Ar), 34.31 (Ar*C*(CH$_3$)$_3$), 31.62 (ArC(*C*H$_3$)$_3$), 28.17 (Ar*C*H(CH$_3$)$_2$), 23.76 (ArCH(*C*H$_3$)$_2$), 23.63 (ArCH(*C*H$_3$)$_2$), 20.93 (Ar*C*H$_3$), 18.60 (Ar*C*H$_3$) ppm. HRMS (FAB+) Calcd. for $C_{55}H_{71}N_2O_2$: 791.5516. Found: 791.5515.

Compound 43-s. The imine condensation with 2,6-diisopropylaniline and **41-s** was accomplished using a procedure analogous to the synthesis of **7**. The desired product was isolated as a pale yellow solid in 47 % yield (2.39 g). ^{1}H NMR (400 MHz, C_6D_6) δ = 13.35 (s, 2H, ArO*H*), 8.04 (s, 2H, NC*H*) 7.49 (d, *J*=1.6 Hz, 2H, Ar*H*), 7.26 (d, *J*=1.6 Hz, 2H, Ar*H*), 7.10 (s, 6H, Ar*H*), 3.44 (s, 3H, ArOCH_3), 3.02 (sept, *J*=6.8 Hz, 4H, ArC*H*(CH$_3$)$_2$), 2.42 (s, 6H, ArCH_3), 2.37 (s, 3H, ArCH_3), 1.22 (s, 18H, ArC(CH_3)$_3$), 1.05 (d, *J*=7.0 Hz, 12H, ArCH(CH_3)$_2$), 1.03 (d, *J*=7.0 Hz, 12H, ArCH(CH_3)$_2$) ppm. ^{13}C NMR (101 MHz, C_6D_6) δ = 167.81 (Ar), 157.57 (Ar), 155.81 (Ar), 147.28 (Ar), 141.69 (Ar), 138.95 (Ar), 137.37 (Ar), 133.37 (Ar), 131.45 (Ar), 130.71 (Ar), 129.47 (Ar), 127.83 (Ar), 125.74 (Ar), 123.48 (Ar), 118.74 (Ar), 59.50 (O*C*H$_3$), 34.16 (Ar*C*(CH$_3$)$_3$), 31.54 (ArC(*C*H$_3$)$_3$), 28.58 (Ar*C*H(CH$_3$)$_2$), 23.53 (ArCH(*C*H$_3$)$_2$), 23.44 (ArCH(*C*H$_3$)$_2$), 18.98 (Ar*C*H$_3$), 14.52 (Ar*C*H$_3$) ppm. HRMS (ES+) Calcd. for $C_{56}H_{73}N_2O_3$: 821.5621. Found: 821.5641.

Synthesis of dinickel complexes

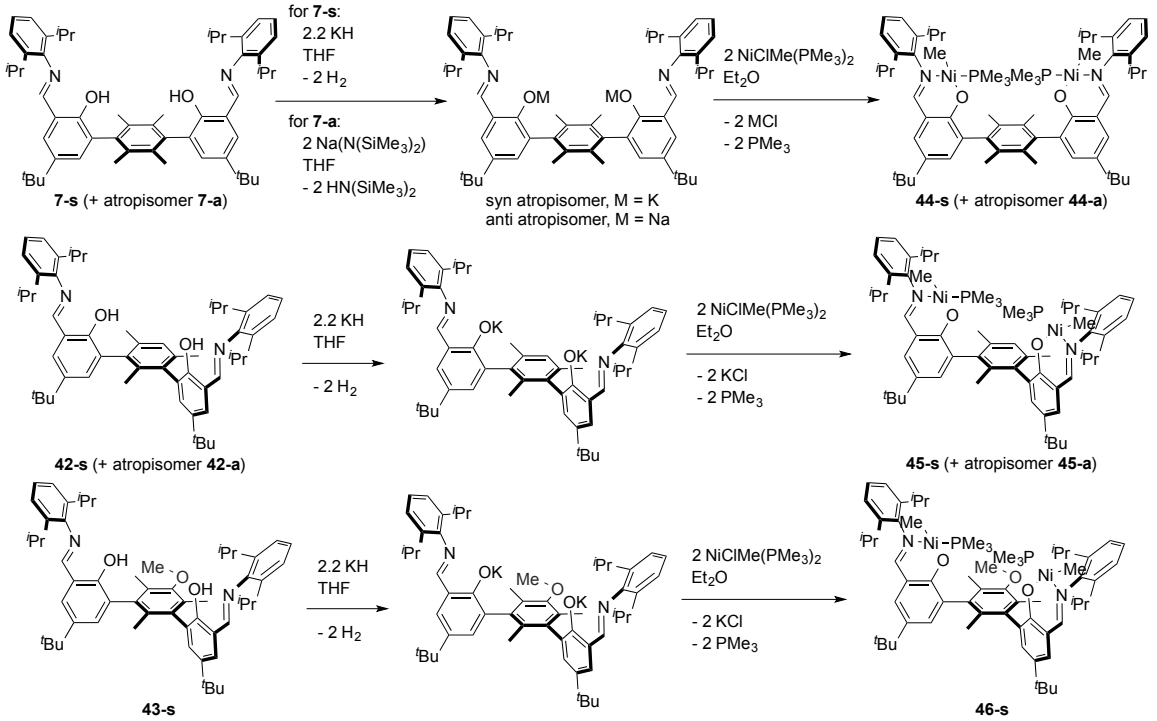

Scheme 4.4. Synthesis of dinickel complexes.

Compound 44-a. Prior to metallation, **7-a** was deprotonated with $Na(N(SiMe_3)_2)$. A scintillation vial equipped with a stirbar was charged with $Na(N(SiMe_3)_2)$ (0.018 g, 0.099 mmol, 2 equiv) and toluene (1 mL). A solution of **7-a** (0.040 g, 0.050 mmol) in toluene (2 mL) was added and the mixture was stirred at room temperature for 2 h, and then concentrated in vacuo to yield a bright yellow solid. The amine side product was removed by two cycles of suspending the product in hexanes and removing the volatiles under vacuum. The solid was used without further purification. ^{1}H NMR (400 MHz, $CDCl_3$) δ = 8.37 (s, 2H, NC*H*), 7.39 (d, *J*=2.5 Hz, 2H, Ar*H*), 7.31 (d, *J*=2.5 Hz, 2H, Ar*H*), 7.18 (m, 6H, Ar*H*), 3.06 (sept, *J*=6.7 Hz, 4H, ArC*H*$(CH_3)_2$), 2.09 (s, 12H ArCH_3), 1.35 (s, 18H, ArC$(CH_3)_3$), 1.19 (d, *J*=6.7 Hz, 24H, ArCH$(CH_3)_2$) ppm.

Metallations with $Ni(PMe_3)_2MeCl$ were carried out using literature conditions.[49] A solution of deprotonated **7-a** (0.114 g, 0.134 mmol, 1 equiv) in Et_2O (4 mL) was added dropwise to a solution of $Ni(PMe_3)_2MeCl$ (0.070 g, 0.266 mmol, 1.98 equiv) in Et_2O (3 mL) and the resulting solution was stirred for 14 h, and then concentrated in vacuo to yield a dark orange brown solid. The solid was suspended in hexanes and filtered over Celite. The hexanes washes were discarded and the desired product was flushed through the Celite with benzene and then concentrated in vacuo to yield 0.12 g of bright orange solid (81 % yield). ^{1}H NMR (600 MHz, C_6D_6) δ = 8.02 (d, *J*=8.9 Hz, 2H, NC*H*), 7.38 (d, *J*=2.7 Hz, 2H, Ar*H*), 7.15 (m, 8H, Ar*H*), 3.93 (sept, *J*=6.9 Hz, 4H, ArC*H*$(CH_3)_2$), 2.15 (s, 12H, ArCH_3), 1.38 (s, 18H, ArC$(CH_3)_3$), 1.37 (d, *J*=6.9 Hz, 12H, ArCH$(CH_3)_2$), 1.05 (d, *J*=6.9 Hz, 12H, ArCH$(CH_3)_2$), 0.70 (d, *J*=9.7 Hz, 18H, P$(CH_3)_3$), -1.14 (d, *J*=7.2 Hz, 6H, NiCH_3) ppm. ^{31}P NMR (121 MHz, C_6D_6) δ = -8.36 (s) ppm. ^{13}C NMR (126 MHz, C_6D_6) δ = 165.88 (N*C*H), 163.83 (Ar), 150.03 (Ar), 141.47 (Ar), 139.97 (Ar), 136.02 (Ar), 135.47 (Ar), 132.99 (Ar), 132.36 (Ar), 128.35 (Ar), 126.29 (Ar), 123.60 (Ar), 118.76 (Ar), 33.90 (Ar*C*$(CH_3)_3$), 31.76 (ArC$(CH_3)_3$), 28.55 (Ar*C*H$(CH_3)_2$), 25.00 (ArCH$(CH_3)_2$), 23.22 (ArCH$(CH_3)_2$), 18.28 (Ar*C*H_3), 12.48 (d, *J*=27.38 Hz, P$(CH_3)_3$), -14.13 (d, *J*=42.36 Hz, NiCH_3) ppm. Anal. Calcd. for $C_{64}H_{94}N_2Ni_2O_2P_2$: C, 69.70; H, 8.59, N, 2.54. Found: C, 69.56; H, 8.50, N, 2.57.

Compound 44-s. Prior to metallation, **7-s** was deprotonated with KH. A scintillation vial equipped with a stirbar was charged with KH (0.005 g, 0.117 mmol, 2 equiv) and THF (1 mL) and frozen in the glovebox cold well. A solution of **7-s** (0.050 g, 0.059 mmol) in THF (2 mL) was also frozen in the cold well. The solution of **7-s** was added and the solution of KH while thawing, and the mixture was stirred at room

temperature for 2 h, and then concentrated in vacuo to yield a bright yellow solid. The solid was taken up in Et_2O, filtered over Celite, concentrated in vacuo, and used without further purification. ^{1}H NMR (300 MHz, C_6D_6) δ = 8.17 (s, 2H, NC*H*), 7.36 (d, *J*=2.7 Hz, 2H, Ar*H*), 7.29 (d, *J*=2.7 Hz, 2H, Ar*H*), 7.07 (bs, 6H, Ar*H*), 3.05 (sept, *J*=6.8 Hz, 4H, ArC*H*$(CH_3)_2$), 2.06 (s, 12H, ArC*H*$_3$), 1.32 (s, 18H, ArC(C*H*$_3)_3$), 1.09 (d, *J*=6.8 Hz, 24H, ArCH(C*H*$_3)_2$) ppm.

A solution of deprotonated **7-s** (0.151 g, 0.171 mmol, 1 equiv) in Et_2O (5 mL) was added dropwise to a solution of $Ni(PMe_3)_2MeCl$ (0.089 g, 0.340 mmol, 1.98 equiv) in Et_2O (4 mL) and the resulting solution was stirred for 14 h, filtered over Celite, and then concentrated in vacuo to yield a red orange solid. The ^{1}H and ^{31}P NMR spectra still indicated the presence of $Ni(PMe_3)_2MeCl$ so an additional 0.15 equiv of deprotonated 6-s was added to the red orange solid in Et_2O (9 mL) and the reaction was stirred an additional 14 h, filtered over Celite, and then concentrated in vacuo. 0.16 g of red orange solid was collected (84 % yield). ^{1}H NMR (600 MHz, C_6D_6) δ = 8.04 (s, 2H, NC*H*), 7.34 (d, *J*=2.8 Hz, 2H, Ar*H*), 7.15 (bs, 6H, Ar*H*), 7.10 (d, *J*=2.8 Hz, 2H, Ar*H*), 3.95 (sept, *J*=6.9 Hz, 4H, ArC*H*$(CH_3)_2$), 2.24 (s, 12H, ArC*H*$_3$), 1.34 (d, *J*=6.9 Hz, 12H, ArCH(C*H*$_3)_2$), 1.24 (s, 18H, ArC(C*H*$_3)_3$), 1.03 (d, *J*=6.9 Hz, 12H, ArCH(C*H*$_3)_2$), 0.80 (d, *J*=9.5 Hz, 18H, P(C*H*$_3)_3$), -1.06 (s, 6H, NiC*H*$_3$) ppm. ^{31}P NMR (121 MHz, C_6D_6) δ = -7.92 (s) ppm. ^{13}C NMR (126 MHz, C_6D_6) δ = 166.48 (N*C*H), 164.19 (Ar), 149.84 (Ar), 141.61 (Ar), 140.53 (Ar), 135.85 (Ar), 135.82 (Ar), 135.44 (Ar), 132.85 (Ar), 128.96 (Ar), 126.34 (Ar), 123.66 (Ar), 119.09 (Ar), 33.84 (Ar*C*$(CH_3)_3$), 31.57 (ArC(*C*$H_3)_3$), 28.53 (Ar*C*H$(CH_3)_2$), 25.08 (ArCH(*C*$H_3)_2$), 23.18 (ArCH(*C*$H_3)_2$), 19.08 (Ar*C*H_3), 13.17 (d,

J=27.82 Hz, P(*C*H$_3$)$_3$), -12.70 (d, *J*=44.90 Hz, Ni*C*H$_3$) ppm. Anal. Calcd. for $C_{64}H_{94}N_2Ni_2O_2P_2$: C, 69.70; H, 8.59, N, 2.54. Found: C, 69.64; H, 8.62, N, 2.51.

Compound 45-a. Deprotonation of **42-a** was accomplished using a procedure analogous to the deprotonation of **7-s** (with KH). The deprotonated material was then dissolved in Et_2O, filtered over Celite, and metallated with Ni(PMe$_3$)$_2$MeCl using the same procedure as for **44-a**. **45-a** was purified by precipitation from pentane. ^{1}H NMR (500 MHz, C_6D_6) δ = 7.99 (d, *J*=8.6 Hz, 2H, NC*H*), 7.34 (d, *J*=2.7 Hz, 2H, Ar*H*), 7.14 (m, 6H, Ar*H*), 7.10 (d, *J*=2.7 Hz, 2H, Ar*H*), 7.03 (s, 1H, Ar*H*), 3.90 (ddt, *J*=13.8, 9.7, 6.8 Hz, 4H, ArC*H*(CH$_3$)$_2$), 2.26 (s, 6H, ArC*H*$_3$), 2.14 (s, 3H, ArC*H*$_3$), 1.37 (d, *J*=6.9 Hz, 6H, ArCH(C*H*$_3$)$_2$), 1.35 (d, J=6.9 Hz, 6H, ArCH(C*H*$_3$)$_2$), 1.34 (s, 18H, ArC(C*H*$_3$)$_3$), 1.05 (d, *J*=6.9 Hz, 6H, ArCH(C*H*$_3$)$_2$), 1.01 (d, *J*=6.9 Hz, 6H, ArCH(C*H*$_3$)$_2$), 0.77 (d, *J*=9.7 Hz, 18H, P(C*H*$_3$)$_3$), -1.14 (d, *J*=6.9 Hz, 6H, NiC*H*$_3$) ppm. ^{31}P NMR (121 MHz, C_6D_6) δ = -7.81 (s) ppm. ^{13}C NMR (126 MHz, C_6D_6) δ = 165.45 (N*C*H), 163.33 (Ar), 149.61 (Ar), 141.11 (Ar), 141.02 (Ar), 138.43 (Ar), 135.90 (Ar), 135.04 (Ar), 134.44 (Ar), 134.39 (Ar) 132.58 (Ar), 128.09 (Ar), 125.87 (Ar), 123.16 (Ar), 118.41 (Ar), 33.49 (Ar*C*(CH$_3$)$_3$), 31.33 (ArC(*C*H$_3$)$_3$), 28.14 (Ar*C*H(CH$_3$)$_2$), 24.60 (ArCH(*C*H$_3$)$_2$), 24.50 (ArCH(*C*H$_3$)$_2$), 22.82 (ArCH(*C*H$_3$)$_2$), 22.74 (ArCH(*C*H$_3$)$_2$), 20.88 (Ar*C*H$_3$), 18.08 (Ar*C*H$_3$), 12.25 (d, *J*=27.39 Hz, P(*C*H$_3$)$_3$), -14.54 (d, *J*=42.19 Hz, Ni*C*H$_3$) ppm. Anal. Calcd. for $C_{63}H_{92}N_2Ni_2O_2P_2$: C, 69.50; H, 8.52, N, 2.57. Found: C, 69.45; H, 8.56, N, 2.59.

Compound 45-s. Deprotonation of **42-a** was accomplished using a procedure analogous to the deprotonation of **7-s** (with KH). The deprotonated material was then dissolved in hexanes, filtered over Celite, and metallated with Ni(PMe$_3$)$_2$MeCl using the same procedure as for **44-s**. **45-s** was purified by recrystallization from pentane. ^{1}H

NMR (500 MHz, C_6D_6) δ = 8.01 (d, *J*=8.4 Hz, 2H, NC*H*), 7.42 (d, *J*=2.8 Hz, 2H, Ar*H*), 7.17 (m, 6H, Ar*H*), 7.07 (d, *J*=2.8 Hz, 2H, Ar*H*), 7.02 (s, 1H, Ar*H*), 3.97 (sept, *J*=6.8 Hz, 4H, C*H*(CH_3)$_2$), 2.35 (s, 6H, ArCH_3), 2.25 (s, 3H, ArCH_3), 1.43 (d, *J*=6.9 Hz, 6H, ArCH(CH_3)$_2$), 1.40 (d, *J*=6.9 Hz, 6H, ArCH(CH_3)$_2$), 1.22 (s, 18H, ArC(CH_3)$_3$), 1.07 (d, *J*=6.9 Hz, 6H, ArCH(CH_3)$_2$), 1.02 (d, *J*=6.9 Hz, 6H, ArCH(CH_3)$_2$), 0.92 (d, *J*=9.6 Hz, 18H, P(CH_3)$_3$), -1.06 (d, *J*=6.6 Hz, 6H, NiCH_3) ppm. ^{31}P NMR (121 MHz, C_6D_6) δ = -8.58 (s) ppm. ^{13}C NMR (126 MHz, C_6D_6) δ = 165.99 (N*C*H), 163.42 (Ar), 149.45 (Ar), 141.20 (Ar), 141.09 (Ar), 139.27 (Ar), 135.99 (Ar), 135.47 (Ar), 135.36 (Ar), 133.85 (Ar) 128.73 (Ar), 125.94 (Ar), 123.33 (Ar), 123.19 (Ar), 118.89 (Ar), 33.38 (Ar*C*(CH_3)$_3$), 31.11 (ArC(*C*H_3)$_3$), 28.18 (Ar*C*H(CH_3)$_2$), 24.72 (ArCH(*C*H_3)$_2$), 24.58 (ArCH(*C*H_3)$_2$), 22.92 (ArCH(*C*H_3)$_2$), 22.87 (ArCH(*C*H_3)$_2$), 21.34 (Ar*C*H_3), 20.34 (Ar*C*H_3), 13.22 (d, *J*=27.75 Hz, P(*C*H_3)$_3$), -12.97 (d, *J*=42.27 Hz, Ni*C*H_3) ppm. Anal. Calcd. for $C_{63}H_{92}N_2Ni_2O_2P_2$: C, 69.50; H, 8.52, N, 2.57. Found: C, 69.45; H, 8.43, N, 2.53.

Compound 46-s. Deprotonation of **42-a** was accomplished using a procedure analogous to the deprotonation of **7-s** (with KH). The deprotonated material was then dissolved in hexanes, filtered over Celite, and metallated with Ni(PMe_3)$_2$MeCl using the same procedure as for **44-s**. **46-s** was purified by precipitation from cold hexanes. The assignment of this product as the syn atropisomer was confirmed by ^{1}H-^{1}H NOESY NMR (Figure 4.6). ^{1}H NMR (600 MHz, C_6D_6) δ = 8.01 (d, *J*=7.8 Hz, 2H, NC*H*), 7.42 (d, *J*=2.8 Hz, 2H, Ar*H*), 7.17 (m, 6H, Ar*H*), 7.09 (d, *J*=2.8 Hz, 2H, Ar*H*), 3.97 (sept, *J*=6.8 Hz, 4H, ArC*H*(CH_3)$_2$), 3.54 (s, 3H, ArOCH_3), 2.40 (s, 6H, ArCH_3), 2.19 (s, 3H, ArCH_3), 1.43 (d, *J*=6.9 Hz, 6H, ArCH(CH_3)$_2$), 1.39 (d, *J*=6.9 Hz, 6H, ArCH(CH_3)$_2$), 1.23 (s, 18H, ArC(CH_3)$_3$), 1.08 (d, *J*=6.9 Hz, 6H, ArCH(CH_3)$_2$), 1.02 (d, *J*=6.9 Hz, 6H,

ArCH(CH_3)$_2$), 0.93 (d, *J*=9.5 Hz, 18H, P(CH_3)$_3$), -1.07 (d, *J*=5.7 Hz, 6H, NiCH_3) ppm. ^{31}P NMR (121 MHz, C_6D_6) δ = -8.66 (s) ppm. ^{13}C NMR (126 MHz, C_6D_6) δ = 165.98 (N*C*H), 163.38 (Ar), 154.70 (Ar), 149.43 (Ar), 141.20 (Ar), 141.06 (Ar), 140.70 (Ar), 135.39 (Ar), 133.89 (Ar), 131.65 (Ar), 128.80 (Ar), 125.95 (Ar), 123.35 (Ar), 123.17 (Ar), 118.94 (Ar), 58.99 (ArO*C*H$_3$), 33.38 (Ar*C*(CH$_3$)$_3$), 31.12 (ArC(*C*H$_3$)$_3$), 28.19 (Ar*C*H(CH$_3$)$_2$), 28.16 (Ar*C*H(CH$_3$)$_2$), 24.73 (ArCH(*C*H$_3$)$_2$), 24.58 (ArCH(*C*H$_3$)$_2$), 22.92 (ArCH(*C*H$_3$)$_2$), 22.86 (ArCH(*C*H$_3$)$_2$), 20.26 (Ar*C*H$_3$), 14.65 (Ar*C*H$_3$), 13.18 (d, *J*=27.73 Hz, P(*C*H$_3$)$_3$), -13.03 (d, *J*=44.35 Hz, Ni*C*H$_3$) ppm. Anal. Calcd. for $C_{64}H_{94}N_2Ni_2O_3P_2$: C, 68.71; H, 8.47, N, 2.50. Found: C, 68.66; H, 8.39, N, 2.47.

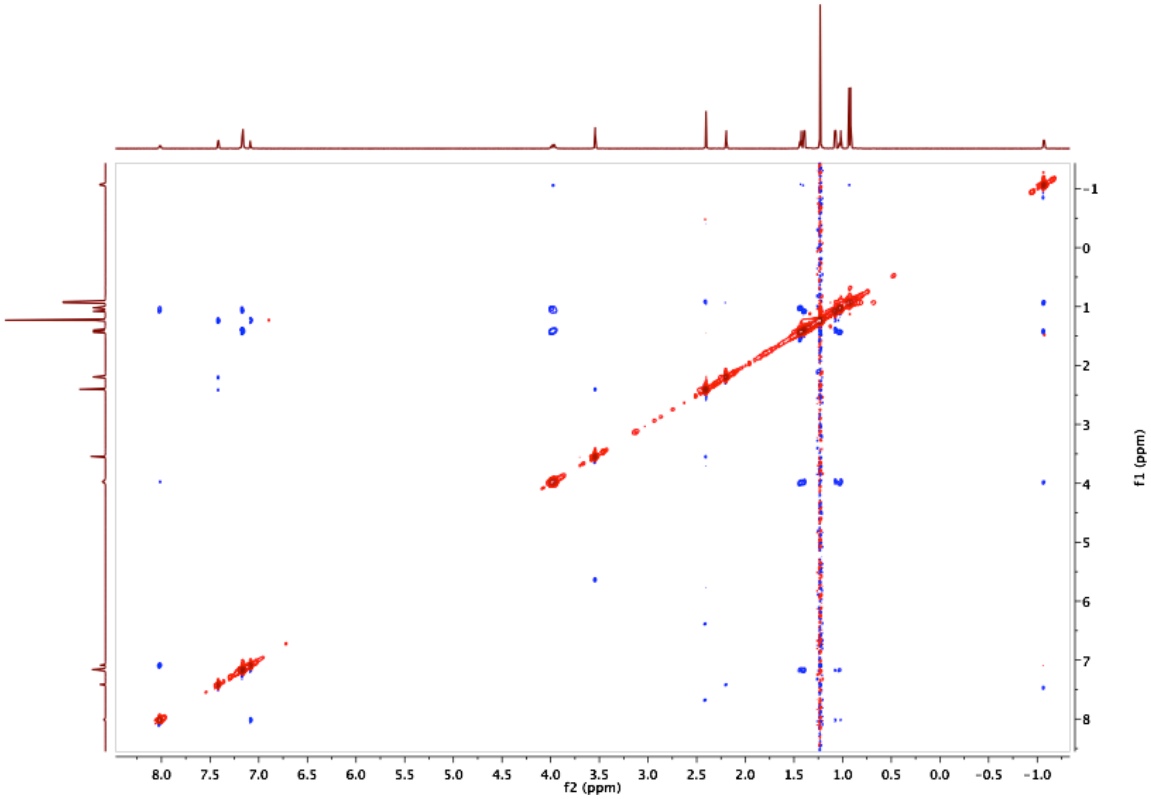

Figure 4.6. ^{1}H-^{1}H NOESY spectrum of **46-s** in C_6D_6 (no cross peaks between the PMe_3 and any aryl peaks, confirming syn atropisomer).

Synthesis of amino olefins

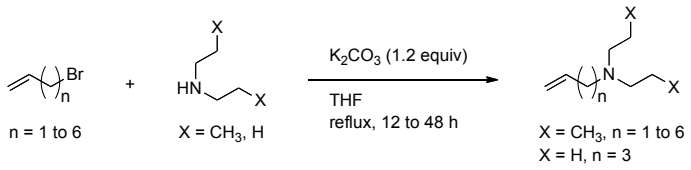

Scheme 4.5. General synthesis of amino olefins.

Representative procedure: Synthesis of N(pentenyl)(^{n}Pr)$_2$. Under ambient conditions, K_2CO_3 (7.00 g, 50.65 mmol, 1.2 equiv), THF (42 mL), HN(^{n}Pr)$_2$ (7.52 mL, 54.87 mmol, 1.3 equiv), and 5-bromo-1-pentene (5.00 mL, 42.21 mmol, 1 equiv) were added, in that order, to a Schlenk tube equipped with a stirbar. The reaction vessel was sealed and heated to 75 °C for 40 h. The complete consumption of the bromide was confirmed by GCMS. The reaction mixture was filtered and the salts were rinsed with THF. The filtrates were then combined and fractionally distilled under static vacuum to separate the product from solvent, excess starting amine, and non-volatile side products. The clear, colorless oil collected in the second fraction was filtered over about 30 mL of silica gel in a frit with about 150 mL of pentane. This pentane fraction was then fractionally distilled under static vacuum to separate the product from pentane. The product was obtained as a clear, colorless oil in the second fraction and was dried by stirring over CaH_2 overnight, degassing on the Schlenk line, bringing into the glovebox and filtering over an alumina pipette plug (3.45 g, 48 % yield).

N(allyl)(^{n}Pr)$_2$. ^{1}H NMR (400 MHz, $CDCl_3$) δ = 5.84 (m, 1H, C*H*), 5.11 (m, 2H, CH_2), 3.06 (dt, *J*=6.5 Hz, 1.4, 2H, NCH_2), 2.36 (m, 4H, NCH_2), 1.43 (m, 4H, CH_2), 0.85 (t, *J*=7.4 Hz, 6H, CH_3) ppm. ^{13}C NMR (101 MHz, $CDCl_3$) δ = 136.50 (olefinic), 116.78 (olefinic), 57.54 (N*C*H$_2$), 56.01 (N*C*H$_2$), 20.35 (*C*H$_2$), 12.05 (*C*H$_3$) ppm. HRMS (FAB+) Calcd. for $C_9H_{20}N$: 142.1596. Found: 142.1597.

N(butenyl)(^{n}Pr)$_2$. ^{1}H NMR (500 MHz, $CDCl_3$) δ = 5.80 (m, 1H, C*H*), 5.00 (m, 2H, CH_2), 2.49 (m, 2H, NCH_2), 2.38 (m, 4H, NCH_2), 2.19 (m, 2H, CH_2), 1.44 (m, 4H, CH_2), 0.87 (t, *J*=7.4 Hz, 6H, CH_3) ppm. ^{13}C NMR (126 MHz, $CDCl_3$) δ = 137.37 (olefinic), 115.37 (olefinic), 56.30 (N*C*H$_2$), 53.75 (N*C*H$_2$), 31.65 (*C*H$_2$), 20.43 (*C*H$_2$), 12.14 (*C*H$_3$) ppm. HRMS (EI+) Calcd. for $C_{10}H_{21}N$: 155.1674. Found: 155.1690.

N(pentenyl)(^{n}Pr)$_2$. ^{1}H NMR (500 MHz, $CDCl_3$) δ = 5.82 (m, 1H, C*H*), 4.96 (m, 2H, CH_2), 2.40 (m, 2H, NCH_2), 2.35 (m, 4H, NCH_2), 2.04 (m, 2H, CH_2), 1.52 (m, 2H, CH_2), 1.43 (m, 4H, CH_2), 0.86 (t, *J*=7.3 Hz, 6H, CH_3) ppm. ^{13}C NMR (126 MHz, $CDCl_3$) δ = 139.01 (olefinic), 114.47 (olefinic), 56.45 (N*C*H$_2$), 53.83 (N*C*H$_2$), 31.90 (*C*H$_2$), 26.51 (*C*H$_2$), 20.42 (*C*H$_2$), 12.13 (*C*H$_3$) ppm. HRMS (EI+) Calcd. for $C_{11}H_{23}N$: 169.1830. Found: 169.1837.

N(hexenyl)(^{n}Pr)$_2$. ^{1}H NMR (500 MHz, $CDCl_3$) δ = 5.81 (m, 1H, C*H*), 4.97 (m, 2H, CH_2), 2.39 (m, 2H, NCH_2), 2.35 (m, 4H, NCH_2), 2.06 (m, 2H, CH_2), 1.41 (m, 8H, CH_2), 0.86 (t, *J*=7.4 Hz, 6H, CH_3) ppm. ^{13}C NMR (126 MHz, $CDCl_3$) δ = 139.16 (olefinic), 114.43 (olefinic), 56.45 (N*C*H$_2$), 54.21 (N*C*H$_2$), 33.90 (*C*H$_2$), 27.09 (*C*H$_2$), 26.72 (*C*H$_2$), 20.41 (*C*H$_2$), 12.16 (*C*H$_3$) ppm. HRMS (FAB+) Calcd. for $C_{12}H_{26}N$: 184.2065. Found: 184.2056.

N(heptenyl)(^{n}Pr)$_2$. ^{1}H NMR (500 MHz, $CDCl_3$) δ = 5.80 (m, 1H, C*H*), 4.96 (m, 2H, CH_2), 2.36 (m, 6H, NCH_2), 2.04 (m, 2H, CH_2), 1.42 (m, 8H, CH_2), 1.28 (m, 2H, CH_2), 0.86 (t, *J*=7.4 Hz, 6H, CH_3) ppm. ^{13}C NMR (126 MHz, $CDCl_3$) δ = 139.25 (olefinic), 114.33 (olefinic), 56.47 (N*C*H$_2$), 54.39 (N*C*H$_2$), 33.96 (*C*H$_2$), 29.08 (*C*H$_2$), 27.30 (*C*H$_2$), 27.11 (*C*H$_2$), 20.39 (*C*H$_2$), 12.16 (*C*H$_3$) ppm. HRMS (FAB+) Calcd. for $C_{13}H_{28}N$: 198.2222. Found: 198.2227.

N(octenyl)(^{n}Pr)$_2$. ^{1}H NMR (500 MHz, $CDCl_3$) δ = 5.80 (m, 1H, C*H*), 4.95 (m, 2H, CH_2), 2.36 (m, 6H, NCH_2), 2.03 (m, 2H, CH_2), 1.39 (m, 14H, CH_2), 0.86 (t, *J*=7.4 Hz, 6H, CH_3) ppm. ^{13}C NMR (126 MHz, $CDCl_3$) δ = 139.32 (olefinic), 114.27 (olefinic), 56.46 (N*C*H$_2$), 54.44 (N*C*H$_2$), 33.92 (*C*H$_2$), 29.28 (*C*H$_2$), 29.08 (*C*H$_2$), 27.66 (*C*H$_2$), 27.21 (*C*H$_2$), 20.39 (*C*H$_2$), 12.16 (*C*H$_3$) ppm. HRMS (FAB+) Calcd. for $C_{14}H_{30}N$: 212.2378. Found: 212.2381.

N(pentenyl)(Et)$_2$. ^{1}H NMR (500 MHz, $CDCl_3$) δ = 5.81 (m, 1H, C*H*), 4.97 (m, 2H, CH_2), 2.50 (q, *J*=7.2 Hz, 4H, NCH_2), 2.40 (m, 2H, NCH_2), 2.03 (m, 2H, CH_2), 1.53 (m, 2H, CH_2), 1.00 (t, *J*=7.2 Hz, 6H, CH_3) ppm. ^{13}C NMR (126 MHz, $CDCl_3$) δ = 138.84 (olefinic), 114.55 (olefinic), 52.53 (N*C*H$_2$), 47.06 (N*C*H$_2$), 31.95 (*C*H$_2$), 26.36 (*C*H$_2$), 11.86 (*C*H$_3$) ppm. HRMS (FAB+) Calcd. for $C_9H_{20}N$: 142.1596. Found: 142.1581.

Representative synthesis: Attempted syntheses of amino acid based monomers. Under ambient conditions, K_2CO_3 (7.30 g, 52.79 mmol, 2.1 equiv), THF (25 mL), H_2O (25 mL), L-phenylglycine (3.80 g, 25.14 mmol, 1 equiv), and 5-bromo-1-pentene (6.25 mL, 52.79 mmol, 2.1 equiv) were added, in that order, to a Schlenk tube equipped with a stirbar. The reaction vessel was sealed and heated to 75 °C for 65 h. Volatiles were removed under vacuum and the remainder was extracted between H_2O and DCM. The organics were dried with $MgSO_4$, filtered, and volatiles were again removed under vacuum. ^{1}H NMR spectroscopy revealed that the desired product was present in the organic fraction. Various attempts to purify by distillation or extraction were unsuccessful. Other than L-phenylglycine, L-valine and (1*S*,2*R*)-(+)-norephedrine were used as precursors.

(*R*,*R*)-*N*,*N'*-dipentenyl-*N*,*N'*-dimethylcyclohexane-1,2-diamine. Under ambient conditions, K_2CO_3 (6.20 g, 44.85 mmol, 2.2 equiv), THF (40 mL), (*R*,*R*)-*N*,*N'*-dimethylcyclohexane-1,2-diamine (2.90 g, 20.39 mmol, 1 equiv), and 5-bromo-1-pentene (5.31 mL, 44.85 mmol, 2.2 equiv) were added, in that order, to a Schlenk tube equipped with a stirbar. The reaction vessel was sealed and heated to 75 °C for 65 h. The reaction mixture was filtered and the salts were rinsed with THF. The filtrates were then combined and volatiles were removed in vacuo. The desired product was purified by Kugelrohr distillation. The product transferred as a yellow oil (2.6 g, 46 % yield). ^{1}H NMR (500 MHz, $CDCl_3$) δ = 5.82 (m, 2H, C*H*), 4.96 (m, 4H, CH_2), 2.49 (2m, 2H, NC*H*, 4H, NCH_2), 2.23 (m, 6H, NCH_3), 2.06 (sept, *J*=7.3, 6.6 Hz, 4H, CH_2), 1.73 (ddd, *J*=37.9, 9.4, 3.8 Hz, 4H, CH_2), 1.53 (m, 4H, CH_2), 1.12 (m, 4H, CH_2) ppm. ^{13}C NMR (126 MHz, $CDCl_3$) δ = 139.30 (olefinic), 114.29 (olefinic), 63.46 (N*C*H$_2$), 54.18 (N*C*H$_3$), 36.71 (*C*H$_2$), 31.99 (*C*H$_2$), 27.95 (*C*H$_2$), 26.05 (*C*H$_2$) ppm. HRMS (FAB+) Calcd. for $C_{18}H_{33}N_2$: 277.2644. Found: 277.2642.

N(pentenyl)(CH_2CH_2OH)$_2$. Under ambient conditions, K_2CO_3 (5.13 g, 37.14 mmol, 1.1 equiv), THF (34 mL), diethanolamine (4.85 g, 50.65 mmol, 1.5 equiv), and 5-bromo-1-pentene (4.00 mL, 33.77 mmol, 1 equiv) were added, in that order, to a Schlenk tube equipped with a stirbar. The reaction vessel was sealed and heated to 75 °C for 54 h. The reaction mixture was filtered and the salts were rinsed with THF. The filtrates were then combined and fractionally distilled under static vacuum to separate the product and excess starting amine from solvent and non-volatile side products. The excess amine was removed by extraction between H_2O and a mixture of $CHCl_3$ and ^{i}PrOH (x4). The organic fractions were washed with H_2O, dried with $MgSO_4$, filtered,

and the volatiles were removed under vacuum (at ambient temperature). The product was further purified by Kugelrohr distillation.^{1}H NMR (500 MHz, $CDCl_3$) δ = 5.79 (m, 1H, C*H*), 4.99 (m, 2H, CH_2), 3.60 (t, *J*=5.3 Hz, 4H, OCH_2), 2.88 (bs, 2H, O*H*), 2.64 (t, 2H, *J*=5.4 Hz, 4H, NCH_2), 2.53 (m, 2H, NCH_2), 2.05 (m, 2H, CH_2), 2.56 (p, *J*=7.4 Hz, 2H, CH_2) ppm. ^{13}C NMR (126 MHz, $CDCl_3$) δ = 138.40 (olefinic), 115.00 (olefinic), 59.78 (O*C*H_2), 56.15 (N*C*H_2), 54.25 (N*C*H_2), 31.52 (*C*H_2), 26.28 (*C*H_2) ppm. HRMS (FAB+) Calcd. for $C_9H_{20}NO_2$: 174.1494. Found: 174.1488.

HN(pentenyl)(*t*Bu). Under ambient conditions, K_2CO_3 (6.42 g, 46.43 mmol, 1.1 equiv), THF (42 mL), H_2N(*t*Bu) (13.31 mL, 126.62 mmol, 3.0 equiv), and 5-bromo-1-pentene (5.00 mL, 42.21 mmol, 1 equiv) were added, in that order, to a Schlenk tube equipped with a stirbar. The reaction vessel was sealed and heated to 75 °C for 40 h. The reaction mixture was filtered and the salts were rinsed with THF. The filtrates were then combined and fractionally distilled under static vacuum to separate the product from solvent, excess starting amine, and non-volatile side products. The product was obtained as a clear, colorless oil in the second fraction. Freeze-pump-thaw cycles were used to degas the product, which was then brought into the glovebox dried by storing over molecular sieves (4 Å) for several days (1.6 g, 27 % yield). ^{1}H NMR (500 MHz, CDCl3) δ = 5.81 (m, 1H, C*H*), 4.98 (m, 2H, CH_2), 2.54 (m, 2H, NCH_2), 2.09 (q, *J*=8.1, 7.5 Hz, 2H, NCH_2), 1.55 (p, *J*=7.4 Hz, 2H, CH_2), 1.08 (s, 9H, C(CH_3)$_3$) ppm. ^{13}C NMR (126 MHz, $CDCl_3$) δ = 138.69 (olefinic), 114.70 (olefinic), 50.38 (N*C*(CH$_3$)$_3$), 42.16 (N*C*H_2), 31.88 (*C*H_2), 30.35 (*C*H_2), 29.20 (NC(*C*H$_3$)$_3$) ppm. HRMS (FAB+) Calcd. for $C_9H_{20}N$: 142.1596. Found: 142.1594.

[N(Me)(pentenyl)(^{n}Pr)$_2$][I]. Synthesis of the ammonium salt [N(Me)(pentenyl)(^{n}Pr)$_2$][I] was accomplished via the reaction of N(pentenyl)(^{n}Pr)$_2$ with MeI using literature conditions.[62] N(pentenyl)(^{n}Pr)$_2$ (0.50 g, 2.95 mmol, 1 equiv), MeI (0.28 mL, 4.45 mmol, 1.5 equiv), and acetone (5 mL) were added to a 3-neck round bottom flask equipped with a stirbar under positive N_2 flow. The mixture was stirred at ambient temperature for 19 h at which point 5 mL of pentane was added. The mixture separated into two layers and the bottom layer was collected. Volatiles were removed in vacuo, and the resulting pale yellow solid was placed under vacuum on the Schlenk line for 12 h to yield the desired product as a white solid (0.78 g, 85 % yield). ^{1}H NMR (500 MHz, C_6D_6) δ = 5.80 (m, 1H, C*H*), 5.12 (m, 2H, CH_2), 3.20 (m, 2H, NCH_2), 3.16 (s, 3H, NCH_3), 3.08 (m, 4H, NCH_2), 2.05 (q, *J*=7.7, 7.0 Hz, 2H, CH_2), 1.51 (m, 2H, CH_2), 1.31 (m, 2H, CH_2), 0.80 (t, *J*=7.2 Hz, 6H, CH_3) ppm.

NMR scale experiments with Ni(COD)$_2$ or 44-s

To monitor the reactions between the functionalized monomers and Ni(COD)$_2$ or **44-s**, 4 equivalents of the monomer, 1 equivalent of Ni(COD)$_2$ or **44-s** and about 1 mL of C_6D_6 were added to a J. Young tube. A ^{1}H NMR spectrum of the mixture was recorded immediately and then at different time intervals out to several days.

General polymerization procedures

A 3 oz. Andrews glass pressure reaction vessel equipped with Swagelok valves and a gauge was used for all high pressure polymerizations. A syringe was loaded with a solution of the desired organometallic complex and scavenger, and the needle was sealed with a rubber septum. The high-pressure setup was brought into the glovebox with a magnetic stirbar and charged with the desired amount of solvent (minus that

which was used to make the solution of complex and scavenger). The desired amount of additive or comonomer was also added to the setup, if applicable, and the setup was sealed. The syringe and setup were brought out of the box and the setup was clamped firmly over a hot plate with a mineral oil bath previously regulated to the desired temperature (25 °C). The solution was stirred vigorously (1200 rpm). A nylon core hose equipped with quick connect adaptors was purged with ethylene for 1 minute and the pressure was set to 15 psig. The hose was connected to the setup and the setup was filled with ethylene. A bleed needle was inserted into a Teflon septum at the top of the high pressure setup and flushed with ethylene. The solution of organometallic complex and scavenger was added via syringe and the top of the setup was closed. The pressure was increased to the desired level (100 psig). After the desired time, the ethylene hose was disconnected, the setup was vented and the reaction mixture was quenched with acidified methanol (3 times the reaction volume) to precipitate the polymer, which was collected as a white solid by filtration over a fine frit. If only a small amount of polymer was precipitated, the entire mixture was collected and volatile materials were removed under vacuum. All polymers were dried on the Schlenk line for a minimum of 8 hours before a mass was recorded.

Representative ^{1}H and ^{13}C NMR spectra of polymers

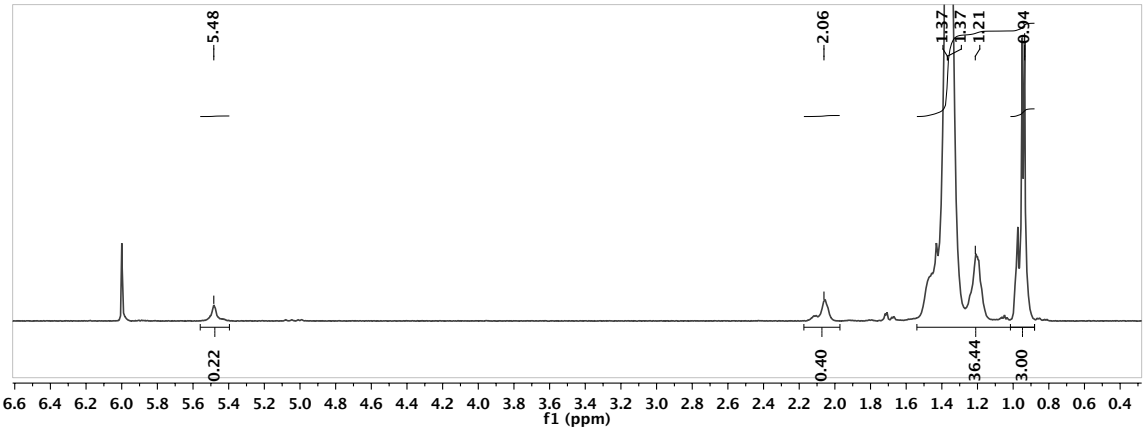

Figure 4.7. ^{1}H NMR spectrum in tetrachloroethane-D_2 at 130 °C of the ethylene/1-hexene copolymer made with **44-s**. The integral of the multiplet at 0.94 ppm was set to 3 for the determination of the extent of branching in the polymer chain.

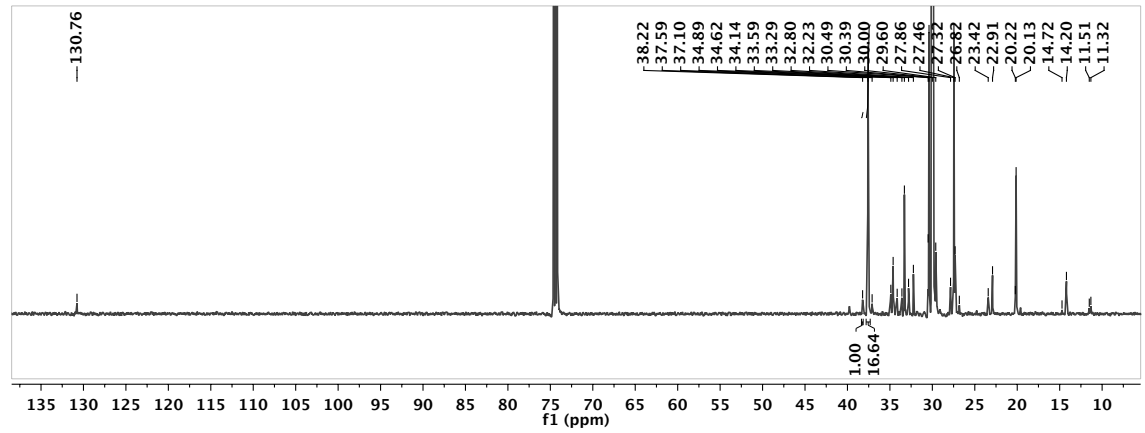

Figure 4.8. ^{13}C NMR spectrum in tetrachloroethane-D_2 at 130 °C of the ethylene/1-hexene copolymer made with **44-s**. The peak at 30 ppm is off scale. The integrated peaks at 37.59 and 38.25 ppm were used to compare the amount of methyl vs. butyl branching in the polymer.

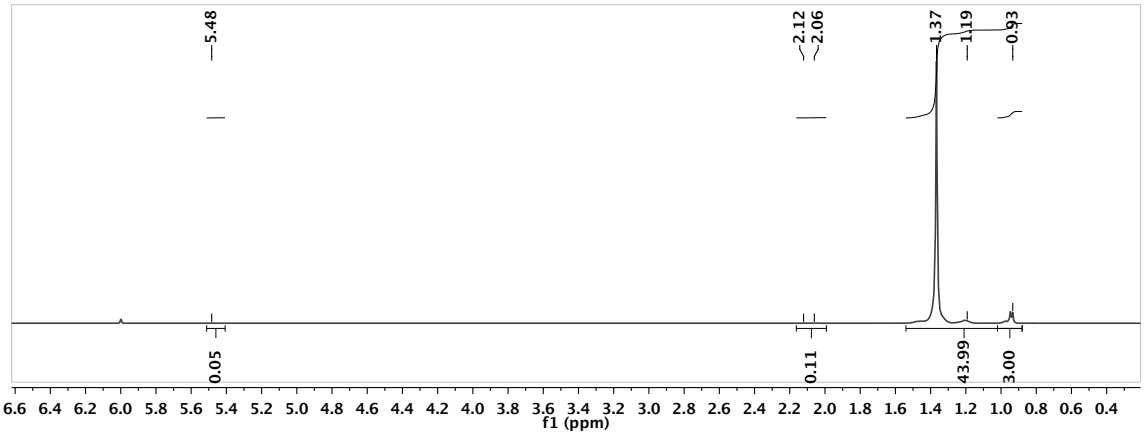

Figure 4.9. ^{1}H NMR spectrum in tetrachloroethane-D_2 at 130 °C of the ethylene/1-hexene copolymer made with **45-s**. The integral of the multiplet at 0.93 ppm was set to 3 for the determination of the extent of branching in the polymer chain.

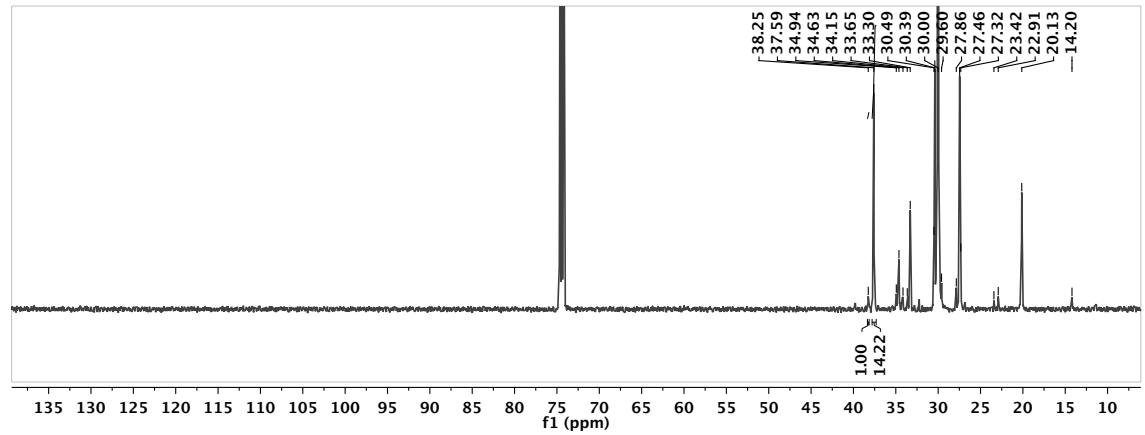

Figure 4.10. ^{13}C NMR spectrum in tetrachloroethane-D_2 at 130 °C of the ethylene/1-hexene copolymer made with **45-s**. The peak at 30 ppm is off scale. The integrated peaks at 37.59 and 38.25 ppm were used to compare the amount of methyl vs. butyl branching in the polymer.

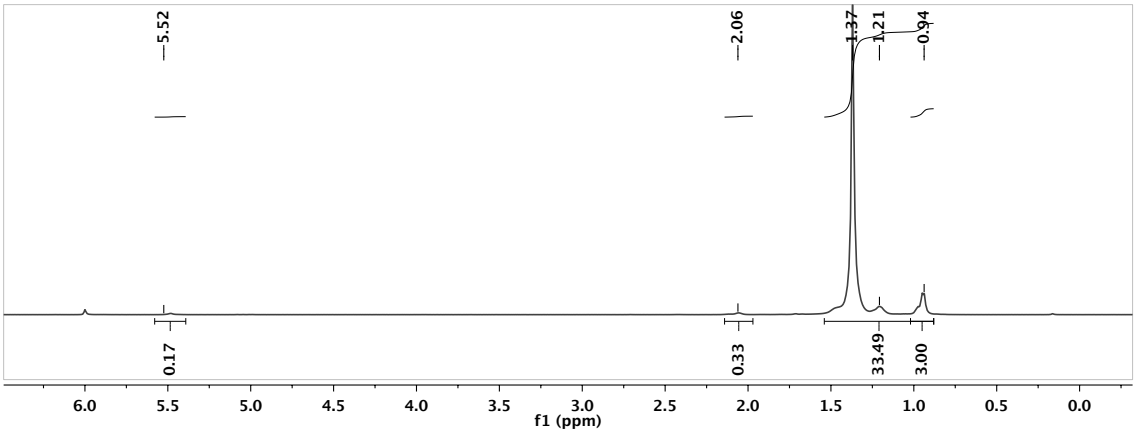

Figure 4.11. ^{1}H NMR spectrum in tetrachloroethane-D_2 at 130 °C of the ethylene/1-hexene copolymer made with **44-s** in the presence of NMe(^{n}Pr)$_2$.

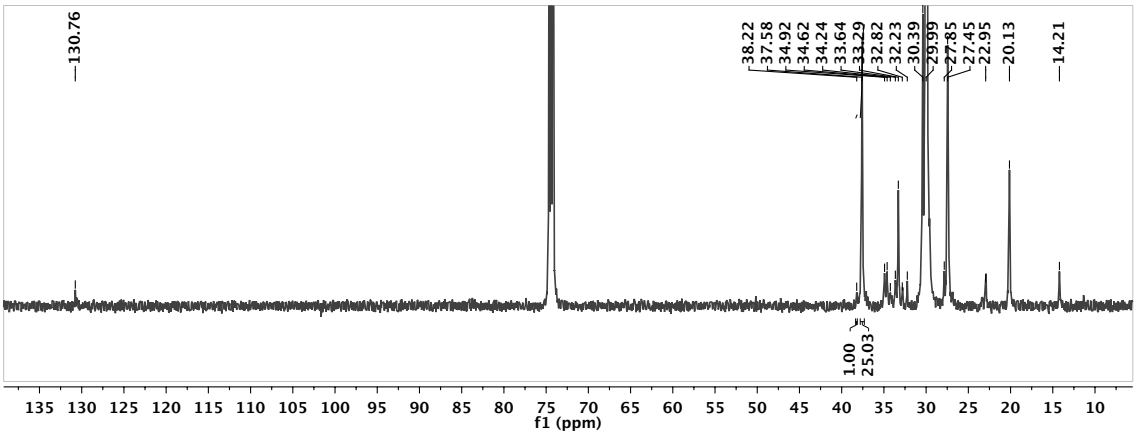

Figure 4.12. ^{13}C NMR spectrum in tetrachloroethane-D_2 at 130 °C of the ethylene/1-hexene copolymer made with **44-s** in the presence of NMe(^{n}Pr)$_2$. The peak at 30 ppm is off scale.

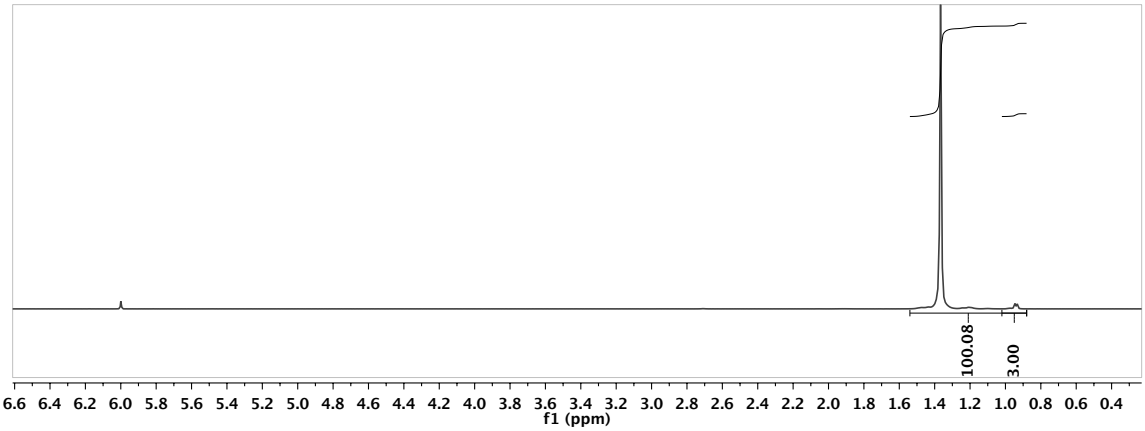

Figure 4.13. ^{1}H NMR spectrum in tetrachloroethane-D_2 at 130 °C of the ethylene/1-hexene copolymer made with **45-s** in the presence of NMe(^{n}Pr)$_2$.

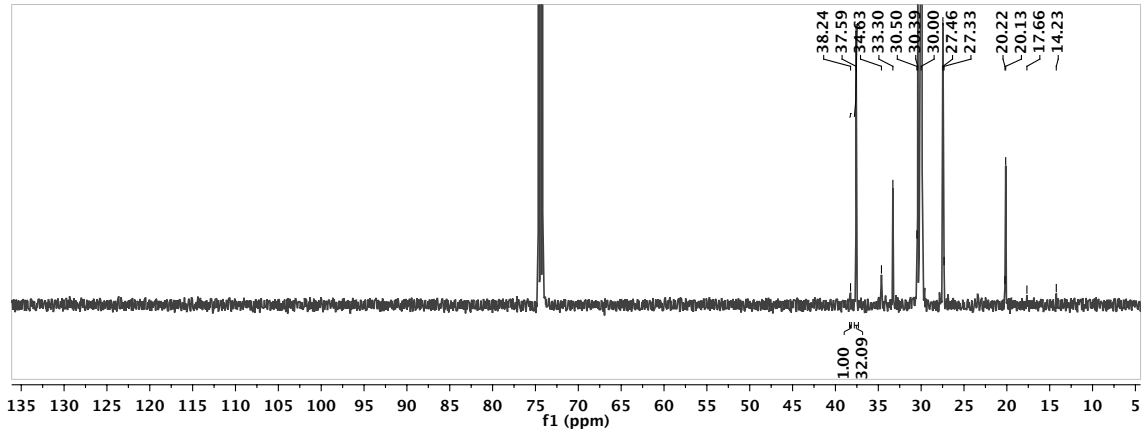

Figure 4.14. ^{13}C NMR spectrum in tetrachloroethane-D_2 at 130 °C of the ethylene/1-hexene copolymer made with **45-s** in the presence of NMe(^{n}Pr)$_2$. The peak at 30 ppm is off scale.

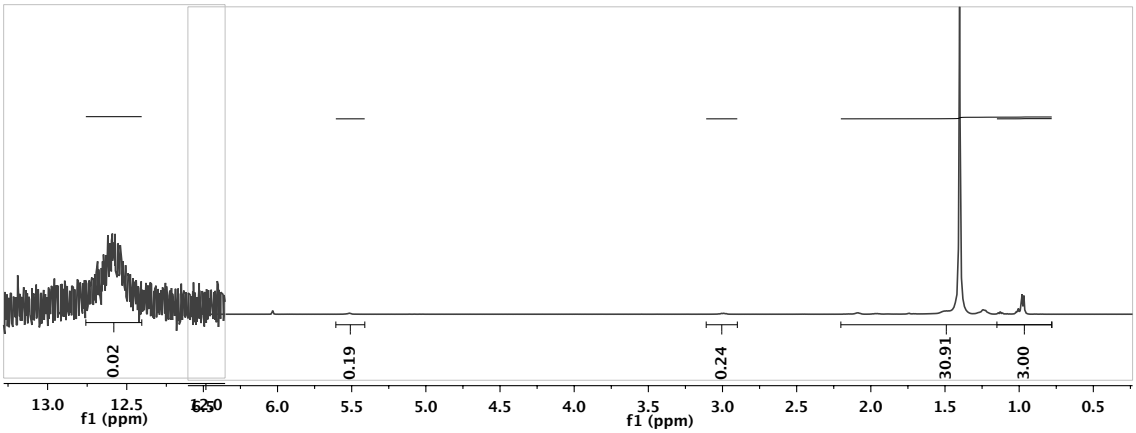

Figure 4.15. ^{1}H NMR spectrum in tetrachloroethane-D_2 at 130 °C of the ethylene/N(pentenyl)(^{n}Pr)$_2$ copolymer made with **44-s**. The blown up peak (left) at 12.6 ppm is the ammonium proton.

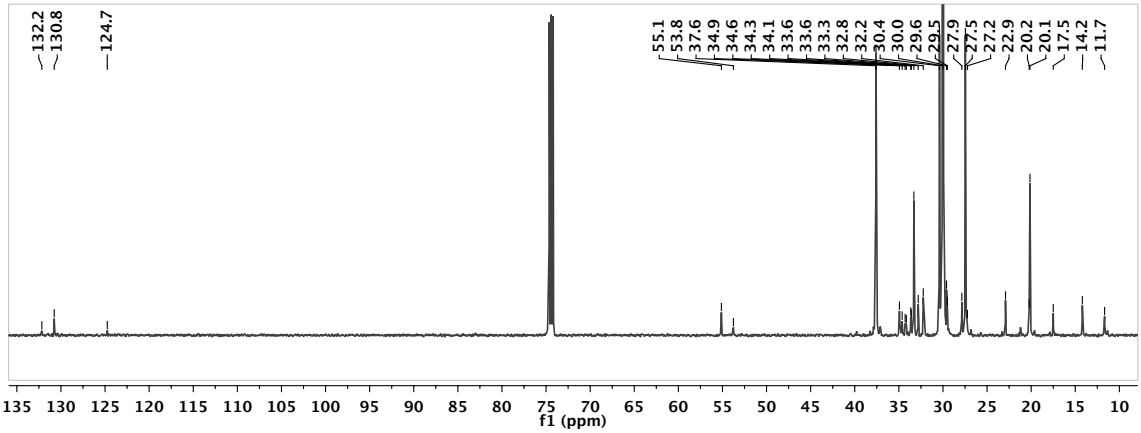

Figure 4.16. ^{13}C NMR spectrum in tetrachloroethane-D_2 at 130 °C of the ethylene/N(pentenyl)(^{n}Pr)$_2$ copolymer made with **44-s**. The peak at 30 ppm is off scale.

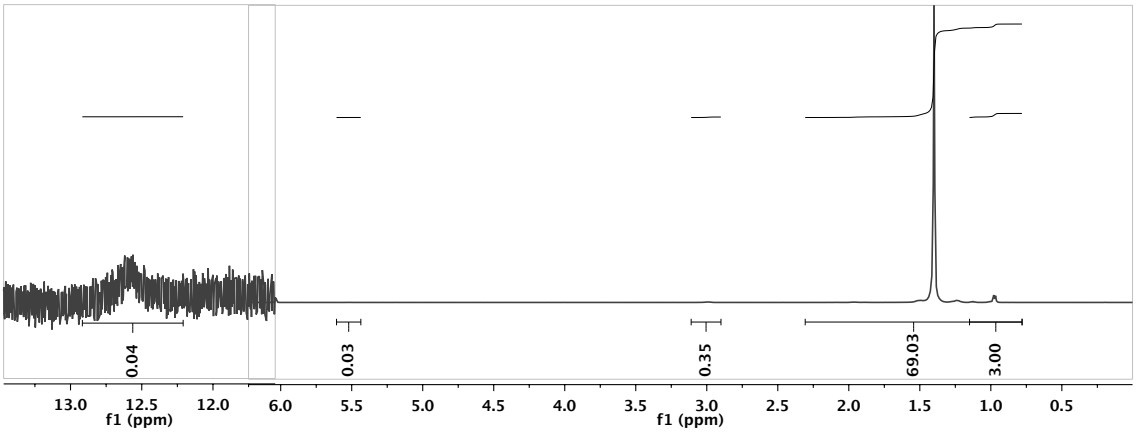

Figure 4.17. ^{1}H NMR spectrum in tetrachloroethane-D_2 at 130 °C of the ethylene/N(pentenyl)(^{n}Pr)$_2$ copolymer made with **45-s**. The blown up peak (left) at 12.6 ppm is the ammonium proton.

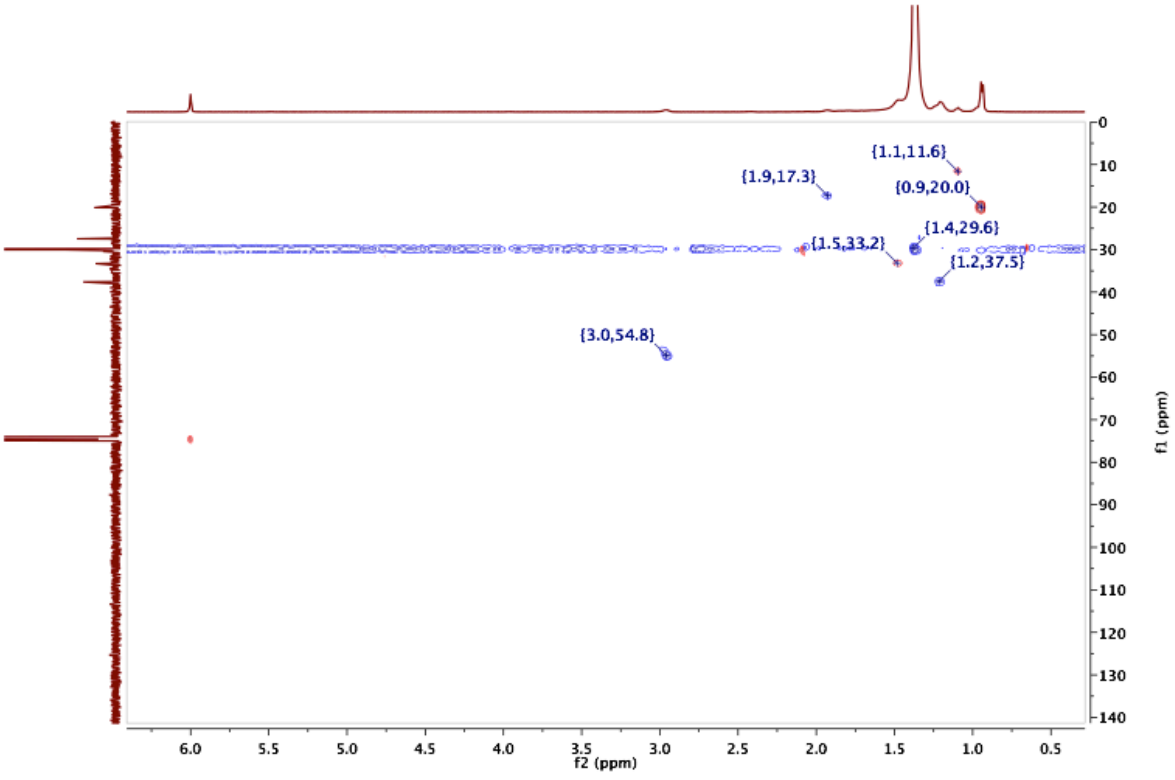

Figure 4.18. ^{1}H-^{13}C HSQCAD NMR spectrum in tetrachloroethane-D_2 at 130 °C of the ethylene/N(pentenyl)(^{n}Pr)$_2$ copolymer made with **45-s** with the largest cross peaks labeled. The peaks around 55 ppm were too small to observe in the ^{13}C NMR spectrum.

Crystallographic Information

Table 4.7. Crystal and refinement data for complexes **44-s** and **45-s**.

	44-s	**45-s**
CCDC number	937340	980857
empirical formula	$C_{86.50}H_{148}N_2Ni_2O_2P_2$	$C_{86.80}H_{119.20}N_2Ni_2O_2P_2$
formula wt	1427.42	1395.93
T (K)	100	100
a, Å	13.408(2)	13.284(4)
b, Å	14.878(2)	21.951(7)
c, Å	23.068(4)	27.971(9)
α, deg	104.541(8)	91.115(7)
β, deg	90.001(9)	97.107(8)
γ, deg	116.551(8)	101.877(7)
V, Å^3	3950.8(12)	7912(4)
Z	2	4
cryst syst	triclinic	triclinic
space group	P -1	P -1
dcalcd, g/cm^3	1.200	1.171
θ range, deg	1.6 to 29.0	1.8 to 27.7
μ, mm^{-1}	0.56	0.56
abs cor	Semi-empirical from equivalents	Semi-empirical from equivalents
GOF	1.77	1.91
R1,[a] wR2[b] (I > 2θ (I))	R1 = 0.1425, wR2 = 0.3256	R1 = 0.1615, wR2 = 0.3432

[a] $R_1 = \sum||F_o| - |F_c||/\sum|F_o|$. [b] $wR_2 = [\sum[w(F_o^2-F_c^2)^2]/\sum[w(F_o^2)^2]]^{1/2}$.

REFERENCES

1. Koning, C.; van Duin, M.; Pagnoulle, C.; Jerome, R. *Prog. Poly. Sci.* **1998**, *23*, 707-757.
2. Ren, Y.; Jiang, X.; Liu, R.; Yin, J. *J. Polym. Sci., Part A: Polym. Chem.* **2009**, *47*, 6353-6361.
3. Ren, Y.; Jiang, X.; Yin, J. *J. Polym. Sci., Part A: Polym. Chem.* **2009**, *47*, 1292-1297.
4. Meyer, J.; Keul, H.; Moeller, M. *Macromolecules* **2011**, *44*, 4082-4091.
5. Dhende, V. P.; Samanta, S.; Jones, D. M.; Hardin, I. R.; Locklin, J. *ACS Appl. Mat. Inter.* **2011**, *3*, 2830-2837.
6. Jones, E. R.; Semsarilar, M.; Blanazs, A.; Armes, S. P. *Macromolecules* **2012**, *45*, 5091-5098.
7. Zhang, C.; Maric, M. *J. Polym. Sci., Part A: Polym. Chem.* **2012**, *50*, 4341-4357.
8. Yang, Y.; Mijalis, A. J.; Fu, H.; Agosto, C.; Tan, K. J.; Batteas, J. D.; Bergbreiter, D. E. *J. Am. Chem. Soc.* **2012**, *134*, 7378-7383.
9. Imuta, J.; Kashiwa, N.; Toda, Y. *J. Am. Chem. Soc.* **2002**, *124*, 1176-1177.
10. Amin, S. B.; Marks, T. J. *Angew. Chem. Int. Ed.* **2008**, *47*, 2006-2025.
11. Itagaki, K.; Nomura, K. *Macromolecules* **2009**, *42*, 5097-5103.
12. Alidedeoglu, A. H.; York, A. W.; McCormick, C. L.; Morgan, S. E. *J. Polym. Sci., Part A: Polym. Chem.* **2009**, *47*, 5405-5415.
13. Nomura, K. *J. Synth. Org. Chem. Jpn.* **2010**, *68*, 1150-1158.
14. Hibi, Y.; Ouchi, M.; Sawamoto, M. *Angew. Chem. Int. Ed.* **2011**, *50*, 7434-7437.
15. Janoschka, T.; Teichler, A.; Krieg, A.; Hager, M. D.; Schubert, U. S. *J. Polym. Sci., Part A: Polym. Chem.* **2012**, *50*, 1394-1407.
16. Leonard, J. K.; Wei, Y.; Wagener, K. B. *Macromolecules* **2012**, *45*, 671-680.
17. Holler, H. V.; Youngman, E. A. **1973**, *US 3 761 458*.
18. Johnson, L. K.; Mecking, S.; Brookhart, M. *J. Am. Chem. Soc.* **1996**, *118*, 267-268.
19. Boffa, L. S.; Novak, B. M. *Chem. Rev.* **2000**, *100*, 1479-1493.
20. Drent, E.; van Dijk, R.; van Ginkel, R.; van Oort, B.; Pugh, R. I. *Chem. Commun.* **2002**, 744-745.
21. Szuromi, E.; Shen, H.; Goodall, B. L.; Jordan, R. F. *Organometallics* **2008**, *27*, 402-409.
22. Nakamura, A.; Ito, S.; Nozaki, K. *Chem. Rev.* **2009**, *109*, 5215-5244.
23. Chen, E. Y. X. *Chem. Rev.* **2009**, *109*, 5157-5214.
24. Guironnet, D.; Roesle, P.; Runzi, T.; Gottker-Schnetmann, I.; Mecking, S. *J. Am. Chem. Soc.* **2009**, *131*, 422-423.
25. Ito, S.; Kanazawa, M.; Munakata, K.; Kuroda, J.-i.; Okumura, Y.; Nozaki, K. *J. Am. Chem. Soc.* **2011**, *133*, 1232-1235.

26. Giannini, U.; Bruckner, G.; Pellino, E.; Cassata, A. *J. Polym. Sci., Part B: Polym. Lett.* **1967**, *5*, 527-533.
27. Giannini, U.; Bruckner, G.; Pellino, E.; Cassata, A. *J. Polym. Sci., Part C: Polym. Symp.* **1968**, *22*, 157-175.
28. Giannini, U.; Bruckner, G. **1969**, *US 3 476 726*.
29. Kesti, M. R.; Coates, G. W.; Waymouth, R. M. *J. Am. Chem. Soc.* **1992**, *114*, 9679-9680.
30. Schneider, M. J.; Schafer, R.; Mulhaupt, R. *Polymer* **1997**, *38*, 2455-2459.
31. Stehling, U. M.; Stein, K. M.; Kesti, M. R.; Waymouth, R. M. *Macromolecules* **1998**, *31*, 2019-2027.
32. Stehling, U. M.; Malmstrom, E. E.; Waymouth, R. M.; Hawker, C. J. *Macromolecules* **1998**, *31*, 4396-4398.
33. Stehling, U. M.; Stein, K. M.; Fischer, D.; Waymouth, R. M. *Macromolecules* **1999**, *32*, 14-20.
34. Mustonen, I.; Hukka, T.; Pakkanen, T. *Macromol. Rapid Commun.* **2000**, *21*, 1286-1290.
35. Wilen, C. E.; Auer, M.; Stranden, J.; Nasman, J. H.; Rotzinger, B.; Steinmann, A.; King, R. E.; Zweifel, H.; Drewes, R. *Macromolecules* **2000**, *33*, 5011-5026.
36. Hakala, K.; Helaja, T.; Lofgren, B. *Polym. Bull.* **2001**, *46*, 123-130.
37. Hagihara, H.; Tsuchihara, K.; Sugiyama, J.; Takeuchi, K.; Shiono, T. *Macromolecules* **2004**, *37*, 5145-5148.
38. Naga, N.; Toyota, A.; Ogino, K. *J. Polym. Sci., Part A: Polym. Chem.* **2005**, *43*, 911-915.
39. Park, M. H.; Huh, J. O.; Do, Y.; Lee, M. H. *J. Polym. Sci., Part A: Polym. Chem.* **2008**, *46*, 5816-5825.
40. Hagihara, H.; Tsuchihara, K.; Sugiyama, J.; Takeuchi, K.; Shiono, T. *J. Polym. Sci., Part A: Polym. Chem.* **2004**, *42*, 5600-5607.
41. Hagihara, H.; Tsuchihara, K.; Takeuchi, K.; Murata, M.; Ozaki, H.; Shiono, T. *J. Polym. Sci., Part A: Polym. Chem.* **2004**, *42*, 52-58.
42. Dong, J. Y.; Wang, Z. M.; Hong, H.; Chung, T. C. *Macromolecules* **2002**, *35*, 9352-9359.
43. Younkin, T. R.; Conner, E. F.; Henderson, J. I.; Friedrich, S. K.; Grubbs, R. H.; Bansleben, D. A. *Science* **2000**, *287*, 460-462.
44. Sujith, S.; Joe, D. J.; Na, S. J.; Park, Y. W.; Chow, C. H.; Lee, B. Y. *Macromolecules* **2005**, *38*, 10027-10033.
45. Delferro, M.; Marks, T. J. *Chem. Rev.* **2011**, *111*, 2450-2485.
46. Ittel, S. D.; Johnson, L. K.; Brookhart, M. *Chem. Rev.* **2000**, *100*, 1169-1204.
47. Stockland, R. A.; Foley, S. R.; Jordan, R. F. *J. Am. Chem. Soc.* **2003**, *125*, 796-809.

48. Heyndrickx, W.; Occhipinti, G.; Bultinck, P.; Jensen, V. R. *Organometallics* **2012**, *31*, 6022-6031.

49. Rodriguez, B. A.; Delferro, M.; Marks, T. J. *Organometallics* **2008**, *27*, 2166-2168.

50. Radlauer, M. R.; Day, M. W.; Agapie, T. *Organometallics* **2012**, *31*, 2231-2243.

51. Radlauer, M. R.; Day, M. W.; Agapie, T. *J. Am. Chem. Soc.* **2012**, *134*, 1478-1481.

52. Bauers, F. M.; Mecking, S. *Macromolecules* **2001**, *34*, 1165-1171.

53. Wehrmann, P.; Mecking, S. *Organometallics* **2008**, *27*, 1399-1408.

54. Connor, E. F.; Younkin, T. R.; Henderson, J. I.; Hwang, S. J.; Grubbs, R. H.; Roberts, W. P.; Litzau, J. J. *J. Polym. Sci., Part A: Polym. Chem.* **2002**, *40*, 2842-2854.

55. Zuideveld, M. A.; Wehrmann, P.; Rohr, C.; Mecking, S. *Angew. Chem. Int. Ed.* **2004**, *43*, 869-873.

56. Connor, E. F.; Younkin, T. R.; Henderson, J. I.; Waltman, A. W.; Grubbs, R. H. *Chem. Commun.* **2003**, 2272-2273.

57. The quality of the data set for 45-s precluded determination of anisotropic structural parameters.

58. Wehrmann, P.; Zuideveld, M.; Thomann, R.; Mecking, S. *Macromolecules* **2006**, *39*, 5995-6002.

59. Martín, R.; Jiménez, L.; Alvaro, M.; Scaiano, J. C.; Garcia, H. *Chem. Eur. J.* **2010**, *16*, 7282-7292.

60. Noonan, K. J. T.; Hugar, K. M.; Kostalik, H. A.; Lobkovsky, E. B.; Abruña, H. D.; Coates, G. W. *J. Am. Chem. Soc.* **2012**, *134*, 18161-18164.

61. Kostalik, H. A.; Clark, T. J.; Robertson, N. J.; Mutolo, P. F.; Longo, J. M.; Abruña, H. c. D.; Coates, G. W. *Macromolecules* **2010**, *43*, 7147-7150.

62. Clark, T. J.; Robertson, N. J.; Kostalik Iv, H. A.; Lobkovsky, E. B.; Mutolo, P. F.; Abruña, H. c. D.; Coates, G. W. *J. Am. Chem. Soc.* **2009**, *131*, 12888-12889.

63. Hibbs, M. R.; Fujimoto, C. H.; Cornelius, C. J. *Macromolecules* **2009**, *42*, 8316-8321.

64. Schwesinger, R.; Link, R.; Wenzl, P.; Kossek, S.; Keller, M. *Chem. Eur. J.* **2006**, *12*, 429-437.

65. Pangborn, A. B.; Giardello, M. A.; Grubbs, R. H.; Rosen, R. K.; Timmers, F. J. *Organometallics* **1996**, *15*, 1518-1520.

66. Kiesewetter, E. T.; Randoll, S.; Radlauer, M.; Waymouth, R. M. *J. Am. Chem. Soc.* **2010**, *132*, 5566-5567.

67. Kaur, I.; Jazdzyk, M.; Stein, N. N.; Prusevich, P.; Miller, G. P. *J. Am. Chem. Soc.* **2010**, *132*, 1261-1263.

68. Mitchell, R. H.; Iyer, V. S.; Khalifa, N.; Mahadevan, R.; Venugopalan, S.; Weerawarna, S. A.; Zhou, P. Z. *J. Am. Chem. Soc.* **1995**, *117*, 1514-1532.

69. Klein, H. F.; Karsch, H. H. *Chem. Ber. Recl.* **1973**, *106*, 1433-1452.

70. Dahl, O. *Acta Chim. Scand.* **1969**, *23*, 2342-2354.

71. Stead, D.; O'Brien, P.; Sanderson, A. *Org. Lett.* **2008**, *10*, 1409-1412.

72. Agapie, T.; Bercaw, J. E. *Organometallics* **2007**, *26*, 2957-2959.

73. Fischer, A.; Henderson, G. N. *Can. J. Chem. Rev. Can. Chem.* **1983**, *61*, 1045-1052.

74. Yan, Y.; Qin, B.; Shu, Y. L.; Chen, X. Y.; Yip, Y. K.; Zhang, D. W.; Su, H. B.; Zeng, H. Q. *Org. Lett.* **2009**, *11*, 1201-1204.

CHAPTER 5

Bimetallic Zirconium Di[amine bis(phenolate)] Polymerization Catalysts for the Enhancement of Stereoregularity of Polypropylene and Poly(1-Hexene)

ABSTRACT

Di[amine bis(phenolate)] ligands with a rigid *p*-terphenyl backbone were designed to support two zirconium centers locked in close proximity. Polymerizations of propylene or 1-hexene with bimetallic precatalysts resulted in polymers with up to 79 % *mmmm* pentads. C_S symmetric monometallic zirconium amine bisphenolate catalysts have been reported to have high polymerization activity to produce stereoirregular polymers. The synthesized bimetallic precatalysts were shown to retain high activity (up to 10^5 (g poly(1-hexene)) or 10^4 (g polypropylene) (mmol Zr)$^{-1}$(h)$^{-1}$), while concurrently increasing polymer isotacticity. To discern the origin of stereoregularity, C_1 symmetric monometallic complexes were synthesized that better mimic the local steric environment around zirconium in the bimetallic system. In the case where a pentamethylaryl substituent was appended to one of the phenolate moieties, partial stereoregularity was observed, up to 39 % *mmmm*, indicating that the second sphere interactions provided by the second metal center are required for optimal stereocontrol in these systems.

INTRODUCTION

Single-site catalysts can be used to modulate a variety of polymer properties including tacticity and molecular weight.[1-4] The mechanisms responsible for stereoregulation in the polymerization of propylene and α-olefins have been studied extensively using homogeneous polymerization catalysts.[1-10] Still, design of stable and inexpensive polymerization catalysts with high activity, regioselectivity, and stereoselectivity remains an ongoing challenge. Bridged zirconocene catalysts are the most successful systems for pairing high activity and stereoselectivity yielding up to 10^6 (g polypropylene)(mmol Zr)$^{-1}$(h)$^{-1}$ isotactic (*mmmm* > 99 %),[11] or up to 10^7 (g polypropylene)(mmol Zr)$^{-1}$(h)$^{-1}$ syndiotactic (*rrrr* > 80 %)[10] polymers.

Numerous non-metallocene catalysts have been reported exhibiting either high activity or stereoselectivity.[2,12-19] Among these are several complexes bearing bisphenolate ligands (Chart 5.1). For example, Kol and coworkers reported highly active C_S symmetric tetradentate amine bisphenolate zirconium complexes.[13,20-22] These monometallic complexes produced up to 10^5 (g poly(1-hexene)) or 10^4 (g polypropylene) (mmol Zr)$^{-1}$(h)$^{-1}$ of stereoirregular polymer.[13,21] Altering the ligand framework such that C_2 symmetric complexes were obtained led to increased isospecificity coupled with a decrease in activity.[23-26] Indeed, tacticity and activity appeared inversely related as increases in steric bulk of phenoxide substituents that lead to high isotacticity resulted in much lower activity.[26] Variation of the amine bisphenolate ligand framework to include both imine and amine donors provided titanium catalysts able to produce highly isospecific polypropylene and poly(1-hexene) at higher activities: up to 10^4 (g poly(1-hexene)) or 10^4 (g polypropylene) (mmol Zr)$^{-1}$(h)$^{-1}$.[18] A separate class of bisphenolate ether hafnium complexes also proved capable of combining high activity with improved tactic control: up to 10^3 (g poly(1-hexene)) or 10^4 (g polypropylene) (mmol Zr)$^{-1}$(h)$^{-1}$.[17,19]

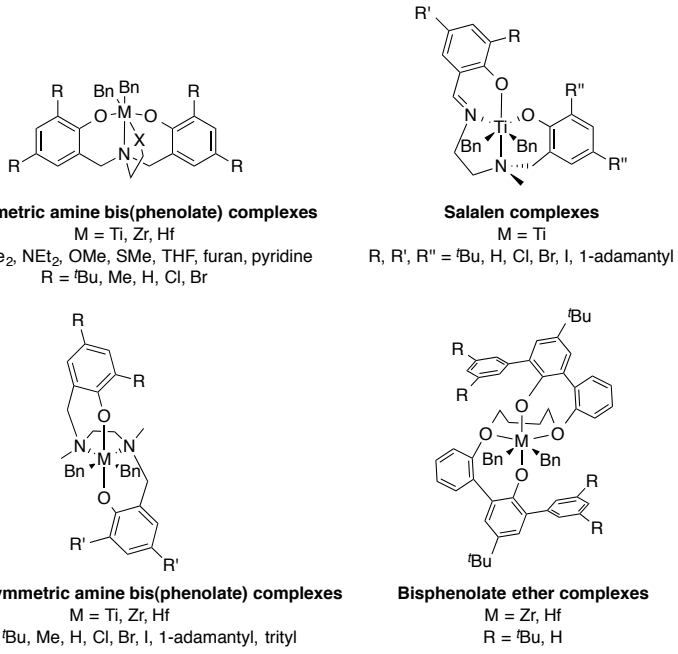

Chart 5.1. Examples of literature non-metallocene catalysts with bisphenolate ligands that have been utilized for propylene and 1-hexene polymerizations.[13,17-26]

A variety of bimetallic polymerization catalysts have been reported to alter the polymerization relative to their monometallic counterparts.[27] Increasing nuclearity has led to enhancement of activity, molecular weight, or comonomer incorporation depending on the specifics of the system. With regards to stereoselectivity, Noh and coworkers have reported improved syndioselectivity in styrene polymerization with linked dititanium systems relative to their monometallic analogues.[28-32] Panunzi and coworkers reported dipalladium catalysts that produced moderately isotactic CO/styrene copolymers, whereas the monometallic palladium system led to stereoirregular polymer.[33] Sita and coworkers described dinuclear bis-propagators that, in the presence of $ZnEt_2$ as a chain transfer agent, allowed for the retention of stereoselectivity generally observed with the monometallic without $ZnEt_2$, thereby overcoming a limitation of chain transfer polymerization.[34]

We have recently reported dinickel bisphenoxyiminato polymerization catalysts based on a rigid terphenyl ligand framework (Chapter 2).[35-37] The locked conformation of these complexes allowed for the isolation and purification of syn and anti atropisomers early

in the synthesis.[36] While the lower oxophilicity of these complexes aided in the tolerance and incorporation of amines (Chapters 3 and 4), the applications of the dinickel catalyst systems were somewhat limited by their low activity. Early transition metal catalysts generally exhibit higher activity than late transition metal catalysts.[2,4,38-39] Thus, to expand the utility of our bimetallic systems, a variety of early transition metal analogues were targeted. Appendix B details work toward a selection of bimetallic zirconium and titanium complexes based on our rigid *p*- and *m*-terphenyl ligand framework and presents future directions with those projects.

For the present chapter, the permethylated *p*-terphenyl backbone was utilized with altered donor sets to target the synthesis of di[amine bis(phenolate)] dizirconium systems analogous to C_S symmetric monometallic systems reported by Kol and coworkers (Scheme 5.1).[20-22] Only the syn atropisomers of these dinucleating ligand precursors were synthesized, as the primary focus of these studies was to examine the effect of a proximal metal center. A series of compounds was targeted with methoxy or dimethylamino donors (X) and chloride, bromide, methyl or *t*-butyl substituents (R and R') on the non-terphenyl phenoxide moieties.

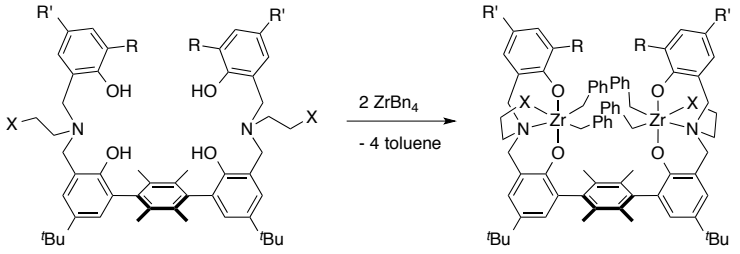

Scheme 5.1. Targeted di[amine bis(phenol)] ligand precursors and dizirconium complexes.

RESULTS AND DISCUSSION

Synthesis of dizirconium complexes

The synthesis of the binucleating ligands is based on precedented procedures (Scheme 5.2). Imine condensation of salicylaldehydes **47** with 2-methoxyethylamine or *N*,*N*-dimethylethylenediamine afforded salicylaldimines **48-X**, which were reduced with $NaBH_4$ to provide amines **49-X** in high yield. Terphenyl **3**, synthesized via Negishi coupling as a mixture of the syn and anti atropisomers (Chapter 2),[36] was deprotected with excess BBr_3, and the atropisomers of the resulting bisphenol terphenyl compound, **50**, were separated via column chromatography. The syn atropisomer was then carried forward to dibromide **51** using analogous literature conditions.[40] Substitution reactions between dibromide **51** and amines **49-X** under basic conditions led to ligand precursors **52-X**, which were purified by aqueous extraction and column chromatography prior to metallation.

The dizirconium complexes (**53-X**) were synthesized by the addition of one equivalent of **52-X** to two equivalents of $ZrBn_4$. In all cases, two major species were observed in the crude reaction mixture by ^{1}H NMR spectroscopy (e.g., Figure 5.2). Purification of one of the two major species was achieved via recrystallization or precipitation, and the resultant ^{1}H NMR spectrum included 8 doublets corresponding to benzyl protons, 4 multiplets corresponding to methylene protons, 2 singlets corresponding to ArCH_3 protons (except in the case of **53c-OMe**) and 1 singlet corresponding to $C(CH_3)_3$ protons (except in the case of **53d-OMe**). Based on the number of peaks for each type of proton, these spectra are consistent with either a *pseudo*-C_2 symmetric species in which the axis of symmetry runs through the center of the central arene of the terphenyl backbone or a *pseudo*-C_S symmetric species in which the mirror plane cuts perpendicularly through the central arene (Figure 5.1). The

isolable compound displayed two diagnostic benzyl peaks between 3 and 4 ppm, which have a larger separation between peaks than what was observed for the second major species in the crude reaction mixture. Additionally, one of these peaks is consistently farther downfield (between 3.8 and 4.2 ppm) for the isolable species.

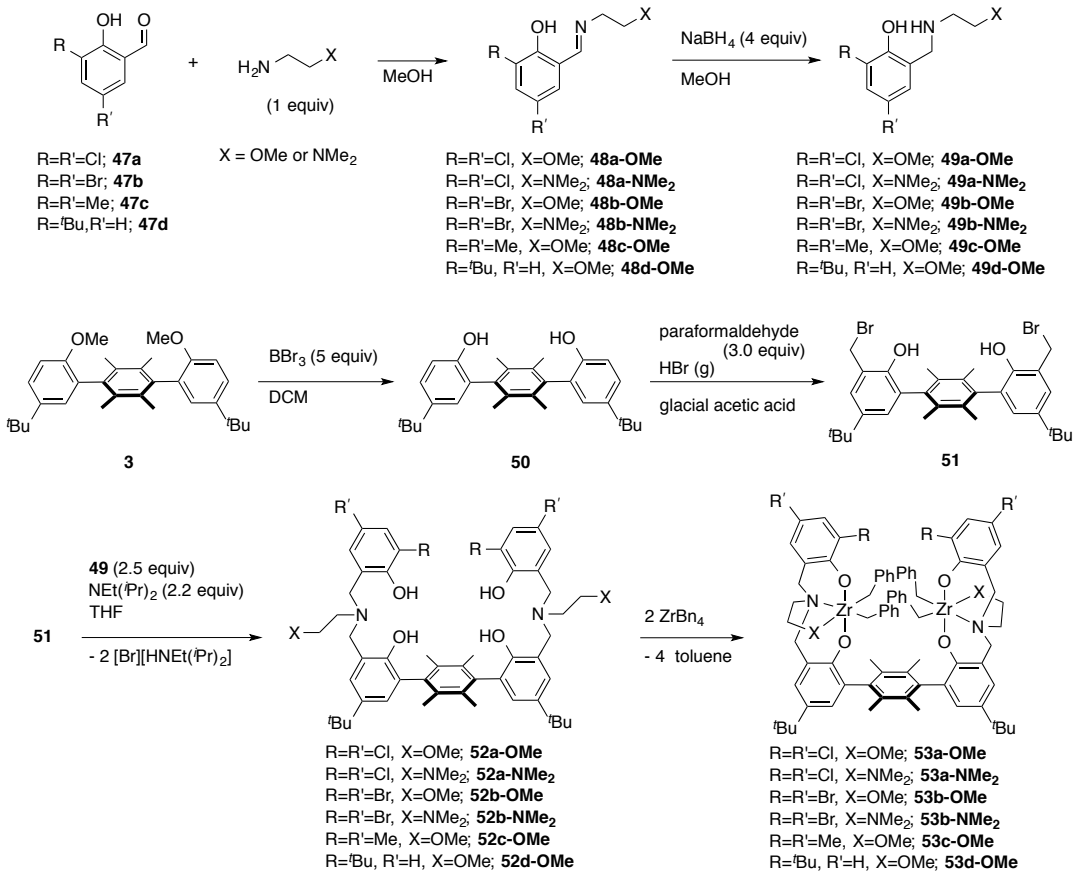

Scheme 5.2. Synthesis and metallation of dinucleating ligands.

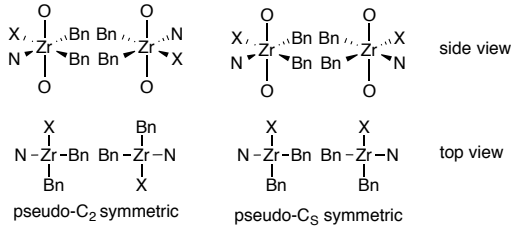

Figure 5.1. Truncated representations of the possible metallation isomers of the dizirconium complexes.

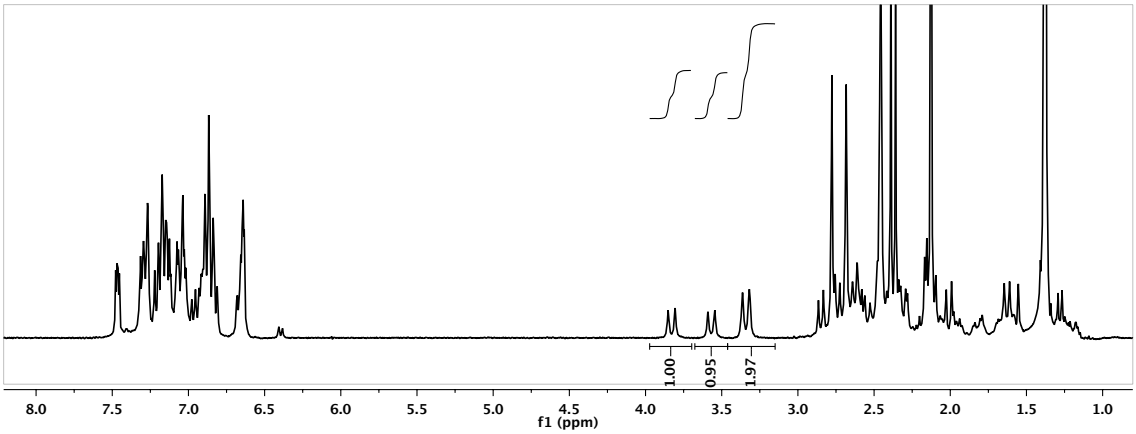

Figure 5.2. ^{1}H NMR spectrum of the crude reaction mixture from the metallation of **52a-OMe** with $ZrBn_4$, in C_6D_6. A mixture of metallation isomers is observed and the diagnostic peaks are integrated. $ZrBn_4$ and solvent impurities are also present.

Structures of dizirconium complexes

X-ray quality crystals of **53a-OMe** and **53a-NMe$_2$** were obtained from liquid diffusion of hexanes into concentrated toluene solutions of the complexes at -35 °C. X-ray diffraction studies indicated that *pseudo*-C_2 symmetric complexes had been synthesized (Figures 5.3 and 5.4). The observed Zr–Zr distances were both 7.6 Å. Distortion of the side aryl rings of the terphenyl backbone from a perpendicular dihedral is symptomatic of the steric interaction of the benzyl substituents on the two adjacent zirconium centers. These steric interactions indicate that appropriate substrates could be affected concurrently by both metal centers.

In the case of **53c-OMe**, as with all of the bimetallic complexes, the *pseudo*-C_2 symmetric complex recrystallized first from the crude mixture (assigned by diagnostic benzyl peaks in the ^{1}H NMR spectrum, vide supra). Uniquely, collection of this *pseudo*-C_2 symmetric complex via filtration and recrystallization of the filtrate yielded X-ray quality crystals of the second species. The ^{1}H NMR spectrum was again consistent with either a *pseudo*-C_2 or a *pseudo*-C_S *s*ymmetric complex based on the number of peaks and

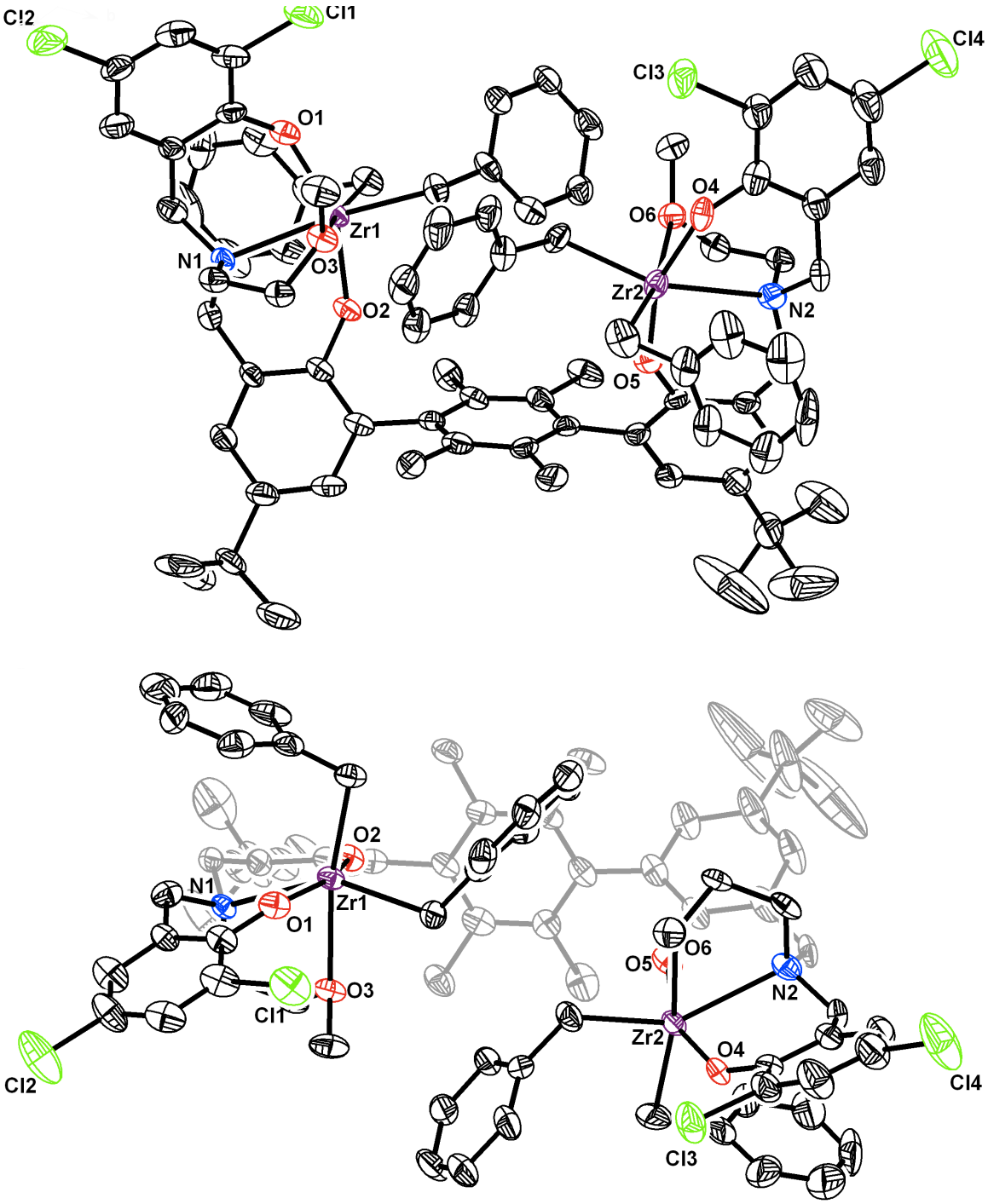

Figure 5.3. Side and top views of the solid-state structure of **53a-OMe** with thermal ellipsoids at the 50 % probability level. For clarity, hydrogen atoms and solvent molecules are omitted.

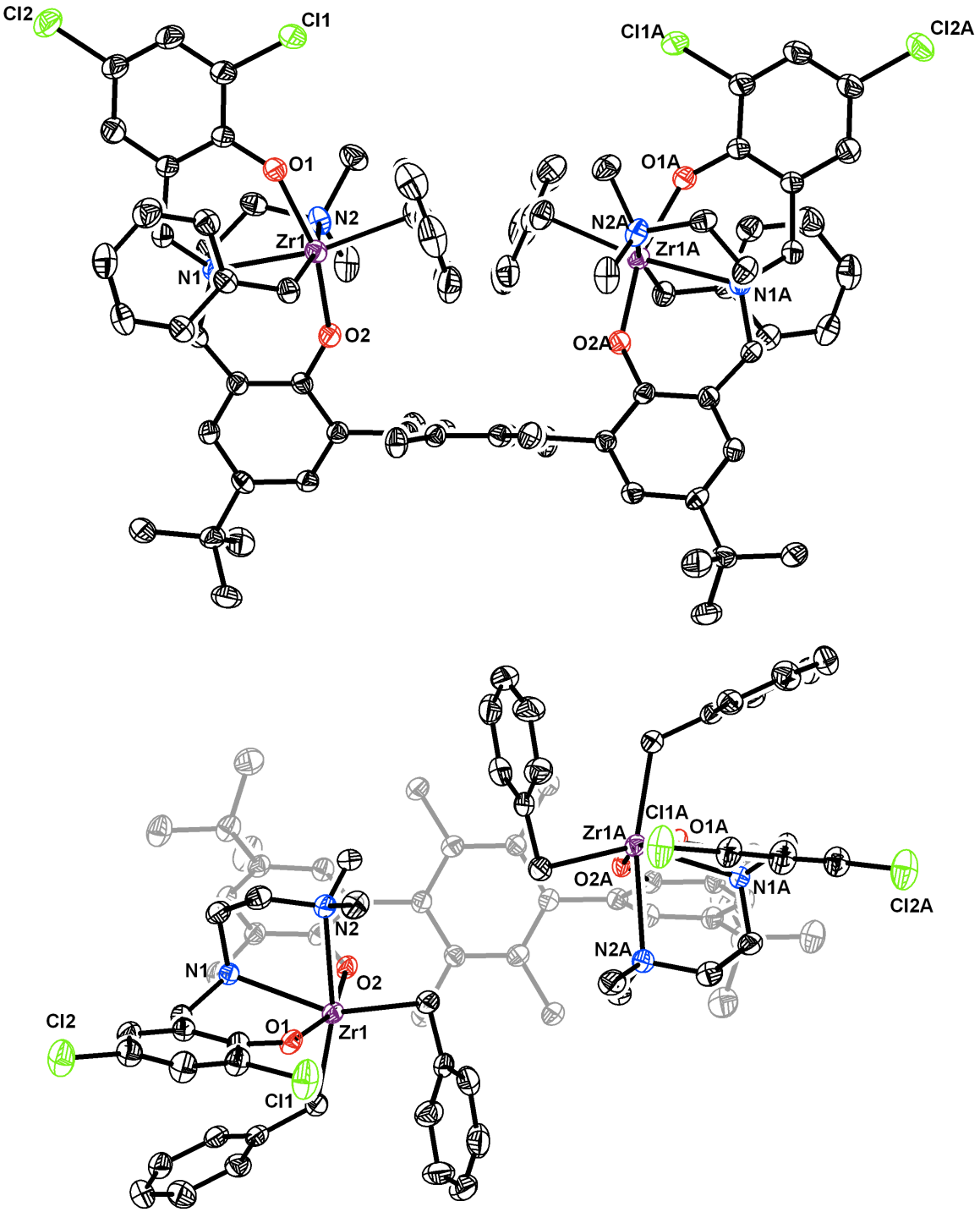

Figure 5.4. Side and top views of the solid-state structure of **53a-NMe$_2$** with thermal ellipsoids at the 50 % probability level. For clarity, hydrogen atoms and solvent molecules are omitted.

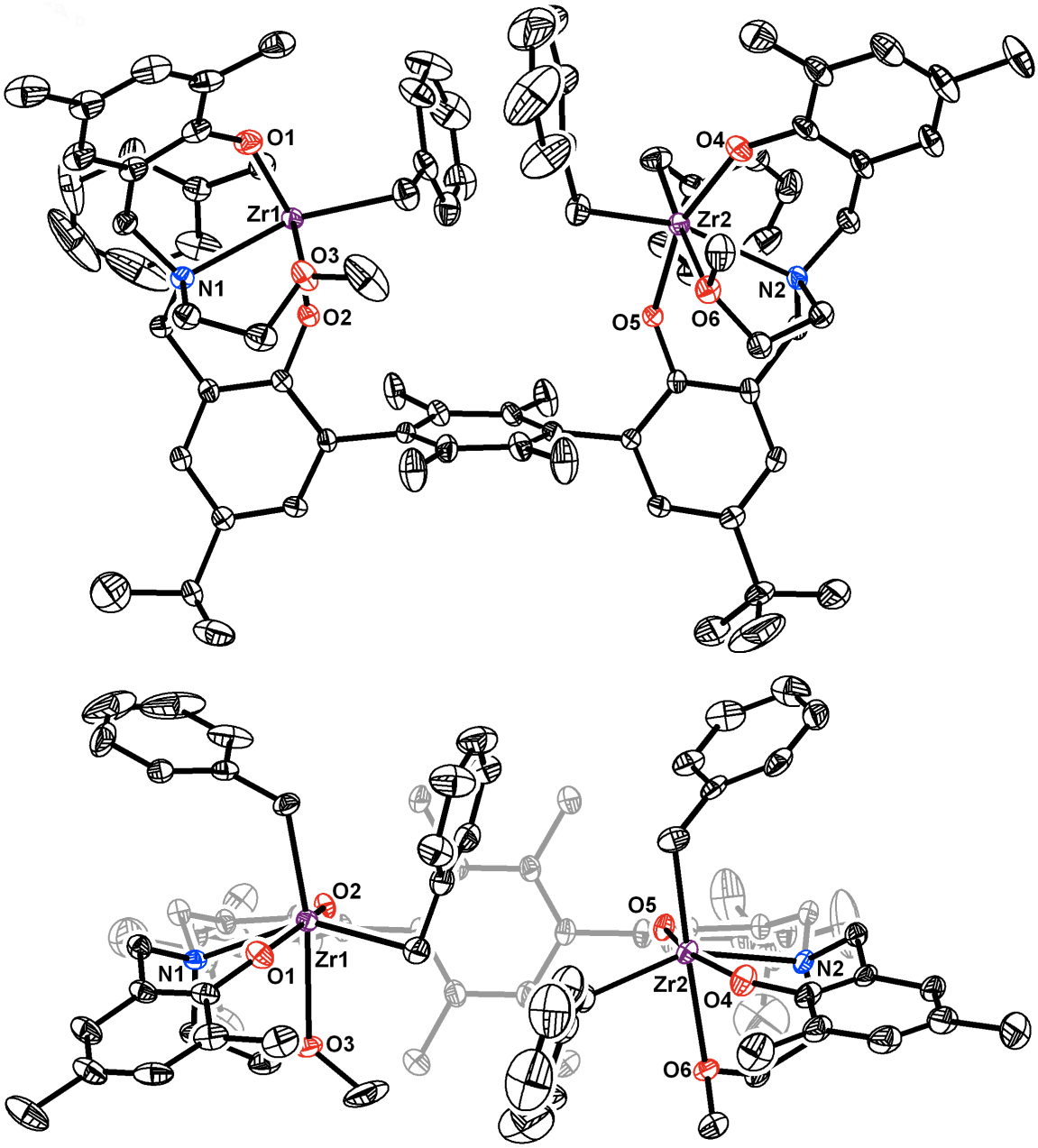

Figure 5.5. Side and top views of the solid-state structure of **53c-OMe** with thermal ellipsoids at the 50 % probability level. For clarity, hydrogen atoms and solvent molecules are omitted.

their relative integrations. The solid-state structure was obtained, identifying the second species as a *pseudo*-C_S symmetric metallation isomer (Figure 5.5). For this structure, a Zr–Zr distance of 7.3 Å was measured and the side aryls of the terphenyl were closer to perpendicular relative to the central arene.

1-Hexene polymerizations

Having obtained pure **53-X**, these complexes were tested for 1-hexene polymerization (Tables 5.1 and 5.2). Literature complexes **54-X** (Chart 5.2),[22] were also tested for polymerization activity under identical conditions. The monometallic and bimetallic catalysts were both very active for 1-hexene polymerization causing a significant exotherm upon stoichiometric activation with $[CPh_3][B(C_6F_5)_4]$ diluted in 2.5 mL chlorobenzene. Indeed, in polymerizations run lasting between 2 and 20 minutes, greater than 60 % of the 2.5 mL of 1-hexene used had been converted to poly-1-hexene (Table 5.1).

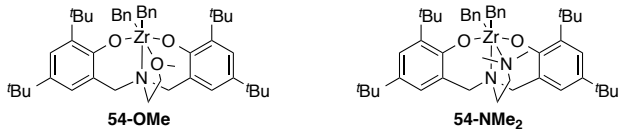

Chart 5.2. Literature monozirconium amine bisphenolate complexes used herein.

^{13}C NMR spectrum of the polymer made with the bimetallic catalyst systems displayed 6 broad singlets rather than multiplets, indicative of enhanced stereoregularity (Figure 5.6).[41] Integration of the ^{13}C NMR spectra was used to determine the stereoregularity of the polymers.[41] As expected from literature reports, **54-X**[22] produced stereoirregular polymers with 6 to 10 % *mmmm* (Table 5.1, entries 1–4). In contrast, the bimetallic complexes produced polymers with increased isotacticity such that % *mmmm* values between 17 and 50 were observed (Table 5.1, entries 5–19). The isotacticity of

the polymers obtained by the bimetallic complexes follows the trend **53a-OMe** > **53b-OMe** > **53a-NMe$_2$** > **53b-NMe$_2$** > **53c-OMe** > **53d-OMe**. Compounds with the same phenoxide substituents, but different X donors, produced polymers with different activity (precatalysts with NMe_2 donors were more active) and stereoregularity (precatalysts with OMe donors produced polymers with higher isotacticity). Using a mixture of the two metallation isomers for **53a-OMe** or **53a-NMe$_2$** did not alter either the activity or the stereoselectivity of the complexes (Table 5.1, entries 9 and 12). Similarly, in the case of **53c-OMe**, where the second isomer was isolated and purified, polymerizations with each isomer were found to be very similar in activity and stereoselectivity (Table 5.1, entry 16). These data imply that the relative orientation of the coordination sites involved in polymerization does not effect their stereoselectivity.

Table 5.1. 1-Hexene polymerizations.[a]

entry	complex	time (min)	yield (g)	conversion of 1-hexene (%)	activity[b]	% *mmmm*[c]
1	**54-OMe**	10	1.60	95	2.4	6
2	**54-OMe**	10	1.62	96	2.4	6
3	**54-OMe**	10	1.58	94	2.4	6
4	**54-NMe$_2$**	10	1.56	93	2.3	10
5	**53a-OMe**	20	1.34	80	1.0	44
6	**53a-OMe**	20	1.32	79	1.0	44
7	**53a-OMe**	20	1.19	71	0.9	50
8	**53a-OMe**	10	1.00	60	1.5	43
9	**53a-OMe**[d]	10	1.08	64	1.6	45
10	**53a-NMe$_2$**	10	1.45	86	2.2	35
11	**53a-NMe$_2$**	2	1.39	83	10.4	36
12	**53a-NMe$_2$**[d]	2	1.04	62	7.8	39
13	**53b-OMe**	20	1.45	86	1.1	46
14	**53b- NMe$_2$**	2	1.12	67	8.4	30
15	**53c-OMe**	20	1.27	76	1.0	29
16	**53c-OMe**[e]	20	1.36	81	1.0	28
17	**53d-OMe**	20	1.54	92	1.2	19
18	**53d-OMe**	20	1.37	82	1.0	17
19	**53d-OMe**	20	1.40	83	1.1	19

[a]Polymerizations were run at ambient temperature with 5000 equivalents of 1-hexene (2.5 mL, 1.683 g) in chlorobenzene (2.5 mL) with 4 μmol [Zr] and 1 equivalent of $[CPh_3][B(C_6F_5)_4]$ per zirconium. [b]Activity, defined as mass of polymer (in kg) per mmol of Zr per hour. [c]Determined by integration of the C3 peak in the ^{13}C NMR spectra as demonstrated in the literature.[41] [d]Mixture of metallation isomers. [e]*pseudo-C*$_s$ symmetric metallation isomer.

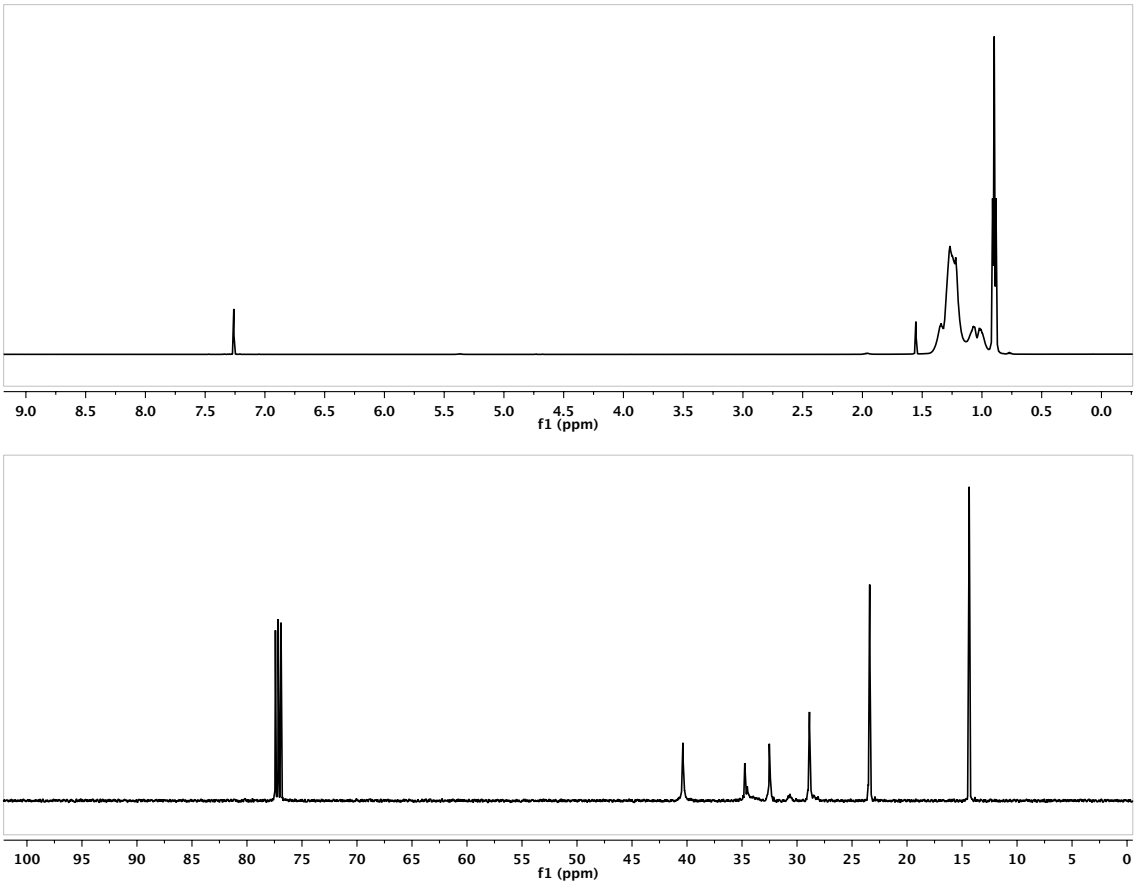

Figure 5.6. ^{1}H (top) and ^{13}C (bottom) NMR spectra in $CDCl_3$ of poly(1-hexene) made with **53a-OMe** at ambient temperature.

Further 1-Hexene homopolymerization trials were performed with the most active (**53a-NMe$_2$**) and most stereoselective (**53a-OMe**) precatalysts to determine the effect of activator and solvent (Table 5.2, entries 9–16). Literature complexes **54-X** were also tested under these conditions as controls (Table 5.2, entries 1–8). Variations of the solvent from PhCl to toluene did not have a significant effect on **54-X**, but greatly reduced the activity of **53a-X**. The drop in activity for the bimetallic systems probably reflects the insolubility of the active catalyst in toluene. Switching to alternate activators (stoichiometric $B(C_6F_5)_4$ or excess MAO (250 equivalents)) likewise did not significantly effect polymerizations with **54-X**, but decreased the activity observed for **53a-X**. Once

more, insolubility of the active species may have contributed to the lower activity, especially in the case of activation of **53a-OMe** with $B(C_6F_5)_4$ where inhomogeneity was visually observed throughout the polymerization reaction. The isotacticity of the polymer made with **53a-NMe$_2$** using excess MAO as the activator was increased by more than 10 % relative to the polymers produced with the stoichiometric activators, but this was accompanied by the aforementioned decrease in activity. Polymerization reactions under conditions that resulted in lower activity did not exotherm as strongly as the cases with higher activity. The increase in isoselectivity of **53a-NMe$_2$** in toluene or with MAO may have stemmed from a decrease in temperature rather than from the use of a different solvent or activator (vide infra).

Table 5.2. 1-Hexene polymerizations varying activators and solvent.[a]

entry	complex	activator	solvent	time (min)	yield (g)	activity[b]	% *mmmm*[c]
1	**54-OMe**	$[CPh_3][(B_6F_5)_4]$	PhCl	10	1.60	2.4	6
2	**54-OMe**	$[CPh_3][(B_6F_5)_4]$	toluene	10	1.61	2.4	6
3	**54-OMe**	$(B_6F_5)_3$	PhCl	10	1.36	2.1	6
4	**54-OMe**	MAO	PhCl	10	1.51	2.3	5
5	**54-NMe$_2$**	$[CPh_3][(B_6F_5)_4]$	PhCl	10	1.56	2.3	10
6	**54-NMe$_2$**	$[CPh_3][(B_6F_5)_4]$	toluene	10	1.57	2.4	9
7	**54-NMe$_2$**	$(B_6F_5)_3$	PhCl	10	1.51	2.3	6
8	**54-NMe$_2$**	MAO	PhCl	10	1.58	2.4	7
9	**53a-OMe**	$[CPh_3][(B_6F_5)_4]$	PhCl	10	1.00	1.5	43
10	**53a-OMe**	$[CPh_3][(B_6F_5)_4]$	toluene	10	0.17	0.3	50
11	**53a-OMe**	$(B_6F_5)_3$	PhCl	10	0.01	0.01	nm[d]
12	**53a-OMe**	MAO	PhCl	10	0.01	0.01	nm[d]
13	**53a-NMe$_2$**	$[CPh_3][(B_6F_5)_4]$	PhCl	10	1.45	2.2	35
14	**53a-NMe$_2$**	$[CPh_3][(B_6F_5)_4]$	toluene	10	0.36	0.5	40
15	**53a-NMe$_2$**	$(B_6F_5)_3$	PhCl	10	1.42	2.1	33
16	**53a-NMe$_2$**	MAO	PhCl	10	1.21	1.8	53

[a]Polymerizations were run at ambient temperature with 5000 equivalents of 1-hexene (2.5 mL, 1.683 g) in the desired solvent (2.5 mL) with 4 μmol [Zr] and 1 equivalent of $[CPh_3][B(C_6F_5)_4]$ or $B(C_6F_5)_3$ or 250 equivalents of MAO per zirconium. [b]Activity, defined as mass of polymer (in kg) per mmol of Zr per hour. [c]Determined by integration of the C3 peak in the ^{13}C NMR spectra as demonstrated in the literature.[41] [d]Not measured due to insufficient sample size (< 10 mg).

Propylene polymerizations

Polymerizations of propylene were also run with precatalysts **53-X** and **54-X** using MAO as an activator and scavenger (Tables 5.3 and 5.4). As with the 1-hexene polymerizations, the bimetallic complexes produced isotactically enriched polymer as determined by ^{13}C NMR spectroscopy.[8,41,42] The first polymerizations attempted utilized 1000 equivalents of MAO and, under these conditions, very low activity was observed for **53a-OMe**. Reducing the number of equivalents of MAO to 250 improved the activity of **53a-OMe**, though isoselectivity was also reduced slightly. The isotacticity of the propylene polymers obtained by the bimetallic complexes (with 250 equivalents of MAO) follows the trend **53a-OMe** > **53c-OMe** > **53b-NMe$_2$** > **53a-NMe$_2$** > **53b-OMe** > **53d-OMe**. The precatalysts bearing NMe_2 donors proved to be significantly more active than their methoxy analogs, and optimization of the polymerization conditions for isoselectivity was attempted by concurrently decreasing precatalyst loading and increasing the equivalents of MAO. At 75-fold reduction of [Zr] and 60-fold increase in MAO equivalents (15000 equivalents of MAO), 43 % *mmmm* and 4.7 * 10^4 (g polypropylene)(mmol Zr)$^{-1}$(h)$^{-1}$ were achieved with **53a-NMe$_2$** (Table 5.3, entry 17). Reducing the temperature of the reaction to -30 °C did not improve the observed stereoselectivity (Table 5.3, entry 18).

The effects of solvent and activator were investigated (Tables 5.3 and 5.4). Using the optimized conditions for **53a-X** and changing the solvent to toluene led to slight reduction of isoselectivity for both catalysts (Table 5.3, entries 7 and 19). The activity of **53a-OMe** increased slightly, whereas the activity of **53a-NMe$_2$** decreased by an order of magnitude, potentially reflecting poor solubility. Employing 3 equivalents of

Table 5.3. Propylene polymerizations using MAO as an activator and scavenger.[a]

entry	complex	precatalyst loading in μmol	MAO/Zr	solvent	time (min)	yield (g)	activity[b]	% *mmmm*[c]
1	**54-OMe**	10	1000	PhCl	240	3.11	0.08	2
2	**54-OMe**	10	500	PhCl	110	6.01[d]	0.3	2
3	**54-OMe**	10	250	PhCl	100	6.31[d]	0.4	2
4	**54-OMe**	10	250	PhCl	15	0.72	0.3	2
5	**53a-OMe**	5	1000	PhCl	240	0.02	--	35
6	**53a-OMe**	5	250	PhCl	240	0.42	0.01	29
7	**53a-OMe**	5	250	toluene	240	1.34	0.03	26
8	**53b-OMe**	5	250	PhCl	240	3.90	0.1	20
9	**53c-OMe**	5	250	PhCl	240	1.59	0.04	27
10	**53d-OMe**	5	1000	PhCl	240	0.49	0.01	6
11	**53d-OMe**	5	250	PhCl	60	5.53[d]	0.6	8
12	**53d-OMe**	5	250	PhCl	15	5.30	2.1	7
13	**54-NMe_2**	10	250	PhCl	2	4.14	12	5
14	**54-NMe_2**	0.13	15000	PhCl	10	0.01	0.2	4
15	**53a-NMe_2**	5	250	PhCl	4	5.15[d]	7.7	22
16	**53a-NMe_2**	1	1000	PhCl	6	3.44	17	31
17	**53a-NMe_2**	0.07	15000	PhCl	10	1.04	47	43
18	**53a-NMe_2**	0.07	15000	PhCl[e]	180	0.67	1.6	44
19	**53a-NMe_2**	0.07	15000	toluene	10	0.09	4.0	38
20	**53b-NMe_2**	5	250	PhCl	3	4.75	9.5	26
21	**53b-NMe_2**	0.07	15000	PhCl	10	0.53	23	20

[a]Polymerizations were run at 0 ºC with 10.3 mL liquid propylene (measured at 0 ºC) in 2 mL of the desired solvent. [b]Activity, defined as mass of polymer (in kg) per mmol of Zr per hour. [c]Determined by integration of the methyl peak in the ^{13}C NMR spectra as demonstrated in the literature.[8,41-42] [d]The stirbar was arrested within the polymerization time. [e]Run at -30 ºC.

Table 5.4. Propylene polymerizations using $[CPh_3][(B_6F_5)_4]$ (3 equivalents) as an activator and Al^iBu_3 (35 equivalents) as a scavenger.[a]

entry	complex	precatalyst loading in μmol	time (min)	yield (g)	activity[b]	% *mmmm*[c]
1	**54-OMe**	10	50	5.81[d]	0.70	3
2[e]	**54-OMe**	10	50	4.40[d]	0.53	2
3	**53a-OMe**	5	240	0.50	0.01	17
4[e]	**53a-OMe**	5	240	0.27	0.01	13
5	**53b-OMe**	5	130	5.34	0.25	10
6[e]	**53c-OMe**	5	240	0.08	--	11
7[e]	**53d-OMe**	5	30	4.99[d]	1.00	19

[a]Polymerizations were run at 0 ºC with 15000 equivalents (10.3 mL) liquid propylene (measured at 0 ºC) in 2 mL of chlorobenzene. [b]Activity, defined as mass of polymer (in kg) per mmol of Zr per hour. [c]Determined by integration of the methyl peak in the ^{13}C NMR spectra as demonstrated in the literature.[8,41-42] [d]The stirbar was arrested within the polymerization time. [e]Order of addition was changed so that the Zr precatalyst was added last.

$[CPh_3][B(C_6F_5)_4]$ and 35 equivalents of Al^iBu_3 as activator and scavenger, respectively, led to similar yields, but considerably decreased stereoselectivity for complexes **53-OMe** (Table 5.4). Significant changes in activity and tacticity upon switching between activators have previously been attributed to different catalyst–counteranion interactions, which may affect the rate of site epimerization.[18,43]

Synthesis of monometallic control complexes

The bimetallic systems combine the high activity of the monometallic analogues with increased stereoregularity and investigation into the mechanisms that lead to this desirable combination could prove useful in the further development of polymerization catalysts. To that end, four monometallic controls were synthesized using analogous procedures to those for the bimetallic complexes (Scheme 5.3). Complexes **57-X** were targeted to determine whether steresoselectivity could be engendered in a monometallic system via desymmetrization. Complexes **61-X** were targeted to determine if steric interactions with the central arene are responsible for stereoselectivity in the bimetallic systems. These monometallic complexes were characterized by ^1H and ^{13}C NMR spectroscopy, which indicated the expected asymmetry such that, for example, none of the benzyl protons are the same. X-ray diffraction (XRD) studies of **57-OMe** revealed a structure very similar to the C_S symmetric literature complexes (Figure 5.7).[20,22]

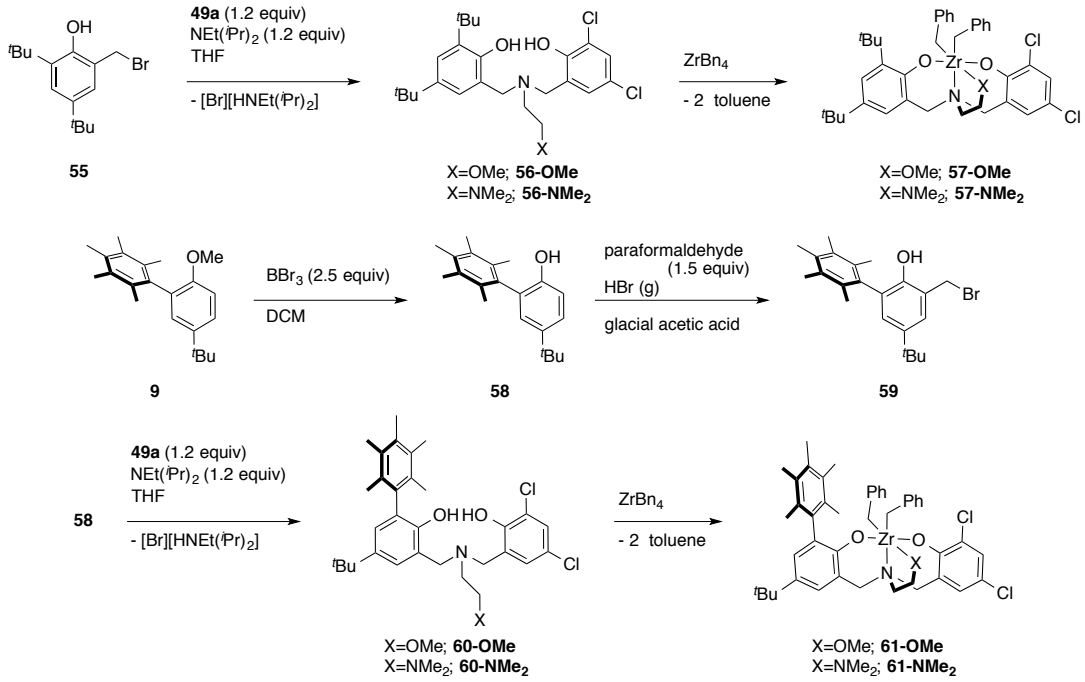

Scheme 5.3. Synthesis and metallation of mononucleating ligands.

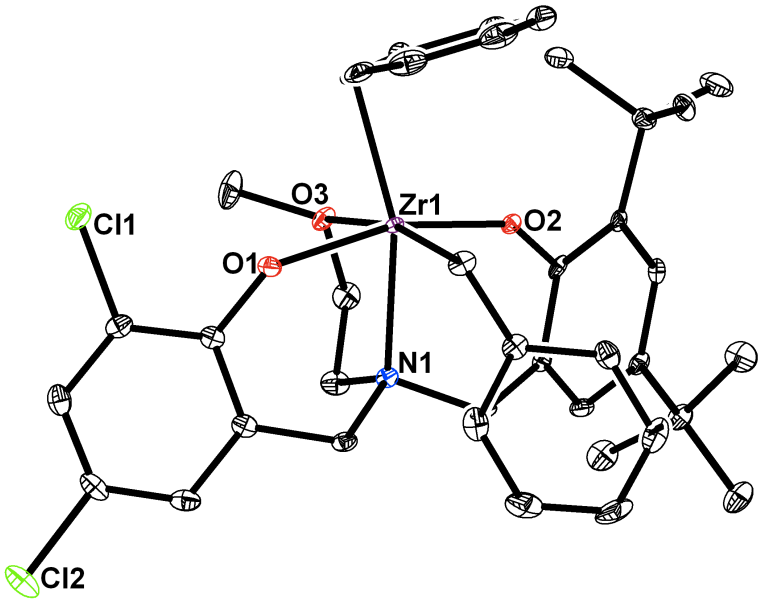

Figure 5.7. Side and top views of the solid-state structure of **56-OMe** with thermal ellipsoids at the 50 % probability level. For clarity, hydrogen atoms are omitted.

Comparison of the polymerization activity of the mono- and bi-metallic complexes

1-Hexene and propylene polymerizations were performed with **57-X** and **61-X** to compare with the bimetallic analogues (Tables 5.5 and 5.6). **57-X** produced stereoirregular polymers (Table 5.5, entries 1–10; Table 5.6, entries 1 and 2). In contrast, **61-X** produced polymers with some isotactic enhancement (Table 5.5, entries 11–20; Table 5.6, entries 3–7), though in lower quantities than with the analogous bimetallics and at lower activities. Comparison of the ^{13}C NMR spectra of the polypropylene samples illustrates the differences in the polymers (Figures 5.8 and 5.9). **57-OMe** and **61-OMe** both produce stereoirregular polymers with regioerrors. Conversely, regioerrors are not seen in polymers produced by **57-NMe$_2$** or **61-NMe$_2$**. Polymers produced by **53a-OMe**, **53a-NMe$_2$** and **61-NMe$_2$** have the same pentads present, but for **61-NMe$_2$** the *mmmr* and *mmrr* peaks are much larger indicating a higher number of stereoerrors for the monometallic complex in propylene polymerizations.

Polymerizations of 1-hexene were exothermic and high conversions of the monomer were observed, but disparities were observed in exotherm intensity in different complexes. Variation of the polymerization temperature and decreased concentration of the precatalysts were therefore expected to yield results more representative of the catalysts' capabilities. Complexes **53a-X**, **57-X**, and **61-X** were tested at various temperatures and concentrations (Table 5.7; Figures 5.10 and 5.11). Reducing the concentration of zirconium complex 2-fold from previous trials (Tables 5.1, 5.2 and 5.5) revealed that **53a-NMe$_2$** is an order of magnitude more active than **53a-OMe**, though under the same conditions, **53a-OMe**, yields more isotactic polymers achieving up to 76 % *mmmm* at –30 °C (Table 5.7, entry 7). Optimization of activity, at

Table 5.5. 1-Hexene polymerizations with monometallic complexes **57-X** and **61-X**.[a]

entry	complex	activator	solvent	time (min)	yield (g)	activity[b]	% *mmmm*[c]
1	**57-OMe**	$[CPh_3][(B_6F_5)_4]$	PhCl	20	1.55	1.2	9
2	**57-OMe**	$[CPh_3][(B_6F_5)_4]$	PhCl	20	1.58	1.2	8
3	**57-OMe**	$[CPh_3][(B_6F_5)_4]$	toluene	10	0.58	0.9	8
4	**57-OMe**	$(B_6F_5)_3$	PhCl	10	0.59	0.9	8
5	**57-OMe**	MAO	PhCl	10	--	--	nm[d]
6	**57-NMe$_2$**	$[CPh_3][(B_6F_5)_4]$	PhCl	10	1.43	2.2	8
7	**57-NMe$_2$**	$[CPh_3][(B_6F_5)_4]$	PhCl	10	1.42	2.1	8
8	**57-NMe$_2$**	$[CPh_3][(B_6F_5)_4]$	toluene	10	0.80	1.2	6
9	**57-NMe$_2$**	$(B_6F_5)_3$	PhCl	10	1.27	1.9	7
10	**57-NMe$_2$**	MAO	PhCl	10	0.24	0.4	10
11	**61-OMe**	$[CPh_3][(B_6F_5)_4]$	PhCl	10	0.14	0.2	25
12	**61-OMe**	$[CPh_3][(B_6F_5)_4]$	PhCl	10	0.09	0.1	24
13	**61-OMe**	$[CPh_3][(B_6F_5)_4]$	toluene	10	0.09	0.1	26
14	**61-OMe**	$(B_6F_5)_3$	PhCl	10	0.13	0.2	27
15	**61-OMe**	MAO	PhCl	10	0.01	0.01	nm[d]
16	**61-NMe$_2$**	$[CPh_3][(B_6F_5)_4]$	PhCl	10	0.97	1.5	31
17	**61-NMe$_2$**	$[CPh_3][(B_6F_5)_4]$	PhCl	10	1.28	1.9	32
18	**61-NMe$_2$**	$[CPh_3][(B_6F_5)_4]$	toluene	10	1.22	1.8	39
19	**61-NMe$_2$**	$(B_6F_5)_3$	PhCl	10	1.24	1.9	30
20	**61-NMe$_2$**	MAO	PhCl	10	1.09	1.6	25

[a]Polymerizations were run at ambient temperature with 5000 equivalents of 1-hexene (2.5 mL, 1.683 g) in the desired solvent (2.5 mL) with 4 μmol [Zr] and 1 equivalent of $[CPh_3][B(C_6F_5)_4]$ or $B(C_6F_5)_3$ or 250 equivalents of MAO per zirconium. [b]Activity, defined as mass of polymer (in kg) per mmol of Zr per hour. [c]Determined by integration of the C3 peak in the ^{13}C NMR spectra as demonstrated in the literature.[41] [d]Not measured due to insufficient sample size (< 10 mg).

Table 5.6. Propylene polymerizations with monometallic complexes **57-X** and **61-X**.[a]

entry	complex	precatalyst loading in μmol	MAO/Zr	solvent	time (min)	yield (g)	activity[b]	% *mmmm*[c]
1	**57-OMe**	10	250	PhCl	240	0.43	0.01	3
2	**57-NMe$_2$**	0.13	15000	PhCl	35	0.41	5.3	4
3	**61-OMe**	10	250	PhCl	900	0.41	--	6
4	**61-OMe**	10	250	PhCl	240	0.07	--	4
5	**61-NMe$_2$**	2	1000	PhCl	180	0.80	0.1	22
6	**61-NMe$_2$**	0.13	15000	PhCl	180	1.15	2.9	31
7	**61-NMe$_2$**	0.13	15000	PhCl	180	0.27	0.7	32

[a]Polymerizations were run at 0 °C with 10.3 mL liquid propylene (measured at 0 °C) in 2 mL of the desired solvent. [b]Activity, defined as mass of polymer (in kg) per mmol of Zr per hour. [c]Determined by integration of the methyl peak in the ^{13}C NMR spectra as demonstrated in the literature.[8,41-42] [d]The stirbar was arrested within the polymerization time. [e]Run at -30 °C.

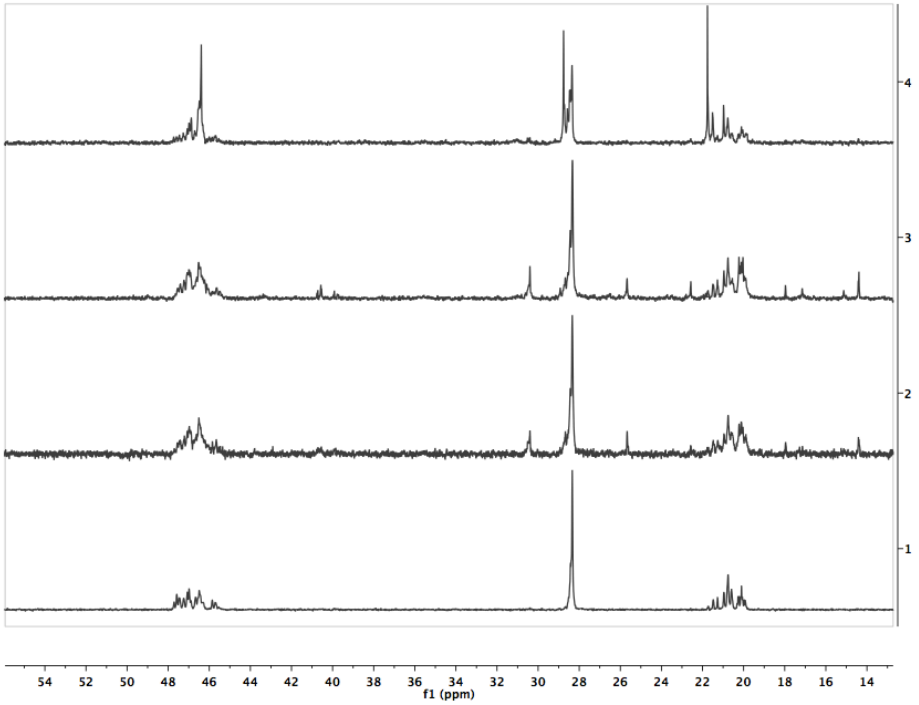

Figure 5.8. ^{13}C NMR spectra in tetrachloroethane-D_2 at 130 °C of polypropylene made with (from bottom to top) **54-OMe** (1), **57-OMe** (2), **61-OMe** (3), and **53a-OMe** (4).

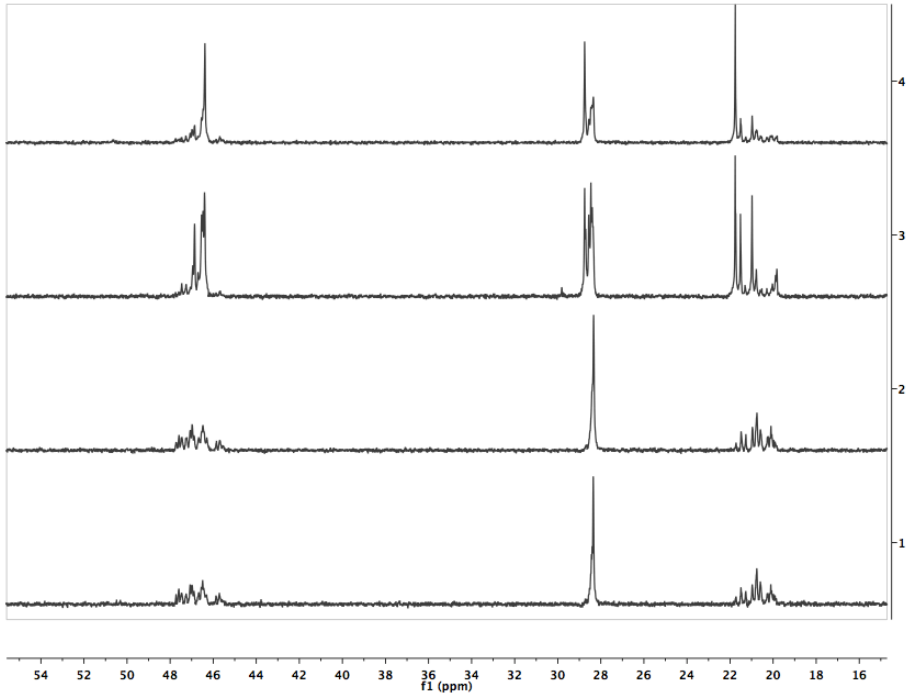

Figure 5.9. ^{13}C NMR spectra in tetrachloroethane-D_2 at 130 °C of polypropylene made with (from bottom to top) **54-NMe$_2$** (1), **57-NMe$_2$** (2), **61-NMe$_2$** (3), and **53a-NMe$_2$** (4).

$1.23 * 10^5$ (g poly(1-hexene))(mmol Zr)$^{-1}$(h)$^{-1}$, was achieved by 5-fold further reduction in **53a-NMe$_2$** concentration at ambient temperature (Table 5.7, entry 25). Reduction of the temperature to -30 °C again had a significant impact on the stereoselectivity and poly(1-hexene) with 79 % *mmmm* was obtained. This polymer also exhibited high molecular weight of $1.2 * 10^6$ Daltons and low polydispersity of 1.1 as determined by size exclusion chromatography. Precatalysts **57-X** produced stereoirregular polymers at all temperatures and were an order of magnitude less active than their bimetallic analogues. **61-OMe** and **61-NMe$_2$** produced polymers with about 25 and 35 % *mmmm*, respectively, though this quantity was not altered by temperature. Activity of **61-X** decreased with temperature, as expected, and was consistently lower than the bimetallic counterparts. The differences in activity between the mono and bimetallic systems are not well understood at this point. The results with complexes **61-X** show that the central arene is partially responsible for the observed stereochemistry, but also that the "local" symmetry and sterics cannot be used to fully explain the reactivity observed with the bimetallic systems.

Table 5.7. 1-Hexene polymerizations at various temperatures. [a]

entry	complex, loading in μmol	A, S[b]	T (°C)	time (min)	yield (g)	activity[c]	% *mmmm*[d]	M_n (x10^3)[e]	PDI[e]
1	**53a-OMe, 1**	1, 5	ambient	10	0.75	2.3	50		
2	**53a-OMe, 1**	1, 5	60	10	0.67	2.0	37		
3	**53a-OMe, 1**	1, 5	25	10	0.65	2.0	53		
4	**53a-OMe, 1**	1, 5	25	10	0.68	2.0	47	108	1.8
5	**53a-OMe, 1**	1, 5	0	480	0.78	0.05	57	13.3	2.6
6	**53a-OMe, 1**	1, 5	0	480	0.70	0.04	45	21.6	2.4
7	**53a-OMe, 1**	1, 5	-30	480	0.01	--	76		
8	**57-OMe, 2**	1, 5	ambient	10	0.06	0.2	7		
9	**57-OMe, 2**	1, 5	60	10	0.12	0.4	7		
10	**57-OMe, 2**	1, 5	25	10	0.06	0.2	8		
11	**57-OMe, 2**	1, 5	0	480	0.11	0.01	9	7.8	2.0
12	**61-OMe, 2**	1, 5	ambient	10	0.01	0.02	nm[f]		
13	**61-OMe, 2**	1, 5	60	10	0.04	0.1	26		
14	**61-OMe, 2**	1, 5	25	10	0.04	0.1	23		
15	**61-OMe, 2**	1, 5	0	480	0.04	--	23	1.4	1.3
16	**53a-NMe_2, 1**	1, 5	ambient	1	1.17	35	38		
17	**53a-NMe_2, 1**	1, 5	60	1	0.65	19	33		
18	**53a-NMe_2, 1**	1, 5	25	2	1.28	19	33		
19	**53a-NMe_2, 1**	1, 5	0	2	1.42	21	38	110	3.6
20	**53a-NMe_2, 1**	1, 5	-20	5	1.51	9.0	58	217	3.0
21	**53a-NMe_2, 0.2**	3, 15	ambient	1	0.82	124	41		
22	**53a-NMe_2, 0.2**	3, 15	60	2	0.58	43	34		
23	**53a-NMe_2, 0.2**	3, 15	25	2	0.62	46	41	596	1.5
24	**53a-NMe_2, 0.2**	3, 15	0	8	1.39	26	48	517	1.6
25	**53a-NMe_2, 0.2**	3, 15	-30	10	0.18	2.7	79	1220	1.1
26	**57-NMe_2, 0.4**	3, 15	ambient	10	0.43	6.5	8		
27	**57-NMe_2, 0.4**	3, 15	60	10	0.24	3.6	7		
28	**57-NMe_2, 0.4**	3, 15	25	10	--	--	nm[f]		
29	**57-NMe_2, 0.4**	3, 15	0	60	0.03	0.01	11	281	1.2
30	**57-NMe_2, 0.4**	3, 15	-30	60	--	--	nm[f]		
31	**61-NMe_2, 0.4**	3, 15	ambient	10	0.58	8.7	34		
32	**61-NMe_2, 0.4**	3, 15	60	10	0.13	2.0	36		
33	**61-NMe_2, 0.4**	3, 15	25	10	0.58	8.7	32		
34	**61-NMe_2, 0.4**	3, 15	0	30	0.61	3.0	35	228	1.6
35	**61-NMe_2, 0.4**	3, 15	-30	480	0.17	0.01	33	346	1.4

[a]Polymerizations were run at the desired temperature with 2.5 mL of 1-hexene (1.683 g) in chlorobenzene (2.5 mL). [b]Activator and scavenger: $[CPh_3][(B_6F_5)_4]$ and Al^iBu_3 in equivalents per Zr. [c]Activity, defined as mass of polymer (in kg) per mmol of Zr per hour. [d]Determined by integration of the C3 peak in the ^{13}C NMR spectra as demonstrated in the literature.[41] [e]Determined by GPC. [f]Not measured due to insufficient sample size (< 10 mg).

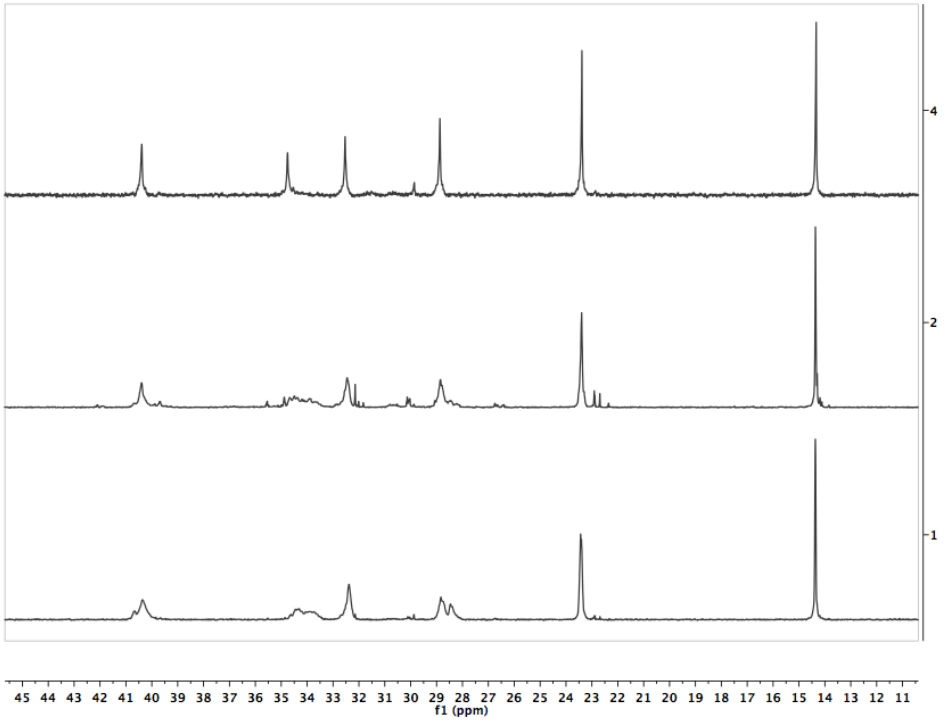

Figure 5.10. ^{13}C NMR spectra in $CDCl_3$ of poly(1-hexene) made with (from bottom to top) **57-OMe** at 0°C (1), **61-OMe** at 0°C (2), and **53a-OMe** at -30°C (3).

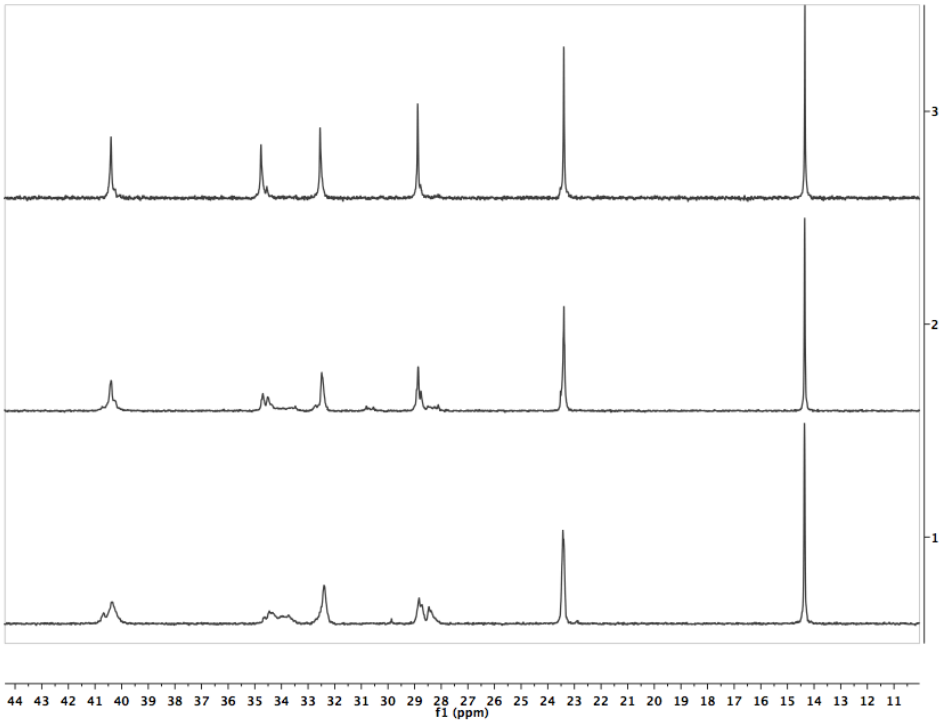

Figure 5.11. ^{13}C NMR spectra in $CDCl_3$ of poly(1-hexene) made with (from bottom to top) **57-NMe$_2$** at 0°C (1), **61-NMe$_2$** at -30°C (2), and **53a-NMe$_2$** at -30°C (3).

Mechanistic proposal

In enantiomorphic site control, the symmetry of the catalyst directs the orientation of the polymer chain, which, in turn, guides the orientation of the monomer such that the insertion step yields a specific stereochemistry.[1,3] Each metal center in the bimetallic systems, if viewed separately, is C_1-symmetric. As observed in the solid-state structure, however, the substituents on each phenoxide moiety eclipse only one of the two coordination sites involved in polymerization (i.e. the sites occupied by benzyl groups in the precatalyst), and would therefore only be expected to affect the orientation of the polymer chain when it is located in that site. An additional process is therefore required to engender isoselectivity. Taking the proximal metal center into consideration, it is expected that positioning of the polymer chain between the two metal centers would be disfavored by steric repulsion (Scheme 5.4). Site epimerization could occur to alleviate that repulsion, and the steric driving force for this process could explain the differences between monometallic systems, **61-X**, and the bimetallic systems, **53a-X**. For the monometallic systems, the polymer chain can be trans to either N or the X donor and the polymer chain can orient either "up" or "down" (towards one set of phenoxide substituents or the other). Though the "up" and "down" positions are sufficiently differentiated for some stereocontrol with **61-X**, several options for orientation and location of the polymer chain. For the bimetallic systems, the polymer chain prefers to be trans to X and thus eliminates some of the options present for the monometallic system. Together, the effects of the phenoxide substituents and the favorable site epimerization could account for the observed stereoselectivity trends.

Because the substituents on both phenoxide moieties affect the same site, the relative favorability of one orientation is improved as the difference in size of the two substituents increases. The permethylated central arene is very large relative to a chloride substituent, and therefore significant isoselectivity is observed with **53a-X**. On the other hand, the size difference between the permethylated central arene and a *tert*-butyl moiety is small, and the stereoselectivity of **53d-OMe** is correspondingly poor. Under the proposed mechanism, little difference is expected between the metallation isomers of a single complex because all of the factors affecting isoselectivity are the same, and this is confirmed in experimental observations.

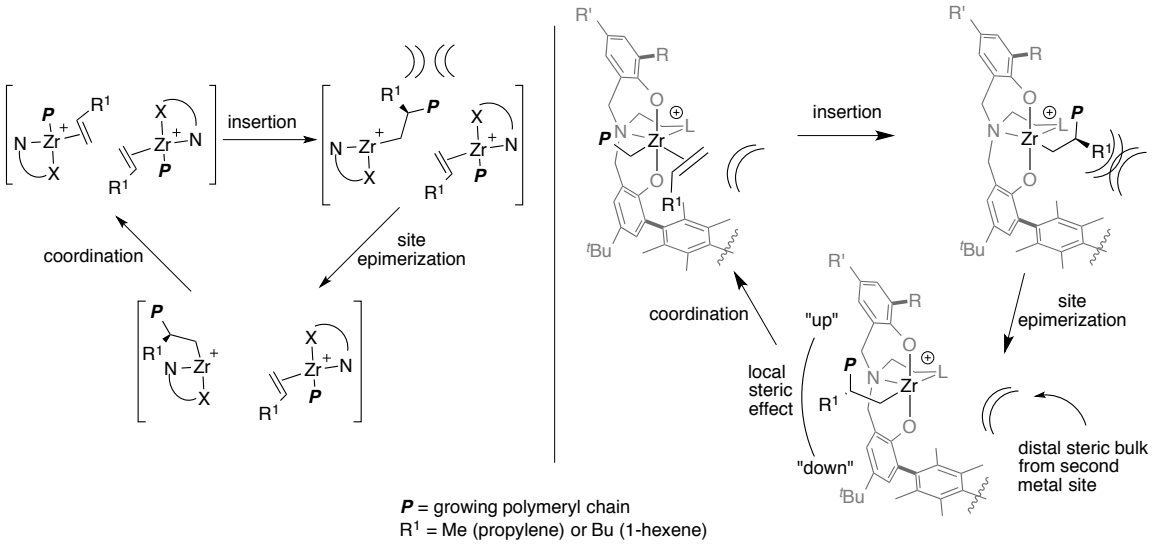

Scheme 5.4. Mechanism for tactic control by bimetallic complexes. Truncated top (left) and side (right) perspectives.

A two-site statistical model for stereospecific polymerization was presented by Chûjô and coworkers wherein one site is under enatiomorphic site control and the other follows a Bernoullian model.[44] The parameters of such a model are based on the probability of different stereoerrors in the polymers depending on the mechanisms involved.[45] Treatment of the data from propylene polymerizations with **53-X** reveals a

distribution of pentads that is not consistent with either strict enantiomorphic site control or chain-end control (Markovian or Bernoullian models). Instead, the values align with a two-site model, consistent with the proposed mechansim for the bimetallic systems.

CONCLUSIONS

In summary, we have synthesized a series of dizirconium di(amine bisphenolate) precatalysts that are effective for the isoselective polymerization of propylene and 1-hexene. Studies on the variation of the polymerization conditions including catalyst loading, activator, solvent and temperature were performed, and at low temperatures polymers with > 75 % *mmmm* could be obtained with the most stereoselective precatalysts (**53a-NMe_2** and **53a-OMe)**. Comparisons with a variety of monometallic analogues indicate that the isoselectivity of the bimetallic systems requires steric effects both in the immediate and secondary coordination spheres of the zirconium metal centers. A mechanism was proposed wherein one coordination site is controlled by the relative size of the phenolic substituents and site epimerization follows each insertion. This site epimerization is driven by the steric bulk of the proximal metal center; the polymer chain does not stay in between the two metal centers, a position which is disfavored sterically. Future efforts will focus on using these dizirconium catalyst systems to synthesize more complicated stereoregular materials based on monomers with additional functionality. Initial work on α-olefin/diene copolymerizations is presented in Appendix B.

EXPERIMENTAL SECTION

General considerations and instrumentation

All air- and/or water-sensitive compounds were manipulated using an inert atmosphere glovebox or standard Schlenk line techniques with an N_2 atmosphere. The solvents for air- and moisture-sensitive reactions were dried over sodium/benzophenone ketyl, calcium hydride, or by the method of Grubbs.[46] All NMR solvents were purchased from Cambridge Isotopes Laboratories, Inc. Toluene for polymerizations and C_6D_6 were dried over sodium/benzophenone ketyl and vacuum transferred prior to use. Chlorobenzene and 1-hexene for polymerizations were refluxed over CaH_2 for greater than 72 h and vacuum transferred prior to use. Toluene, C_6D_6, chlorobenzene, and 1-hexene were further purified by filtration over activated alumina. Propylene was purchased from Matheson and equipped with a PUR-Gas in-line trap to remove oxygen and moisture before use. All ^1H and ^{13}C NMR spectra of small organic and organometallic compounds were recorded on Varian Mercury 300 MHz, Varian 400 MHz, or Varian INOVA-500 or 600 MHz spectrometers at room temperature. ^1H and ^{13}C NMR spectra of poly(1-hexene) samples were recorded on a Varian INOVA-500 MHz spectrometer at room temperature in $CDCl_3$. ^1H and ^{13}C NMR spectra of polypropylene samples were recorded on a Varian INOVA-500 MHz spectrometer at 130 °C in tetrachloroethane-D_2. For ^1H and ^{13}C NMR spectra, chemical shifts are reported with respect to residual internal deuterated solvent: 7.16 and 128.06 (t) ppm (C_6D_6); 7.26 and 77.16 (t) ppm ($CDCl_3$); 6.00 and 74.22 (t) ppm ($C_2D_2Cl_4$); for ^1H and ^{13}C data. J coupling are reported in Hz. Combustion analyses (C, H, and N) were performed by Robertson Microlit Laboratories, Ledgewood, NJ.

Synthetic protocols

2-hydroxybenzaldehydes **47c** and **47d**,[47,48] 2-(bromomethyl)-4,6-bis(*tert*-butyl)phenol (**55**),[40] **54-OMe**,[22] and **54-NMe$_2$**[20] were synthesized according to literature procedures. Diphenyl **9** and terphenyl **3** were synthesized according to literature procedures and the latter was obtained as a mixture of the syn and anti atropisomers.[36]

$ZrBn_4$ was synthesized by alteration of literature procedures.[49,50] All of the manipulations to synthesize $ZrBn_4$ were performed in the dark because the product is light sensitive. Solid benzylmagnesium chloride (20 g, 4.5 equiv) and 180 mL of Et_2O were added to a 500 mL round bottom flask with a stirbar and frozen in the glovebox cold well. $ZrCl_4$ (7 g) was added as a solid in portions to the thawing Grignard. The resulting mixture was stirred (allowing it to warm to ambient temperature) for 4 h before volatiles were removed under vacuum. Hexanes (20 mL) were added to the residue and the slurry was filtered over Celite. The precipitate was then washed with more hexanes (20 mL x 2), Et_2O (20 mL x 2), and toluene (20 mL x 4). The filtrates were combined and the volatiles were removed under vacuum to yield the product as a crystalline orange solid (4.9 g, 36 % yield).

General synthesis of phenoxyimines 48-X. 2-methoxyethylamine or *N*,*N*-dimethylethylenediamine (1 equiv), 2-hydroxybenzaldehydes **47** (1 equiv) and MeOH (4 mL per mmol **47**) were added to a round bottom flask equipped with a stirbar and a reflux condenser and heated to reflux with stirring for 12 h over which time the reaction mixture turned bright yellow. The reaction mixture was cooled to room temperature and volatiles were removed under vacuum to yield imines **48-X**.

Compound 48a-OMe. 48a-OMe was collected in quantitative yield as an orange solid. ^{1}H NMR (300 MHz, $CDCl_3$) δ = 14.45 (s, 1H, ArO*H*), 8.25 (t, *J*=1.1, 1H, C*H*N), 7.40 (d, *J*=2.5, 1H, Ar), 7.15 (d, *J*=2.5, 1H, Ar), 3.79 (t, *J*=5.4, 2H, CH_2), 3.66 (t, *J*=5.4, 2H, CH_2), 3.35 (s, 3H, OCH_3) ppm. ^{13}C NMR (101 MHz, $CDCl_3$) δ = 164.95 (*C*HN), 157.83 (Ar), 132.47 (Ar), 129.20 (Ar), 123.32 (Ar), 122.25 (Ar), 119.30 (Ar), 71.33 (O*C*H_3), 59.17 (*C*H_2), 57.95 (*C*H_2) ppm.

Compound 48a-NMe$_2$. 48a-NMe$_2$ was collected in quantitative yield as an orange oil. ^{1}H NMR (400 MHz, $CDCl_3$) δ = 8.24 (s, 1H, C*H*N), 7.39 (d, *J*=2.4, 1H, Ar), 7.12 (d, *J*=2.4, 1H, Ar), 3.74 (t, *J*=6.3, 2H, CH_2), 2.68 (t, *J*=6.3, 2H, CH_2), 2.31 (s, 6H, N(CH_3)$_2$) ppm. ^{13}C NMR (101 MHz, $CDCl_3$) δ = 164.41 (*C*HN), 158.56 (Ar), 132.64 (Ar), 129.20 (Ar), 123.58 (Ar), 121.85 (Ar), 118.93 (Ar), 59.31 (*C*H_2), 55.63 (*C*H_2), 45.67 (N(*C*H_3)$_2$) ppm.

Compound 48b-OMe. 48b-OMe was collected in quantitative yield as a yellow solid. ^{1}H NMR (300 MHz, $CDCl_3$) δ = 8.21 (s, 1H, C*H*N), 7.69 (d, *J*=2.3, 1H, Ar), 7.33 (d, *J*=2.3, 1H, Ar), 3.79 (t, *J*=5.0, 2H, CH_2), 3.65 (t, *J*=5.1, 2H, CH_2), 3.35 (s, 3H, OCH_3) ppm. ^{13}C NMR (101 MHz, $CDCl_3$) δ = 164.80 (*C*HN), 159.46 (Ar), 137.96 (Ar), 132.96 (Ar), 119.65 (Ar), 113.10 (Ar), 108.94 (Ar), 71.27 (O*C*H_3), 59.16 (*C*H_2), 57.63 (*C*H_2) ppm.

Compound 48b-NMe$_2$. 48b-NMe$_2$ was collected in quantitative yield as an orange oil. ^{1}H NMR (500 MHz, $CDCl_3$) δ = 8.19 (s, 1H, C*H*N), 7.68 (d, *J*=2.4, 1H, Ar), 7.29 (d, *J*=2.4, 1H, Ar), 3.71 (t, *J*=6.4, 2H, CH_2), 2.62 (t, *J*=6.4, 2H, CH_2), 2.27 (s, 6H, N(CH_3)$_2$) ppm. ^{13}C NMR (126 MHz, $CDCl_3$) δ = 163.99 (*C*HN), 160.19 (Ar), 138.03 (Ar), 132.90 (Ar), 119.35 (Ar), 113.51 (Ar), 108.49 (Ar), 59.39 (*C*H_2), 55.57 (*C*H_2), 45.78 (N(*C*H_3)$_2$) ppm.

Compound 48c-OMe. 48c-OMe was collected in quantitative yield as a yellow oil. ^{1}H NMR (300 MHz, $CDCl_3$) δ = 13.41 (s, 1H, ArO*H*), 8.30 (s, 1H, C*H*N), 7.00 (bs, 1H, Ar), 6.89 (bs, 1H, Ar), 3.75 (t, *J*=5.5, 2H, CH_2), 3.66 (t, *J*=5.5, 2H, CH_2), 3.36 (s, 3H, OCH_3), 2.26 (s, 3H, ArCH_3), 2.25 (s, 3H, ArCH_3) ppm. ^{13}C NMR (101 MHz, $CDCl_3$) δ = 166.59 (*C*HN), 157.30 (Ar), 134.35 (Ar), 129.07 (Ar), 127.09 (Ar), 125.71 (Ar), 117.82 (Ar), 72.09 (O*C*H_3), 59.22 (*C*H_2), 59.10 (*C*H_2) 20.44 (Ar*C*H_3), 15.54 (Ar*C*H_3) ppm.

Compound 48d-OMe. 48d-OMe was collected in quantitative yield as an orange oil. ^{1}H NMR (300 MHz, $CDCl_3$) δ = 13.94 (s, 1H, ArO*H*), 8.37 (t, *J*=1.1, 1H, C*H*N), 7.31 (dd, *J*=7.7, 1.7, 1H, Ar), 7.11 (dd, *J*=7.6, 1.7, 1H, Ar), 6.80 (t, *J*=7.7, 1H, Ar), 3.76 (m, 2H, CH_2), 3.68 (m, 2H, CH_2), 3.38 (s, 3H, O*C*H_3), 1.43 (s, 9H, C(CH_3)$_3$) ppm. ^{13}C NMR (101 MHz, $CDCl_3$) δ = 167.21 (*C*HN), 160.61 (Ar), 137.48 (Ar), 129.86 (Ar), 129.48 (Ar), 118.80 (Ar), 117.87 (Ar), 72.07 (O*C*H_3), 59.10 (*C*H_2), 50.95 (*C*H_2) 34.95 (*C*(CH$_3$)$_3$), 29.47 (C(*C*H_3)$_3$) ppm.

General synthesis of phenoxyamines 49-X. 48-X (1 equiv) and MeOH (4 mL per mmol **48-X**) were added to a round bottom flask equipped with a stirbar. $NaBH_4$ (4 equiv) was added as a solid in portions causing an exotherm and bubbling of the solution. The bright yellow suspension was stirred at room temperature, turning colorless and mostly clear within 0.5 h. After a total of 2 h of stirring, 1M HCl was added (in 1 mL aliquots until the solution was at pH = 7) to quench the reaction and the product was extracted with DCM (x3). The combined organic fractions were dried with $MgSO_4$, filtered, and volatiles were removed under vacuum to yield amine **49-X**.

Compound 49a-OMe. 49a-OMe was collected in quantitative yield as a light yellow solid. ^{1}H NMR (300 MHz, $CDCl_3$) δ = 7.24 (d, *J*=2.5, 1H, Ar), 6.88 (d, *J*=2.5, 1H, Ar), 6.41

(bs, 1H, N*H*) 3.99 (s, 2H, ArCH_2), 3.51 (t, *J*=4.9, 2H, CH_2), 3.36 (s, 3H, OCH_3), 2.80 (t, *J*=4.9, 2H, CH_2) ppm. ^{13}C NMR (101 MHz, $CDCl_3$) δ = 153.19 (Ar), 128.59 (Ar), 126.66 (Ar), 124.46 (Ar), 123.29 (Ar), 121.75 (Ar), 70.72 (O*C*H$_3$), 59.01 (*C*H$_2$), 51.98 (*C*H$_2$), 47.90 (Ar*C*H$_2$) ppm.

Compound 49a-NMe$_2$. 49a-NMe$_2$ was collected in 66 % yield as a pale pink solid. ^{1}H NMR (500 MHz, $CDCl_3$) δ = 7.23 (d, *J*=2.5, 1H, Ar), 6.87 (d, *J*=2.5, 1H, Ar), 6.79 (bs, 1H, N*H*), 3.97 (s, 2H, ArCH_2), 2.69 (t, *J*=5.7, 2H, CH_2), 2.46 (t, *J*=5.7, 2H, CH_2), 2.23 (s, 6H, N(CH_3)$_2$) ppm. ^{13}C NMR (126 MHz, $CDCl_3$) δ = 153.35 (Ar), 128.54 (Ar), 126.62 (Ar), 124.72 (Ar), 123.12 (Ar), 121.75 (Ar), 57.86 (*C*H$_2$), 52.05 (*C*H$_2$), 45.51 (Ar*C*H$_2$), 45.40 (N(*C*H$_3$)$_2$) ppm.

Compound 49b-OMe. 49b-OMe was collected in 87 % yield as a white solid. ^{1}H NMR (300 MHz, $CDCl_3$) δ = 7.54 (d, *J*=2.4, 1H, Ar), 7.06 (d, *J*=2.4, 1H, Ar), 3.99 (s, 2H, ArCH_2), 3.51 (t, *J*=4.9, 2H, CH_2), 3.36 (s, 3H, OCH_3), 2.81 (t, *J*=4.9, 2H, CH_2), ppm. ^{13}C NMR (101 MHz, $CDCl_3$) δ = 154.66 (Ar), 134.07 (Ar), 130.21 (Ar), 124.85 (Ar), 111.32 (Ar), 110.46 (Ar), 70.66 (O*C*H$_3$), 59.02 (*C*H$_2$), 51.91 (*C*H$_2$), 47.87 (Ar*C*H$_2$) ppm.

Compound 49b-NMe$_2$. 49b-NMe$_2$ was collected in 98 % yield as an off-white solid. ^{1}H NMR (500 MHz, $CDCl_3$) δ = 7.52 (d, *J*=2.2, 1H, Ar), 7.04 (d, *J*=2.2, 1H, Ar), 5.84 (bs, 1H, N*H*), 3.96 (s, 2H, ArCH_2), 2.68 (t, *J*=5.7, 2H, CH_2), 2.44 (t, *J*=5.7, 2H, CH_2), 2.22 (s, 6H, N(CH_3)$_2$) ppm. ^{13}C NMR (126 MHz, $CDCl_3$) δ = 154.85 (Ar), 133.95 (Ar), 130.12 (Ar), 125.12 (Ar), 111.32 (Ar), 110.24 (Ar), 57.82 (*C*H$_2$), 52.02 (*C*H$_2$), 45.53 (Ar*C*H$_2$), 45.41 (N(*C*H$_3$)$_2$) ppm.

Compound 49c-OMe. 49c-OMe was collected in quantitative yield as a pale yellow oil. ^{1}H NMR (300 MHz, $CDCl_3$) δ = 6.86 (bs, 1H, Ar), 6.65 (bs, 1H, Ar), 3.95 (s, 2H, ArCH_2), 3.52 (t, *J*=5.0, 2H, CH_2), 3.36 (s, 3H, OCH_3), 2.81 (t, *J*=5.0, 2H, CH_2), 2.21 (s, 3H, ArCH_3), 2.20 (s, 3H, ArCH_3) ppm. ^{13}C NMR (101 MHz, $CDCl_3$) δ = 153.91 (Ar), 130.38 (Ar), 127.33 (Ar), 126.42 (Ar), 124.70 (Ar), 121.40 (Ar), 71.05 (O*C*H$_3$), 58.75 (*C*H$_2$), 52.34 (*C*H$_2$), 47.82 (Ar*C*H$_2$), 20.36 (Ar*C*H$_3$), 15.58 (Ar*C*H$_3$) ppm.

Compound 49d-OMe. 49d-OMe was collected in quantitative yield as a pale peach oil. ^{1}H NMR (300 MHz, $CDCl_3$) δ = 7.19 (dd, *J*=7.8, 1.7, 1H, Ar), 6.87 (m, 1H, Ar), 6.71 (t, *J*=7.4, 1.4, 1H, Ar), 3.98 (s, 2H, ArCH_2), 3.52 (t, *J*=4.8, 2H, CH_2), 3.36 (s, 3H, OCH_3), 2.82 (t, *J*=4.8, 2H, CH_2), 1.42 (s, 9H, C(CH_3)$_3$) ppm. ^{13}C NMR (101 MHz, $CDCl_3$) δ = 157.43 (Ar), 136.87 (Ar), 126.65 (Ar), 126.03 (Ar), 122.84 (Ar), 118.29 (Ar), 71.14 (O*C*H$_3$), 58.98 (*C*H$_2$), 52.87 (*C*H$_2$), 47.91 (Ar*C*H$_2$), 34.81 (*C*(CH$_3$)$_3$), 29.66 (C(*C*H$_3$)$_3$) ppm.

Compound 50. **3** (2.12 g, 8.98 mmol) was dried under vacuum for 8 h in a large Schlenk tube. DCM (225 mL) was transferred via canula into the Schlenk tube with N_2 pressure. The solution was cooled to 0 ºC in an ice water bath. With the Schlenk tube under N_2, BBr_3 (4.3 mL, 44.91 mmol, 5 equiv) was dripped in via syringe over several minutes. The colorless solution turned bright yellow over the addtion of BBr_3 and continued to darken to golden orange as the reaction was allowed to gradually warm to ambient temperature. After stirring for 17 h, the reaction was quenched by the slow addition of H_2O (6 mL). Another 100 mL of water was added and the product extracted with dichloromethane. Organic fractions were dried over $MgSO_4$ and filtered, and volatile materials were removed by rotary evaporation. Column chromatography was utilized to separate the atropisomers (5/1 hexanes/ethyl acetate, R_f=0.6 (anti) and 0.2

(syn)) and the desired syn isomer was collected as a white solid (1.4 g, 36 % yield). ^{1}H NMR (500 MHz, $CDCl_3$) δ = 7.31 (dd, *J*=8.5, 2.5, 2H, Ar), 7.07 (d, *J*=2.4, 2H, Ar), 6.95 (d, *J*=8.5, 2H, Ar), 4.58 (bs, 2H, ArO*H*), 2.02 (s, 12H, ArCH_3), 1.32 (s, 18H, C(CH_3)$_3$) ppm. ^{13}C NMR (126 MHz, $CDCl_3$) δ = 150.23 (Ar), 143.66 (Ar), 136.14 (Ar), 134.49 (Ar), 127.36 (Ar), 127.19 (Ar), 125.61 (Ar), 114.60 (Ar), 34.35 (*C*(CH_3)$_3$), 31.78 (C(*C*H_3)$_3$), 17.86 (Ar*C*H_3) ppm.

Compound 51. Bis(bromomethyl phenol) **51** was synthesized by alteration of literature procedures.[40] **50** (1.40 g, 3.25 mmol), paraformaldehyde (0.49 g, 16.26 mmol, 5 equiv), and glacial acetic acid (14.5 mL, 4.5 mL per mmol **50**) were combined in a 3-neck round bottom flask equipped with a stirbar. A thermometer was secured in one arm of the flask, another arm was equipped with a small Teflon tube secured in a septum and the third was connected via hosing to a series of bubblers with water and dilute base. HBr(g) was bubbled through the Teflon tube directly into the stirring mixture for 15 minutes (with a maximum exotherm to 60 °C), at which point the tube was lifted out of the solution and the flask was sealed and left to stir an additional 12 h. During the bubbling, the reaction mixture became temporarily homogeneous, then thickened and turned peach-colored. The desired material was extracted into hexanes and the aqueous fractions were washed with DCM. The organic fractions were combined, dried with $MgSO_4$, filtered, and the volatiles were removed under vacuum. The residue was dissolved in warm hexanes and then cooled so that the desired product precipitated. **51** was collected via filtration as a white solid (1.39 g, 69 % yield). ^{1}H NMR (500 MHz, $CDCl_3$) δ = 7.34 (d, *J*=2.4, 2H, Ar), 7.05 (d, *J*=2.5, 2H, Ar), 4.83 (bs, 2H, ArO*H*), 4.67 (s, 4H, ArCH_2), 2.00 (s, 12H, ArCH_3), 1.32 (s, 18H, C(CH_3)$_3$) ppm. ^{13}C

NMR (126 MHz, $CDCl_3$) δ = 148.64 (Ar), 143.76 (Ar), 135.69 (Ar), 134.71 (Ar), 128.19 (Ar), 127.81 (Ar), 126.90 (Ar), 123.35 (Ar), 34.39 ($C(CH_3)_3$), 31.67 ($C(CH_3)_3$), 30.21 ($ArCH_2$), 17.90 ($ArCH_3$) ppm.

General synthesis of di(amine bisphenol)s 52-X. Amine **49-X** (2.5 equiv), diisopropylethylamine (2.2 equiv) and THF (0.7 mL per 0.01 mmol **51**) were added to a round bottom flask equipped with a stirbar. The solution was stirred until homogeneous and cooled to 0 ºC in an ice water bath. **51** (1 equiv) was dissolved in THF (0.3 mL per 0.01 mmol **51**) and added dropwise over several minutes to the cooled solution. The reaction was stirred, allowing it to gradually warm to ambient temperature, for 3 to 6 hours, over which time the solution became cloudy, indicating precipitation of diisopropylethylammonium bromide. After the desired reaction time, volatiles were removed under vacuum. Aqueous K_2CO_3 was added to the residue and the product extracted with dichloromethane. Organic fractions were washed with water, and then dried over $MgSO_4$ and filtered, and volatile materials were removed by rotary evaporation. Column chromatography was utilized to purify the product.

Compound 52a-OMe. Column chromatography (4/1 hexanes/ethyl acetate, R_f = 0.2) yielded the product as an off-white solid (0.27 g, 89 % yield). ^{1}H NMR (500 MHz, C_6D_6) δ = 8.48 (s, 4H, ArO*H*), 7.24 (d, *J*=2.5, 2H, Ar), 7.19 (t, *J*=2.5, 2H, Ar), 7.16 (bs, 2H, Ar), 6.68 (d, *J*=2.5, 2H, Ar), 3.59 (s, 4H, $ArCH_2$), 3.40 (s, 4H, $ArCH_2$), 3.10 (t, *J*=5.3, 4H, CH_2), 2.89 (s, 6H, OCH_3), 2.40 (t, *J*=5.3, 4H, CH_2), 2.17 (s, 12H, $ArCH_3$), 1.34 (s, 18H, $C(CH_3)_3$) ppm. ^{13}C NMR (126 MHz, C_6D_6) δ = 153.03 (Ar), 150.81 (Ar), 142.98 (Ar), 137.38 (Ar), 134.02 (Ar), 129.46 (Ar), 129.13 (Ar), 128.35 (Ar), 127.92 (Ar), 127.80 (Ar), 127.39 (Ar), 125.33 (Ar), 123.59 (Ar), 122.37 (Ar), 122.17 (Ar), 70.54

(O*C*H$_3$), 58.57 (*C*H$_2$), 56.88 (*C*H$_2$), 55.62 (*C*H$_2$), 52.35 (*C*H$_2$), 34.28 (*C*(CH$_3$)$_3$), 31.82 (C(*C*H$_3$)$_3$), 18.19 (Ar*C*H$_3$) ppm. HRMS (EI+) Calcd. for $C_{52}H_{65}Cl_4N_2O_6$: 955.3578. Found: 955.3576.

Compound 52a-NMe$_2$. Column chromatography (10/2/1 ethyl acetate/hexanes/MeOH, R_f = 0.14) yielded the product as an off-white solid (0.40 g, 88 % yield). ^{1}H NMR (400 MHz, C_6D_6) δ = 9.55 (s, 4H, ArO*H*), 7.25 (s, 2H, Ar), 7.19 (s, 2H, Ar), 7.13 (s, 2H, Ar), 6.75 (s, 2H, Ar), 3.35 (s, 4H, ArC*H*$_2$), 3.15 (s, 4H, ArC*H*$_2$), 2.19 (s, 12H, N(C*H*$_3$)$_2$), 2.11 (s, 4H, C*H*$_2$), 1.89 (s, 4H, C*H*$_2$), 1.74 (s, 12H, ArC*H*$_3$), 1.33 (s, 18H, C(C*H*$_3$)$_3$) ppm. ^{13}C NMR (101 MHz, C_6D_6) δ = 153.13 (Ar), 151.78 (Ar), 142.23 (Ar), 138.26 (Ar), 133.24 (Ar), 130.29 (Ar), 129.63 (Ar), 128.50 (Ar), 128.17 (Ar), 127.94 (Ar), 126.78 (Ar), 125.71 (Ar), 123.09 (Ar), 123.04 (Ar), 122.19 (Ar), 55.81 (*C*H$_2$), 55.50 (*C*H$_2$), 55.44 (*C*H$_2$), 49.34 (*C*H$_2$), 44.46 (N(*C*H$_3$)$_2$), 34.19 (*C*(CH$_3$)$_3$), 31.86 (C(*C*H$_3$)$_3$), 18.37 (Ar*C*H$_3$) ppm. HRMS (EI+) Calcd. for $C_{54}H_{71}Cl_4N_4O_4$: 981.4212. Found: 981.4251.

Compound 52b-OMe. Column chromatography (4/1 hexanes/ethyl acetate, R_f = 0.2) yielded the product as an off-white solid (0.18 g, 49 % yield). ^{1}H NMR (500 MHz, C_6D_6) δ = 8.56 (s, 4H, ArO*H*), 7.52 (d, *J*=2.4, 2H, Ar), 7.23 (d, *J*=2.5, 2H, Ar), 7.20 (d, *J*=2.5, 2H, Ar), 6.84 (d, *J*=2.3, 2H, Ar), 3.57 (s, 4H, ArC*H*$_2$), 3.36 (s, 4H, ArC*H*$_2$), 3.08 (t, *J*=5.3, 4H, C*H*$_2$), 2.87 (s, 6H, OC*H*$_3$), 2.37 (t, *J*=5.3, 4H, C*H*$_2$), 2.18 (s, 12H, ArC*H*$_3$), 1.35 (s, 18H, C(C*H*$_3$)$_3$) ppm. ^{13}C NMR (126 MHz, C_6D_6) δ = 154.50 (Ar), 150.77 (Ar), 143.00 (Ar), 137.37 (Ar), 134.57 (Ar), 134.06 (Ar), 131.23 (Ar), 129.47 (Ar), 128.35 (Ar), 127.93 (Ar), 127.47 (Ar), 125.66 (Ar), 122.15 (Ar), 111.93 (Ar), 110.82 (Ar), 70.53 (O*C*H$_3$), 58.56 (*C*H$_2$), 56.88 (*C*H$_2$), 55.50 (*C*H$_2$), 52.28 (*C*H$_2$), 34.30 (*C*(CH$_3$)$_3$),

31.84 (C(CH_3)$_3$), 18.22 (ArCH_3) ppm. HRMS (EI+) Calcd. for $C_{52}H_{65}Br_4N_2O_6$: 1133.1544. Found: 1133.1545.

Compound 52b-NMe$_2$. Column chromatography (20/5/1 ethyl acetate/hexanes/MeOH) yielded the product as an off-white solid (0.24 g, 51 % yield). ^{1}H NMR (400 MHz, C_6D_6) δ = 9.52 (s, 4H, ArO*H*), 7.58 (s, 2H, Ar), 7.19 (s, 2H, Ar), 7.13 (s, 2H, Ar), 6.92 (s, 2H, Ar), 3.33 (s, 4H, ArCH_2), 3.14 (s, 4H, ArCH_2), 2.21 (s, 12H, N(CH_3)$_2$), 2.09 (s, 4H, CH_2), 1.88 (s, 4H, CH_2), 1.74 (s, 12H, ArCH_3), 1.34 (s, 18H, C(CH_3)$_3$) ppm. ^{13}C NMR (101 MHz, C_6D_6) δ = 154.52 (Ar), 151.74 (Ar), 142.24 (Ar), 138.26 (Ar), 135.07 (Ar), 133.31 (Ar), 131.82 (Ar), 130.26 (Ar), 128.50 (Ar), 127.93 (Ar), 126.89 (Ar), 126.07 (Ar), 122.18 (Ar), 112.61 (Ar), 110.36 (Ar), 55.80 (*C*H$_2$), 55.56 (*C*H$_2$), 55.21 (*C*H$_2$), 49.31 (*C*H$_2$), 44.49 (N(*C*H$_3$)$_2$), 34.21 (*C*(CH$_3$)$_3$), 31.88 (C(*C*H$_3$)$_3$), 18.38 (Ar*C*H$_3$) ppm. HRMS (EI+) Calcd. for $C_{54}H_{71}Br_4N_4O_4$: 1159.2177. Found: 1159.2148.

Compound 52c-OMe. Column chromatography (4/1 hexanes/ethyl acetate, R_f = 0.2) yielded the product as an off-white solid (0.21 g, 74 % yield). ^{1}H NMR (500 MHz, C_6D_6) δ = 8.23 (s, 4H, ArO*H*), 7.32 (d, *J*=2.5, 2H, Ar), 7.20 (t, *J*=2.5, 2H, Ar), 6.85 (d, *J*=2.1, 2H, Ar), 6.66 (d, *J*=2.0, 2H, Ar), 3.76 (s, 4H, ArCH_2), 3.69 (s, 4H, ArCH_2), 3.18 (t, *J*=5.3, 4H, CH_2), 2.92 (s, 6H, OCH_3), 2.57 (t, *J*=5.3, 4H, CH_2), 2.37 (s, 6H, ArCH_3), 2.21 (s, 6H, ArCH_3), 2.17 (s, 12H, ArCH_3), 1.34 (s, 18H, C(CH_3)$_3$) ppm. ^{13}C NMR (126 MHz, C_6D_6) δ = 153.98 (Ar), 151.14 (Ar), 142.62 (Ar), 137.76 (Ar), 133.73 (Ar), 131.42 (Ar), 129.57 (Ar), 128.35 (Ar), 128.11 (Ar), 127.76 (Ar), 127.48 (Ar), 127.33 (Ar), 125.32 (Ar), 122.74 (Ar), 121.76 (Ar), 71.14 (O*C*H$_3$), 58.57 (*C*H$_2$), 57.88 (*C*H$_2$), 55.87 (*C*H$_2$), 52.10 (*C*H$_2$), 34.27 (*C*(CH$_3$)$_3$), 31.85 (C(*C*H$_3$)$_3$), 20.70 (Ar*C*H$_3$), 18.26

(Ar*C*H$_3$), 16.30 (Ar*C*H$_3$) ppm. HRMS (EI+) Calcd. for $C_{56}H_{77}N_2O_6$: 873.5782. Found: 873.5761.

Compound 52d-OMe. Column chromatography (4/1 hexanes/ethyl acetate, R_f = 0.5) yielded the product as a pale peach solid (0.28 g, 94 % yield). ^{1}H NMR (500 MHz, C_6D_6) δ = 7.34 (d, *J*=2.5, 2H, Ar), 7.32 (dd, *J*=7.0, 2.5, 2H, Ar), 7.21 (d, *J*=2.5, 2H, Ar), 6.83 (q, *J*=7.0, 2H, Ar), 3.71 (s, 4H, ArC*H*$_2$), 3.68 (s, 4H, ArC*H*$_2$), 3.15 (t, *J*=5.4, 4H, C*H*$_2$), 2.91 (s, 6H, OC*H*$_3$), 2.51 (t, *J*=5.4, 4H, C*H*$_2$), 2.24 (s, 12H, ArC*H*$_3$), 1.63 (s, 18H, C(C*H*$_3$)$_3$), 1.33 (s, 18H, C(C*H*$_3$)$_3$) ppm. ^{13}C NMR (126 MHz, C_6D_6) δ = 157.11 (Ar), 150.85 (Ar), 142.80 (Ar), 137.74 (Ar), 136.97 (Ar), 133.91 (Ar), 129.41 (Ar), 128.35 (Ar), 127.79 (Ar), 127.61 (Ar), 126.65 (Ar), 123.04 (Ar), 122.72 (Ar), 118.95 (Ar), 70.96 (O*C*H$_3$), 58.53 (*C*H$_2$), 58.27 (*C*H$_2$), 55.58 (*C*H$_2$), 51.92 (*C*H$_2$), 35.09 (*C*(CH$_3$)$_3$), 34.27(*C*(CH$_3$)$_3$), 31.84 (C(*C*H$_3$)$_3$), 29.95 (C(*C*H$_3$)$_3$), 18.22 (Ar*C*H$_3$) ppm. HRMS (EI+) Calcd. for $C_{60}H_{85}N_2O_6$: 929.6408. Found: 929.6403.

General synthesis of dizirconium complexes 53-X. In an inert atmosphere glovebox, a solution of $ZrBn_4$ (2 equiv) in toluene (2 mL per mmol $ZrBn_4$) was added to a scintillation vial equipped with a stirbar. To this, a solution of **52-X** (1 equiv) in toluene (2 mL per mmol $ZrBn_4$) was added at room temperature, and the reaction was stirred in the dark for 2 to 6 hours. After the desired reaction time, the volatiles were removed *in vacuo*. After metallation, the reaction was no longer considered to be light sensitive. Before purification, a ^{1}H NMR spectrum was obtained, and two metallation isomers were observed as the major products in all cases. X-ray diffraction (XRD) studies were correlated with ^{1}H NMR spectra to identify diagnostic benzyl peaks for each metallation isomer in the ^{1}H NMR spectra between 3 and 4 ppm. The *pseudo-C*$_2$

symmetric isomer displays benzyl peaks farther downfield and with more separation than those of the *pseudo*-C_S symmetric isomer. Different purification methods including fractionation and recrystallization were used to separate and purify both metallation isomers, though in some cases, only the *pseudo*-C_2 symmetric isomer could be obtained in high purity. Therefore, for many of the precatalysts, only the *pseudo*-C_2 symmetric isomer is reported with regards to characterization and polymerization. There are a few examples where the *pseudo*-C_S symmetric isomer was purified, namely with **53c-OMe**, of which X-ray quality crystals were grown and XRD provided a structure (Figure 5.5). In other cases, a mixture of metallation isomers was used for polymerizations to determine differences that occur using a mixture of isomers. In those instances, NMR spectra of the second isomer or mixture of isomers are presented alongside the NMR data for the *pseudo*-C_2 symmetric isomer.

Compound 53a-OMe. Et_2O (10 mL) was added to the crude residue and stirred at room temperature. The resulting precipitate was collected via filtration and recrystallized from toluene via liquid diffusion of hexanes to yield pale yellow crystals. These crystals were collected via filtration (0.073 g, 30 % yield) and determined by ^{1}H NMR spectroscopy and XRD (Figure 5.3) to be purely the *pseudo*-C_2 symmetric isomer. ^{1}H NMR (600 MHz, C_6D_6) δ = 7.46 (d, *J*=2.3, 2H, Ar), 7.31 (d, *J*=2.4, 2H, Ar), 7.27 (d, *J*=7.9, 4H, Ar), 7.13 (t, *J*=7.5, 4H, Ar), 7.05 (d, *J*=2.2, 2H, Ar), 6.94 (t, *J*=7.3, 2H, Ar), 6.88 (t, *J*=7.4, 3H, Ar), 6.81 (d, *J*=7.8, 3H, Ar), 6.65 (t, *J*=7.3, 2H, Ar), 6.62 (d, *J*=2.4, 2H, Ar), 3.82 (d, *J*=13.7, 2H, ArCH_2), 3.33 (d, *J*=13.5, 2H, ArCH_2), 2.76 (s, 6H, ArCH_3), 2.72 (d, *J*=9.4, 2H, ArCH_2), 2.65 (d, *J*=13.8, 2H, ArCH_2), 2.46 (d, *J*=9.5, 2H, ArCH_2), 2.44 (s, 6H, ArCH_3), 2.41 (m, 2H, CH_2), 2.38 (s, 6H, OCH_3), 2.29 (d, *J*=13.5, 2H,

ArCH_2), 2.08 (m, 4H, CH_2), 2.00 (d, J=10.6, 2H, ArCH_2), 1.62 (d, J=10.6, 2H, ArCH_2), 1.58 (m, 2H, CH_2), 1.37 (s, 18H, C(CH_3)$_3$) ppm. ^{13}C NMR (126 MHz, C_6D_6) δ = 156.53 (Ar), 156.13 (Ar), 151.89 (Ar), 141.89 (Ar), 141.45 (Ar), 138.82 (Ar), 137.90 (Ar), 134.21 (Ar), 131.95 (Ar), 131.09 (Ar), 130.82 (Ar), 130.11 (Ar), 130.01 (Ar), 129.91 (Ar), 129.33 (Ar), 126.78 (Ar), 125.87 (Ar), 125.70 (Ar), 124.82 (Ar), 123.84 (Ar), 123.50 (Ar), 122.64 (Ar), 120.41 (Ar), 72.46 (O*C*H$_2$), 67.12 (Ar*C*H$_2$), 63.98 (Ar*C*H$_2$), 62.56 (Ar*C*H$_2$), 62.38 (Ar*C*H$_2$), 61.22 (O*C*H$_3$), 51.53 (N*C*H$_2$), 34.35 (*C*(CH$_3$)$_3$), 31.91 (C(*C*H$_3$)$_3$), 20.05 (Ar*C*H$_3$), 19.34 (Ar*C*H$_3$) ppm. Elemental analysis was not obtained for **53a-OMe** due to issues with decomposition. Additional recrystallizations to collect more **53a-OMe** from the filtrates yielded only the *pseudo-C*$_2$ symmetric isomer or a mixture of the two metallation isomers. One such mixture was used in a 1-hexene polymerization and the corresponding ^{1}H NMR spectrum is provided below (Figure 5.12).

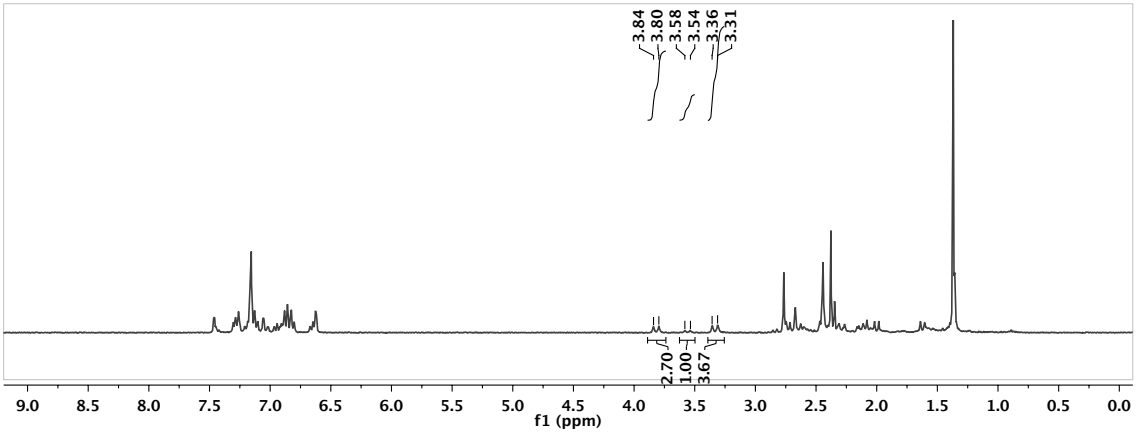

Figure 5.12. ^{1}H NMR spectrum of **53a-OMe**, mixture of isomers, in C_6D_6.

Compound 53a-NMe$_2$. 53a-NMe$_2$ was recrystallized from toluene via liquid diffusion of hexanes to yield yellow crystals. These crystals were collected via filtration (0.052 g, 45 % yield) and determined by ^{1}H NMR spectroscopy and XRD (Figure 5.4) to

be purely the *pseudo-*C_2 symmetric isomer. ^{1}H NMR (400 MHz, C_6D_6) δ = 7.45 (d, *J*=2.2, 2H, Ar), 7.28 (d, *J*=7.4, 4H, Ar), 7.27 (m, 2H, Ar), 7.14 (m, 4H, Ar), 7.12 (d, *J*=2.1, 2H, Ar), 6.98 (t, *J*=7.4, 2H, Ar), 6.88 (t, *J*=7.6, 4H, Ar), 6.75 (d, *J*=7.4, 4H, Ar), 6.63 (d, *J*=2.6, 2H, Ar), 6.62 (t, *J*=7.2, 2H, Ar), 4.14 (d, *J*=13.7, 2H, ArCH_2), 3.36 (d, *J*=13.9, 2H, ArCH_2), 2.74 (s, 6H, ArCH_3), 2.70 (d, *J*=10.2, 2H, ArCH_2), 2.65 (d, *J*=9.3, 2H, ArCH_2), 2.44 (d, *J*=9.0, 2H, ArCH_2), 2.41 (s, 6H, ArCH_3), 2.25 (d, *J*=14.0, 2H, ArCH_2), 2.19 (m, 2H, CH_2), 1.93 (d, *J*=10.4, 2H, ArCH_2), 1.66 (s, 6H, N(CH_3)$_2$), 1.55 (m, 4H, CH_2), 1.47 (s, 6H, N(CH_3)$_2$), 1.38 (s, 18H, C(CH_3)$_3$), 1.30 (m, 2H, CH_2), 1.14 (d, *J*=10.5, 2H, ArCH_2) ppm. ^{13}C NMR (101 MHz, C_6D_6) δ = 156.33 (Ar), 155.78 (Ar), 153.19 (Ar), 142.02 (Ar), 140.27 (Ar), 138.90 (Ar), 134.54 (Ar), 131.79 (Ar), 131.18 (Ar), 130.33 (Ar), 130.16 (Ar), 130.10 (Ar), 129.34 (Ar), 128.59 (Ar), 128.57 (Ar), 126.32 (Ar), 126.18 (Ar), 125.70 (Ar), 125.45 (Ar), 124.73 (Ar), 123.12 (Ar), 122.78 (Ar), 120.02 (Ar), 66.93 (Ar*C*H$_2$), 64.24 (Ar*C*H$_2$), 62.98 (Ar*C*H$_2$), 60.18 (Ar*C*H$_2$), 59.87 (N*C*H$_2$), 52.23 (N*C*H$_2$), 47.65 (N(*C*H$_3$)$_2$), 34.38 (*C*(CH$_3$)$_3$), 31.90 (C(*C*H$_3$)$_3$), 20.05 (Ar*C*H$_3$), 19.17 (Ar*C*H$_3$) ppm. Anal. Calcd. for $C_{82}H_{94}Cl_4N_4O_4Zr_2$: C, 64.63; H, 6.22, N, 3.68. Found: C, 64.42; H, 6.39, N, 3.15. As with **53a-OMe**, additional recrystallizations to collect more **53a-NMe$_2$** from the filtrate yielded only the *pseudo-*C_2 symmetric isomer or a mixture of the two metallation isomers. One such mixture was used in a 1-hexene polymerization and the corresponding ^{1}H NMR spectrum is provided below (Figure 5.13).

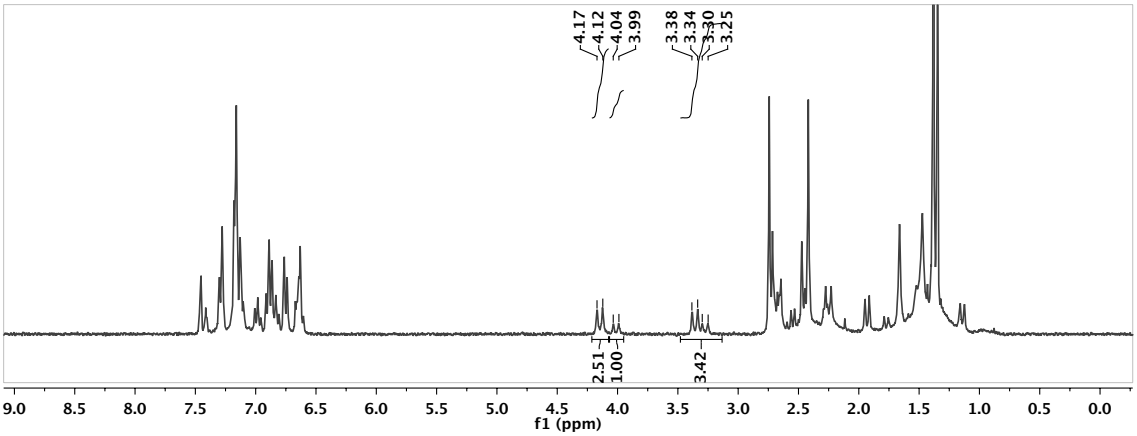

Figure 5.13. ^{1}H NMR spectrum of **53a-NMe$_2$**, mixture of isomers, in C_6D_6.

Compound 53b-OMe. 53b-OMe was recrystallized from toluene via liquid diffusion of hexanes to yield pale yellow precipitate. This precipitate was collected via filtration (0.034 g, 23 % yield) and determined by ^{1}H NMR spectroscopy to be purely the *pseudo-C*$_2$ symmetric isomer. ^{1}H NMR (600 MHz, C_6D_6) δ = 7.61 (d, *J*=2.3, 2H, Ar), 7.45 (d, *J*=2.4, 2H, Ar), 7.31 (d, *J*=7.6, 4H, Ar), 7.15 (t, *J*=7.9, 4H, Ar), 7.05 (d, *J*=2.4, 2H, Ar), 6.96 (t, *J*=7.3, 2H, Ar), 6.87 (t, *J*=7.6, 4H, Ar), 6.81 (d, *J*=7.8, 4H, Ar), 6.80 (d, *J*=2.3, 2H, Ar), 6.64 (t, *J*=7.2, 2H, Ar), 3.82 (d, *J*=13.7, 2H, ArCH_2), 3.35 (d, *J*=13.4, 2H, ArCH_2), 2.78 (d, *J*=9.4, 2H, ArCH_2), 2.76 (s, 6H, ArCH_3), 2.65 (d, *J*=13.9, 2H, ArCH_2), 2.47 (d, *J*=9.4, 2H, ArCH_2), 2.44 (s, 6H, ArCH_3), 2.42 (m, 2H, CH_2), 2.39 (s, 6H, OCH_3), 2.28 (d, *J*=13.6, 2H, ArCH_2), 2.07 (m, 4H, CH_2), 1.97 (d, *J*=10.6, 2H, ArCH_2), 1.62 (d, *J*=10.6, 2H, ArCH_2), 1.56 (m, 2H, CH_2), 1.36 (s, 18H, C(CH_3)$_3$) ppm. ^{13}C NMR (126 MHz, C_6D_6) δ = 157.54 (Ar), 156.53 (Ar), 151.94 (Ar), 141.95 (Ar), 141.45 (Ar), 138.89 (Ar), 135.56 (Ar), 134.19 (Ar), 131.98 (Ar), 131.83 (Ar), 131.06 (Ar), 130.90 (Ar), 130.05 (Ar), 129.94 (Ar), 128.59 (Ar), 127.68 (Ar), 126.78 (Ar), 125.87 (Ar), 124.81 (Ar), 123.90 (Ar), 120.42 (Ar), 113.69 (Ar), 109.86 (Ar), 72.52 (O*C*H$_2$), 67.30

(Ar*C*H_2), 63.96 (Ar*C*H_2), 62.62 (Ar*C*H_2), 62.32 (Ar*C*H_2), 61.32 (O*C*H_3), 51.56 (N*C*H_2), 34.36 (*C*(CH_3)$_3$), 31.91 (C(*C*H_3)$_3$), 20.03 (Ar*C*H_3), 19.27 (Ar*C*H_3) ppm. Elemental analysis was not obtained for **53b-OMe** due to issues with decomposition.

Compound 53b-NMe_2. 53b-NMe_2 was fractioned over Celite with hexanes, Et_2O and benzene. The Et_2O and benzene fractions both contained both metallation isomers. To obtain a single isomer, recrystallizations from toluene via liquid diffusion of hexanes were performed, yielding yellow crystals. These crystals were collected via filtration (0.041 g, 28 % yield) and determined by ^{1}H NMR spectroscopy to be purely the *pseudo-C*$_2$ symmetric isomer. ^{1}H NMR (400 MHz, C_6D_6) δ = 7.58 (d, *J*=2.5, 2H, Ar), 7.44 (d, *J*=2.3, 2H, Ar), 7.32 (d, *J*=7.4, 4H, Ar), 7.12 (m, 2H, Ar), 7.02 (m, 6H, Ar), 6.87 (t, *J*=7.4, 4H, Ar), 6.81 (d, *J*=2.3, 2H, Ar), 6.73 (d, *J*=7.5, 4H, Ar), 6.61 (t, *J*=7.1, 2H, Ar), 4.15 (d, *J*=13.5, 2H, ArC*H*$_2$), 3.37 (d, *J*=14.3, 2H, ArC*H*$_2$), 2.73 (s, 6H, ArC*H*$_3$), 2.71 (d, *J*=9.4, 2H, ArC*H*$_2$), 2.68 (d, *J*=12.8, 2H, ArC*H*$_2$), 2.45 (d, *J*=9.3, 2H, ArC*H*$_2$), 2.41 (s, 6H, ArC*H*$_3$), 2.24 (d, *J*=13.9, 2H, ArC*H*$_2$), 2.20 (m, 2H, C*H*$_2$), 1.89 (d, *J*=10.5, 2H, ArC*H*$_2$), 1.67 (s, 6H, N(C*H*$_3$)$_2$), 1.53 (m, 4H, C*H*$_2$), 1.48 (s, 6H, N(C*H*$_3$)$_2$), 1.37 (s, 18H, C(C*H*$_3$)$_3$), 1.24 (m, 2H, C*H*$_2$), 1.11 (d, *J*=10.3, 2H, ArC*H*$_2$) ppm. ^{13}C NMR (101 MHz, C_6D_6) δ = 157.17 (Ar), 156.33 (Ar), 153.29 (Ar), 142.03 (Ar), 140.10 (Ar), 138.92 (Ar), 135.53 (Ar), 134.54 (Ar), 131.79 (Ar), 131.67 (Ar), 131.31 (Ar), 131.16 (Ar), 130.39 (Ar), 130.17 (Ar), 129.34 (Ar), 128.57 (Ar), 126.32 (Ar), 126.19 (Ar), 125.44 (Ar), 124.86 (Ar), 120.02 (Ar), 113.37 (Ar), 110.03 (Ar), 66.95 (Ar*C*H_2), 64.22 (Ar*C*H_2), 63.02 (Ar*C*H_2), 59.86 (Ar*C*H_2), 59.82 (N*C*H_2), 52.24 (N*C*H_2), 47.64 (N(*C*H_3)$_2$), 34.38 (*C*(CH_3)$_3$), 31.89 (C(*C*H_3)$_3$), 20.06 (Ar*C*H_3), 19.13 (Ar*C*H_3) ppm. Elemental analysis was not obtained for **53b-NMe_2** due to issues with decomposition.

Compound 53c-OMe. 53c-OMe was recrystallized from toluene via liquid diffusion of hexanes to yield pale yellow precipitate. This precipitate was collected via filtration (0.045 g, 27 % yield) and determined by ^{1}H NMR spectroscopy to be purely the *pseudo*-C_2 symmetric isomer. ^{1}H NMR (600 MHz, C_6D_6) δ = 7.50 (d, *J*=2.8, 2H, Ar), 7.24 (d, *J*=7.3, 4H, Ar), 7.15 (t, *J*=7.9, 4H, Ar), 7.09 (d, *J*=2.5, 2H, Ar), 6.90 (m, 12H, Ar), 6.65 (t, *J*=7.0, 2H, Ar), 6.52 (d, *J*=1.7, 2H, Ar), 3.82 (d, *J*=13.7, 2H, ArCH_2), 3.57 (d, *J*=13.2, 2H, ArCH_2), 2.89 (s, 6H, ArCH_3), 2.76 (d, *J*=13.9, 2H, ArCH_2), 2.62 (d, *J*=9.6, 2H, ArCH_2), 2.56 (d, *J*=13.3, 2H, ArCH_2), 2.49 (s, 6H, ArCH_3), 2.45 (d, *J*=9.7, 2H, ArCH_2), 2.41 (s, 6H, ArCH_3), 2.40 (m, 2H, CH_2), 2.37 (s, 6H, OCH_3), 2.27 (m, 2H, CH_2), 2.20 (d, *J*=10.4, 2H, ArCH_2), 2.18 (s, 6H, ArCH_3), 2.14 (m, 2H, CH_2), 1.90 (d, *J*=10.3, 2H, ArCH_2), 1.85 (m, 2H, CH_2), 1.39 (s, 18H, C(CH_3)$_3$) ppm. ^{13}C NMR (126 MHz, C_6D_6) δ = 157.63 (Ar), 156.89 (Ar), 151.46 (Ar), 143.87 (Ar), 141.28 (Ar), 139.00 (Ar), 134.36 (Ar), 132.12 (Ar), 131.98 (Ar), 131.14 (Ar), 130.03 (Ar), 129.84 (Ar), 129.43 (Ar), 128.35 (Ar), 128.32 (Ar), 127.41 (Ar), 126.95 (Ar), 125.85 (Ar), 125.53 (Ar), 125.16 (Ar), 124.17 (Ar), 122.67 (Ar), 120.23 (Ar), 72.83 (O*C*H$_2$), 65.32 (Ar*C*H$_2$), 64.21 (Ar*C*H$_2$), 63.73 (Ar*C*H$_2$), 63.40 (Ar*C*H$_2$), 60.87 (O*C*H$_3$), 51.37 (N*C*H$_2$), 34.35 (*C*(CH$_3$)$_3$), 31.98 (C(*C*H$_3$)$_3$), 20.78 (Ar*C*H$_3$), 20.16 (Ar*C*H$_3$), 19.56 (Ar*C*H$_3$), 16.53 (Ar*C*H$_3$) ppm. Anal. Calcd. for $C_{84}H_{100}N_2O_6Zr_2$: C, 71.24; H, 7.12, N, 1.98. Found: C, 71.41; H, 7.32, N, 1.77. Additional recrystallizations to collect more **53c-OMe** from the filtrate yielded X-ray quality crystals of the *pseudo*-C_S symmetric isomer in low yield (0.011 g, 7 % yield). XRD provided a structure (Figure 5.5). ^{1}H NMR (600 MHz, C_6D_6) δ = 7.47 (d, *J*=2.5, 2H, Ar), 7.23 (m, 8H, Ar), 7.05 (d, *J*=2.4, 2H, Ar), 6.90 (m, 12H, Ar), 6.66 (t, *J*=7.0, 2H, Ar), 6.53 (d, *J*=1.6, 2H, Ar), 3.59 (d, *J*=13.3, 4H, ArCH_2), 2.77 (d, *J*=9.8, 2H, ArCH_2),

2.74 (s, 6H, ArCH_3), 2.69 (d, *J*=13.5, 2H, ArCH_2), 2.65 (m, 2H, CH_2), 2.58 (d, *J*=12.3, 2H, ArCH_2), 2.55 (d, *J*=9.1, 2H, ArCH_2), 2.46 (s, 6H, ArCH_3), 2.42 (s, 6H, ArCH_3), 2.31 (d, *J*=10.1, 2H, ArCH_2), 2.26 (s, 6H, OCH_3), 2.25 (d, *J*=8.9, 2H, ArCH_2), 2.20 (s, 6H, ArCH_3), 2.07 (m, 2H, CH_2), 1.99 (m, 2H, CH_2), 1.93 (m, 2H, CH_2), 1.38 (s, 18H, C(CH_3)$_3$) ppm.

Compound 53d-OMe. Et_2O (10 mL) was added to the crude residue and stirred at room temperature. The resulting pale yellow precipitate was collected via filtration (0.092 g, 39 % yield) and was determined to be the *pseudo-*C_2 symmetric isomer by ^{1}H NMR spectroscopy. ^{1}H NMR (300 MHz, C_6D_6) δ = 7.50 (d, *J*=2.5, 2H, Ar), 7.32 (m, 6H, Ar), 7.12 (t, *J*=7.6, 4H, Ar), 7.09 (d, *J*=2.3, 2H, Ar), 6.86 (m, 10H, Ar), 6.75 (d, *J*=5.1, 4H, Ar), 6.62 (m, 2H, Ar), 3.94 (d, *J*=13.6, 2H, ArCH_2), 3.40 (d, *J*=13.9, 2H, ArCH_2), 2.91 (s, 6H, ArCH_3), 2.70 (d, *J*=13.8, 2H, ArCH_2), 2.57 (d, *J*=12.2, 2H, ArCH_2), 2.52 (s, 6H, ArCH_3), 2.46 (s, 6H, OCH_3), 2.46 (m, 2H, ArCH_2), 2.40 (d, *J*=11.0, 2H, ArCH_2), 2.24 (d, *J*=11.0, 2H, ArCH_2), 2.18 (m, 4H, CH_2), 1.85 (m, 2H, CH_2), 1.72 (d, *J*=10.2, 2H, ArCH_2), 1.62 (s, 18H, C(CH_3)$_3$), 1.43 (m, 2H, CH_2), 1.40 (s, 18H, C(CH_3)$_3$) ppm. ^{13}C NMR (126 MHz, C_6D_6) δ = 160.47 (Ar), 157.01 (Ar), 152.00 (Ar), 143.29 (Ar), 141.31 (Ar), 139.35 (Ar), 137.19 (Ar), 134.39 (Ar), 132.16 (Ar), 131.36 (Ar), 130.26 (Ar), 129.91 (Ar), 129.46 (Ar), 129.33 (Ar), 128.59 (Ar), 128.57 (Ar), 126.64 (Ar), 125.99 (Ar), 125.88 (Ar), 125.04 (Ar), 122.96 (Ar), 120.22 (Ar), 118.87 (Ar), 73.00 (O*C*H$_2$), 66.93 (Ar*C*H$_2$), 64.23 (Ar*C*H$_2$), 63.96 (Ar*C*H$_2$), 63.44 (Ar*C*H$_2$), 61.83 (O*C*H$_3$), 51.62 (N*C*H$_2$), 35.11 (*C*(CH$_3$)$_3$), 34.35 (*C*(CH$_3$)$_3$), 31.99 (C(*C*H$_3$)$_3$), 30.00 (C(*C*H$_3$)$_3$), 20.34 (Ar*C*H$_3$), 19.26 (Ar*C*H$_3$) ppm. Anal. Calcd. for $C_{88}H_{108}N_2O_6Zr_2$: C, 71.79; H, 7.39, N, 1.90. Found: C, 72.25; H, 7.31, N, 1.74.

General synthesis of amine bisphenols 56-X. Mononucleating ligand precursors (**56-X**) were synthesized from **49a-X** (1.2 equiv), diisopropylethylamine (1.2 equiv), and **55** (1 equiv), using THF (1 mL per 0.02 mmol **55**) as the solvent and analogous synthetic and workup procedures to those used for the synthesis and workup of the dinucleating ligands (**52-X**).

Compound 56-OMe. Column chromatography (4/1 hexanes/ethyl acetate, R_f = 0.5) yielded the product as a white solid (0.41 g, 87 % yield). ^{1}H NMR (500 MHz, C_6D_6) δ = 8.80 (s, 2H, ArO*H*), 7.51 (d, *J*=2.5, 1H, Ar), 7.12 (d, *J*=2.6, Ar), 6.90 (d, *J*=2.5, 1H, Ar), 6.74 (d, *J*=2.6, 1H, Ar), 3.35 (s, 2H, ArCH_2), 3.24 (s, 2H, ArCH_2), 2.90 (t, *J*=5.7, 2H, CH_2), 2.88 (s, 3H, OCH_3), 2.15 (t, *J*=5.7, 2H, CH_2), 1.66 (s, 9H, C(CH_3)$_3$), 1.38 (s, 9H, C(CH_3)$_3$) ppm. ^{13}C NMR (126 MHz, C_6D_6) δ = 153.91 (Ar), 151.59 (Ar), 141.34 (Ar), 136.75 (Ar), 129.38 (Ar), 129.23 (Ar), 125.24 (Ar), 124.92 (Ar), 124.19 (Ar), 123.97 (Ar), 122.58 (Ar), 121.79 (Ar), 70.87 (*C*H$_2$), 58.57 (O*C*H$_3$), 58.33 (*C*H$_2$), 55.46 (*C*H$_2$), 51.45 (*C*H$_2$), 35.43 (*C*(CH$_3$)$_3$), 34.40 (*C*(CH$_3$)$_3$), 31.98 (C(*C*H$_3$)$_3$), 30.06 (C(*C*H$_3$)$_3$) ppm. HRMS (EI+) Calcd. for $C_{25}H_{36}Cl_2NO_3$: 468.2072. Found: 468.2066.

Compound 56-NMe$_2$. Column chromatography (4/1 hexanes/ethyl acetate, R_f = 0.05) yielded the product as an off-white solid (0.39 g, quantitative yield). ^{1}H NMR (500 MHz, C_6D_6) δ = 10.40 (s, 2H, ArO*H*), 7.47 (d, *J*=2.5, 1H, Ar), 7.25 (d, *J*=2.6, 1H, Ar), 6.90 (d, *J*=2.4, 1H, Ar), 6.74 (d, *J*=2.6, 1H, Ar), 3.22 (s, 2H, ArCH_2), 2.92 (s, 2H, ArCH_2), 1.99 (t, *J*=5.6, 2H, CH_2), 1.82 (s, 6H, N(CH_3)$_2$), 1.79 (t, *J*=5.9, 2H, CH_2), 1.58 (s, 9H, C(CH_3)$_3$), 1.38 (s, 9H, C(CH_3)$_3$) ppm. ^{13}C NMR (126 MHz, C_6D_6) δ = 153.71 (Ar), 153.08 (Ar), 141.18 (Ar), 136.60 (Ar), 130.02 (Ar), 129.05 (Ar), 125.24 (Ar), 124.67 (Ar), 123.80 (Ar), 123.67 (Ar), 122.86 (Ar), 121.91 (Ar), 58.38 (*C*H$_2$), 55.29 (*C*H$_2$), 54.25

(CH_2), 48.93 (CH_2), 44.35 ($N(CH_3)_2$), 35.33 ($C(CH_3)_3$), 34.38 ($C(CH_3)_3$), 32.00 ($C(CH_3)_3$), 30.02 ($C(CH_3)_3$) ppm. HRMS (EI+) Calcd. for $C_{26}H_{39}Cl_2N_2O_2$: 481.2389. Found: 481.2366.

General synthesis of monozirconium complexes 57-X. In an inert atmosphere glovebox, a solution of $ZrBn_4$ (1 equiv) in toluene (2 mL per mmol $ZrBn_4$) was added to a scintillation vial equipped with a stirbar. To this, a solution of **56-X** (1 equiv) in toluene (2 mL per mmol $ZrBn_4$) was added at room temperature, and the reaction was stirred in the dark for 5 hours. After the desired reaction time, the volatiles were removed *in vacuo*. After metallation, the reaction was no longer considered to be light sensitive.

Compound 57-OMe. 57-OMe was fractioned over Celite with hexanes, Et_2O and benzene. The ^{1}H NMR spectrum of the benzene fraction was purely the desired complex (pale yellow solid, 0.033 g, 35 % yield). X-ray quality crystals were obtained via recrystallization of the Et_2O soluble fraction from toluene via liquid diffusion of pentane (Figure 5.7). ^{1}H NMR (600 MHz, C_6D_6) δ = 7.74 (d, *J*=7.3, 2H, Ar), 7.57 (d, *J*=2.4, 1H, Ar), 7.34 (d, *J*=2.6, 1H, Ar), 7.32 (t, *J*=7.7, 2H, Ar), 7.06 (t, *J*=7.4, 1H, Ar), 6.83 (m, 5H, Ar), 6.64 (m, 2H, Ar), 3.50 (d, *J*=13.5, 1H, ArCH_2), 3.38 (d, *J*=13.5, 1H, ArCH_2), 2.93 (d, *J*=10.0, 1H, ArCH_2), 2.77 (d, *J*=10.0, 1H, ArCH_2), 2.49 (d, *J*=13.5, 1H, ArCH_2), 2.46 (m, 1H, CH_2), 2.42 (s, 3H, OCH_3), 2.28 (d, *J*=13.5, 1H, ArCH_2), 2.21 (d, *J*=10.3, 1H, ArCH_2), 2.13 (d, *J*=10.3, 1H, ArCH_2), 1.87 (m, 1H, CH_2), 1.79 (s, 9H, $C(CH_3)_3$), 1.71 (m, 1H, CH_2), 1.61 (m, 1H, CH_2), 1.34 (s, 9H, $C(CH_3)_3$) ppm. ^{13}C NMR (126 MHz, C_6D_6) δ = 157.99 (Ar), 156.13 (Ar), 149.40 (Ar), 143.28 (Ar), 141.79 (Ar), 136.61 (Ar), 130.20 (Ar), 129.83 (Ar), 128.72 (Ar), 128.58 (Ar), 128.35 (Ar), 127.48 (Ar),

127.29 (Ar), 125.22 (Ar), 125.11 (Ar), 124.68 (Ar), 123.93 (Ar), 123.65 (Ar), 122.75 (Ar), 121.04 (Ar), 72.64 (O*C*H_2), 66.24 (Ar*C*H_2), 64.86 (Ar*C*H_2), 64.23 (Ar*C*H_2), 62.41 (Ar*C*H_2), 60.59 (O*C*H_3), 50.76 (N*C*H_2), 35.50 (*C*(CH_3)$_3$), 34.47 (*C*(CH_3)$_3$), 31.92 (C(*C*H_3)$_3$), 30.12 (C(*C*H_3)$_3$) ppm. Anal. Calcd. for $C_{39}H_{47}Cl_2NO_2Zr_2$: C, 63.31; H, 6.40, N, 1.89. Found: C, 63.96; H, 6.47, N, 1.86.

Compound 57-NMe_2. 57-NMe_2 was fractioned over Celite with hexanes, Et_2O and benzene. The ^{1}H NMR spectrum of the benzene fraction was the desired pure complex (yellow solid, 0.045 g, 48 % yield). ^{1}H NMR (400 MHz, C_6D_6) δ = 7.76 (d, *J*=7.7, 2H, Ar), 7.59 (d, *J*=2.1, 1H, Ar), 7.34 (m, 3H, Ar), 7.07 (t, *J*=7.3, 1H, Ar), 6.87 (d, *J*=2.1, 1H, Ar), 6.80 (t, *J*=7.5, 2H, Ar), 6.74 (d, *J*=7.3, 2H, Ar), 6.67 (d, *J*=2.3, 1H, Ar), 6.58 (t, *J*=7.1, 1H, Ar), 3.55 (d, *J*=13.6, 1H, ArC*H*$_2$), 3.38 (d, *J*=13.8, 1H, ArC*H*$_2$), 2.80 (d, *J*=10.0, 1H, ArC*H*$_2$), 2.72 (d, *J*=10.0, 1H, ArC*H*$_2$), 2.47 (d, *J*=13.6, 1H, ArC*H*$_2$), 2.24 (d, *J*=13.9, 1H, ArC*H*$_2$), 2.11 (d, *J*=10.1, 1H, ArC*H*$_2$), 2.05 (m, 1H, C*H*$_2$), 1.95 (d, *J*=10.2, 1H, ArC*H*$_2$), 1.79 (s, 9H, C(C*H*$_3$)$_3$), 1.60 (s, 3H, N(*C*H$_3$)$_2$), 1.51 (m, 1H, C*H*$_2$), 1.44 (s, 3H, N(*C*H$_3$)$_2$), 1.34 (s, 9H, C(C*H*$_3$)$_3$), 1.33 (m, 2H, C*H*$_2$) ppm. ^{13}C NMR (101 MHz, C_6D_6) δ = 157.23 (Ar), 155.51 (Ar), 150.62 (Ar), 142.43 (Ar), 141.40 (Ar), 136.06 (Ar), 129.81 (Ar), 129.71 (Ar), 129.50 (Ar), 128.17 (Ar), 126.41 (Ar), 125.12 (Ar), 124.84 (Ar), 124.54 (Ar), 123.83 (Ar), 122.86 (Ar), 122.48 (Ar), 119.92 (Ar), 66.53 (Ar*C*H_2), 64.10 (Ar*C*H_2), 64.04 (Ar*C*H_2), 62.68 (Ar*C*H_2), 59.50 (N*C*H_2), 51.44 (N*C*H_2), 46.75 (N(*C*H_3)$_2$), 35.26 (*C*(CH_3)$_3$), 34.05 (*C*(CH_3)$_3$), 31.49 (C(*C*H_3)$_3$), 30.23 (C(*C*H_3)$_3$) ppm. Anal. Calcd. for $C_{40}H_{50}Cl_2N_2O_2Zr$: C, 63.81; H, 6.69, N, 3.72. Found: C, 64.30; H, 6.67, N, 3.44.

Compound 58. Phenol **58** was synthesized from **9** (1.14 g, 3.67 mmol) using BBr_3 (0.9 mL, 9.18 mmol, 2.5 equiv) and an analogous procedure to the synthesis of **50**. Column chromatography was utilized to purify the product (5/1 hexanes/ethyl acetate, R_f=0.8), which was collected as a white solid (1.02 g, 94 % yield). ^{1}H NMR (500 MHz, $CDCl_3$) δ = 7.29 (dd, *J*=8.5, 2.5, 1H, Ar), 7.02 (d, *J*=2.5, 1H, Ar), 6.92 (d, *J*=8.5, 1H, Ar), 2.32 (s, 3H, ArCH_3), 2.28 (s, 6H, ArCH_3), 1.99 (s, 6H, ArCH_3), 1.31 (s, 9H, C(CH_3)$_3$) ppm. ^{13}C NMR (126 MHz, $CDCl_3$) δ = 150.32 (Ar), 143.46 (Ar), 135.40 (Ar), 133.38 (Ar), 133.30 (Ar), 133.00 (Ar), 127.81 (Ar), 127.51 (Ar), 125.30 (Ar), 114.21 (Ar), 34.29 (*C*(CH$_3$)$_3$), 31.76 (C(*C*H$_3$)$_3$), 17.97 (Ar*C*H$_3$), 17.00 (Ar*C*H$_3$), 16.86 (Ar*C*H$_3$) ppm.

Compound 59. Bromomethyl phenol **59** was synthesized from **58** (0.94 g, 3.17 mmol) using paraformaldehyde (0.14 g, 4.76 mmol, 1.5 equiv) in glacial acetic acid (4 mL), and an analogous procedure to the synthesis of **51**. No product precipitated from hexanes so the material was used at the purity it was obtained (1.34 g, quantitative yield, >90 % purity). ^{1}H NMR (500 MHz, $CDCl_3$) δ = 7.30 (d, *J*=2.4, 1H, Ar), 7.00 (d, *J*=2.5, 1H, Ar), 4.81 (s, 1H, ArO*H*), 4.65 (s, 2H, ArCH_2), 2.31 (s, 3H, ArCH_3), 2.27 (s, 6H, ArCH_3), 1.96 (s, 6H, ArCH_3), 1.30 (s, 9H, C(CH_3)$_3$) ppm. ^{13}C NMR (126 MHz, $CDCl_3$) δ = 148.77 (Ar), 143.48 (Ar), 135.68 (Ar), 133.45 (Ar), 133.33 (Ar), 132.25 (Ar), 128.50 (Ar), 128.45 (Ar), 126.54 (Ar), 122.91 (Ar), 34.32 (*C*(CH$_3$)$_3$), 31.65 (C(*C*H$_3$)$_3$), 18.01 (Ar*C*H$_3$), 17.02 (Ar*C*H$_3$), 16.86 (Ar*C*H$_3$) ppm.

General synthesis of amine bisphenols 60-X. Mononucleating ligand precursors (**60-X**) were synthesized from **49a-X** (1.2 equiv), diisopropylethylamine (1.2 equiv), and **59** (1 equiv), using THF (1 mL per 0.02 mmol **59**) as the solvent and

analogous synthetic and workup procedures to those used for the synthesis and workup of the dinucleating ligands (**52-X**).

Compound 60-OMe. Column chromatography (5/1 hexanes/ethyl acetate) yielded the product as a white solid (0.30 g, 70 % yield). ^{1}H NMR (400 MHz, C_6D_6) δ = 8.36 (s, 2H, ArO*H*), 7.26 (d, *J*=2.2, 1H, Ar), 7.19 (d, *J*=2.3, 1H, Ar), 7.11 (d, *J*=2.3, 1H, Ar), 6.65 (d, *J*=1.9, 1H, Ar), 3.62 (s, 2H, ArCH_2), 3.39 (s, 2H, ArCH_2), 3.11 (t, *J*=5.3, 2H, CH_2), 2.92 (s, 3H, OCH_3), 2.43 (t, *J*=5.2, 2H, CH_2), 2.14 (s, 3H, ArCH_3), 2.09 (s, 6H, ArCH_3), 2.07 (s, 6H, ArCH_3), 1.33 (s, 9H, C(CH_3)$_3$) ppm. ^{13}C NMR (101 MHz, C_6D_6) δ = 153.30 (Ar), 150.39 (Ar), 143.02 (Ar), 134.87 (Ar), 133.87 (Ar), 133.04 (Ar), 133.02 (Ar), 129.69 (Ar), 129.06 (Ar), 127.76 (Ar), 127.58 (Ar), 127.40 (Ar), 125.40 (Ar), 123.42 (Ar), 122.35 (Ar), 122.07 (Ar), 70.39 (OCH$_2$), 58.50 (OCH$_3$), 56.99 (ArCH$_2$), 55.21 (ArCH$_2$), 52.57 (NCH$_2$), 34.27 (C(CH$_3$)$_3$), 31.81 (C(CH$_3$)$_3$) 18.22 (ArCH$_3$), 16.85 (ArCH$_3$), 16.78 (ArCH$_3$) ppm. HRMS (EI+) Calcd. for $C_{32}H_{42}Cl_2NO_3$: 558.2542. Found: 558.2540.

Compound 60-NMe2. Column chromatography (20/5/1 ethyl acetate/hexanes/MeOH, R_f = 0.5) yielded the product as a white solid (0.39 g, 89 % yield). ^{1}H NMR (400 MHz, C_6D_6) δ = 9.73 (s, 2H, ArO*H*), 7.19 (s, 1H, Ar), 7.16 (s, 1H, Ar), 7.10 (s, 1H, Ar), 6.72 (s, 1H, Ar), 3.32 (s, 2H, ArCH_2), 3.11 (s, 2H, ArCH_2), 2.15 (s, 9H, ArCH_3), 2.12 (s, 6H, ArCH_3), 2.06 (s, 2H, CH_2), 1.85 (s, 2H, CH_2), 1.74 (s, 6H, N(CH_3)$_2$), 1.34 (s, 9H, C(CH_3)$_3$) ppm. ^{13}C NMR (126 MHz, C_6D_6) δ = 152.96 (Ar), 151.99 (Ar), 142.05 (Ar), 136.42 (Ar), 133.75 (Ar), 132.37 (Ar), 132.28 (Ar), 131.08 (Ar), 129.69 (Ar), 128.72 (Ar), 128.59 (Ar), 127.74 (Ar), 126.26 (Ar), 125.49 (Ar), 123.10 (Ar), 121.83 (Ar), 56.02 (ArCH$_2$), 55.69 (ArCH$_2$), 55.48 (NCH$_2$), 49.24 (NCH$_2$), 44.45

($N(CH_3)_2$), 34.17 ($C(CH_3)_3$), 31.88 ($C(CH_3)_3$) 18.52 ($ArCH_3$), 16.82 ($ArCH_3$), 16.80 ($ArCH_3$) ppm. HRMS (EI+) Calcd. for $C_{33}H_{45}Cl_2N_2O_2$: 571.2858. Found: 571.2864.

General synthesis of monozirconium complexes 61-X. In an inert atmosphere glovebox, a solution of $ZrBn_4$ (1 equiv) in toluene (2 mL per mmol $ZrBn_4$) was added to a scintillation vial equipped with a stirbar. To this, a solution of **60-X** (1 equiv) in toluene (2 mL per mmol $ZrBn_4$) was added at room temperature, and the reaction was stirred in the dark for 5 hours. After the desired reaction time, the volatiles were removed *in vacuo*. After metallation, the reaction was no longer considered to be light sensitive.

Compound 61-OMe. 61-OMe was fractioned over Celite with hexanes, Et_2O and benzene. The ^1H NMR spectrum of the benzene fraction was purely the desired complex (pale yellow solid, 0.041 g). Recrystallization of the Et_2O soluble fraction from toluene via liquid diffusion of pentane yielded additional product (0.051 g, 62 % yield overall). ^1H NMR (400 MHz, C_6D_6) δ = 7.35 (d, *J*=2.5, 1H, Ar), 7.31 (d, *J*=2.4, 1H, Ar), 7.07 (m, 3H, Ar), 6.96 (d, *J*=2.5, 1H, Ar), 6.86 (t, *J*=7.5, 2H, Ar), 6.77 (m, 4H, Ar), 6.66 (m, 2H, Ar), 3.54 (d, *J*=13.8, 1H, $ArCH_2$), 3.54 (d, *J*=13.8, 1H, $ArCH_2$), 3.48 (d, *J*=13.8, 1H, $ArCH_2$), 2.67 (d, *J*=8.7, 1H, $ArCH_2$), 2.57 (m, 1H, CH_2), 2.54 (s, 3H, OCH_3), 2.53 (d, J=13.2, 1H, $ArCH_2$), 2.41 (s, 3H, $ArCH_3$), 2.35 (s, 3H, $ArCH_3$), 2.34 (d, J=13.2, 1H, $ArCH_2$), 2.31 (s, 3H, $ArCH_3$), 2.27 (s, 3H, $ArCH_3$), 2.22 (d, *J*=8.7, 1H, $ArCH_2$), 2.14 (s, 3H, $ArCH_3$), 1.98 (m, 2H, CH_2), 1.78 (d, *J*=10.3, 1H, $ArCH_2$), 1.65 (m, 1H, CH_2), 1.49 (d, *J*=10.3, 1H, $ArCH_2$), 1.32 (s, 9H, $C(CH_3)_3$) ppm. ^{13}C NMR (101 MHz, C_6D_6) δ = 156.18 (Ar), 156.14 (Ar), 151.43 (Ar), 142.37 (Ar), 139.90 (Ar), 136.96 (Ar), 134.04 (Ar), 132.67 (Ar), 132.55 (Ar), 132.05 (Ar), 131.47 (Ar), 131.26 (Ar), 131.06 (Ar), 130.12 (Ar),

130.01 (Ar), 129.01 (Ar), 128.67 (Ar), 127.04 (Ar), 125.00 (Ar), 124.57 (Ar), 124.39 (Ar), 123.56 (Ar), 122.49(Ar), 120.46 (Ar), 72.39 (O*C*H_2), 64.90 (Ar*C*H_2), 64.08 (Ar*C*H_2), 62.42 (Ar*C*H_2), 61.70 (Ar*C*H_2), 60.56 (O*C*H_3), 51.77 (N*C*H_2), 34.32 (*C*(CH_3)$_3$), 31.90 (C(*C*H_3)$_3$), 18.64 (Ar*C*H_3), 18.44 (Ar*C*H_3), 17.11 (Ar*C*H_3), 16.91 (Ar*C*H_3), 16.87 (Ar*C*H_3) ppm. Anal. Calcd. for $C_{46}H_{53}Cl_2NO_3Zr$ • toluene (C_7H_8): C, 69.03; H, 6.67, N, 1.52. Found: C, 69.32; H, 6.84, N, 1.54.

Compound 61-NMe$_2$. 61-NMe$_2$ was fractioned over Celite with hexanes, Et_2O and benzene. The ^{1}H NMR spectrum of the benzene fraction was purely the desired complex (yellow solid, 0.085 g). Recrystallization of the Et_2O soluble fraction from toluene via liquid diffusion of pentane yielded additional product (0.012 g, 66 % yield overall). ^{1}H NMR (400 MHz, C_6D_6) δ = 7.32 (d, *J*=1.7, 2H, Ar), 7.23 (t, *J*=7.5, 2H, Ar), 7.12 (d, *J*=7.5, 2H, Ar), 7.06 (m, 2H, Ar), 6.88 (t, *J*=7.5, 2H, Ar), 6.77 (d, *J*=7.6, 2H, Ar), 6.65 (m, 2H, Ar), 4.01 (d, *J*=13.7, 1H, ArC*H*$_2$), 3.35 (d, *J*=13.8, 1H, ArC*H*$_2$), 2.63 (d, *J*=13.8, 1H, ArC*H*$_2$), 2.49 (s, 3H, ArC*H*$_3$), 2.48 (d, 1H, ArC*H*$_2$), 2.43 (s, 3H, ArC*H*$_3$), 2.27 (s, 3H, ArC*H*$_3$), 2.25 (s, 3H, ArC*H*$_3$), 2.24 (d, 1H, ArC*H*$_2$), 2.19 (m, 1H, C*H*$_2$), 2.13 (d, J=9.0, 1H, ArC*H*$_2$), 2.10 (s, 3H, ArC*H*$_3$), 1.88 (d, *J*=10.3, 1H, ArC*H*$_2$), 1.56 (m, 1H, C*H*$_2$), 1.38 (d, *J*=10.3, 1H, ArC*H*$_2$), 1.47 (s, 6H, N(C*H*$_3$)$_2$), 1.33 (s, 9H, C(C*H*$_3$)$_3$) 1.25 (m, 2H, C*H*$_2$) ppm. ^{13}C NMR (101 MHz, C_6D_6) δ = 156.17 (Ar), 155.84 (Ar), 152.45 (Ar), 142.04 (Ar), 140.85 (Ar), 136.65 (Ar), 134.00 (Ar), 133.55 (Ar), 132.60 (Ar), 132.25 (Ar), 130.92 (Ar), 130.63 (Ar), 130.29 (Ar), 130.26 (Ar), 130.07 (Ar), 128.59 (Ar), 128.21 (Ar), 126.60 (Ar), 125.57 (Ar), 125.05 (Ar), 124.68 (Ar), 123.23 (Ar), 122.71 (Ar), 120.13 (Ar), 66.21 (Ar*C*H_2), 64.37 (Ar*C*H_2), 63.01 (Ar*C*H_2), 60.89 (Ar*C*H_2), 59.89 (N*C*H_2), 52.16 (N*C*H_2), 46.90 (N(C*H*$_3$)$_2$), 34.31 (*C*(CH_3)$_3$), 31.86 (C(*C*H_3)$_3$), 19.46 (Ar*C*H_3), 19.00

(Ar*C*H_3), 17.20 (Ar*C*H_3), 17.03 (Ar*C*H_3), 16.94 (Ar*C*H_3) ppm. Anal. Calcd. for $C_{47}H_{56}Cl_2N_2O_2Zr$ • toluene (C_7H_8): C, 69.35; H, 6.90, N, 3.00. Found: C, 68.93; H, 6.78, N, 3.00.

General polymerization procedures.

The setup of all the polymerizations was conducted in a nitrogen atmosphere glovebox.

1-Hexene polymerizations without temperature control. In polymerizations where $[CPh_3][B(C_6F_5)_4]$ or $B(C_6F_5)_3$ was used as the activator, 1-hexene (2.5 mL), solvent (1.5 mL) and the desired zirconium precatalyst (4.0 μmol of Zr) were added to a Schlenk tube equipped with a stirbar. The activator ($[CPh_3][B(C_6F_5)_4]$ or $B(C_6F_5)_3$) was dissolved in the remaining 1 mL solvent. The activator solution was added all at once and the timer was started. The tube was sealed and brought out of the glovebox. After stirring the reaction for the appointed amount of time, the reaction was opened and quenched with 5 mL of hexanes and 0.5 mL of MeOH. The quenched reaction was filtered over Celite and washed with additional hexanes. The filtrate was transferred to a tared flask and volatiles were removed on the Schlenk line at 100 °C overnight.

In polymerizations where MAO was used as the activator, MAO was added as a solid to the Schlenk tube equipped with a stirbar along with 1-hexene (2.5 mL) and solvent (1.5 mL). The desired zirconium complex (4.0 μmol of Zr) was dissolved in the remaining 1 mL solvent. The zirconium precatalyst solution was added in one fraction and the timer was started. The tube was sealed and brought out of the glovebox. After stirring the reaction for the appointed amount of time, the reaction was opened and quenched with 5 mL of hexanes and 0.5 mL of MeOH. The quenched reaction was

filtered over Celite and washed with additional hexanes. The filtrate was transferred to a tared flask and volatiles were removed on the Schlenk line at 100 °C overnight.

1-Hexene polymerizations with temperature control. 1-hexene (2.5 mL), chlorobenzene (1.0 mL), the desired amount of Al^iBu_3 (measured in a microsyringe), and the desired zirconium precatalyst (2.0 μmol or 0.4 μmol of Zr) dissolved in 1.0 mL chlorobenzene were added to a Schlenk tube equipped with a stirbar in that order. The tube was sealed, brought out of the glovebox, and regulated to the desired temperature: no bath for those run at ambient temperature, an oil bath regulated at 60 or 25 °C, an ice water bath at 0 °C, or an ethanol/ethylene glycol/dry ice bath at -20 or -30 °C. The tube was connected to the Schlenk line via a rubber hose, which was evacuated and backfilled with N_2. In the glovebox, $[CPh_3][B(C_6F_5)_4]$ (1 or 3 equivalents per Zr) was dissolved in 0.5 mL of chlorobenzene and loaded into a 1 mL syringe. The needle was sealed with a rubber septum and the syringe was brought out of the glovebox. The activator solution was syringed into the reaction quickly under N_2, the timer was started, and the reaction was sealed. After stirring the reaction for the appointed amount of time, the reaction was opened and quenched with 5 mL of hexanes and 0.5 mL of MeOH. The quenched reaction was filtered over Celite and washed with additional hexanes. The filtrate was transferred to a tared flask and volatiles were removed on the Schlenk line at 100 °C overnight.

Propylene polymerizations with MAO. A 3 oz. Andrews glass pressure reaction vessel equipped with Swagelok valves and a gauge was used for all high pressure polymerizations. In the glovebox, a syringe was loaded with a solution of the desired zirconium precatalyst in 1 mL of solvent, and the needle was sealed with a

rubber septum. The high-pressure setup was brought into the glovebox with a magnetic stirbar and charged with the desired amount of MAO and 1 mL solvent, and the setup was sealed. The syringe and setup were brought out of the glovebox and the setup was clamped firmly over a hot plate with an ice bath. The solution was stirred vigorously. A nylon core hose equipped with quick connect adaptors was attached to the setup and was evacuated and backfilled with propylene at greater than 100 psig pressure. The hose was opened to the setup and approximately 10.3 mL propylene was condensed into the setup. The setup was closed and the hose was disconnected. The solution of organometallic complex was added via syringe through the top of the setup, the setup was closed, and the timer was started. The pressure of the reaction at 0 °C was approximately 80 psig, though for some of the more active systems, a spike in pressure was observed shortly after injection of the catalyst. After the desired time, the setup was vented and the reaction mixture was quenched with 10 mL of 10 % HCl in methanol. An additional 10 mL of acidified methanol was added and the mixure was left stirring for greater than 1 h. The precipitated polymer was collected by filtration over a fine frit. All polymers were dried on the Schlenk line for a minimum of 8 hours before a mass was recorded.

Propylene polymerizations with $[CPh_3][B(C_6F_5)_4]$ and Al^iBu_3. In the glovebox, a syringe was loaded with a solution of the desired zirconium precatalyst in 1 mL of PhCl. A second syringe was loaded with a solution of $[CPh_3][B(C_6F_5)_4]$ in 1 mL of PhCl. Both needles were sealed with rubber septa. The high-pressure setup was brought into the glovebox with a magnetic stirbar and charged with the desired amount of Al^iBu_3, and the setup was sealed. The syringes and setup were brought out of the

glovebox and the setup was clamped firmly over a hot plate with an ice bath. The solution was stirred vigorously. A nylon core hose equipped with quick connect adaptors was attached to the setup and was evacuated and backfilled with propylene at great than 100 psig pressure. The hose was opened to the setup and approximately 10.3 mL propylene was condensed into the setup. The setup was closed and the hose was disconnected. The contents of the two syringes were added through the top of the setup (order of addition is specified in the data tables), the setup was closed, and the timer was started. From this point, the procedure exactly matches that of the propylene polymerizations with MAO.

Polymer Characterization Methods.

NMR. All polymer NMR spectra were recorded on a Varian-INOVA 500 MHz NMR instrument. ^{1}H and ^{13}C NMR spectra of 1-hexene homopolymers were taken in $CDCl_3$ at room temperature. 1-Hexene ^{13}C NMR spectra were assigned according to literature.[41,51] ^{1}H and ^{13}C NMR spectra of propylene homopolymers were taken in $C_2D_2Cl_4$ at 130 °C. The polypropylene peaks were assigned according to literature.[8,42,52]

GPC. Poly(1-hexene) molecular weights were determined utilizing THF as the eluent by multi-angle laser light scattering (MALLS) gel permeation chromatography (GPC) using a miniDAWN TREOS light scattering detector, a Viscostar viscometer, and an OptilabRex refractive index detector, all from Wyatt Technology. An Agilent 1200 UV-Vis detector was also present in the detector stack. Absolute molecular weights were determined using dn/dc values calculated by assuming 100% mass recovery of the polymer sample injected into the GPC.

Crystallographic Information

Table 5.8. Crystal and refinement data for complexes **53a-OMe**, **53a-NMe$_2$**, **53c-OMe**, and **57-OMe**.

	53a-OMe	**53a-NMe$_2$**	**53c-OMe**	**57-OMe**
CCDC #	9080844	980855	980843	980845
empirical formula	$C_{107}H_{118}Cl_4N_2O_6Zr_2$	$C_{115}H_{138}Cl_4N_4O_4Zr_2$	$C_{84}H_{100}N_2O_6Zr_2$	$C_{39}H_{47}Cl_2NO_3Zr$
formula wt	1852.27	1964.53	1416.09	739.89
T (K)	100	100	100	100
a, Å	16.9447(8)	15.1035(15)	9.6061(4)	10.100(2)
b, Å	19.0668(10)	25.847(3)	29.2804(13)	21.150(4)
c, Å	29.5530(17)	26.584(3)	17.7516(8)	17.180(3)
α, deg	90	90	90	90
β, deg	90	90	105.5095(17)	101.11(3)
γ, deg	90	90	90	90
V, Å^3	9548.0(9)	10377.7(18)	4811.2(4)	3601.1(13)
Z	4	4	2	4
cryst syst	orthorhombic	orthorhombic	monoclinic	monoclinic
space group	P 21 21 21	P c c n	P 1 21 1	P 1 21/n 1
d_{calcd}, g/cm^3	1.289	1.257	0.978	1.365
θ range, deg	1.6 to 30.6	1.5 to 35.7	1.2 to 34.2	2.1 to 34.0
μ, mm^{-1}	0.38	0.36	0.26	1.14
abs cor	Semi-empirical from equivalents	Semi-empirical from equivalents	Semi-empirical from equivalents	Semi-empirical from equivalents
GOF	1.04	1.10	0.99	1.11
R1,[a] wR2[b] (I > 2θ (I))	R1 = 0.0757, wR2 = 0.1896	R1 = 0.0839, wR2 = 0.1805	R1 = 0.0502, wR2 = 0.0879	R1 = 0.0328, wR2 = 0.0737

[a] $R_1 = \sum||F_o| - |F_c||/\sum|F_o|$. [b] $wR_2 = [\sum[w(F_o^2-F_c^2)^2]/\sum[w(F_o^2)^2]]^{1/2}$.

REFERENCES

1. Brintzinger, H. H.; Fischer, D.; Mulhaupt, R.; Rieger, B.; Waymouth, R. M. *Angew. Chem. Int. Ed.* **1995**, *34*, 1143-1170.
2. Britovsek, G. J. P.; Gibson, V. C.; Wass, D. F. *Angew. Chem. Int. Ed.* **1999**, *38*, 428-447.
3. Coates, G. W. *Chem. Rev.* **2000**, *100*, 1223-1252.
4. Gibson, V. C.; Spitzmesser, S. K. *Chem. Rev.* **2003**, *103*, 283-315.
5. Miller, S. A. *J. Organomet. Chem.* **2007**, *692*, 4708-4716.
6. Miller, S. A.; Bercaw, J. E. *Organometallics* **2006**, *25*, 3576-3592.
7. Miller, S. A.; Bercaw, J. E. *Organometallics* **2004**, *23*, 1777-1789.
8. Busico, V.; Cipullo, R. *Prog. Poly. Sci.* **2001**, *26*, 443-533.
9. Resconi, L.; Cavallo, L.; Fait, A.; Piemontesi, F. *Chem. Rev.* **2000**, *100*, 1253-1345.
10. Veghini, D.; Henling, L. M.; Burkhardt, T. J.; Bercaw, J. E. *J. Am. Chem. Soc.* **1999**, *121*, 564-573.
11. Spaleck, W.; Kueber, F.; Winter, A.; Rohrmann, J.; Bachmann, B.; Antberg, M.; Dolle, V.; Paulus, E. F. *Organometallics* **1994**, *13*, 954-963.
12. Ward, B. D.; Bellemin-Laponnaz, S.; Gade, L. H. *Angew. Chem. Int. Ed.* **2005**, *44*, 1668-1671.
13. Gendler, S.; Groysman, S.; Goldschmidt, Z.; Shuster, M.; Kol, M. *J. Polym. Sci., Part A: Polym. Chem.* **2006**, *44*, 1136-1146.
14. Senda, T.; Hanaoka, H.; Hino, T.; Oda, Y.; Tsurugi, H.; Mashima, K. *Macromolecules* **2009**, *42*, 8006-8009.
15. Ward, B. D.; Lukesova, L.; Wadepohl, H.; Bellemin-Laponnaz, S.; Gade, L. H. *Eur. J. Inorg. Chem.* **2009**, 866-871.
16. Cai, Z.; Ohmagari, M.; Nakayama, Y.; Shiono, T. *Macromol. Rapid Commun.* **2009**, *30*, 1812-1816.
17. Kiesewetter, E. T.; Randoll, S.; Radlauer, M.; Waymouth, R. M. *J. Am. Chem. Soc.* **2010**, *132*, 5566-5567.
18. Press, K.; Cohen, A.; Goldberg, I.; Venditto, V.; Mazzeo, M.; Kol, M. *Angew. Chem. Int. Ed.* **2011**, *50*, 3529-3532.
19. Kiesewetter, E. T.; Waymouth, R. M. *Macromolecules* **2013**, *46*, 2569-2575.
20. Tshuva, E. Y.; Goldberg, I.; Kol, M.; Weitman, H.; Goldschmidt, Z. *Chem. Commun.* **2000**, 379-380.
21. Groysman, S.; Tshuva, E. Y.; Reshef, D.; Gendler, S.; Goldberg, I.; Kol, M.; Goldschmidt, Z.; Shuster, M.; Lidor, G. *Isr. J. Chem.* **2002**, *42*, 373-381.

22. Tshuva, E. Y.; Groysman, S.; Goldberg, I.; Kol, M.; Goldschmidt, Z. *Organometallics* **2002**, *21*, 662-670.

23. Tshuva, E. Y.; Goldberg, I.; Kol, M. *J. Am. Chem. Soc.* **2000**, *122*, 10706-10707.

24. Busico, V.; Cipullo, R.; Ronca, S.; Budzelaar, P. H. M. *Macromol. Rapid Commun.* **2001**, *22*, 1405-1410.

25. Segal, S.; Goldberg, I.; Kol, M. *Organometallics* **2005**, *24*, 200-202.

26. Yeori, A.; Goldberg, I.; Shuster, M.; Kol, M. *J. Am. Chem. Soc.* **2006**, *128*, 13062-13063.

27. Delferro, M.; Marks, T. J. *Chem. Rev.* **2011**, *111*, 2450-2485.

28. Lee, D. H.; Yoon, K. B.; Lee, E. H.; Noh, S. K.; Byun, G. G.; Lee, C. S. *Macromol. Rapid Commun.* **1995**, *16*, 265-268.

29. Linh, N. T. B.; Huyen, N. T. D.; Noh, S. K.; Lyoo, W. S.; Lee, D.-H.; Kim, Y. *J. Organomet. Chem.* **2009**, *694*, 3438-3443.

30. Noh, S. K.; Byun, G. G.; Lee, C. S.; Lee, D.; Yoon, K. B.; Kang, K. S. *J. Organomet. Chem.* **1996**, *518*, 1-6.

31. Noh, S. K.; Jung, W.; Oh, H.; Lee, Y. R.; Lyoo, W. S. *J. Organomet. Chem.* **2006**, *691*, 5000-5006.

32. Noh, S. K.; Kim, S.; Yang, Y.; Lyoo, W. S.; Lee, D. H. *Eur. Polym. J.* **2004**, *40*, 227-235.

33. Casalino, M.; De Felice, V.; Fraldi, N.; Panunzi, A.; Ruffo, F. *Inorg. Chem.* **2009**, *48*, 5913-5920.

34. Wei, J.; Hwang, W.; Zhang, W.; Sita, L. R. *J. Am. Chem. Soc.* **2013**, *135*, 2132-2135.

35. Radlauer, M. R.; Buckley, A. K.; Henling, L. M.; Agapie, T. *J. Am. Chem. Soc.* **2013**, *135*, 3784-3787.

36. Radlauer, M. R.; Day, M. W.; Agapie, T. *Organometallics* **2012**, *31*, 2231-2243.

37. Radlauer, M. R.; Day, M. W.; Agapie, T. *J. Am. Chem. Soc.* **2012**, *134*, 1478-1481.

38. Ittel, S. D.; Johnson, L. K.; Brookhart, M. *Chem. Rev.* **2000**, *100*, 1169-1204.

39. Makio, H.; Terao, H.; Iwashita, A.; Fujita, T. *Chem. Rev.* **2011**, *111*, 2363-2449.

40. Appiah, W. O.; DeGreeff, A. D.; Razidlo, G. L.; Spessard, S. J.; Pink, M.; Young, V. G.; Hofmeister, G. E. *Inorg. Chem.* **2002**, *41*, 3656-3667.

41. Asakura, T.; Demura, M.; Nishiyama, Y. *Macromolecules* **1991**, *24*, 2334-2340.

42. Busico, V.; Cipullo, R.; Monaco, G.; Vacatello, M.; Segre, A. L. *Macromolecules* **1997**, *30*, 6251-6263.

43. Bochmann, M. *J. Organomet. Chem.* **2004**, *689*, 3982-3998.

44. Inoue, Y.; Itabashi, Y.; Chûjô, R.; Doi, Y. *Polymer* **1984**, *25*, 1640-1644.

45. Bruce, M. D.; Waymouth, R. M. *Macromolecules* **1998**, *31*, 2707-2715.

46. Pangborn, A. B.; Giardello, M. A.; Grubbs, R. H.; Rosen, R. K.; Timmers, F. J. *Organometallics* **1996**, *15*, 1518-1520.

47. Gisch, N.; Balzarini, J.; Meier, C. *J. Med. Chem.* **2007**, *50*, 1658-1667.

48. Knight, P. D.; O'Shaughnessy, P. N.; Munslow, I. J.; Kimberley, B. S.; Scott, P. *J. Organomet. Chem.* **2003**, *683*, 103-113.

49. Covert, K. J.; Mayol, A. R.; Wolczanski, P. T. *Inorg. Chim. Acta* **1997**, *263*, 263-278.

50. Rong, Y.; Al-Harbi, A.; Parkin, G. *Organometallics* **2012**, *31*, 8208-8217.

51. Galland, G. B.; Da Silva, L. F.; Nicolini, A. *J. Polym. Sci., Part A: Polym. Chem.* **2005**, *43*, 4744-4753.

52. Busico, V.; Cipullo, R.; Corradini, P.; Landriani, L.; Vacatello, M.; Segre, A. L. *Macromolecules* **1995**, *28*, 1887-1892.

APPENDIX A

TOWARD PALLADIUM CATALYSTS WITH PENDANT LEWIS ACIDS FOR INSERTION POLYMERIZATION OF POLAR MONOMERS

Reproduced in part by permission of The Royal Society of Chemistry:
Kelley, P.; Radlauer, M. R.; Yanez, A. J.; Day, M. W.; Agapie, T. *Dalton Trans.* **2012**, *41*, 8086-8092.
http://pubs.rsc.org/en/content/articlehtml/2012/dt/c2dt30285c

ABSTRACT

The targeted palladium complexes with pendant Lewis acids were intended for insertion polymerization of polar monomers. The pendant Lewis acids would coordinate the polar moieties, disfavoring deactivation pathways and allowing polymerization to proceed. Dioximato ligands were designed to support a palladium via the oxime nitrogens and two Lewis acids via the oxime oxygens. The dioximato ligand structure could be metallated with palladium(II), but the addition of Lewis acid precursors resulted in intractable mixtures. Similarly, reactivity between Lewis acid precursors and dioximato framework went cleanly, but the subsequent addition of palladium(II) precursors yielded complex mixtures. Pure complexes were obtained from these mixtures wherein two dioximato ligands were bound to a single palladium center with aluminum bridging the oxime oxygens on either side. Peaks consistent with the [$PdAl_2$] complexes were present in the NMR spectra of most of the attempts to make the desired mono-dioximato complexes. The ligand was therefore altered. Diimine bis-*o*-phenolate frameworks were developed and metallated with palladium(II), but the addition of pendant Lewis acids was again unsuccesful. To increase the number of donors present on the ligand framework for binding to the Lewis acid, a diimine backbone was designed with pendant aminediol moieties. Again, metallation with palladium(II) provided isolable complexes. The addition of pendant Lewis acids, however, resulted in very reactive speices whose isolation remained elusive. Preliminary ethylene/methyl acrylate copolymerizations were performed using *in situ* activation of the palladium speceis, but were not effective. Efforts toward further purification of the desired complexes proved unsuccessful.

INTRODUCTION

Polymers consisting of or incorporating polar monomers are used in a variety of industries because of their many useful properties including improved adhesion to substrates, response to stimuli, and increased compatibility with other materials for use in polymer blends and composites.[1-8] Tens of millions of tons of functionalized polymers such as polyvinyl chloride (PVC) are synthesized world-wide each year.[9] The free-radical polymerization method currently used for the industrial scale synthesis of PVC, polyacrylates, and several other polymers incorporating polar monomers often does not allow for much control over the polymer microstructure (e.g., tacticity, branching, functionality incorporation, molecular weight),[4,6,10-16] such that the investigation of other methods for polar monomer polymerization is desirable.[17-23] To that end, examples of polymers incorporating a range of functionality produced by coordination polymerization or metathesis polymerization have been reported, though systems that produce polymers at sufficient rates and productivities for commercial viability have yet to be developed.[17-39]

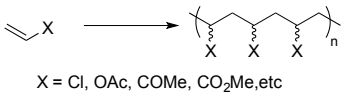

Scheme A.1. Polymerization of polar monomers.

Early transition metal catalyzed polymerizations of ethylene, propylene, and α-olefins provide high yields and control over a variety of polymer characteristics.[40-45] Late transition metal catalysts cannot match this activity due to β-hydride elimination from the agostic catalyst resting state competing with coordination and insertion of the next monomer.[19] Early transition metal complexes, however, are generally too oxophilic for

insertion polymerization of polar olefins, and the catalysts are deactivated by coordination of the polar moiety.[25,46] Coordination polymerization of a limited set of polar monomers can be achieved with early transition metal catalysts by taking advantage of their oxophilicity (Scheme A.2).[20,37,39] In these polymerizations, the polar functionality binds to the metal and the polymerization proceeds through Michael additions of subsequent monomers. High stereospecificity has been achieved in this manner.[37,39]

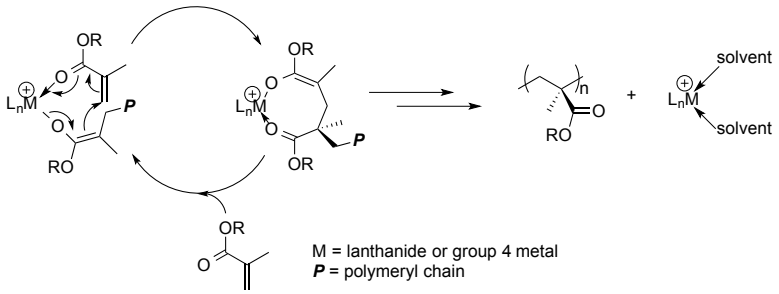

Scheme A.2. Coordination polymerization of methyl methacrylate mediated by early transition metal catalysts.

Late transition metal catalysts may offer access to a wide variety of polymers incorporating polar monomers through insertion polymerization.[17-23,45] Such catalysts are generally more tolerant of polar groups because of their reduced oxophilicity. Many groups have developed catalysts for the insertion polymerization of polar monomers, and the most successful polymerizations to date have utilized cationic or neutral palladium(II) and nickel(II) catalyst systems (Chart A.1).[18-23] These include cationic palladium(II) and nickel(II) complexes with sterically bulky diimine ligands (**A**), neutral nickel(II) phenoxyiminato complexes (**B**), and neutral palladium(II) phoshine-sulfonate catalyst systems (**C**). Systems **A** produce highly branched polyethylene and copolymers of ethylene and α-olefins; the polymers produced with palladium(II) catalysts are

generally more branched than those produced with nickel(II) analogues.[47-48] The ortho substituents on the aryl rings of the diimine hinder the approach of olefins to the axial positions of palladium thereby decreasing the likelihood of associative displacement and chain transfer and increasing the average molecular weight of the polymer.[47] **A** and derivatives of **A** display copolymerization activity of acrylates[25,49] or silyl vinyl ethers[50] with ethylene and α-olefins, though incorporation of the polar monomer is limited (less than 20%), and no success has been reported with vinyl halides[33,51-52] or vinyl acetates.[53] Systems **B** have proven to be efficient for ethylene homopolymerization and tolerant of a variety of functional groups allowing for the incorporation of monomers with distal functionality, such as norbornenyl acetate.[26,54,55] Systems **C** have been shown to be active for ethylene homopolymerization, ethylene-polar olefin copolymerization and homooligomerization of polar monomers.[21,23,29] Copolymerization of ethylene and methyl acrylate by **C** produced polymer with upwards of 50 % incorporation of methyl acrylate, but with a much lower activity than that seen with the α-diimine systems.[36]

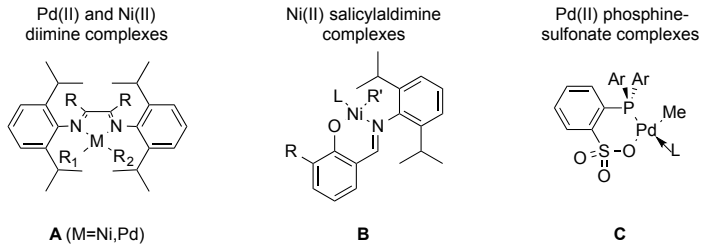

Chart A.1. Examples of Ni(II) and Pd(II) catalyst systems for polar monomer polymerizations.

Mechanistic studies, especially of α-diimine palladium systems, have detailed the limitations for polar monomer incorporation due to chain walking and β-eliminations. These processes lead to metal halides (**D**), stable 5- or 6-membered chelates (**E**), or enolates (**F**), effectively deactivating the system (Scheme A.3).[33,46,51-53,56-61] Finding

systems capable of combining of high incorporation, high molecular weight and high activity remains a challenge.[21,23]

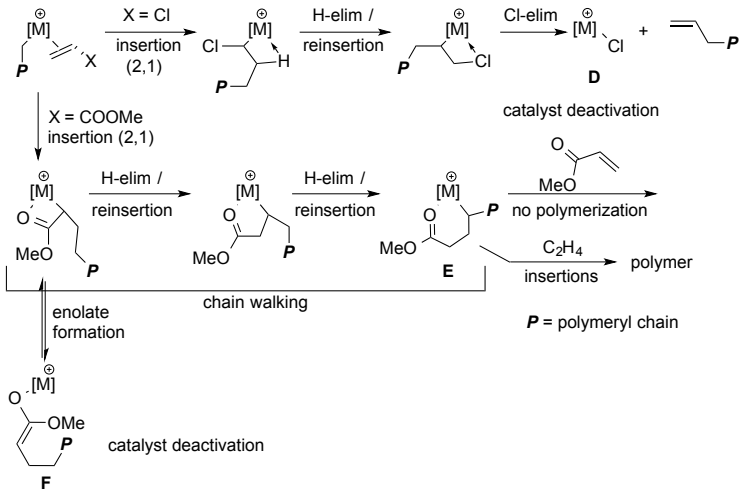

Scheme A.3. Deactivation of catalysts via chain walking, β-hydride or β-chloride elimination, and enolate formation.

The strategy presented herein uses Lewis acidic groups pendant to a palladium based polymerization center to coordinate the polar moiety of functionalized olefins, disfavoring deactivation pathways. The pendant Lewis acidic groups on the catalysts will serve multiple purposes (Scheme A.4). The oxophilic Lewis acid is expected to coordinate the polar moiety of the growing polymer chain to impede heteroatom coordination to palladium and subsequent chelate formation or β-elimination. The Lewis acid will also coordinate the polar moieties of free monomer to favor coordination of the olefinic moiety to palladium. Additionally, the Lewis acidic group is designed to provide sufficient steric bulk in the axial positions of palladium to lower the rate of chain transfer to monomer and resultant polymer termination.

In the present work, two backbone designs were pursued: a dioxime backbone in which the Lewis acids would be bound directly to the oxime oxygens (**G**) and a diimine

backbone which contains phenol or aminediol binding sites for Lewis acids (**H** and **I**) (Figure A.1). The dioxime/diimine backbone was chosen because of the promising copolymerization activity with polar monomers and the detailed mechanistic studies completed with previously reported palladium diimine systems.[19,53,56,62-63] A variety of Lewis acids were selected to access a range of Lewis acidities. The pendant Lewis acidic groups must be suitably oxophilic for polar functionality to preferentially bind to the Lewis acid over palladium. The coordination of the polar monomer to the Lewis acid cannot be too strong, however, because good turnover of monomer is necessary for effective polymerization.

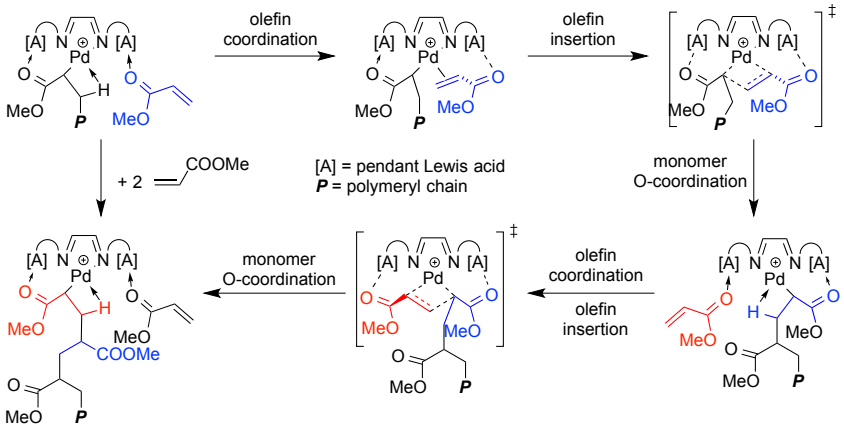

Scheme A.4. Interactions in proposed [PdA_2] catalysts between Lewis acids and the polar moieties of methyl acrylate during polymerization.

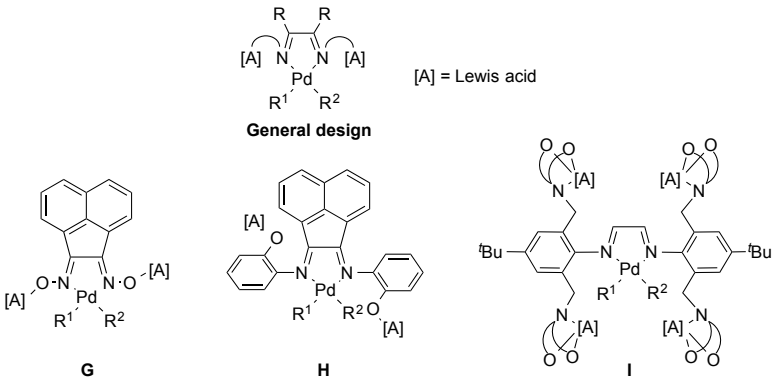

Figure A.1. General design of catalyst system (above). Three targets pursued in the present work (below).

RESULTS AND DISCUSSION

Complexes with a dioxime backbone

The proposed catalyst systems can divided into three pieces: the organic backbone, the palladium(II) precursor, and the Lewis acids. A rigid α-dioxime based off of acenaphthenequinone was chosen. Acenaphthenequinonedioxime (**62**) was synthesized via an analogous literature procedure[64] from the condensation of two equivalents of hydroxylamine onto acenaphthenequinone (Scheme A.5). Two metal precursors – palladium metallocycle **63** and (COD)PdMeCl (**64**) (Scheme A.6; COD = 1,5-cyclooctadiene) – were synthesized according to literature procedures.[65-67] Reactions between these precursors and acenaphthenequinonedioxime resulted in metallation at the oxime nitrogens (Scheme A.6). X-ray quality crystals were obtained of palladium complexes **65** and **66**. X-ray diffraction (XRD) studies revealed that metallation with **63** resulted in a dimeric structure, while metallation with **64** yielded the expected monomeric complex **66** (Figure A.2). To form dimer **65**, the metallocycle was protonolyzed and the palladium coordinated to oxygen from the second dioxime molecule. The dimeric nature of **65** was not intended, but is not expected to limit further reactivity because the oxime oxygen will bind more favorably to a Lewis acidic metal than to palladium.

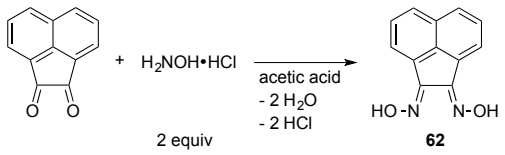

Scheme A.5. Synthesis of acenaphthenequinonedioxime.

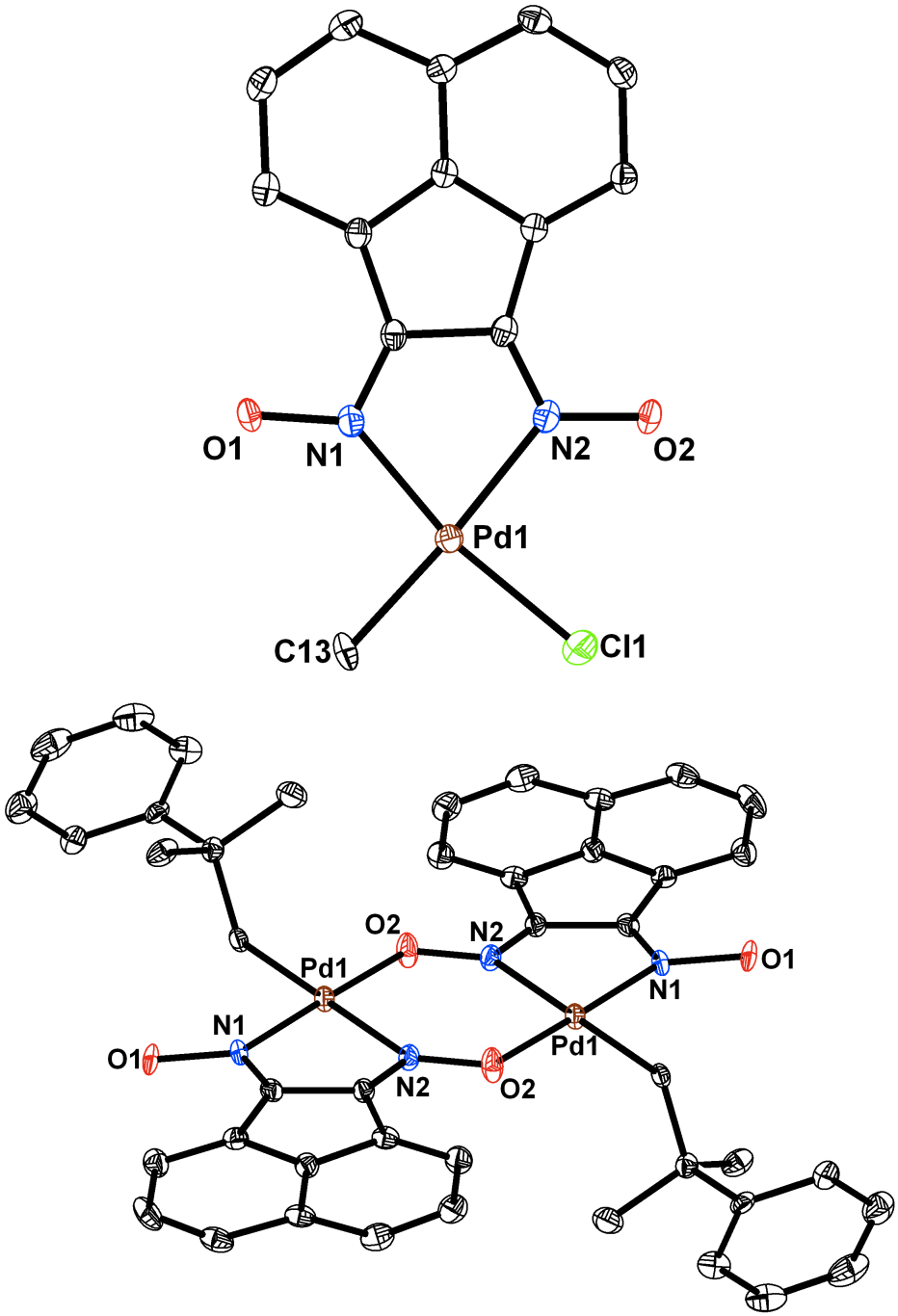

Figure A.2. Solid-state structures of **65** (above) and **66** (below) with thermal ellipsoids at the 50 % probability level.[68] For clarity, hydrogen atoms and solvent molecules are omitted.

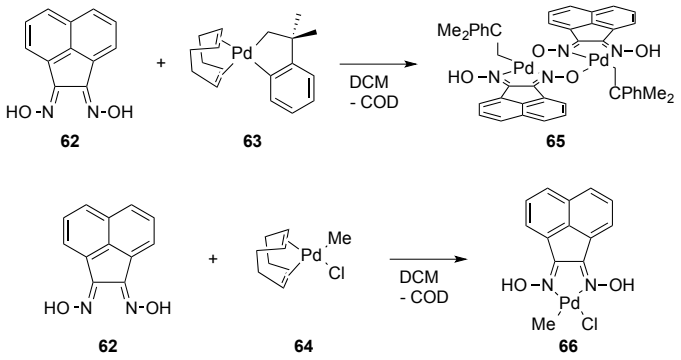

Scheme A.6. Metallation of acenaphthenequinonedioxime (**62**) with palladium precursors **63** and **64**.

A variety of Lewis acid precursors were synthesized or purchased (Chart A.2). Reactions were conducted by adding two equivalents of the Lewis acid precursor per palladium to the palladium-dioxime complex **65** or **66** with the intent of binding the Lewis acid compounds to the dioxime oxygens (Scheme A.7). A variety of conditions for these reactions were utilized, but primarily resulted in intractable mixtures. Reactions were run in benzene, toluene, dichloromethane or tetrahydrofuran. When Lewis acid precursors with halides were used, one equivalent of triethylamine per equivalent of Lewis acid was added to quench the acidic byproduct. The scales of the reactions were varied (0.015–0.05 mmol of palladium complex and 0.03–0.1 mmol of Lewis acid precursor). The reactions were monitored after the first hour and periodically thereafter. They were run until most of the starting material was converted or for 48 h. In most of the reactions between **65** or **66** and Lewis acid precursors, at least some palladium black was formed. ^{1}H NMR spectra indicated mixtures of species, generally including unreacted starting material. Some of the ^{1}H NMR spectra included peaks indicative of a species with dioxime bound to two Lewis acid complexes based on the location and number of peaks and their integration, but the data were not

conclusive. Efforts to isolate these species were unsuccessful though recrystallizations did eventually yield X-ray quality crystals, *vide infra*.

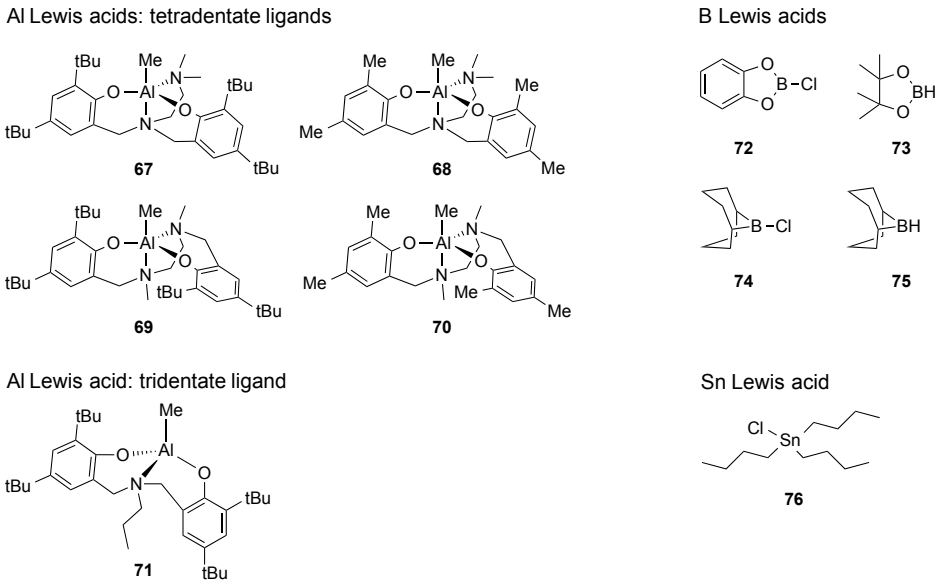

Chart A.2. Lewis acid precursors.

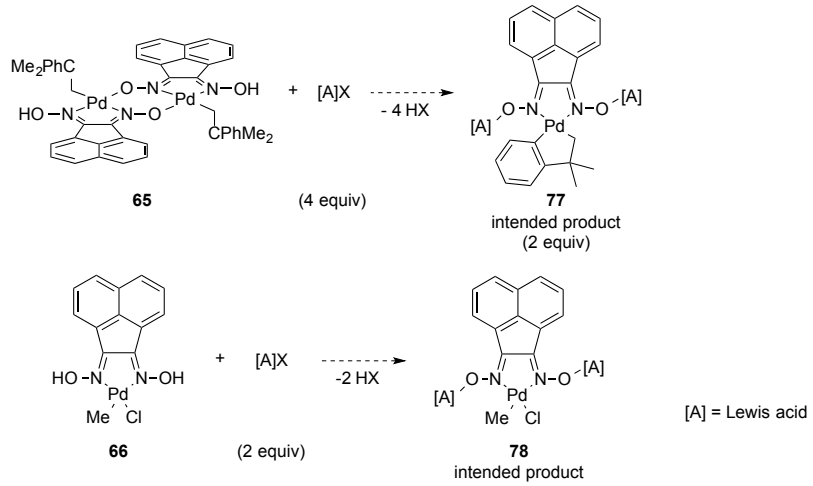

Scheme A.7. Intended reactivity between **65** or **66** and the Lewis acid precursors.

Because of the difficulties met when adding Lewis acids to the palladium-dioxime complexes, a separate route was attempted in which Lewis acids were bound to **62** before coordination of palladium (Scheme A.8). ^{1}H NMR spectroscopy data supported the synthesis of several Lewis acid-dioxime complexes. Specifically, reactions

between dioxime **62** and aluminum Lewis acids **67**, **68**, and **71**, and boron Lewis acids **73** and **75** all resulted in single products by ^{1}H NMR spectroscopy. Unfortunately, as with reactions combining the palladium-dioxime complexes and Lewis acids, reactions combining Lewis acid-dioxime complexes and palladium precursors resulted in complicated mixtures. Again, efforts to purify these mixtures did not provide interpretable ^{1}H NMR spectra. A challenge with the oxime ligand design may the proximity of the palladium and Lewis acid binding sites, which may affect the coordinating abilities to these centers both by steric and electronic effects. Hence a new ligand framework where oxygen is not directly bound to the nitrogen was targeted.

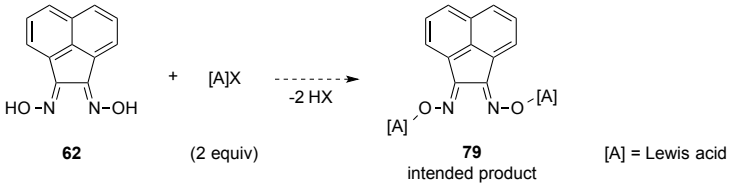

Scheme A.8. Intended reactivity between **62** and the Lewis acid precursors.

Complexes with a diimine backbone and pendant phenolic donors[69]

To spatially separate the binding sites for palladium from those for the Lewis acids, a rigid α-diimine based off of acenaphthenequinone was chosen wherein phenols off of the oxime nitrogens would provide the oxygenic donor for the Lewis acids. The synthesis of diimine **80** proceeded through diimine condensation of two equivalents of 6-amino-*m*-cresol onto acenaphthenequinone. This diimine was metallated with (COD)PdMeCl to yield complexes **81** (Scheme A.9). XRD studies of a single crystal of **81** confirmed that a monomeric palladium complex had been synthesized (Figure A.3). Subsequent reactions with Lewis acid precursors again resulted in complex product mixtures.

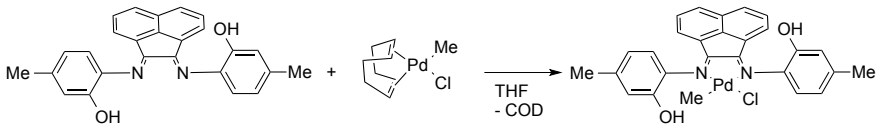

80 64 81

Scheme A.9. Metallation of diimine **80** with palladium precursor **64**.

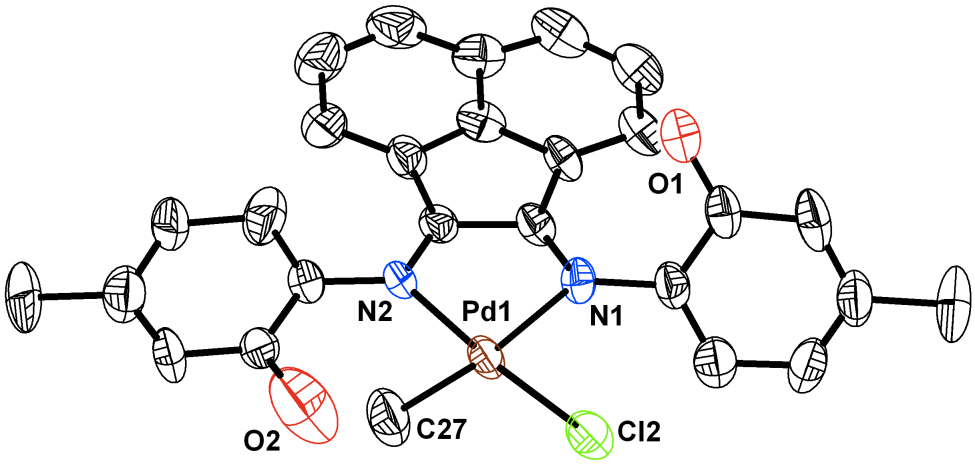

Figure A.3. Solid-state structure of **81** with thermal ellipsoids at the 50 % probability level.[70] For clarity, hydrogen atoms and solvent molecules are omitted.

Aluminum-bridged bis(dioximato) complexes of palladium

Concurrent with attempts to optimize the backbone design, X-ray quality crystals were obtained from the reaction of palladium complex **65** with aluminum complex **68**. The compound indicated by XRD was not the intended product with palladium bound to one dioxime molecule bearing two aluminum complexes (**77**), but rather the palladium was bound to two dioximato ligands bridged on either side by aluminum (**82**) (Figure A.4 and Scheme A.10). Two isomers were discovered in the solid-state: one with both aluminum bridges on the same side of the palladium (**82-cis**), the other with the aluminum bridges on opposite sides (**82-trans**). **82** was independently synthesized in 63% yield by treatment of the product of the reaction between $Pd(OAc)_2$ and two equivalents of **62** with two equivalents of aluminum complex **68** (Scheme

A.11). The reaction product, **82**, was confirmed through unit cell determination. Comparison of the ^{1}H NMR spectra of the unintentional and direct syntheses of **82** indicated that it accounted for no more than a quarter of the reaction mixture of the reaction between **65** and **68**. Thus, the intended product may have also been synthesized, but has not been isolated.

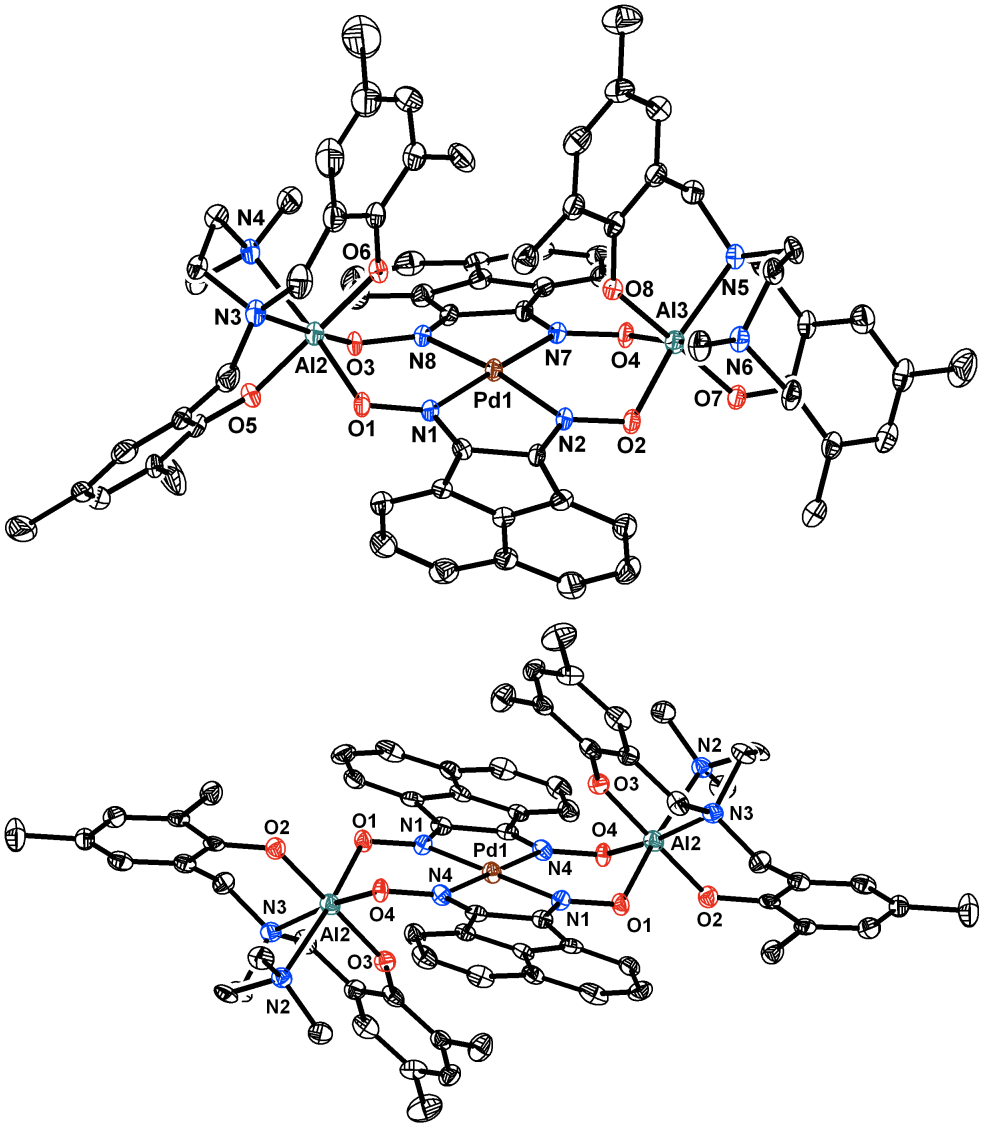

Figure A.4. Solid-state structures of **82-cis** (above) and **82-trans** (below) with thermal ellipsoids at the 50 % probability level. For clarity, hydrogen atoms and solvent molecules are omitted.

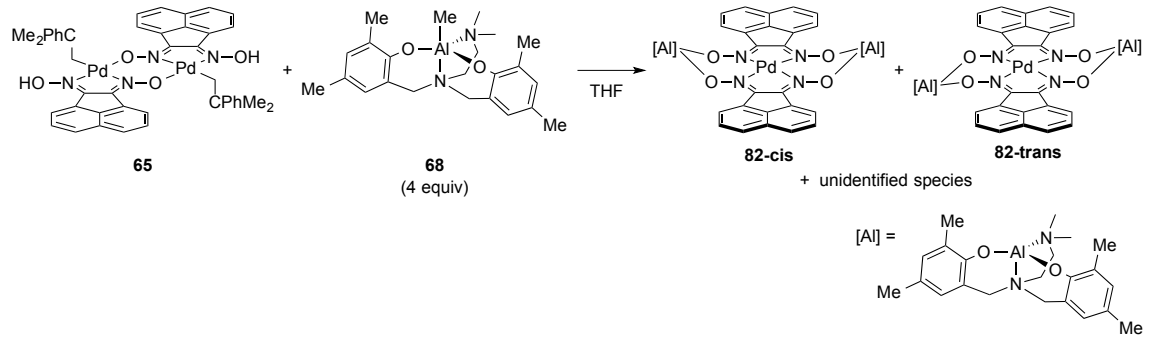

Scheme A.10. Reaction between **65** and **68**.

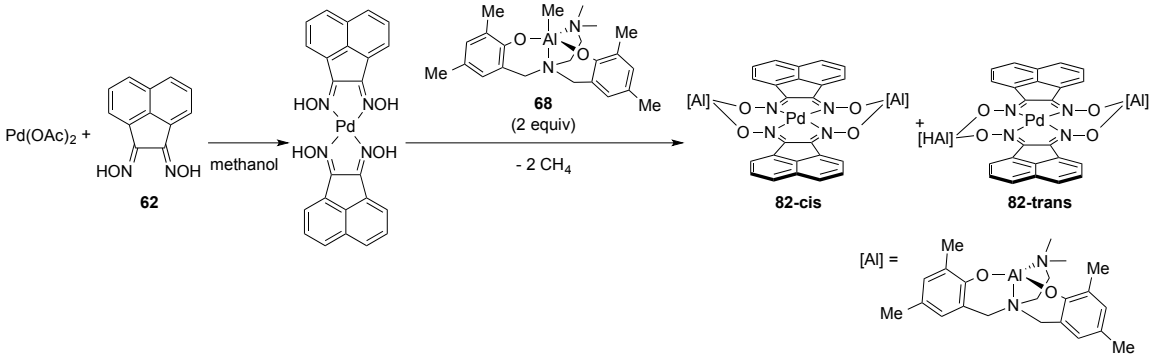

Scheme A.11. Direct synthesis of **82**.

The reaction of one equivalent of acenaphthenequinonedioxime and two equivalents of aluminum complex **67** was intended to produce a Lewis acid-dioxime complex in which an aluminum molecule was bound to each of the oxime oxygens. While integration of the ^{1}H NMR spectrum provided evidence for the desired product, **83**, XRD studies of crystals grown from the reaction of **62** and **67** produced a macrocyclic structure with two oximes bridged on either side by aluminum (complex **84**, Scheme A.12 and Figure A.5). One explanation for the discrepancy between the integration of the ^{1}H NMR spectrum and the crystal structure is that during the period it to took to recrystallize the product from the reaction between **62** and **67**, the product disproportionated. Direct synthesis of macrocycle **85** (an analogue of **84** with Me substituents on the phenoxy rings) could be achieved in 74 % yield by the 1:1 addition

of **62** to **68** (Scheme A.13). NMR analysis of compound **85** reveals that the methyl groups ortho to the phenoxide oxygen and the $N(CH_3)_2$ groups display single peaks, respectively. The C*H* protons at the 2 and 7 positions of the naphthalene moiety display different signals in NMR spectra. These data support an average structure that has C_{2h} symmetry, suggesting a fast fluxional process that exchanges the methyl groups on the NMR time scale, but preserves the C_2 axis. Additionally, a peak slightly downfield of 14 ppm indicated protonation of two of the nitrogen atoms of the dioximato moiety. A single crystal XRD study reveals the cis isomer of the dialuminum-bridged bisglyoximato macrocycle with pseudo-C_2 symmetry (Figure A.5). Notably, palladium complex **82** could be accessed via addition of $Pd(OAc)_2$ to this macrocyclic dialuminum complex, **85** (Scheme A.13).

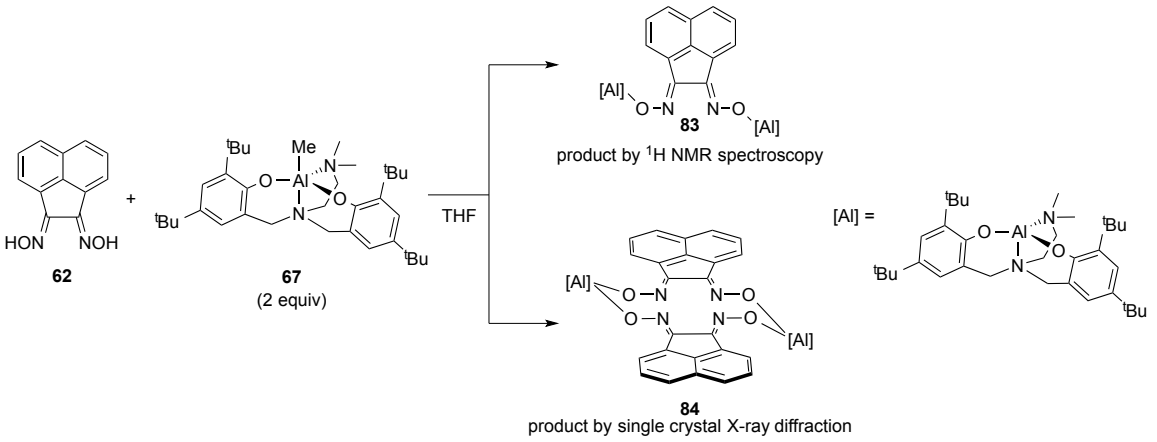

Scheme A.12. Reaction between **62** and **67**. Different products were identified by ^1H NMR spectroscopy (top) and single crystal XRD (bottom).

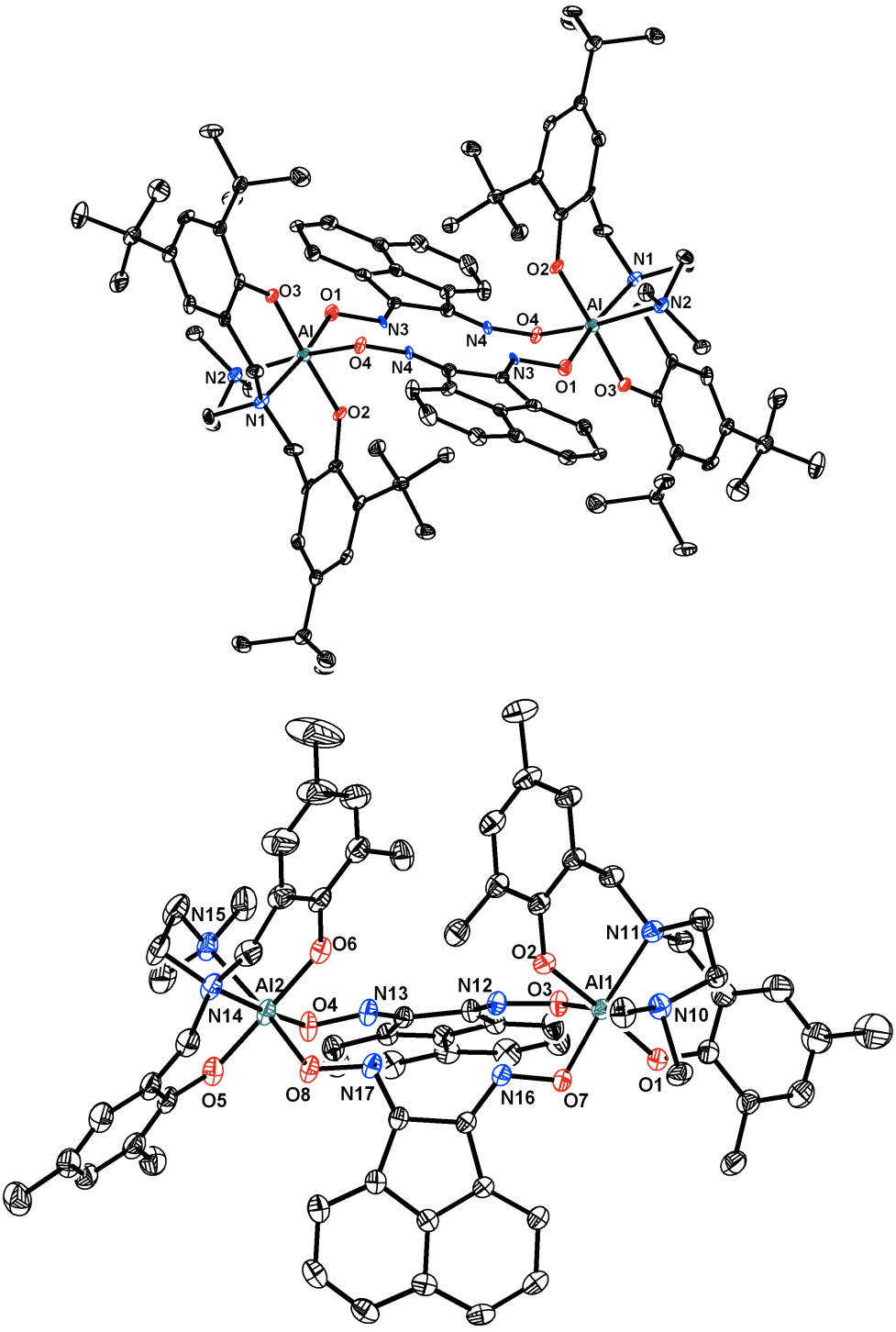

Figure A.5. Solid-state structures of **84** (above) and **85** (below) with thermal ellipsoids at the 50 % probability level. For clarity, hydrogen atoms and solvent molecules are omitted.

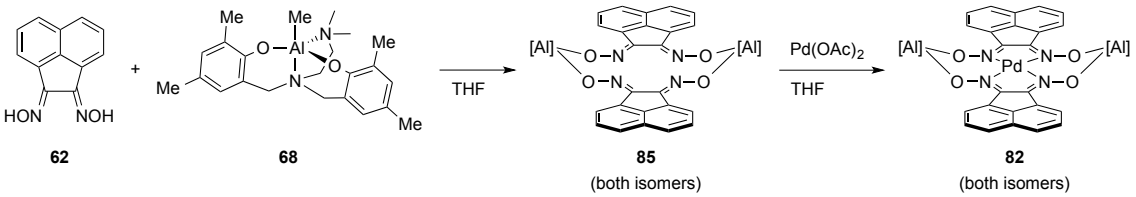

Scheme A.13. Direct synthesis of **85** and subsequent synthesis of **82**.

Complex **82** is not applicable as a polar monomer polymerization catalyst because there are no open coordination sites on palladium to coordinate monomers. Because the intended complexes **77** or **78** with acenaphthenequinone-based backbones could not be isolated, a different target complex was deemed desirable.

Complexes with a diimine backbone and pendant aminediol donors

A ligand framework was designed with a diimine backbone and pendant aminediol moieties to increase the number of donors available to bind to each Lewis acid (Chart A.3). A diimine was targeted because inductive and steric effects may have made synthesis of the full complex with the dioxime more difficult. The pendant aminodiol moieties are expected to be bulky enough to block the axial positions of palladium, which is important for limiting chain transfer events during polymerization. Because there are several Lewis acid coordinating groups covalently linked to the diimine, greater reliability of the reactions between the palladium diimine complex and Lewis acid precursors is expected.

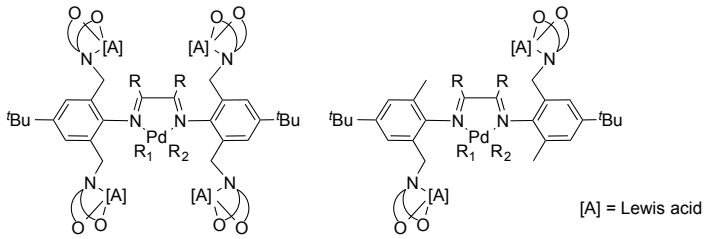

Chart A.3. Target palladium diimine complexes with pendant Lewis acids coordinated to the aminediol moieties.

Synthesis of the palladium diimine complex with pendant aminediol moieties was accomplished with established procedures (Scheme A.14). Nitration of 5-*tert*-butyl-*m*-xylene resulted in substituted nitrobenzene (**86**).[71] Treatment of **86** with two equivalents of N-bromosuccinimide (NBS) in carbon tetrachloride with benzoyl peroxide as a radical initiator, was intended to yield the dibromide, but even after several days of reflux, the major product was the monobromide (**87**), which was separated from the remaining starting material and the dibromide via column chromatography. While the dibromide was synthesized in low yield (<10%) the moderate yield of monobromide (~20%) made it reasonable to continue the synthesis with the latter and pursue the disubstituted complex after optimizing the synthesis with the monosubstituted variant. Aminediol **88** was synthesized from isobutylene oxide and an excess of ammonium hydroxide via literature procedures.[72] The reaction between an equimolar amount of **87** and **88** in the presence of one equivalent of Hünig's base over 50 h gave the monobenzylaminediol (**89**) in about 70% yield.[73] Reduction with lithium aluminum hydride (LAH) to the aniline (**90**) proceeded with greater than 75% yield after 18 h.[73] After obtaining aniline **90**, imine condensation onto an α-dione was required to complete the ligand synthesis. Diimine condensations onto acenaphthenequinone or 2,3-butadione were attempted under a variety of conditions, but were unsuccessful. The condensation of two equivalents of **90** onto glyoxal resulted in a bright yellow solid that corresponded to diimine **91** by ^{1}H NMR spectroscopy.

Metallation of diimine **91** was accomplished via addition of one equivalent of palladium precursor **63** or **64** at ambient temperature. With **63** or **64**, the ^{1}H-NMR spectrum displayed twice the number of peaks expected for the desired complexes,

consistent with the generation of atropisomers. The presence of atropisomers was confirmed by a variety of 2D NMR spectra. Chart A.4 illustrates the atropisomers of palladium diimine complexes **92** and **93**.

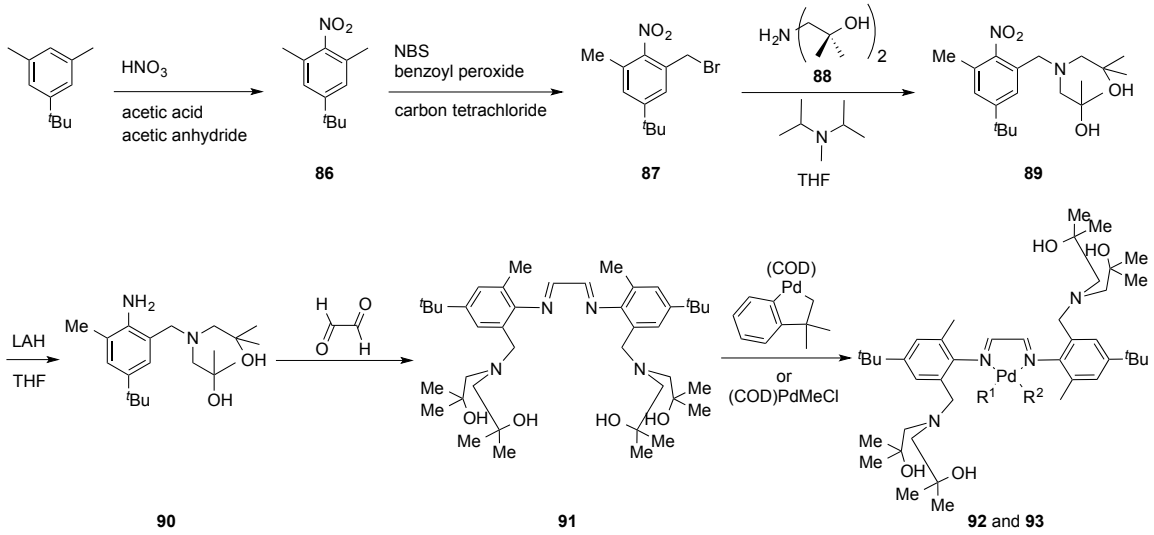

Scheme A.14. Synthesis of the palladium α-diimine complex with pendant aminediol moieties.

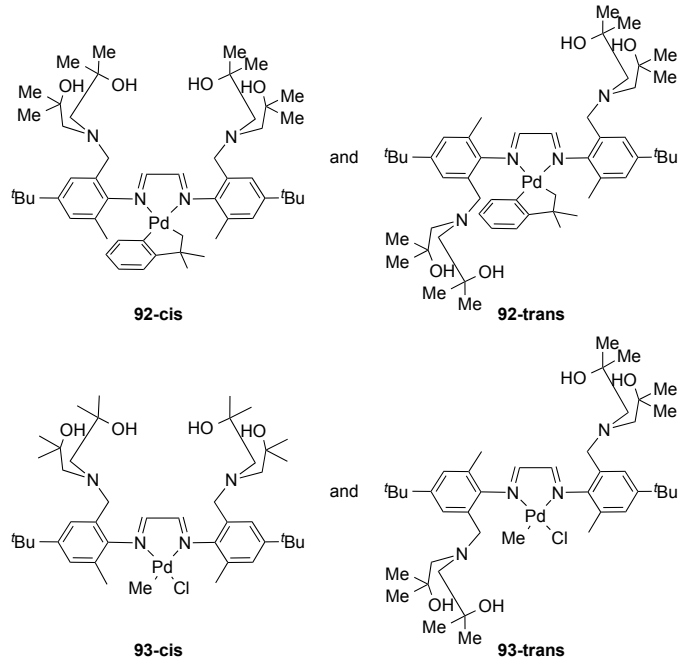

Chart A.4. Atropisomers of palladium diimine complexes **92** and **93**.

Synthesis of the target palladium diimine complexes with pendant Lewis acids was attempted by treating the palladium diimine complexes with two equivalents of a Lewis acid precursor. No reaction occurred between the palladium diimine complexes and $Zn(OMe)_2$. Complex mixtures resulted from reactions between the palladium diimine complexes and $Zn(OTf)_2$, $ZnEt_2$, $B(OMe)_3$, $Ti(NMe_2)_4$, and $Al(O^tBu)_3$. With $ZnMe_2$, promising crude ^1H NMR spectra were obtained indicating a new species. The ^1H NMR spectrum of a dark solid (yellow when in solution) isolated from the reaction of **93** with two equivalents of $ZnMe_2$ was consistent with a symmetric product, possibly a dimethyl palladium species. Reactions between either **92** or **93** with $Ti(O^iPr)_4$ provided promising ^1H NMR spectra with peaks shifted from those of the starting material and only one major species. These complexes were thermally unstable and thus difficult to purify. Neither the palladium-zinc nor palladium-titanium complexes were successfully isolated.

In addition to palladium diimine complexes **92** and **93** and their pendant Lewis acid bearing forms, another analogue was targeted. The complex with four aminediol moieties (**94**, Chart A.5) is more bulky, which may aid in blocking the axial sites of palladium during polymerization. The added symmetry of palladium diimine **94** removes the complexity of the ^1H NMR data that comes from having atropisomers in solution. Low yields of the dibromide, *vide supra*, and difficulties with the imine condensation after aniline synthesis limited the overall yield of the diimine. Additionally, while the complex was expected to crystallize more easily than **92** or **93** because there is only one potential isomer, reactions to assemble **94** from the ligand and palladium precursors led to highly insoluble product mixtures and no further efforts were made toward **94**.

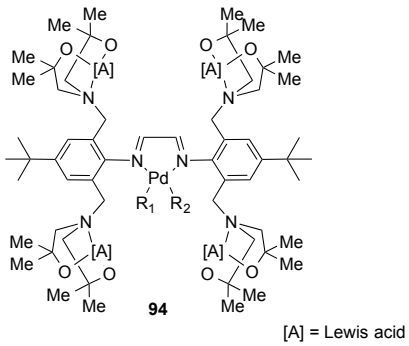

Chart A.5. Target palladium-Lewis acid complex bearing four aminediol moieties to bind Lewis acidic metals.

Preliminary polymerizations

Preliminary homopolymerizations of ethylene to test the palladium and putative palladium dizinc systems for polymerization activity were attempted using one of Brookhart's palladium α-diimine complexes as a control, **93**, and the product from the reaction of **93** with two equivalents of $ZnMe_2$. These complexes were activated to form **95**, **96**, and **97**, respectively, by the abstraction of the chloride or one of the methyls using $Na[B(3,5\text{-}(CF_3)_2C_6H_3)_4]$ or $[H(OEt_2)_2][B(3,5\text{-}(CF_3)_2C_6H_3)_4]$ (Chart A.6).[47] The activated complexes were dissolved (without further purification) in DCM to make 1 mM solutions and transferred into Schlenk flasks. After evacuating the headspace, the flasks were backfilled with 1 atm of ethylene. The polymerization reactions were stirred for 20 h under ethylene and then quenched with methanol. The resultant polymers were extracted into petroleum ether.

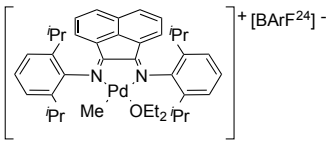

95

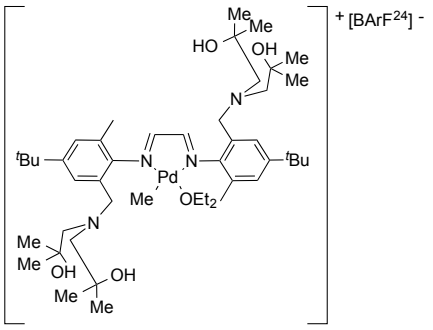

96

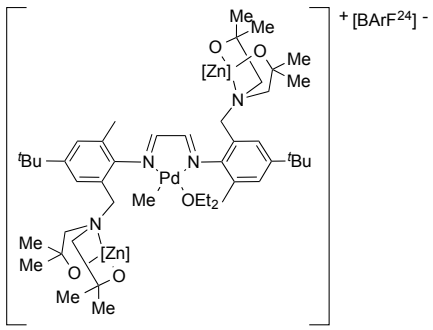

97

Chart A.6. Cationic palladium complexes with $BArF^{24}$ counterions ($BArF^{24}$ = $B(3,5\text{-}(CF_3)_2C_6H_3)_4$).

All three polymerizations resulted in polymer. Brookhart system **95** produced ten times as much polymer as the palladium diimine(diaminediol) systems **96** and **97**. The difference in yield may have been due to the impurities in **96** and **97**. The ^1H NMR spectra of the polymers made with palladium systems **96** and **97** were identical to one another (Figure A.7). The number and location of the peaks in the ^{13}C NMR spectrum of the polymer made with **95** confirms that the polymer is highly branched polyethylene (Figure A.6). Conversely, there are only a few peaks in the ^{13}C NMR spectra of the polymers made with **96** and **97**, consistent with minimal branching. GPC data indicated molecular weights of roughly 10^4 Daltons for all three polymers.

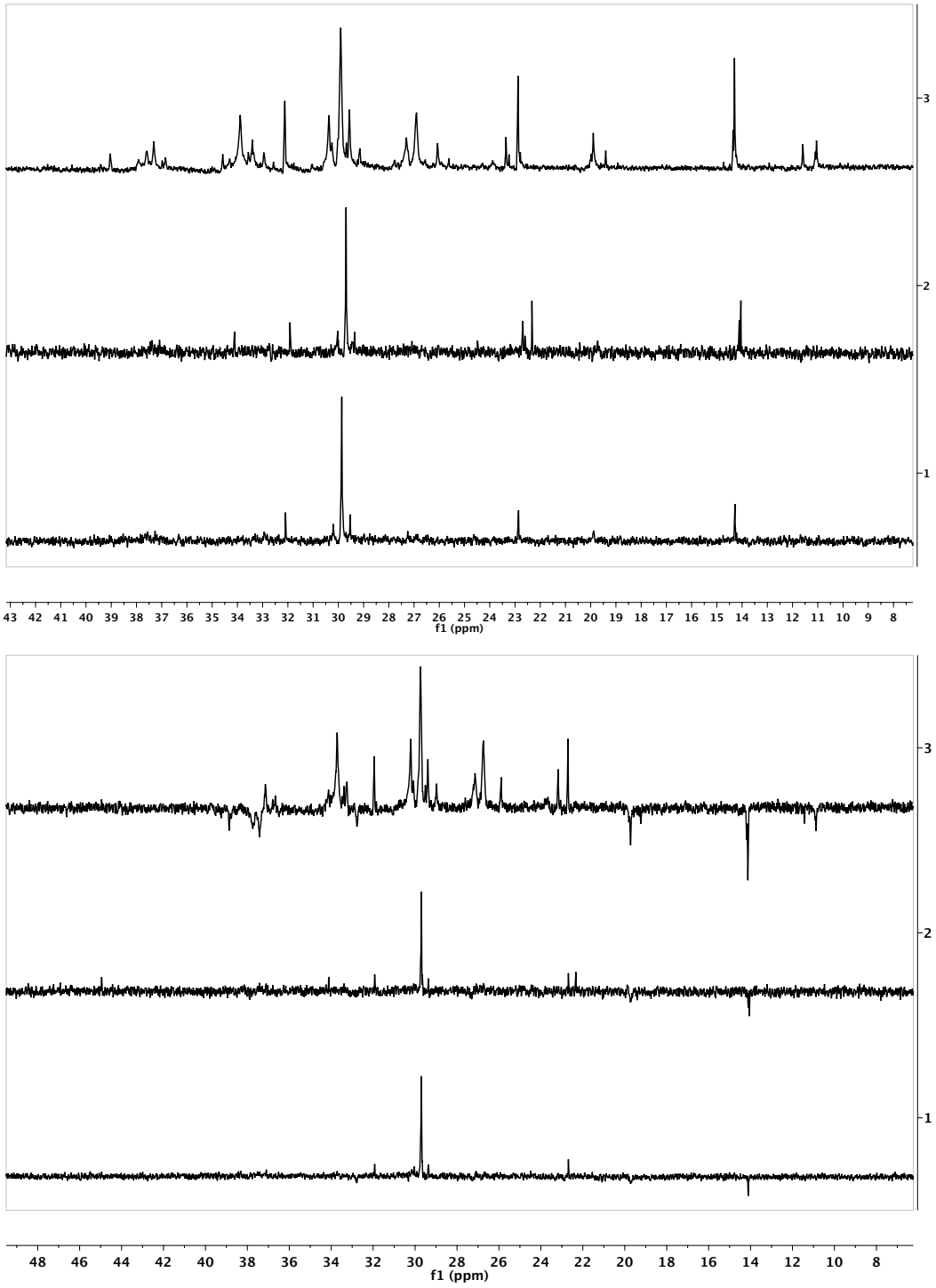

Figure A.6. ^{13}C (above) and DEPT (below) NMR spectra in $CDCl_3$ of polyethylene made with (from top to bottom) **95** (3), **96** (2), and **97** (1).

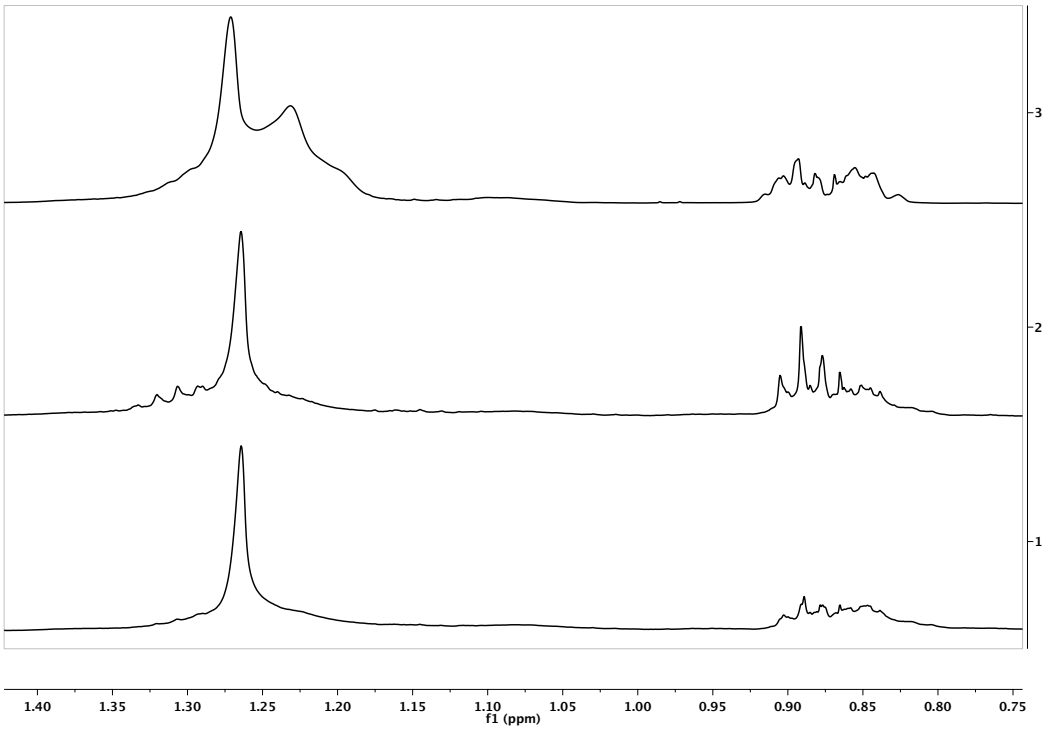

Figure A.7. ^{1}H NMR spectra in $CDCl_3$ of polyethylene made with (from top to bottom) **95** (3), **96** (2), and **97** (1).

Copolymerizations of ethylene and methyl acrylate were run with complexes **95**, **93** and the product from the reaction of **93** with two equivalents of $ZnMe_2$. As expected, the control polymerizations provided to results similar to previous reports.[25] Because the syntheses of **96** and **97** did not proceed cleanly, *in situ* activation was utilized. Activator ($Na[B(3,5\text{-}(CF_3)_2C_6H_3)_4]$, $[H(OEt_2)_2][B(3,5\text{-}(CF_3)_2C_6H_3)_4]$, or MAO) was added to the palladium or putative palladium dizinc complex and allowed to react for 30 minutes. Then methyl acrylate and ethylene were added. While these polymerizations were not successful, polymerizations with the control system were also unsuccessful if *in situ* activation was employed.

Further attempts to cleanly activate the palladium diimine complexes with or without Lewis acids were made using $Na[B(3,5\text{-}(CF_3)_2C_6H_3)_4]$ or $[H(OEt_2)_2][B(3,5\text{-}$

$(CF_3)_2C_6H_3)_4]$. By ^{1}H NMR spectroscopy, no clean activation was achieved of **92**, **93**, or the complexes formed from reactions between **92** and **93** and $ZnMe_2$ or $Ti(O^iPr)_4$. Purification of the mixtures from these reactions was unsuccessful. X-ray quality crystals were obtained from the mixture produced in the reaction between palladium-diimine complex **93**, $Ti(O^iPr)_4$, and $Na[B(3,5\text{-}(CF_3)_2C_6H_3)_4]$ (Figure A.8). The compound indicated by XRD was not the intended product – the diimine binding a cationic palladium etherate and each aminediol binding titanium with two additional isopropoxide ligands – but rather a tetrameric barrel in which each palladium bridges to another palladium via a chloride ligand and the titaniums are shared between aminediol moeities on two ligands. While this was not the intended product, this structure indicated that palladium and titanium were bound to the ligand in the expected locations. Additionally, the solid-state structure obtained may not have been the major species produced in the reaction.

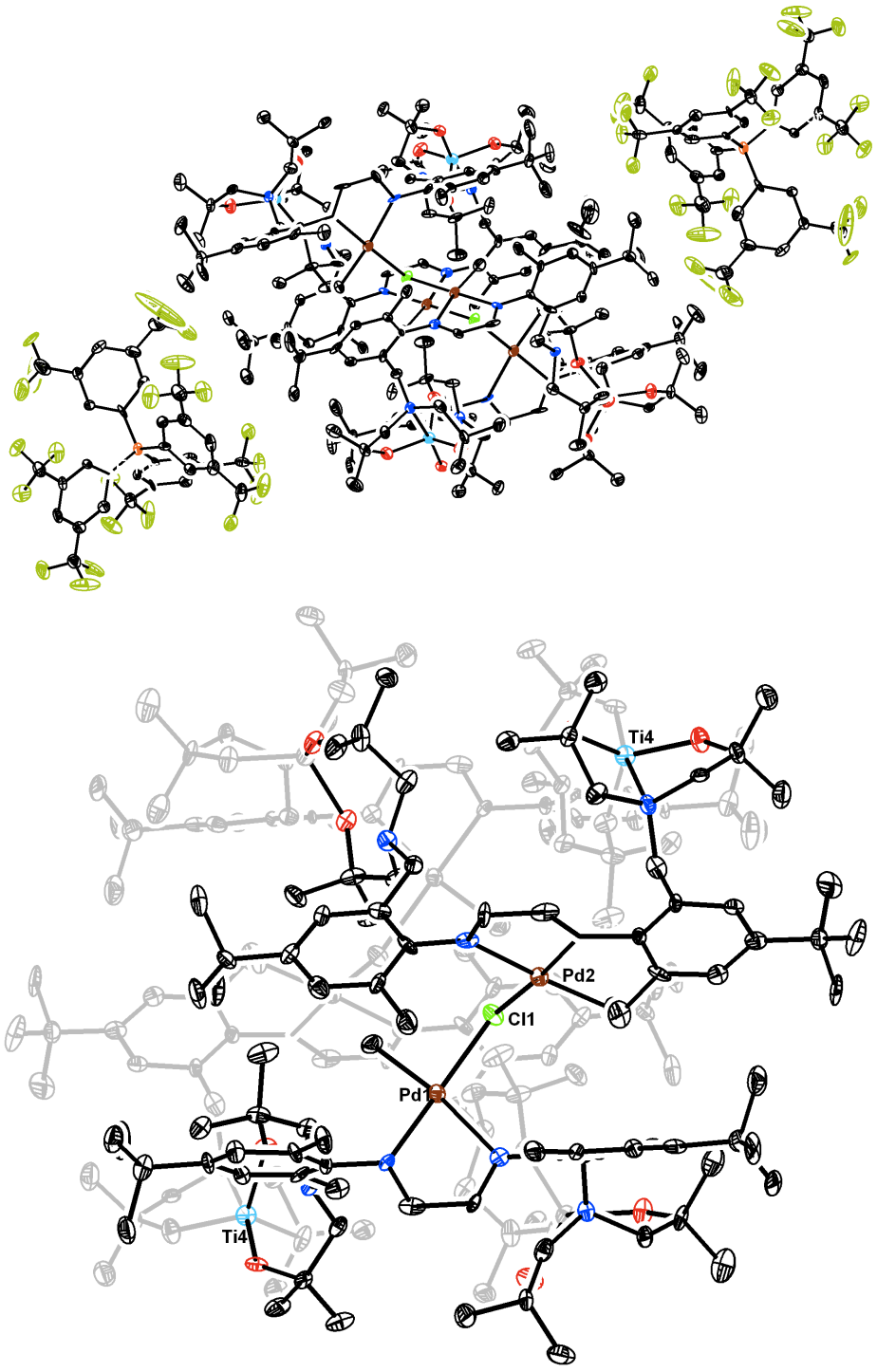

Figure A.8. Solid-state structure of the Pd_4Ti_4 complex with thermal ellipsoids at the 50 % probability level (above).[74] For clarity, hydrogen atoms and solvent molecules are omitted (Pd = brown; Ti = cyan; B = orange; Cl = neon green; F = olive green; N = blue; O = red). A view of the tetrameric barrel without the counterions and the back half of the barrel greyed out (below).

CONCLUSIONS

The syntheses of palladium complexes with pendant Lewis acids have been targeted. Using acenaphthenequinonedioxime or acenaphthenequinonediimine as the backbone led to successful metallation with palladium, but subsequent reactions with Lewis acid precursors resulted primarily in intractable mixtures. The crystal structure of one compound (**82**) isolated from the reaction of palladium dioxime **65** with aluminum Lewis acid precursor **68** indicated that palladium was bound to two dioximato ligands, leaving no open sites for monomer coordination. **82** could also be synthesized directly, and comparison of the ^{1}H NMR spectrum of **82** with that of the crude reaction of **65** and **68** indicated that **82** was only part of the reaction mixture. Indeed, the desired product may have been synthesized, but was not isolable. Therefore, a new backbone was designed bearing multiple ligands for both palladium and Lewis acidic metals. Using this design, palladium diimine-di(aminediol) complexes **92** and **93** were synthesized. These complexes were identified by ^{1}H NMR and 2D NMR experiments; efforts to grow X-ray quality crystals were ineffective. Complexes **92** and **93** were combined with a variety of Lewis acid precursors with varying success. Reactions with $ZnMe_2$ and $Ti(O^iPr)_4$ provided promising NMR data, but isolation of the targets proved unsuccessful.

Preliminary polymerization trials with activated complexes **95**, **96**, and **97** each yielded polymer, though the activation of **92** and **93** to obtain **96** and **97** did not proceed cleanly. Copolymerizations with ethylene and methyl acrylate were performed utilizing *in situ* activation, but no polymer was formed, even with the literature system. From the reaction mixture of an attempt to activate the impure palladium complex with pendant

titaniums synthesized from **93** and $Ti(O^iPr)_4$, a Pd_4Ti_4 cationic complex was obtained, whose solid-state structure indicated that the metals were bound to the expected moieties and that treatment with $Na[B(3,5\text{-}(CF_3)_2C_6H_3)_4]$ abstracted a chloride. Isolation of this or any palladium complex with pendant Lewis acids in sufficient yield to use for polymerizations proved unsuccessful, possibly due to the high reactivity of the Lewis acidic moieties. To reduce complexity, homobimetallic complexes were pursued and the results of that research are detailed in Chapters 2–5 and Appendix B of this thesis.

EXPERIMENTAL SECTION

General considerations and instrumentation

All air- and/or water-sensitive compounds were manipulated using an inert atmosphere glovebox or standard Schlenk line techniques with an N_2 atmosphere. The solvents for air- and moisture-sensitive reactions were dried over sodium/benzophenone ketyl, calcium hydride, or by the method of Grubbs.[75] All NMR solvents were purchased from Cambridge Isotopes Laboratories, Inc. and dried over sodium/benzophenone ketyl or calcium hydride. All ^{1}H, ^{13}C, and 2D NMR spectra were recorded on Varian Mercury 300 MHz, or Varian INOVA-500 or 600 MHz spectrometers at ambient temperature. Chemical shifts are reported with respect to residual internal deuterated solvent. J coupling are reported in Hz. *B*-chlorocatecholborane (**72**), pinacolborane (**73**), 9-BBN (**75**), (^{n}Bu)$_3$SnCl (**76**), 5-^{t}Bu-*m*-xylene and 2,3-butanedione were purchased from Aldrich. Glyoxal (40% in water) and acenaphthenequinone were purchased from Alfa Aesar. Palladium metallocycle (**63**),[66-67] (COD)PdMeCl (**64**),[65] aluminum Lewis acids (**67–71**),[76-82] *B*-Cl-9-BBN (**74**),[83] 2,6-dimethyl-4-tertbutyl-nitrobenzene (**86**),[71] aminediol (**88**),[72] Na[B(3,5-(CF$_3$)$_2$C$_6$H$_3$)$_4$],[84] and [H(OEt$_2$)$_2$][B(3,5-(CF$_3$)$_2$C$_6$H$_3$)$_4$][85] were synthesized according to literature procedures.

Synthetic protocols

Compound 62. Acenaphthenequinonedioxime was synthesized according to the analogous synthesis of acenaphthenediimine.[64] ^{1}H NMR (300 MHz, (CD$_3$)$_2$CO) δ = 11.47 (s, 2H, O*H*), 8.47 (d, *J*=7.1, 2H, Ar*H*), 8.02 (d, *J*=8.2, 2H, Ar*H*), 7.72 (dd, *J*=8.3, 7.1, 2H, Ar*H*) ppm.

Compound 65. A solution of **63** (0.0400 g, 0.1153 mmol, 1 equiv) in DCM (5 mL) was added to a suspension of **62** (0.0262 g, 0.1233 mmol, 1.07 equiv) in DCM (5 mL). After stirring for 16 h at ambient temperature, volatiles were removed *in vacuo*. Benzene (10 mL) was added to the solid and the resulting suspension was stirred for 10 minutes. An orange precipitate was collected via filtration over a fine frit and X-ray quality crystals were obtained via recrystallization of the precipitate from THF via liquid diffusion of hexanes (Figure A.2). NMR data was not acquired for **65** due to extremely low solubility.

Compound 66. A solution of **64** (0.100 g, 0.380 mmol, 1 equiv) in DCM (3 mL) was added to a suspension of **62** (0.082 g, 0.384 mmol, 1.01 equiv) in DCM (3 mL). After stirring for 16 h at ambient temperature, volatiles were removed *in vacuo*. X-ray quality crystals were obtained via recrystallization of the yellow-orange solid from THF via liquid diffusion of hexanes (Figure A.2). NMR data was not acquired for **66** due to extremely low solubility.

General methods for the attempted syntheses of compounds of the form of **77**, **78**, and **79.** In the glovebox, a solution of a Lewis acid precursor (2 equiv) in toluene or THF (2 mL per 0.05 mmol of Lewis acid precursor) was added to a suspension of **62**, **65**, or **66** (1 equiv) in toluene or THF (2 mL per 0.025 mmol of **62**, **65**, or **66**). Volatile materials were removed *in vacuo* after between 2 and 50 h of stirring at ambient temperature. Fractions of the material were collected by filtration through a glass filter paper pipette plug with hexanes, diethylether, toluene and THF. For all fractions, volatile materials were removed under vacuum. In the reaction between **65** and Lewis acid precursor **68**, X-ray quality crystals of **85** were obtained via recrystallization of the

toluene soluble fraction from minimal THF via vapor diffusion of hexanes. In the reaction between **62** and Lewis acid precursor **67**, precipitation yielded a nearly pure species by ^{1}H NMR spectroscopy that was assigned by integration and ^{1}H-^{1}H COSY to be the desired compound, **83**. Recrystallization of the precipitate from minimal THF via liquid diffusion of hexanes at -35 ºC resulted in X-ray quality crystals of **84**. Complex **84** took several weeks to crystallize. A ^{1}H NMR spectrum of the crystals was not obtained. Data for **83** are as follows. ^{1}H NMR (500 MHz, C_6D_6) δ = 9.69 (d, *J*=6.8, 2H, acenaphthyl-Ar*H*), 7.79 (m, 2H, acenaphthyl-Ar*H*), 7.74 (d, *J*=7.7, 2H, acenaphthyl-Ar*H*), 7.64 (d, *J*=2.5, 4H, Ar*H*), 6.83 (bs, 4H, Ar*H*), 3.28 (bs, 8H, ArCH_2), 2.22 (s, 12H, NCH_3), 1.97 (m, 4H, NCH_2), 1.80 (s, 36H, C(CH_3)$_3$), 1.65 (m, 4H, NCH_2), 1.44 (s, 36H, C(CH_3)$_3$) ppm.

Compound 80. Diimine **80** was synthesized by a procedure analogous to literature.[64] ^{1}H NMR (300 MHz, $CDCl_3$) δ = 8.13 (d, *J*=7.5, 1H, Ar*H*), 7.97 (d, *J*=8.3, 1H, Ar*H*), 7.85 (d, *J*=8.6, 1H, Ar*H*), 7.74 (m, 1H, Ar*H*), 7.58 (d, *J*=7.9, 1H, Ar*H*), 7.44 (dd, *J*=8.4, 7.0, 1H, Ar*H*), 7.24 (d, *J*=6.8, 1H, Ar*H*), 7.18 (d, *J*=1.1, 1H, Ar*H*), 7.03 (dd, *J*=7.2, 3.2, 2H, Ar*H*), 6.69 (dd, *J*=7.7, 2.1, 1H, Ar*H*), 6.56 (d, *J*=1.5, 1H, Ar*H*), 5.65 (s, 2H, O*H*), 2.47 (s, 3H, ArCH_3), 2.29 (s, 3H, ArCH_3) ppm.

Compound 81. **81** was synthesized by a procedure analogous to the synthesis of **66**. ^{1}H NMR (300 MHz, $(CD_3)_2CO$) δ = 8.26 (m, 2H, Ar*H*), 7.65 (m, 2H, Ar*H*), 7.38 (m, 1H, Ar*H*), 7.14 (m, 3H, Ar*H*), 6.93 (m, 4H, Ar*H*), 2.40 (s, 6H, ArCH_3), 0.72 (s, 3H, PdCH_3) ppm.

Synthesis of 82 starting from 62. $Pd(OAc)_2$ (0.10 g, 0.45 mmol) and **62** (0.19 g, 0.89 mmol, 2 equiv) were added to a Schlenk tube with methanol (10 mL) and the mixture was stirred for 3 h resulting in a color change of the heterogeneous mixture to

orange. Volatiles were removed under vacuum, dry THF (10 mL) was added via cannula and then removed *in vacuo* twice. **68** (0.35 g, 0.89 mmol, 2 equiv) and dry THF (10 mL) were added by syringe and the reaction was stirred for 12 h. Volatiles were removed under vacuum and the resulting yellow orange solid was brought into the glovebox. Stirred solid in THF (10 mL) for 1 h and collected yellow orange precipitate (0.36 g, 63 % yield) which includes 2 sets of peaks by ^{1}H NMR spectroscopy in a 10:1 ratio. X-ray quality crystals were grown from vapor diffusion of hexanes into THF. See below for labeled drawings correlated to the NMR peak assignments. ^{1}H NMR (600 MHz, C_6D_6) *major species* δ = 8.37 (2H, d, *J*=7.0, A), 8.16 (2H, d, *J*=7.0, A), 7.37 (2H, d, *J*=8.2, B), 7.32 (2H, d, *J*=8.4, B), 7.25 (2H, dd, *J*=7.2, *J*=8.0, C), 7.09 (2H, dd, *J*=7.0, *J*=8.3, C), 6.96 (4H, d, *J*=1.6, D), 6.74 (4H, d, *J*=1.9, E), 5.10 (2H, d, *J*=12.6, F), 3.01 (2H, d, *J*=12.7, F), 2.39 (12H, s, G), 2.36 (4H, t, *J*=5.8, H), 2.26 (12H, s, I), 2.17 (12H, s, J), 1.71 (4H, t, *J*=6.0, K) ppm; *minor species* δ = 8.66 (2H, d, *J*=6.7, A), 7.81 (2H, d, *J*=7.0, A), 7.44 (2H, d, *J*=8.2, B), 7.32 (2H, d, B), 7.22 (2H, dd, C), 7.04 (2H, dd, C), 6.95 (4H, d, *J*=1.6, D), 6.55 (4H, d, E), 4.93 (2H, d, *J*=13.0, F), 2.98 (2H, d, *J*=12.7, F), 2.63 (12H, s, G), 2.26 (6H, s, J), 2.23 (4H, t, H), 2.19 (12H, s, I), 2.11 (6H, s, J), 1.78 (4H, t, *J*=6.1, K) ppm. ^{13}C NMR (from 2D spectra, C_6D_6) δ = 158.7 (1), 153.1 (2), 140.8 (3), 132.6 (4), 131.2 (5), 128.3 (6), 127.9 (6), 127.4 (7), 127.2 (8), 127.0 (9), 126.9 (8), 126.5 (5), 122.5 (10), 122.5 (11), 122.4 (11), 121.0 (12), 64.6 (13), 64.5 (13), 57.8 (14), 50.0 (15), 47.9 (16), 20.8 (17), 16.7 (18) ppm. Anal. Calcd. for $C_{68}H_{72}Al_2N_8O_8Pd$: C, 63.33; H, 5.63; N, 8.69. Found: C, 63.20; H, 5.48; N, 8.39.

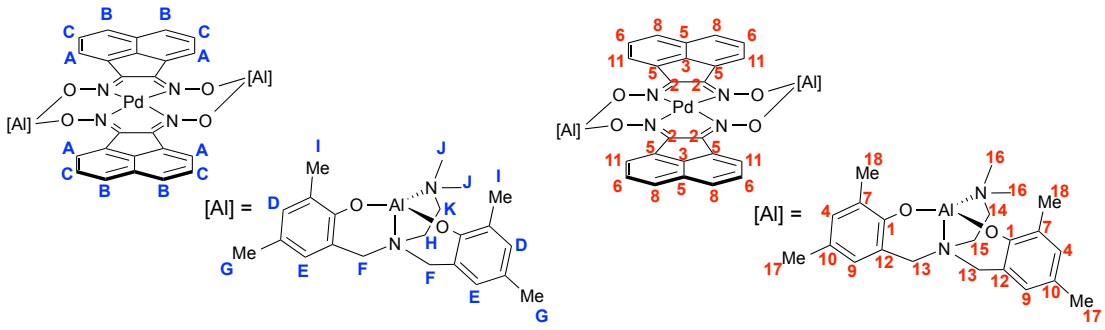

Synthesis of 82 starting from 85. 82 was also synthesized by the addition of **85** (0.050 g, 0.042 mmol) to $Pd(OAc)_2$ (0.021 g, 0.095 mmol, 2.25 equiv) in THF (5 mL) in a 20 mL vial in the glovebox at ambient temperature. The mixture was stirred over 13 h during which time the mixture turned dark orange brown with precipitate. Volatiles were removed under vacuum and the desired product was isolated by washing over Celite with hexanes and collecting the filtrate from toluene. Volatiles were again removed *in vacuo*, and 0.033 g of pale orange solid was collected (61 % yield).

Direct synthesis of 85. 68 (0.17 g, 0.43 mmol, 1 equiv), **62** (0.09 g, 0.43 mmol, 1 equiv), and THF (10 mL) were added to 20 mL vial with a stirbar at -35 °C in the glovebox and the mixture was stirred for 12 h. Volatiles were removed under vacuum to yield a yellow orange residue (0.19 g, 74 % yield). **85** was used without any further purification in the reaction with $Pd(OAc)_2$, *vide supra*. X-ray quality crystals were grown from a vapor diffusion of pentane into toluene. See below for labeled drawings correlated to the NMR peak assignments. ^{1}H NMR (400 MHz, CD_2Cl_2) δ = 14.33 (2H, s, A), 8.60 (2H, d, *J*=7.1, B), 8.35 (2H, d, *J*=7.0, B'), 7.94 (2H, d, *J*=8.2, C), 7.77 (2H, d, *J*=8.3, C'), 7.68 (2H, dd, *J*=8.3, 7.0, D), 7.56 (2H, dd, *J*=8.4, 7.0, D'), 6.74 (4H, d, *J*=2.4, E), 6.72 (4H, d, *J*=2.5, E), 4.97 (4H, d, *J*=12.7, F), 3.29 (4H, d, *J*=12.8, F), 2.76 (4H, t, *J*=6.0, G), 2.28 (2s, 24H, H, I), 2.12 (4H, t, *J*=6.0, J), 1.82 (s, 12H, K). ^{13}C NMR (101 MHz, C_6D_6) δ = 158.59 (1), 144.92 (2), 144.71 (3),

137.09 (4), 132.67 (5), 130.65 (6), 129.98 (7), 129.18 (8), 128.33 (9), 127.92 (6), 127.56 (10), 126.74 (11), 126.18 (12), 125.66 (13), 123.86 (14), 123.06 (15), 121.25 (16), 64.56 (17), 58.11 (18), 50.24 (19), 48.18 (20), 20.64 (21), 16.06 (22) ppm. Anal. Calcd. for $C_{68}H_{74}Al_2N_8O_8$: C, 68.90; H, 6.29; N, 9.45. Found: C, 63.17; H, 5.96; N, 8.14.

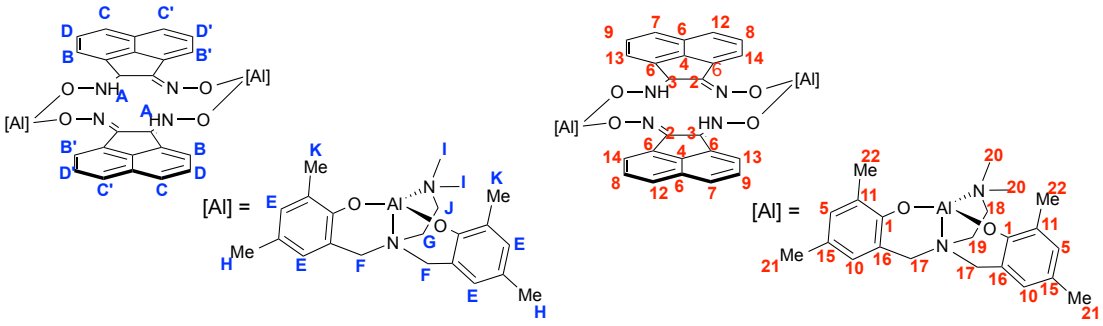

Compound 87. **86** (7.00 g, 33.77 mmol, 1 equiv), N-bromosuccinimide (12.02 g, 67.54 mmol, 2 equiv) and CCl_4 (50 mL) were combined in an oven-dried Schlenk tube under N_2 and heated to 80 ºC at which point benzoyl peroxide (0.41 g, 1.69 mmol, 0.05 equiv) was added and the Schlenk tube was sealed. Stirring at 80 ºC for two days yielded a dark red solution, which was filtered over Celite and purified by column chromatography (10/1 hexanes/DCM). Remaining starting material and an unidentified impurity eluted first, followed by monobromide **87** and the dibromide. 1.74 g (18% yield) of **87** was collected as a light yellow solid. ^{1}H NMR (300 MHz, $CDCl_3$) δ = 7.32 (d, 1H, Ar*H*), 7.25 (d, 1H, Ar*H*), 4.50 (s, 2H, ArCH_2), 2.36 (s, 3H, ArCH_3), 1.36 (s, 9H, C(CH_3)$_3$) ppm. 0.7810 g (6% yield) of the dibromide was collected as a light yellow solid. ^{1}H NMR (300 MHz, $CDCl_3$) δ = 7.47 (s, 2H, Ar*H*), 4.53 (s, 4H, ArCH_2), 1.32 (s, 9H, C(CH_3)$_3$) ppm.

Compound 89. The syntheses and workup of **89** and the disubstituted analogue were completed analogously to the literature synthesis and workup of 1-(3,5-di-*tert*-

butyl-2-nitrobenzyl)-4,7-dimethyl-1,4,7-triazacyclononane.[73] Data for **89**. ^{1}H NMR (500 MHz, $CDCl_3$) δ = 7.50 (s, 1H, Ar*H*), 7.18 (s, 1H, Ar*H*), 3.77 (s, 2H, ArCH_2), 3.51 (bs, 2H, O*H*), 2.63 (s, 4H, NCH_2), 2.30 (s, 3H, ArCH_3), 1.32 (s, 9H, C(CH_3)$_3$), 1.14 (s, 12H, CH_3) ppm. ^{13}C NMR (500 MHz, $CDCl_3$) δ = 153.30, 149.47, 130.90, 129.26, 127.31, 125.45, 71.71, 68.07, 59.24, 34.95, 31.24, 28.22, 17.78 ppm. Data for the disubstituted analogue. ^{1}H NMR (300 MHz, $CDCl_3$) δ = 7.58 (s, 2H, Ar*H*), 3.74 (s, 4H, ArCH_2), 3.48 (s, 4H, O*H*), 2.61 (s, 8H, NCH_2), 1.33 (s, 9H, C(CH_3)$_3$), 1.12 (s, 24H, CH_3) ppm. ^{13}C NMR (500 MHz, $CDCl_3$) δ = 153.05, 149.24, 130.86, 127.11, 71.65, 68.01, 59.04, 35.05, 31.21, 28.25 ppm.

Compound 90. The syntheses of **90** and the disubstituted analogue were completed analogously to the literature synthesis of 1-(2-amino-3,5-di-*tert*-butylbenzyl)-4,7-dimethyl-1,4,7-triazacyclononane.[73] In the glovebox, an oven-dried three-neck round bottom was charged with $LiAlH_4$ (0.486 g, 12.805 mmol, 10 equiv) and dry THF (5 mL). The vessel was sealed, brought out of the box, and put under N_2 on the Schlenk line. A solution of **89** (0.469 g, 1.281 mmol, 1 equiv) in THF (15mL) was transferred gradually into the reaction vessel via cannula. The reaction vessel was equipped with a reflux condenser and stirred with reflux for 16 h. After cooling to ambient temperature, aqueous $Na_2S_2O_2$ (40 mL) was added in four portions. This suspension was stirred at ambient temperature for 20 minutes after which the solid was removed by filtration and washed with water and diethylether. The product was extracted from the filtrate into Et_2O. Saturated aqueous KOH (20 mL) was added to the aqueous phase and a second extraction into Et_2O was completed. The Et_2O layers were combined, dried with $MgSO_4$, filtered and the volatiles were removed under vacuum. The residue was

purified by column chromatography (5/1 hexanes/EtOAc until after the first (bright yellow) impurity came off the column and then 1/5 hexanes/EtOAc). **90** was collected as a nearly colorless solid (0.281 g, 65 % yield). Data for **90**. ^{1}H NMR (300 MHz, $CDCl_3$) δ = 7.00 (d, 1H, Ar*H*), 6.87 (d, 1H, Ar*H*), 3.72 (s, 2H, ArCH_2), 2.62 (s, 4H, NCH_2), 2.04 (s, 3H, ArCH_3), 1.27 (s, 9H, C(CH_3)$_3$), 1.13 (s, 12H, CH_3) ppm. ^{13}C NMR (500 MHz, $CDCl_3$) δ = 142.14, 140.16, 126.54, 125.97, 122.84, 121.82, 71.68, 68.20, 63.68, 33.84, 31.76, 28.72, 17.82 ppm. Data for the disubstituted analogue. ^{1}H NMR (300 MHz, $CDCl_3$) δ = 6.97 (d, 2H, Ar*H*), 3.70 (s, 4H, ArCH_2), 2.61 (s, 8H, NCH_2), 1.25 (s, 9H, C(CH_3)$_3$), 1.13 (s, 24H, CH_3) ppm. ^{13}C NMR (500 MHz, $CDCl_3$) δ = 143.68, 139.28, 127.22, 123.20, 71.48, 67.99, 62.85, 33.74, 31.69, 28.68 ppm.

Compound 91. Diimine **91** and the analogue with four aminediol moieties were synthesized via diimine condensations analogous to a literature procedure.[86] A suspension of glyoxal (40% solution in water) (0.14 ml, 1.19 mmol, 1 equiv) and $MgSO_4$ (2.72 g, 22.58 mmol, 19 equiv) in DCM (5 mL) was stirred in a Schlenk tube under nitrogen atmosphere at ambient temperature for 10 minutes. Aniline **90** (0.80 g, 2.38 mmol, 2 equiv) and formic acid (0.004 g, 0.083 mmol, 0.07 equiv) in DCM (5 mL) were added to the suspension and the Schlenk tube was sealed and stirred at ambient temperature for 25 h. The resulting suspension was filtered over Celite to remove the solids. Volatiles were removed under vacuum. Acetonitrile (10 mL) was added to the dark yellow oil and the solution was stirred until yellow solid had precipitated (about 1 h). This yellow solid was collected via filtration yielding 0.33 g (40% yield) of **91**. Data for **91**. ^{1}H NMR ($CDCl_3$, 300 MHz) δ = 8.13 (bs, 2H, NC*H*), 7.28 (d, 2H, Ar*H*), 7.18 (d,

2H, Ar*H*), 3.82 (bs, 4H, ArCH_2), 3.70 (s, 4H, O*H*), 2.64 (s, 8H, NCH_2), 2.20 (s, 6H, ArCH_3), 1.33 (s, 18H, C(CH_3)$_3$), 1.09 (s, 24H, CH_3) ppm. ^{13}C NMR ($CDCl_3$, 500 MHz) δ = 164.20, 147.81, 147.56, 129.25, 127.20, 125.53, 71.23, 67.83, 59.85, 34.40, 31.51, 28.48, 19.04 ppm. Data for the analogue with four aminediol moieties. ^{1}H NMR ($CDCl_3$, 300 MHz) δ = 8.08 (s, 2H, NC*H*), 7.48 (s, 4H, Ar*H*), 3.71 (s, 8H, ArCH_2), 2.61 (s, 16H, NCH_2), 1.35 (s, 18H, C(CH_3)$_3$), 1.11 (s, 48H, CH_3) ppm.

Compound 92. A solution of **91** (0.074 g, 0.107 mmol, 1 equiv) in DCM (5 mL) was added to a solution **63** (0.037 g, 0.107 mmol, 1 equiv) in DCM (5 mL) and stirred for 24 h at ambient temperature. Volatiles were removed under vacuum. The dark solid was washed with hexanes, Et_2O and toluene, and 0.0734 g (74% yield) of dark red THF-soluble solid was collected. See below for labeled drawings to correlated to the NMR peak assignments. ^{1}H NMR (600 MHz, CD_2Cl_2) δ = 8.33 (two singlets, 1H, I), 8.29 (two singlets, 1H, I), 7.64 (two singlets, 1H, E), 7.59 (two singlets, 1H, E), 7.33 (two singlets, 1H, G), 7.28 (two singlets, 1H, G), 6.65 (t, 1H, D'), 6.55 (d, 1H, C'), 6.30 (t, 1H, E'), 5.86 (d, 1H, F'), 4.32–3.57 (eight doublets, 4H, D), 3.40 (s, 1H, A), 3.30 (s, 1H, A), 3.19 (s, 1H, A), 3.09 (s, 1H, A), 2.82–2.50 (8 peaks, 8H, C), 2.38 (two singlets, 3H, H), 2.31 (two singlets, 3H, H), 2.29–1.59 (four doublets, 2H, A'), 1.42 (s, 9H, F), 1.40 (s, 9H, F), 1.20–0.89 (twelve singlets, 30H, B, B') ppm. ^{13}C NMR (from 2D spectra, C_6D_6) δ = 169.5 (4'), ~165 (2 peaks, 14), 157.2 (9'), 149.2 (7), 145.2 (13), 133.8 (8'), 130.4 (5), 129.2 (5), 127.9 (11), 125.8 (10), 125.6 (10), 123.4 (6), 123.2 (6'), 123.0 (7'), 123.0 (6), 121.2 (5'), 71.9 (1), 71.6 (1), 68.0 (3), 67.6 (3), 59.2 (4), 59.0 (4), 58.9 (4), 58.8 (4) 46.9 (2'), 46.1 (1'), 45.9 (1'), 35.5 (3'), 34.3 (8), 34.3 (3'), 32.1 (3'), 30.9 (9), 30.6 (3'), 27.8 (2), 27.4 (2), 18.1 (12), 17.9 (12) ppm.

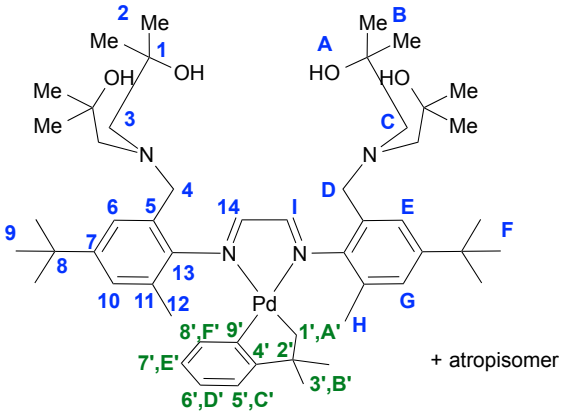

Compound 93. A solution of **91** (0.200 g, 0.288 mmol, 1 equiv) in DCM (6 mL) was added to a solution of **64** (0.076 g, 0.288 mmol, 1 equiv) in DCM (6 mL) in a vial. After stirring for 2.5 h at ambient temperature, volatile materials were removed under vacuum. DCM (10 mL) was added to the orange solid, and the suspension was stirred for 30 minutes. The vial was cooled to -35 °C in the freezer. The suspension was then filtered over a fine frit and the orange precipitate was rinsed with cold DCM yielding 0.170 g (69%) of **93**. ^{1}H NMR (300 MHz, CD_2Cl_2) δ = 8.29 (two singlets, 1H, NC*H*), 8.09 (two singlets, 1H, NC*H*), 7.63 (s, 1H, Ar*H*), 7.57 (s, 1H, Ar*H*), 7.28 (s, 1H, Ar*H*), 7.24 (s, 1H, Ar*H*), 3.91 (m, 4H, ArCH_2), 3.07 (m, 4H, O*H*), 2.78 (m, 8H, NCH_2), 2.35 (m, 6H, ArCH_3), 1.37 (s, 18H, C(CH_3)$_3$), 1.21 (m, 24H, CH_3), 0.62 (s, 3H, PdCH_3) ppm.

Reaction of 93 with $ZnMe_2$. A solution of **93** (0.050 g, 0.059 mmol, 1 equiv) in THF (5 mL) and a solution of 2 M $ZnMe_2$ in toluene (0.059 ml, 0.117 mmol, 2 equiv) in THF (5 mL) were both frozen in the glovebox cold well chilled with liquid N_2. The solution of $ZnMe_2$was transferred into the solution of **93** while thawing. Volatiles were removed under vacuum after 40 minutes of stirring. Hexanes (10 mL) and toluene (1 mL) were added. The resulting suspension was stirred for 10 minutes and the solid was collected by filtration. ^{1}H NMR (300 MHz, CD_2Cl_2) δ = 8.25 (m, 2H), 7.57 (bs, 2H),

7.25 (bs, 2H), 4.00 (m, 4H), 3.48 (m, 2H), 3.24 (m, 2H), 2.73 (m, 8H), 2.27 (m, 6H), 1.37 (m, 18H), 1.18 (m, 24H), –0.15 (m, 6H) ppm.

Reaction of 92 with $ZnMe_2$. A solution of **92** (0.030 g, 0.032 mmol, 1 equiv) in DCM (3 mL) and a solution of 2 M $ZnMe_2$ in toluene (0.032 ml, 0.064 mmol, 2 equiv) in DCM (2 mL) were both frozen in the glovebox cold well chilled with liquid N_2. The solution of $ZnMe_2$ was transferred into the solution of **92** while thawing. Volatiles were removed under vacuum after 16 h of stirring.

Reaction of 92 with $Ti(O^iPr)_4$. A solution of **92** (0.042 g, 0.045 mmol, 1 equiv) in THF (5 mL) and a solution of $Ti(O^iPr)_4$ (0.027 ml, 0.090 mmol, 2 equiv) in THF (5 mL) were both frozen in the glovebox cold well chilled with liquid N_2. The solution of **92** was transferred into the solution of $Ti(O^iPr)_4$ while thawing. Volatiles were removed under vacuum after 1 h of stirring.

Reaction of 93 with $Ti(O^iPr)_4$. A solution of **93** (0.040 g, 0.047 mmol, 1 equiv) in THF (5 mL) and a solution of $Ti(O^iPr)_4$ (0.028 ml, 0.094 mmol, 2 equiv) in THF (5 mL) were both frozen in the glovebox cold well chilled with liquid N_2. The solution of **93** was transferred into the solution of $Ti(O^iPr)_4$ while thawing. Volatiles were removed under vacuum after 1 h of stirring.

Compounds 95 and 96. Solutions of one equivalent of either **93** or (ArN=C(H)-C(H)=NAr)PdMeCl (Ar = 2,6-$C_6H_3(^iPr)_2$) in DCM were added to $Na^+[B(3,5\text{-}(CF_3)_2C_6H_3)_4]^-$ (1 equiv) and Et_2O (1 equiv). After 45 minutes of mixing, volatile materials were removed under vacuum. Data for **95**. ^1H NMR (300 MHz, CD_2Cl_2) δ = 8.12 (m, 2H), 7.80 (s, 8H), 7.60 (s, 4H), 7.39 (m, 4H), 6.61 (m, 2H), 3.54 (m, 3H), 3.21 (m, 3H), 1.46 (m, 2H), 1.35-0.85 (m, 24H) ppm. The reaction between

$Na^+[B(3,5\text{-}(CF_3)_2C_6H_3)_4]^-$ and the product of the reaction between **93** and $Ti(O^iPr)_4$ was also carried out under these conditions.

Compound 97. Activation of the product from the reaction of **93** with $ZnMe_2$ to make complex **97** was performed according to an analogous literature procedure.[47] A solution of the product from the reaction of **93** with $ZnMe_2$ (0.010 g, 0.010 mmol, 1 equiv) in DCM (2 mL) and a solution of $[H(OEt_2)_2]^+[B(3,5\text{-}(CF_3)_2C_6H_3)_4]^-$ in 2 mL of Et_2O were frozen in the cold well. The $[H(OEt_2)_2]^+[B(3,5\text{-}(CF_3)_2C_6H_3)_4]^-$ solution was added to the solution of the product from the reaction of **93** with $ZnMe_2$ and the mixture was stirred for 30 minutes while warming to ambient temperature. Volatiles were removed under vacuum. The reactions between $[H(OEt_2)_2]^+[B(3,5\text{-}(CF_3)_2C_6H_3)_4]^-$ and **92**, the product of the reaction between **92** and $ZnMe_2$, and the product of the reaction between **92** and $Ti(O^iPr)_4$ were also carried out under these conditions.

General polymerization procedures

Homopolymerizations of ethylene were performed under conditions from literature.[47] The activated complexes **95** (0.009 g, 0.005 mmol), **96** (0.093 g, 0.005 mmol), and **97** (0.010 g, 0.005 mmol) were each dissolved (without further purification) in DCM in an inert atmosphere glovebox to make 1 mM solutions and transferred into 100 ml Schlenk flasks. The Schlenk flasks were attached to a high vacuum line. After a freeze-pump-thaw cycle, the headspace of the flasks was backfilled with 1 atm of ethylene. The polymerization reactions were stirred for 20 h under ethylene before being quenched in methanol, and the polymer extracted into petroleum ether. Polymerization with **95** produced 51 mg of polymer. Polymerization with **96** produced 5 mg of polymer. Polymerization with **97** produced 3 mg of polymer.

Crystallographic Information

Table A.1. Crystal and refinement data for complexes **66**, **82-trans**, and **82-cis**.

	66	**82-trans**	**82-cis**
CCDC #	744726	861065	862109
empirical formula	$C_{13}H_{11}N_2O_2ClPd$ • C_4H_8O	$C_{68}H_{72}N_8O_8Al_2Pd$ • $6(C_4H_8O)$	$C_{68}H_{72}N_8O_8Al_2Pd$ • $0.5(C_6H_{14})$ • $1.45(C_4H_8O)$
formula wt	441.19	1722.32	1437.33
T (K)	100	100	100
a, Å	13.0726(4)	10.9146(3)	18.5492(17)
b, Å	13.8440(4)	16.3913(5)	19.7138(17)
c, Å	19.8059(7)	24.2331(7)	20.515(2)
α, deg	79.203(2)	90	90
β, deg	72.134(4)	101.8030(10)	102.794(3)
γ, deg	80.569(2)	90	90
V, $Å^3$	3329.40(18)	4243.7(2)	7315.5(12)
Z	8	2	4
cryst syst	triclinic	monoclinic	monoclinic
space group	P-1	P $2_1/c$	P $2_1/n$
d_{calcd}, g/cm^3	1.760	1.348	1.305
θ range, deg	1.51 to 39.36	1.51 to 25.38	1.34 to 30.52
μ, mm^{-1}	1.293	0.309	0.340
abs cor	Semi-empirical from equivalents	Semi-empirical from equivalents	Semi-empirical from equivalents
GOF	1.849	2.000	1.788
R1,[a] wR2[b] (I > 2θ (I))	R1 = 0.0422, wR2 = 0.0675	R1 = 0.0567, wR2 = 0.0814	R1 = 0.0504, wR2 = 0.0681

[a] $R_1 = \sum||F_o| - |F_c||/\sum|F_o|$. [b] $wR_2 = [\sum[w(F_o^2-F_c^2)^2]/\sum[w(F_o^2)^2]]^{1/2}$.

Table A.2. Crystal and refinement data for complexes **84** and **85**.

	84	**85**
CCDC #	861066	867795
empirical formula	$C_{92}H_{120}N_8O_8Al_2 \bullet 4(C_4H_8O)$	$C_{68}H_{70}Al_2N_8O_8$
formula wt	1808.34	1181.28
T (K)	100	100
a, Å	11.9403(6)	12.0569(6)
b, Å	12.7271(7)	18.5625(10)
c, Å	17.7934(9)	18.9548(11)
α, deg	98.660(2)	78.418(3)
β, deg	103.176(2)	76.313(3)
γ, deg	106.624(2)	76.094(3)
V, Å^3	2454.4(2)	3954.1(4)
Z	1	2
cryst syst	triclinic	triclinic
space group	P-1	P-1
d_{calcd}, g/cm^3	1.223	0.992
θ range, deg	1.21 to 27.71	1.72 to 30.00
μ, mm^{-1}	0.095	0.086
abs cor	Semi-empirical from equivalents	Semi-empirical from equivalents
GOF	3.445	1.096
R1,[a] wR2[b] (I > 2θ (I))	R1 = 0.0643, wR2 = 0.0858	R1 = 0.0515, wR2 = 0.1498

[a] $R_1 = \sum||F_o| - |F_c||/\sum|F_o|$. [b] $wR_2 = [\sum[w(F_o^2-F_c^2)^2]/\sum[w(F_o^2)^2]]^{1/2}$.

REFERENCES

1. Koning, C.; van Duin, M.; Pagnoulle, C.; Jerome, R. *Prog. Poly. Sci.* **1998**, *23*, 707-757.
2. Ren, Y.; Jiang, X.; Liu, R.; Yin, J. *J. Polym. Sci., Part A: Polym. Chem.* **2009**, *47*, 6353-6361.
3. Ren, Y.; Jiang, X.; Yin, J. *J. Polym. Sci., Part A: Polym. Chem.* **2009**, *47*, 1292-1297.
4. Meyer, J.; Keul, H.; Moeller, M. *Macromolecules* **2011**, *44*, 4082-4091.
5. Dhende, V. P.; Samanta, S.; Jones, D. M.; Hardin, I. R.; Locklin, J. *ACS Appl. Mat. Inter.* **2011**, *3*, 2830-2837.
6. Jones, E. R.; Semsarilar, M.; Blanazs, A.; Armes, S. P. *Macromolecules* **2012**, *45*, 5091-5098.
7. Zhang, C.; Maric, M. *J. Polym. Sci., Part A: Polym. Chem.* **2012**, *50*, 4341-4357.
8. Yang, Y.; Mijalis, A. J.; Fu, H.; Agosto, C.; Tan, K. J.; Batteas, J. D.; Bergbreiter, D. E. *J. Am. Chem. Soc.* **2012**, *134*, 7378-7383.
9. McGinty, K. M.; Brittain, W. J. *Polymer* **2008**, *49*, 4350-4357.
10. Imuta, J.; Kashiwa, N.; Toda, Y. *J. Am. Chem. Soc.* **2002**, *124*, 1176-1177.
11. Amin, S. B.; Marks, T. J. *Angew. Chem. Int. Ed.* **2008**, *47*, 2006-2025.
12. Itagaki, K.; Nomura, K. *Macromolecules* **2009**, *42*, 5097-5103.
13. Alidedeoglu, A. H.; York, A. W.; McCormick, C. L.; Morgan, S. E. *J. Polym. Sci., Part A: Polym. Chem.* **2009**, *47*, 5405-5415.
14. Nomura, K. *J. Synth. Org. Chem. Jpn.* **2010**, *68*, 1150-1158.
15. Hibi, Y.; Ouchi, M.; Sawamoto, M. *Angew. Chem. Int. Ed.* **2011**, *50*, 7434-7437.
16. Janoschka, T.; Teichler, A.; Krieg, A.; Hager, M. D.; Schubert, U. S. *J. Polym. Sci., Part A: Polym. Chem.* **2012**, *50*, 1394-1407.
17. Ittel, S. D.; Johnson, L. K.; Brookhart, M. *Chem. Rev.* **2000**, *100*, 1169-1204.
18. Boffa, L. S.; Novak, B. M. *Chem. Rev.* **2000**, *100*, 1479-1493.
19. Guan, Z.; Popeney, C. S. *Top Organomet Chem* **2009**, *26*, 179-220.
20. Chen, E. Y. X. *Chem. Rev.* **2009**, *109*, 5157-5214.
21. Nakamura, A.; Ito, S.; Nozaki, K. *Chem. Rev.* **2009**, *109*, 5215-5244.
22. Heyndrickx, W.; Occhipinti, G.; Bultinck, P.; Jensen, V. R. *Organometallics* **2012**, *31*, 6022-6031.
23. Nakamura, A.; Anselment, T. M. J.; Claverie, J.; Goodall, B.; Jordan, R. F.; Mecking, S.; Rieger, B.; Sen, A.; van Leeuwen, P. W. N. M.; Nozaki, K. *Acc. Chem. Res.* **2013**, *46*, 1438-1449.

24. Vanasselt, R.; Gielens, E.; Rulke, R. E.; Vrieze, K.; Elsevier, C. J. *J. Am. Chem. Soc.* **1994**, *116*, 977-985.

25. Johnson, L. K.; Mecking, S.; Brookhart, M. *J. Am. Chem. Soc.* **1996**, *118*, 267-268.

26. Younkin, T. R.; Conner, E. F.; Henderson, J. I.; Friedrich, S. K.; Grubbs, R. H.; Bansleben, D. A. *Science* **2000**, *287*, 460-462.

27. Gibson, V. C.; Tomov, A. *Chem. Commun.* **2001**, 1964-1965.

28. Boone, H. W.; Athey, P. S.; Mullins, M. J.; Philipp, D.; Muller, R.; Goddard, W. A. *J. Am. Chem. Soc.* **2002**, *124*, 8790-8791.

29. Drent, E.; van Dijk, R.; van Ginkel, R.; van Oort, B.; Pugh, R. I. *Chem. Commun.* **2002**, 744-745.

30. Drent, E.; van Dijk, R.; van Ginkel, R.; van Oort, B.; Pugh, R. I. *Chem. Commun.* **2002**, 964-965.

31. Guan, Z. B.; Marshall, W. J. *Organometallics* **2002**, *21*, 3580-3586.

32. Chen, G. H.; Ma, X. S.; Guan, Z. B. *J. Am. Chem. Soc.* **2003**, *125*, 6697-6704.

33. Foley, S. R.; Stockland, R. A.; Shen, H.; Jordan, R. F. *J. Am. Chem. Soc.* **2003**, *125*, 4350-4361.

34. Sujith, S.; Joe, D. J.; Na, S. J.; Park, Y. W.; Chow, C. H.; Lee, B. Y. *Macromolecules* **2005**, *38*, 10027-10033.

35. Bahuleyan, B. K.; Kim, J. H.; Seo, H. S.; Oh, J. M.; Ahn, I. Y.; Ha, C. S.; Park, D. W.; Kim, I. *Catal. Lett.* **2008**, *126*, 371-377.

36. Guironnet, D.; Roesle, P.; Runzi, T.; Gottker-Schnetmann, I.; Mecking, S. *J. Am. Chem. Soc.* **2009**, *131*, 422-423.

37. Zhang, Y. T.; Ning, Y. L.; Caporaso, L.; Cavallo, L.; Chen, E. Y. X. *J. Am. Chem. Soc.* **2010**, *132*, 2695-2709.

38. Delferro, M.; Marks, T. J. *Chem. Rev.* **2011**, *111*, 2450-2485.

39. Chen, X.; Caporaso, L.; Cavallo, L.; Chen, E. Y. X. *J. Am. Chem. Soc.* **2012**, *134*, 7278-7281.

40. Spaleck, W.; Kueber, F.; Winter, A.; Rohrmann, J.; Bachmann, B.; Antberg, M.; Dolle, V.; Paulus, E. F. *Organometallics* **1994**, *13*, 954-963.

41. Brintzinger, H. H.; Fischer, D.; Mulhaupt, R.; Rieger, B.; Waymouth, R. M. *Angew. Chem. Int. Ed.* **1995**, *34*, 1143-1170.

42. Britovsek, G. J. P.; Gibson, V. C.; Wass, D. F. *Angew. Chem. Int. Ed.* **1999**, *38*, 428-447.

43. Coates, G. W. *Chem. Rev.* **2000**, *100*, 1223-1252.

44. Gibson, V. C.; Spitzmesser, S. K. *Chem. Rev.* **2003**, *103*, 283-315.

45. Makio, H.; Terao, H.; Iwashita, A.; Fujita, T. *Chem. Rev.* **2011**, *111*, 2363-2449.

46. Stockland, R. A.; Jordan, R. F. *J. Am. Chem. Soc.* **2000**, *122*, 6315-6316.
47. Johnson, L. K.; Killian, C. M.; Brookhart, M. *J. Am. Chem. Soc.* **1995**, *117*, 6414-6415.
48. Gates, D. P.; Svejda, S. K.; Onate, E.; Killian, C. M.; Johnson, L. K.; White, P. S.; Brookhart, M. *Macromolecules* **2000**, *33*, 2320-2334.
49. Popeney, C. S.; Camacho, D. H.; Guan, Z. B. *J. Am. Chem. Soc.* **2007**, *129*, 10062-10063.
50. Luo, S.; Jordan, R. F. *J. Am. Chem. Soc.* **2006**, *128*, 12072-12073.
51. Foley, S. R.; Shen, H.; Qadeer, U. A.; Jordan, R. F. *Organometallics* **2004**, *23*, 600-609.
52. Kilyanek, S. M.; Stoebenau, E. J.; Vinayavekhin, N.; Jordan, R. F. *Organometallics* **2010**, *29*, 1750-1760.
53. Williams, B. S.; Leatherman, M. D.; White, P. S.; Brookhart, M. *J. Am. Chem. Soc.* **2005**, *127*, 5132-5146.
54. Connor, E. F.; Younkin, T. R.; Henderson, J. I.; Hwang, S. J.; Grubbs, R. H.; Roberts, W. P.; Litzau, J. J. *J. Polym. Sci., Part A: Polym. Chem.* **2002**, *40*, 2842-2854.
55. Connor, E. F.; Younkin, T. R.; Henderson, J. I.; Waltman, A. W.; Grubbs, R. H. *Chem. Commun.* **2003**, 2272-2273.
56. Mecking, S.; Johnson, L. K.; Wang, L.; Brookhart, M. *J. Am. Chem. Soc.* **1998**, *120*, 888-899.
57. Tempel, D. J.; Johnson, L. K.; Huff, R. L.; White, P. S.; Brookhart, M. *J. Am. Chem. Soc.* **2000**, *122*, 6686-6700.
58. Stockland, R. A.; Foley, S. R.; Jordan, R. F. *J. Am. Chem. Soc.* **2003**, *125*, 796-809.
59. Wu, F.; Foley, S. R.; Burns, C. T.; Jordan, R. F. *J. Am. Chem. Soc.* **2005**, *127*, 1841-1853.
60. Popeney, C. S.; Guan, Z. B. *J. Am. Chem. Soc.* **2009**, *131*, 12384-12393.
61. Chen, C.; Luo, S.; Jordan, R. F. *J. Am. Chem. Soc.* **2010**, *132*, 5273-5284.
62. Shultz, L. H.; Tempel, D. J.; Brookhart, M. *J. Am. Chem. Soc.* **2001**, *123*, 11539-11555.
63. Philipp, D. M.; Muller, R. P.; Goddard, W. A.; Storer, J.; McAdon, M.; Mullins, M. *J. Am. Chem. Soc.* **2002**, *124*, 10198-10210.
64. Vanasselt, R.; Elsevier, C. J.; Smeets, W. J. J.; Spek, A. L.; Benedix, R. *Recl. Trav. Chim. Pays-Bas* **1994**, *113*, 88-98.
65. Rulke, R. E.; Ernsting, J. M.; Spek, A. L.; Elsevier, C. J.; Vanleeuwen, P.; Vrieze, K. *Inorg. Chem.* **1993**, *32*, 5769-5778.
66. Gutierrez, E.; Nicasio, M. C.; Paneque, M.; Ruiz, C.; Salazar, V. *J. Organomet. Chem.* **1997**, *549*, 167-176.
67. Campora, J.; Lopez, J. A.; Palma, P.; del Rio, D.; Carmona, E.; Valerga, P.; Graiff, C.; Tiripicchio, A. *Inorg. Chem.* **2001**, *40*, 4116-4126.

68. The XRD data for **66** was not fully refined. The displayed image is a preliminary structure.

69. The preparation and metallation of diimines **81** and **82** were completed by undergraduate researcher Andreas Wierschen.

70. The XRD data for **82** was not fully refined. The displayed image is a preliminary structure.

71. Liu, J.; Li, Y.; Li, Y.; Hu, N. *J. Appl. Polym. Sci.* **2008**, *109*, 700-707.

72. Bonningue, C.; Houalla, D.; Wolf, R.; Jaud, J. *J. Chem. Soc., Perkin Trans. 2* **1983**, 773-776.

73. Penkert, F. N.; Weyhermuller, T.; Bill, E.; Hildebrandt, P.; Lecomte, S.; Wieghardt, K. *J. Am. Chem. Soc.* **2000**, *122*, 9663-9673.

74. The XRD data for the cationic Pd_4Ti_4 complex was not fully refined. The displayed image is a preliminary structure.

75. Pangborn, A. B.; Giardello, M. A.; Grubbs, R. H.; Rosen, R. K.; Timmers, F. J. *Organometallics* **1996**, *15*, 1518-1520.

76. Tshuva, E. Y.; Goldberg, I.; Kol, M. *J. Am. Chem. Soc.* **2000**, *122*, 10706-10707.

77. Tshuva, E. Y.; Goldberg, I.; Kol, M.; Goldschmidt, Z. *Inorg. Chem.* **2001**, *40*, 4263-4270.

78. Chen, C. T.; Huang, C. A.; Huang, B. H. *Dalton Trans.* **2003**, 3799-3803.

79. Chen, C. T.; Huang, C. A.; Huang, B. H. *Macromolecules* **2004**, *37*, 7968-7973.

80. Hormnirun, P.; Marshall, E. L.; Gibson, V. C.; White, A. J. P.; Williams, D. J. *J. Am. Chem. Soc.* **2004**, *126*, 2688-2689.

81. Tang, Z. H.; Gibson, V. C. *Eur. Polym. J.* **2007**, *43*, 150-155.

82. Clegg, W.; Davidson, M. G.; Graham, D. V.; Griffen, G.; Jones, M. D.; Kennedy, A. R.; O'Hara, C. T.; Russo, L.; Thomson, C. M. *Dalton Trans.* **2008**, 1295-1301.

83. Brown, H. C.; Kulkarni, S. U. *J. Organomet. Chem.* **1979**, *168*, 281-293.

84. Yakelis, N. A.; Bergman, R. G. *Organometallics* **2005**, *24*, 3579-3581.

85. Brookhart, M.; Grant, B.; Volpe, A. F. *Organometallics* **1992**, *11*, 3920-3922.

86. Jia, Y. X.; Hillgren, J. M.; Watson, E. L.; Marsden, S. P.; Kundig, E. P. *Chem. Commun.* **2008**, 4040-4042.

APPENDIX B

Towards Bimetallic Polymerization Catalysts with Early Transition Metals and Preliminary Polymerization Results

ABSTRACT

The results with dinickel bisphenoxyiminato complexes detailed in Chapters 2, 3 and 4 present the possibility that similar bimetallic complexes with early transition metals may demonstrate interesting effects in polymerization catalysis. Bimetallic titanium and zirconium bisphenoxyiminato complexes were synthesized, but the isolated complexes were not very active for ethylene polymerizations. To improve activity, tetraphenoxyiminato complexes and bisphenoxyiminato complexes with pendant thiolate or thioether donors were targeted. No pure tetraphenoxyiminato complexes could be isolated. Synthesis of the bisphenoxyiminato ligand precursor with pendant thiolate donors resulted in the isolation of a bisthiazole, rather than the desired compound. More success was achieved towards bisphenoxyiminato complexes with pendant thioether donors, and dititanium complexes were obtained in >90 % purity. Further purification, however, remains a challenge. Dinucleating bisphenoxyiminato ligand precursors with pendant ether donors were synthesized. Metallation to form the bimetallic titanium complexes for ethylene oligomerization was unsuccessful in preliminary attempts. A series of bimetallic titanium and zirconium di[amine bis(phenolate)] complexes were designed and synthesized. 1-Hexene and propylene homopolymerizations with dizirconium complexes **53** are discussed in Chapter 5. Preliminary 1-hexene polymerization trials in the presence of polar additives and 1-hexene/diene copolymerizations with **53** are reported herein. Asymmetric bimetallic complexes were designed with one polymerizing metal center and one metal center providing steric bulk. A couple asymmetric monometallic precursors were synthesize,

though addition of the second metal precursor resulted in complex mixtures, and additional efforts towards these complexes is required.

INTRODUCTION

The syn atropisomers of dinickel bisphenoximinato complexes based on a rigid *p*- or *m*-terphenyl backbone demonstrate increased tolerance of amine moieties due to a steric interaction between ligands bound to the two nickel centers (Chapter 3).[1] This bimetallic effect allowed the polymerization of ethylene in the presence of primary, secondary, and tertiary amines as well as the incorporation of tertiary amino olefins with olefinic chains containing at least two methylene units (Chapter 4).[2] The nickel complexes exhibited only limited ability for incorporation of comonomers: up to 4.8 mol % incorporation of 1-hexene with 3200 equivalents per nickel, or up to 1.2 mol % incorporation of 1-hexene with 500 equivalents per nickel (using 100 psig ethylene in both cases).[2,3] Similarly, with 500 equivalents of amino olefin per nickel and 100 psig ethylene, a maximum of 0.8 mol % incorporation was achieved.[2] The low incorporation is consistent with previous reports on monometallic nickel phenoxyiminato complexes.[4,5] Alternatively, many early transition metal polymerization catalysts are known to incorporate high mole percentages of α-olefins, as well as significantly higher polymerization activity than nickel catalysts.[6-8] Therefore, it has been our intent to extend the bimetallic strategy developed using nickel complexes to early transition metal complexes.

Early transition metal systems based on the terphenyl framework were targeted due to the monometallic systems' abilities to incorporate over 50 % of an α-olefin comonomer in copolymerizations with ethylene,[6] copolymerize ethylene and α-olefins with activities of up to four orders of magnitude higher than with the nickel systems,[6,8] and homopolymerize α-olefins with high turnover frequencies.[8-10] While early transition

metal complexes are generally more sensitive to the presence of polar moieties than late transition metal complexes due to the higher oxophilicity of the former, it is expected that the syn atropisomers of the terphenyl-based systems will utilize the steric interactions around the metal center to decrease that sensitivity. An inhibiting effect of the polar additive or polar monomer is likely, but the increases in expected activity and percent incorporation of comonomer will counterbalance the inhibitory effect such that the resultant polymers will be more desirable than those synthesized with the nickel complexes.

This Appendix, along with Chapter 5, details the research on bimetallic systems incorporating early transition metals. Bisphenoxyiminato ligands and derivatives thereof were studied with titanium and zirconium. Preliminary polymerization results are presented. Di[amine bis(phenolate)] ligands were explored with titanium and zirconium. Preliminary studies of the dizirconium di[amine bis(phenolate)] complexes for the polymerization of a variety of monomers (including dienes) or in the presence of polar additives are discussed. Use of these dizirconium complexes for the stereoselective polymerization of propylene and 1-hexene is described in Chapter 5. This Appendix also covers efforts toward heterobimetallic complexes based on the terphenyl framework.

RESULTS AND DISCUSSION

Dititanium and dizirconium bisphenoxyiminato-type complexes

Monophenoxyimine complexes were reported for ethylene and ethylene/1-hexene copolymerizations.[11-14] These catalyst systems are not very active, and less than 10 % α-olefin comonomer incorporation was observed.[13,14] Bimetallic variants explored by Marks and coworkers show improvement of both activity and comonomer incorporation relative to their monomeric counterparts,[13,14] indicating that analogous bimetallic compounds on the terphenyl backbone (**A**) have the potential to be effective polymerization catalysts (Chart B.1). Addition of a second set of phenoxyiminato ligands to the complexes (**B**) is likely to improve activity and comonomer incorporation, as monometallic bisphenoxyiminato catalysts with early transition metals display remarkable ethylene polymerization activity.[15] The extra bulk of the second ligand set may also enhance the bimetallic effects. Complexes based on tridentate variants of monophenoxyimine ligands exhibit increased activity over the monophenoxyiminato complexes and, in some cases, higher incorporation of comonomers than the monometallic bisphenoxyiminato catalysts.[7,16-20] Some of these systems were found to be very active and selective for oligomerization under the appropriate conditions.[21] Therefore, alterations of the terphenyl ligand to accommodate a third donor were also performed and the titanium complexes were targeted (**C**).

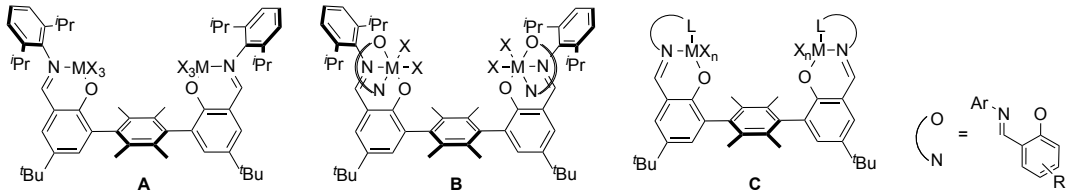

Chart B.1. Targeted dititanium and dizirconium bisphenoxyimine complexes (anti atropisomer not shown).

Bisphenoxyimine complexes

Metallations of bis-salicylaldimine **7** were performed to target bimetallic bis(phenoxyiminato) complexes **A**. Reactions between $Ti(O^iPr)_4$ and **7** and between $TiCl(O^iPr)_3$ and the deprotonated ligand precursors resulted in the same major species by ^1H NMR spectroscopy (Scheme B.1). Yellow solids were isolated and assigned as the desired products (**98**) based on the number and integration of the peaks in the ^1H NMR spectra. Pale yellow X-ray quality single crystals of **98-a** and **98-s** were grown by evaporation of hexanes at –35 °C (Figure B.1) confirming the identity of the dititanium compound. The Ti–Ti distance of 7.2 Å measured for **98-s** is similar to the Ni–Ni distance of 7.1 Å in the solid-state structure of **25-s**.

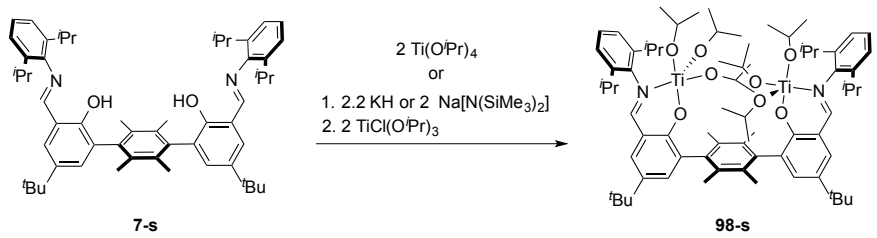

Scheme B.1. Synthesis of dititanium complexes **98** (anti atropisomer not shown).

Ethylene polymerizations with **98-s** and **98-a** were run with MAO as an activator (Table B.1). Monophenoxyimine titanium complexes with chloride ligands display turnover frequencies (TOFs) of up to 440 (g of polyethylene) $(mmol\ Ti)^{-1}\ (h)^{-1}$ at 15 psi

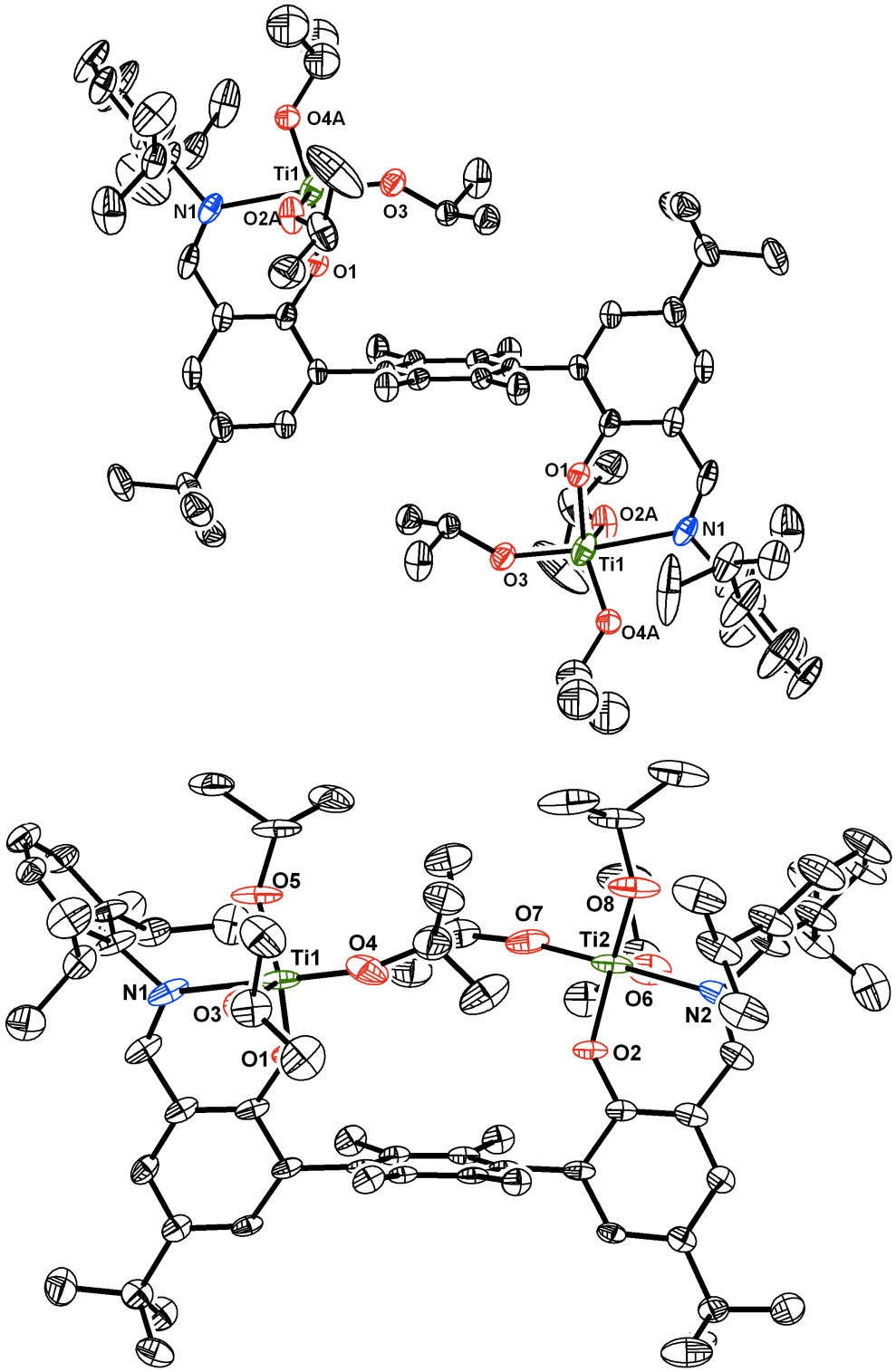

Figure B.1. Solid-state structures of **98-a** (top) and **98-s** (bottom) with thermal ellipsoids at the 50 % probability level. For clarity, hydrogen atoms and solvent molecules are omitted.

of ethylene.[11-12] Complexes **98**, however, did not achieve TOFs higher than 6.2 (g of polyethylene) (mmol Ti)$^{-1}$ (h)$^{-1}$ at 20 psi, indicating inefficient activation by MAO.[22] In an attempt to exchange the alkoxide ligands for more easily abstracted chloride ligands, **98-a** and **98-s** were treated with a 9-fold excess of Me_3SiCl, but no reaction took place. Alternative titanium precursors were therefore used for the metallation in order to target a more active catalyst system for ethylene and α-olefin polymerizations. Still, **98** may be useful for ring-opening polymerization (ROP) of lactides as titanium alkoxide complexes have been reported as effective ROP initiators,[23] and efforts will be made to used **98** for ROP.

Table B.1. Ethylene polymerizations with **98-s** and **98-a**.[a]

entry	complex	precatalyst loading in μmol	MAO/Zr	time (min)	yield (g)	TOF[b]
1	**98-s**	0.25	500	0.5	0.001	2.4
2	**98-s**	2.5	500	1.3	0.023	3.5
3	**98-a**	2.5	500	1.3	0.006	0.9
4	**98-s**	2.5	1000	1.3	0.042	6.2
5	**98-a**	2.5	1000	1.3	0.007	1.1

[a]All polymerizations were run at 0 °C under 20 psig of ethylene in toluene (25 mL) with MAO as an activator and scavenger. [b]Turnover frequency, defined as mass of polymer (in g) per mmol of Ti per h.

Metallations of **7** with $TiBn_4$ and $ZrBn_4$ were used to access dititanium benzyl complexes **99** and dizirconium benzyl complexes **100** (Scheme B.2). **99-s** and **99-a** were each precipitated from hexanes to yield deep red compounds with one major species by ^{1}H NMR spectroscopy, but attempts to further purify these complexes proved unsuccessful. Complexes **100**, on the other hand were isolable. For the syn atropisomer, the reaction mixture was washed over Celite with hexanes, the product-containing fraction was filtered through with benzene, and precipitation from hexanes yielded **100-s** as a bright orange solid. For the anti atropisomer, the reaction mixture was washed

over Celite with benzene, the product-containing fraction was filtered through with dichloromethane (DCM), and **100-a** was obtained as a bright orange solid.

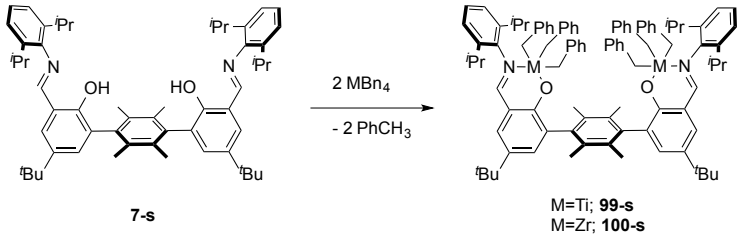

Scheme B.2. Synthesis of dititanium complexes **99** and dizirconium complexes **100** (anti atropisomers not shown).

Polymerizations with **100-s** and **100-a** were run with MAO as an activator (Table B.2). In ethylene homopolymerizations, a TOF of 17 (g polymer) $(\text{mmol Zr})^{-1}$ $(\text{h})^{-1}$ $(\text{atm})^{-1}$ was reported for monophenoxyimine zirconium complexes with chloride ligands and diisopropyl substituted aryl groups on the imine moiety of the ancillary ligand.[11-12] Bimetallic analogues reported by Marks, et al. displayed similar activity in ethylene homopolymerizations and up to 15 mol % incorporation of α-olefins and unfunctionalized dienes.[13-14] Complexes **100** achieved TOFs up to 190 (g polymer) $(\text{mmol Zr})^{-1}$ $(\text{h})^{-1}$ $(\text{atm})^{-1}$, but only incorporated 2 to 3 mol % of 1-hexene (Table B.2).

Table B.2. Polymerizations with **100-s** and **100-a**.[a]

entry	complex	comonomer	equivalents of comonomer per Zr	yield (g)	TOF[b]	branching[c]	I[d]
1	**100-s**			0.285	190		
2	**100-a**			0.183	122		
3	**100-s**	1-hexene	3600	0.162	108	9.8	2.0
4	**100-a**	1-hexene	3600	0.094	62	14.8	3.2

[a]All polymerizations were run at 20 °C under 15 psig of ethylene in toluene (25 mL total) with 0.003 mmol Zr, and 1000 equivalents of MAO/Zr for 30 minutes. [b]Turnover frequency, defined as mass of polymer (in g) per mmol of Zr per h per atm. [c]Branching was determined from ^{1}H NMR spectroscopy and is reported as the number of branches per 1000 carbons. [d]Mole percent incorporation of comonomer was calculated from the overall branching as only butyl branches were apparent in the ^{13}C NMR spectra.

Tetraphenoxyimine complexes

Because complexes **100** were neither highly active nor efficient at incorporating comonomers, efforts were focused on appending a second phenoxyimine donor set to target bimetallic tetraphenoxyiminato complexes **B**. Three previously reported monophenoxyimines with a phenyl group in the ortho position of the phenol and variation in the aryl group of the imine (Ph, 4-^{t}BuPh, and 3,5-di-^{t}BuPh) were synthesized according to literature procedures. Upon reaction of either **99** or **100** with two equivalents of a monophenoxyimine, the reaction components become much more soluble than the starting materials such that the crude reaction mixtures are fully solubilized by non-polar solvents. In one case, precipitation from hexanes yielded a solid with a promising ^{1}H NMR spectrum whose peaks could be assigned as two imine peaks, several of aromatic peaks, 4 benzyl peaks, 2 methine peaks, 2 aryl-methyl peaks, 4 isopropyl peaks, and 1 *tert*-butyl peak, which would account for all the protons in the desired product (**101**, Figure B.2). **101** is depicted in Figure B.2 as the *psuedo*-C_2 symmetric isomer, but a *pseudo*-C_S symmetric isomer is also possible and would have the same number of peaks by ^{1}H NMR spectroscopy. Unfortunately, further purification was ineffective and the yield was extremely low. In all other cases, intractable mixtures were formed and neither precipitations nor recrystallizations yielded pure desired product.

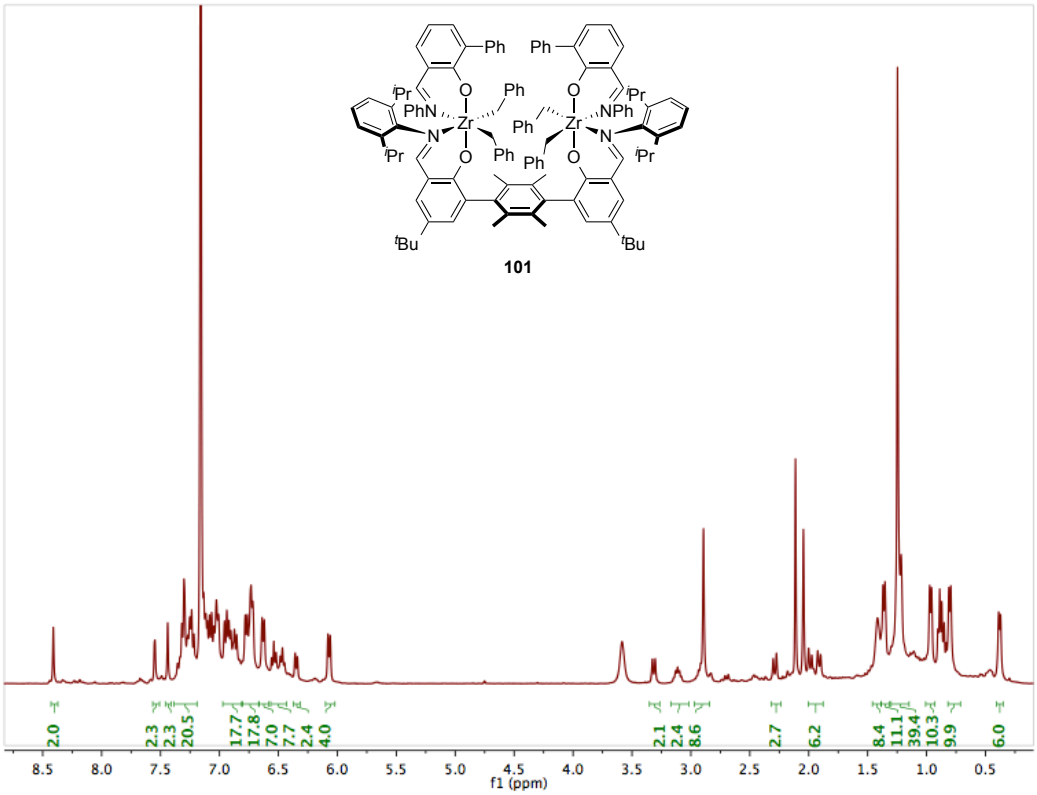

Figure B.2. ^{1}H NMR spectrum (C_6D_6) of the hexanes precipitate from the reaction of a second set of phenoxyimine donors with **100-s**, assigned as dizirconium tetraphenoxyimine complex **101**.

In order to access isolable complexes expected to have higher activity than **98** and **100**, the amide- and chloride-ligated bimetallic tetraphenoxyimine analogues were targeted by both stepwise and *in situ* syntheses (Scheme B.3). Metallation of **7** with Ti(O^{i}Pr)Cl_3 and Ti$(NMe_2)_4$ led to intractable mixtures. Deprotonation of **7**, followed by metallation with $TiCl_4$, $TiCl_4(THF)_2$, or $ZrCl_4(THF)_2$ yielded, in most cases, a single major species by ^{1}H NMR spectroscopy, but attempts to purify the products via washings, precipitations, or recrystallizations resulted in decomposition to a complex mixture, with greater decomposition if the material had been exposed to Et_2O or THF. To avoid the need for isolation of the unstable bis(phenoxyiminato) complexes, a one-pot synthesis of the tetraphenoxyiminato complexes was pursued by adding a slight

excess of deprotonated monophenoxyimine (**102**) to the crude reaction mixtures of the metallations. The ^{1}H NMR spectra indicated products with new imine peaks, but in all cases, resonances were observed for at least two species and efforts to isolate a single species failed.

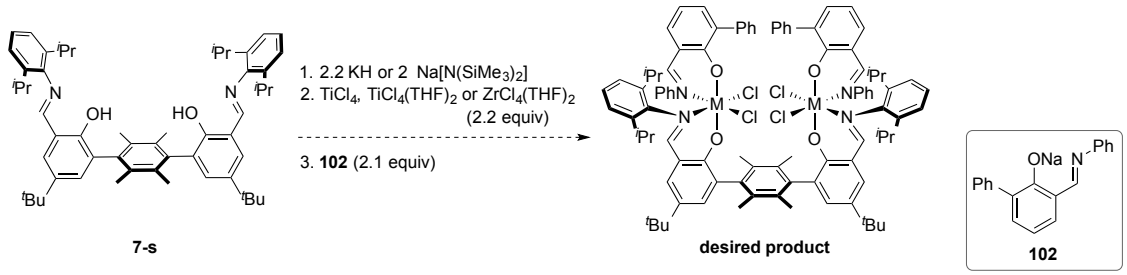

Scheme B.3. Synthetic route toward dititanium or dizirconium tetraphenoxyiminato chloride complexes (anti atropisomers not shown).

Bisphenoxyimine complexes with pendant donors

A set of bisphenoxyimine ligands were targeted wherein the aryl group of the imine was substituted with a thiol or thioether which could serve as a third donor for the metal center and thereby eliminate the complications of adding a second set of phenoxyimine donors (**103** and **104**, Scheme B.4). Complexes obtained from the metallation of the mononucleating analogues of **103** and **104** were reported to have significantly higher activity (up to 10^3 (g polymer) (mmol M)$^{-1}$ (h)$^{-1}$ (atm)$^{-1}$) and comonomer incorporation (up to 30 mol %) in ethylene/1-hexene copolymerizations than their monophenoxyimine counterparts.[7,16] To generate the dinucleating ligand precursors with pendant thiol or thioether moieties, an imine condensation of the terphenyl bisaldehyde precursor **6** with 2.2 equivalents of 2-aminothiophenol was performed under the same conditions as the imine condensation to form **7**. Instead of producing the desired bisphenoxyimine-thiophenol **103**, a bisthiazole was synthesized,

as confirmed by ^{1}H and ^{13}C NMR spectroscopy and HRMS, potentially due to oxidation by O_2. The conditions were altered to rigorously exclude O_2, but the desired product (**103**) was not obtained in appreciable yield for either atropisomer. Both atropisomers of **104** were successfully synthesized and purified from the reaction between **6** and 2.2 equivalents of 2-aminophenyl phenyl sulfide; unreacted aldehyde was removed by resubmitting to the reaction conditions with another 0.4 equivalents of 2-aminophenyl phenyl sulfide and the imine containing impurity was removed via column chromatography.

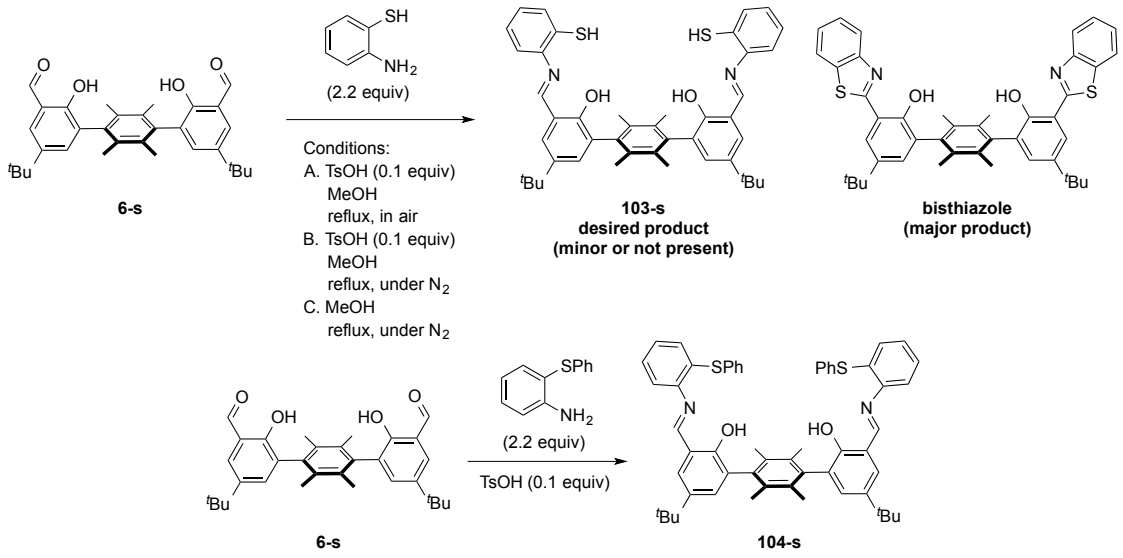

Scheme B.4. Synthesis of dinucleating bisphenoxyiminato ligand precursors with pendant thiolate or thioether donors (anti atropisomers not shown).

104 was deprotonated with KH (**105**) and subsequently metallated with $TiCl_4$ or $TiCl_4(THF)_2$ (Scheme B.5). Both atropisomers were found to be unstable toward prolonged exposure to THF, so THF could not be used for purification, but the compounds were stable to chlorinated solvents. Dititanium complex **106-a** was purified via precipitation from DCM by the addition of hexanes and cooling to –35 °C. For the

syn atropisomer, however, the products and impurities present were highly insoluble; coprecipitated of the product with the impurities occurred under the variety of conditions that were tried. Instead of continuing attempts to purify **106-s** post-metallation, which were not promising, further purification of the precursors was attempted. Bisaldehyde **6-s**, a precursor that was generally moved on to the imine condensation without purification, was purified to >90 % purity via column chromatography. After the imine condensation, bisphenoxyimine **104-s** was purified via precipitation from methanol and drying on the Schlenk line to remove additional volatile impurities. Deprotonation in the glovebox with KH was followed by precipitation from pentane, filtration over a fine frit to remove the pentane soluble materials, washing through with benzene to collect the product and leave excess salts behind, and lyophilization from benzene to yield the clean desired product, **105-s**. These purification methods successfully eliminated a number of impurities from the deprotonated ligand, but metallation attempts with $TiCl_4$ did not yield pure product.

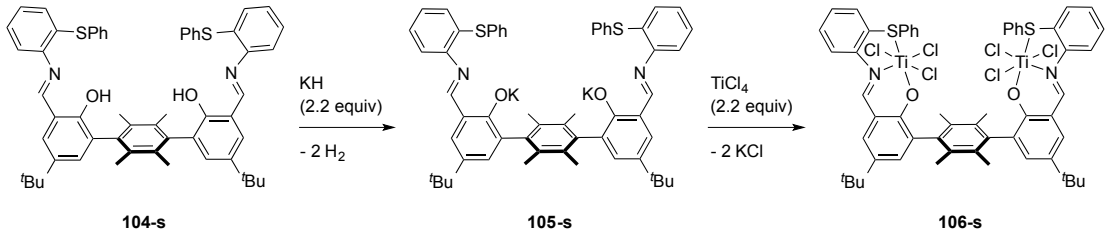

Scheme B.5. Synthesis of dititanium complexes **106** (anti atropisomers not shown).

To access an isolable complex, the alkylated analogues of **106** were targeted. One of the difficulties in the purification of **106-s** was its insolubility in most solvents, and the complexes with alkyl rather than chloride ligands were expected to increase solubility. Reactions of either atropisomer of **106** with methyl Grignard formed dark

green, nearly black reaction mixtures with broad ^{1}H NMR spectra. Reactions of **106** with benzyl Grignard formed dark red reaction mixtures with ^{1}H NMR spectra containing no resonances consistent with imine protons (e.g. downfield of 8 ppm). A nearly identical ^{1}H NMR spectrum was obtained from the reaction of **104** with $TiBn_4$. A significant upfield shift of the imine resonance would be consistent with a reaction occurring at the imino carbon. Indeed, a doublet of doublets was present at 5.2 ppm in all reactions. In a 2D NMR study (^{1}H-^{13}C gHSQCAD), the proton signals at 5.2 ppm were found to couple to a tertiary carbon signal at 76.3 ppm. From these data, the product was assigned as a dititanium complex with one phenoxide, one amido, one thioether and two benzyl donors per titanium (**107**, Scheme B.6). This assignment is consistent with literature examples of benzyl migration to the imino carbon in a variety of group 4 transition metal complexes.[24,25] Gibson, *et al.* reported that monometallic zirconium and hafnium complexes bearing a phenoxy(benzimidazolyl) amide ligand displayed no ethylene homopolymerization activity, though the analogous titanium complexes were not reported.[24] Efforts towards the purification of **107** were unproductive.

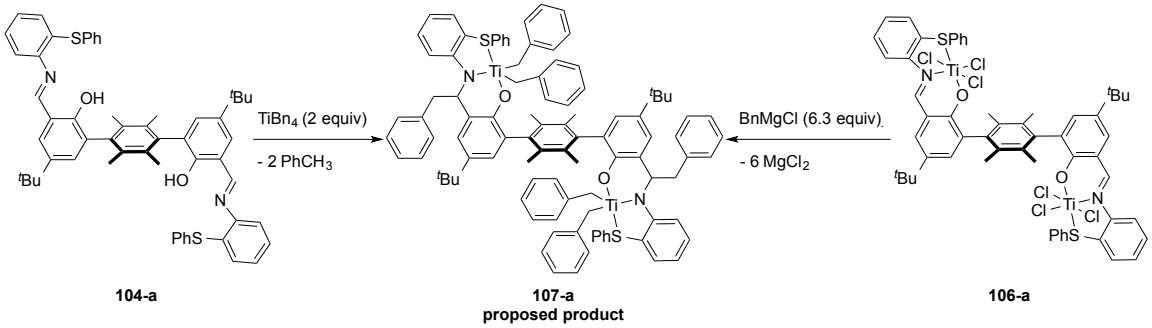

Scheme B.6. Reactions of **104** with $TiBn_4$ and **106** with benzyl Grignard to form **107** (syn atropisomer not shown)**.**

A dititanium bisphenoxyimine complex with pendant ether donors was targeted for the oligomerization of ethylene (**110**, Chart B.2). The monometallic complex (**109**, Chart B.2) has been reported to selectively oligomerize ethylene to 1-hexene with very high activity.[21] Changes in selectivity may occur with the bimetallic analogue as from steric or cooperative bimetallic effects favoring a particular ring size, assuming the reaction proceeds through a metallacycle mechanism. If different selectivity is observed, mechanistic insight into the involvement of a second metal center could be made.

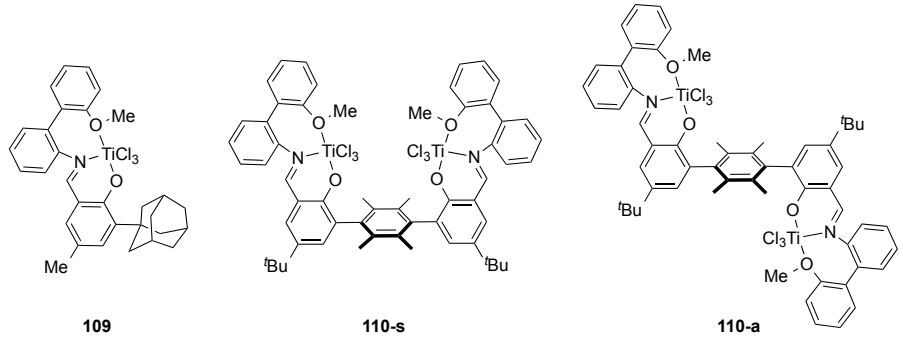

Chart B.2. Mono- and dititanium phenoxyimine complexes with pendant aryl-OMe donors**.**

The bisphenoxyimine ligand precursors with pendant aryl-OMe donors (**112**) were synthesized via imine condensation of bisaldehyde **6** and aniline **111** using the same procedure as for the synthesis of **7** (Scheme B.7). Metallation of **112** with $TiCl_4$ using the literature conditions from the monometallic analogue[21] resulted in one major imine-containing product by ^1H NMR spectroscopy. The number and integration of the peaks of the major species were consistent with desired complexes **110**. Purification attempts resulted in decomposition for both atropisomers and efforts to obtain pure species were unsuccessful. While metallation without deprotonation was reported to be effective for the synthesis of monotitanium complex **109**, deprotonation of **112** prior to metallation

may improve the stability of the products, as HCl is the expected biproduct of the reaction of $TiCl_4$ with **112**.

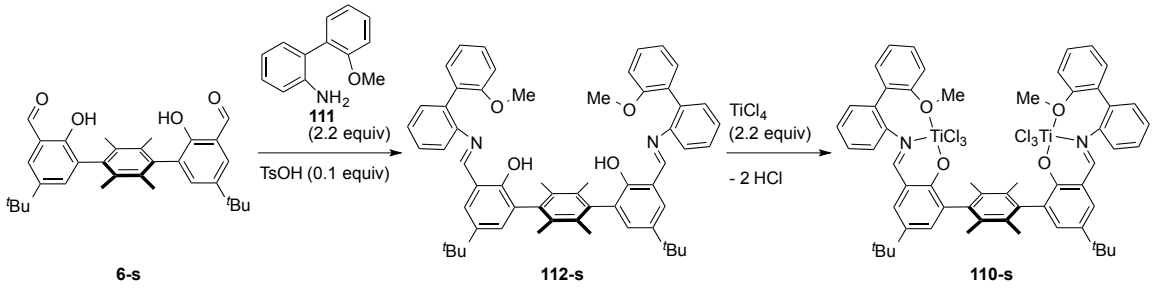

Scheme B.7. Intended synthesis of bisphenoxyimine ligand precursors with pendant aryl-OMe donors (**112**) and subsequent metallation to dititanium complex **110** (anti atropisomer not shown).

Titanium and zirconium di[amine bis(phenolate)] complexes

Literature on group IV ONXO-type amine bis(phenolate) complexes for polymerization focuses primarily on their high activity for polymerization of a-olefins.[10] These C_S-symmetric non-metallocene complexes were first introduced in 1999 by Kol and coworkers and have been studied for the polymerization of 1-hexene and modified such that activities of up to 120,000 (g polymer) x $(\text{mmol Zr})^{-1}$ $(\text{h})^{-1}$ have been achieved.[10,26-36] The most extensively studied of these ONXO-type amine bis(phenolate) complexes are those with $X=NMe_2$, which have been used for propylene, 1-hexene, vinyl cyclohexane, and 4-methyl pentene polymerizations as well as 1-hexene/1-octene block copolymerizations.[6,10,29,33,37] While high activities, high molecular weight polymers, low molecular weight distributions and highly regioregular polymers have been observed, only atactic polymers were made with these C_S complexes.[6,10,29,33,37]

C_1- and C_2-symmetric diamine bis(phenolate) ligands, a derivative ligand set from the ONXO-type amine bis(phenolate), also know as salan ligands were also developed by Kol and coworkers.[38] Group IV salan complexes were found to have only moderate

polymerization activity compared to the ONXO-type amine bis(phenolate) complexes, but the *fac-fac* binding mode of the ligand led to C_2 symmetric complexes with the capability for living isospecific polymerization of 1-hexene at room temperature.[38] Isospecific polymerization of propylene, 1-hexene, vinyl cyclohexane, and 4-methyl pentene as well as cyclopolymerization of 1,5-hexadiene, and copolymerizations of ethylene with propylene, ethylene with 1-hexene, and 1-hexene with 1-octene were studied.[6,39-44] Variations of the ligand set led to increases in activity by the addition of electron withdrawing substituents on the phenoxide rings and increases in isospecificity by the addition of sterically bulky substituents on the phenoxide rings.[42,45-46] These effects were combined and improved upon through the use of an asymmetric ligand.[47-49] The isotacticity, rather than hemitacticity, of the polymers produced by the C_1-symmetric complexes suggested that, unlike metallocenes, the control of polymer tacticity arose from a combined effect of the substituents on both sides of the ligand rather than each site being affected by only one.[47-49] The ^{13}C NMR data support that these polymerizations proceeded with enantiomorphic site control.[47-49] Complexes with *o*-iodide and *p*-iodide substituents on one phenoxide ring and *o*-adamantyl and *p*-methyl on the other were found to produce poly(1-hexene) with up to 95 % *mmmm* and polypropylene with up to 83 % *mmmm* while maintaining relatively high activity and M_w compared to other salan complexes.[47-48]

Both bimetallic bis-salan (**D**) and bimetallic di[amine bis(phenolate)] (**E**) complexes were targeted (Chart B.3). Progress towards the synthesis of dizirconium complexes **D** and dititanium complexes **E** will be discussed. The synthesis, characterization, and 1-hexene and propylene homopolymerization activity of

dizirconium complexes **E** are detailed in Chapter 5. Additional polymerization experiments focused on progress toward polymerizations in the presence of polar groups and the polymerization of dienes to synthesize ladder polymers with the dizirconium di[amine bis(phenolate)] complexes are presented herein.

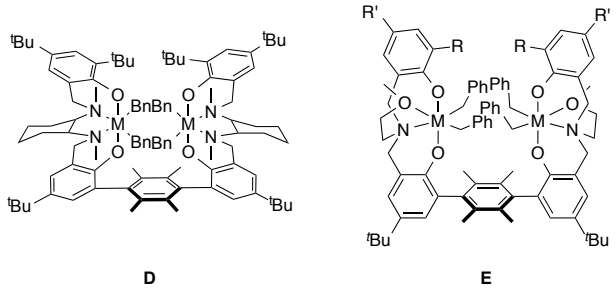

Chart B.3. Targeted dititanium and dizirconium di[amine bis(phenolate)] complexes (anti atropisomer not shown).

Attempted synthesis of enantiopure bis-salan complexes

The synthesis of enantiopure bis-salan framework **115** was accomplished from enantiopure diamine **113** and benzyl bromides **51** and **55** (Scheme B.8). Diamine **114** was synthesized via the reaction of **55** with **113** in the presence of Hünig's base in THF. Bis-salans **115** were obtained in low yield from the reactions of dibromides **51** with slight excess of **114** and purified by column chromatography to >90 % purity. Metallation of **115** with $ZrBn_4$ resulted in complex mixtures whose components were all soluble in non-polar solvents, limiting efforts towards further purification.

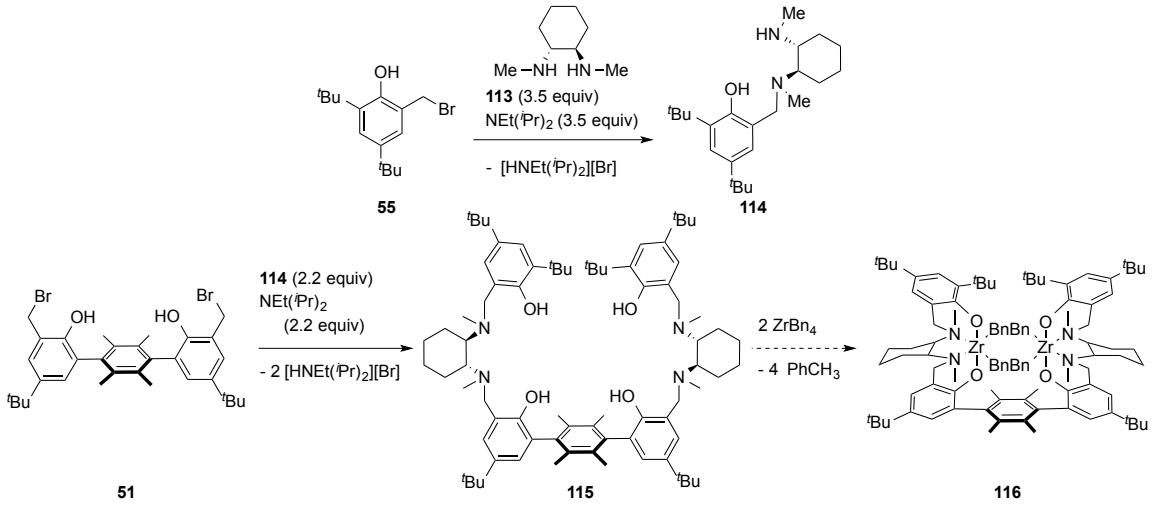

Scheme B.8. Synthesis of bis-salan framework **115** and proposed metallation to zirconium complexes **116** (anti atropisomer not shown)**.**

Synthesis of di[amine bis(phenolate)] complexes

Efforts towards bimetallic di[amine bis(phenolate)] complexes **E** started with the synthesis of a complex with substituents R=R'=^{t}Bu. While this ligand precursor was obtained in significantly higher yield and purity than **115**, similar issues with high solubility impeding purification led to the synthesis of ligand variants with other substituents to decrease the solubility of the resultant complexes and increase the likelihood of obtaining analytically pure complexes for polymerization trials. Accordingly, the synthesis of the syn atropisomers of di[amine bis(phenolate)] ligand precursors **52** and the metallation of these compounds yielded pure dizirconium complexes **53** (Chapter 5). The anti atropisomers of **52a-OMe** and **52d-OMe** were also synthesized via the route detailed in Scheme 5.2. These compounds, **52a-OMe-a** and **52d-OMe-a** were metallated with $ZrBn_4$, but could not be adequately purified for polymerization trials (Chart B.4). Likewise, metallations of both the syn and anti

atropisomers of **52a-OMe** and **52d-OMe** with $TiBn_4$ were attempted targeting dititanium complexes **117** (Chart B.4), but pure complexes could not be obtained.

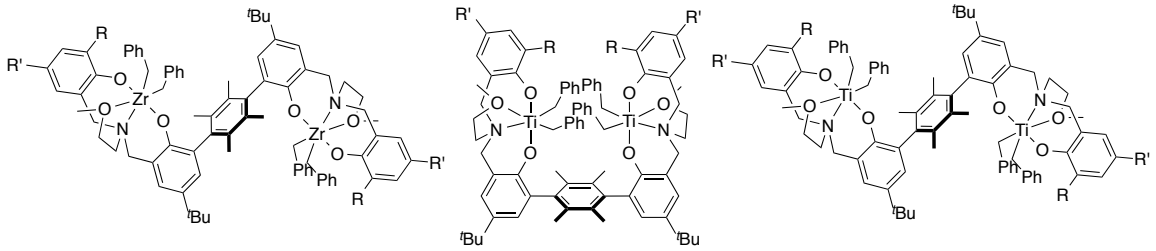

Chart B.4. Anti and dititanium analogues of dizirconium complexes **53a-OMe** and **53d-OMe.**

Attempted polymerizations with di[amine bis(phenolate)] complexes in the presence of polar additives

Attempts were made to extend the bimetallic strategy for tolerance and incorporation of amines achieved with nickel to tolerance and incorporation of ethers and esters by dizirconium complexes **53**. To test for tolerance, polymerizations in the presence of a number of ethers and esters have been attempted with both mono- (**54-OMe** and **57-OMe**) and bimetallic (**53a-OMe** and **53d-OMe**) zirconium complexes (Table B.3, Chart B.5, and Scheme B.9). Thus far, no enhanced tolerance has been observed with the bimetallic complexes for diisopropylether, *tert*-butyl ethyl ether, benzyl ether, or ethyl benzoate. The lack of tolerance may be because the additives are not bulky enough, especially around the oxygen moieties, or because after binding to the additive, there is insufficient space for a 1-hexene molecule to bind to the Zr center. To address these possibilities, bulkier ethers and esters such as dicyclohexyl ether will be employed, and polymerizations of smaller olefins such as propylene or ethylene in the presence of these ethers will be attempted. The lack of tolerance may also stem

from a reaction between the activator and the additive; further experimentation is needed to rule out this possibility.

Table B.3. 1-Hexene polymerizations in the presence of polar additives.[a]

entry	complex	additive	time (min)	yield (g)	activity[b]	C[c]
1	**54-OMe**	none	10	1.60	2390	95
2	**57-OMe**	none	20	1.55	1160	92
3	**53d-OMe**	none	20	1.54	1150	91
4	**53a-OMe**	none	20	1.34	1010	80
5	**54-OMe**	diisopropylether	60	0.047	12	3
6	**57-OMe**	diisopropylether	60	0.015	4	1
7	**53d-OMe**	diisopropylether	60	0.048	12	3
8	**53a-OMe**	diisopropylether	60	0.011	3	1
9	**54-OMe**	*tert*-butyl ethyl ether	60	0.015	4	1
10	**57-OMe**	*tert*-butyl ethyl ether	60	0.009	2	1
11	**53d-OMe**	*tert*-butyl ethyl ether	60	0.010	3	1
12	**53a-OMe**	*tert*-butyl ethyl ether	60	0.006	2	0
13	**54-OMe**	benzyl ether	60	0.015	4	1
14	**57-OMe**	benzyl ether	60	0.019	5	1
15	**53d-OMe**	benzyl ether	60	0.012	3	1
16	**53a-OMe**	benzyl ether	60	0.022	6	1
17	**54-OMe**	ethyl benzoate	60	0.004	1	0
18	**57-OMe**	ethyl benzoate	60	0.003	1	0
19	**53d-OMe**	ethyl benzoate	60	0.022[d]	5[d]	1[d]
20	**53a-OMe**	ethyl benzoate	60	0.003	1	0

[a]Polymerizations were run at ambient temperature with 5000 equivalents of 1-hexene (2.5 mL, 1.68 g) in chlorobenzene with 4 μmol [Zr], 4 μmol of $[CPh_3][B(C_6F_5)_4]$, and 50 equivalents of additive per zirconium. Solution volume = 5 mL. [b]Activity, defined as mass of polymer (in g) per mmol of Zr per hour. [c]Percent conversion of 1-hexene [d]Ethyl benzoate was present in ^{1}H NMR spectrum of the polymer sample.

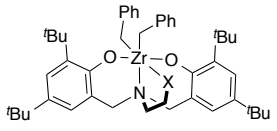

X=OMe; **54-OMe**
X=NMe_2; **54-NMe_2**

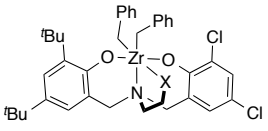

X=OMe; **57-OMe**
X=NMe_2; **57-NMe_2**

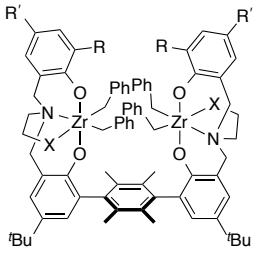

R=R'=Cl, X=OMe; **53a-OMe**
R=R'=Cl, X=NMe_2; **53a-NMe_2**
R=^{t}Bu, R'=H, X=OMe; **53d-OMe**

Chart B.5. Mono- and dizirconium complexes utilized herein**.**

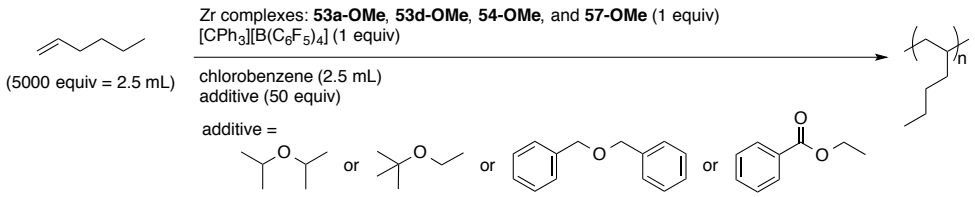

Scheme B.9. 1-Hexene polymerizations in the presence of polar additives**.**

Copolymerizations of 1-hexene with di[amine bis(phenolate)] complexes

Dizirconium complexes **53** are also being applied to the attempted synthesis of ladder polymers. In the copolymerization of an α-olefin with a diene, insertion of the two olefinic moieties of a single diene monomer at both zirconium centers of a single molecule would form a link between the two growing chains (Scheme B.10). This connection would serve to increase the average molecular weight of the polymers and potentially decrease the molecular weight distribution. 1,7-Octadiene, 1,9-decadiene, and 1,3-dibutenylbenzene were chosen as dienes for copolymerizations with 1-hexene (Table B.4). For 1,7-octadiene and 1,9-decadiene evidence of the formation of ladder polymers would primarily come from the comparison of the GPC data with that of polymers made under the same conditions without the diene comonomer. With 1,3-dibutenylbenzene, additional evidence for the ladder polymers could be obtained by using ozonolysis to cleave the arene moieties present within the polymer and comparing the NMR and GPC data before and after ozonolysis.[50] Another advantage of using 1,3-dibutenylbenzene as the diene comonomer is that the monomer is more rigid compared to the aliphatic dienes, decreasing the likelihood that both olefinic moieties of a monomer would be inserted into the same chain. To test if the amine bisphenolate systems would be active for 1-hexene copolymerzation with an aryl comonomer, a copolymerization with 5000 equiv of 1-hexene and 250 equiv of 4-phenyl-1-butene was

run with monozirconium complex **57-NMe$_2$** (entry 1, Table B.5). High activity was observed and incorporation of aryl moiety was observed by ^{1}H and ^{13}C NMR spectroscopy.

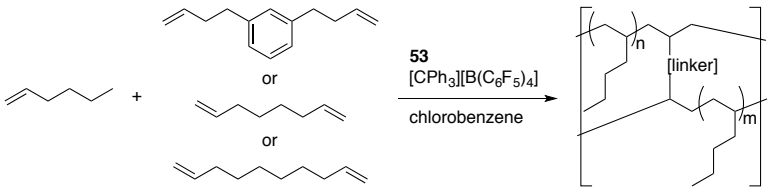

Scheme B.10. Proposed 1-hexene/diene copolymerizations to form ladder polymers.

Preliminary polymerization data with 1,7-octadiene, 1,9-decadiene, and 1,3-dibutenylbenzene are presented in Table B.4. Copolymerizations with monometallic catalysts **54-OMe** and **57-NMe$_2$** produced polymers with NMR spectra containing olefinic peaks, indicating incorporation of the comonomers. Polymers produced by **54-OMe** with 100 equivalents of 1,7-octadiene were soluble in $CDCl_3$ at room temperature and displayed about 5 mol % incorporation by integration of the ^{1}H NMR spectrum (entries 3 and 4, Table B.4). Polymerizations by **54-OMe** with 100 equivalents of 1,9-decadiene produced gel-like polymers that were insoluble in $C_2D_2Cl_4$ even at 130 °C, probably due to crosslinking (entries 5 and 6, Table B.4). Polymer produced by **57-NMe$_2$** with 167 equivalents of 1,7-octadiene were soluble in $CDCl_3$ at room temperature and displayed about 11 mol % incorporation by integration of the ^{1}H NMR spectrum (entry 8, Table B.4). Polymerization by **57-NMe$_2$** with 100 equivalents of 1,3-dibutenylbenzene produced a gel-like polymer that was only sparingly soluble in $C_2D_2Cl_4$ even at 130 °C, probably due to crosslinking (entry 9, Table B.4). Copolymerizations with dizirconium complex **53a-NMe$_2$** produced polymers physically different from those produced by the monometallic analogues. With 1,7-octadiene and

1,3-dibutenylbenzene, highly insoluble gel-like polymers were synthesized with **53a-NMe$_2$** that were qualitatively harder than those produced by the monometallic complexes, possibly due to increased isotacticity or higher molecular weight. The activity of **53a-NMe$_2$** was also increased relative to **57-NMe$_2$** under the same polymerization conditions. These differences between the mono- and bimetallic analogues may not pertain to the formation of ladder polymers and additional trials that access soluble polymers, especially with 1,3-dibutenylbenzene, are necessary. To that end, the number of diene equivalents will be decreased at least 10-fold to reduce extraneous cross-linking. Though many of these polymerizations were run to less than 50 % conversion of the monomer, cross-linking may also be occuring as the concentration of olefin decreases. Limiting olefin consumption may also serve to minimize extraneous cross-linking.

Table B.4. 1-Hexene/diene copolymerizations.[a]

entry	complex, loading in μmol	$[CPh_3][B(C_6F_5)_4]$, Al^{i}Bu (equiv per Zr)	comonomer	time (min)	yield (g)	activity[b]
1	**54-OMe**, 2	1, 5	none	10	0.58	1700
2	**54-OMe**, 2	1, 5	none	100	1.55	460
3	**54-OMe**, 2	1, 5	octadiene	10	0.08	220
4	**54-OMe**, 2	1, 5	octadiene	100	0.12	35
5	**54-OMe**, 2	1, 5	decadiene	7.5	1.15	4600
6	**54-OMe**, 2	1, 5	decadiene	90	1.69	560
7	**54-NMe$_2$**, 0.4	3, 15	none	10	0.09	1400
8	**54-NMe$_2$**, 0.4	3, 15	octadiene	10	0.06	890
9	**54-NMe$_2$**, 0.4	3, 15	1,3-dibutenylbenzene	10	0.19	2900
10	**53a-NMe$_2$**, 0.2	3, 15	none	5	0.71	21000
11	**53a-NMe$_2$**, 0.2	3, 15	octadiene	5	0.44	13000
12	**53a-NMe$_2$**, 0.2	3, 15	1,3-dibutenylbenzene	5	0.56	17000

[a]Polymerizations were run in chlorobenzene at 0 °C. Runs 1–6 were run with 10000 equiv of 1-hexene (2.5 mL, 1.6 g) and 100 equiv comonomer per Zr with a total reaction volume of 5.0 mL. Runs 7–12 were run with 25000 equiv of 1-hexene (1.25 mL, 0.84 g) and 167 equiv comonomer per Zr with a total reaction volume of 2.5 mL. [b]Activity, defined as mass of polymer (in g) per mmol of Zr per hour.

Zirconium complexes **53a-OMe**, **53a-NMe$_2$**, and **57-NMe$_2$** were also used for the homopolymerizations of 1,5-hexadiene and 4-methyl-1-pentene (Table B.5). These

monomers have been stereoselectively polymerized by C_1- and C_2-symmetric zirconium salan complexes. The increased bulk of 4-methyl-1-pentene and the propensity of 1,5-hexadiene for cyclopolymerization were expected to lead to increased stereoselectivity with the bimetallic complexes. This was not, however, observed in preliminary polymerization trials and no further work with these monomers was done.

Table B.5. 1-Hexene/4-phenyl-1-butene and 1-hexene/4-methyl-1-pentene copolymerization and homopolymerization of 1,5-hexadiene and 4-methyl-1-pentene.[a]

entry	complex, loading in μmol	monomers	time (min)	yield (g)	activity[b]	% *mmmm*
1	**57-NMe$_2$**, 4	1-hexene, 4-phenyl-1-butene[c]	10	1.34	2000	<10
2	**57-NMe$_2$**, 4	1,5-hexadiene	2	1.45	11000	nd[d]
3	**53a-NMe$_2$**, 2	1,5-hexadiene	1	0.95	14000	nd[d]
4	**53a-OMe**, 2	1,5-hexadiene	6	0.19	490	nd[d]
5	**57-NMe$_2$**, 4	1-hexene, 4-methyl-1-pentene[e]	10	1.29	1900	<10
6	**57-NMe$_2$**, 2[f]	4-methyl-1-pentene	10	0.57	860	25
7	**53a-NMe$_2$**, 1[f]	4-methyl-1-pentene	10	0.72	1100	40
8	**53a-OMe**, 1[f]	4-methyl-1-pentene	20	0.16	120	53

[a]Polymerizations were run in chlorobenzene at ambient temperature with 1 equiv $[CPh_3][B(C_6F_5)_4]$ and 5000 equiv of monomer per Zr. Total reaction volume of 5.0 mL. [b]Activity, defined as mass of polymer (in g) per mmol of Zr per hour. [c]250 equivalents of 4-phenyl-1-butene were used. [d]Not determined because of reliable NMR data could not be obtained due to issues with insolubility of the polymers. [e]500 equivalents of 4-methyl-1-pentene were used. [f]Total reaction volume of 2.5 mL.

Systems with One Active Metal

The proposed mechanism of amino olefin incorporation detailed in Chapter 4 does not necessitate the presence of a second metal center as long as sufficient steric bulk to disfavor the binding of the bulky polar moiety is available. Therefore, a new set of targets was designed which use a non-polymerizing metal center to provide steric bulk around the active metal center. An example of the potential mechanism for copolymerization of ethylene and amino olefins with titanium isopropoxide as the inactive metal and a nickel alkyl moiety as the polymerizing metal center is illustrated in Scheme B.11. The proposed mechanism is analogous to that of amino olefin incorporation in Scheme 4.3. Without abstracting the isopropoxide ligands on titanium,

the metal center is expected to remain dormant, just as **98** was not an effective polymerization catalyst, even with 1000 equivalents of MAO present. Meanwhile, the nickel center, in the example shown, would serve as the site of polymerization. Instead of nickel, titanium or zirconium could also serve as the active metal center.

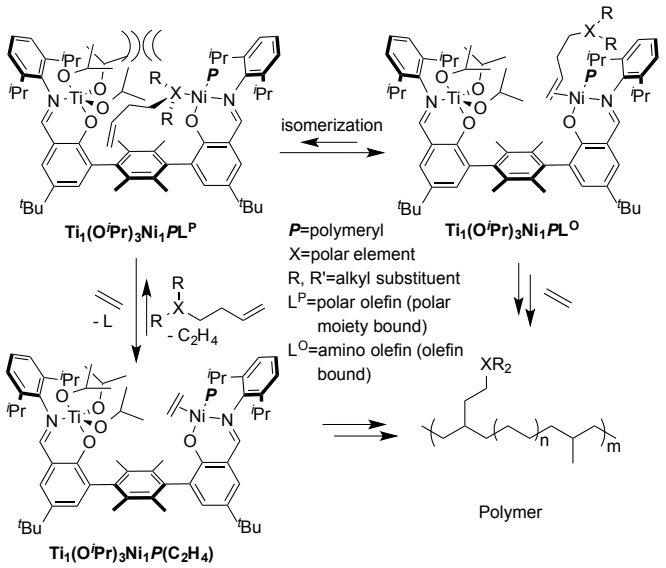

Scheme B.11. Proposed mechanism for polar olefin incorporation by a complex with $Ti(O^iPr)_3$ providing bulk in the system.

Attempts were made to synthesize the desired complexes with one polymerizing metal by the addition of a nickel alkyl precursor and subsequent addition of a titanium alkoxide precursor (Scheme B.12). When metallating bisphenoxyiminato ligand **7-s** with $Ni(Me)_2(tmeda)$ in the presence of 2,6-lutidine (rather than pyridine as is reported in Chapter 2), the major product was found to be a mononickel species (**118**). This mononickel species could be synthesized cleanly by the addition of 1.8 equiv of $Ni(Me)_2(tmeda)$ to **7-s** in the presence of 20 equiv of 2,6-lutidine. Metallation of open phenoxyiminato ligand on **118** with $Ti(O^iPr)_4$ proved unsuccessful, probably due to

steric hindrance. Instead, a titanium precursor with smaller alkoxide substituents may be effective.

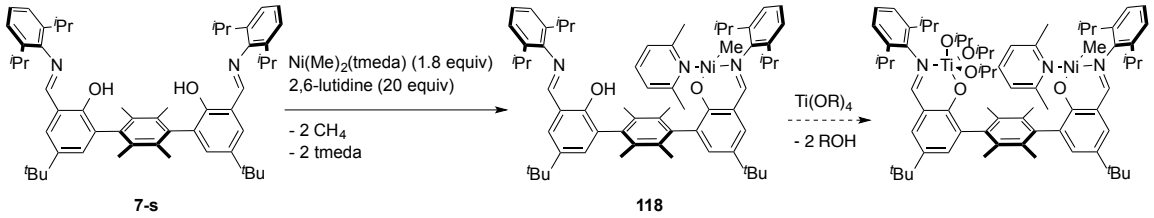

Scheme B.12. Synthesis of **118** and proposed metallation with $Ti(OR)_4$.

The heterobimetallic complexes were also targeted through metallation with the stable titanium alkoxide precursor first (Scheme B.13). This was undertaken by two methods: initial deprotonation of one of the two phenoxyimines followed by metallation with $Ti(O^iPr)_4$ and then a metal source requiring a deprotonated phenoxyimine such as $NiClMe(PMe_3)_2$ or $TiCl_4$ (Route A, Scheme B.13), or installation of titanium isopropoxide followed by deprotonation and metallation or just metallation if the metal source does not require a deprotonated phenoxyimine such as $NiMe_2(tmeda)$ or $TiCl_2(NMe_2)_2$ (Route B, Scheme B.13). In pursuit of Route A, **7-s** was deprotonated with one equivalent of KH to yield the monopotassium salt, **119**. Upon addition of slightly greater than one equivalent of $Ti(O^iPr)_4$ to **119**, a mixture of species was generated with new peaks in all the regions in the ^1H NMR spectrum expected for the desired product, but which still included a species with a phenolic proton. Along Route B, a monotitanium species, **120**, was isolated in >90 % purity from the reaction of one equivalent of $Ti(O^iPr)_4$ and **7-s**. Attempts to deprotonate **120** with KH resulted in decomposition, but metallation attempts with $NiMe_2(tmeda)$ in the presence of excess pyridine or $TiCl_2(NMe_2)_2$ resulted in multiple new species as observed by ^1H NMR spectroscopy. While the reactions yielded multiple products, new $NiCH_3$ and imine

peaks, respectively, were observed, potentially indicating the formation of the desired species In addition to further purification of the current metallation attempts, metallations of **120** with $NiMe_2$(tmeda) in the presence of excess acetonitrile (which would be less sterically bulky) or with $TiCl_2(O^iPr)_2$ or $TiCl_3(O^iPr)$ will also be pursued.

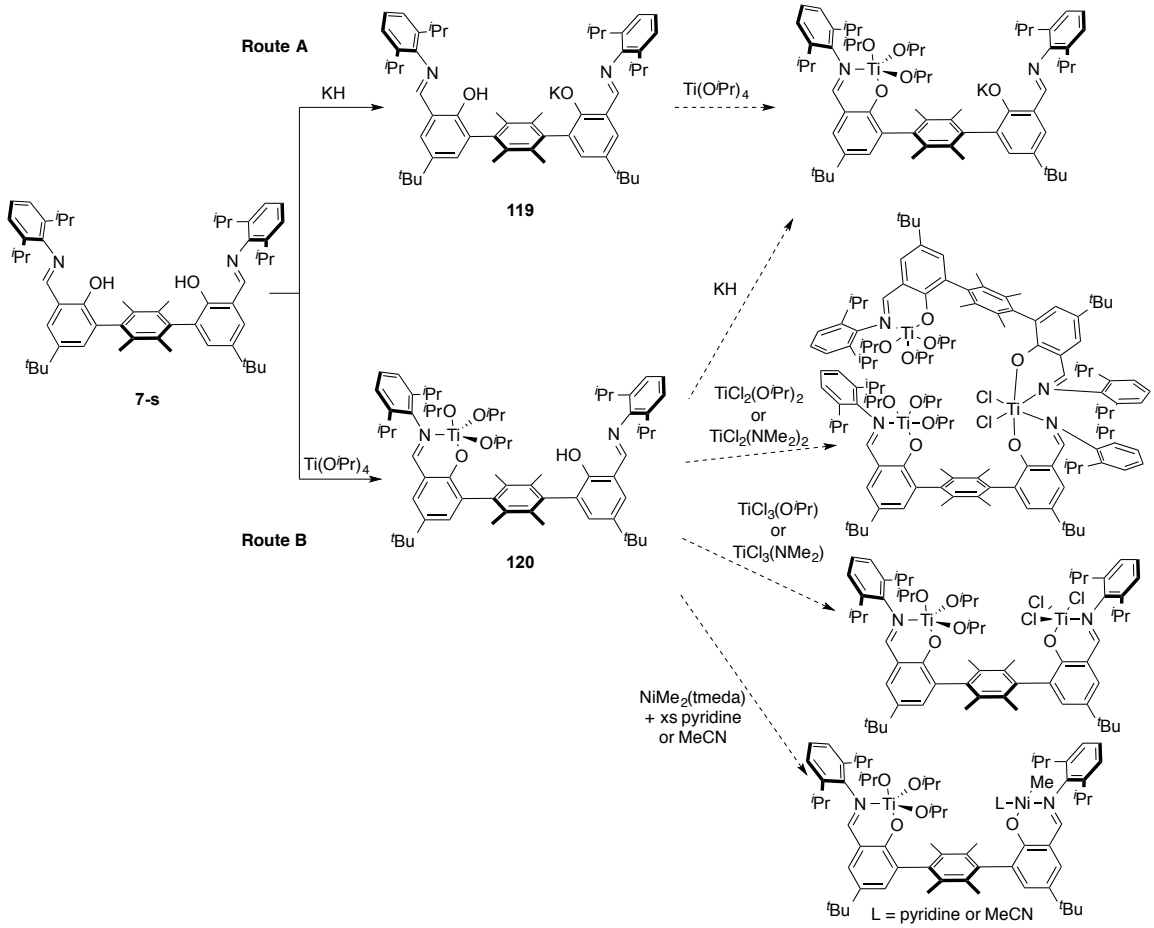

Scheme B.13. Progress toward complexes metallated with $Ti(O^iPr)_4$ to providing steric bulk around the second, active, metal center by metallation with $Ti(O^iPr)_4$ before the addition of the second metal.

CONCLUSIONS

A variety of titanium and zirconium complexes were targeted to explore the potential of the *p*-terphenyl framework to support bimetallic early transition metal complexes that could be utilized for enhanced polymerization catalysis. Dititanium bisphenoxyiminato alkoxide complexes **98** were isolated and structurally characterized. **98** did not exhibit ethylene polymerization activity when activated with MAO, but may be effective initiators for ROP of lactide. Dititanium and dizirconium bisphenoxyiminato complexes **99** and **100** with benzyl rather than isopropoxide ligands were synthesized. Ethylene and ethylene/1-hexene polymerizations with **100** proceeded with low activity <4 mol % incorporation of 1-hexene, similar to that reported for monometallic complexes, indicating that these complexes are not good candidates for copolymerization trials with polar comonomers where high incorporation is desired. Isolation of bimetallic tetraphenoxyiminato complexes was unsuccessful. Dinucleating ligand frameworks with pendant thioether donors for titanium were synthesized (**104**) and metallations yielded the desired the dititanium complexes (**106**) as the major product. Attempts towards the purification of **106-s** were ineffectual. In pursuing an analogous dititanium complex with alkyl (rather than chloride) ligands, benzyl migration to the imino carbon occurred to generate complexes **107**. Bimetallic bisphenoxyiminato complexes with pendant ether donors **110** were targeted for possible ethylene oligomerization activity. The dinucleating ligand precursors were synthesized and metallations are ongoing.

As described in Chapter 5, dizirconium di[amine bis(phenolate)] complexes **53** exhibit stereoselectivity in the polymerization of propylene and 1-hexene. No pure

complexes were obtained in endeavors to isolate the anti atropisomers or the titanium analogues of **53**. Complexes **53** were used in a variety of polymerizations to search for additional applications of these complexes. Polymerizations with ether and ester additives were unproductive. Preliminary 1-hexene/diene copolymerization trials demonstrated that dizirconium di[amine bis(phenolate)] complexes could effectively incorporate dienes, but some of the polymers formed were extremely insoluble, limiting analysis. Further studies will test the potential of the bimetallic systems to incorporate the olefinic moieties of a monomer into the growing polymeryl chains on both zirconium centers in a single complex. Such ladder polymers would be a unique material from well-known and inexpensive monomers. Polymerization of bulky monomers, such as 4-methyl-1-pentene was also explored to determine the effect of the additional bulk on tacticity, but very little difference was observed relative to the analogously synthesized 1-hexene polymers. Exchange of the benzyl ligands on **53** for alkoxides may provide active ROP catalysts.

Asymmetric systems were designed to have one active metal center at which polymerizations would take place and a second dormant metal center that would provide steric bulk proximal to the first metal center. These systems would take advantage of the mechanisms proposed for the tolerance of amines by dinickel complexes **25**, the incorporation of amino olefins by dinickel complexes **44**, **45** and **46**, and the stereoselectivity of dizirconium complexes **53**, which all rely on proximal effects and suggest that steric bulk may work as well as a second metal center at engendering interesting polymerization activity at the first metal center. The dormant metal would provide that steric bulk and specific variation of the size of the dormant moiety could

be tuned for the desired reactivity. Mononickel and monotitanium complexes **118** and **120**, respectively were synthesized, and further efforts will be made to append a second metal center.

Many of the early transition metal complexes reported in this Appendix have potential for use as olefin polymerization or oligomerization catalysts or lactide ROP initiators, though in most cases pure complexes have remained elusive. 1-Hexene/diene copolymerization to make ladder polymers with **53** holds promise. As demonstrated in Chapters 2 through 5, bimetallic complexes on a rigid terphenyl backbone allow for thorough investigation of the nature of bimetallic effects in polymerization, and many more developments are expected using this framework.

EXPERIMENTAL SECTION

General considerations and instrumentation

All air- and/or water-sensitive compounds were manipulated using an inert atmosphere glovebox or standard Schlenk line techniques with an N_2 atmosphere. The solvents for air- and moisture-sensitive reactions were dried over sodium/benzophenone ketyl, CaH_2, or by the method of Grubbs.[51] All NMR solvents were purchased from Cambridge Isotopes Laboratories, Inc. For NMR samples of air- and/or water-sensitive compounds $CDCl_3$ and CD_2Cl_2 were dried over calcium hydride and vacuum transferred prior to use. Toluene for polymerizations and C_6D_6 were dried over sodium/benzophenone ketyl and vacuum transferred prior to use. Chlorobenzene and 1-hexene for polymerizations were refluxed over CaH_2 for greater than 72 h and vacuum transferred prior to use. Toluene, C_6D_6, chlorobenzene, and 1-hexene were further purified by filtration over activated alumina. Ethylene was purchased from Matheson and equipped with a PUR-Gas in-line trap to remove oxygen and moisture before use. Diisopropyl ether, 4-phenyl-1-butene, 1,5-hexadiene, 1,7-octadiene, 1,9-decadiene and 4-methyl-1-pentene were stirred over CaH_2 for greater than 48 h and vacuum transferred prior to use. *tert*-Butyl ethyl ether was stirred over CaH_2 for greater than 48 h and filtered over activated alumina before use. Ethyl benzoate was refluxed over sodium for 1 week, distilled (by Kugelrohr), and filtered over activated alumnia prior to use. Benzyl ether was fractionally distilled (by Kugelrohr) and filtered over activated alumina prior to use. Unless otherwise noted, all other reagents were used as received. All ^{1}H, ^{13}C, and 2D NMR spectra of small organic and organometallic compounds were recorded on Varian Mercury 300 MHz, Varian 400 MHz, or Varian

INOVA-500 or 600 MHz spectrometers at room temperature. ^{1}H and ^{13}C NMR spectra of poly(1-hexene) samples were recorded on a Varian INOVA-500 MHz spectrometer at room temperature in $CDCl_3$. ^{1}H and ^{13}C NMR spectra of polyethylene samples were recorded on a Varian INOVA-500 MHz spectrometer at 130 °C in tetrachloroethane-D_2. For ^{1}H and ^{13}C NMR spectra, chemical shifts are reported with respect to residual internal deuterated solvent: 7.16 and 128.06 (t) ppm (C_6D_6); 7.26 and 77.16 (t) ppm ($CDCl_3$); 6.00 and 74.22 (t) ppm ($C_2D_2Cl_4$); 5.32 and 53.84 ppm (CD_2Cl_2); for ^{1}H and ^{13}C data. J coupling are reported in Hz.

Synthetic protocols

Imino-phenols,[52] $Ti(O^{i}Pr)Cl_3$,[53] $TiBn_4$,[54] $TiCl_4(THF)_2$,[55] $ZrCl_4(THF)_2$,[55] **111**,[21] **113**[56] and 1,3-dibutenylbenzene[57] were prepared according to literature procedures. $ZrBn_4$ was synthesized by modification of literature procedures as detailed in Chapter 5.[58-59]

Compound 98-a. A solution of **7-a** (0.050 g, 0.062 mmol) in THF (3 mL) was added dropwise to a solution of $Ti(O^{i}Pr)_4$ (0.039 g, 0.137 mmol, 2.2 equiv) in THF (2 mL) and the resulting solution was stirred for 20 h, and concentrated *in vacuo*. The material was then dissolved in hexanes and filtered over Celite. The volatiles were removed under vacuum to yield **98-a** as a yellow solid. X-ray quality single crystals were grown by evaporation of hexanes at –35 °C. ^{1}H NMR (300 MHz, C_6D_6) δ = 8.25 (s, 2H, C*H*N), 7.61 (d, *J*=2.6, 2H, Ar*H*), 7.25 (d, *J*=2.5, 2H, Ar*H*), 7.16 (s, 6H, Ar*H*), 4.58 (sept, *J*=6.1, 6H, OC*H*$(CH_3)_2$), 3.47 (sept, *J*=6.8, 4H, ArC*H*$(CH_3)_2$), 2.26 (s, 12H, ArCH_3), 1.35 (bs, 24H, ArCH(C$H_3)_2$), 1.28 (s, 18H, C(C$H_3)_3$), 1.10 (d, *J*=6.1, 36H, OCH(C$H_3)_2$) ppm.

Compound 98-s. A solution of **7-s** (0.092 g, 0.115 mmol) in THF (5 mL) was added dropwise to a solution of $Ti(O^{i}Pr)_4$ (0.072 g, 0.252 mmol, 2.2 equiv) in THF (4 mL) and the

resulting solution was stirred for 22 h, and concentrated *in vacuo*. The material was then dissolved in hexanes and filtered over Celite. The volatiles were removed under vacuum to yield a yellow solid. This solid was reprecipitated from hexanes to yield **98-s**. X-ray quality single crystals were grown by evaporation of hexanes at –35 °C. ^{1}H NMR (300 MHz, C_6D_6) δ = 8.27 (s, 2H, C*H*N), 7.56 (d, *J*=2.6, 2H, Ar*H*), 7.29 (d, *J*=2.6, 2H, Ar*H*), 7.19 (s, 6H, Ar*H*), 4.76 (sept, *J*=6.1, 6H, OC*H*$(CH_3)_2$), 3.59 (p, *J*=6.8, 4H, ArC*H*$(CH_3)_2$), 2.40 (s, 12H, ArC*H*$_3$), 1.40 (s, 24H, ArCH(C*H*$_3)_2$), 1.24 (s, 18H, C(C*H*$_3)_3$), 1.15 (d, *J*=6.1, 36H, OCH(C*H*$_3)_2$) ppm.

Reaction of 98 with Me_3SiCl. Both atropisomers of **98** were treated with Me_3SiCl to exchange the isopropoxide ligands for chlorides using literature conditions,[60] but neither isomer reacted.

Compounds 99-a and 99-s. A cooled solution of **7** (0.050 g, 0.062 mmol) in toluene (3 mL) was added dropwise to a solution of $TiBn_4$ (0.064 g, 0.155 mmol, 2.5 equiv) in toluene (2 mL) at –35 °C and the resulting solution was stirred for 20 h, covered, and concentrated *in vacuo* to yield a deep red solid. For **99-a**, the solid was washed with hexanes, Et_2O, and THF. The remaining deep red material was >90 % pure by ^{1}H NMR spectropscopy. For **99-s**, the solid was reprecipitated from hexanes to yield a single major species in >80 % purity by ^{1}H NMR spectropscopy. Data for **99-a** are as follows. ^{1}H NMR (400 MHz, $CDCl_3$) δ = 8.56 (s, 2H, C*H*N), 7.63 (d, *J*=2.5, 2H, Ar*H*), 7.38 (d, *J*=2.5, 2H, Ar*H*), 7.20 (m, 6H, Ar*H*), 6.94 (t, *J*=7.5, 12H, $CH_2(C_6H_5)$), 6.83 (t, *J*=7.3, 6H, $CH_2(C_6H_5)$), 6.41 (d, *J*=7.2, 12H, $CH_2(C_6H_5)$), 2.60 (s, 12H, C*H*$_2(C_6H_5)$), 2.34 (sept, *J*=6.7, 4H, ArC*H*$(CH_3)_2$), 2.13 (s, 12H, ArC*H*$_3$), 1.31 (s, 18H, C(C*H*$_3)_3$), 1.18 (d, *J*=6.7, 12H, ArCH(C*H*$_3)_2$), 1.03 (d, *J*=6.7, 12H, ArCH(C*H*$_3)_2$) ppm. Data for **99-s** are as follows. ^{1}H

NMR (400 MHz, C_6D_6) δ = 8.33 (s, 2H, C*H*N), 7.54 (d, *J*=2.6, 2H, Ar*H*), 7.24 (d, *J*=2.6, 2H, Ar*H*), 7.07 (d, *J*=6.6, 6H, Ar*H*), 7.02 (t, *J*=7.7, 12H, $CH_2(C_6H_5)$), 6.84 (t, *J*=7.3, 6H, $CH_2(C_6H_5)$), 6.74 (d, *J*=7.2, 12H, $CH_2(C_6H_5)$), 2.99 (s, 12H, $CH_2(C_6H_5)$), 2.65 (sept, *J*=6.7, 4H, ArC*H*$(CH_3)_2$), 2.37 (s, 12H, ArC*H*$_3$), 1.21 (s, 18H, C(C*H*$_3)_3$), 1.06 (m, 12H, ArCH(C*H*$_3)_2$), 1.00 (m, 12H, ArCH(C*H*$_3)_2$) ppm.

Compounds 100-a and 100-s. A cooled solution of **7** (0.050 g, 0.062 mmol) in toluene (3 mL) was added dropwise to a solution of $ZrBn_4$ (0.071 g, 0.155 mmol, 2.5 equiv) in toluene (2 mL) at –35 °C and the resulting solution was stirred for 20 h and concentrated *in vacuo* to yield a bright orange solid. To purify **100-a**, the solid was washed over Celite with benzene and the product was flushed through with dichloromethane. Volatiles were removed *in vacuo* and the resulting bright orange solid was clean by ^{1}H NMR spectropscopy. To purify **100-s**, the solid was washed over Celite with hexanes and the product was flushed through with benzene. Volatiles were removed *in vacuo* and the residue was suspended in hexanes and cooled to –35 °C overnight. **100-s** was collected via filtration as a bright orange solid. Data for **100-a** are as follows. ^{1}H NMR (400 MHz, $CDCl_3$) δ = 8.41 (s, 2H, C*H*N), 7.56 (d, *J*=2.5, 2H, Ar*H*), 7.31 (d, *J*=2.5, 2H, Ar*H*), 7.19 (m, 6H, Ar*H*), 6.88 (t, *J*=7.1, 12H, $CH_2(C_6H_5)$), 6.84 (t, *J*=6.9, 6H, $CH_2(C_6H_5)$), 6.26 (d, *J*=7.1, 12H, $CH_2(C_6H_5)$), 2.51 (sept, *J*=6.7, 4H, C*H*$(CH_3)_2$), 2.09 (s, 12H, C*H*$_2(C_6H_5)$), 1.59 (s, 12H, ArC*H*$_3$), 1.29 (s, 18H, C(C*H*$_3)_3$), 1.22 (d, *J*=6.8, 12H, CH(C*H*$_3)_2$), 1.04 (d, *J*=6.7, 12H, CH(C*H*$_3)_2$) ppm. Data for **100-s** are as follows. ^{1}H NMR (400 MHz, C_6D_6) δ = 8.25 (s, 2H, C*H*N), 7.48 (d, *J*=2.6, 2H, Ar*H*), 7.22 (d, *J*=2.6, 2H, Ar*H*), 7.08 (m, *J*=5.3, 6H, Ar*H*), 7.00 (t, *J*=7.6, 12H, $CH_2(C_6H_5)$), 6.86 (t, *J*=7.3, 6H, $CH_2(C_6H_5)$), 6.61 (d, *J*=7.2, 12H, $CH_2(C_6H_5)$), 2.57 (sept, *J*=6.6, 4H,

C*H*(CH_3)$_2$), 2.32 (s, 12H, CH_2(C_6H_5)), 1.93 (s, 12H, ArCH_3), 1.18 (s, 18H, C(CH_3)$_3$), 1.17 (d, *J*=6.9, 12H, CH(CH_3)$_2$), 1.02 (d, *J*=6.7, 12H, CH(CH_3)$_2$) ppm.

Addition of additional phenoxyimine ligand precursors to 100. A cooled solution of imino-phenol (imine aryl=Ph) (0.015 g, 0.055 mmol, 4 equiv) in toluene (1 mL) was added dropwise to a solution of **100** (0.022 g, 0.015 mmol) in toluene (1 mL) at –35 °C and the resulting solution was stirred for 3 h, and concentrated *in vacuo* to yield an orange solid. Excess monophenoxyimine was removed by washing with cold hexanes. The ^{1}H NMR spectrum of the precipitate from the reaction with **100-s** is presented in Figure B.2 (assigned as complex **101**).

Representative procedure for metallation of 7 with $TiCl_4$, $TiCl_4(THF)_2$, or $ZrCl_4(THF)_2$. All of the metallations with $TiCl_4$, $TiCl_4(THF)_2$, and $ZrCl_4(THF)_2$ were conducted using the same protocol. A cooled solution of **7-a** deprotonated with KH (0.051 g, 0.058 mmol) in toluene (4 mL) was added dropwise to a solution of $TiCl_4$ (0.014 mL, 0.128 mmol, 2.2 equiv) in toluene (4 mL) at –35 °C and the resulting solution was stirred for 24 h, and concentrated *in vacuo* to yield a brownish red solid. The product was partially purified by washing over Celite with hexanes, Et_2O and benzene before flushing the product through with THF and concentrating *in vacuo* to yield a brownish red solid.

Compound 102. A cooled solution of imino-phenol (0.150 g, 0.550 mmol) in THF (10 mL) was added to a solution of NaH (0.066 g, 2.75 mmol, 5 equiv) in THF (5 mL) at –35 °C. The resulting solution was stirred for 2 h, and concentrated *in vacuo* to yield a fine yellow powder with no phenolic peak in the ^{1}H NMR spectrum. ^{1}H NMR

(300 MHz, $CDCl_3$) δ = 8.31 (bs, 2H, C*H*N), 7.65–7.30 (m, 9H, Ar*H*), 6.68 (bs, 4H, Ar*H*) ppm.

Representative procedure for deprotonation and metallation of 7 with $TiCl_4$, $TiCl_4(THF)_2$, or $ZrCl_4(THF)_2$ followed by *in situ* reaction with 2 equiv of 102. All of the metallations with $TiCl_4$, $TiCl_4(THF)_2$, and $ZrCl_4(THF)_2$ followed by *in situ* reactions with 2 equiv of a monophenoxyimine were conducted using the same protocol. A scintillation vial equipped with a stirbar was charged with $Na(N(SiMe_3)_2)$ (0.022 g, 0.117 mmol, 2 equiv) in THF (1 mL). A solution of **7-a** (0.050 g, 0.059 mmol) in THF (2 mL) was added and the mixture was stirred at room temperature for 12 h, before being concentrated *in vacuo* to yield a bright yellow solid. The amine side product was removed by two cycles of suspending the product in hexanes and removing the volatiles under vacuum. The residue was suspended in toluene (4 mL) and added dropwise to a solution of $TiCl_4(THF)_2$ (0.043 mL, 0.129 mmol, 2.2 equiv) in toluene (4 mL) at –35 °C and the resulting solution was stirred for 18 h, before being concentrated *in vacuo* to yield a deep red solid. The solid was resuspended in toluene (4 mL), a solution of **102** (0.036 g, 0.123 mmol, 2.1 equiv) in toluene (4 mL) was added and the mixture was stirred for 12 h before concentrating *in vacuo* to yield a deep red solid.

Attempted syntheses of 103. Terphenyl bisaldehyde **6** (0.050 g, 0.103 mmol), 2-aminothiophenol (0.028 g, 0.226 mmol, 2.2 equiv), tosic acid (0.002 g, 0.010 mmol, 0.1 equiv) and MeOH (5 mL) were combined in a round bottom flask equipped with a stirbar and a reflux condenser. The reaction mixture was heated to reflux with stirring for 4 h and then cooled to room temperature and put into freezer to precipitate for 12 h. The pale solid (which was assigned as the bisthiazole) was collected over a frit. The

reaction conditions were changed to rigorously exclude O_2 using both MeOH and EtOH as solvents with and without tosic acid in order to access **103**, but the desired product was not isolated in appreciable yield in any case.

Compound 104-a. Terphenyl bisaldehyde **6-a** (0.050 g, 0.103 mmol), 2-aminophenyl phenyl sulfide (0.046 g, 0.226 mmol, 2.2 equiv), tosic acid (0.002 g, 0.010 mmol, 0.1 equiv) and MeOH (5 mL) were combined in a round bottom flask equipped with a stirbar and a reflux condenser. The reaction mixture was heated to reflux with stirring for 4 h and then cooled to room temperature and put into freezer to precipitate for 12 h. The pale solid was collected over a frit. Some bisaldehyde starting material was still present so the precipitate was resubmitted to the reaction conditions with 0.4 more equivalents of 2-aminophenyl phenyl sulfide (0.009 g) and 0.1 equivalents of tosic acid (0.002 g) in MeOH (5 mL). The mixture was refluxed for 24 h, cooled to room temperature, and put into the freezer to precipitate. **104-a** was collected as a pale yellow precipitate via filtration. ^{1}H NMR (300 MHz, $CDCl_3$) δ = 12.89 (s, 2H, O*H*), 8.62 (s, 2H, C*H*N), 7.42-7.27 (m, 14H, Ar*H*), 7.24-7.04 (m, 8H, Ar*H*), 2.04 (s, 12H, ArCH_3), 1.34 (s, 18H, C(CH_3)$_3$) ppm.

Compound 104-s. **6-s** (0.174 g, 0.358 mmol), 2-aminophenyl phenyl sulfide (0.159 g, 0.788 mmol, 2.2 equiv), tosic acid (0.007 g, 0.036 mmol, 0.1 equiv) and MeOH (18 mL) were combined in a round bottom flask equipped with a stirbar and a reflux condenser. The reaction mixture was heated to reflux with stirring for 10 h and then cooled to room temperature and reduced under vacuum. Some bisaldehyde starting material was still present as observed by ^{1}H NMR spectroscopy so the residue was resubmitted to the reaction conditions with 1 more equivalents of 2-aminophenyl phenyl sulfide (0.079 g) and 0.05 equivalents of tosic acid (0.003 g) in MeOH (18 mL). The mixture was refluxed for 15 h,

cooled to room temperature and the light yellow precipitate was collected over a medium frit. The precipitate was transferred to a tared vial and volatiles were removed under vacuum yielding 0.244 g (80 % yield) of yellow solid. ^{1}H NMR (600 MHz, C_6D_6) δ = 13.39 (s, 2H, O*H*), 8.15 (s, 2H, C*H*N), 7.41 (d, *J*=2.5, 2H, Ar*H*), 7.32 (dd, *J*=8.0, 1.6, 3H, Ar*H*), 7.17 (d, *J*=2.6, 3H, Ar*H*), 7.12 (dd, *J*=7.9, 1.3, 2H, Ar*H*), 6.92 (td, *J*=7.6, 1.4, 2H, Ar*H*), 6.88 (m, 6H, Ar*H*), 6.81 (td, *J*=7.6, 1.3, 2H, Ar*H*), 6.73 (dd, *J*=7.9, 1.2, 2H, Ar*H*), 2.24 (s, 12H, ArCH_3), 1.29 (s, 18H, C(CH_3)$_3$) ppm.

Compound 105-a. A scintillation vial equipped with a stirbar was charged with KH (0.006 g, 0.159 mmol, 2 equiv) in THF (1 mL) and cooled in the glovebox cold well. A solution of **104-a** (0.068 g, 0.079 mmol) in THF (2 mL) was also cooled in the cold well. The solution of **104-a** was added and the solution of KH while thawing, and the mixture was stirred at room temperature for 2 h during which time the reaction remained cloudy. The suspension was concentrated *in vacuo* to yield a bright yellow solid. ^{1}H NMR spectroscopy indicated that complete deprotonated was not achieved as evidenced by a phenolic peak in the spectrum, so the solid was resubmitted to the reaction conditions with another equivalent of KH. After an hour of stirring the reaction mixture became homogeneous. The resubmitted reaction was stirred for a total of 14 h and then concentrated *in vacuo* to yield **105-a** as a bright yellow solid. ^{1}H NMR (300 MHz, $CDCl_3$) δ = 8.00 (s, 2H, C*H*N), 7.15 (m, 10H, Ar*H*), 6.99 (d, *J*=2.4, 3H, Ar*H*), 6.89 (t, *J*=7.5, 3H, Ar*H*), 6.77 (dd, *J*=11.8, 7.9, 4H, Ar*H*), 6.67 (d, *J*=2.2, 2H, Ar*H*), 2.15 (s, 6H, ArCH_3), 1.54 (s, 6H, ArCH_3), 1.12 (s, 18H, C(CH_3)$_3$) ppm.

Compound 105-s. A scintillation vial equipped with a stirbar was charged with KH (0.007 g, 0.176 mmol, 2 equiv) in THF (2 mL) and the suspension was frozen in the

glovebox cold well. A solution of **104-s** (0.075 g, 0.088 mmol) in THF (3 mL) was also frozen in the cold well. The solution of **104-s** was added and the solution of KH while thawing, and the mixture was stirred at room temperature for 2 h during which time the reaction became homogeneous. The solution was concentrated *in vacuo* to yield a bright orange yellow solid. Pentane (5 mL) was added to the solid and the suspension was stirred vigorously for several hours. The suspension was then filtered over a fine frit to remove the pentane soluble materials and the desired product was washed through with benzene, leaving excess salts behind. The benzene fraction was frozen and the benzene was lyophilized under vacuum to yield 0.076 g (93 % yield) of clean **105-s** as an orange yellow solid. ^{1}H NMR (300 MHz, C_6D_6) δ = 8.04 (s, 2H, C*H*N), 7.39 (d, *J*=2.5, 2H, Ar*H*), 7.20 (m, 6H, Ar*H*), 6.92 (m, 8H, Ar*H*), 6.83 (t, *J*=7.4, 2H, Ar*H*), 6.67 (t, *J*=7.6, 2H, Ar*H*), 6.35 (d, *J*=7.7, 2H, Ar*H*), 1.99 (s, 12H, ArCH_3), 1.41 (s, 18H, C(CH_3)$_3$) ppm.

Compound 106-a. After the deprotonation of **104-a** with KH, the solid was metallated without further purification and assuming quantitative yield of the deprotonated product. **105-a** (0.079 mmol) in toluene (5 mL) was added dropwise to $TiCl_4(THF)_2$ (0.058 g, 0.174 mmol, 2.2 equiv) in toluene (5 mL) and left stirring at room temperature for 12 h. The reaction was then concentrated *in vacuo* to yield a deep red solid. **106-a** was purified via precipitation from DCM by the addition of hexanes and cooling to –35 °C. The red solid was collected via filtration over a frit. ^{1}H NMR (400 MHz, $CDCl_3$) δ = 8.96 (s, 2H, C*H*N), 7.69 (m, 10H, Ar*H*), 7.50 (m, 2H, Ar*H*), 7.31 (m, 10H, Ar*H*), 2.00 (s, 12H, ArCH_3), 1.42 (s, 18H, C(CH_3)$_3$) ppm.

106-s. $TiCl_4$ (0.008 mL, 0.073 mmol, 2.2 equiv) was added via syringe to **105-s** (0.031 g, 0.033 mmol) in toluene (4 mL) and stirred at room temperature for 12 h. The

reaction was then concentrated *in vacuo* to yield a deep red solid. **106-s** was partially purified by washing over Celite with hexanes and benzene before flushing the desired product through with DCM. The product is partially soluble in benzene, so some material was lost using this method of purification. Other precipitation and recrystallization efforts also proved ineffective for the purification of **106-s**.

Metallation of 104 with $TiBn_4$. A cooled solution of **104** (0.030 g, 0.035 mmol) in toluene (1 mL) was added dropwise to a solution of $TiBn_4$ (0.029 g, 0.070 mmol, 2 equiv) in toluene (1 mL) at –35 °C and the resulting solution was stirred for 1 h covered, and concentrated *in vacuo* to yield a deep red solid. ^{1}H NMR spectroscopy provided evidence that the benzyl-migration product **107** was formed.

Reaction of 106 with benzyl Grignard. A 1 M solution of benzyl Grignard (0.073 mL, 0.073 mmol, 6.3 equiv) was added dropwise to suspension of **106** (0.013 g, 0.012 mmol) in toluene (2 mL) at –35 °C and the resulting solution was stirred for 2 h over which time it became clear and darker red. The reaction mixture was concentrated *in vacuo* to yield a deep red solid. The ^{1}H NMR spectrum of this solid matched that of the above reaction, assigned as **107-a**.

Compound 112. The bisphenoxyimine ligand precursor with aryl-OMe pendant donors, **112**, was synthesized via an imine condensation of aniline **111** with bisaldehyde **6** using literature conditions.[3] Data for **112-a**. ^{1}H NMR (400 MHz, $CDCl_3$) δ = 12.58 (s, 2H, O*H*), 8.56 (s, 2H, C*H*N), 7.41 (dd, *J*=16.7, 8.5, 4H, Ar*H*), 7.32 (d, *J*=7.5, 2H, Ar*H*), 7.29 (s, 4H, Ar*H*), 7.21 (d, *J*=7.4, 2H, Ar*H*), 7.17 (d, *J*=7.6, 2H, Ar*H*), 6.95 (t, *J*=7.4, 2H, Ar*H*), 6.85 (d, *J*=7.9, 2H, Ar*H*), 3.62 (s, 6H, OCH_3), 1.92 (s, 12H, ArCH_3), 1.32 (s, 18H, C(CH_3)$_3$) ppm. Data for **112-s**. ^{1}H NMR (400 MHz, $CDCl_3$) δ = 12.55 (s, 2H, O*H*), 8.56 (s, 2H, C*H*N), 7.41

(m, 4H, Ar*H*), 7.33 (m, 4H, Ar*H*), 7.30 (d, *J*=2.4, 2H, Ar*H*), 7.21 (dt, *J*=5.2, 2.2, 6H, Ar*H*), 6.98 (td, *J*=7.4, 0.8, 2H, Ar*H*), 6.90 (d, *J*=8.2, 2H, Ar*H*), 3.67 (s, 6H, OCH_3), 1.94 (s, 12H, ArCH_3), 1.33 (s, 18H, C(CH_3)$_3$) ppm.

Attempted synthesis of 110. The metallation of **112** with $TiCl_4$ was attempted using conditions analogous to literature.[21] In the glovebox, $TiCl_4$ (0.012 mL, 0.110 mmol, 2.2 equiv) and toluene (0.11 mL) were added to a small Schlenk tube and a syringe was charged with **112** (0.0425 g, 0.050 mmol) in toluene (2 ml). The Schlenk tube and syringe were sealed and brought out of the glovebox. The Schlenk tube was cooled to -78 °C in an isopropanol/dry ice bath and the solution of **112** was added dropwise over 20 minutes. The reaction mixture turned deep red. After 12 hours of stirring, the volatiles were removed *in vacuo*. The residues were brought back into the glovebox and separated into fractions by washing with hexanes, benzene, and DCM over Celite. By ^{1}H NMR spectroscopy this purification method was unsuccessful and actually resulted in decomposition of the major imine-containing product that was observed in the crude ^{1}H NMR spectrum.

Compound 114. **55** (0.30 g, 1.00 mmol) in THF (10 mL) was added dropwise into a solution of **113** (0.50 g, 3.51 mmol, 3.5 equiv) and Hünig's base (0.36 g, 3.51 mmol, 3.5 equiv) in THF (10 mL) and cooled to 0 °C in an ice bath over 5 minutes. Over this time the solution turned cloudy. The reaction was stirred for 2 h at 0 °C and for 2.5 h at room temperature. The reaction mixture was filtered over Celite and volatiles were removed under vacuum to yield a pale yellow oily solid. The solid was washed over silica gel with 2/1 EtOAc/hexanes and then flushed through with 2/1 DCM/MeOH. This second fraction was concentrated *in vacuo* to yield **114** as a nearly colorless oily solid in 66 % yield. ^{1}H NMR

(300 MHz, $CDCl_3$) δ = 7.24 (d, *J*=2.4, 1H, Ar*H*), 6.87 (d, *J*=2.4, 1H, Ar*H*), 3.83 (d, *J*=13.1, 1H, CH_2Ar), 3.60 (d, *J*=13.0, CH_2Ar), 2.96 (m, 2H, CH_2), 2.72 (td, *J*=11.1, 3.5, 2H, CH_2), 2.42 (s, 3H, NCH_3), 2.31 (s, 3H, NCH_3), 2.22 (d, *J*=13.5, 2H, CH_2), 2.04 (m, 2H, CH_2), 1.84 (m, 2H, CH_2), 1.41 (s, 9H, C(CH_3)$_3$), 1.28 (s, 9H, C(CH_3)$_3$) ppm.

Compound 115-a. A solution of **114** (0.10 g, 0.28 mmol, 2.2 equiv) and Hünig's base (0.028 g, 0.28 mmol, 2.2 equiv) in THF (7 mL) was cooled in an ice bath and **51-a** (0.078 g, 0.13 mmol) in THF (6 mL) was added dropwise into the solution over 5 minutes. The mixture was stirred while gradually warming to room temperature over 4 h, filtered over Celite and concentrated *in vacuo*. The solid was washed over silica gel with 5/1 EtOAc/hexanes and concentrated *in vacuo*, after which the product was isolated by column chromatography (1/3 EtOAc/hexanes). ^{1}H NMR (400 MHz, $CDCl_3$) δ = 10.02 (s, 4H, O*H*), 7.20 (m, 2H, Ar*H*), 7.04 (d, *J*=2.0, 2H, Ar*H*), 6.97 (s, 2H, Ar*H*), 6.85 (s, 2H, Ar*H*), 4.15 (d, *J*=7.2, 2H, CH_2Ar), 4.11 (d, *J*=7.2, 2H, CH_2Ar), 3.86 (m, 10H, CH_2), 2.72 (m, 5H, CH_2), 2.27 (s, 12H, NCH_3), 2.07 (s, 3H, ArCH_3), 2.05 (s, 3H, ArCH_3), 1.98 (s, 6H, ArCH_3), 1.78 (d, *J*=11.7, 5H, CH_2), 1.34 (s, 18H, C(CH_3)$_3$), 1.28 (s, 36H, C(CH_3)$_3$) ppm. (Note: peak assignments are tentative).

Compound 115-s. A solution of **114** (0.10 g, 0.28 mmol, 2.2 equiv) and Hünig's base (0.028 g, 0.28 mmol, 2.2 equiv) in THF (7 mL) was cooled in an ice bath and **51-s** (0.078 g, 0.13 mmol) in THF (6 mL) was added dropwise into the solution over 5 minutes. The mixture was stirred while gradually warming to room temperature over 4 h, filtered over Celite, and concentrated *in vacuo*. The solid was washed over silica gel with 5/1 EtOAc/hexanes and concentrated *in vacuo* after which the product was isolated by column chromatography (1/2 EtOAc/hexanes). ^{1}H NMR (400 MHz, $CDCl_3$) δ = 7.19 (bs, 2H,

Ar*H*), 7.07 (bs, 2H, Ar*H*), 6.98 (bs, 2H, Ar*H*), 6.84 (bs, 2H, Ar*H*), 4.13 (m), 3.88 (m, 4H, CH_2Ar), 3.63 (m), 2.65 (m), 2.29 (m), 2.19 (s, 3H, ArCH_3), 2.12 (s, 3H, ArCH_3), 2.02 (s, 6H, ArCH_3), 1.30 (several peaks, 54H, C(CH_3)$_3$) ppm. (Note: peak assignments are tentative).

Attempted synthesis of 116. A solution of **115** (0.030 g, 0.025 mmol) in toluene (1 mL) was cooled to –35 °C and added dropwise to a cooled solution of $ZrBn_4$ (0.023 g, 0.051 mmol, 2 equiv) in toluene (1 mL). The reaction mixture was stirred for 6 h over which time the color lightened from bright yellow to pale yellow. Volatiles were removed under vacuum. The ^{1}H NMR spectra of both the syn and anti atropisomers had broad baselines and indicated complex mixtures that could not be purified by fractionation. The resonances in the ^{1}H NMR spectrum did not sharpen in variable temperature experiments (to -30 °C).

Compounds **51-a**, **52a-OMe-a**, and **52d-OMe-a** were synthesized via the same procedures as for the syn isomer of these complexes. Data for **51-a** are as follows. ^{1}H NMR (300 MHz, $CDCl_3$) δ = 7.34 (d, *J*=2.4, 2H, Ar*H*), 7.02 (d, *J*=2.4, 2H, Ar*H*), 4.82 (s, 2H, O*H*), 4.66 (s, 4H, ArCH_2Br), 1.98 (s, 12H, ArCH_3), 1.33 (s, 18H, C(CH_3)$_3$) ppm. Data for **52a-OMe-a** are as follows. ^{1}H NMR (300 MHz, C_6D_6) δ = 8.56 (bs, 4H, O*H*), 7.24 (d, *J*=2.7, 2H, Ar*H*), 7.21 (d, *J*=2.2, 2H, Ar*H*), 6.65 (d, *J*=2.2, 2H, Ar*H*), 3.56 (s, 4H, CH_2Ar), 3.36 (s, 4H, CH_2Ar), 3.04 (t, *J*=5.1, 4H, CH_2), 2.84 (s, 6H, OCH_3), 2.34 (t, *J*=5.1, 4H, CH_2), 2.17 (s, 12H, ArCH_3), 1.37 (s, 18H, C(CH_3)$_3$) ppm. (Note: additional aryl peak is presumably hidden under the solvent peak at 7.16 ppm). Data for **52d-OMe-a** are as follows. ^{1}H NMR (300 MHz, C_6D_6) δ = 7.31 (multiple peaks, 6H, Ar*H*), 6.82 (two peaks, 4H, Ar*H*), 3.69 (s, 4H, CH_2Ar), 3.65 (s, 4H, CH_2Ar), 3.09 (t, *J*=4.6, 4H, CH_2), 2.84 (s, 6H, OCH_3), 2.46 (t, *J*=5.3, 4H, CH_2), 2.26 (s, 12H, ArCH_2), 1.60 (s, 18H, C(CH_3)$_3$), 1.34 (s, 18H, C(CH_3)$_3$) ppm.

Compound 53a-OMe-a. A solution of **52a-OMe-a** (0.100 g, 0.105 mmol) in toluene (4 mL) was added to a solution of $ZrBn_4$ (0.096 g, 0.209 mmol, 2 equiv) in toluene (4 mL) in a covered 20 mL scintillation vial equipped with a stirbar. The reaction mixture was stirred at room temperature for 2 h at which point the volatiles were removed *in vacuo*. The yellow residue was suspended in 5 mL of hexanes and the volatiles were again removed *in vacuo*. Several successive precipitations from Et_2O yielded 0.045 g of >90 % pure product as yellow solid (28 % yield).

Compound 53d-OMe-a. A solution of **52d-OMe-a** (0.100 g, 0.108 mmol) in toluene (4 mL) was added to a solution of $ZrBn_4$ (0.098 g, 0.215 mmol, 2 equiv) in toluene (4 mL) in a covered 20 mL scintillation vial equipped with a stirbar. The reaction mixture was stirred at room temperature for 2 h at which point the volatiles were removed *in vacuo*. The yellow residue was suspended in 5 mL of hexanes and the volatiles were again removed *in vacuo*. The product was precipitated from Et_2O and collected 0.058 g of yellow solid was collected via filtration (37 % yield).

Compound 117a-OMe. A solution of **52a-OMe** (0.035 g, 0.036 mmol) in toluene (2 mL) was added to a solution of $TiBn_4$ (0.030 g, 0.073 mmol, 2 equiv) in toluene (1 mL) in a covered 20 mL scintillation vial equipped with a stirbar. The reaction mixture was stirred at room temperature for 2 h at which point the volatiles were removed *in vacuo*. The brown residue was suspended in 5 mL of hexanes and the volatiles were again removed *in vacuo*. Purifications by precipitation and recrystallization proved unsuccessful.

Compound 117d-OMe. A solution of **52d-OMe** (0.034 g, 0.036 mmol) in toluene (2 mL) was added to a solution of $TiBn_4$ (0.030 g, 0.073 mmol, 2 equiv) in toluene (1 mL) in a covered 20 mL scintillation vial equipped with a stirbar. The reaction mixture was stirred at room temperature for 2 h at which point the volatiles were removed *in vacuo*. The brown residue was suspended in 5 mL of hexanes and the volatiles were again removed *in vacuo*. Purifications by precipitation and recrystallization proved unsuccessful.

Compound 118. A solution of **7-s** (0.20 g, 0.248 mmol, 1 equiv) in Et_2O (5 mL) and a solution of $NiMe_2$(tmeda) (0.092 g, 0.45 mmol, 1.8 equiv) in Et_2O (4 mL) were cooled in the glovebox freezer to –35 °C. The solution of the ligand precursor was added to the solution of nickel precursor. 2,6-Lutidine (0.58 mL, 4.97 mmol, 20 equiv) was syringed into the mixture causing a color change to reddish orange. The reaction was stirred for 5 h and filtered over Celite. Volatiles were removed under vacuum and the residue was suspended in pentane. After stirring and cooling to –35 °C, the suspension was filtered over Celite and the product was dissolved in Et_2O. Volatiles were removed under vacuum to yield **118** as a bright reddish orange solid (0.130 g, 47 % yield). ^{1}H NMR (300 MHz, $CDCl_3$) δ = 13.40 (s, 1H, O*H*), 8.09 (s, 1H, C*H*N), 7.72 (s, 1H, C*H*N), 7.40 (m, 2H, Ar*H*), 7.28 (d, *J*=2.6, 1H, Ar*H*), 7.19 (m, 6H, Ar*H*), 7.12 (d, *J*=2.6, 1H, Ar*H*), 7.08 (m, 1H, Ar*H*), 6.55 (d, *J*=7.6, 2H, Ar*H*), 4.29 (sept, *J*=6.9, 2H, C*H*(CH_3)$_2$), 3.74 (s, 6H, ArCH_3), 3.18 (sept, *J*=6.9, 2H, C*H*(CH_3)$_2$), 2.06 (s, 6H, ArCH_3), 2.02 (s, 6H, ArCH_3), 1.56 (d, *J*=6.9, 6H, CH(CH_3)$_2$), 1.35 (m, 9H, C(CH_3)$_3$), 1.28 (m, 9H, C(CH_3)$_3$), 1.18 (d, *J*=6.9, 12H, CH(CH_3)$_2$), 1.12 (d, *J*=6.9, 6H, CH(CH_3)$_2$), -1.03 (s, 3H, NiCH_3) ppm.

Compound 119. To monodeprotonate **7-s**, a suspension of KH (0.002 g, 0.050 mmol, 1 equiv) in THF (6 mL) and a solution of **7-s** (0.040 g, 0.050 mmol) in THF (6 mL) were frozen in the cold well. The suspension of KH was added to the solution of **7-s** while thawing, and the mixture was stirred at room temperature for 7 h during which time the reaction became homogeneous. The solution was concentrated *in vacuo* to yield a bright yellow solid. The solid was dissolved in benzene and filtered over Celite to remove any remaining KH and the filtrate was frozen and lyophilized to yield 0.040 g (~80 % purity by ^{1}H NMR spectroscopy, 95 % yield) of **119** as a fluffy yellow powder.

Metallation of 119 with Ti(O^{i}Pr)$_4$. A solution of Ti(O^{i}Pr)$_4$ (0.014 mL, 0.047 mmol, 1 equiv) in THF (2 mL) and a solution of **119** (0.040 g, 0.047 mmol) in THF (2 mL) were frozen in the cold well. The solution of Ti(O^{i}Pr)$_4$ was added to the solution of **119** while thawing, and the mixture was stirred at room temperature for 4 h and then concentrated *in vacuo* to yield a bright yellow residue.

Compound 120. A solution of Ti(O^{i}Pr)$_4$ (0.030 mL, 0.099 mmol, 1 equiv) in THF (4 mL) and a solution of **7-s** (0.080 g, 0.099 mmol) in THF (4 mL) were frozen in the cold well. The solution of Ti(O^{i}Pr)$_4$ was added to the solution of **7-s** while thawing, and the mixture was stirred at room temperature for 4 h and then concentrated *in vacuo*. Pentane (5 mL) was added to the residue and the resulting suspension was again concentrated *in vacuo* to yield a bright yellow solid. ^{1}H NMR (300 MHz, C_6D_6) δ = 13.53 (s, 1H, O*H*), 8.38 (s, 1H, C*H*N), 8.14 (s, 1H, C*H*N), 7.63 (d, *J*=2.6, 1H, Ar*H*), 7.57 (d, *J*=2.5, 1H, Ar*H*), 7.38 (d, *J*=2.4, 1H, Ar*H*), 7.36 (d, *J*=2.6, 1H, Ar*H*), 7.28 (s, 3H, Ar*H*), 7.22 (s, 3H, Ar*H*), 4.75 (sept, *J*=6.1, 3H, OC*H*(CH$_3$)$_2$), 3.62 (sept, *J*=6.7, 2H, C*H*(CH$_3$)$_2$), 3.18 (sept, *J*=6.8, 2H, C*H*(CH$_3$)$_2$), 2.42 (s,

6H, ArCH_3), 2.38 (s, 6H, ArCH_3), 1.39 (s, 9H, C(CH_3)$_3$), 1.32 (s, 9H, C(CH_3)$_3$), 1.24 (d, J=6.1, 24H, CH(CH_3)$_2$), 1.20 (d, J=6.8, 18H, OCH(CH_3)$_2$) ppm.

Attempted deprotonation of 120. A suspension of KH (0.001 g, 0.021 mmol, 1 equiv) in THF (2 mL) and a solution of **120** (0.022 g, 0.021 mmol) in THF (1 mL) were frozen in the cold well. The suspension of KH was added to the solution of **120** while thawing, and the mixture was stirred at room temperature for 20 h and then concentrated *in vacuo* to yield a bright yellow residue.

Metallation of 120 with $TiCl_2(NMe_2)_2$. A solution of $TiCl_2(NMe_2)_2$ (0.004 g, 0.019 mmol, 0.5 equiv) in THF (2 mL) and a solution of **120** (0.040 g, 0.039 mmol) in THF (3 mL) were cooled to –35 °C. The solution of $TiCl_2(NMe_2)_2$ was added to the solution of **120**, and the mixture was stirred at room temperature for 3 h, during which time it turned from orange red to golden yellow. The solution was concentrated *in vacuo*. ^{1}H NMR spectroscopy indicated no remaining $TiCl_2(NMe_2)_2$, and that the majority of the material was still **120**. An excess of $TiCl_2(NMe_2)_2$ (about 2 equivalents) in THF was added to the material and the mixture was stirred at ambient temperature for another 36 h before being again concentrated *in vacuo*. The ^{1}H NMR spectrum at this point showed no **120** and no phenolic peaks.

Metallation of 120 with $NiMe_2$(tmeda) in the presence of excess pyridine. A solution of $NiMe_2$(tmeda) (0.010 g, 0.047 mmol, 1.2 equiv) and Et_2O (2 mL) and a solution of **120** (0.040 g, 0.039 mmol) in THF (2 mL) were cooled to –35 °C. The solution of **120** was added to the solution of $NiMe_2$(tmeda), and pyridine (0.03 mL, 0.389 mmol, 10 equiv) was syringed into the reaction. The mixture was stirred at room temperature for 3 h, during which time it turned red. The solution was concentrated *in*

vacuo. ^{1}H NMR spectroscopy indicated a significant amount of $NiMe_2$(tmeda) and **120** were both still present. Another 0.04 mL of pyridine and 4 mL of Et_2O were added to the material, and the mixture was stirred at ambient temperature for another 36 h before being filtered over Celite and concentrated *in vacuo*.

General polymerization procedures

The setup of all the polymerizations was conducted in a nitrogen atmosphere glovebox.

Ethylene polymerizations. A 3 oz. Andrews glass pressure reaction vessel equipped with Swagelok valves and a gauge was used for all high pressure polymerizations. The high-pressure setup was brought into the glovebox with a magnetic stirbar and charged with the desired amounts of solvent and comonomer. A syringe was loaded with a solution of complex and activator and the needle was sealed with a rubber septum. The syringe and setup were brought out of the box and the setup was clamped firmly over a hot plate with a mineral oil bath previously regulated to to 25 °C or 20 °C or an ice bath at 0 °C. The solution was stirred vigorously (1200 rpm). A nylon core hose equipped with quick connect adaptors was purged with ethylene for 1 minute and the pressure was set to 15 psig. The hose was connected to the setup and the setup was filled with ethylene. A bleed needle was inserted into a Teflon septum at the top of the high pressure setup and flushed with ethylene. The solution of nickel or titanium complex was added via syringe and the top of the setup was closed. The pressure was increased to the desired level. After the desired time, the ethylene hose was disconnected, the setup was vented and the reaction mixture was quenched with acidified methanol (3 times the reaction volume) to precipitate the polymer, which was

collected as a white solid by filtration over a fine frit. If only a small amount of polymer was precipitated, the entire mixture was collected and volatile materials were removed under vacuum. All polymers were dried on the Schlenk line for a minimum of 8 hours before a mass was recorded.

1-Hexene polymerizations. In the glovebox, the desired organometallic complex was added to a Schlenk tube equipped with a stirbar with one half of the solvent, or in cases where no solvent was used, with one half of the monomer. The activator was dissolved in the remaining solvent or monomer. The 1-hexene and any comonomer or additive were added to the Schlenk tube. The solution of activator was added and the timer for the polymerization was started upon addition. The Schlenk tube was sealed and brought out of the glovebox. After stirring the reaction for the appointed amount of time, the reaction was opened to air and quenched with 5 mL of hexanes and 0.5 mL of MeOH. The quenched reaction was filtered over Celite and washed with additional hexanes. The filtrate was transferred to a tared flask and volatiles were removed on the Schlenk line at 100 °C overnight.

Polymer characterization methods

NMR. All polymer NMR spectra were recorded on a Varian-INOVA 500 MHz NMR instrument. ^{1}H and ^{13}C NMR spectra of 1-hexene homopolymers were taken in $CDCl_3$ at room temperature. 1-Hexene ^{13}C NMR spectra were assigned according to literature.[61-62] ^{1}H and ^{13}C NMR spectra of ethylene homopolymers were taken in $C_2D_2Cl_4$ at 130 °C. The ethylene peaks were assigned according to literature.[63-65]

GPC. Poly(1-hexene) molecular weights were determined utilizing THF as the eluent by multi-angle laser light scattering (MALLS) gel permeation chromatography

(GPC) using a miniDAWN TREOS light scattering detector, a Viscostar viscometer, and an OptilabRex refractive index detector, all from Wyatt Technology. An Agilent 1200 UV-Vis detector was also present in the detector stack. Absolute molecular weights were determined using dn/dc values calculated by assuming 100% mass recovery of the polymer sample injected into the GPC.

Representative ^{1}H and ^{13}C NMR spectra of polymers

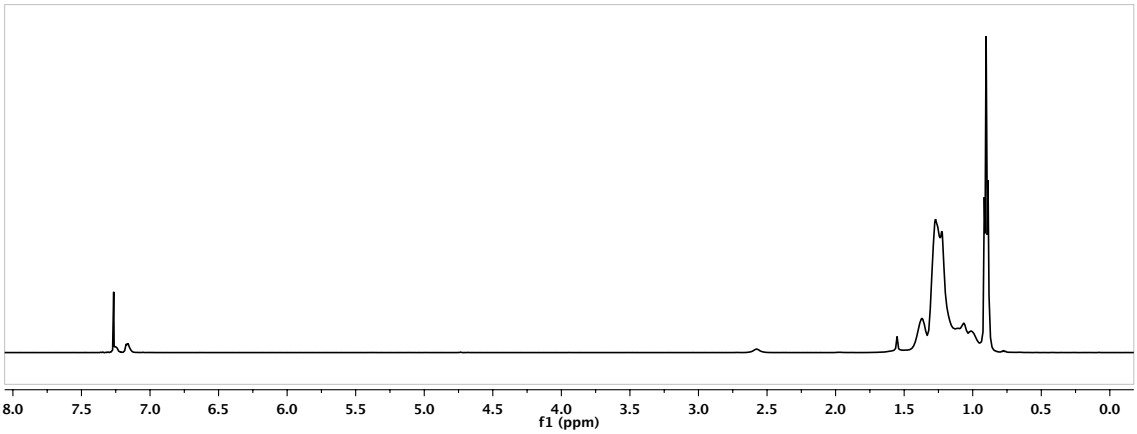

Figure B.3. ^{1}H NMR spectrum of the 1-hexene/4-phenyl-1-butene copolymer synthesized with **57-NMe$_2$**.

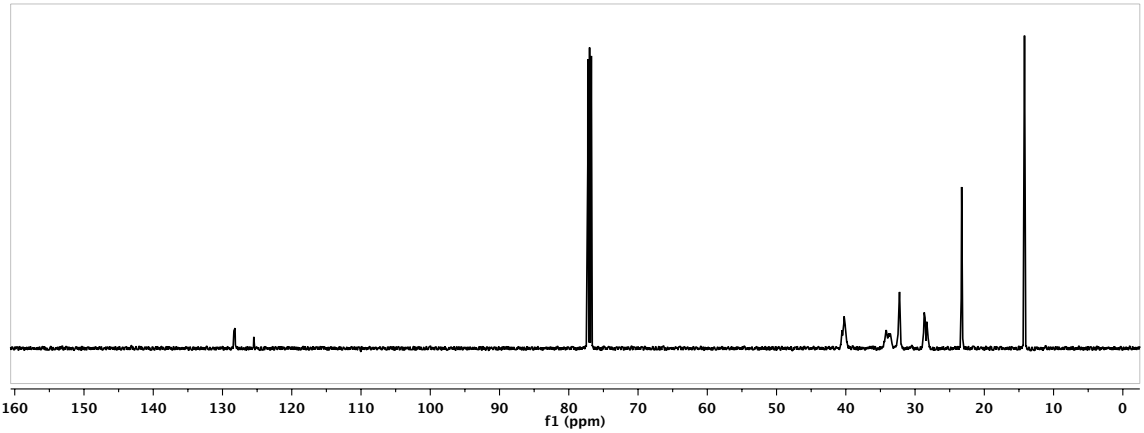

Figure B.4. ^{13}C NMR spectrum of the 1-hexene/4-phenyl-1-butene copolymer synthesized with **57-NMe$_2$**.

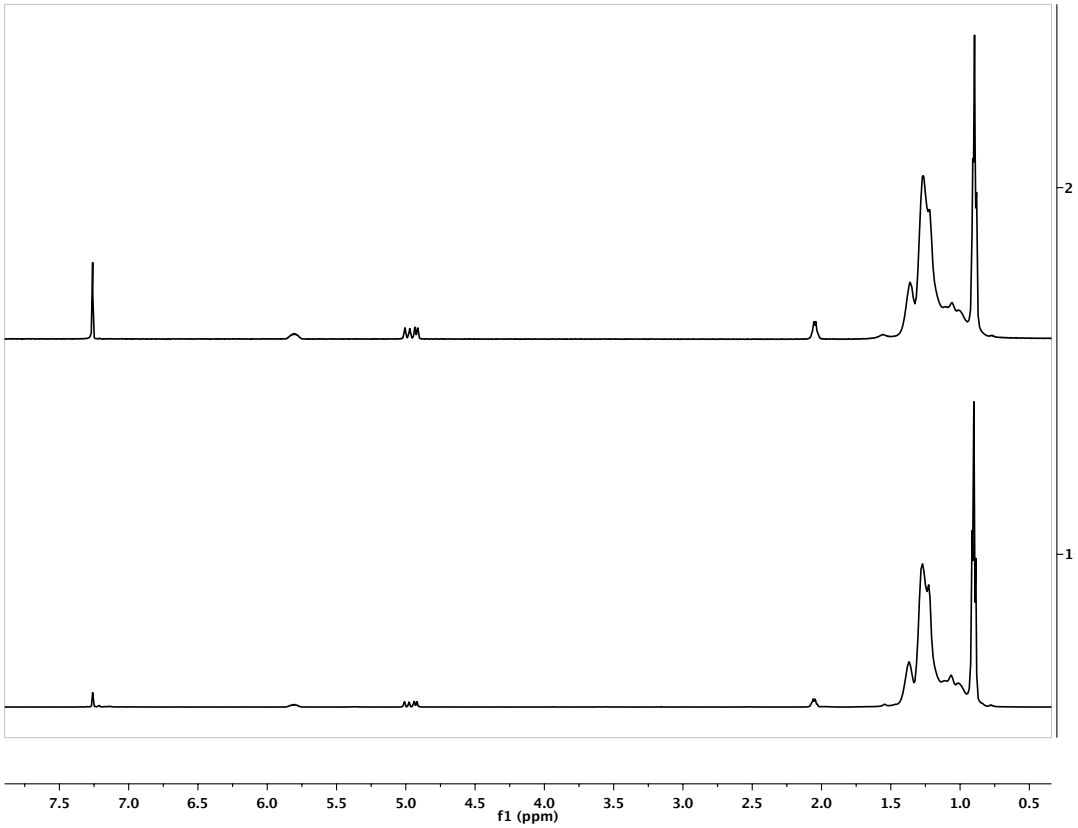

Figure B.5. ^{1}H NMR spectra of the 1-hexene/1,7-octadiene copolymers synthesized with **54-OMe** (below) and **57-NMe$_2$** (above).

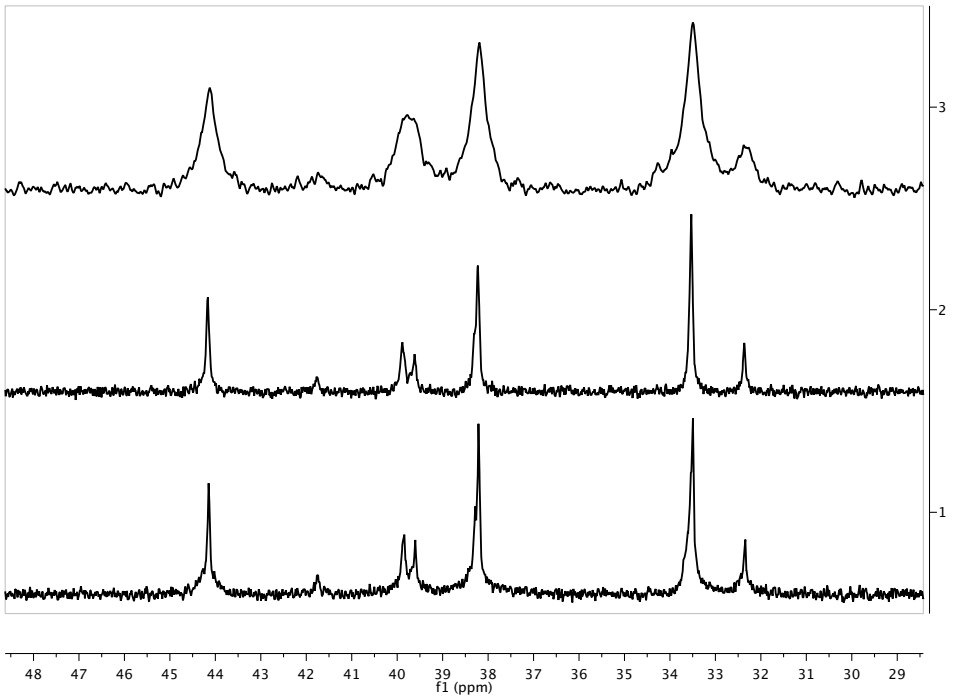

Figure B.6. ^{13}C NMR spectra of cyclopolymerized 1,5-hexadiene synthesized with (from bottom to top) **57-NMe$_2$** (1), **53a-NMe$_2$** (2) and **53a-OMe** (3).

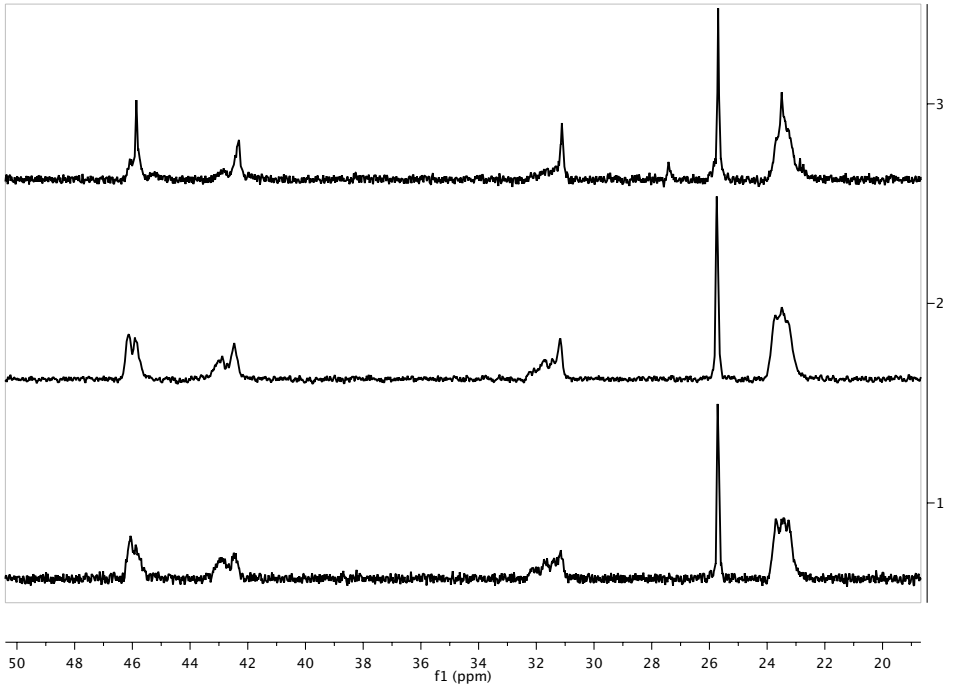

Figure B.7. ^{13}C NMR spectra of 4-methyl-1-pentene homopolymers synthesized with (from bottom to top) **57-NMe$_2$** (1), **53a-NMe$_2$** (2) and **53a-OMe** (3).

Crystallographic Information

Table B.6. Crystal and refinement data for complexes **98-a** and **98-s**.

	98-a	**98-s**
CCDC #	980729	980730
empirical formula	$C_{74}H_{112}N_2O_8Ti_2$	$C_{74}H_{112}N_2O_8Ti_2$
formula wt	1253.45	1253.45
T (K)	100	100
a, Å	30.009(1)	10.7773(5)
b, Å	16.8027(8)	19.410(1)
c, Å	16.0279(7)	20.308(1)
α, deg	90	60.723(3)
β, deg	111.444(2)	83.895(3)
γ, deg	90	90.242(3)
V, Å^3	7522.3(6)	3676.7(3)
Z	4	2
cryst syst	monoclinic	triclinic
space group	C 1 2/c 1	P -1
d_{calcd}, g/cm^3	1.107	1.132
θ range, deg	1.8 to 29.5	1.9 to 25.0
μ, mm^{-1}	0.26	0.27
abs cor	Semi-empirical from equivalents	Semi-empirical from equivalents
GOF	1.49	1.08
R1,[a] wR2[b] (I > 2θ (I))	R1 = 0.0763, wR2 = 0.1410	R1 = 0.0845, wR2 = 0.2296

[a] $R_1 = \sum||F_o| - |F_c||/\sum|F_o|$. [b] $wR_2 = [\sum[w(F_o^2-F_c^2)^2]/\sum[w(F_o^2)^2]]^{1/2}$.

REFERENCES

1. Radlauer, M.; Day, M. W.; Agapie, T. *J. Am. Chem. Soc.* **2012**, *134*, 1478-1481.
2. Radlauer, M. R.; Buckley, A. K.; Henling, L. M.; Agapie, T. *J. Am. Chem. Soc.* **2013**, *135*, 3784-3787.
3. Radlauer, M. R.; Day, M. W.; Agapie, T. *Organometallics* **2012**, *31*, 2231-2243.
4. Wehrmann, P.; Zuideveld, M.; Thomann, R.; Mecking, S. *Macromolecules* **2006**, *39*, 5995-6002.
5. Connor, E. F.; Younkin, T. R.; Henderson, J. I.; Hwang, S. J.; Grubbs, R. H.; Roberts, W. P.; Litzau, J. J. *J. Polym. Sci., Part A: Polym. Chem.* **2002**, *40*, 2842-2854.
6. Reybuck, S. E.; Lincoln, A. L.; Ma, S. D.; Waymouth, R. M. *Macromolecules* **2005**, *38*, 2552-2558.
7. Wang, C.; Ma, Z.; Sun, X.-L.; Gao, Y.; Guo, Y.-H.; Tang, Y.; Shi, L.-P. *Organometallics* **2006**, *25*, 3259-3266.
8. Makio, H.; Terao, H.; Iwashita, A.; Fujita, T. *Chem. Rev.* **2011**, *111*, 2363-2449.
9. Gendler, S.; Zelikoff, A. L.; Kopilov, J.; Goldberg, I.; Kol, M. *J. Am. Chem. Soc.* **2008**, *130*, 2144-2145.
10. Gendler, S.; Groysman, S.; Goldschmidt, Z.; Shuster, M.; Kol, M. *J. Polym. Sci., Part A: Polym. Chem.* **2006**, *44*, 1136-1146.
11. Pennington, D. A.; Clegg, W.; Coles, S. J.; Harrington, R. W.; Hursthouse, M. B.; Hughes, D. L.; Light, M. E.; Schormann, M.; Bochmann, M.; Lancaster, S. J. *Dalton Trans.* **2005**, 561-571.
12. Pennington, D. A.; Hughes, D. L.; Bochmann, M.; Lancaster, S. J. *Dalton Trans.* **2003**, 3480-3482.
13. Salata, M. R.; Marks, T. J. *J. Am. Chem. Soc.* **2008**, *130*, 12-13.
14. Salata, M. R.; Marks, T. J. *Macromolecules* **2009**, *42*, 1920-1933.
15. Makio, H.; Terao, H.; Iwashita, A.; Fujita, T. *Chem. Rev.* **2011**, *111*, 2363-2449.
16. Jia, A.-Q.; Jin, G.-X. *Organometallics* **2009**, *28*, 1872-1877.
17. Gao, M.; Wang, C.; Sun, X.; Qian, C.; Ma, Z.; Bu, S.; Tang, Y.; Xie, Z. *Macromol. Rapid Commun.* **2007**, *28*, 1511-1516.
18. Gao, M.-L.; Gu, Y.-F.; Wang, C.; Yao, X.-L.; Sun, X.-L.; Li, C.-F.; Qian, C.-T.; Liu, B.; Ma, Z.; Tang, Y.; Xie, Z.; Bu, S.-Z.; Gao, Y. *J. Mol. Catal. A: Chem.* **2008**, *292*, 62-66.
19. Gao, M.-L.; Sun, X.-L.; Gu, Y.-F.; Yao, X.-L.; Li, C.-F.; Bai, J.-Y.; Wang, C.; Ma, Z.; Tang, Y.; Xie, Z.; Bu, S.-Z.; Qian, C. *J. Polym. Sci., Part A: Polym. Chem.* **2008**, *46*, 2807-2819.
20. Wang, C.; Sun, X. L.; Guo, Y. H.; Gao, Y.; Liu, B.; Ma, Z.; Xia, W.; Shi, L. P.; Tang, Y. *Macromol. Rapid Commun.* **2005**, *26*, 1609-1614.

21. Suzuki, Y.; Kinoshita, S.; Shibahara, A.; Ishii, S.; Kawamura, K.; Inoue, Y.; Fujita, T. *Organometallics* **2010**, *29*, 2394-2396.

22. Golisz, S. R.; Bercaw, J. E. *Macromolecules* **2009**, *42*, 8751-8762.

23. Sauer, A.; Kapelski, A.; Fliedel, C.; Dagorne, S.; Kol, M.; Okuda, J. *Dalton Trans.* **2013**, *42*, 9007-9023.

24. Cariou, R.; Gibson, V. C.; Tomov, A. K.; White, A. J. P. *J. Organomet. Chem.* **2009**, *694*, 703-716.

25. Giannini, L.; Solari, E.; Deangelis, S.; Ward, T. R.; Floriani, C.; Chiesivilla, A.; Rizzoli, C. *J. Am. Chem. Soc.* **1995**, *117*, 5801-5811.

26. Tshuva, E. Y.; Versano, M.; Goldberg, I.; Kol, M.; Weitman, H.; Goldschmidt, Z. *Inorg. Chem. Commun.* **1999**, *2*, 371-373.

27. Steelman, D. K.; Xiong, S.; Pletcher, P. D.; Smith, E.; Switzer, J. M.; Medvedev, G. A.; Delgass, W. N.; Caruthers, J. M.; Abu-Omar, M. M. *J. Am. Chem. Soc.* **2013**, *135*, 6280-6288.

28. Groysman, S.; Tshuva, E. Y.; Goldberg, I.; Kol, M.; Goldschmidt, Z.; Shuster, M. *Organometallics* **2004**, *23*, 5291-5299.

29. Groysman, S.; Goldberg, I.; Kol, M.; Genizi, E.; Goldschmidt, Z. *Inorg. Chim. Acta* **2003**, *345*, 137-144.

30. Groysman, S.; Goldberg, I.; Kol, M.; Genizi, E.; Goldschmidt, Z. *Organometallics* **2003**, *22*, 3013-3015.

31. Tshuva, E. Y.; Groysman, S.; Goldberg, I.; Kol, M.; Goldschmidt, Z. *Organometallics* **2002**, *21*, 662-670.

32. Tshuva, E. Y.; Goldberg, I.; Kol, M.; Goldschmidt, Z. *Organometallics* **2001**, *20*, 3017-3028.

33. Tshuva, E. Y.; Goldberg, I.; Kol, M.; Goldschmidt, Z. *Chem. Commun.* **2001**, 2120-2121.

34. Tshuva, E. Y.; Goldberg, I.; Kol, M.; Goldschmidt, Z. *Inorg. Chem.* **2001**, *40*, 4263-4270.

35. Tshuva, E. Y.; Goldberg, I.; Kol, M.; Weitman, H.; Goldschmidt, Z. *Chem. Commun.* **2000**, 379-380.

36. Tshuva, E. Y.; Goldberg, I.; Kol, M.; Goldschmidt, Z. *Inorg. Chem. Commun.* **2000**, *3*, 611-614.

37. Groysman, S.; Tshuva, E. Y.; Reshef, D.; Gendler, S.; Goldberg, I.; Kol, M.; Goldschmidt, Z.; Shuster, M.; Lidor, G. *Isr. J. Chem.* **2002**, *42*, 373-381.

38. Tshuva, E. Y.; Goldberg, I.; Kol, M. *J. Am. Chem. Soc.* **2000**, *122*, 10706-10707.

39. Cohen, A.; Kopilov, J.; Lamberti, M.; Venditto, V.; Kol, M. *Macromolecules* **2010**, *43*, 1689-1691.

40. Segal, S.; Yeori, A.; Shuster, M.; Rosenberg, Y.; Kol, M. *Macromolecules* **2008**, *41*, 1612-1617.
41. Yeori, A.; Goldberg, I.; Kol, M. *Macromolecules* **2007**, *40*, 8521-8523.
42. Yeori, A.; Goldberg, I.; Shuster, M.; Kol, M. *J. Am. Chem. Soc.* **2006**, *128*, 13062-13063.
43. Busico, V.; Cipullo, R.; Friederichs, N.; Ronca, S.; Togrou, M. *Macromolecules* **2003**, *36*, 3806-3808.
44. Busico, V.; Cipullo, R.; Ronca, S.; Budzelaar, P. H. M. *Macromol. Rapid Commun.* **2001**, *22*, 1405-1410.
45. Segal, S.; Goldberg, I.; Kol, M. *Organometallics* **2005**, *24*, 200-202.
46. Busico, V.; Cipullo, R.; Pellecchia, R.; Ronca, S.; Roviello, G.; Talarico, G. *Proc. Natl. Acad. Sci. U.S.A.* **2006**, *103*, 15321-15326.
47. Cohen, A.; Coates, G. W.; Kol, M. *J. Polym. Sci., Part A: Polym. Chem.* **2013**, *51*, 593-600.
48. Cohen, A.; Kopilov, J.; Goldberg, I.; Kol, M. *Organometallics* **2009**, *28*, 1391-1405.
49. Cohen, A.; Yeori, A.; Kopilov, J.; Goldberg, I.; Kol, M. *Chem. Commun.* **2008**, 2149-2151.
50. Klein, H.; Steinmetz, A. *Tetrahedron Letters* **1975**, *16*, 4249-4250.
51. Pangborn, A. B.; Giardello, M. A.; Grubbs, R. H.; Rosen, R. K.; Timmers, F. J. *Organometallics* **1996**, *15*, 1518-1520.
52. Terao, H.; Ishii, S.; Mitani, M.; Tanaka, H.; Fujita, T. *J. Am. Chem. Soc.* **2008**, *130*, 17636-17637.
53. Kamigaito, M.; Sawamoto, M.; Higashimura, T. *Macromolecules* **1995**, *28*, 5671-5675.
54. Hamaed, A.; Trudeau, M.; Antonelli, D. M. *J. Am. Chem. Soc.* **2008**, *130*, 6992-6999.
55. Manzer, L. E. *Inorg. Synth.* **1982**, *21*, 135-140.
56. Stead, D.; O'Brien, P.; Sanderson, A. *Org. Lett.* **2008**, *10*, 1409-1412.
57. Kataoka, K.; Yanagi, M.; Katagiri, T. *CrystEngComm* **2011**, *13*, 6342-6344.
58. Covert, K. J.; Mayol, A. R.; Wolczanski, P. T. *Inorg. Chim. Acta* **1997**, *263*, 263-278.
59. Rong, Y.; Al-Harbi, A.; Parkin, G. *Organometallics* **2012**, *31*, 8208-8217.
60. Ahmad, S.; Dey, S. S.; Jousseaume, B.; Toupance, T. *Dalton Trans.* **2011**, *40*, 457-462.
61. Asakura, T.; Demura, M.; Nishiyama, Y. *Macromolecules* **1991**, *24*, 2334-2340.
62. Galland, G. B.; Da Silva, L. F.; Nicolini, A. *J. Polym. Sci., Part A: Polym. Chem.* **2005**, *43*, 4744-4753.
63. Crompton, T. R. *Analysis of Polymers: An Intoduction*; Pargamon Press, 1989.
64. Axelson, D. E.; Levy, G. C.; Mandelkern, L. *Macromolecules* **1979**, *12*, 41-52.

65. De Pooter, M.; Smith, P. B.; Dohrer, K. K.; Bennett, K. F.; Meadows, M. D.; Smith, C. G.; Schouwenaars, H. P.; Geerards, R. A. *Journal of Applied Polymer Science* **1991**, *42*, 399-408.

APPENDIX C

NMR SPECTRA

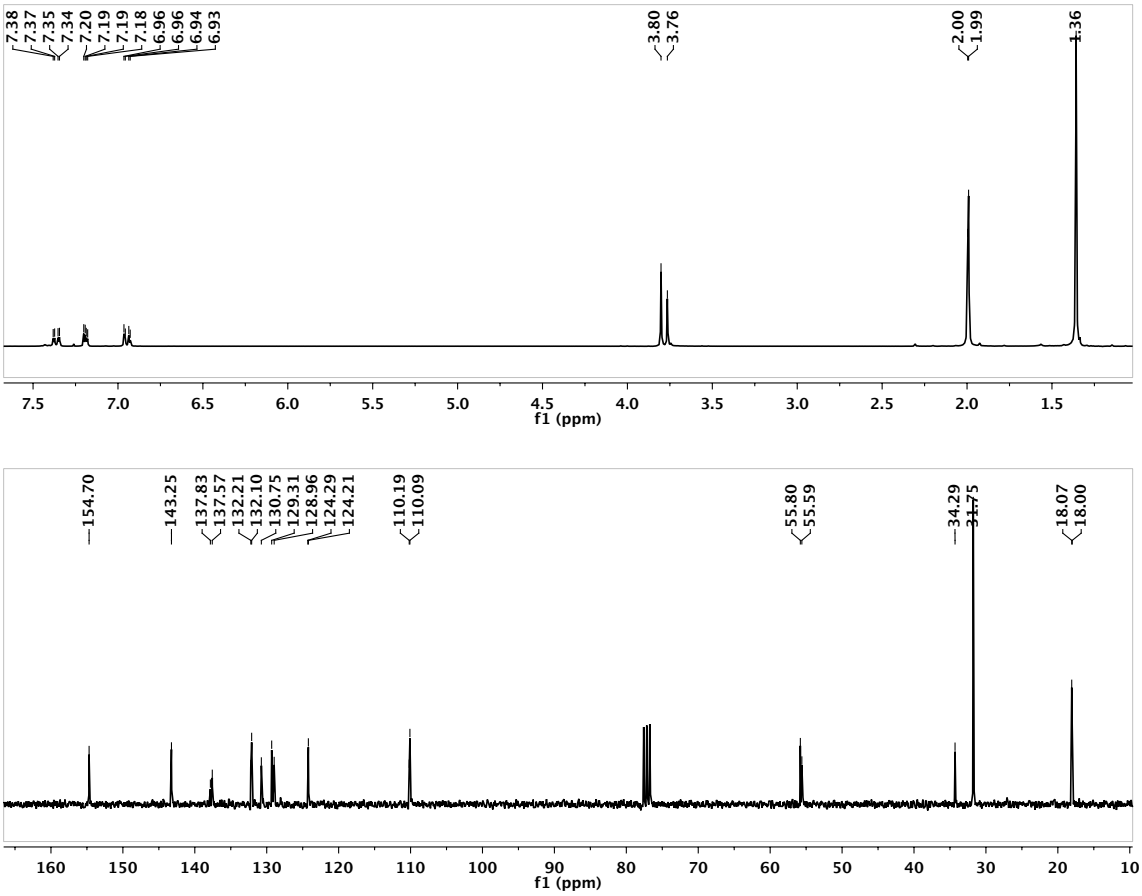

Figure C.1. ^{1}H (above) and ^{13}C (below) NMR spectra of compounds **3** in $CDCl_3$.

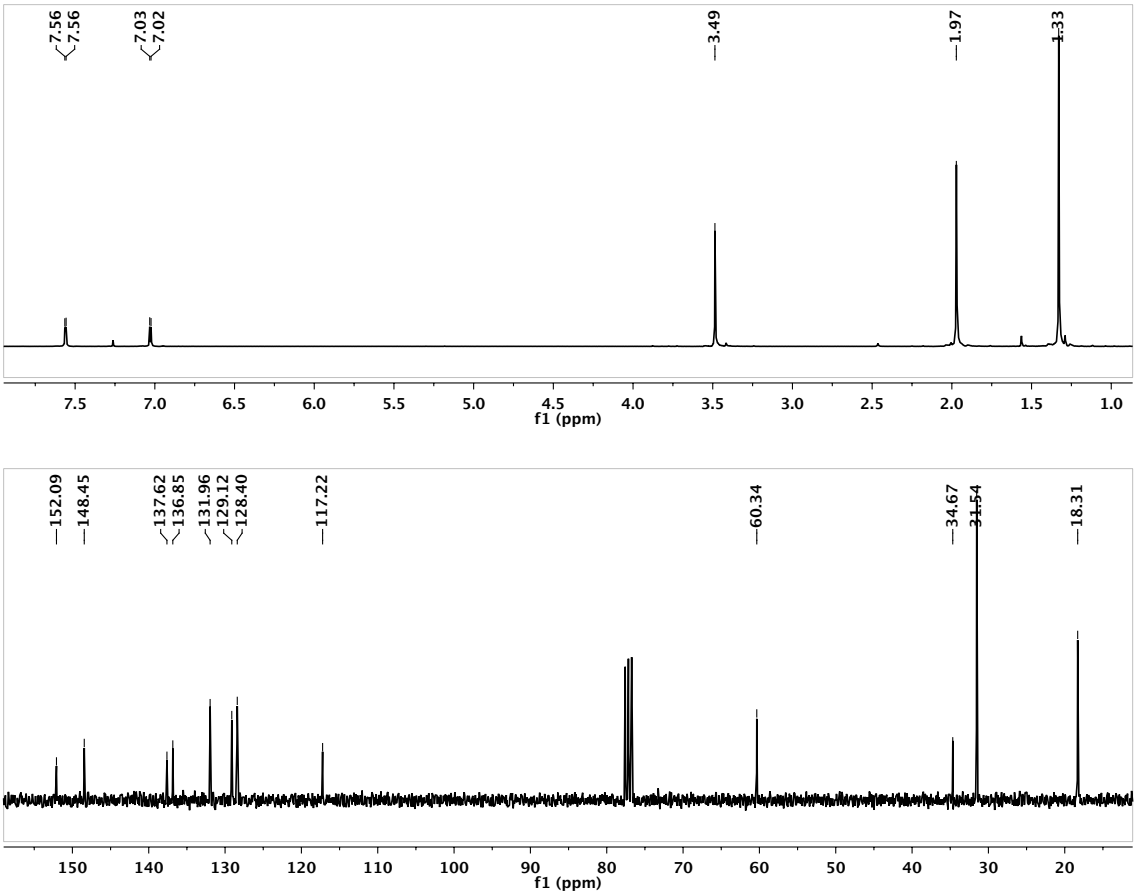

Figure C.2. ^{1}H (above) and ^{13}C (below) NMR spectra of compound **4-a** in $CDCl_3$.

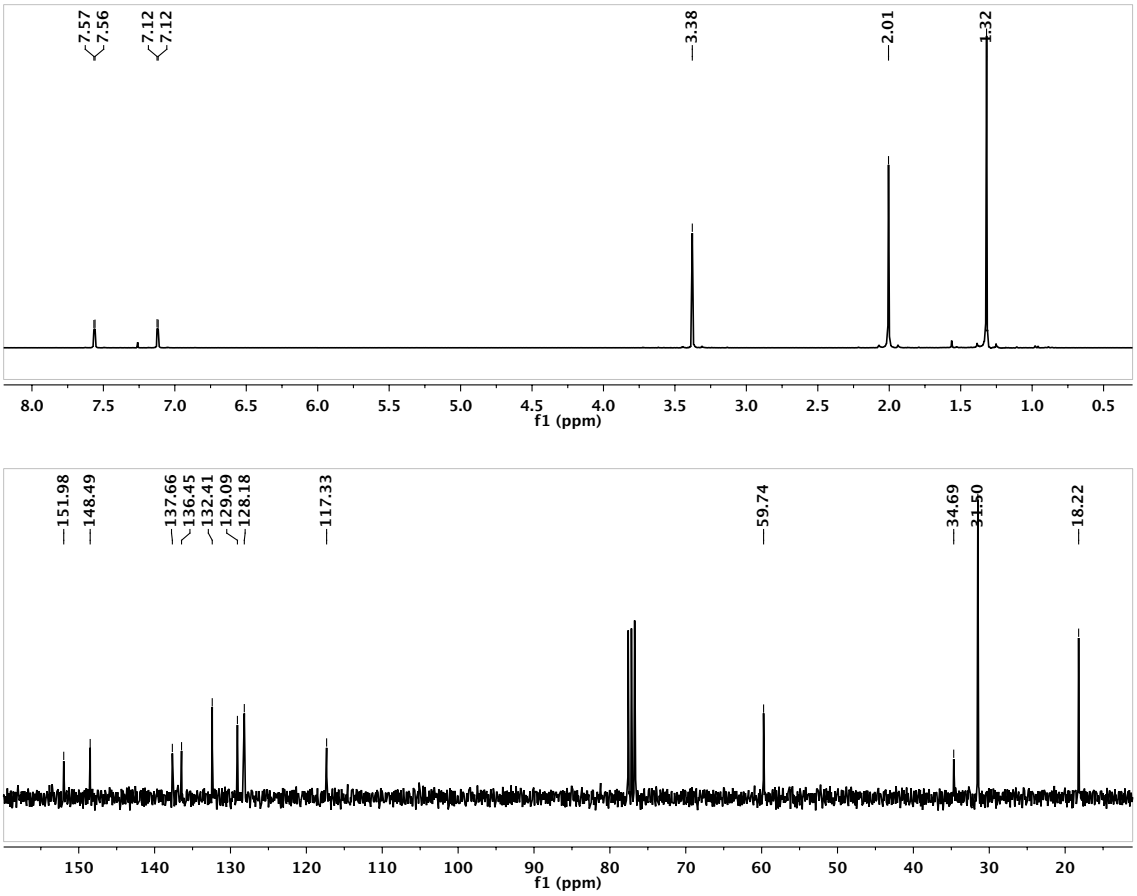

Figure C.3. ^{1}H (above) and ^{13}C (below) NMR spectra of compound **4-s** in $CDCl_3$.

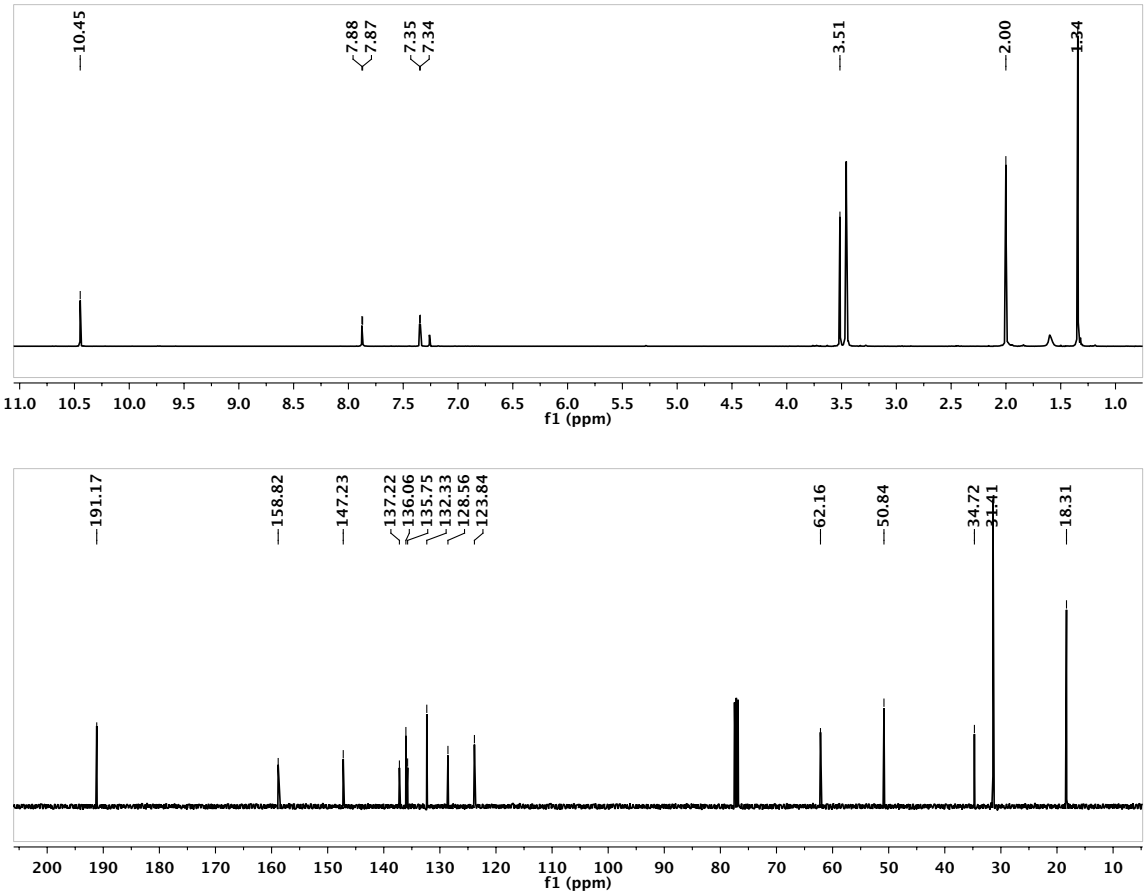

Figure C.4. ^{1}H (above) and ^{13}C (below) NMR spectra of compound **5-a** in $CDCl_3$.

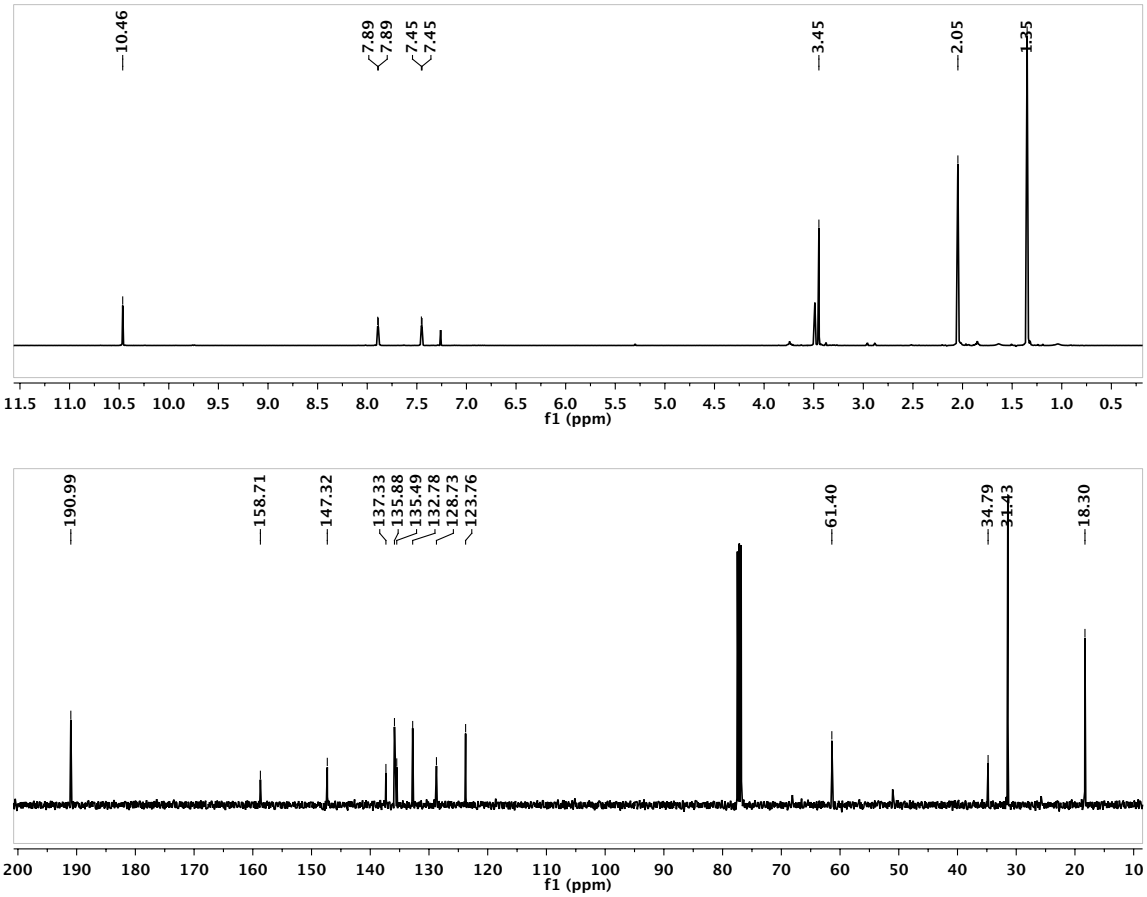

Figure C.5. ^{1}H (above) and ^{13}C (below) NMR spectra of compound **5-s** in $CDCl_3$.

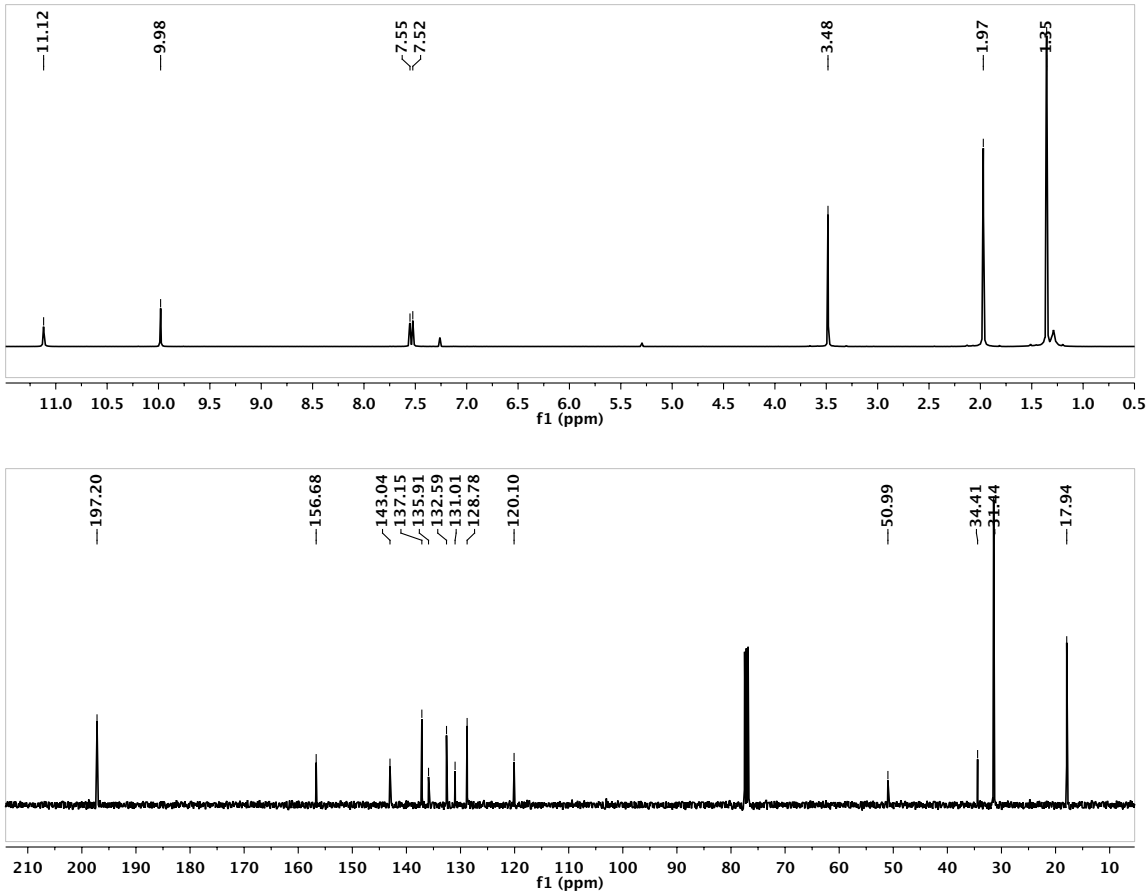

Figure C.6. ^{1}H (above) and ^{13}C (below) NMR spectra of compound **6-a** in $CDCl_3$.

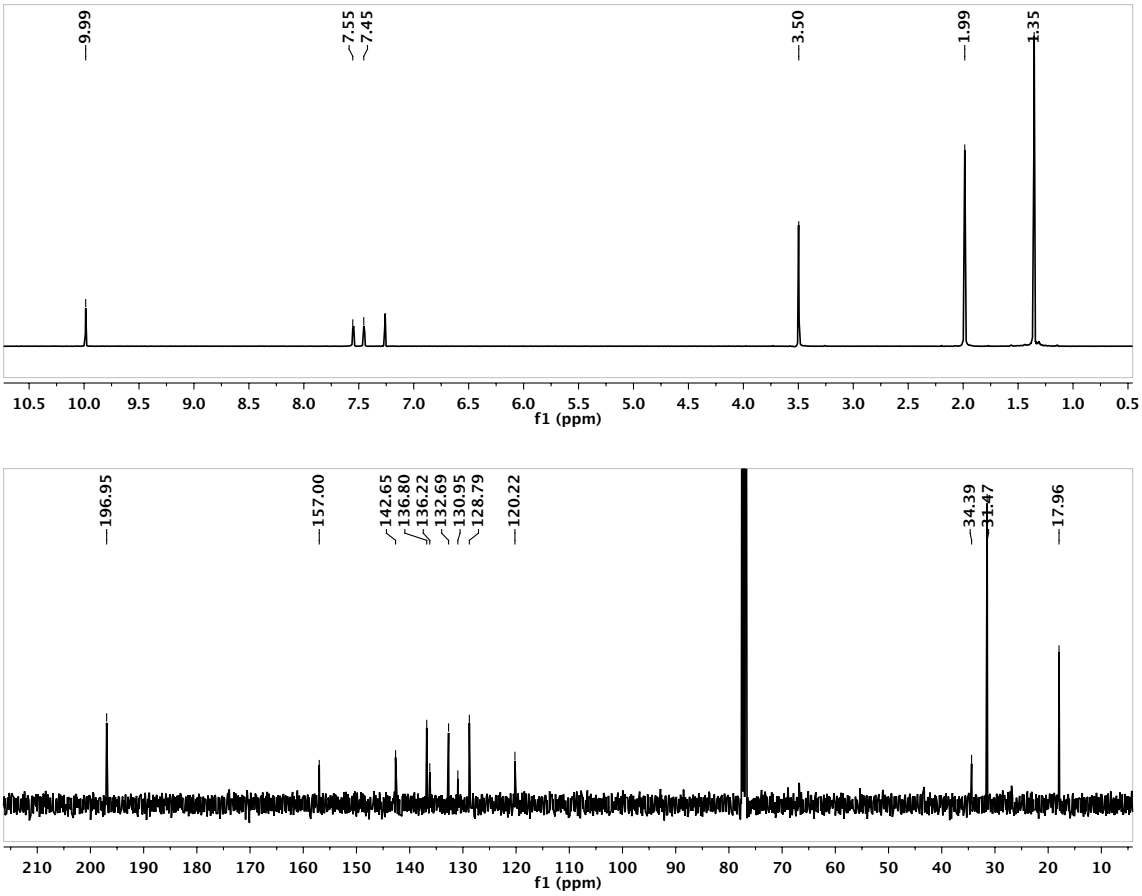

Figure C.7. ^{1}H (above) and ^{13}C (below) NMR spectra of compound **6-s** in $CDCl_3$.

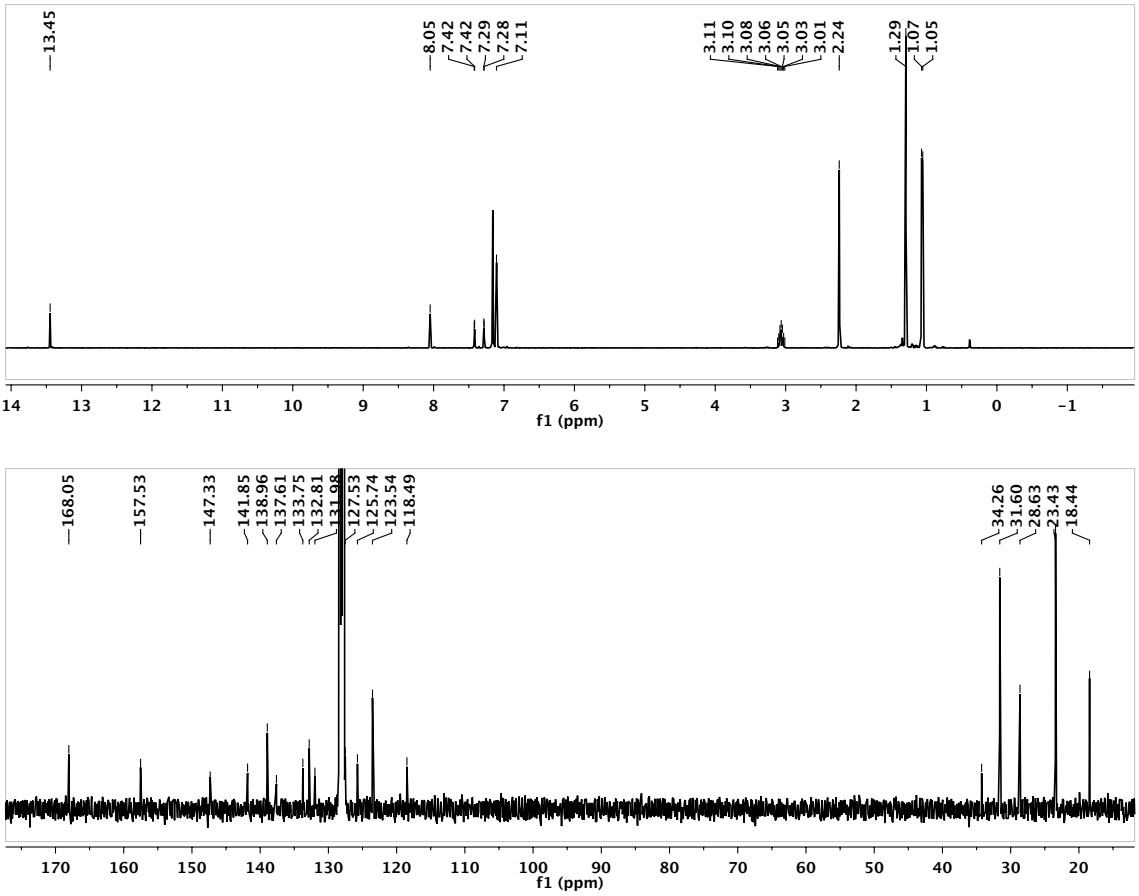

Figure C.8. ^{1}H (above) and ^{13}C (below) NMR spectra of compound **7-a** in C_6D_6.

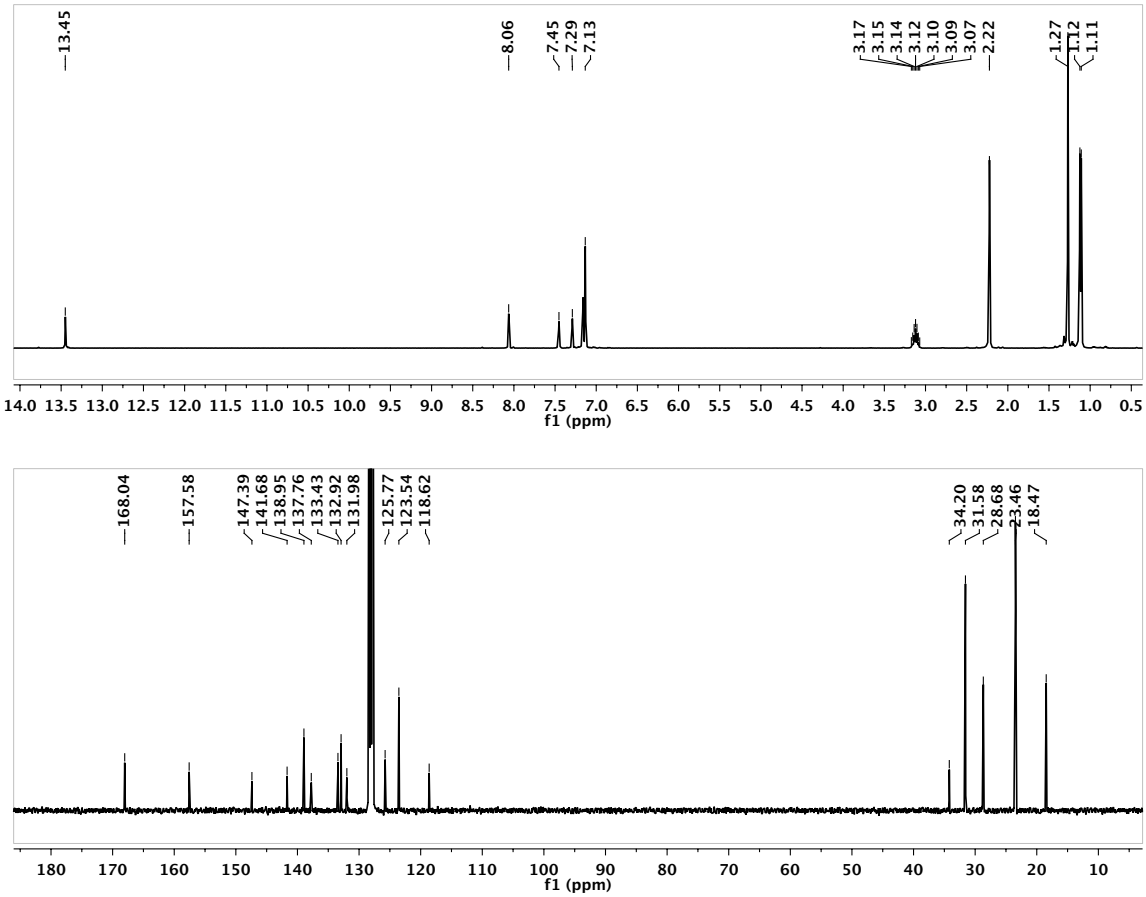

Figure C.9. ^{1}H (above) and ^{13}C (below) NMR spectra of compound **7-s** in C_6D_6.

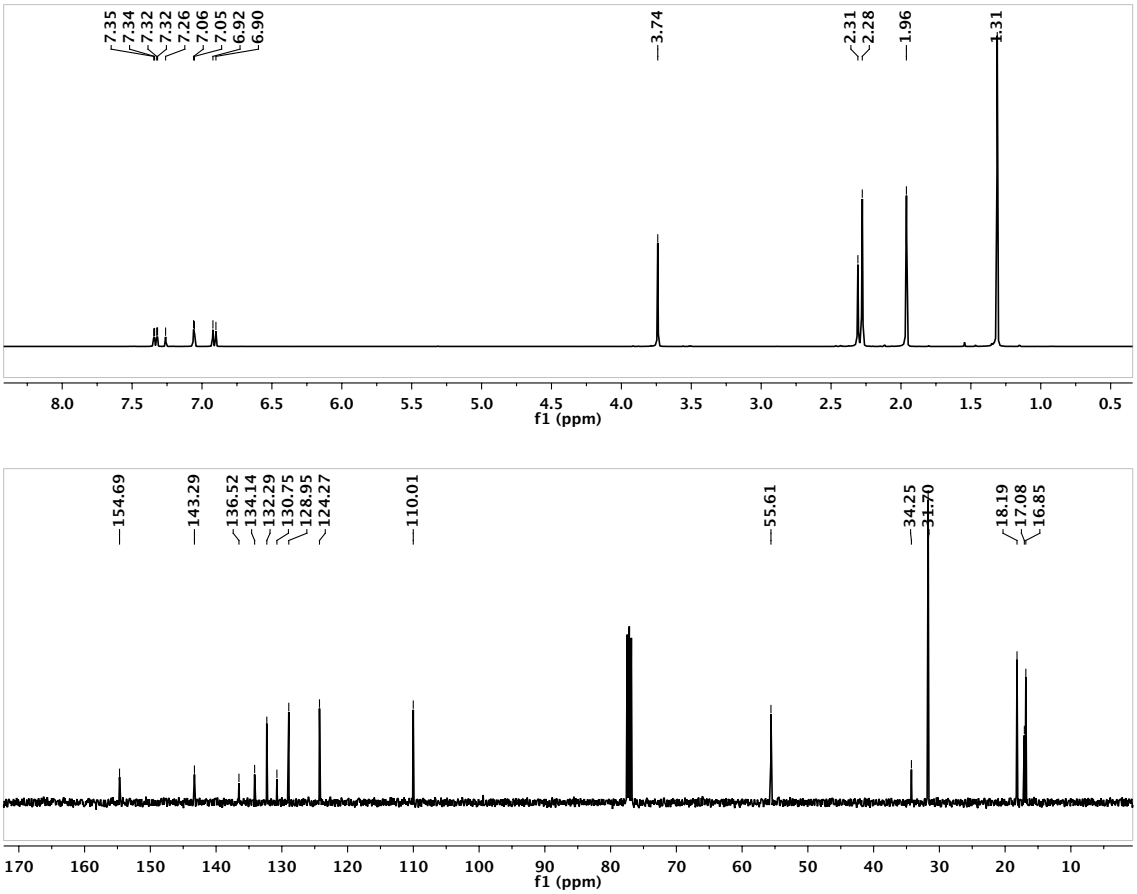

Figure C.10. ^{1}H (above) and ^{13}C (below) NMR spectra of compound **9** in $CDCl_3$.

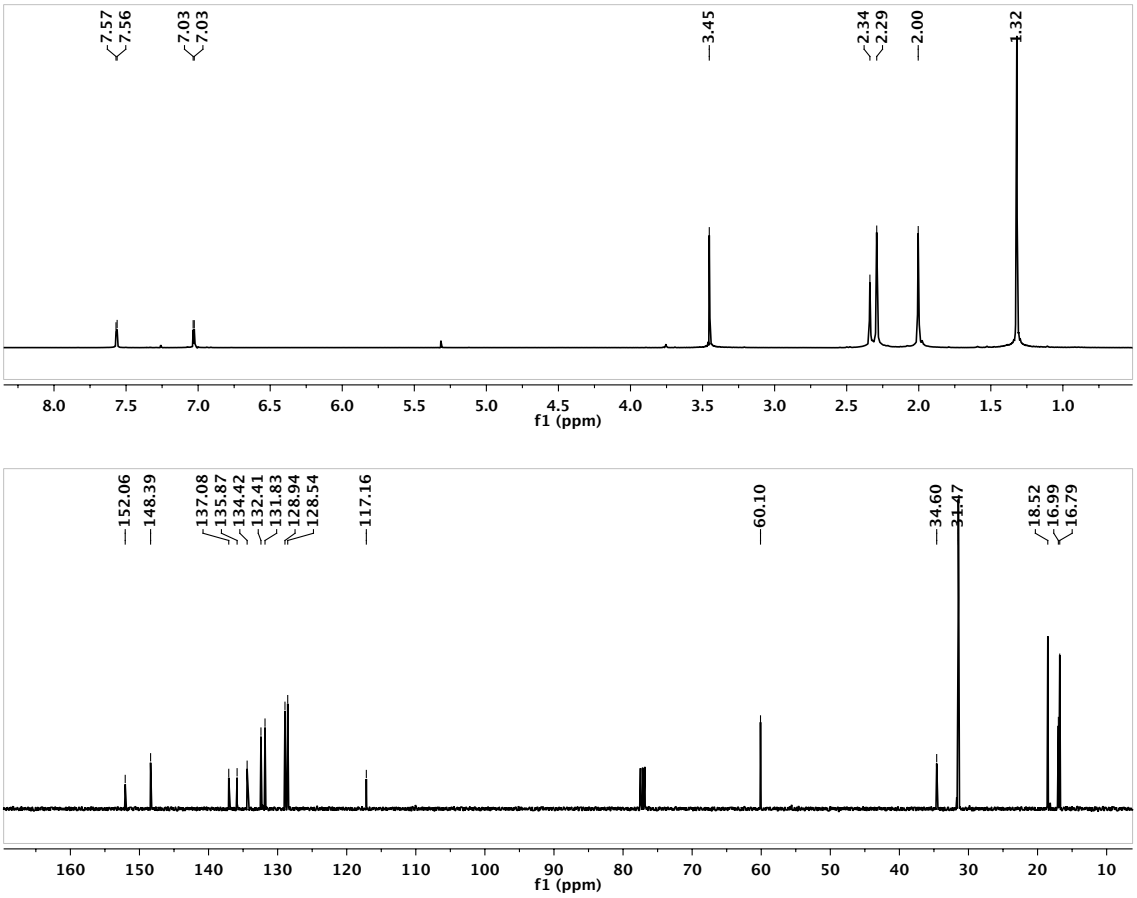

Figure C.11. ^{1}H (above) and ^{13}C (below) NMR spectra of compound **10** in $CDCl_3$.

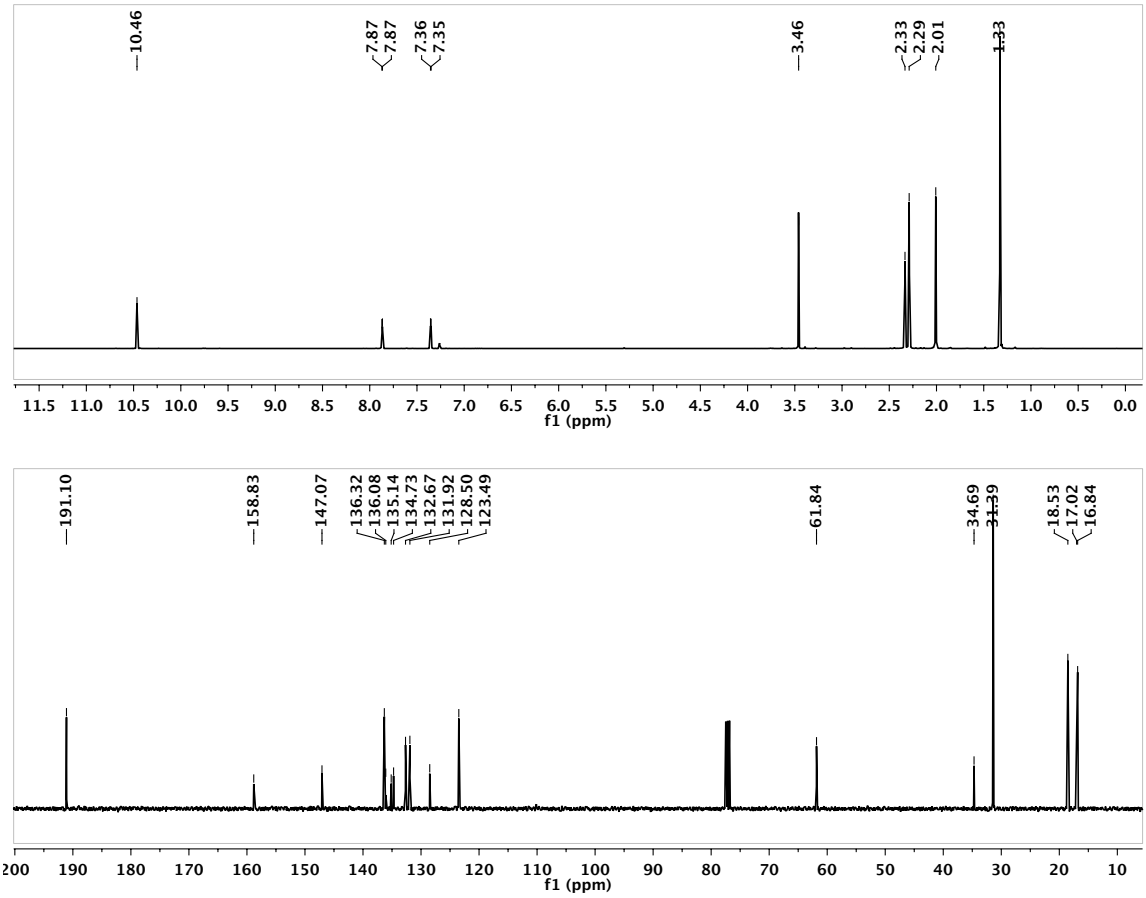

Figure C.12. ^{1}H (above) and ^{13}C (below) NMR spectra of compound **11** in $CDCl_3$.

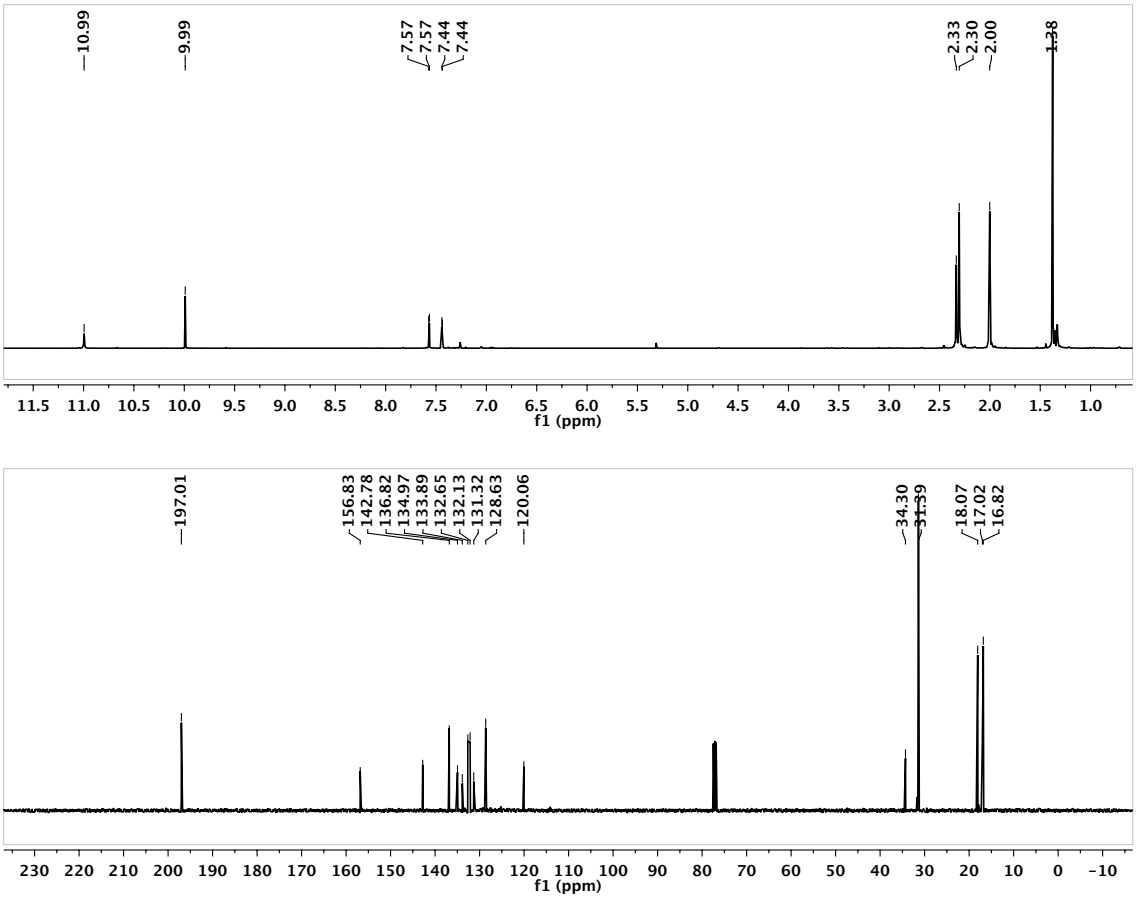

Figure C.13. ^{1}H (above) and ^{13}C (below) NMR spectra of compound **12** in $CDCl_3$.

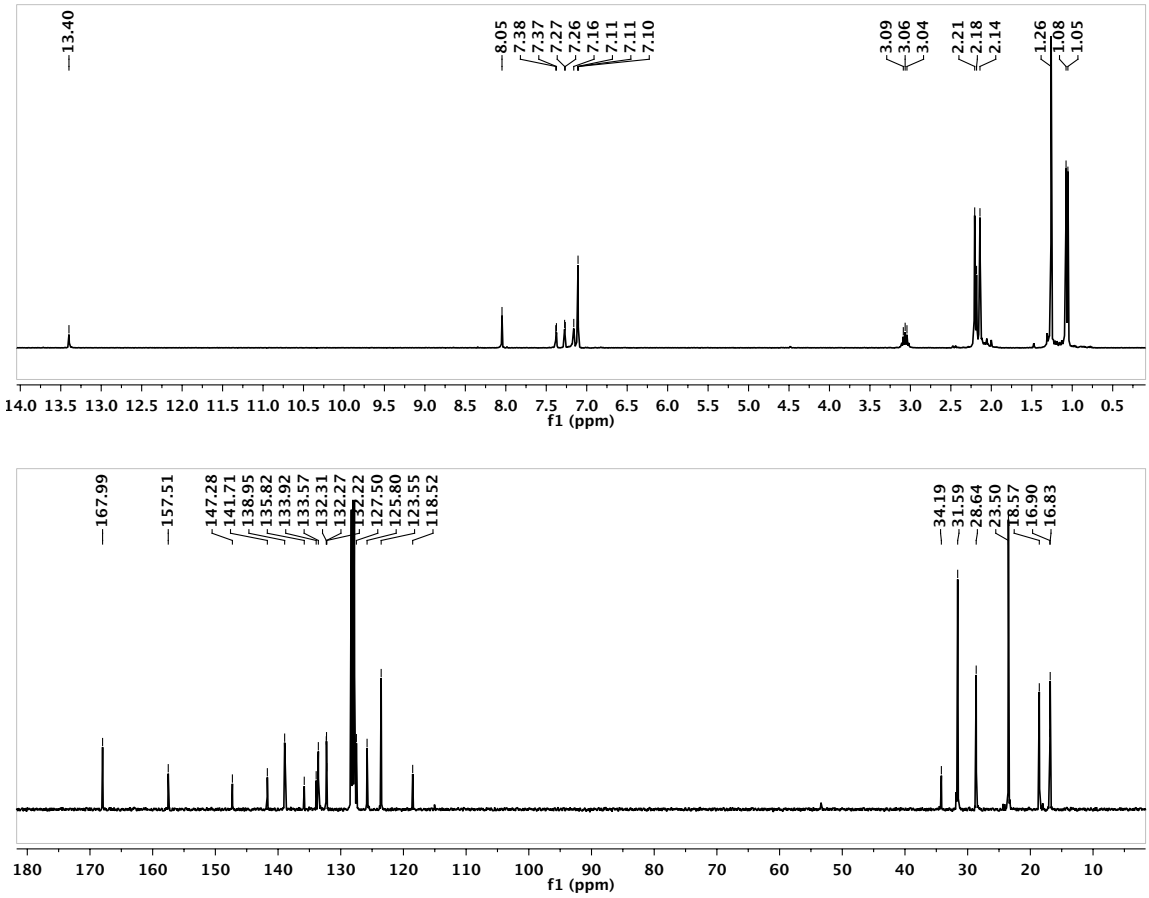

Figure C.14. ^{1}H (above) and ^{13}C (below) NMR spectra of compound **13** in C_6D_6.

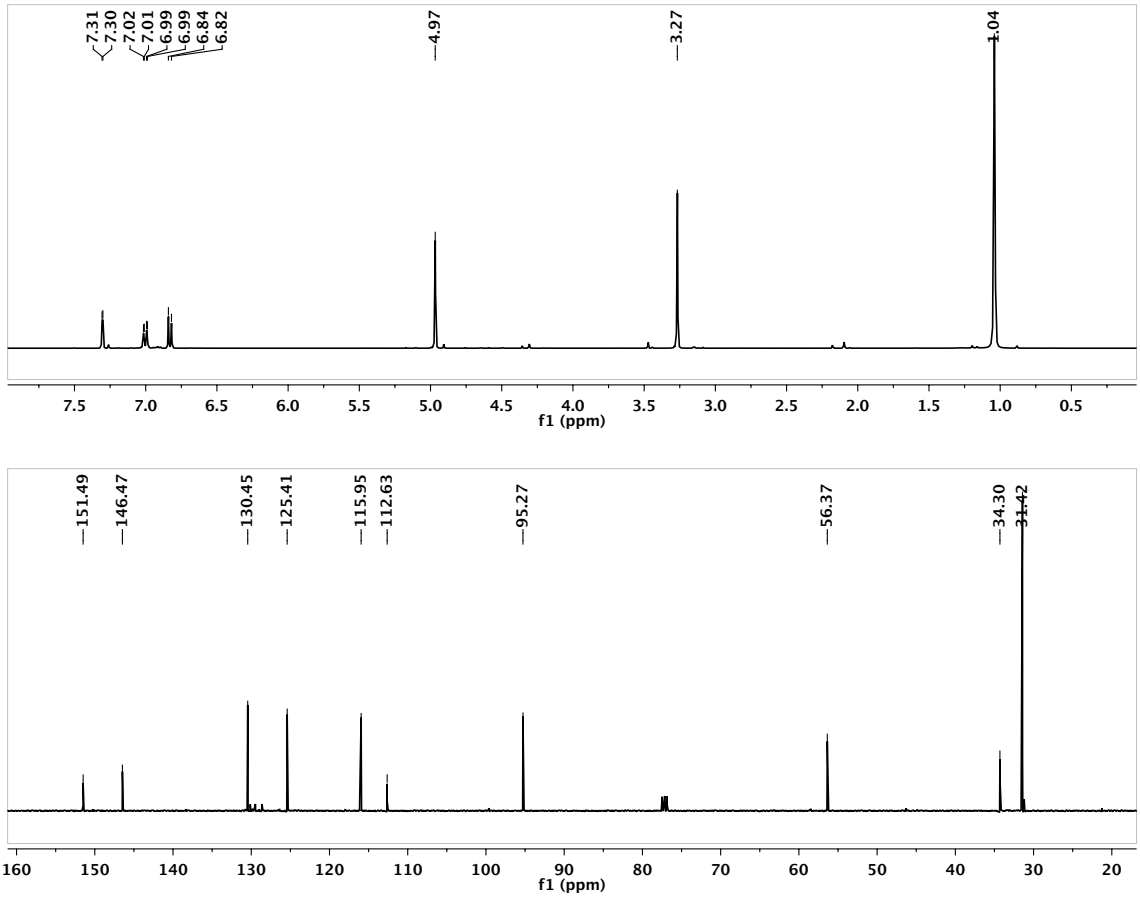

Figure C.15. ^{1}H (above) and ^{13}C (below) NMR spectra of compound **14** in $CDCl_3$.

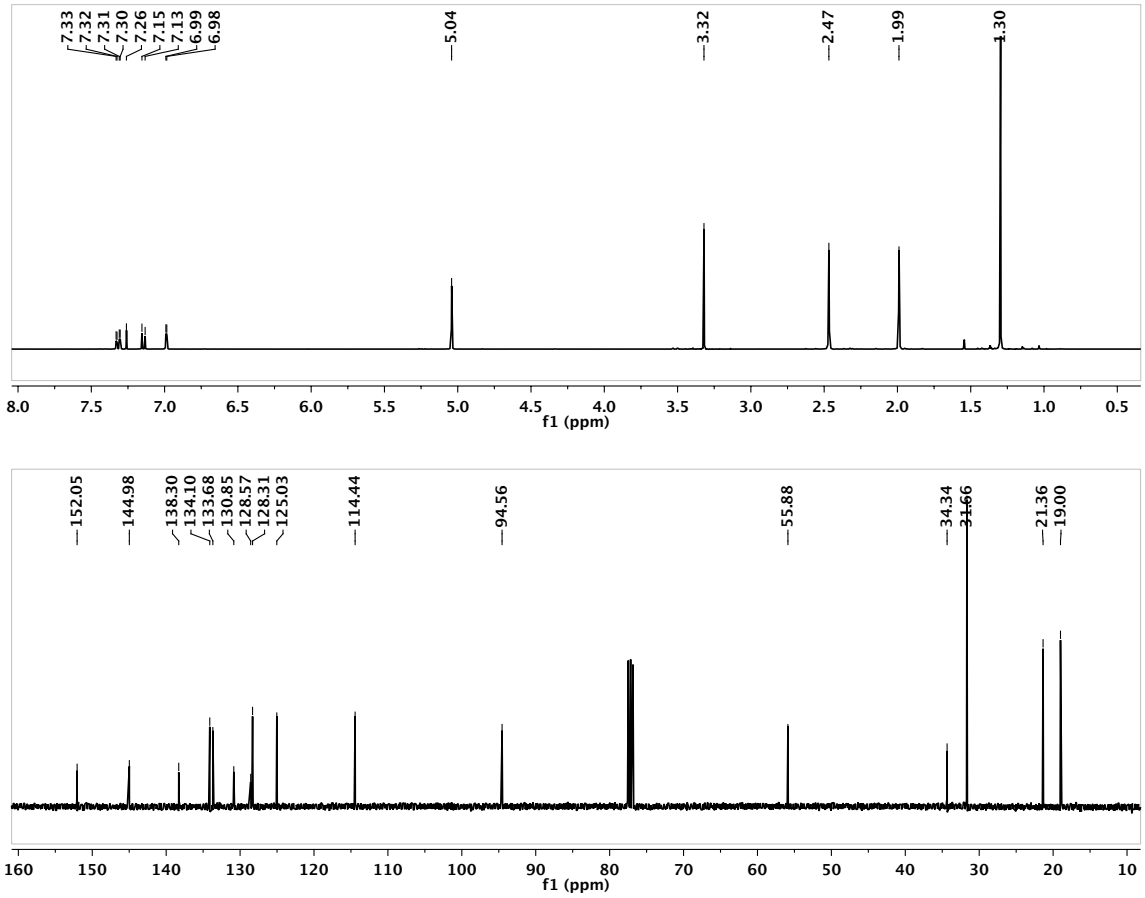

Figure C.16. ^{1}H (above) and ^{13}C (below) NMR spectra of compound **15** in $CDCl_3$.

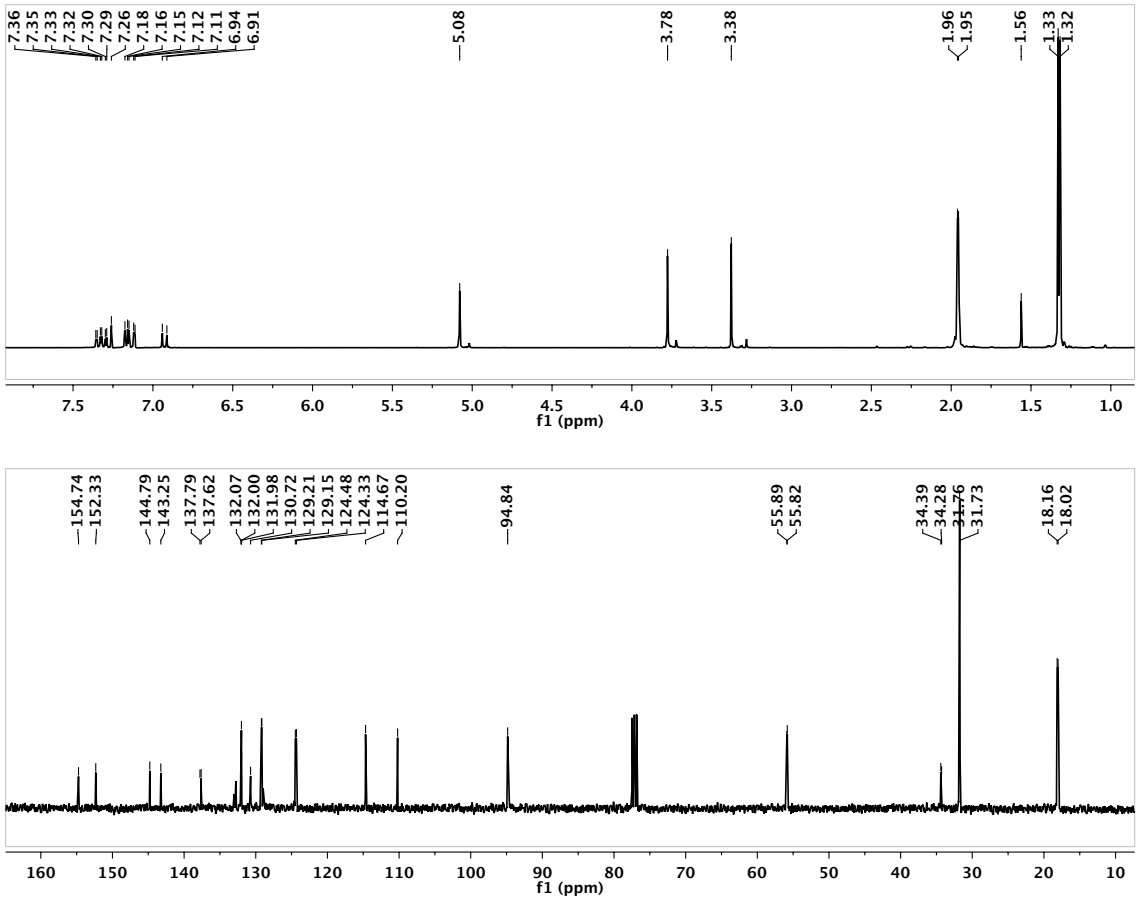

Figure C.17. ^{1}H (above) and ^{13}C (below) NMR spectra of compound **16-a** in $CDCl_3$.

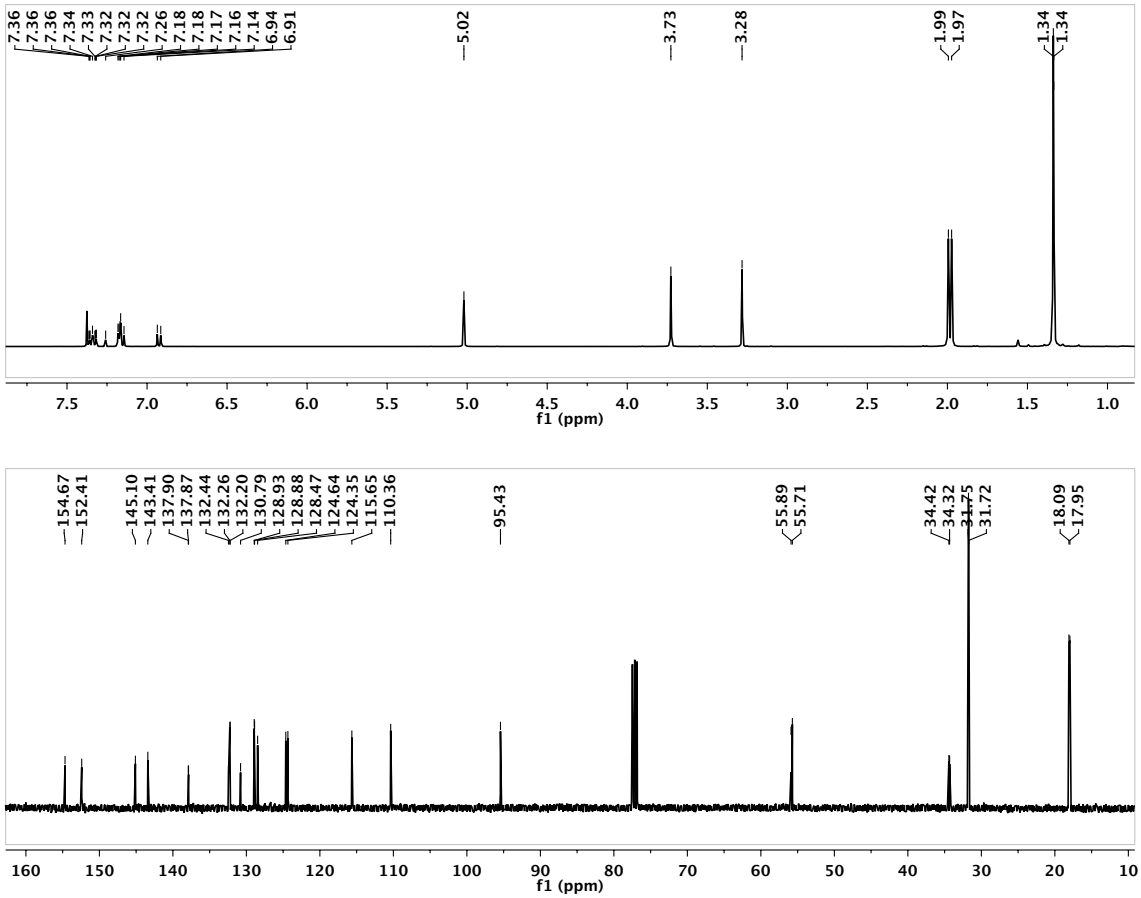

Figure C.18. ^{1}H (above) and ^{13}C (below) NMR spectra of compound **16-s** in $CDCl_3$.

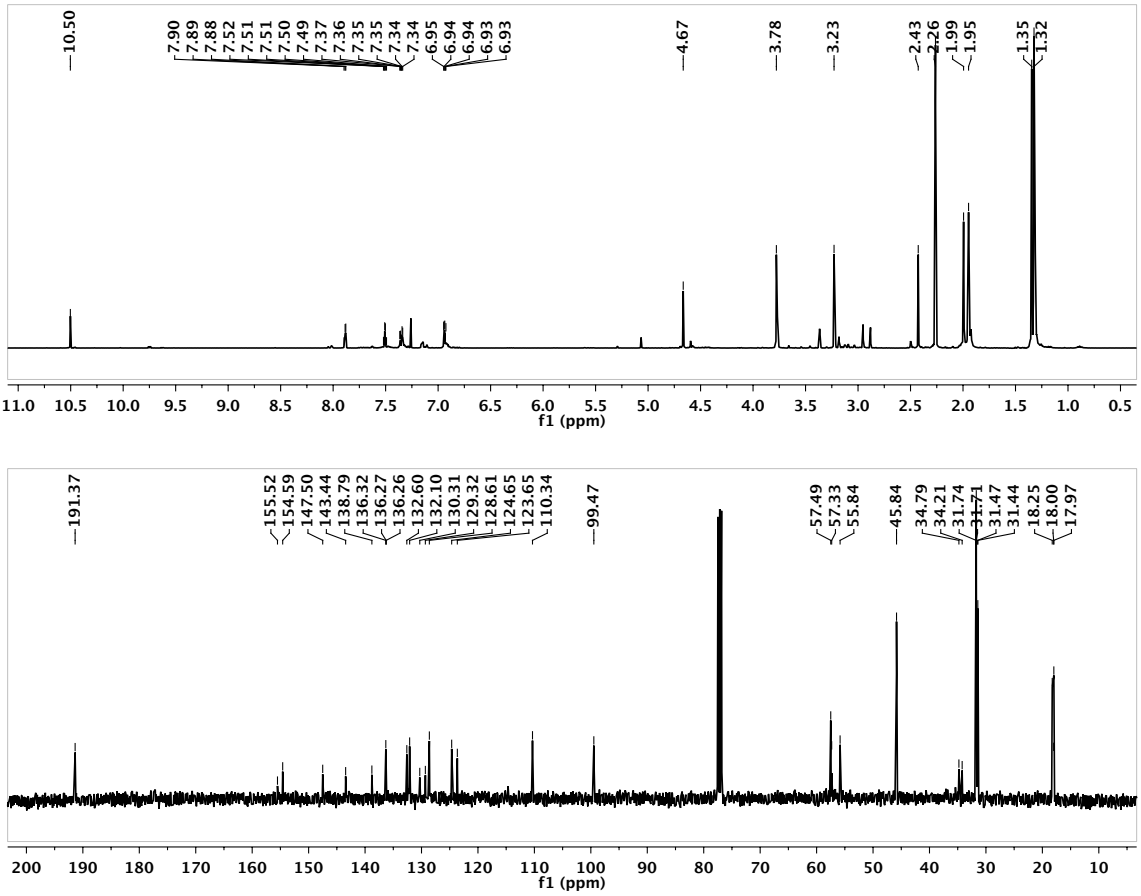

Figure C.19. ^{1}H (above) and ^{13}C (below) NMR spectra of compound **17-a** in $CDCl_3$.

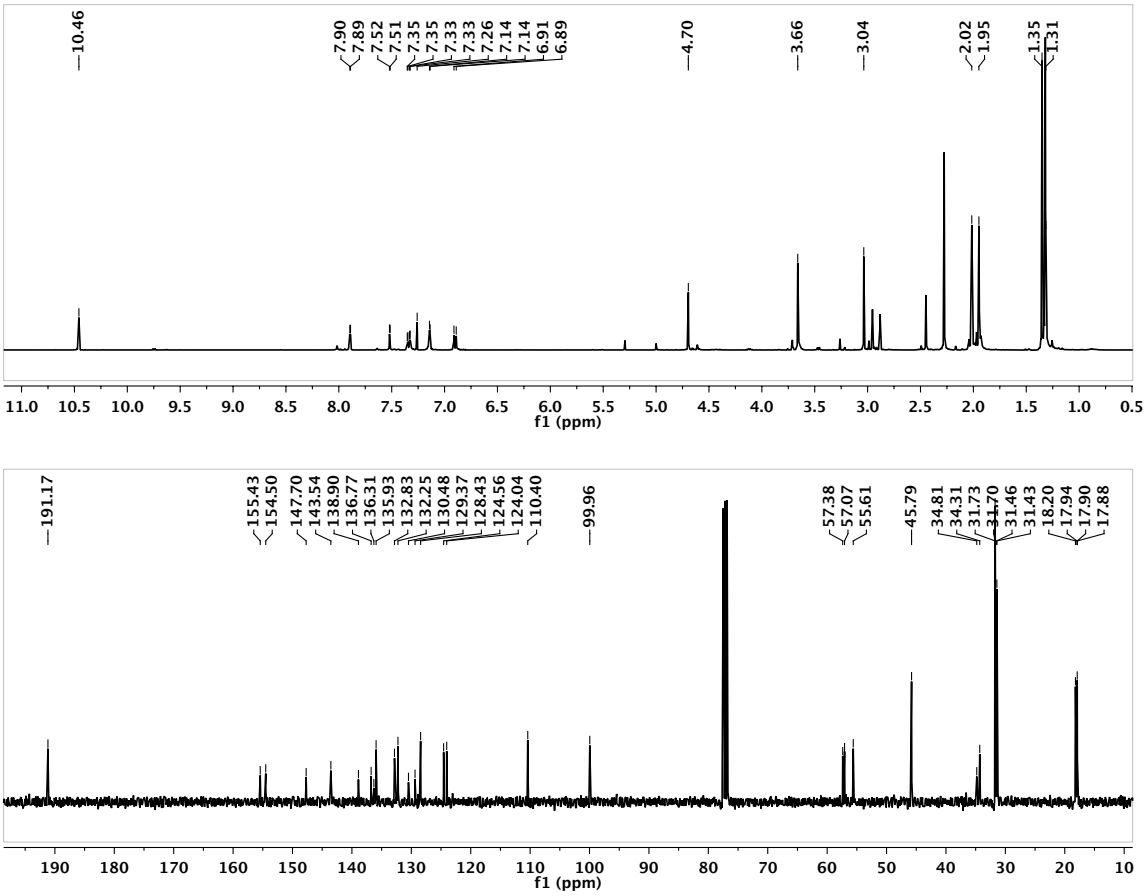

Figure C.20. ^{1}H (above) and ^{13}C (below) NMR spectra of compound **17-s** in $CDCl_3$.

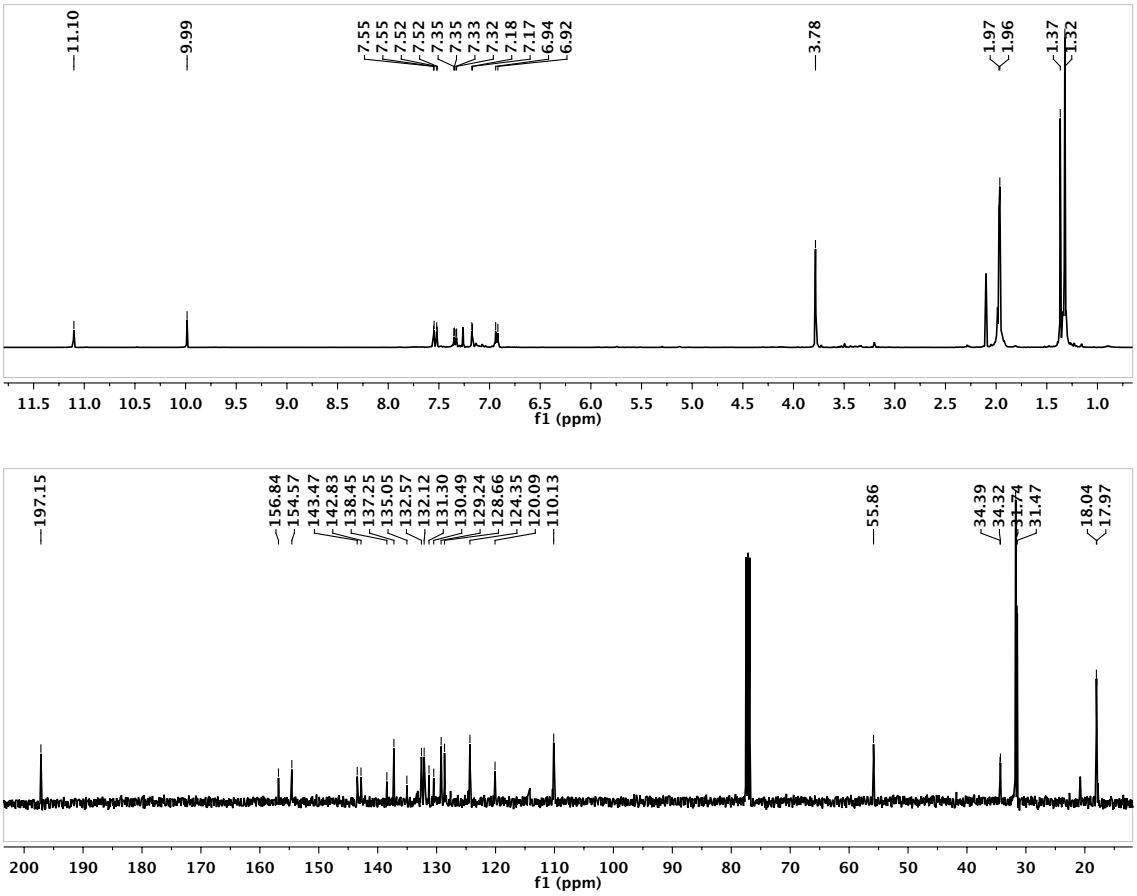

Figure C.21. ^{1}H (above) and ^{13}C (below) NMR spectra of compound **18-a** in $CDCl_3$.

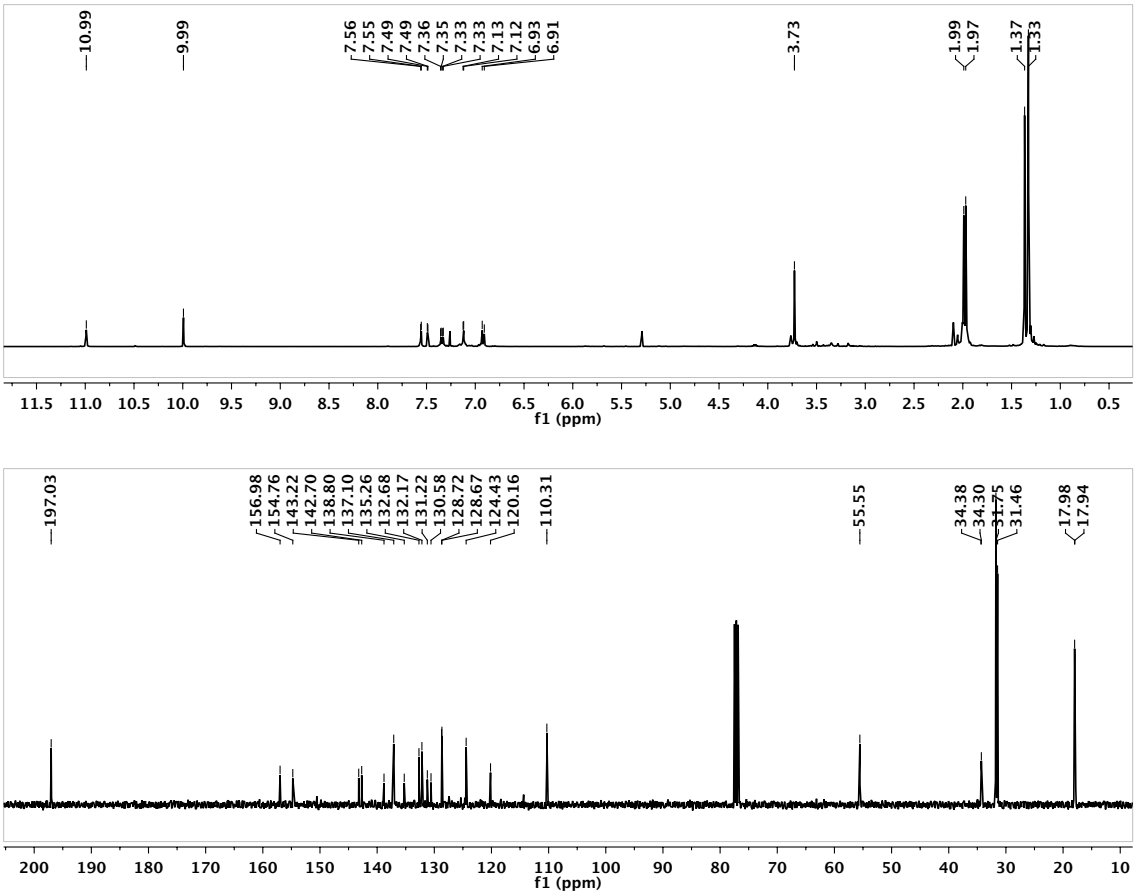

Figure C.22. ^{1}H (above) and ^{13}C (below) NMR spectra of compound **18-s** in $CDCl_3$.

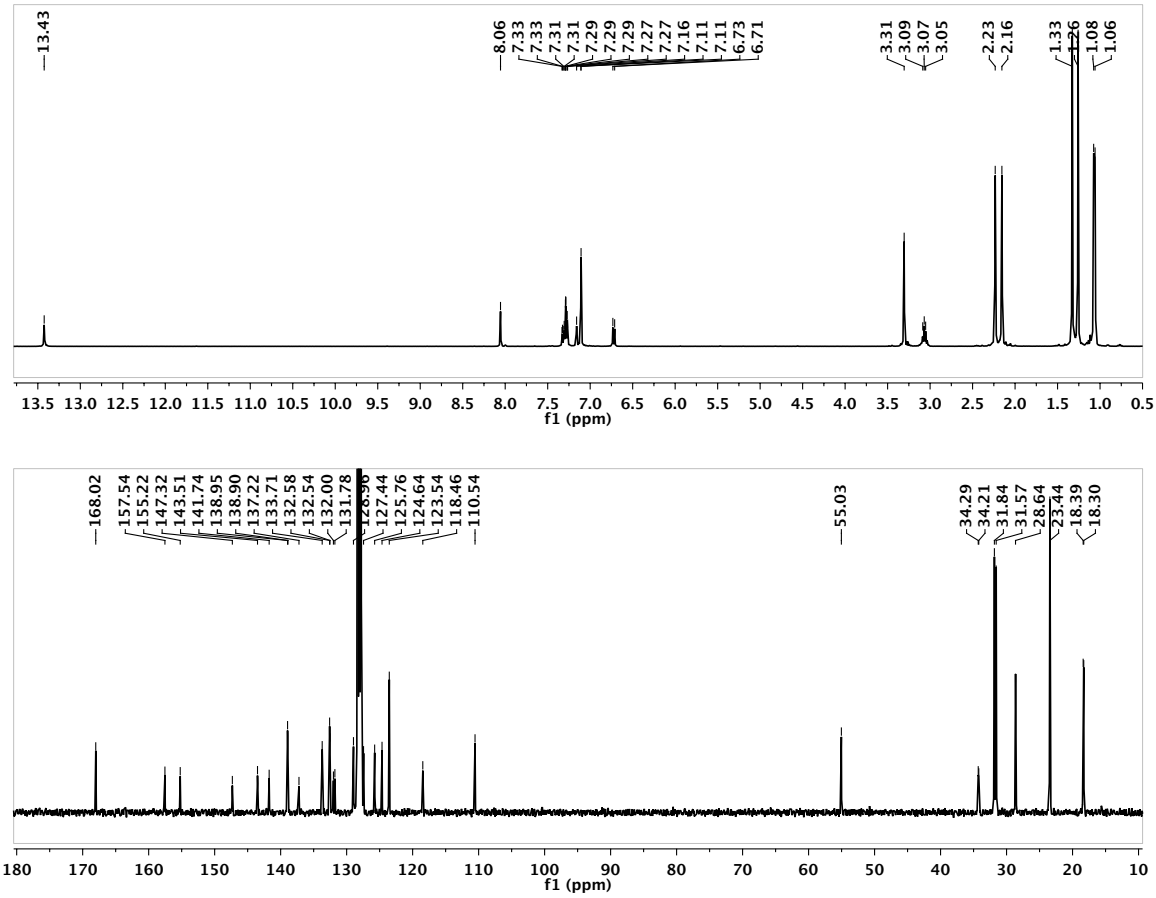

Figure C.23. ^{1}H (above) and ^{13}C (below) NMR spectra of compound **19-a** in C_6D_6.

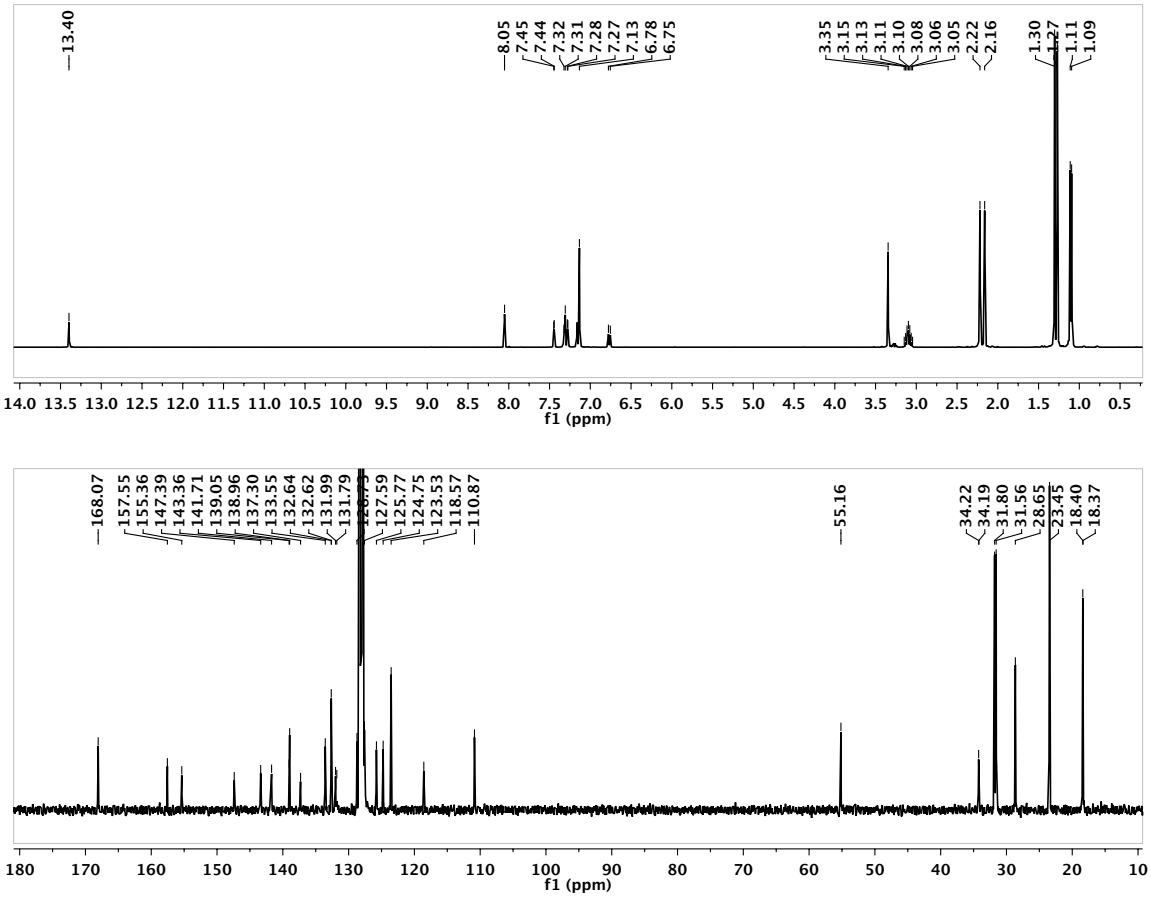

Figure C.24. ^{1}H (above) and ^{13}C (below) NMR spectra of compound **19-s** in C_6D_6.

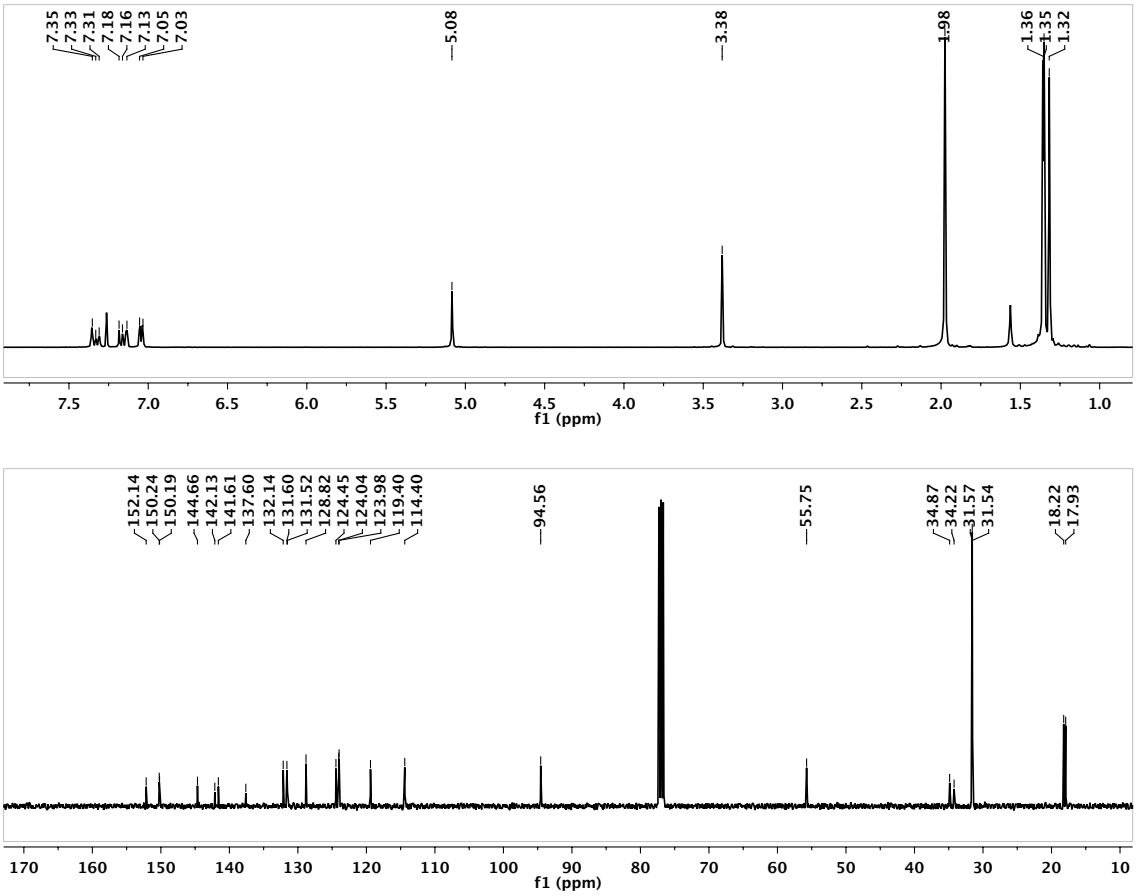

Figure C.25. ^{1}H (above) and ^{13}C (below) NMR spectra of compound **21** in $CDCl_3$.

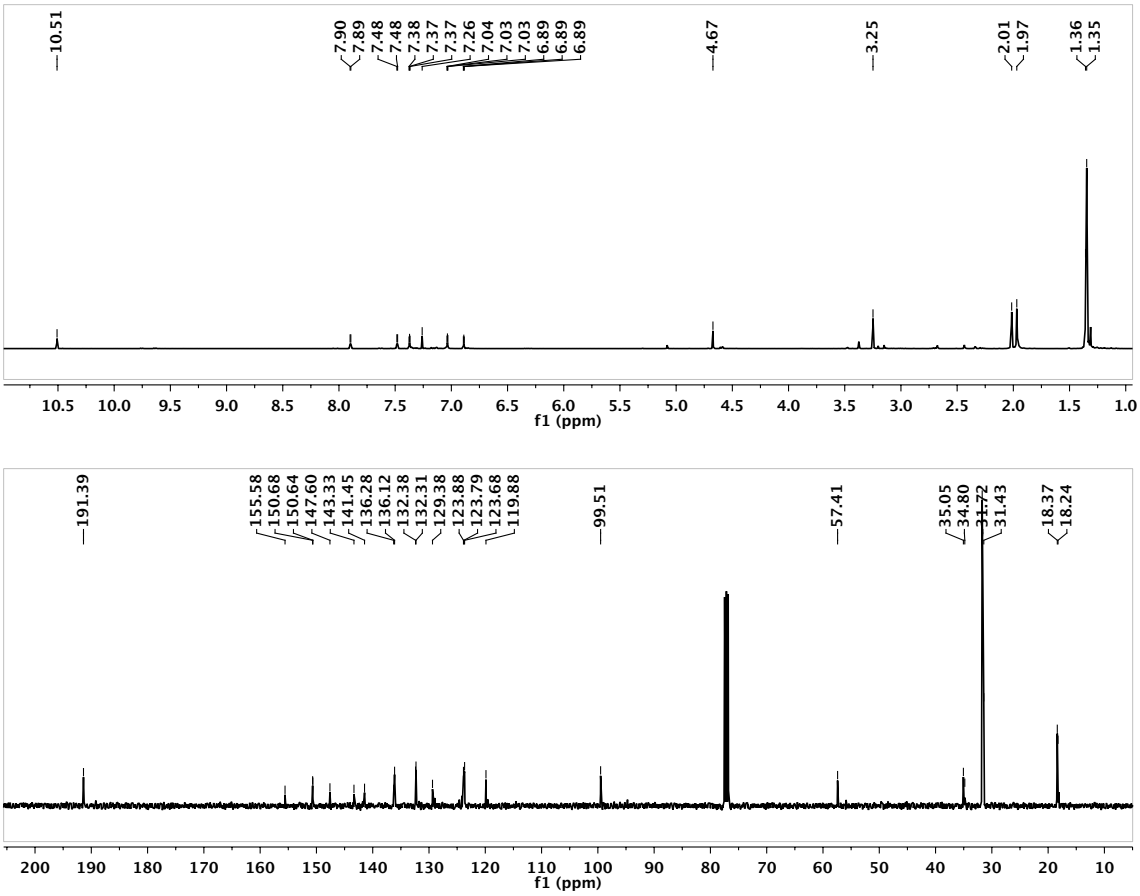

Figure C.26. ^{1}H (above) and ^{13}C (below) NMR spectra of compound **22** in $CDCl_3$.

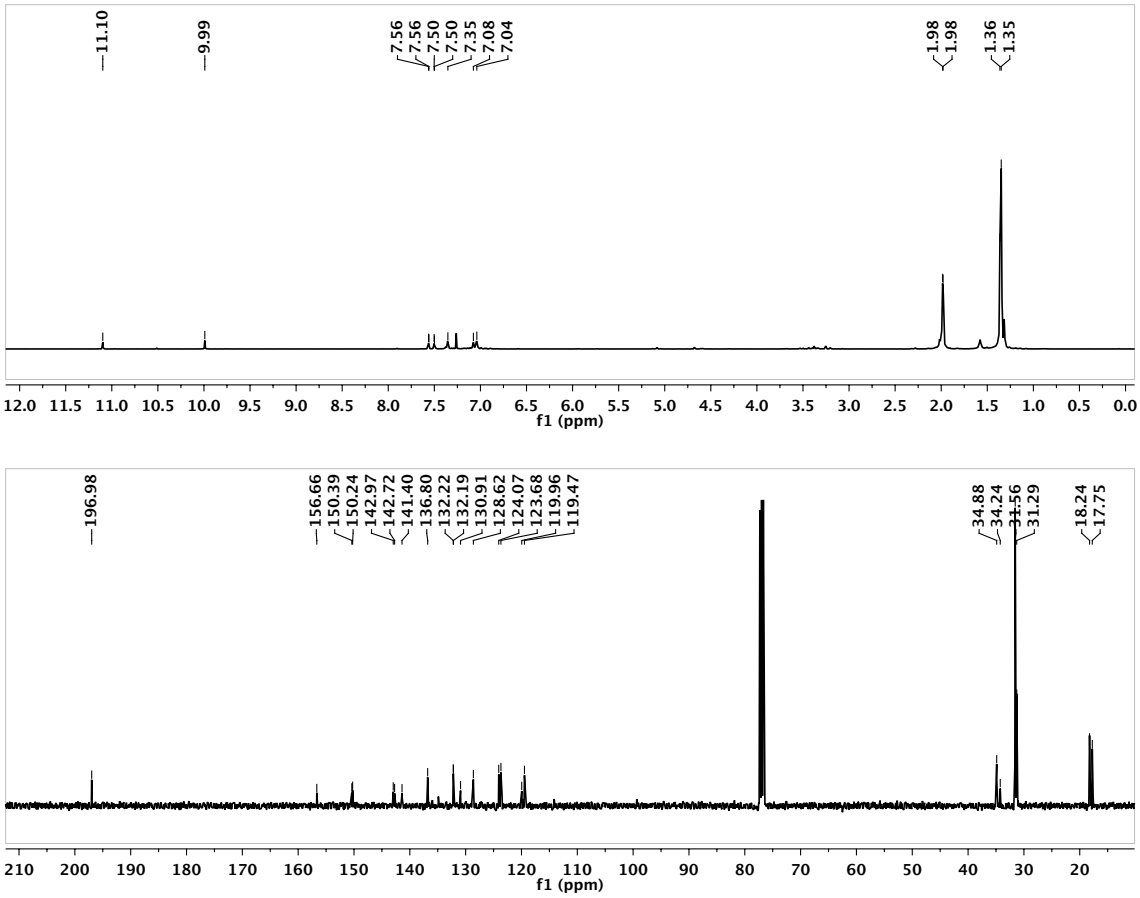

Figure C.27. ^{1}H (above) and ^{13}C (below) NMR spectra of compound **23** in $CDCl_3$.

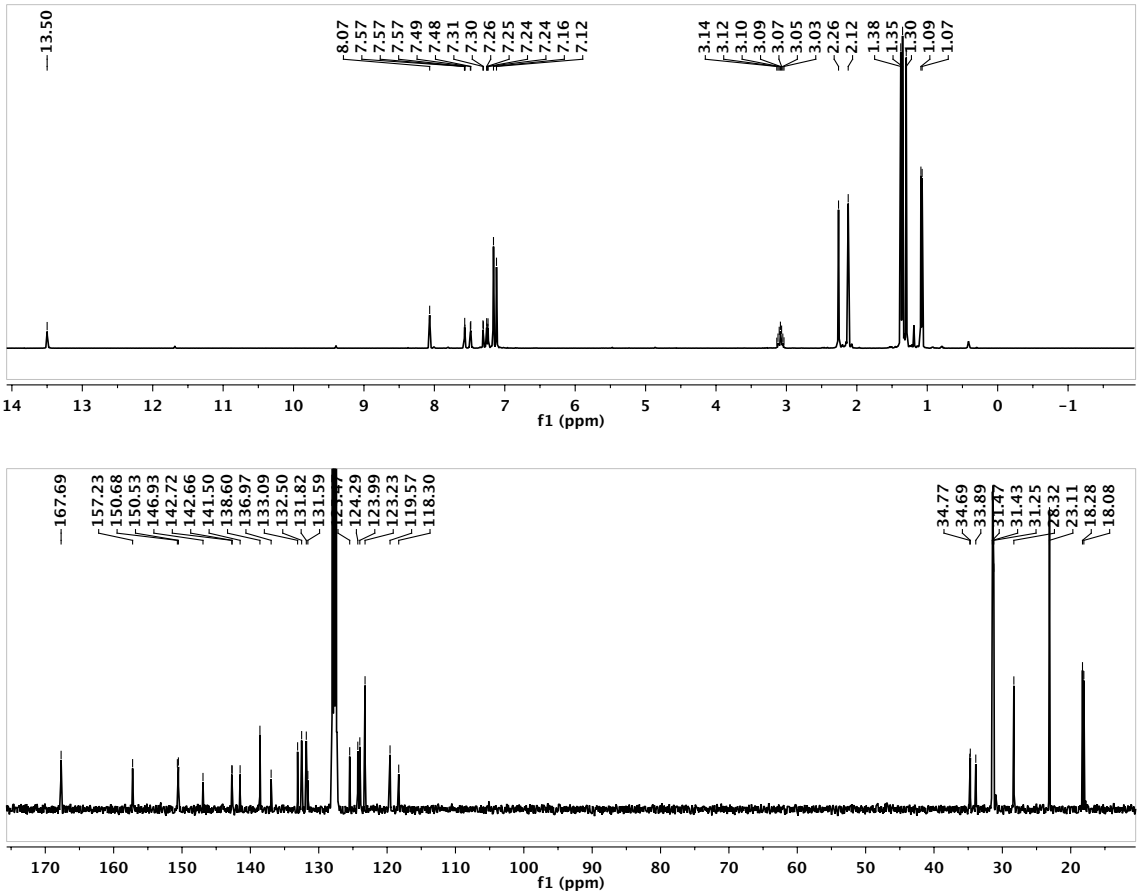

Figure C.28. ^{1}H (above) and ^{13}C (below) NMR spectra of compound **24** in C_6D_6.

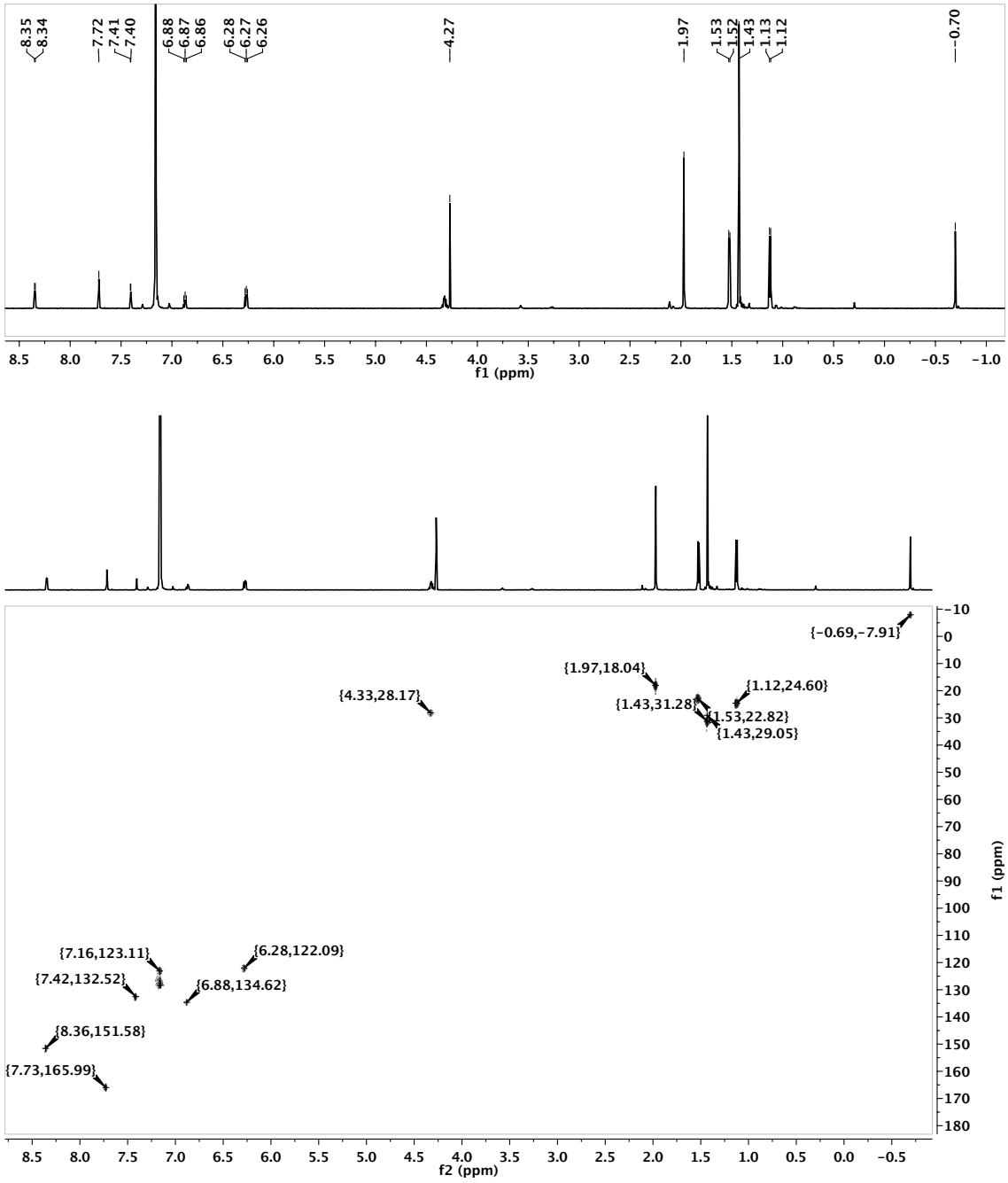

Figure C.29. ^{1}H (above) and ^{1}H-^{13}C gHSQCAD (below) NMR spectra of compound **25-a** in C_6D_6.

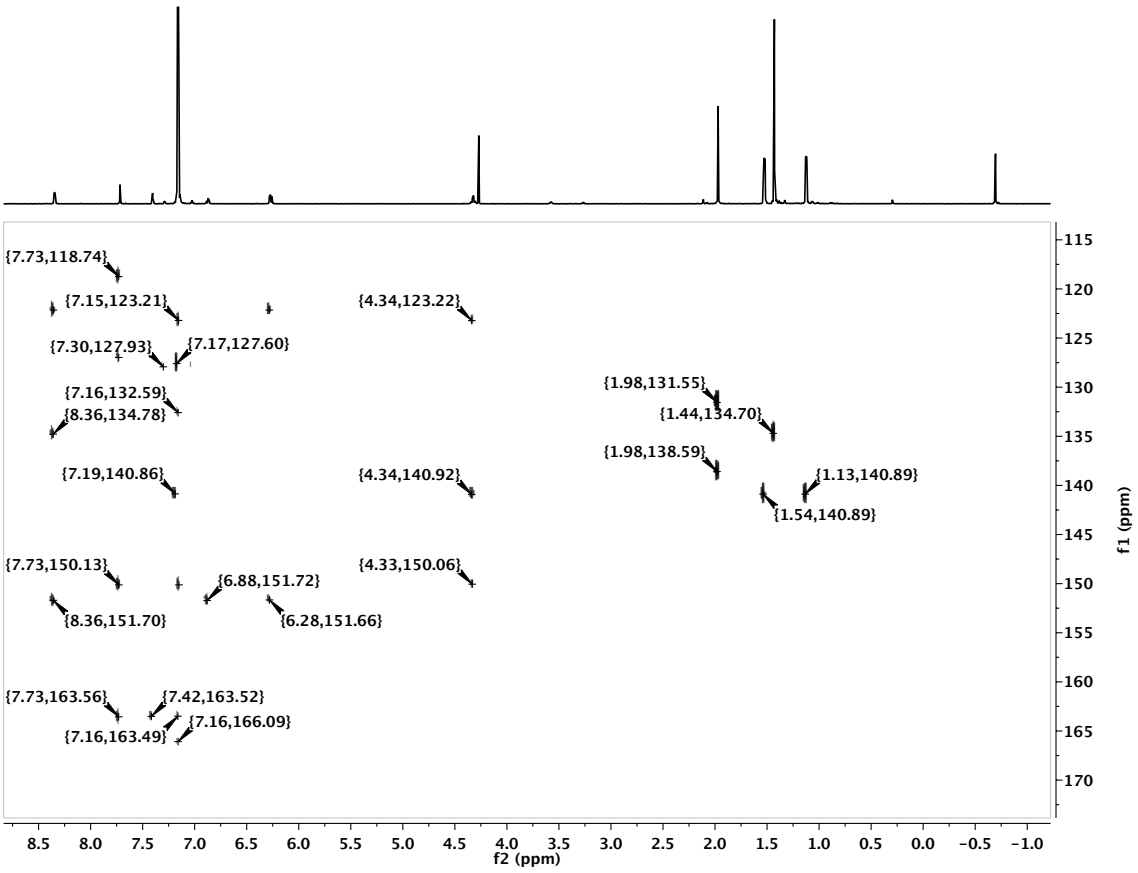

Figure C.30. ^{1}H-^{13}C gHMBCAD NMR spectrum of compound **25-a** in C_6D_6.

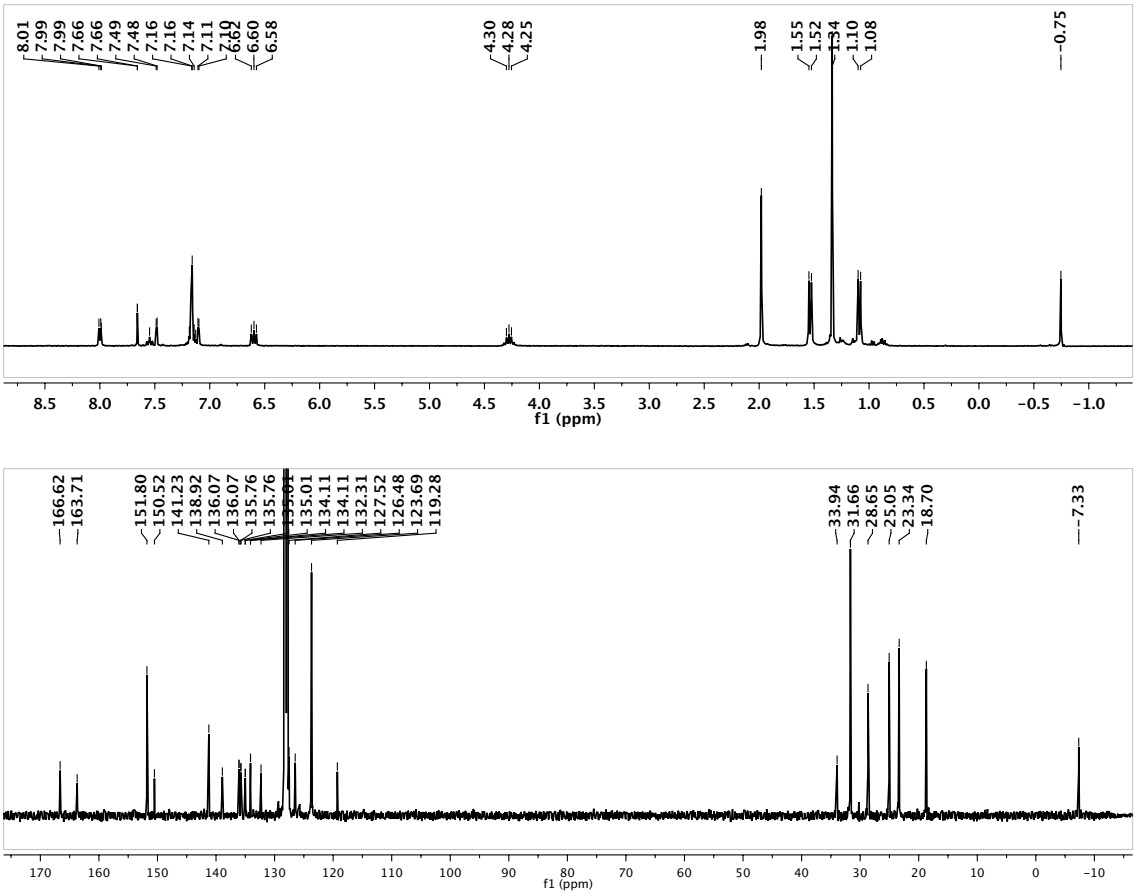

Figure C.31. ^{1}H (above) and ^{13}C (below) NMR spectra of compound **25-s** in C_6D_6.

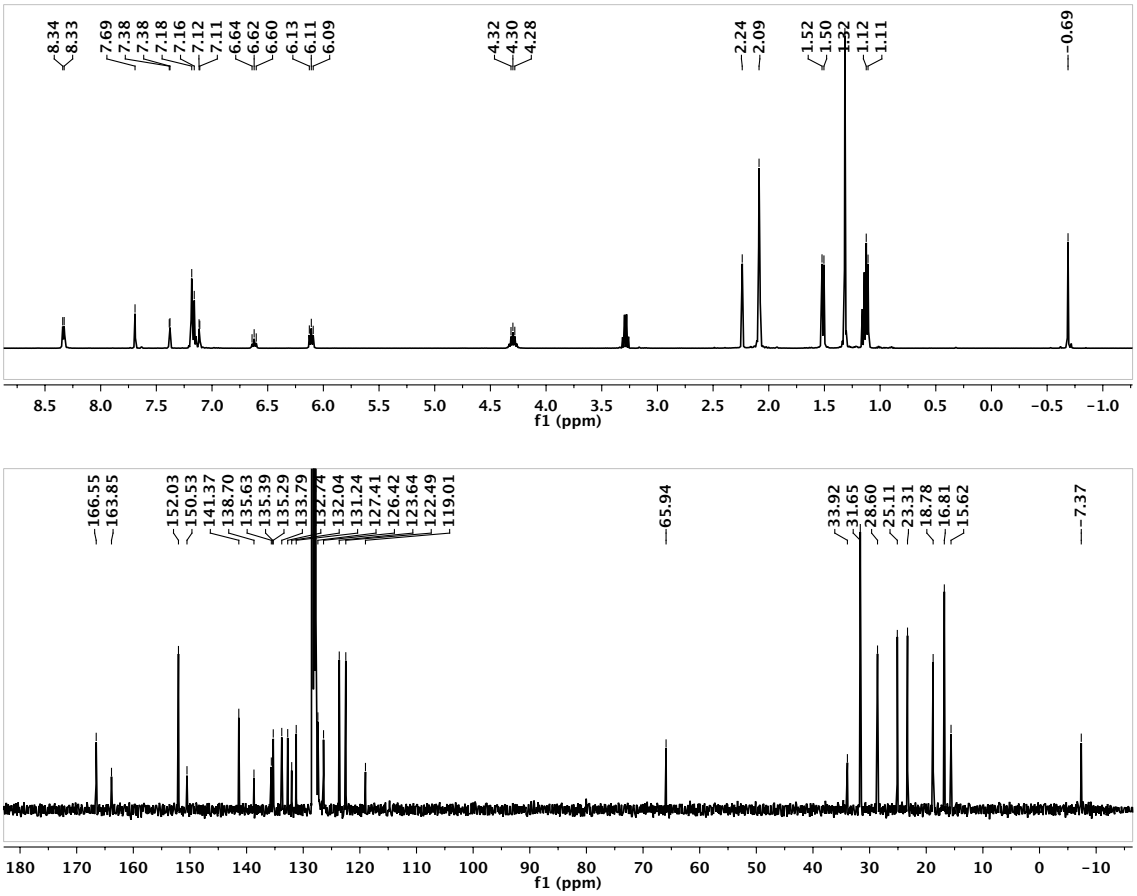

Figure C.32. ^{1}H (above) and ^{13}C (below) NMR spectra of compound **26** in C_6D_6.

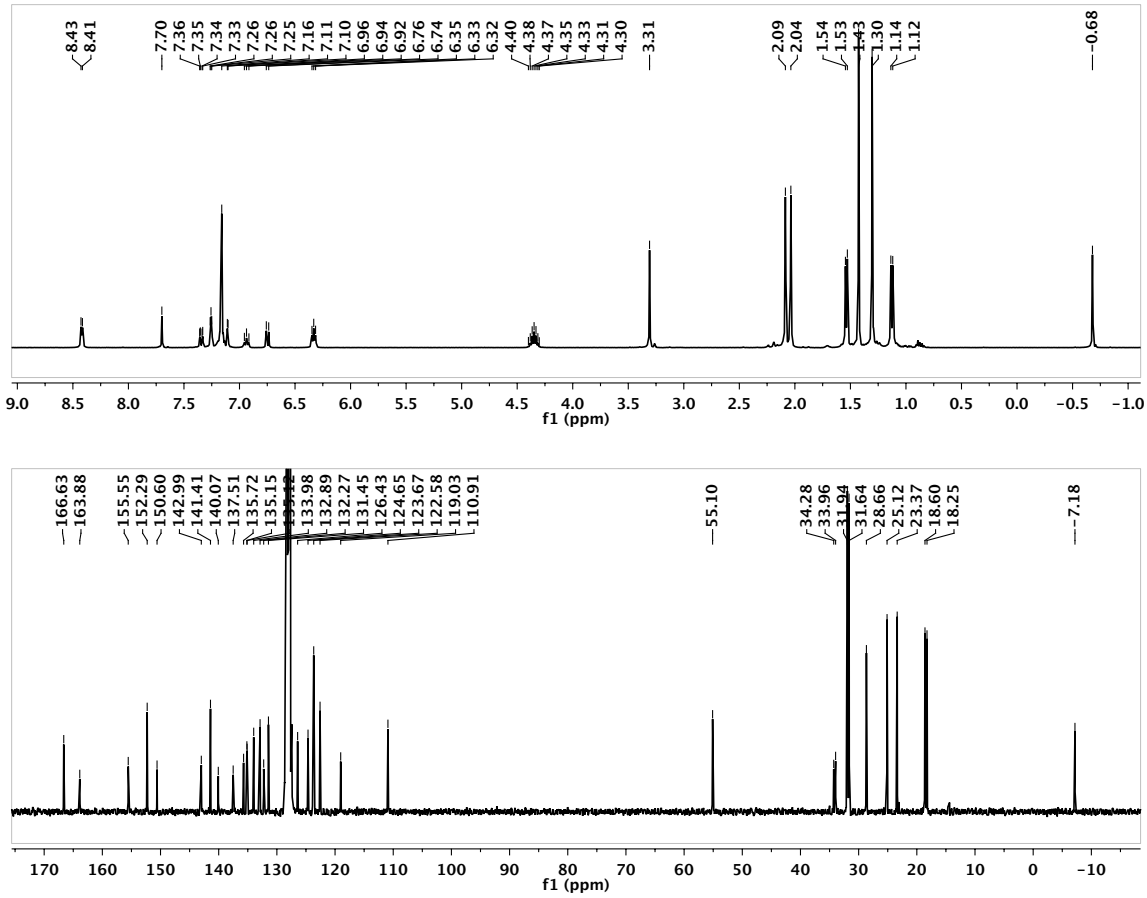

Figure C.33. ^{1}H (above) and ^{13}C (below) NMR spectra of compound **27-a** in C_6D_6.

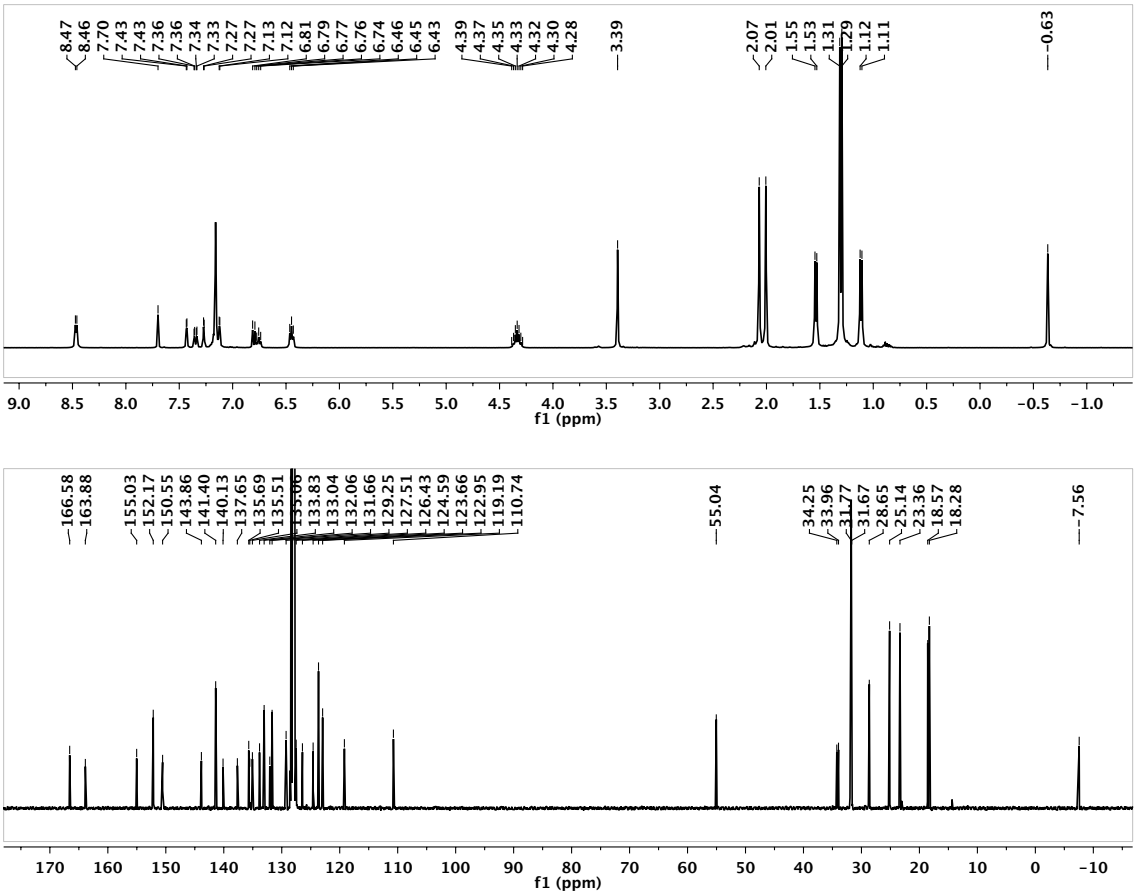

Figure C.34. ^{1}H (above) and ^{13}C (below) NMR spectra of compound **27-s** in C_6D_6.

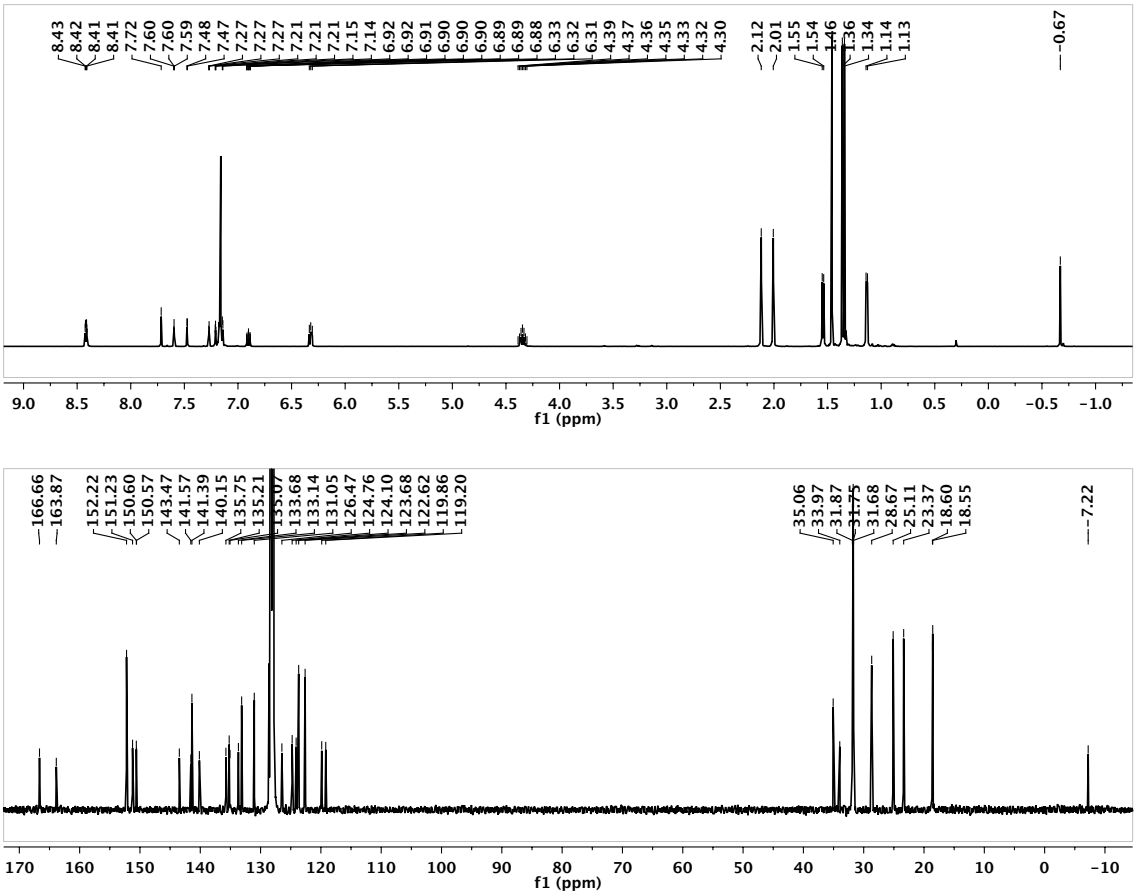

Figure C.35. ^{1}H (above) and ^{13}C (below) NMR spectra of compound **28** in C_6D_6.

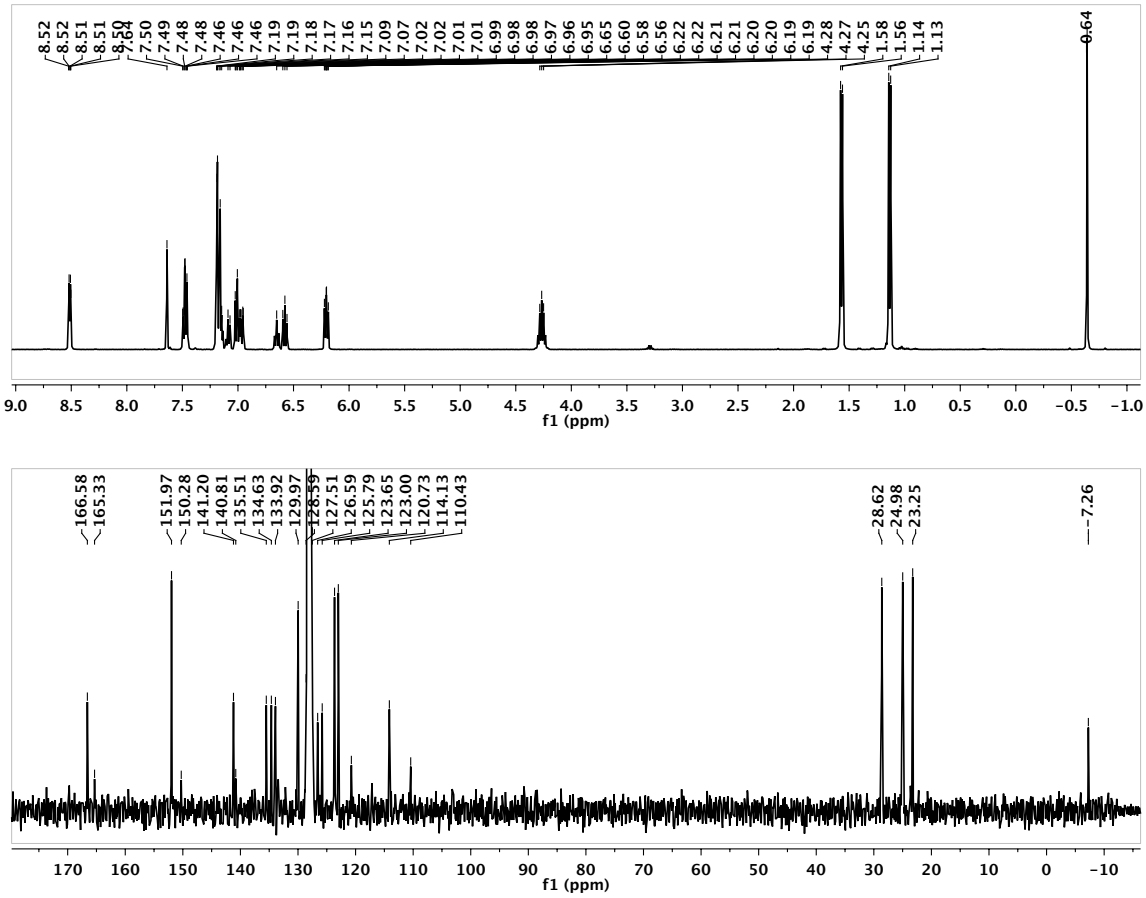

Figure C.36. ^{1}H (above) and ^{13}C (below) NMR spectra of compound **30** in C_6D_6.

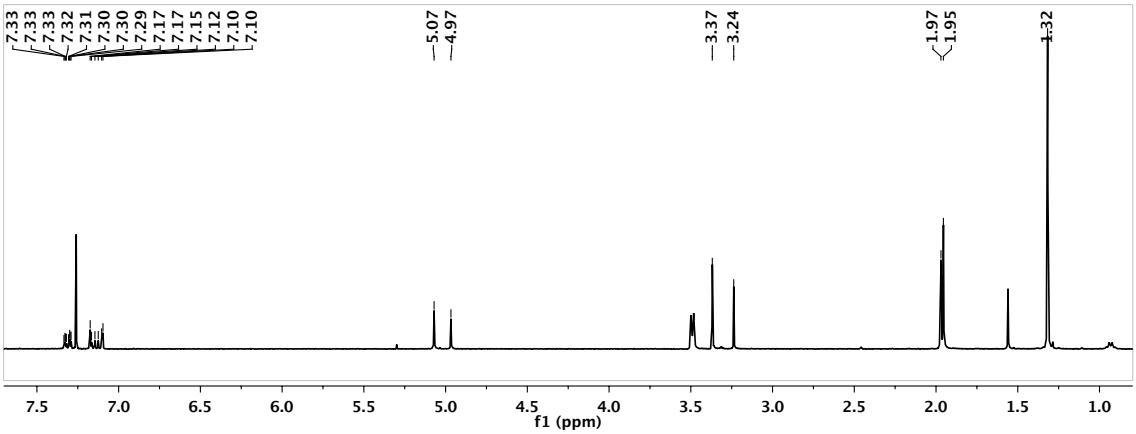

Figure C.37. ^{1}H NMR spectrum of compounds **32** in $CDCl_3$.

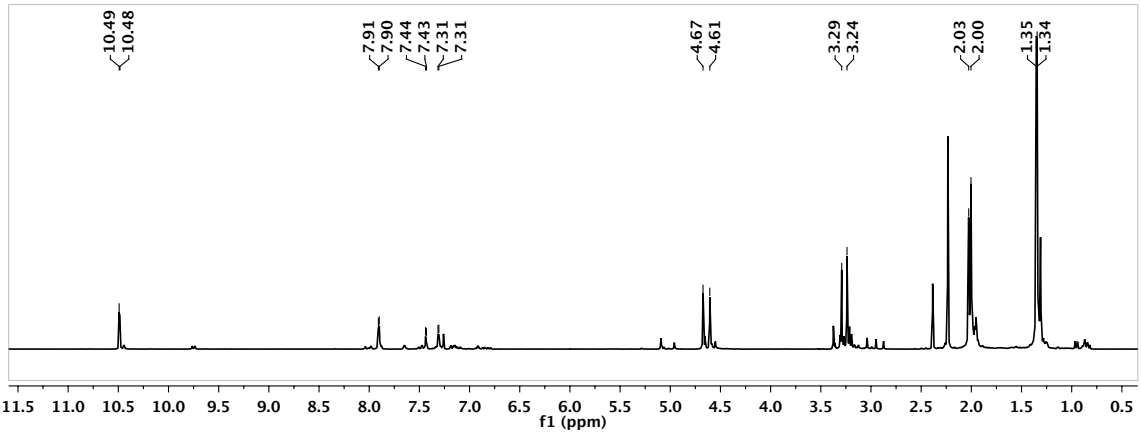

Figure C.38. ^{1}H NMR spectrum of compounds **33** in $CDCl_3$.

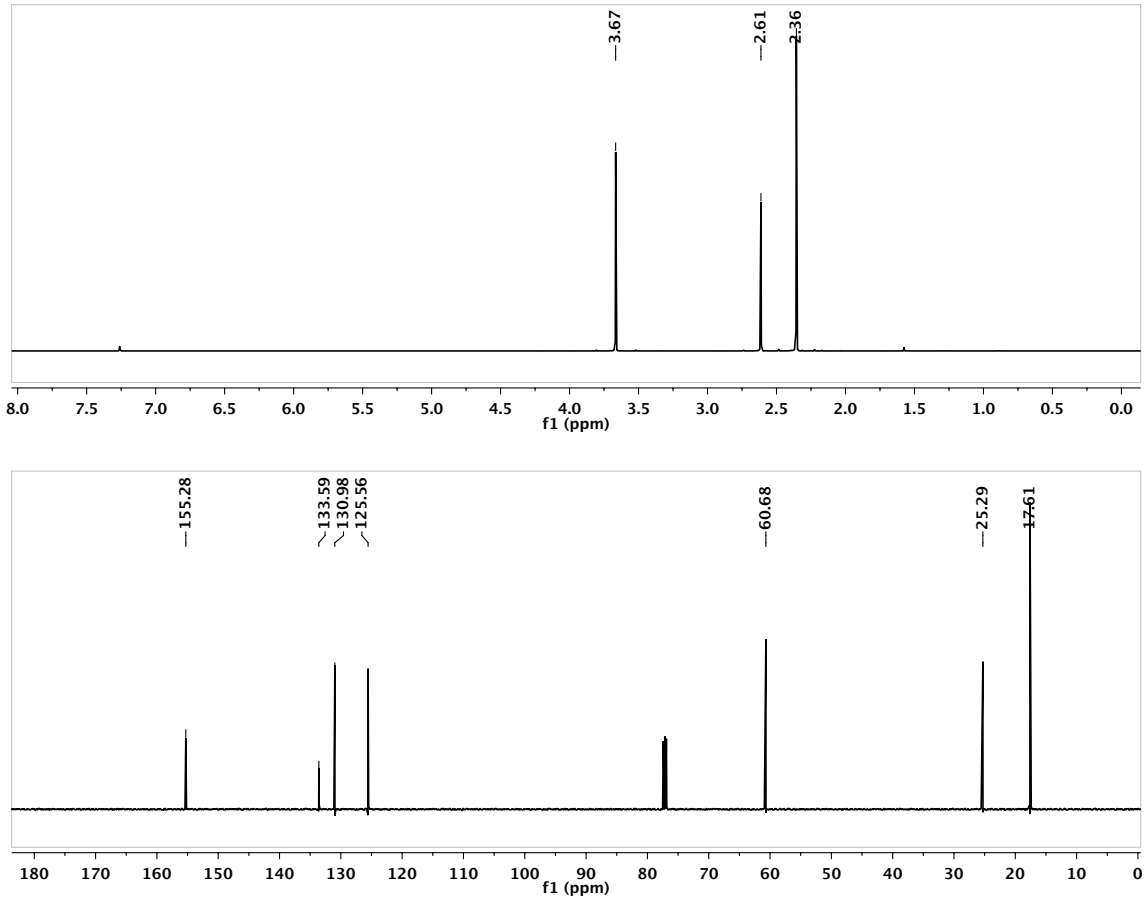

Figure C.39. ^{1}H (above) and ^{13}C (below) NMR spectra of compound **35** in $CDCl_3$.

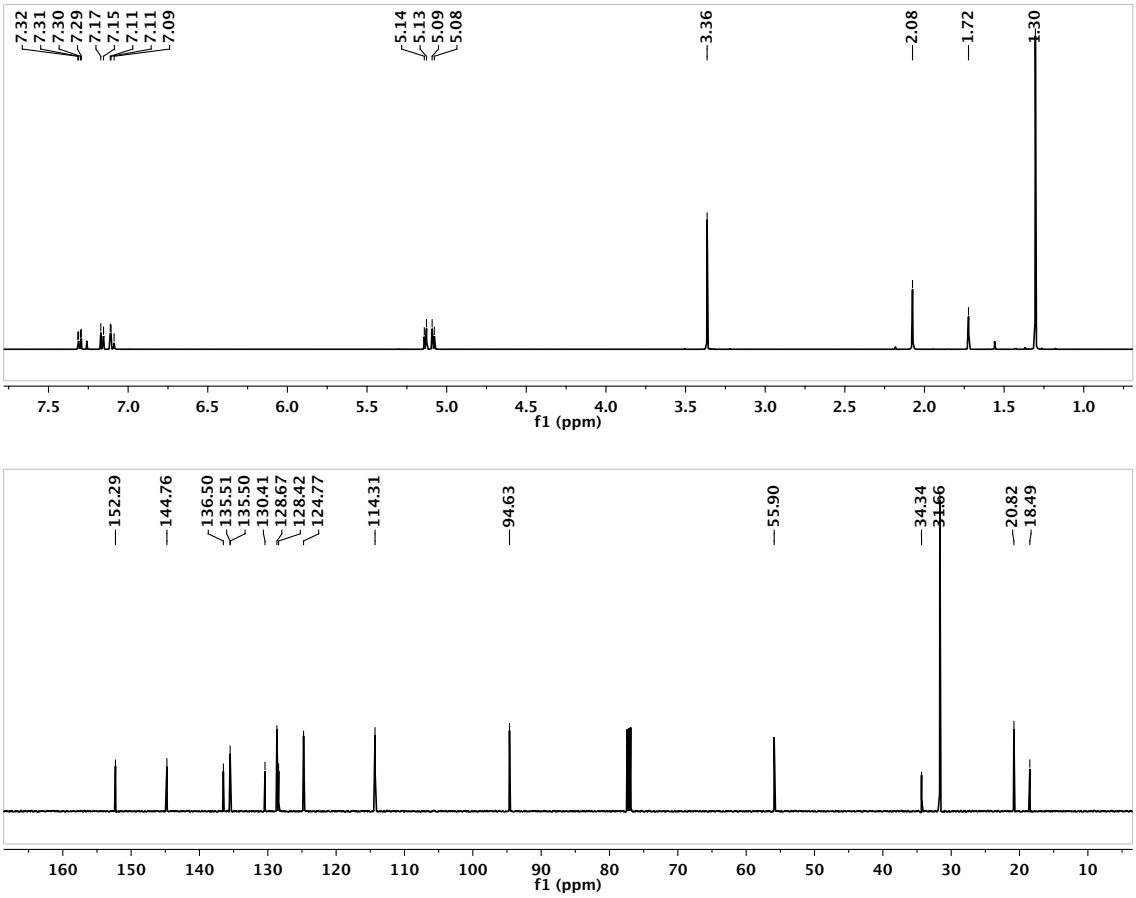

Figure C.40. ^{1}H (above) and ^{13}C (below) NMR spectra of compound **36-a** in $CDCl_3$.

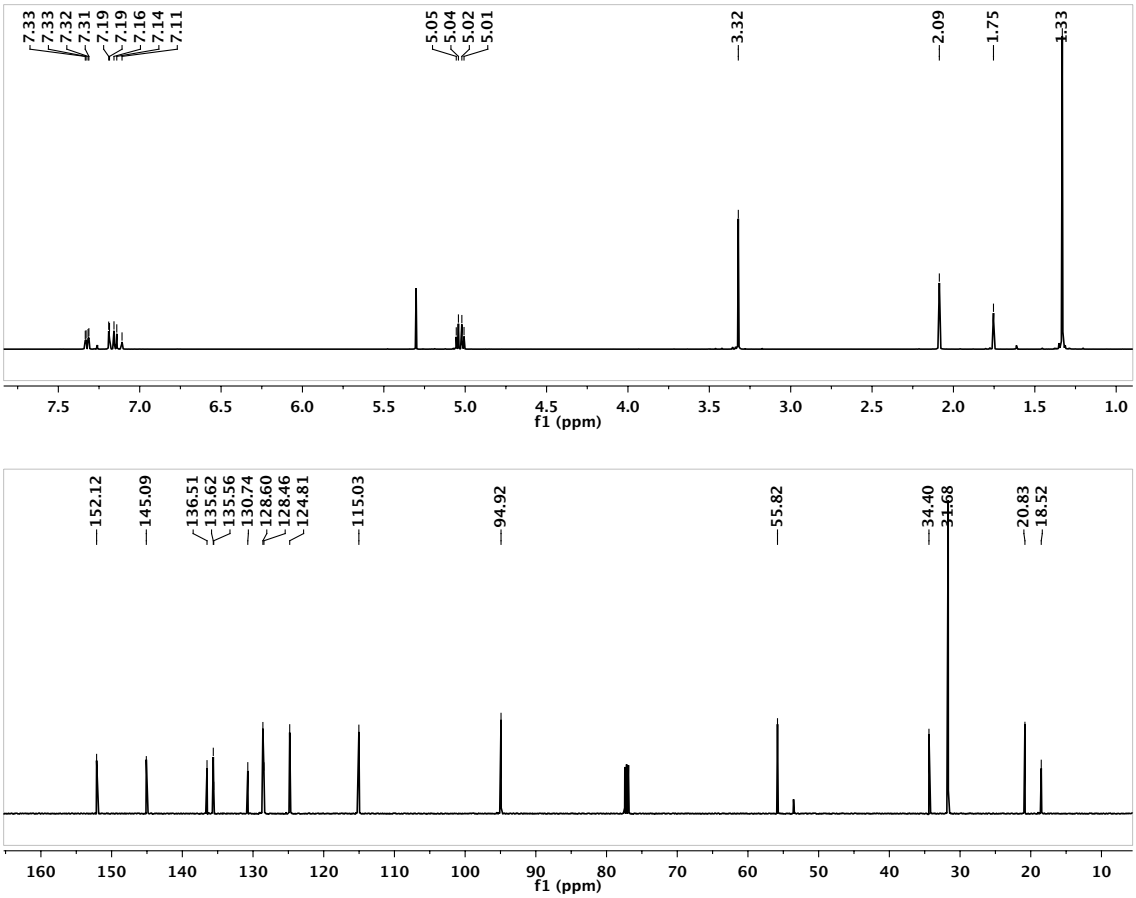

Figure C.41. ^{1}H (above) and ^{13}C (below) NMR spectra of compound **36-s** in $CDCl_3$.

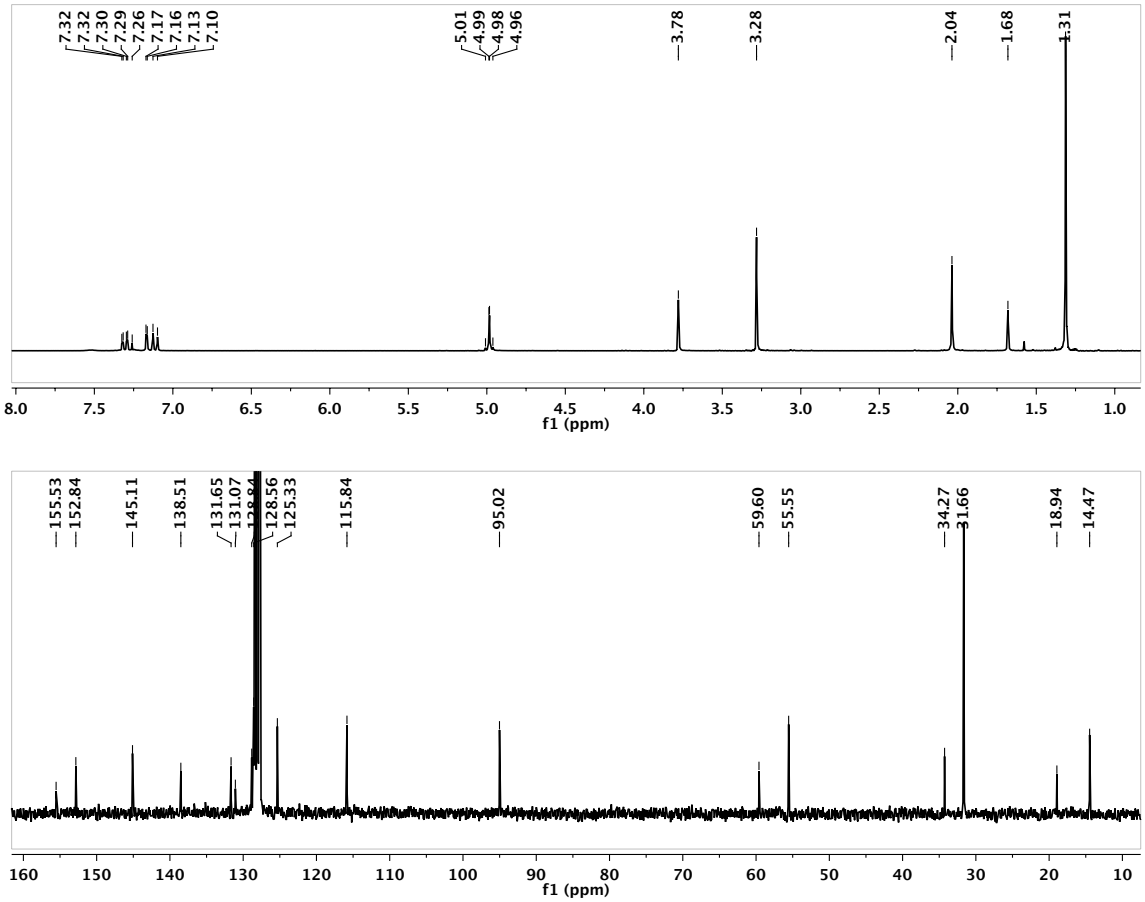

Figure C.42. ^{1}H NMR spectrum in $CDCl_3$ (above) and ^{13}C NMR spectrum in C_6D_6 (below) of compound **37-s**.

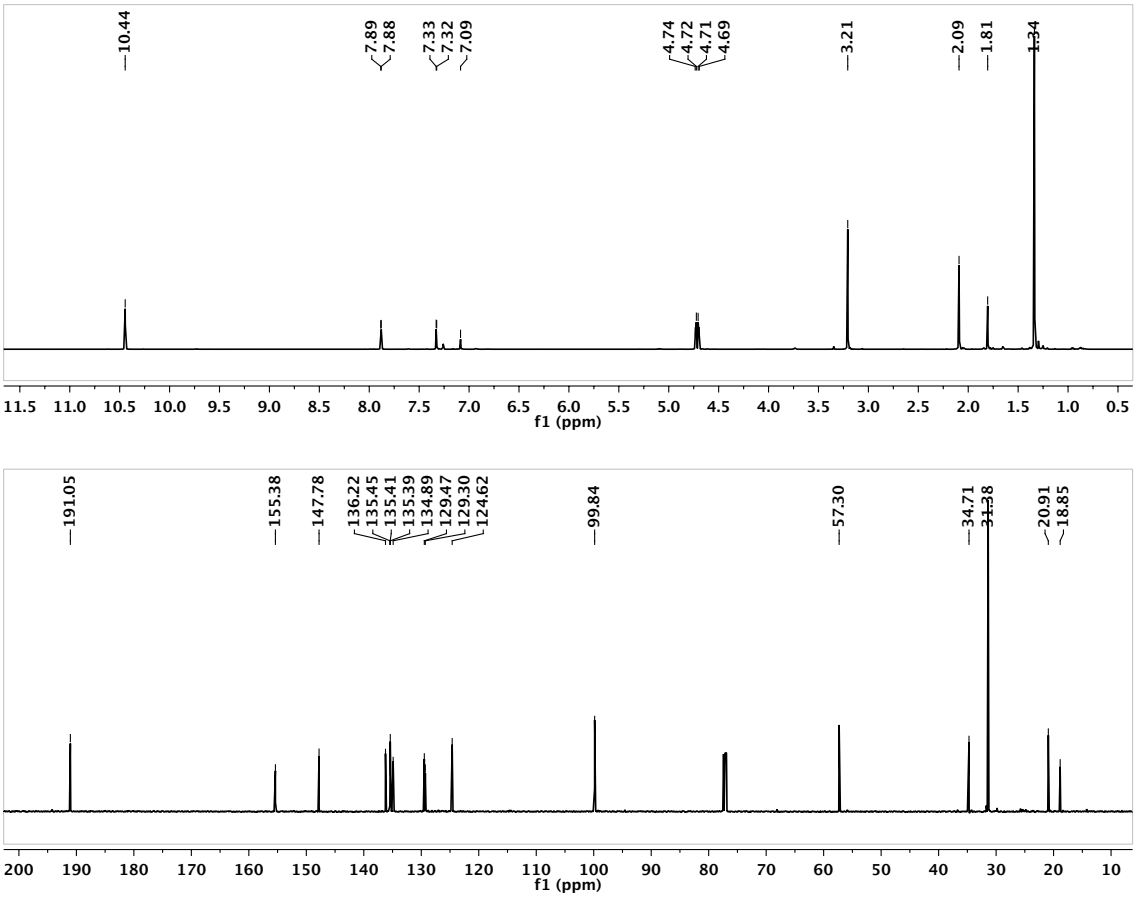

Figure C.43. ^{1}H (above) and ^{13}C (below) NMR spectra of compound **38-a** in $CDCl_3$.

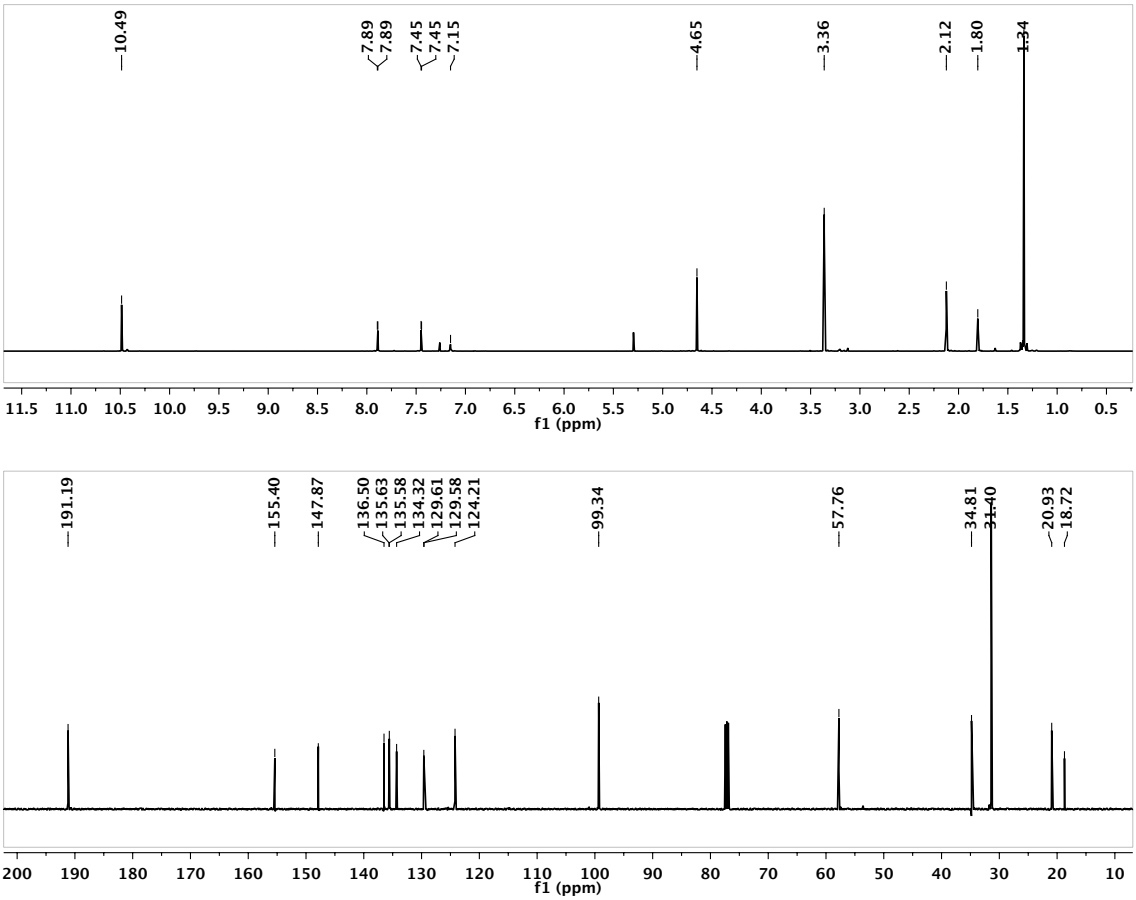

Figure C.44. ^{1}H (above) and ^{13}C (below) NMR spectra of compound **38-s** in $CDCl_3$.

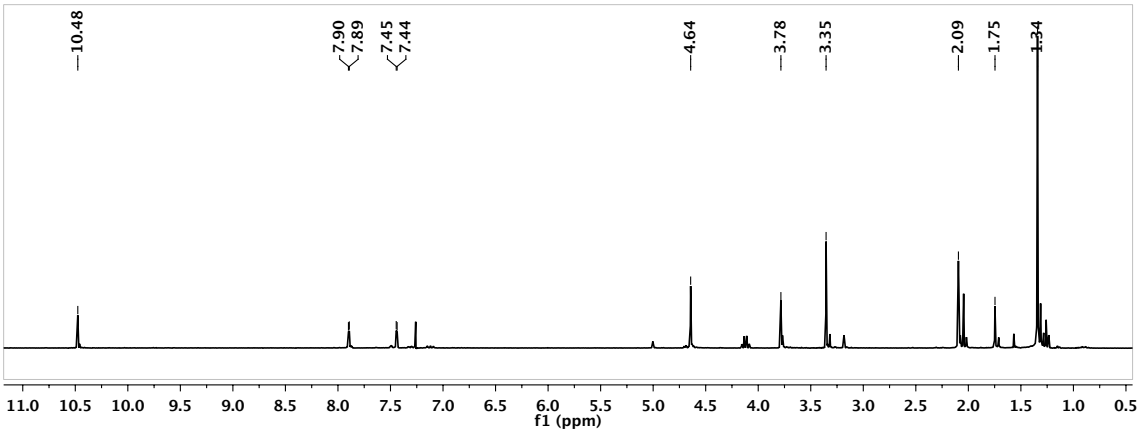

Figure C.45. ^{1}H NMR spectrum of compound **39-s** in $CDCl_3$.

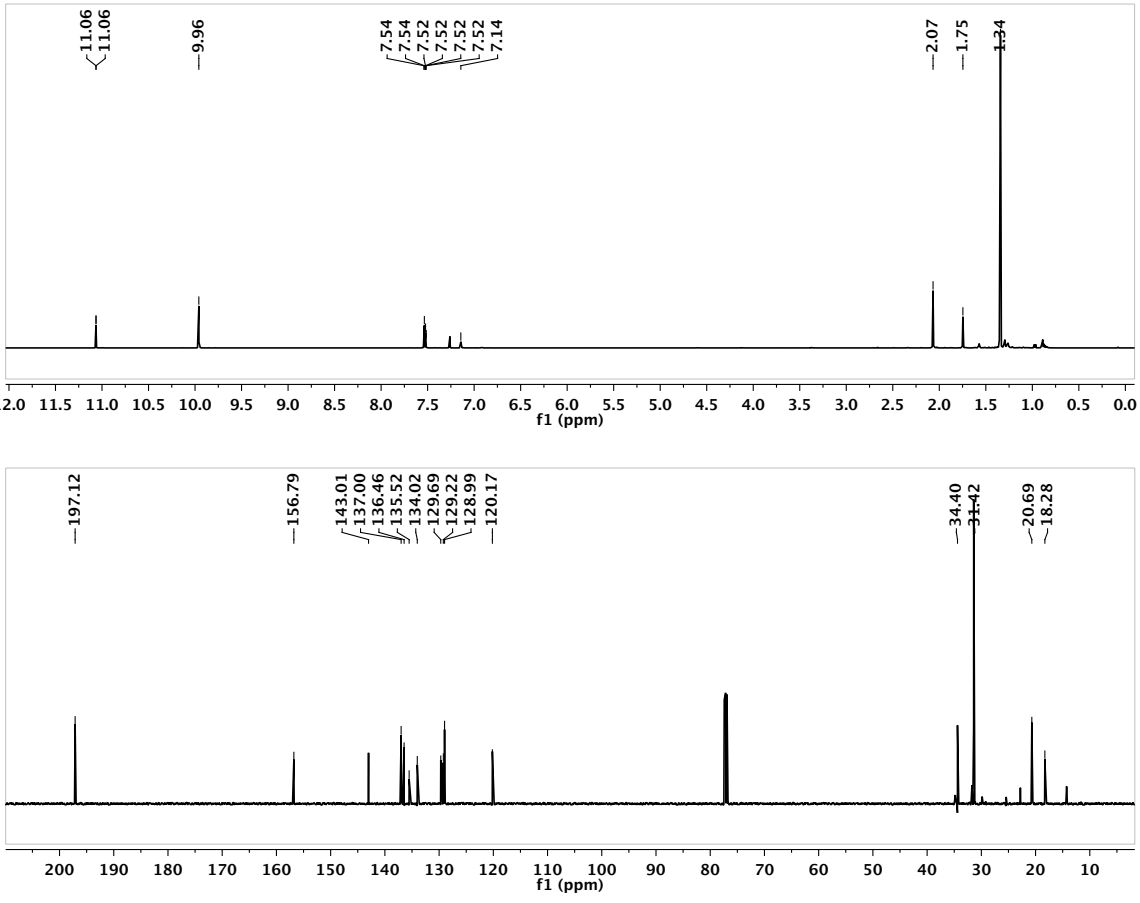

Figure C.46. ^{1}H (above) and ^{13}C (below) NMR spectra of compound **40-a** in $CDCl_3$.

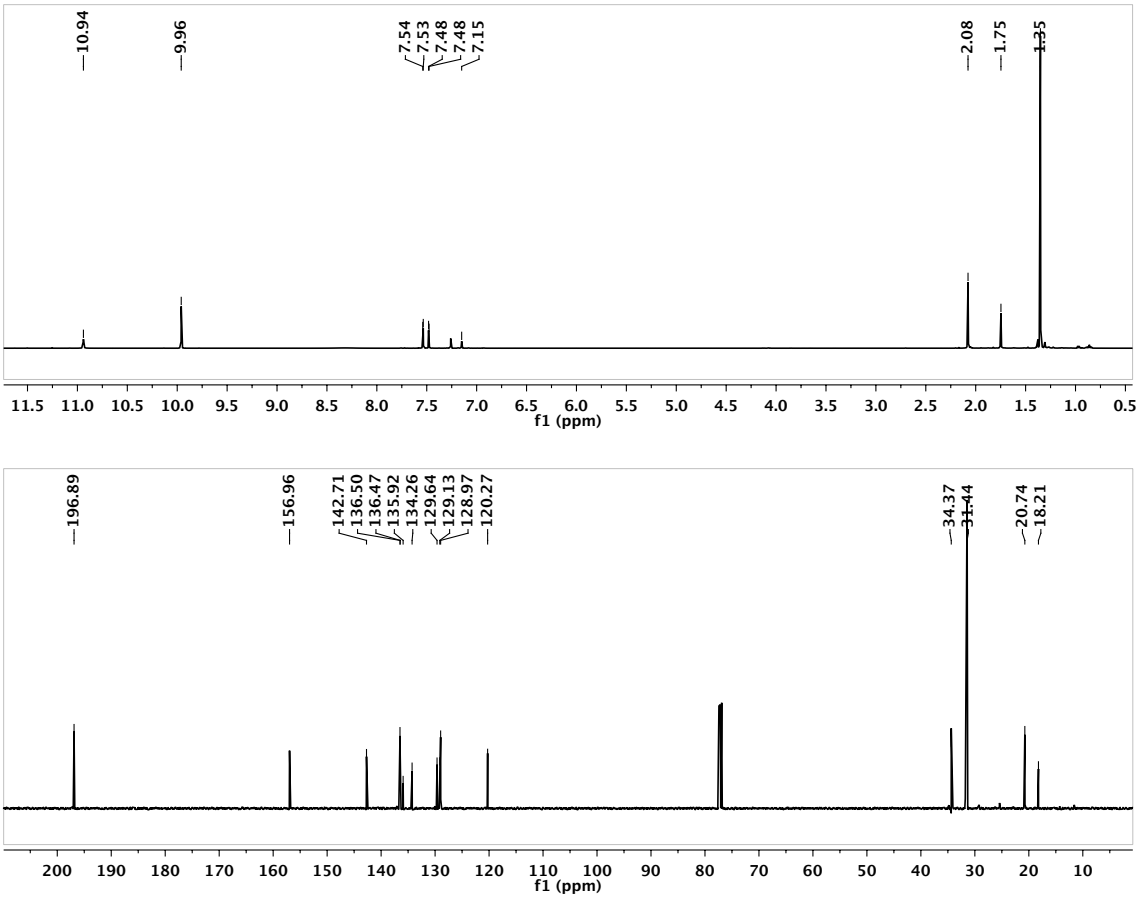

Figure C.47. ^{1}H (above) and ^{13}C (below) NMR spectra of compound **40-s** in $CDCl_3$.

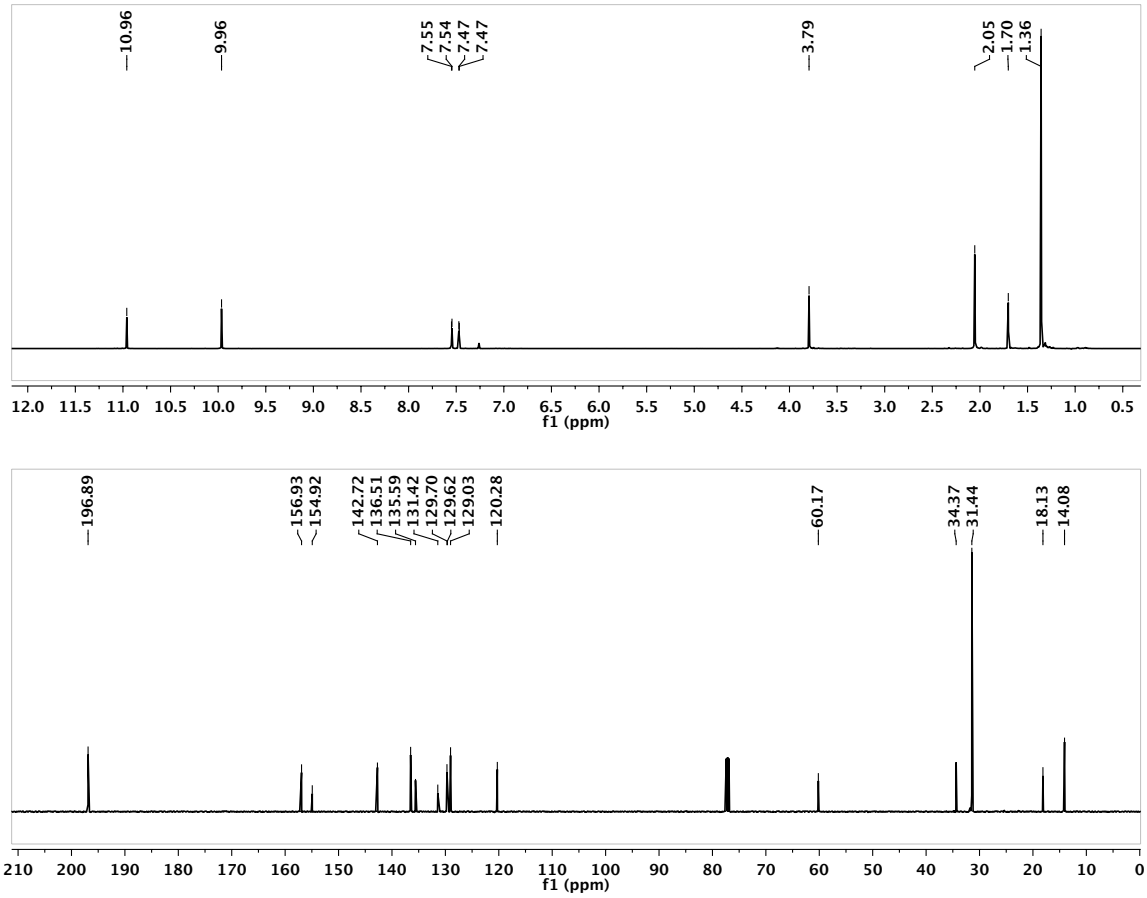

Figure C.48. ^{1}H (above) and ^{13}C (below) NMR spectra of compound **41-s** in $CDCl_3$.

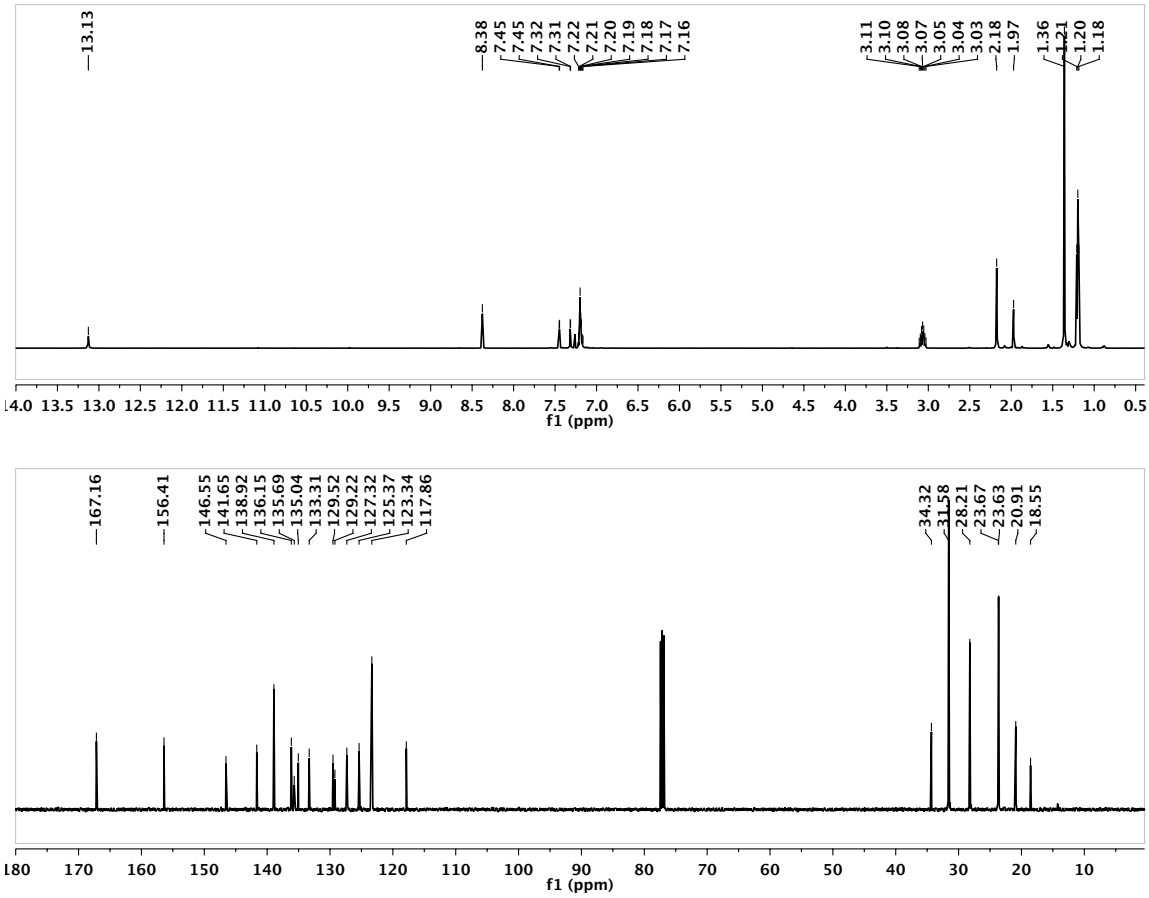

Figure C.49. ^{1}H (above) and ^{13}C (below) NMR spectra of compound **42-a** in $CDCl_3$.

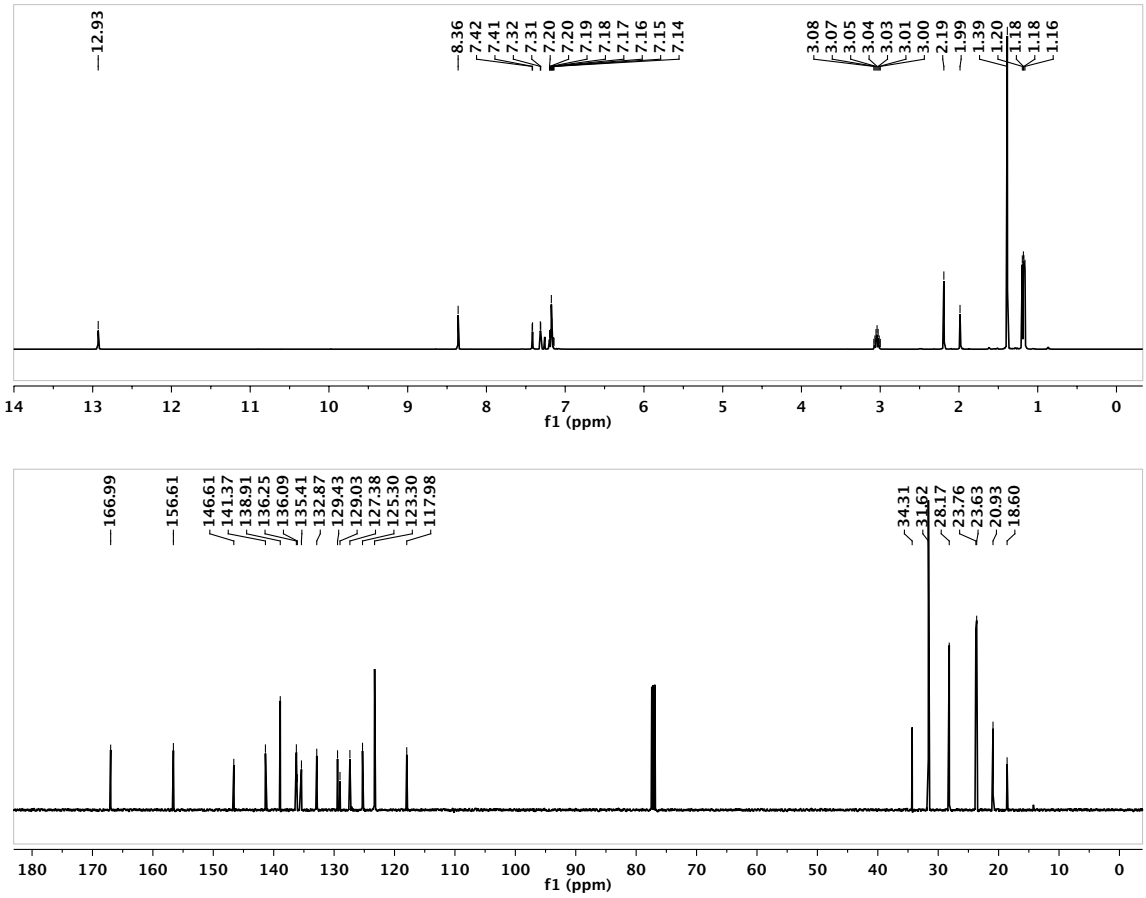

Figure C.50. ^{1}H (above) and ^{13}C (below) NMR spectra of compound **42-s** in $CDCl_3$.

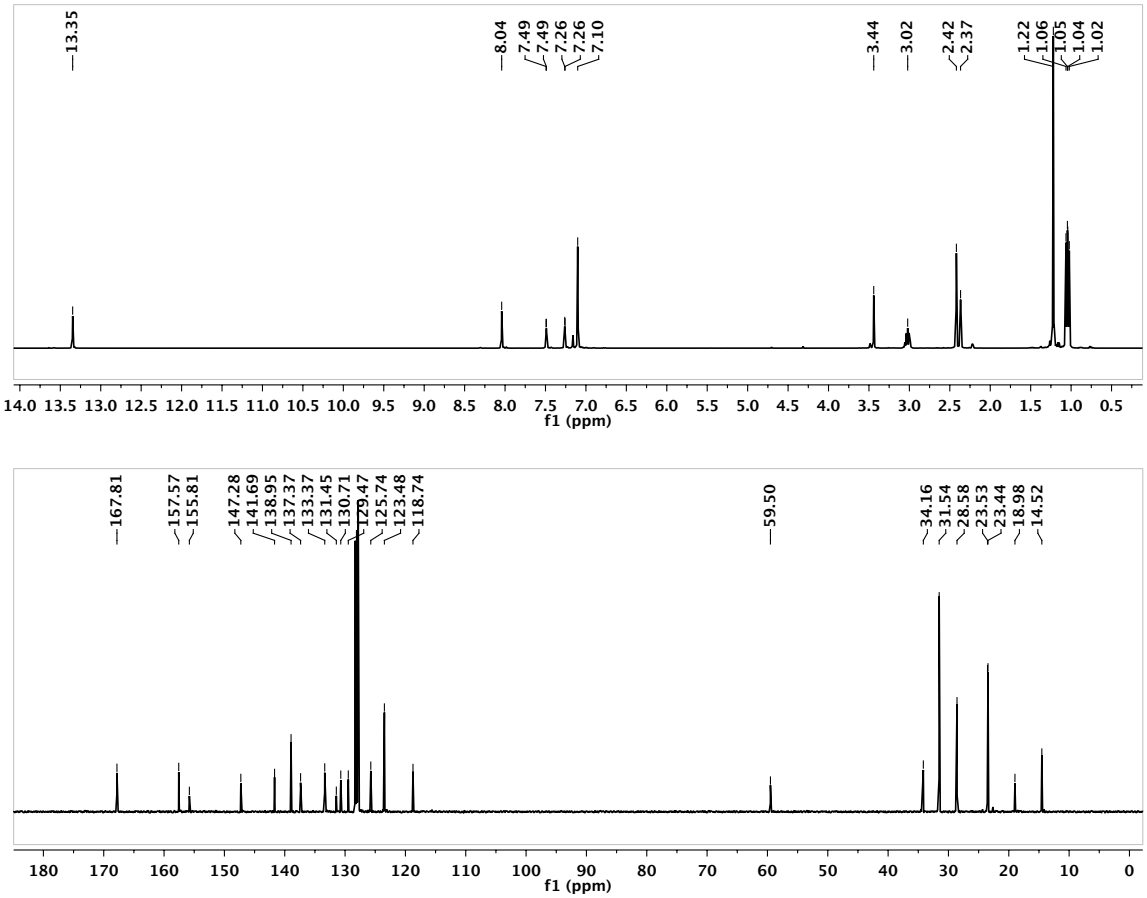

Figure C.51. ^{1}H (above) and ^{13}C (below) NMR spectra of compound **43-s** in C_6D_6.

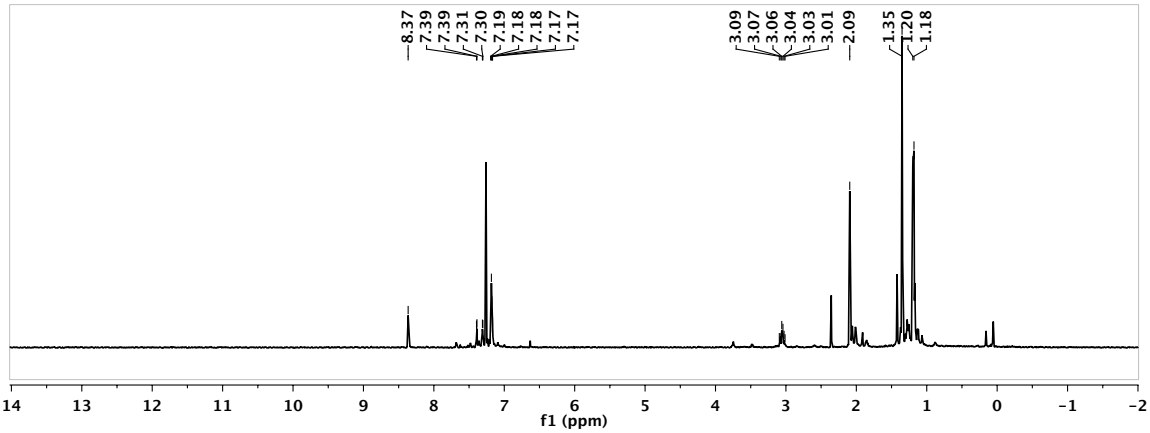

Figure C.52. ^{1}H NMR spectrum in $CDCl_3$ of the deprotonation of compound **7-a**.

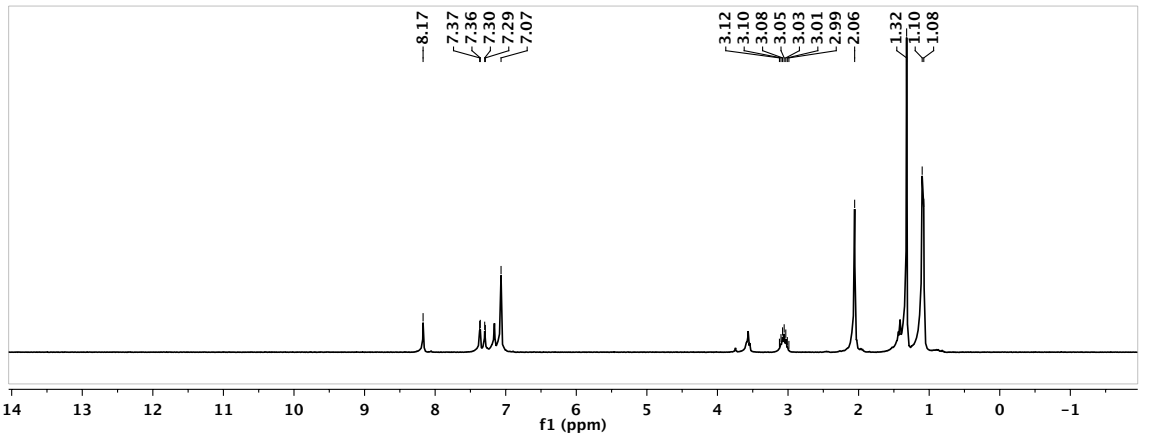

Figure C.53. ^{1}H NMR spectrum in $CDCl_3$ of the deprotonation of compound **7-s**.

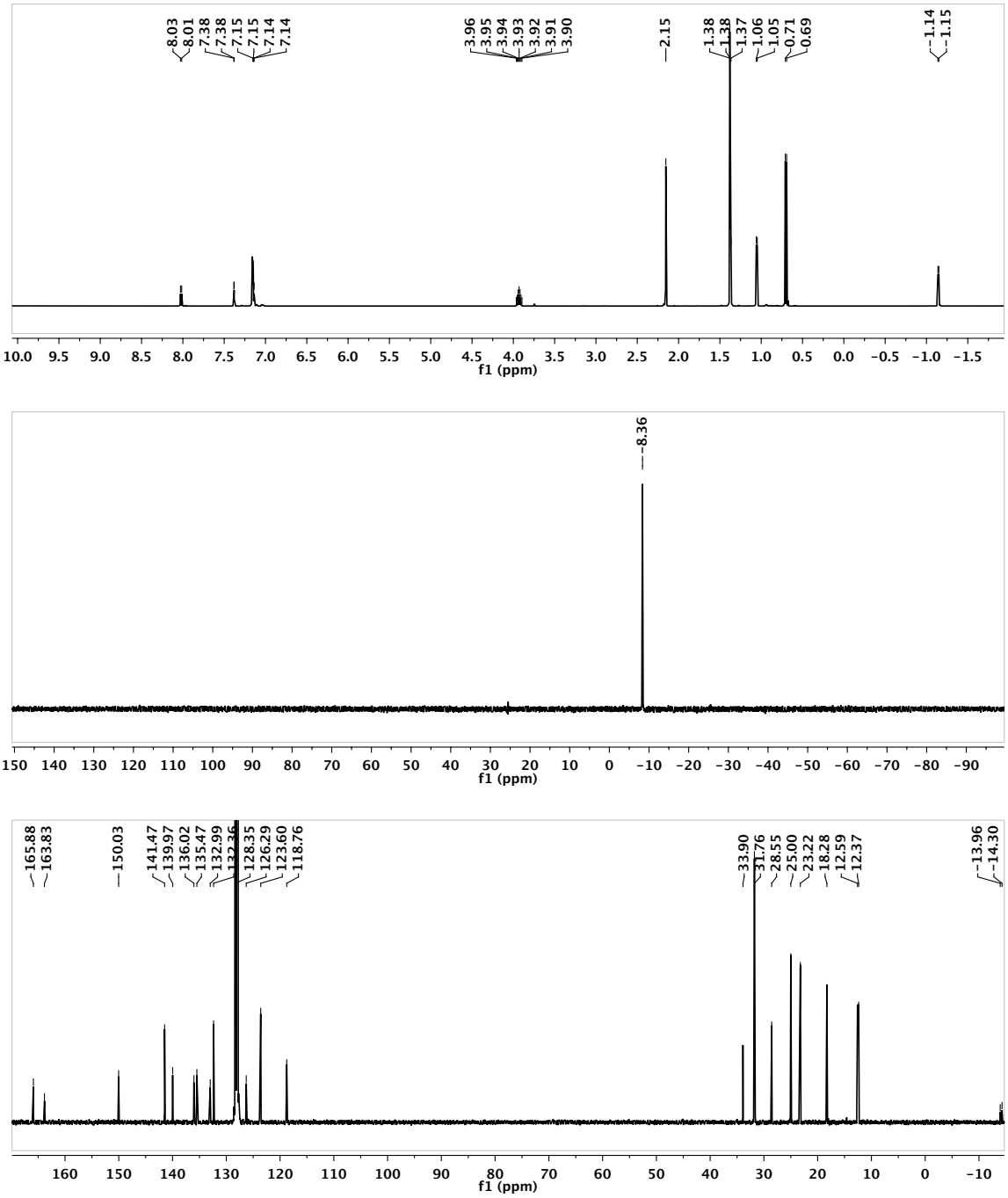

Figure C.54. ^{1}H (top), ^{31}P (middle) and ^{13}C (bottom) NMR spectra of compound **44-a** in C_6D_6.

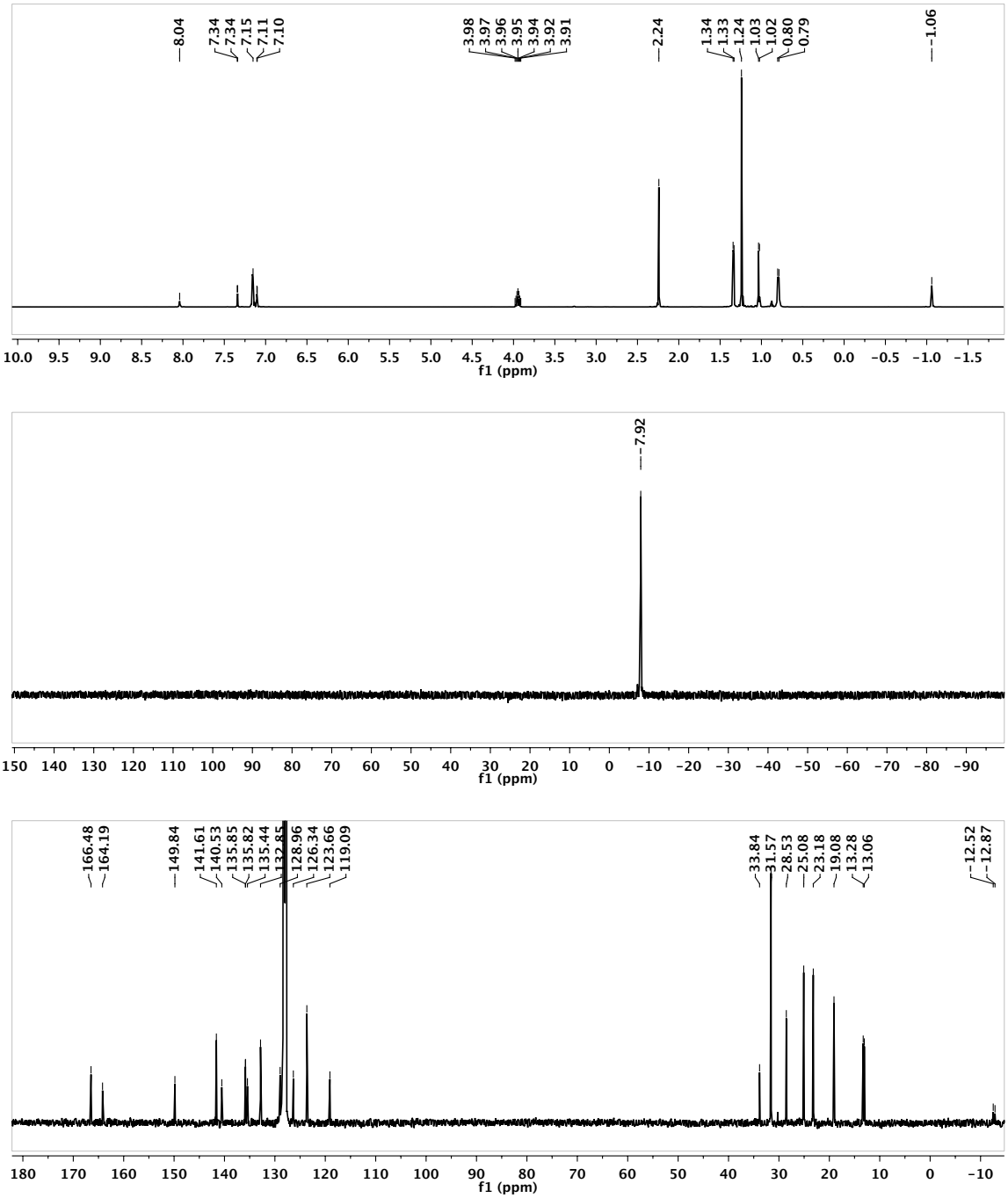

Figure C.55. ^{1}H (top), ^{31}P (middle) and ^{13}C (bottom) NMR spectra of compound **44-s** in C_6D_6.

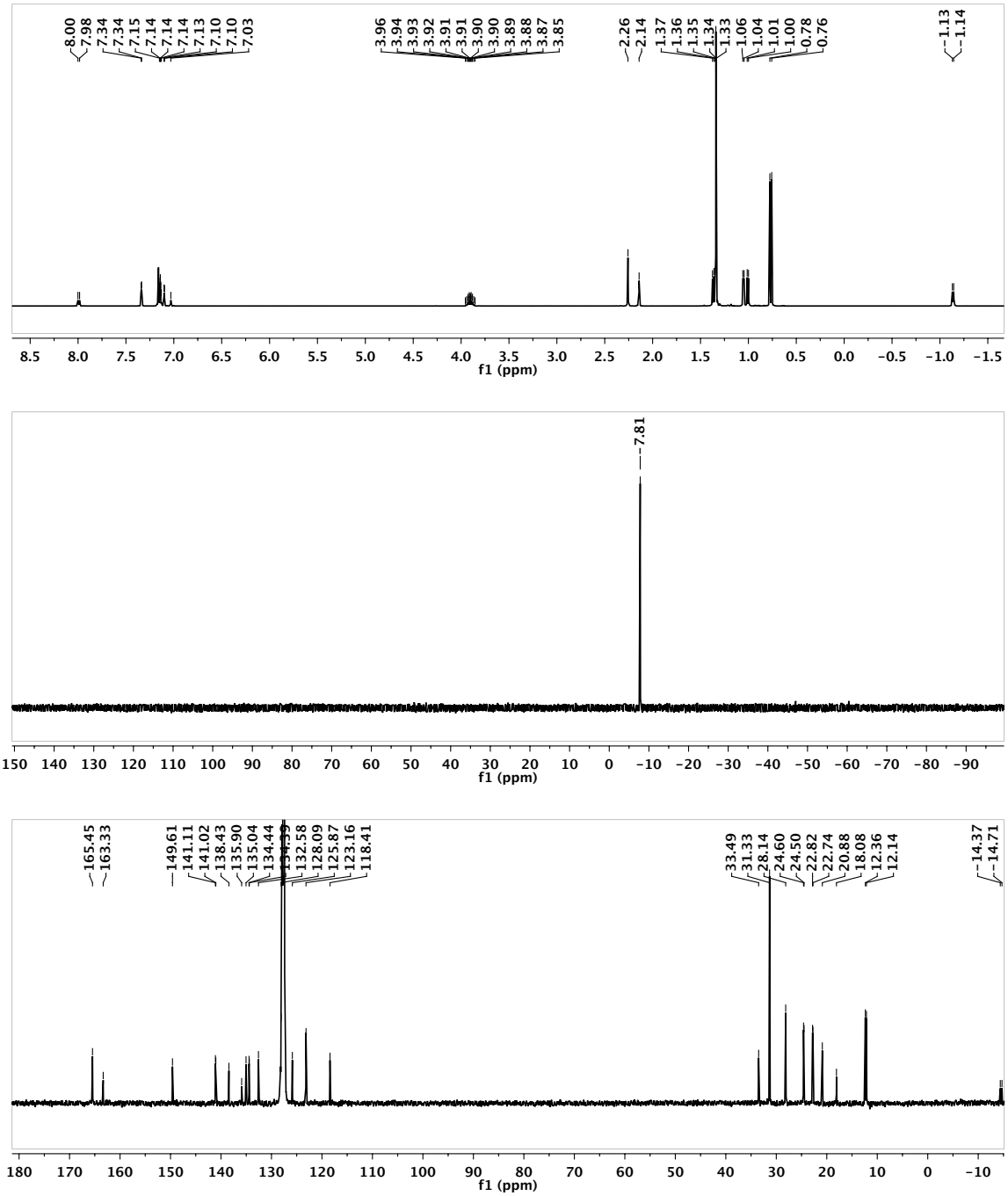

Figure C.56. ^{1}H (top), ^{31}P (middle) and ^{13}C (bottom) NMR spectra of compound **45-a** in C_6D_6.

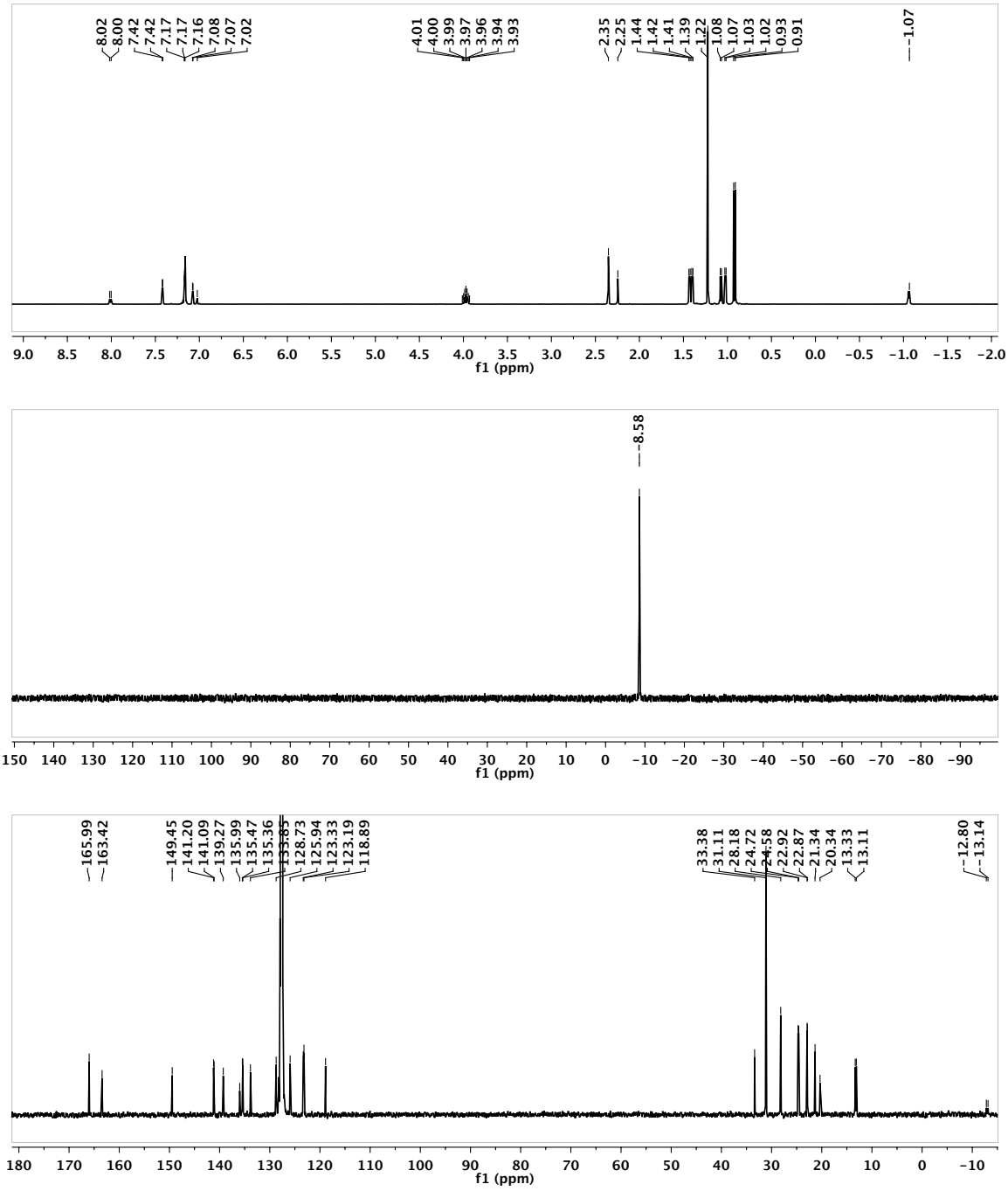

Figure C.57. ^{1}H (top), ^{31}P (middle) and ^{13}C (bottom) NMR spectra of compound **45-s** in C_6D_6.

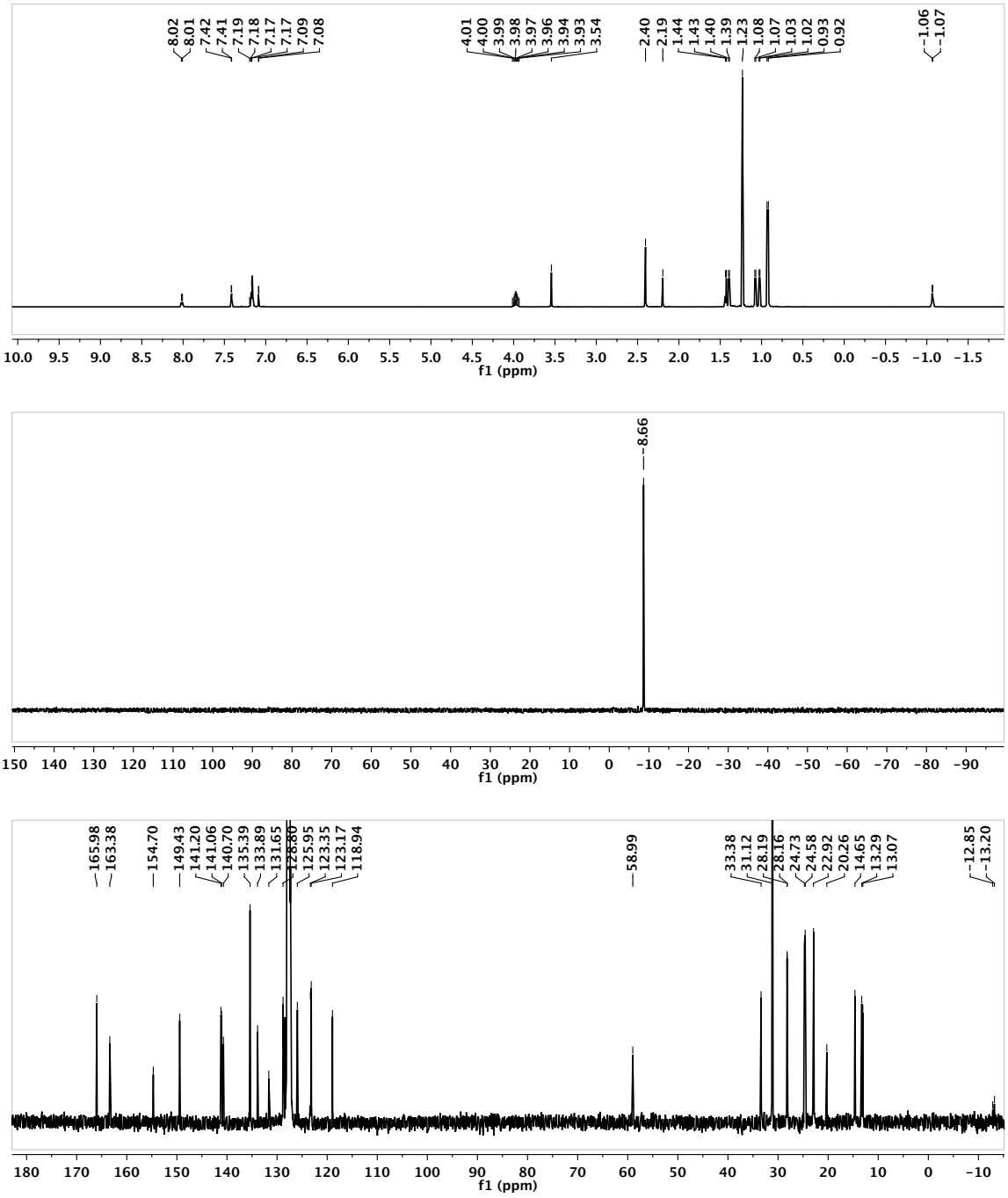

Figure C.58. ^{1}H (top), ^{31}P (middle) and ^{13}C (bottom) NMR spectra of compound **46-s** in C_6D_6.

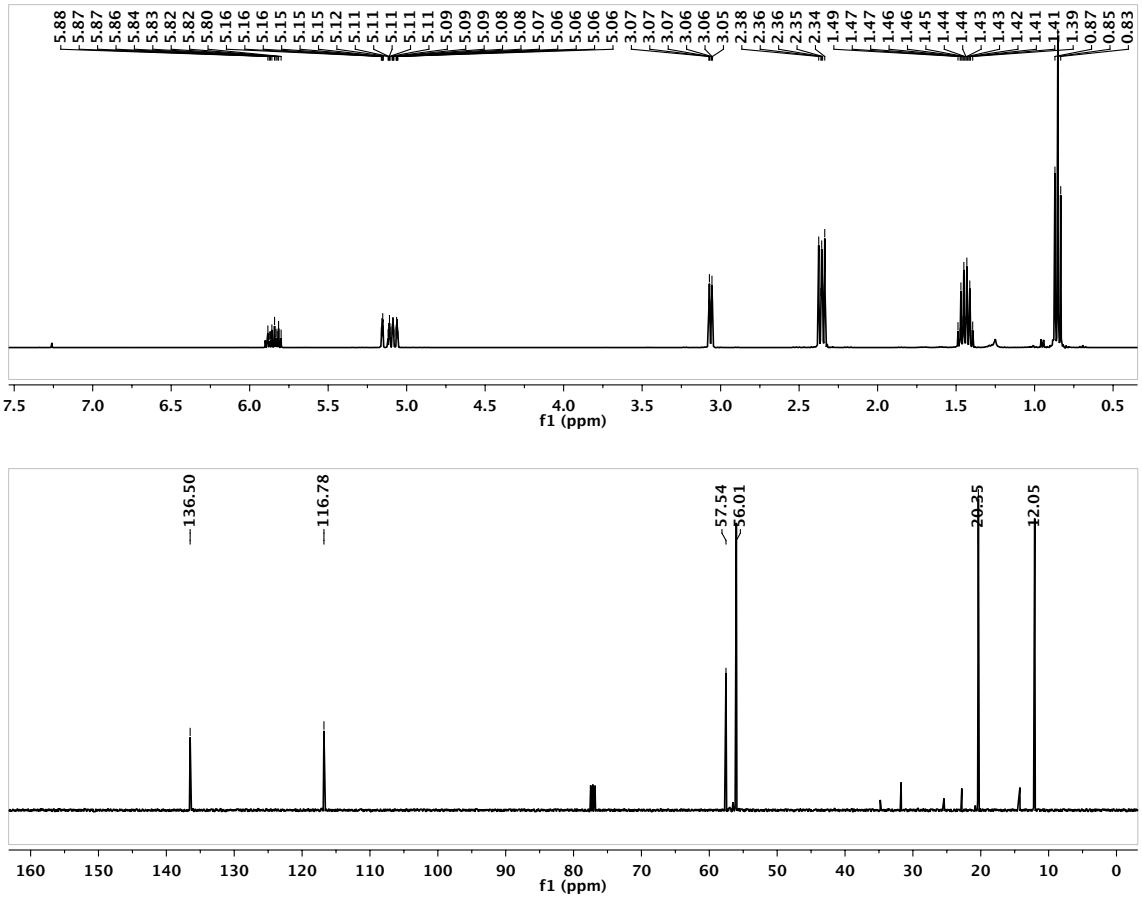

Figure C.59. ^{1}H (above) and ^{13}C (below) NMR spectra of **N(allyl)(ⁿPr)$_2$** in $CDCl_3$.

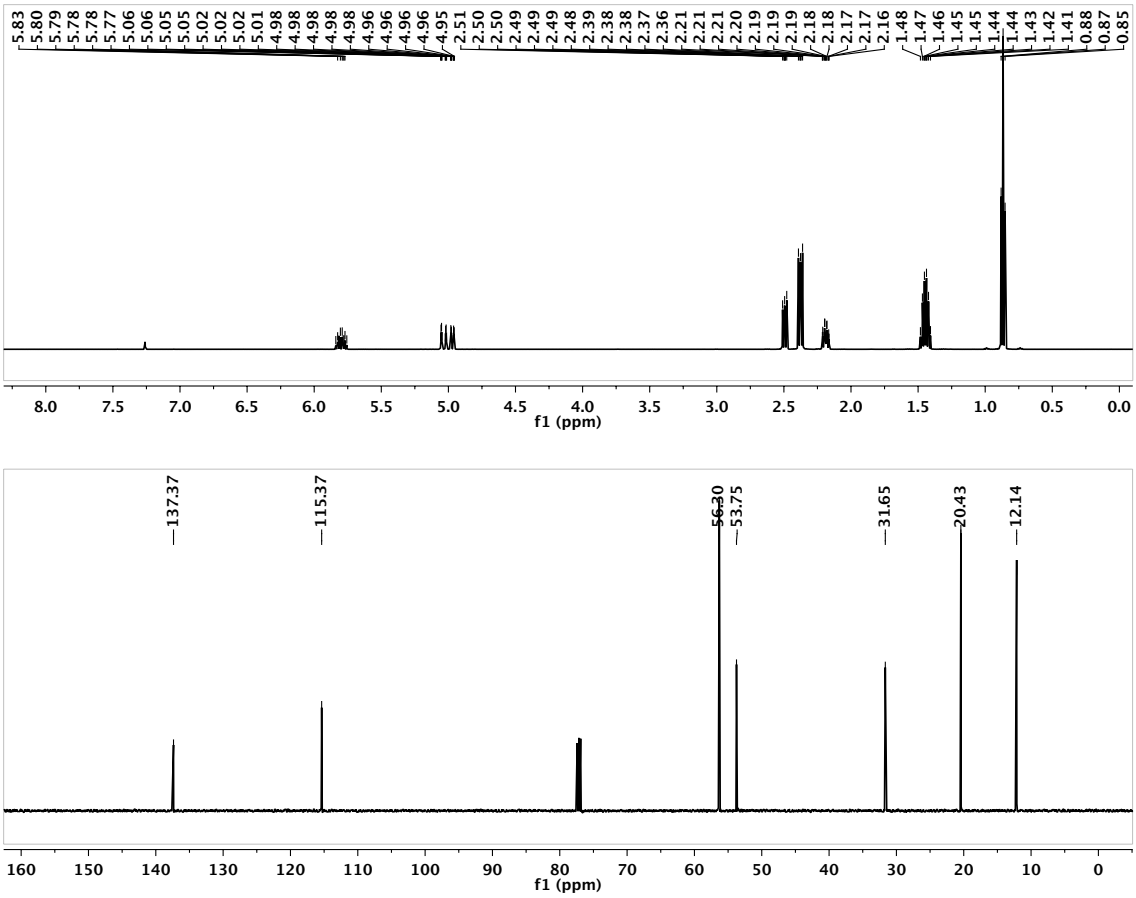

Figure C.60. ^{1}H (above) and ^{13}C (below) NMR spectra of **N(butenyl)(″Pr)$_2$** in $CDCl_3$.

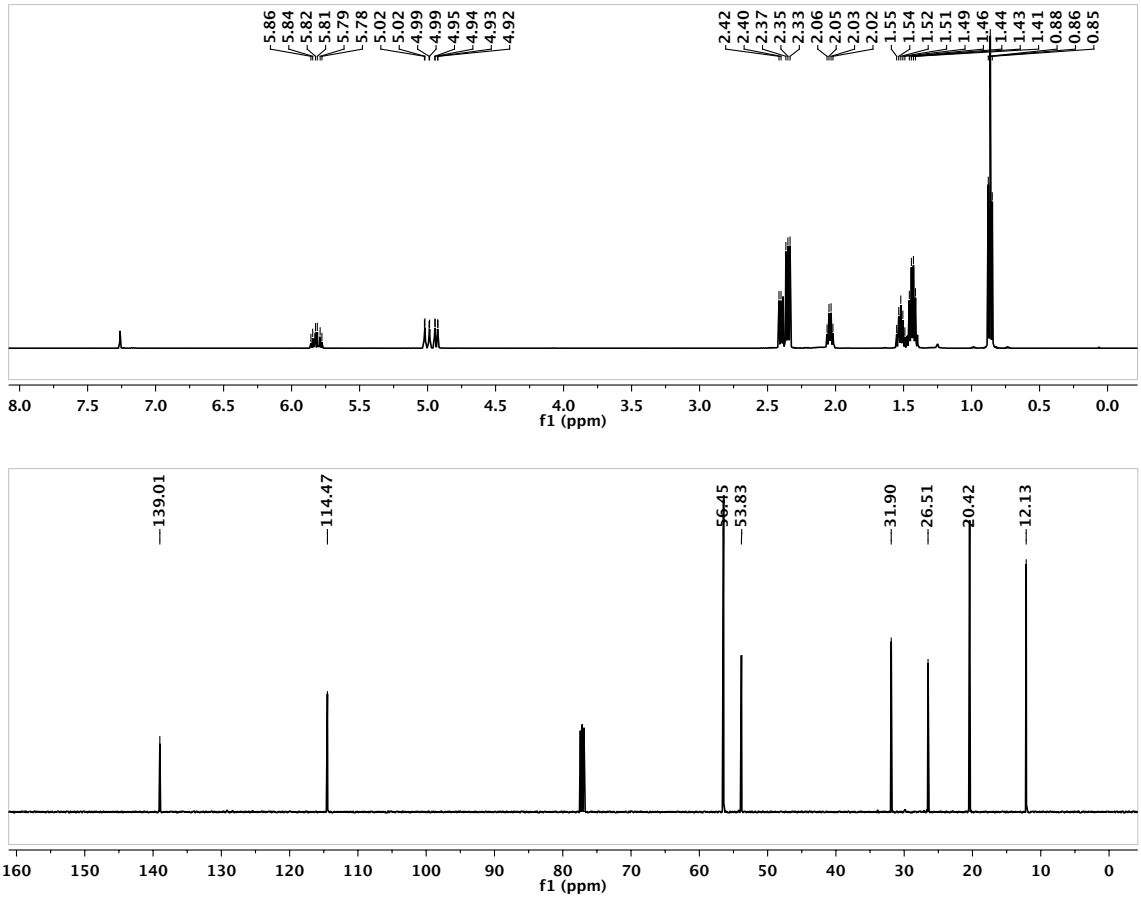

Figure C.61. ^{1}H (above) and ^{13}C (below) NMR spectra of **N(pentenyl)(″Pr)$_2$** in $CDCl_3$.

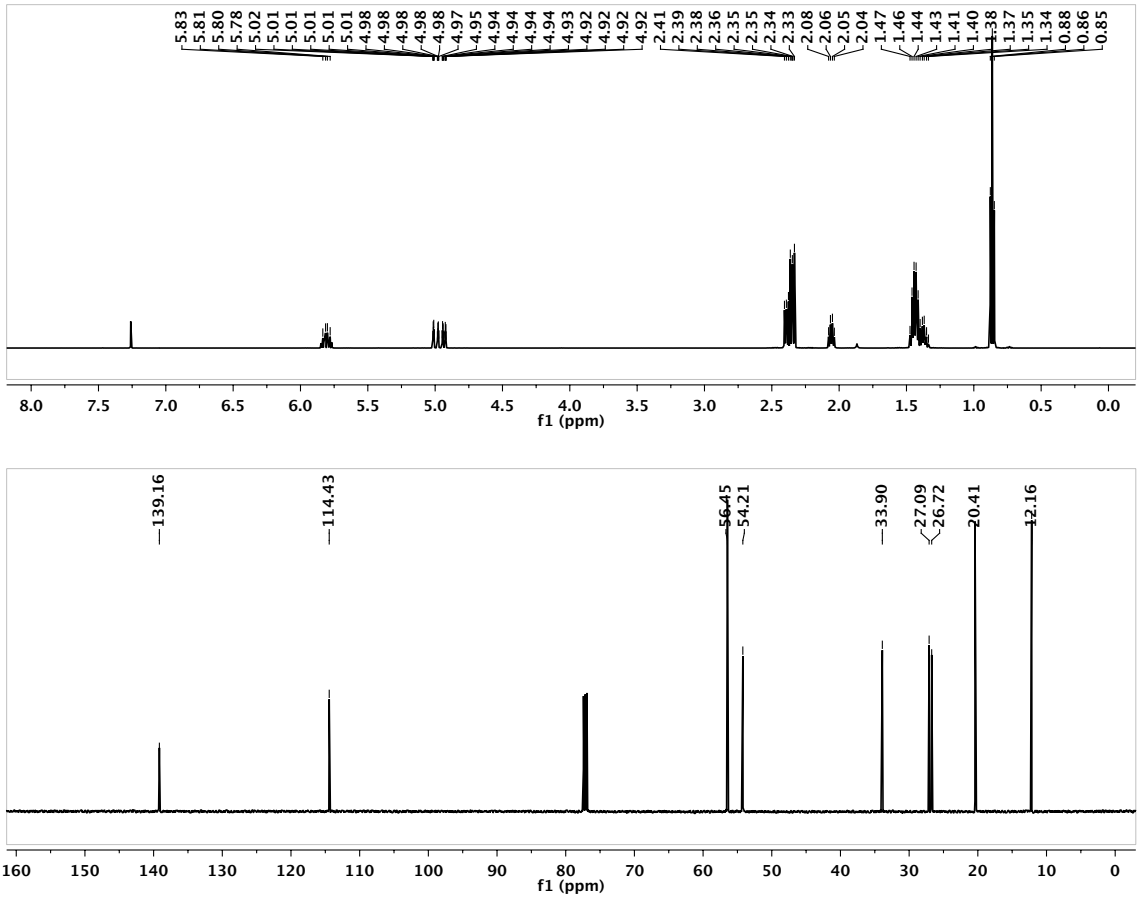

Figure C.62. ^{1}H (above) and ^{13}C (below) NMR spectra of **N(hexenyl)(″Pr)$_2$** in $CDCl_3$.

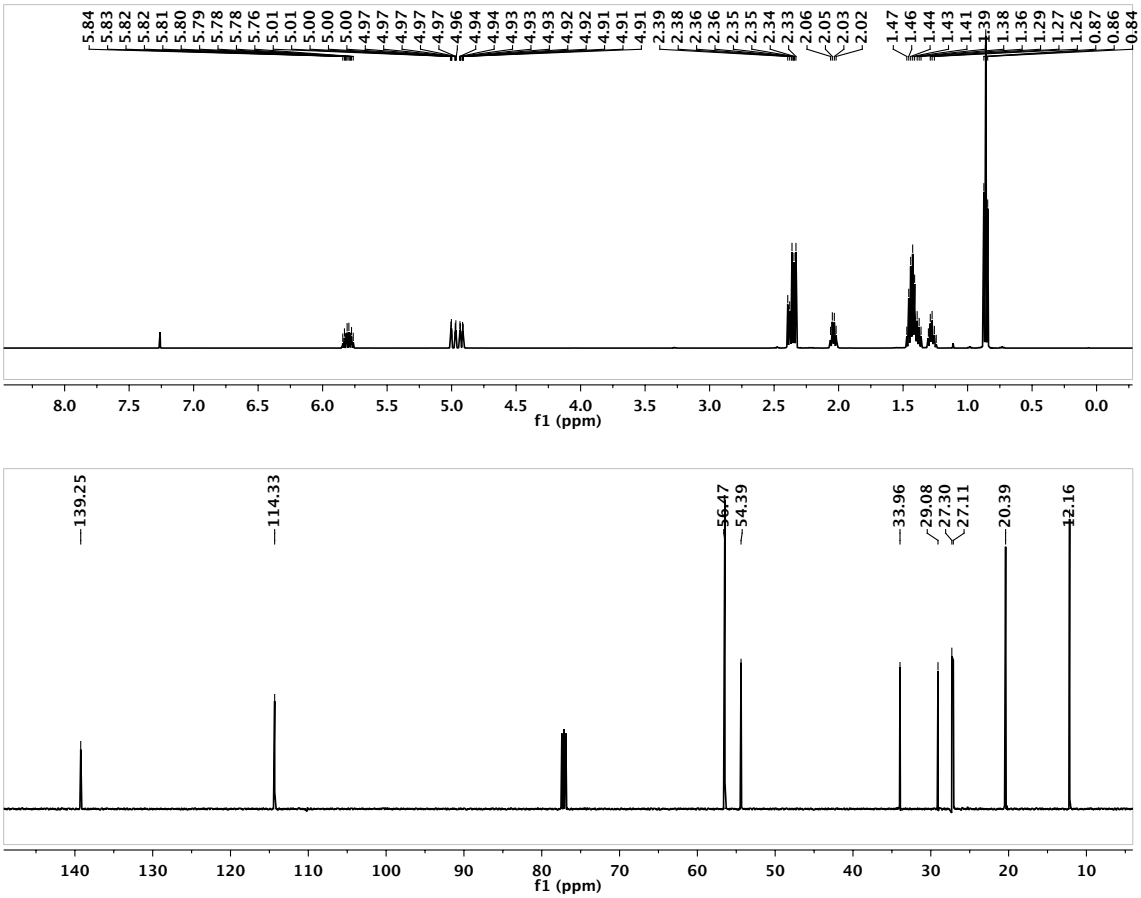

Figure C.63. ^{1}H (above) and ^{13}C (below) NMR spectra of **N(heptenyl)(″Pr)$_2$** in $CDCl_3$.

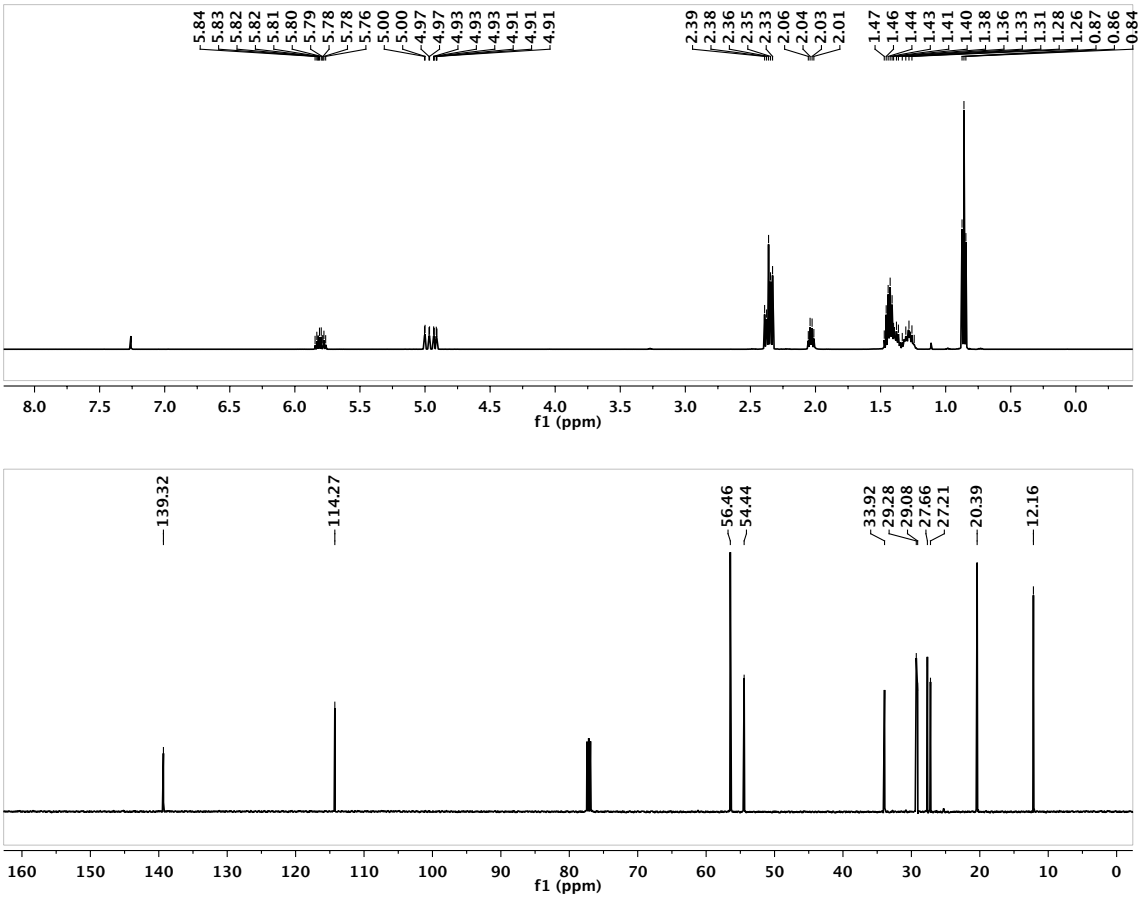

Figure C.64. ^{1}H (above) and ^{13}C (below) NMR spectra of **N(octenyl)(″Pr)$_2$** in $CDCl_3$.

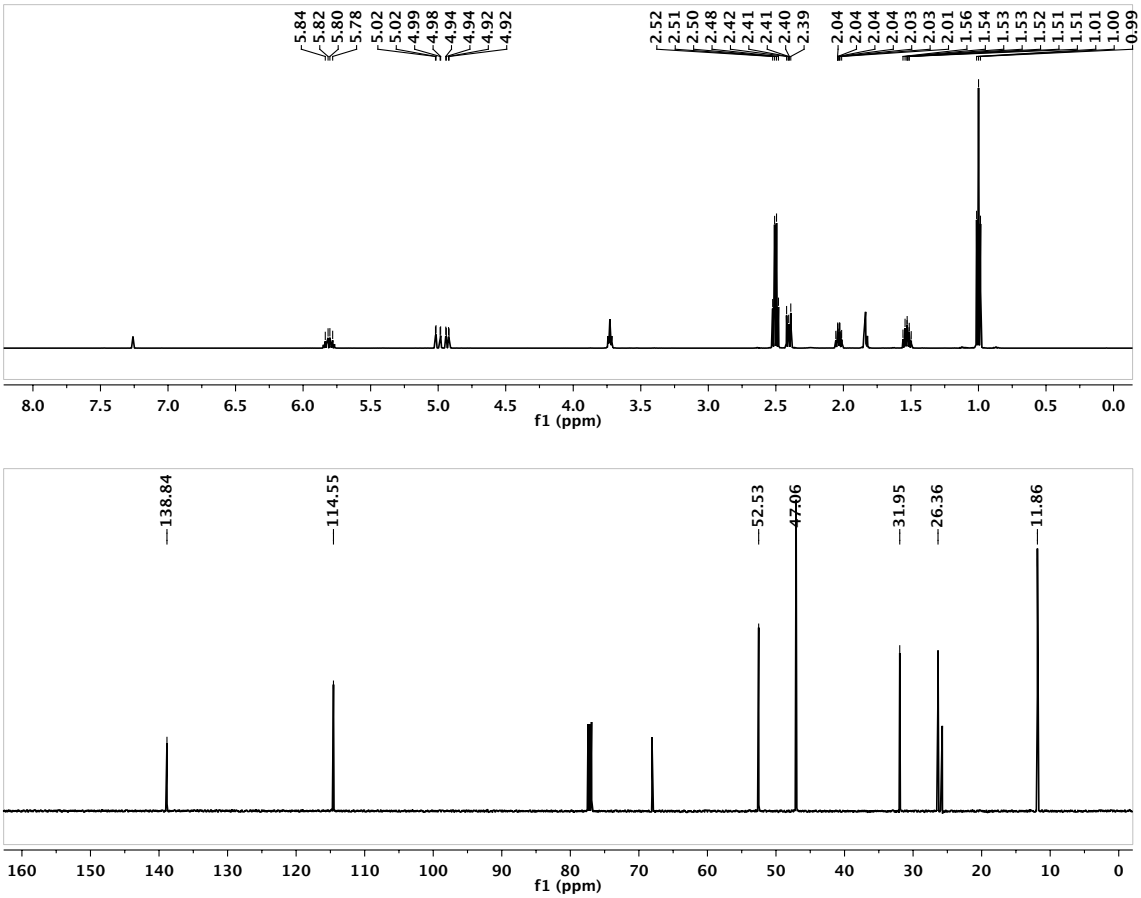

Figure C.65. ^{1}H (above) and ^{13}C (below) NMR spectra of **N(pentenyl)(Et)$_2$** in $CDCl_3$.

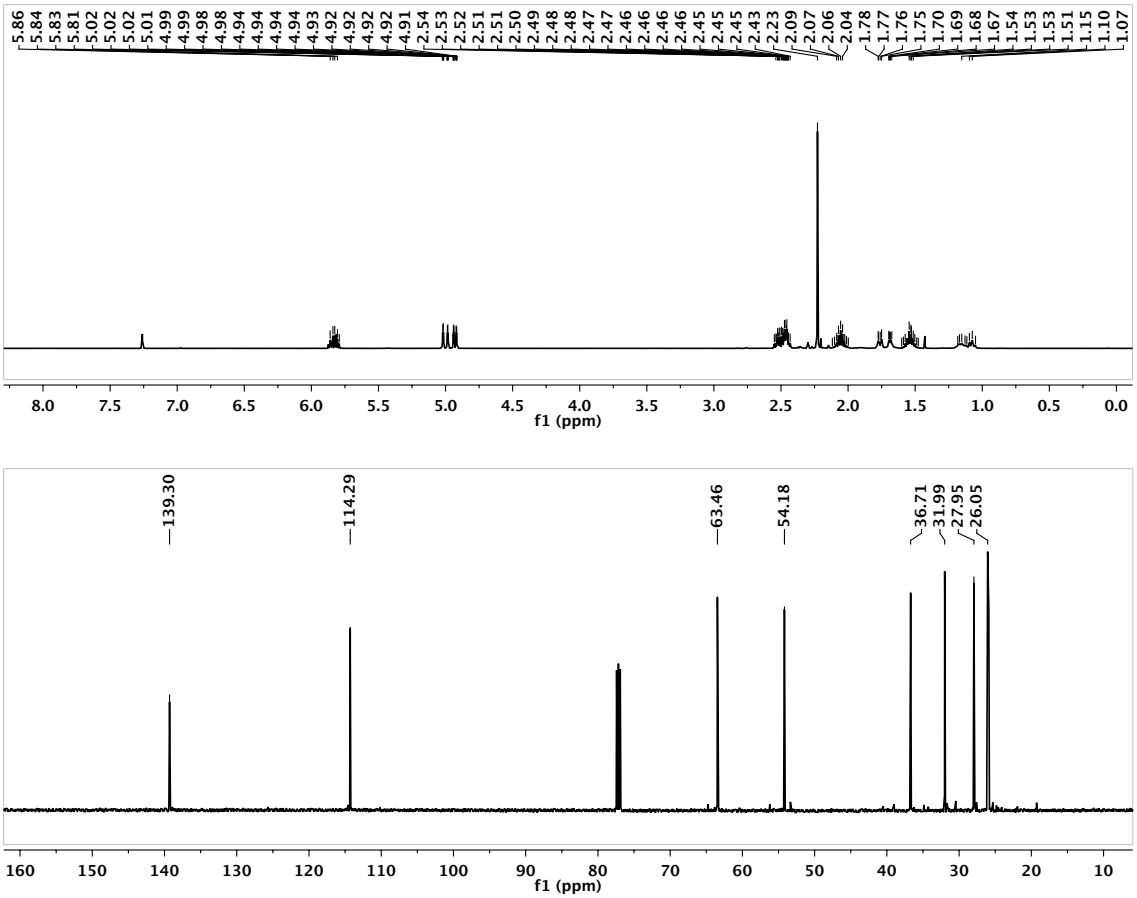

Figure C.66. ^{1}H (above) and ^{13}C (below) NMR spectra of **(*R,R*)-*N,N'*-dipentenyl-*N,N'*-dimethylcyclohexane-1,2-diamine** in $CDCl_3$.

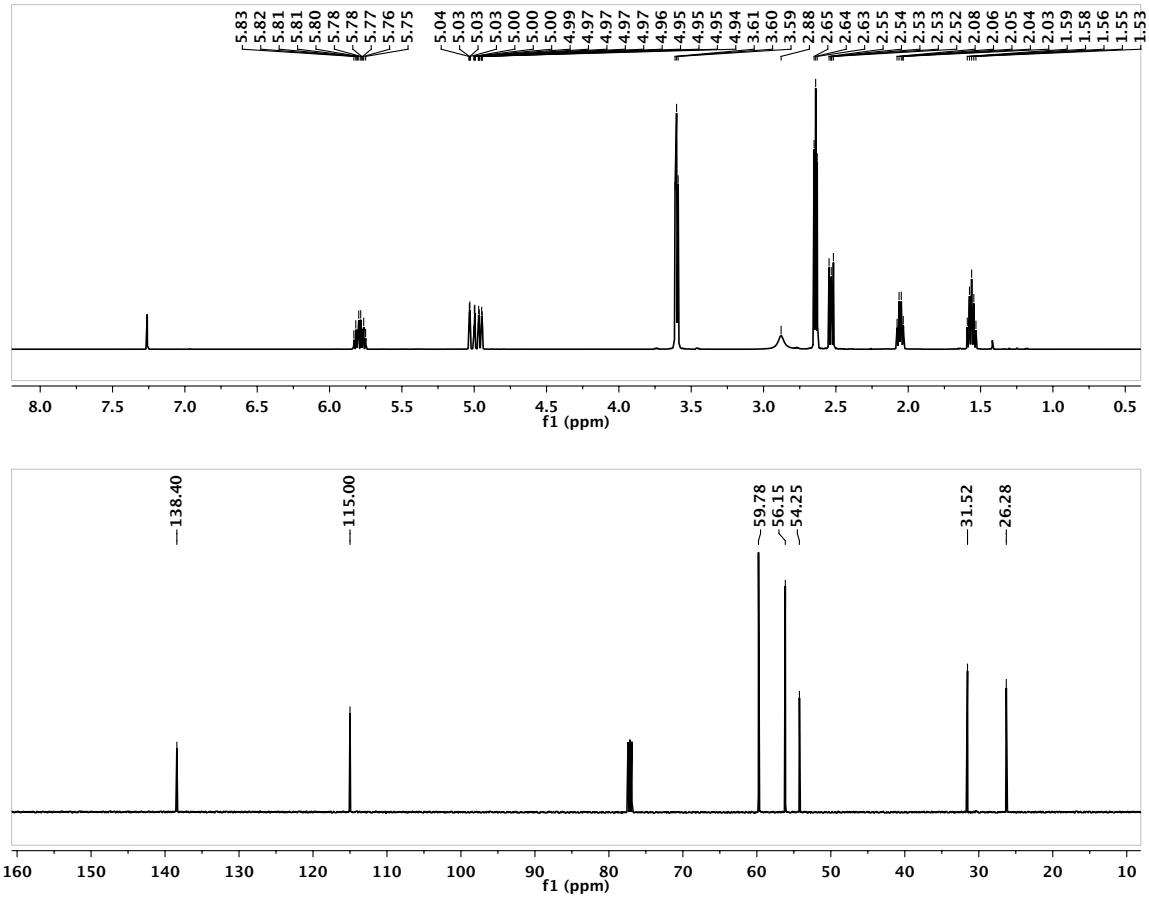

Figure C.67. ^{1}H (above) and ^{13}C (below) NMR spectra of **N(pentenyl)(CH_2CH_2OH)$_2$** in $CDCl_3$.

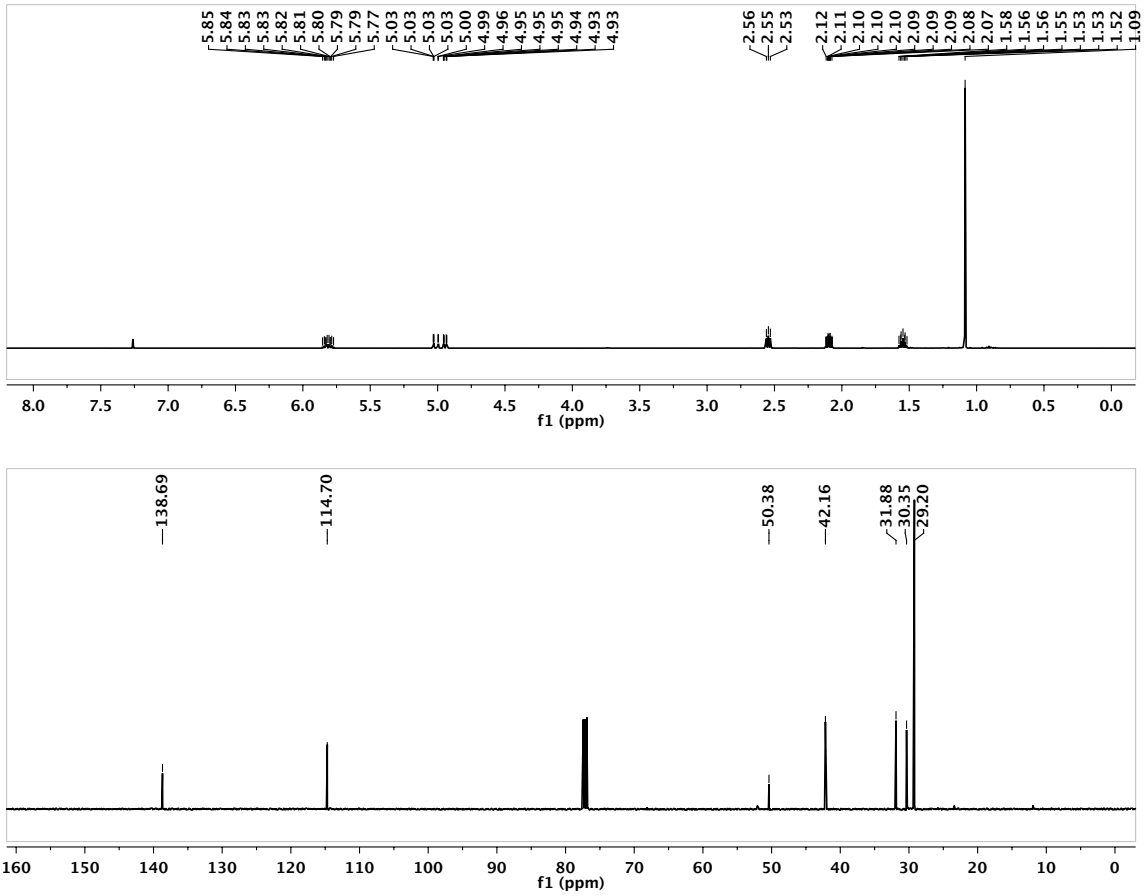

Figure C.68. ^{1}H (above) and ^{13}C (below) NMR spectra of **HN(pentenyl)(*t*Bu)** in $CDCl_3$.

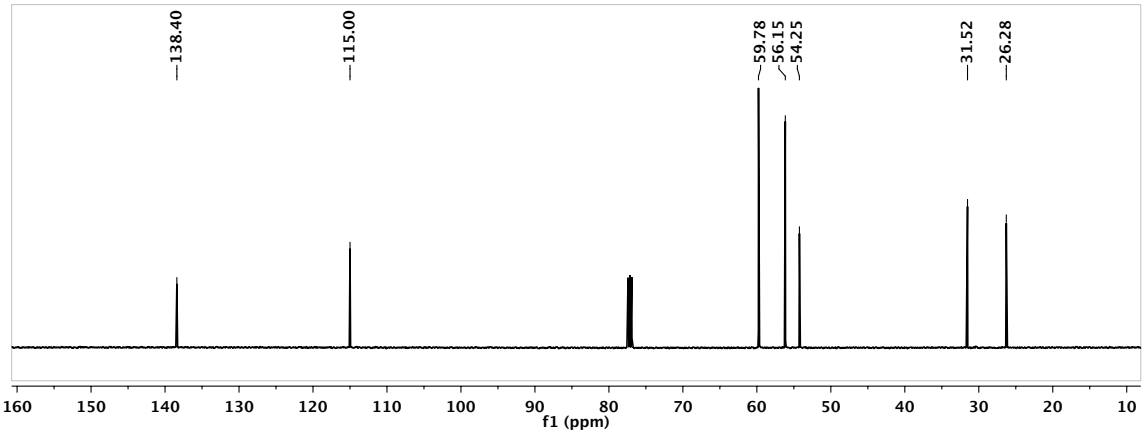

Figure C.69. ^{1}H NMR spectrum of [**N(Me)(pentenyl)(ⁿPr)$_2$][I]** in $CDCl_3$.

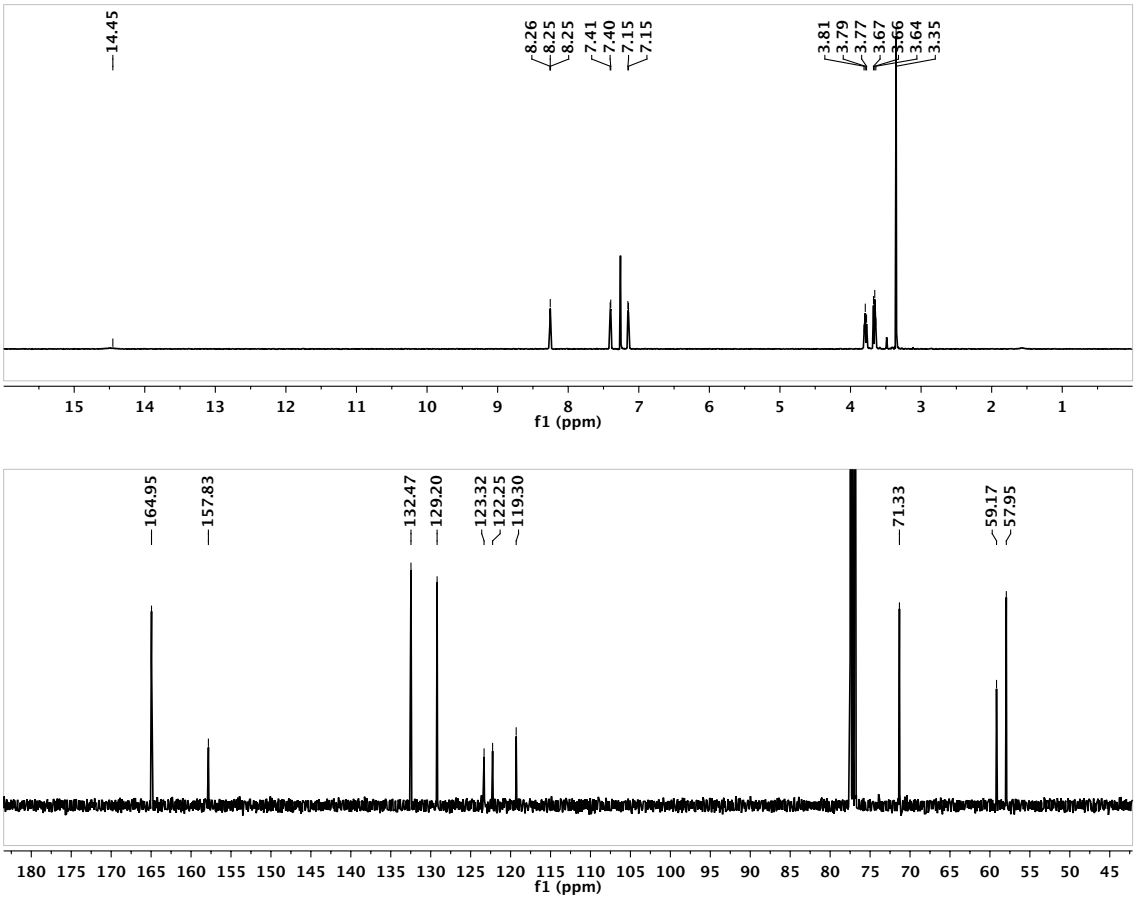

Figure C.70. ^{1}H (above) and ^{13}C (below) NMR spectra of **48a-OMe** in $CDCl_3$.

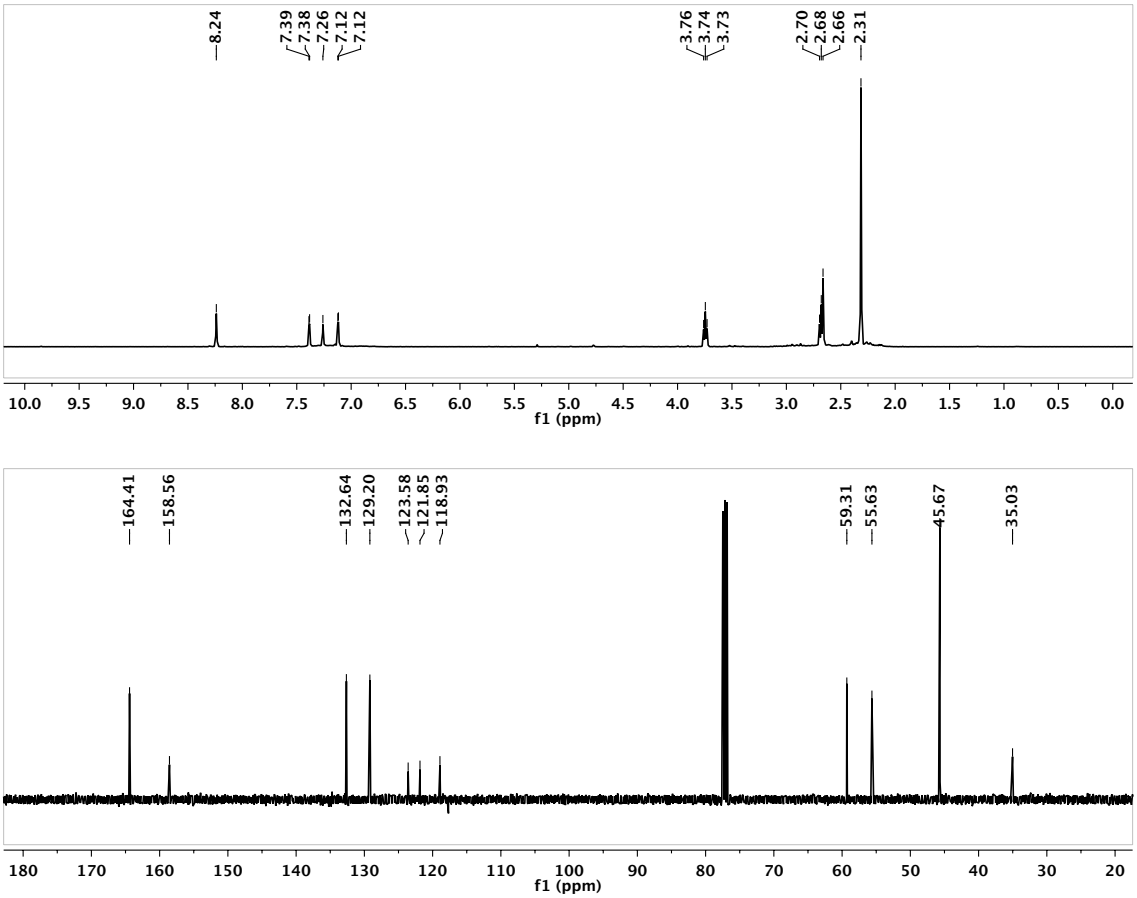

Figure C.71. ^{1}H (above) and ^{13}C (below) NMR spectra of **48a-NMe$_2$** in $CDCl_3$.

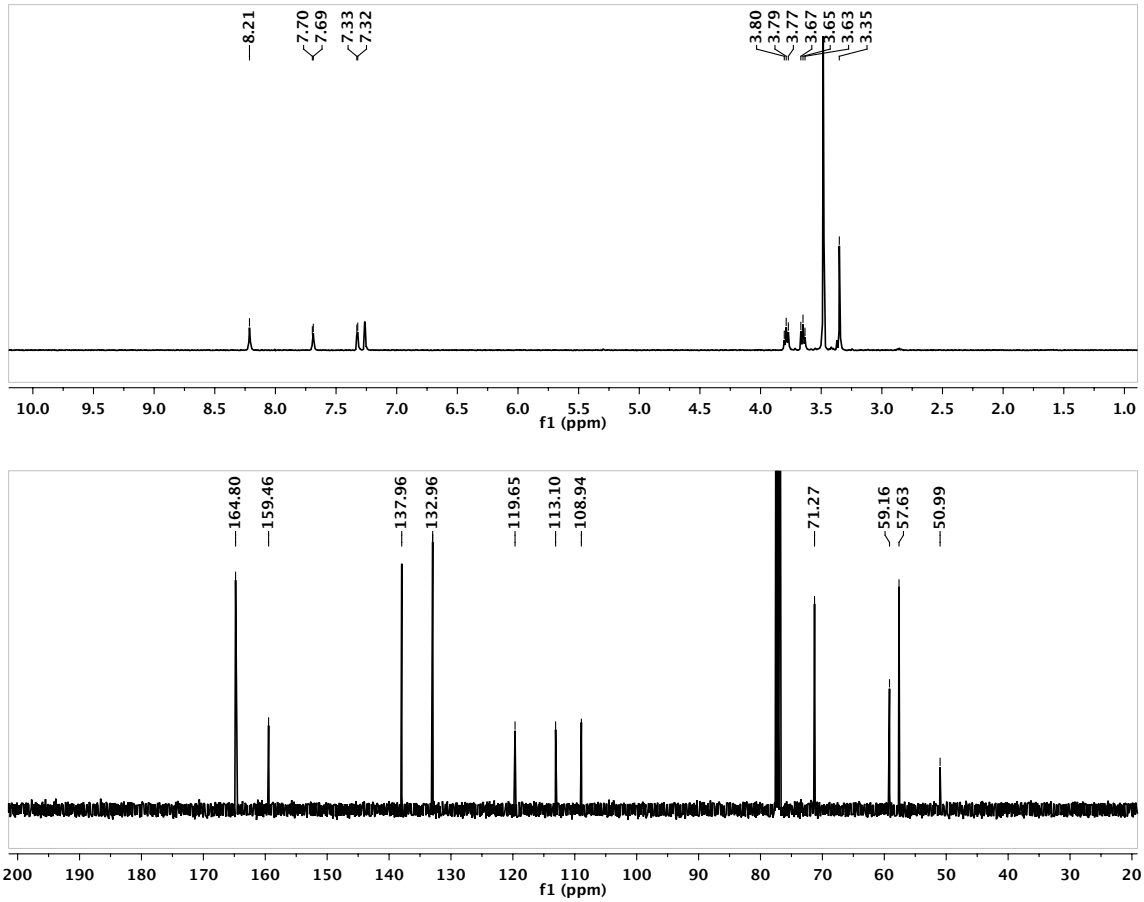

Figure C.72. ^{1}H (above) and ^{13}C (below) NMR spectra of **48b-OMe** in $CDCl_3$.

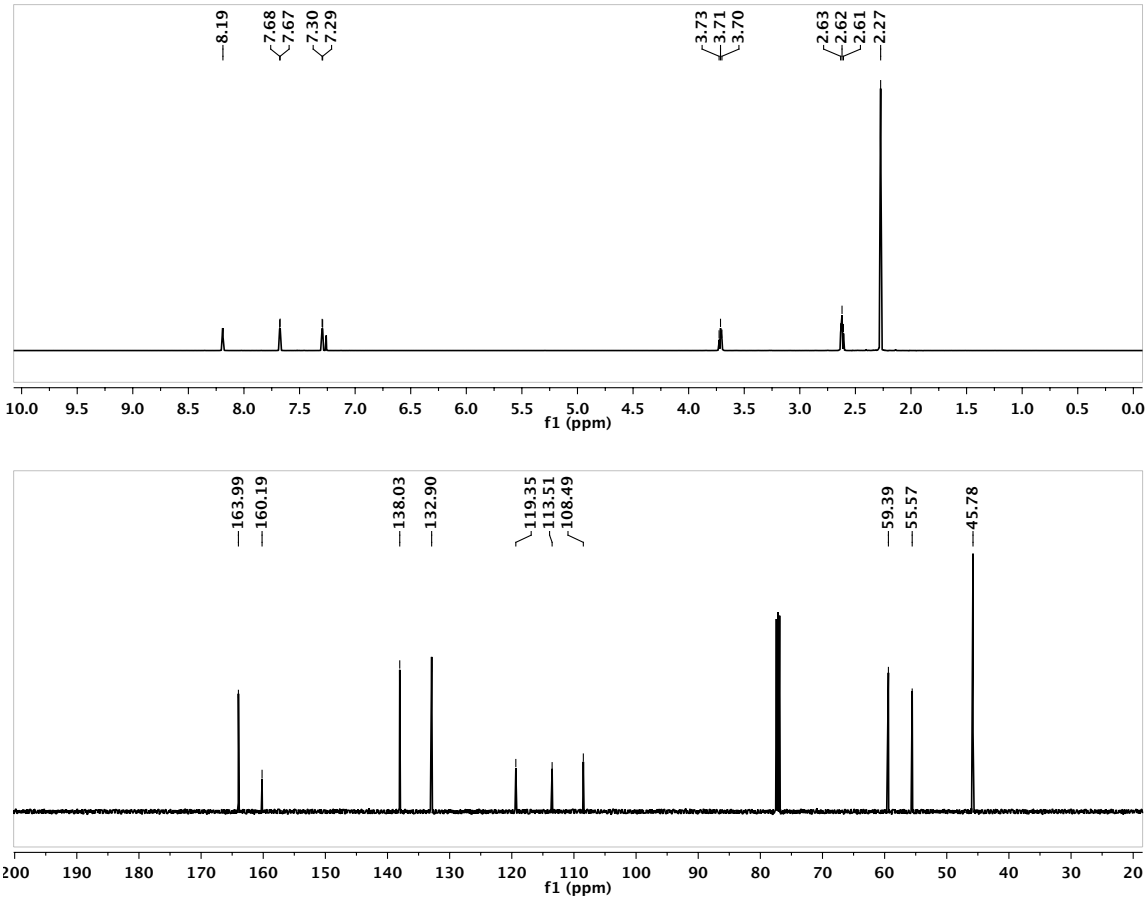

Figure C.73. ^{1}H (above) and ^{13}C (below) NMR spectra of **48b-NMe$_2$** in $CDCl_3$.

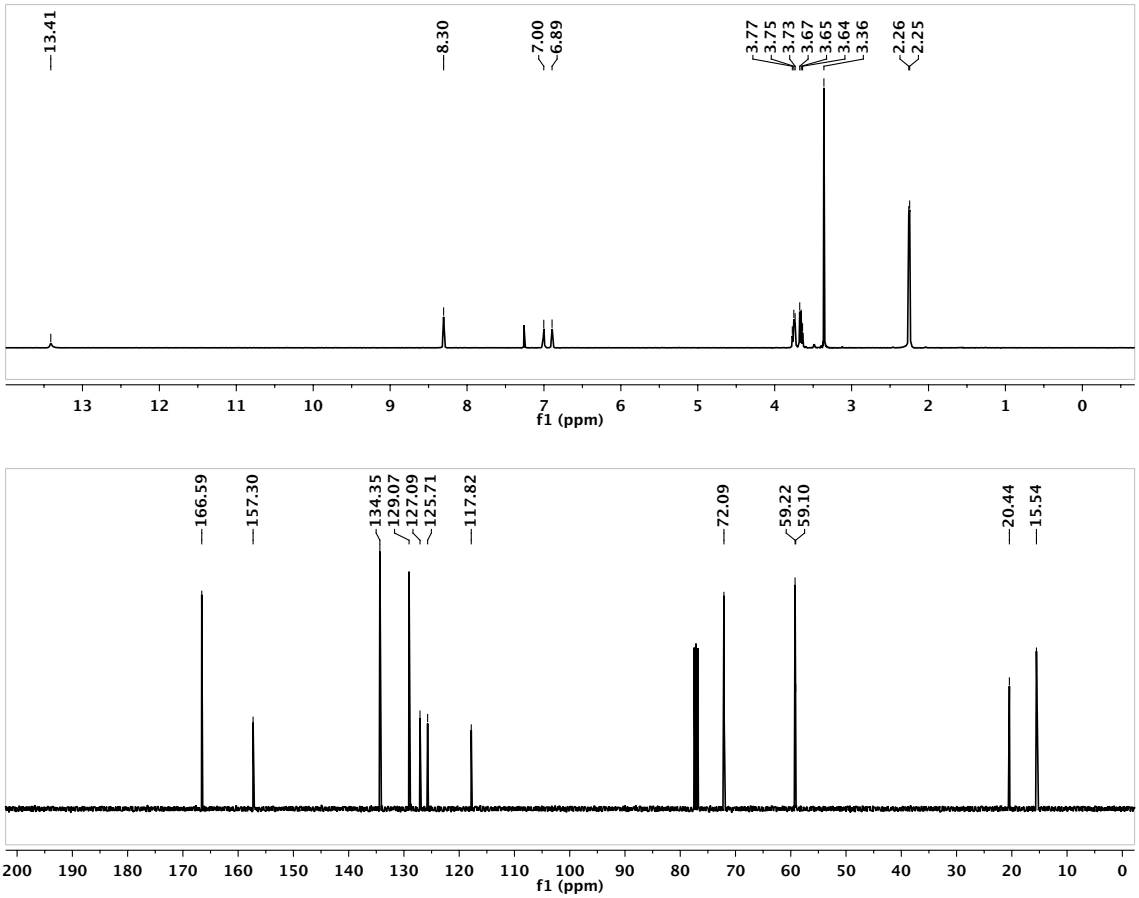

Figure C.74. ^{1}H (above) and ^{13}C (below) NMR spectra of **48c-OMe** in $CDCl_3$.

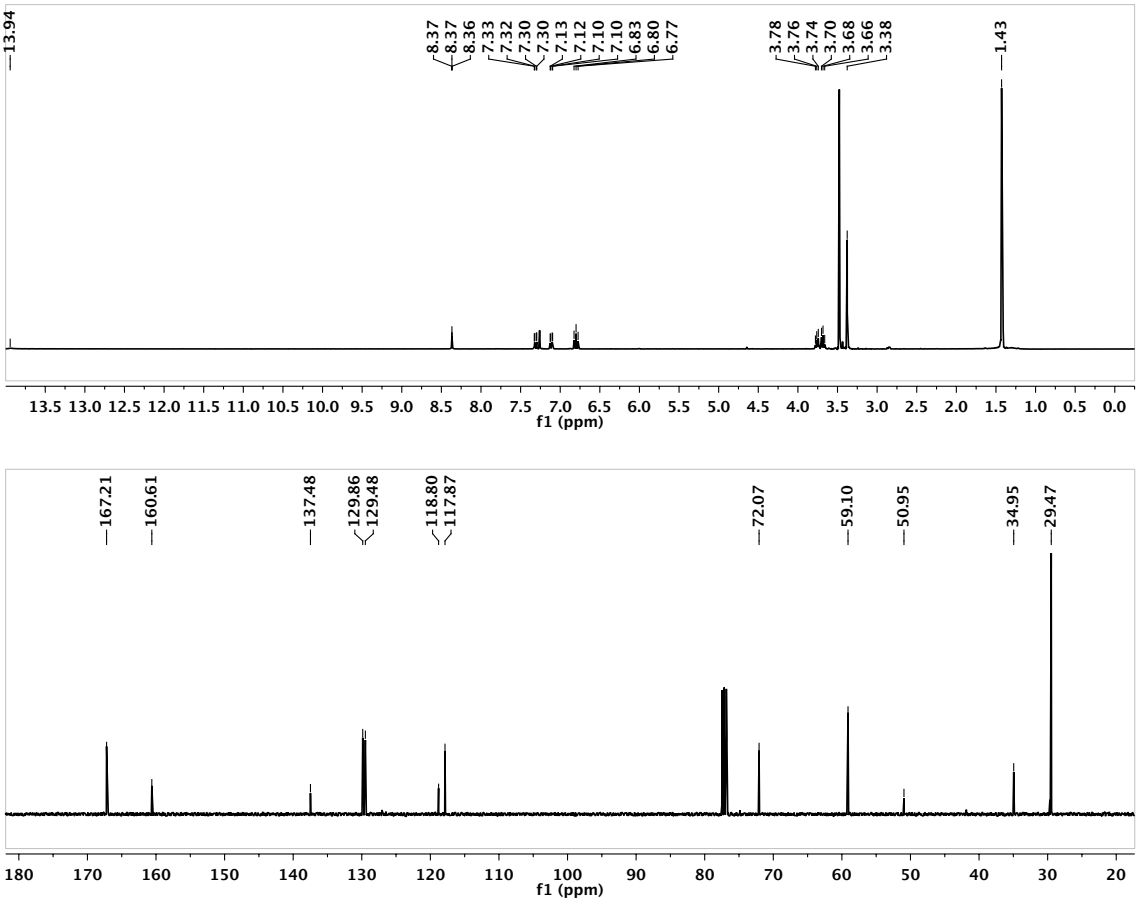

Figure C.75. ^{1}H (above) and ^{13}C (below) NMR spectra of **48d-OMe** in $CDCl_3$.

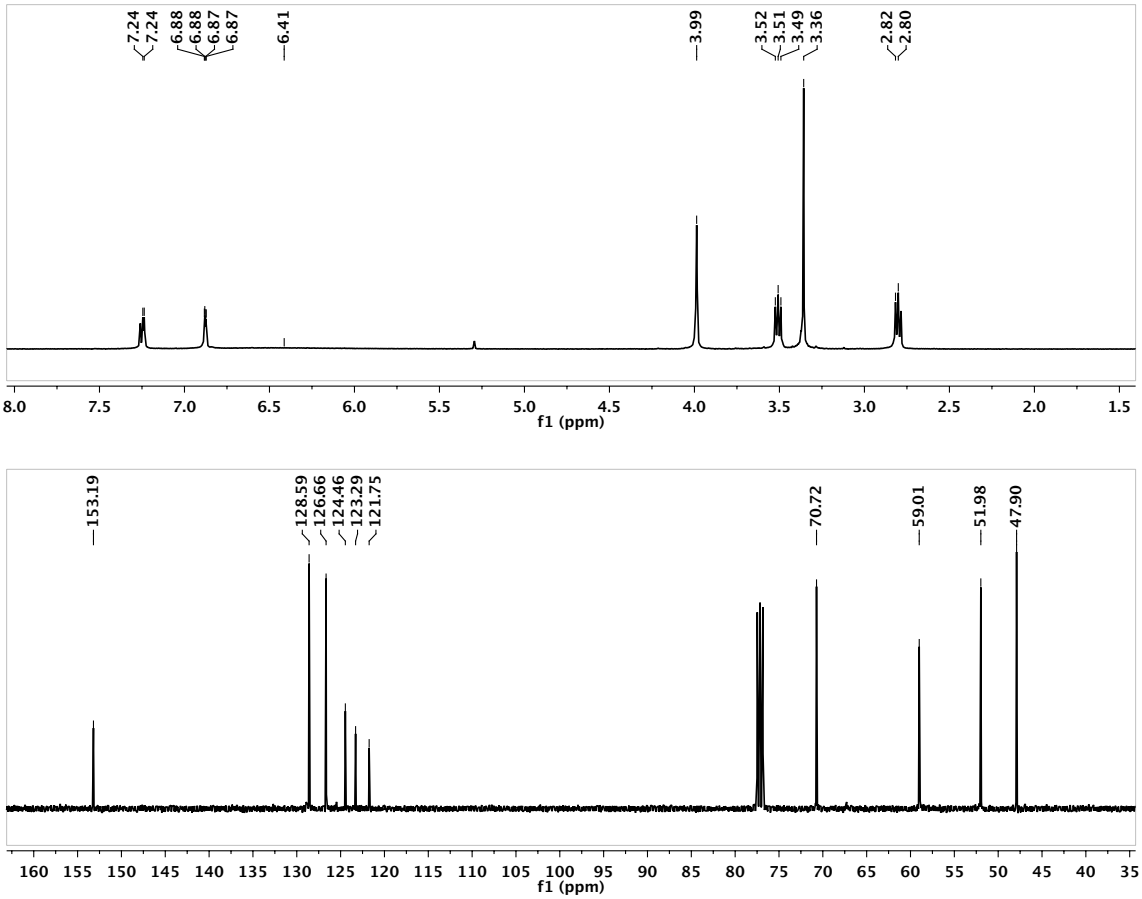

Figure C.76. ^{1}H (above) and ^{13}C (below) NMR spectra of **49a-OMe** in $CDCl_3$.

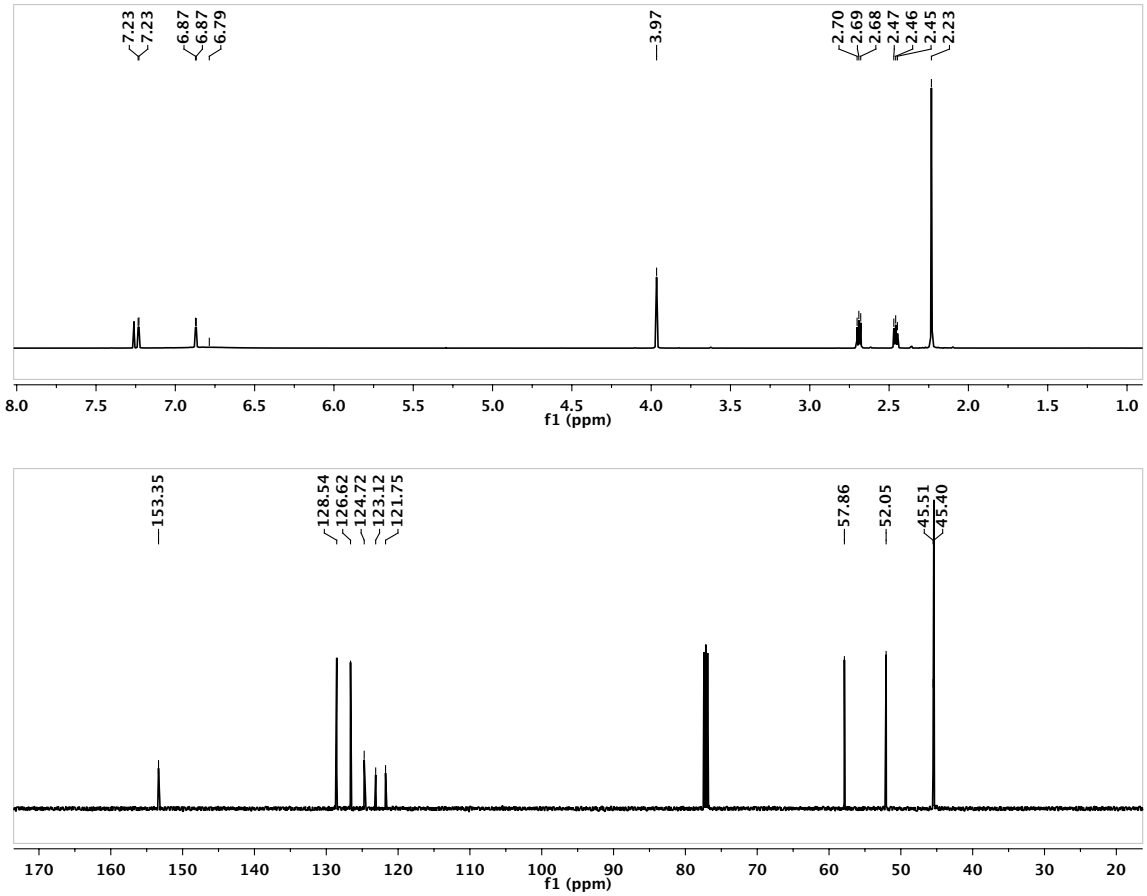

Figure C.77. ^{1}H (above) and ^{13}C (below) NMR spectra of **49a-NMe$_2$** in $CDCl_3$.

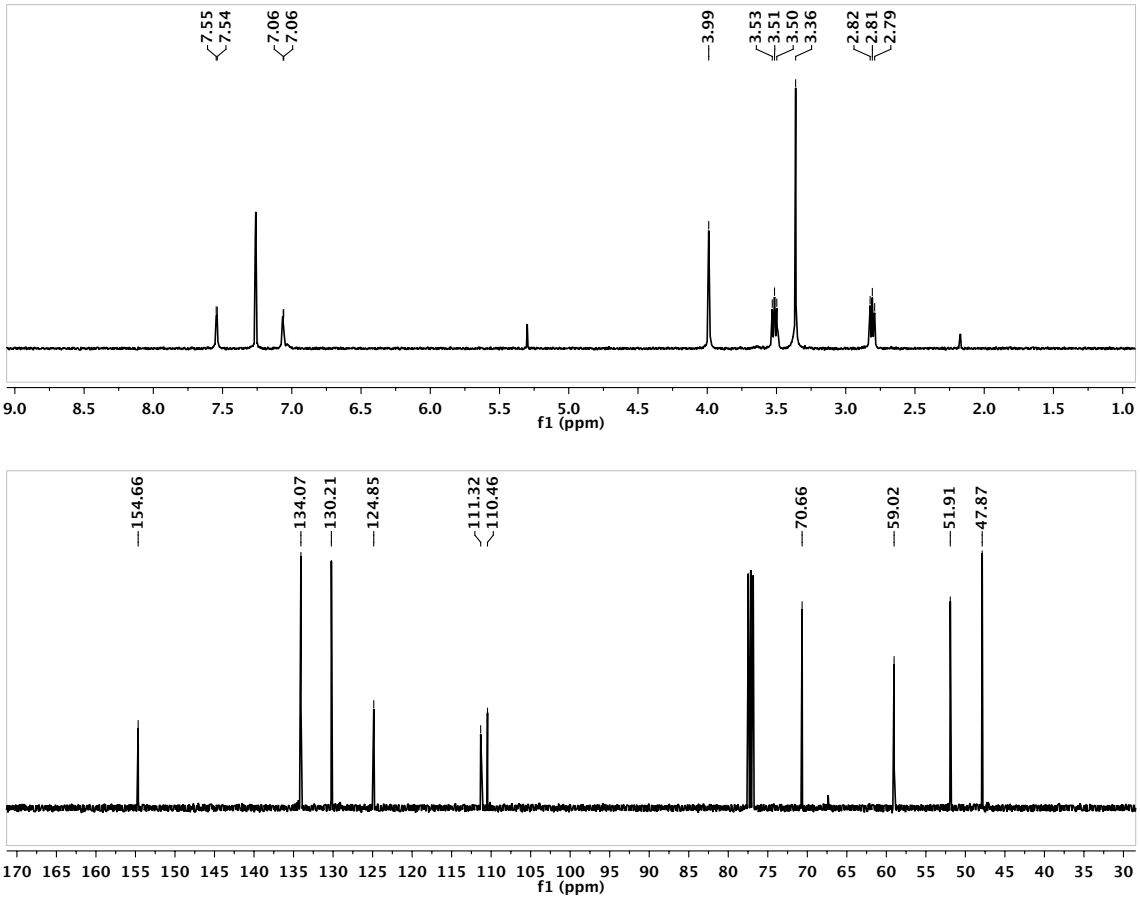

Figure C.78. ^{1}H (above) and ^{13}C (below) NMR spectra of **49b-OMe** in $CDCl_3$.

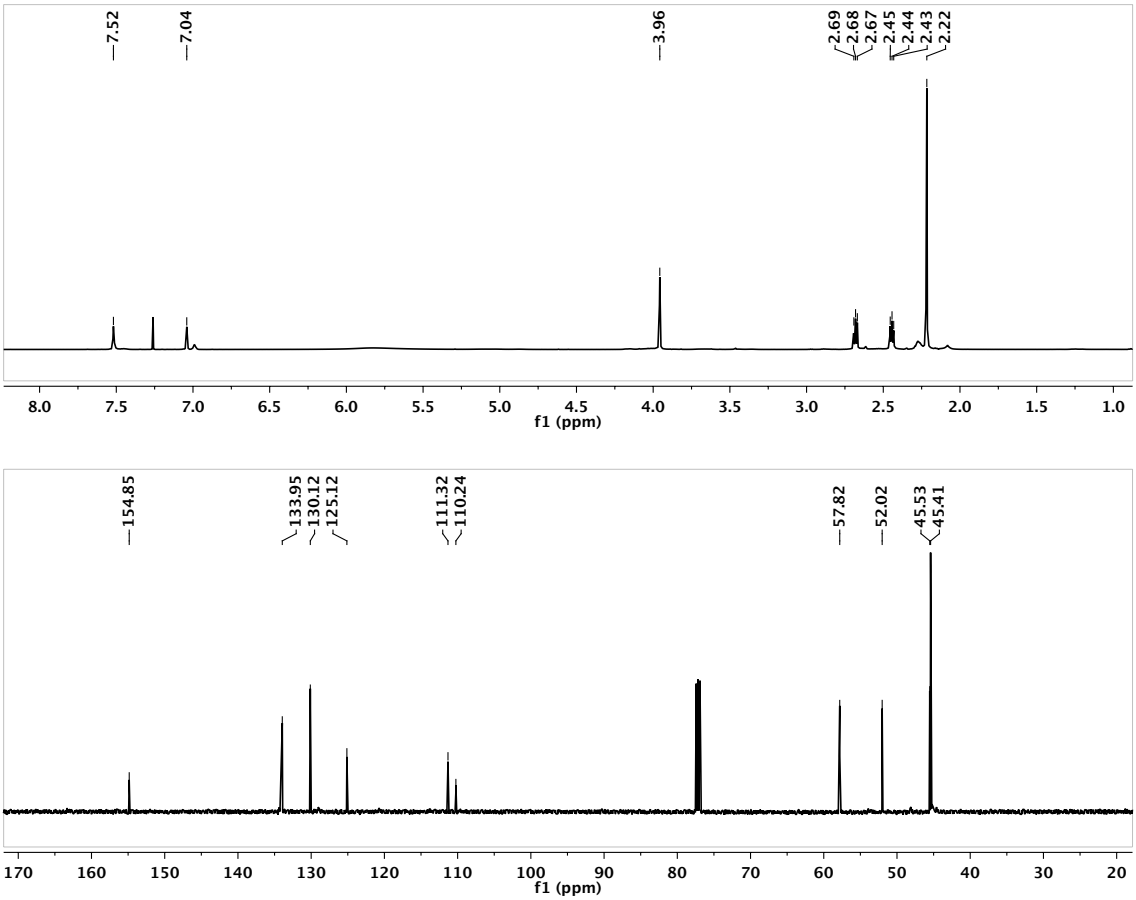

Figure C.79. ^{1}H (above) and ^{13}C (below) NMR spectra of **49b-NMe$_2$** in $CDCl_3$.

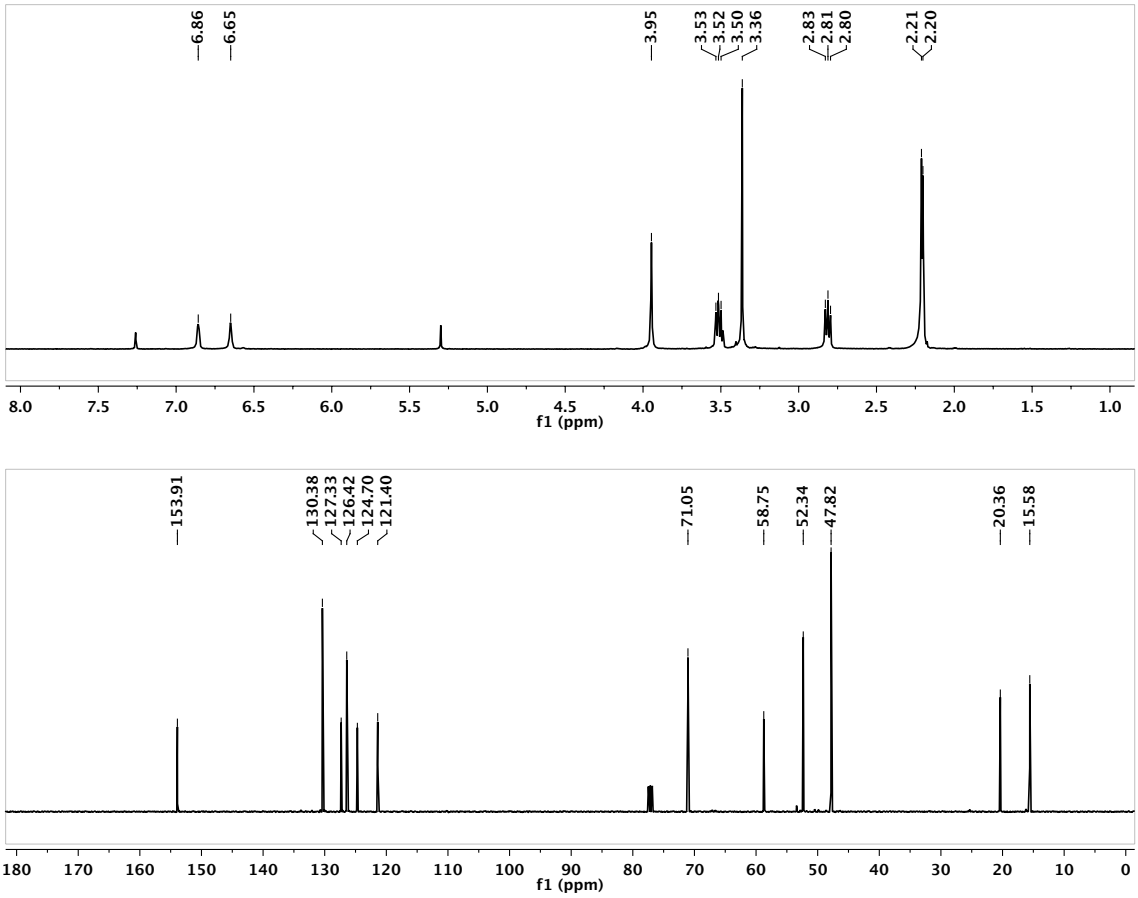

Figure C.80. ^{1}H (above) and ^{13}C (below) NMR spectra of **49c-OMe** in $CDCl_3$.

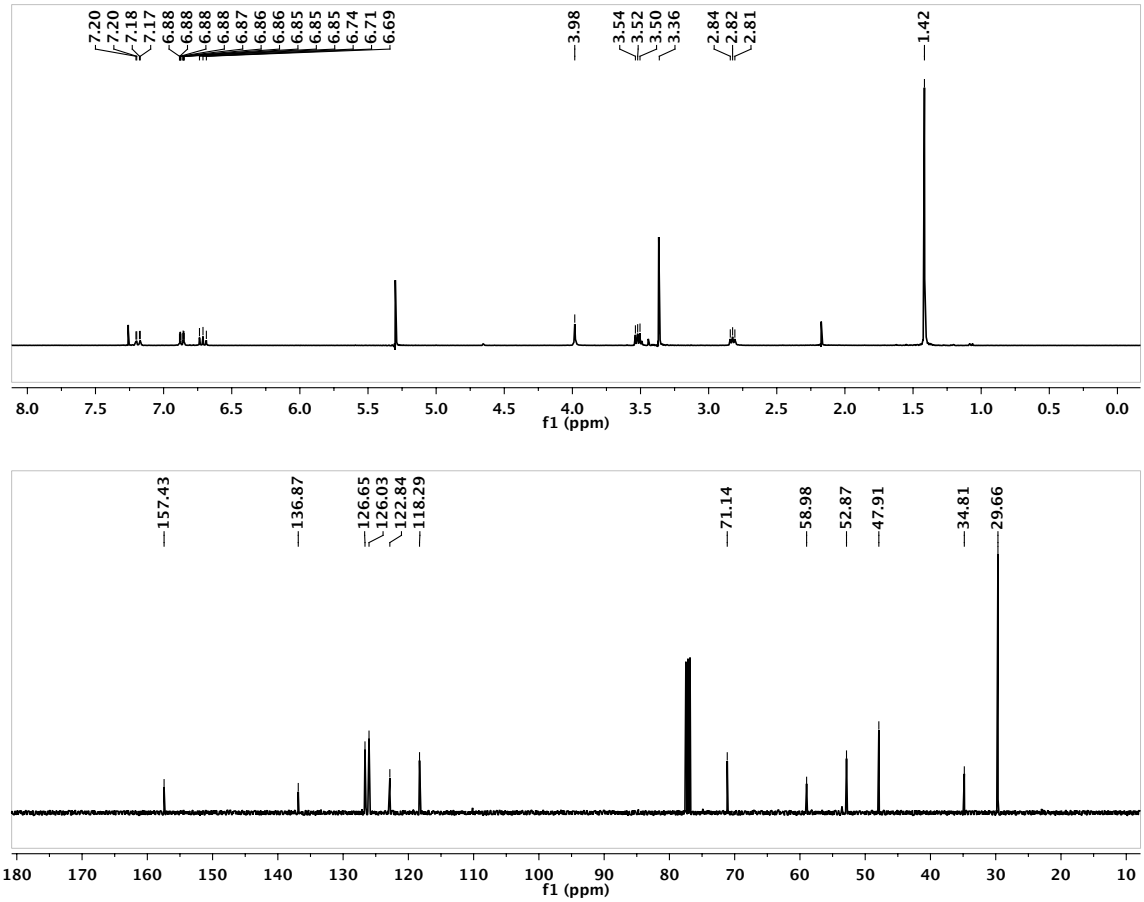

Figure C.81. ^{1}H (above) and ^{13}C (below) NMR spectra of **49d-OMe** in $CDCl_3$.

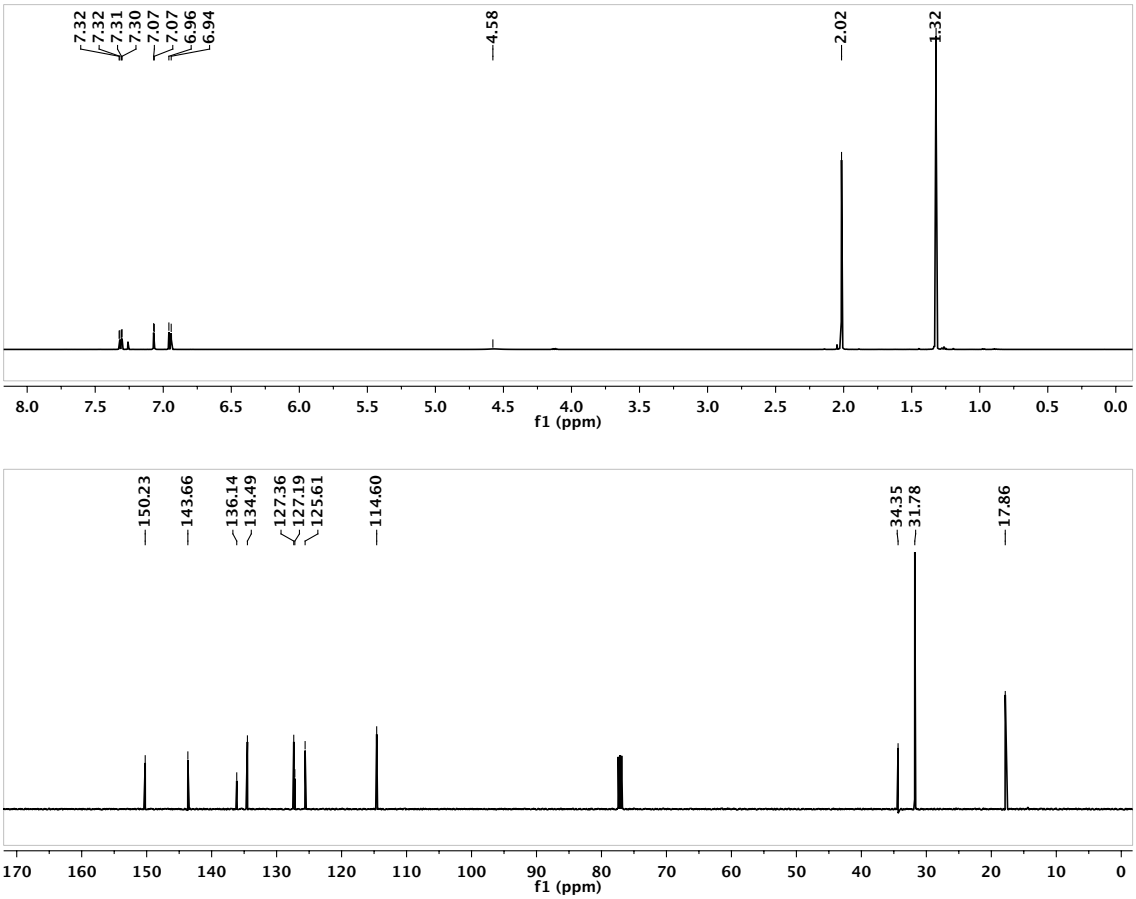

Figure C.82. ^{1}H (above) and ^{13}C (below) NMR spectra of **50** in $CDCl_3$.

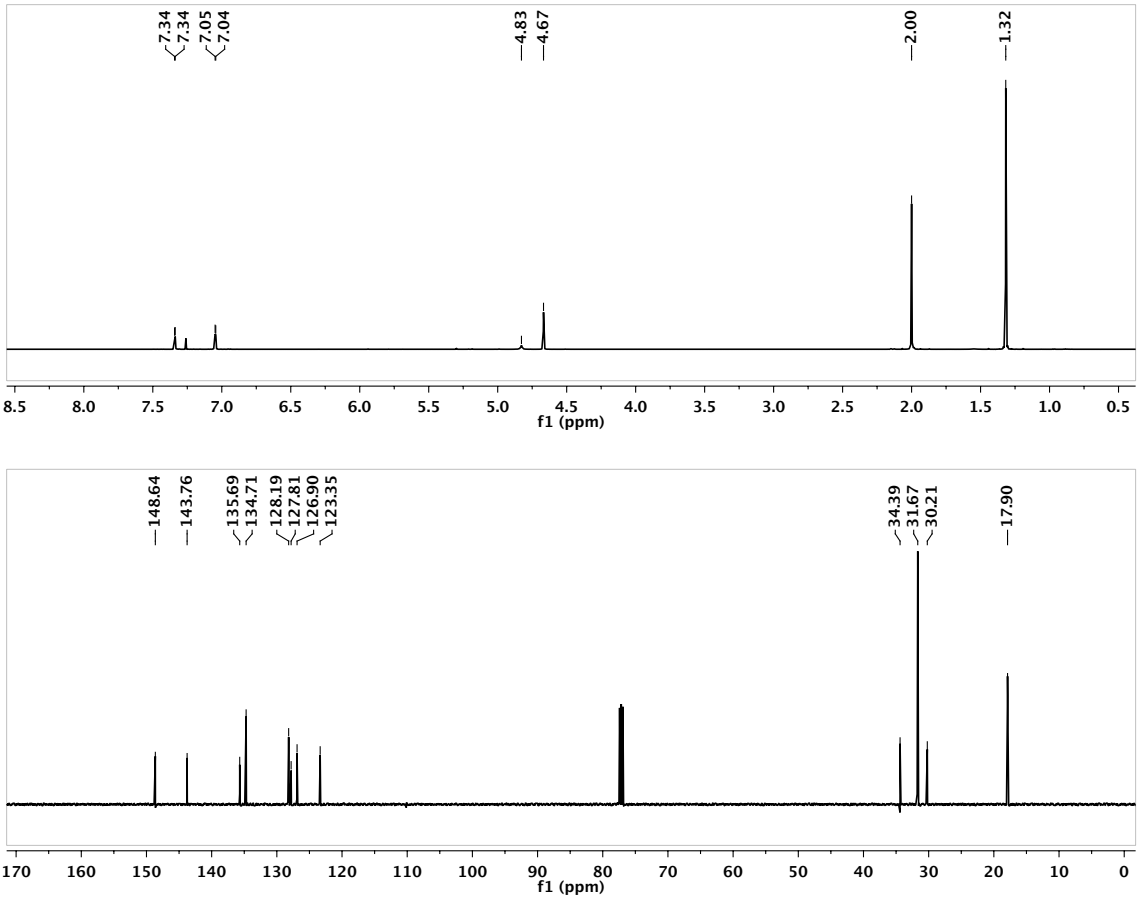

Figure C.83. ^{1}H (above) and ^{13}C (below) NMR spectra of **51** in $CDCl_3$.

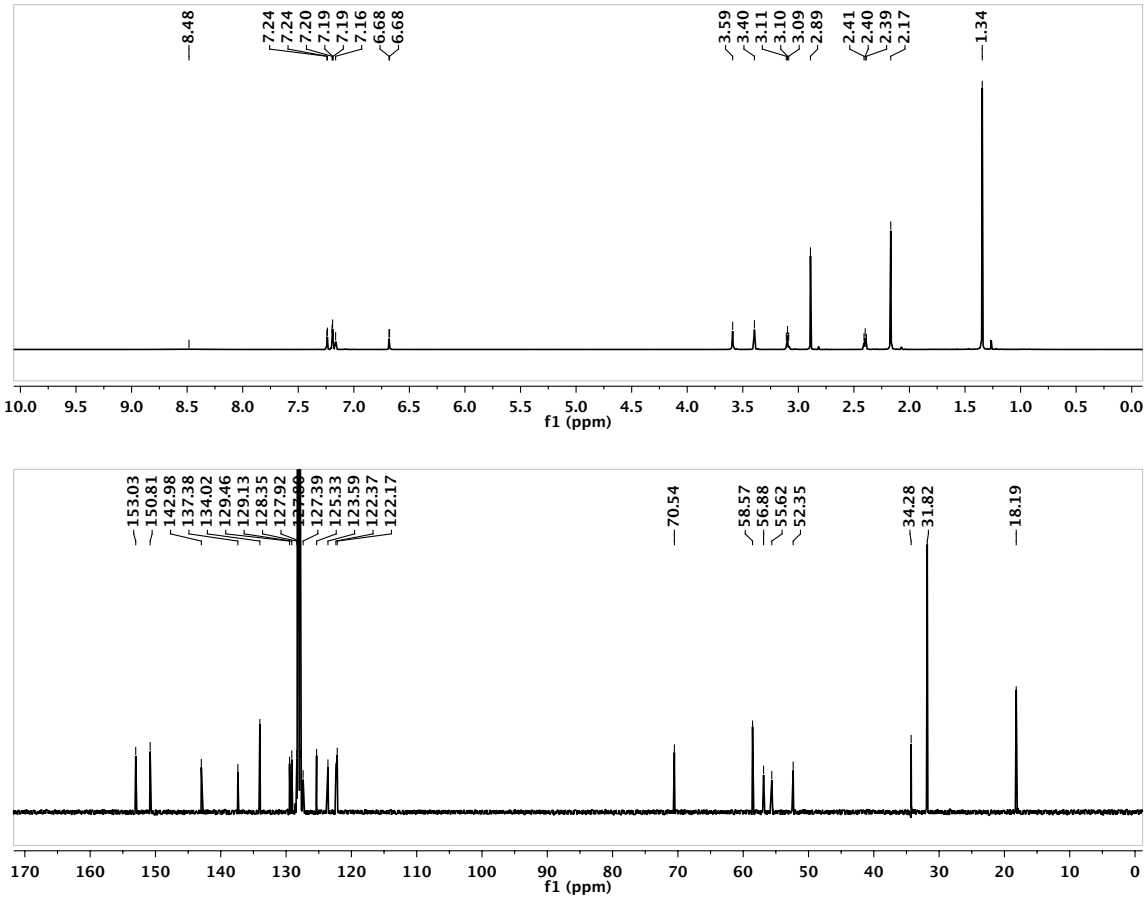

Figure C.84. ^{1}H (above) and ^{13}C (below) NMR spectra of **52a-OMe** in C_6D_6.

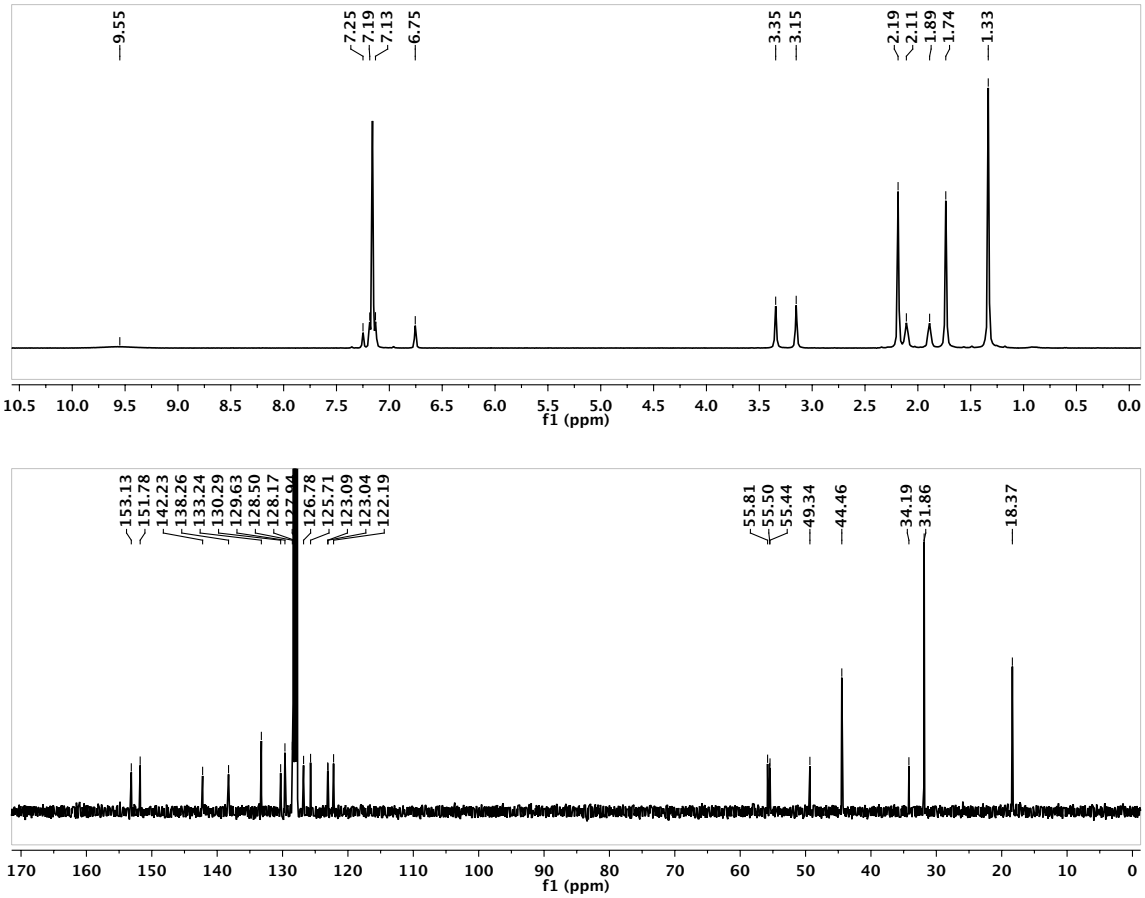

Figure C.85. ^{1}H (above) and ^{13}C (below) NMR spectra of **52a-NMe$_2$** in C_6D_6.

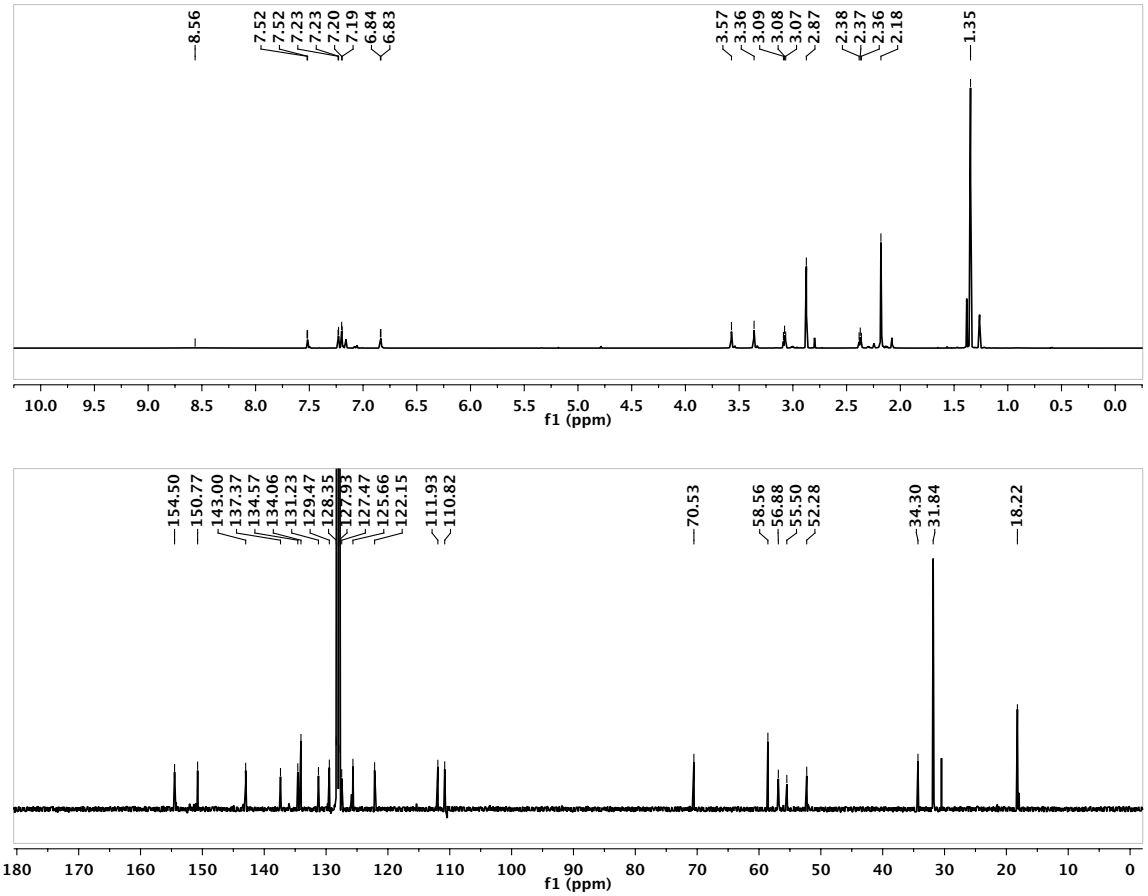

Figure C.86. ^{1}H (above) and ^{13}C (below) NMR spectra of **52b-OMe** in C_6D_6.

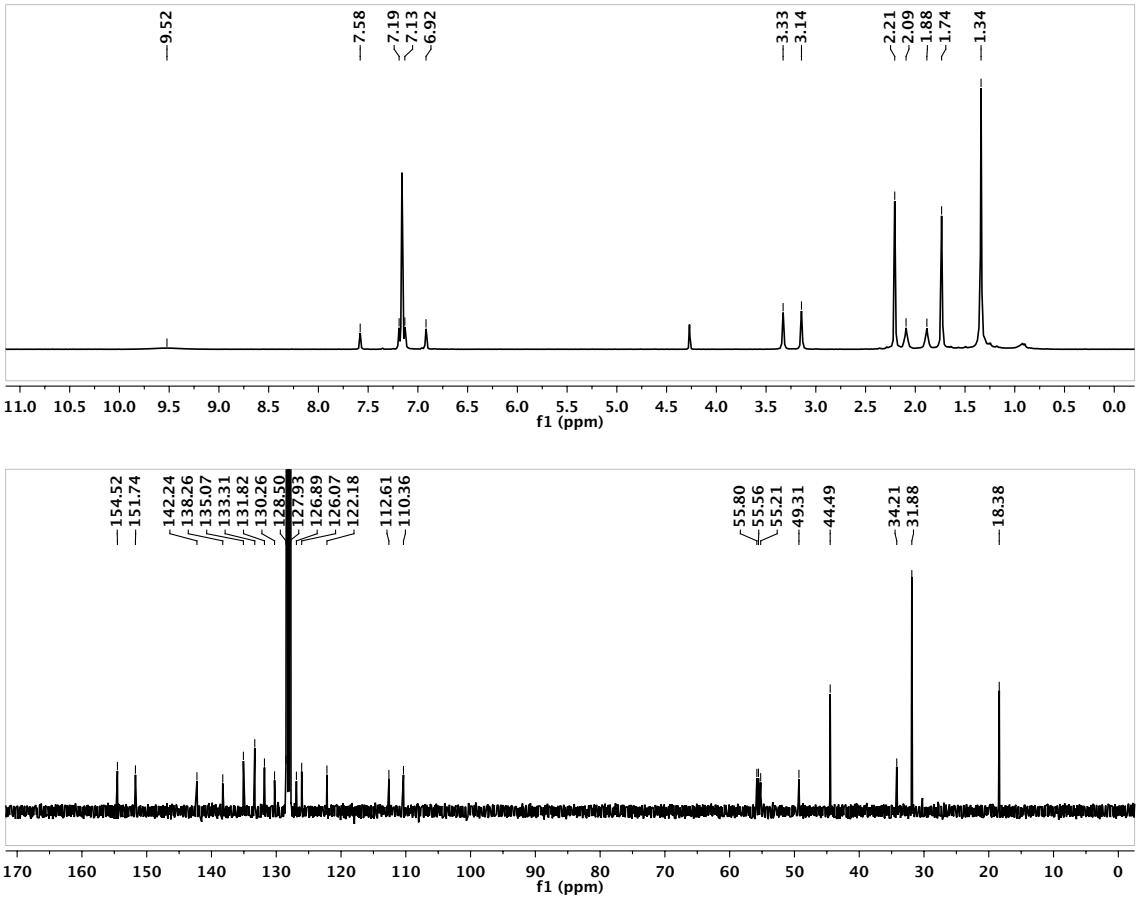

Figure C.87. ^{1}H (above) and ^{13}C (below) NMR spectra of **52b-NMe$_2$** in C_6D_6.

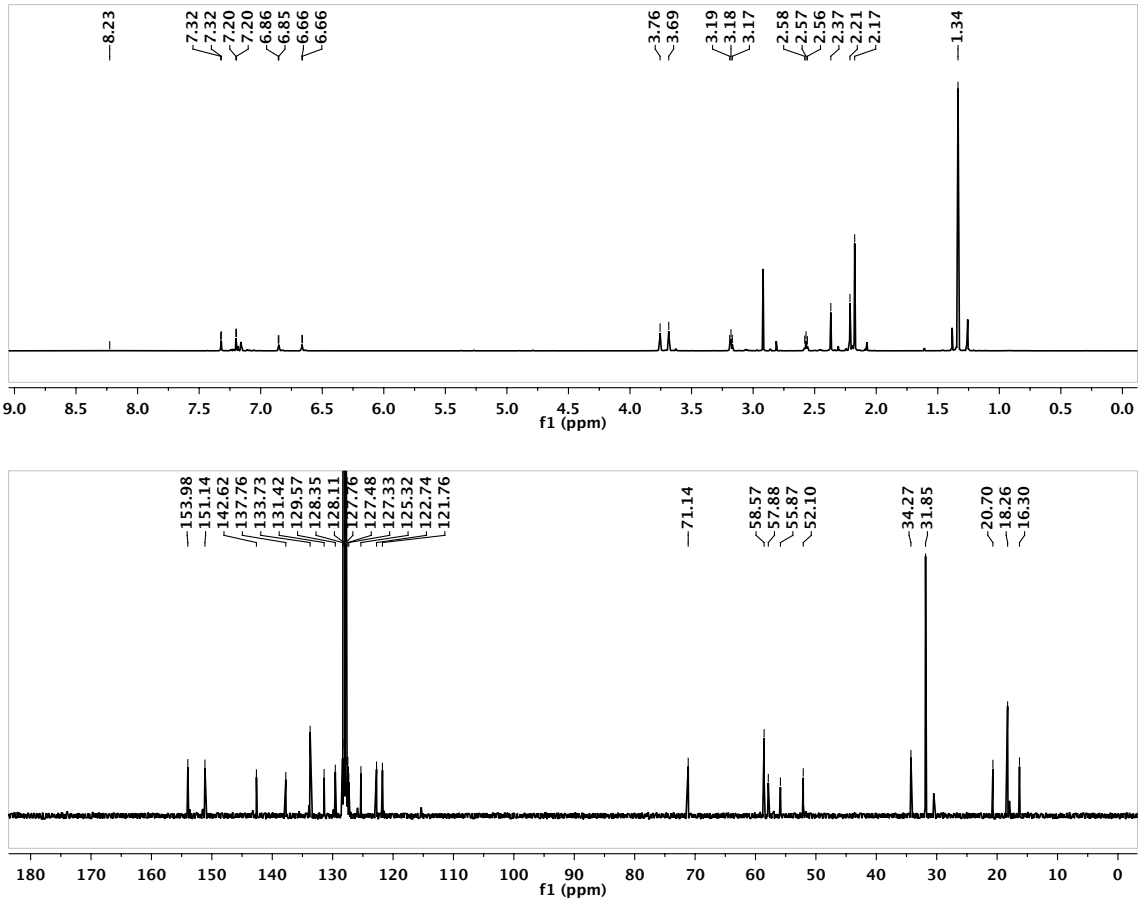

Figure C.88. ^{1}H (above) and ^{13}C (below) NMR spectra of **52c-OMe** in C_6D_6.

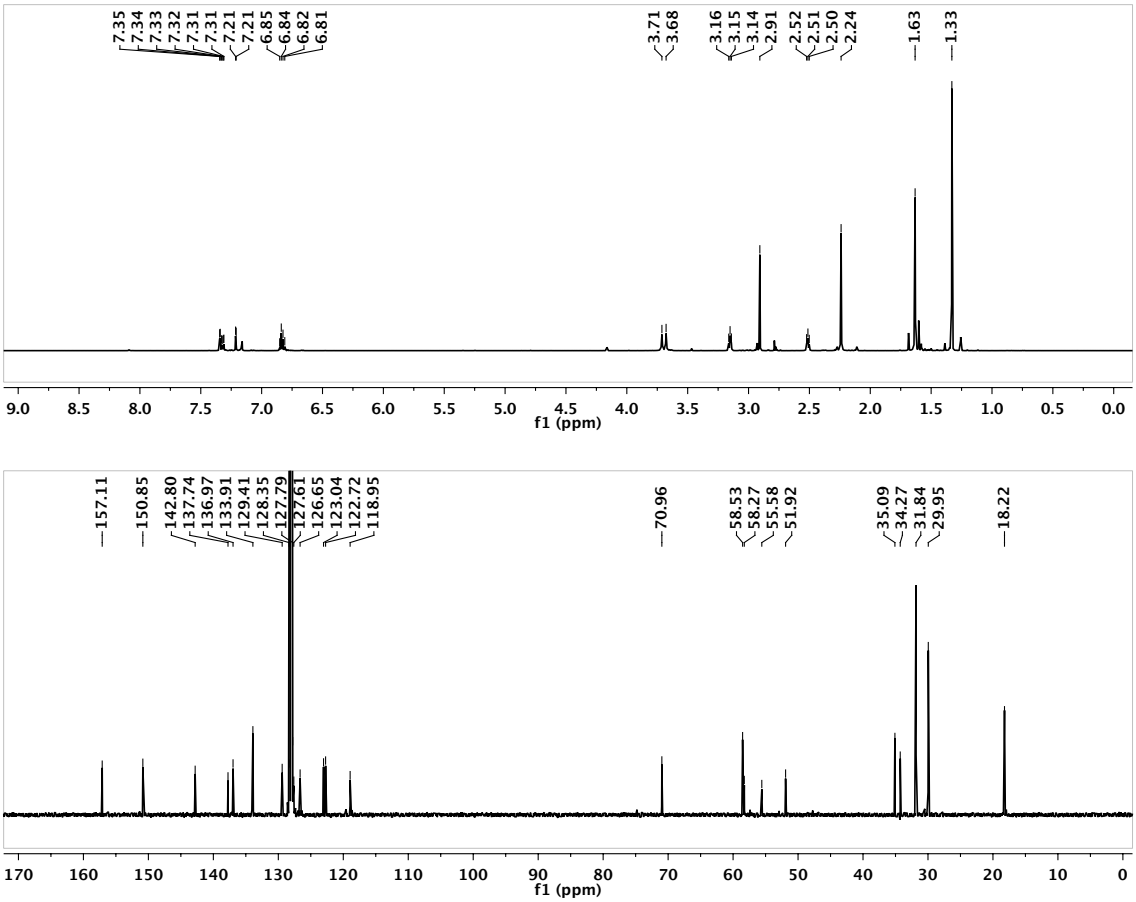

Figure C.89. ^{1}H (above) and ^{13}C (below) NMR spectra of **52d-OMe** in C_6D_6.

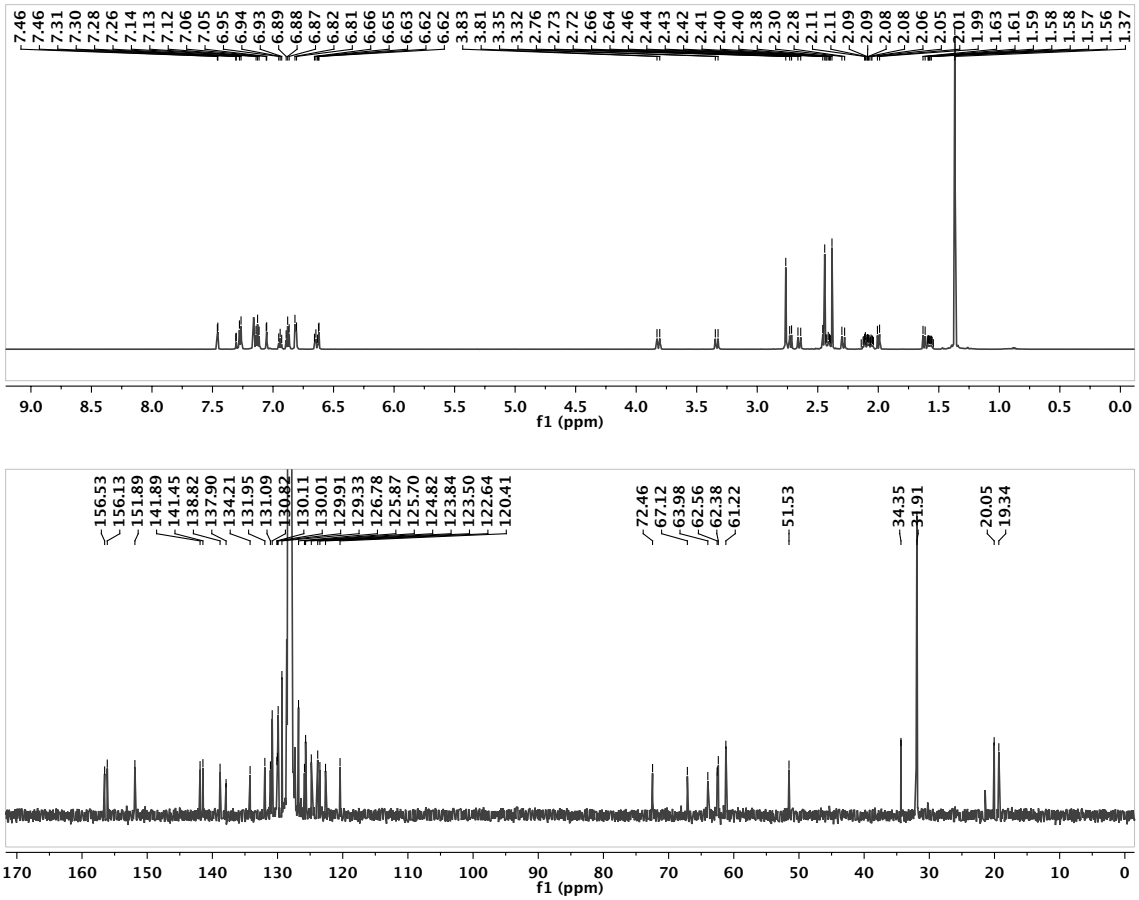

Figure C.90. ^{1}H (above) and ^{13}C (below) NMR spectra of **53a-OMe** in C_6D_6.

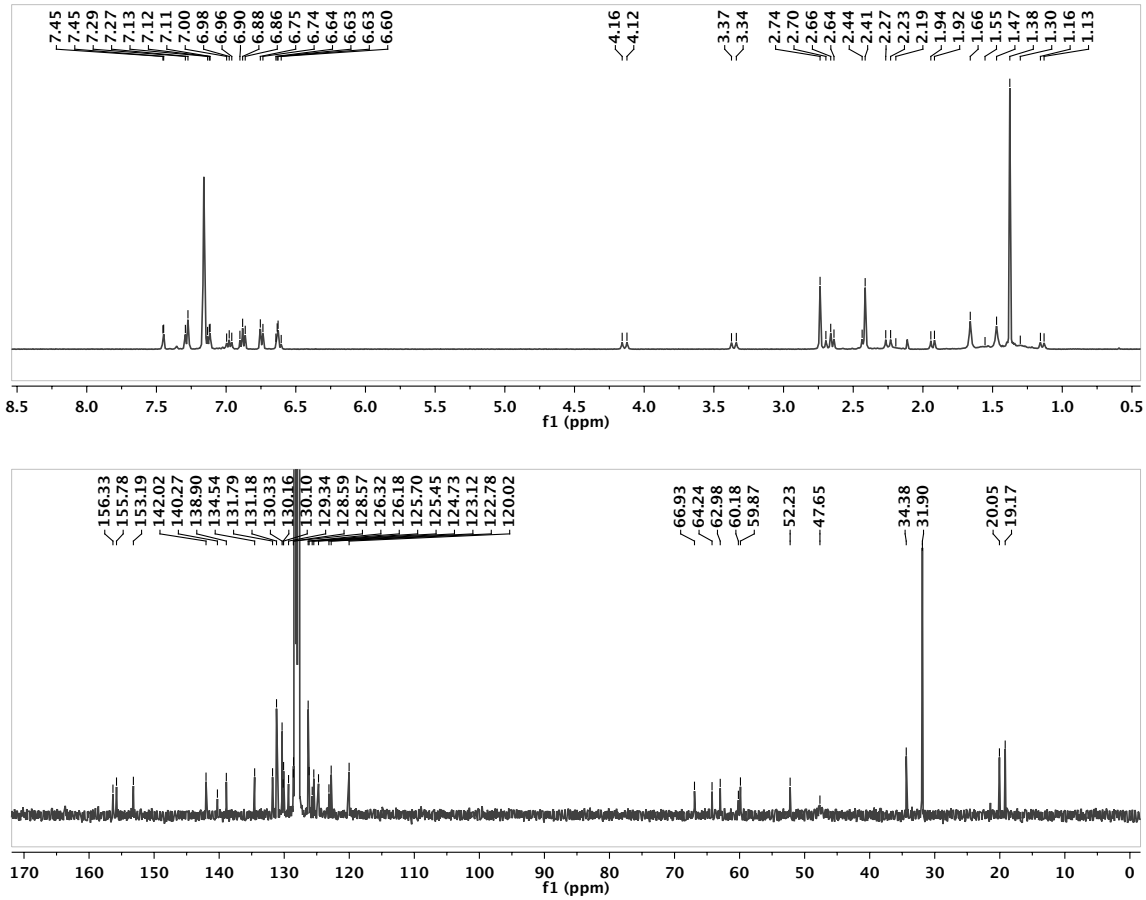

Figure C.91. ^{1}H (above) and ^{13}C (below) NMR spectra of **53a-NMe$_2$** in C_6D_6.

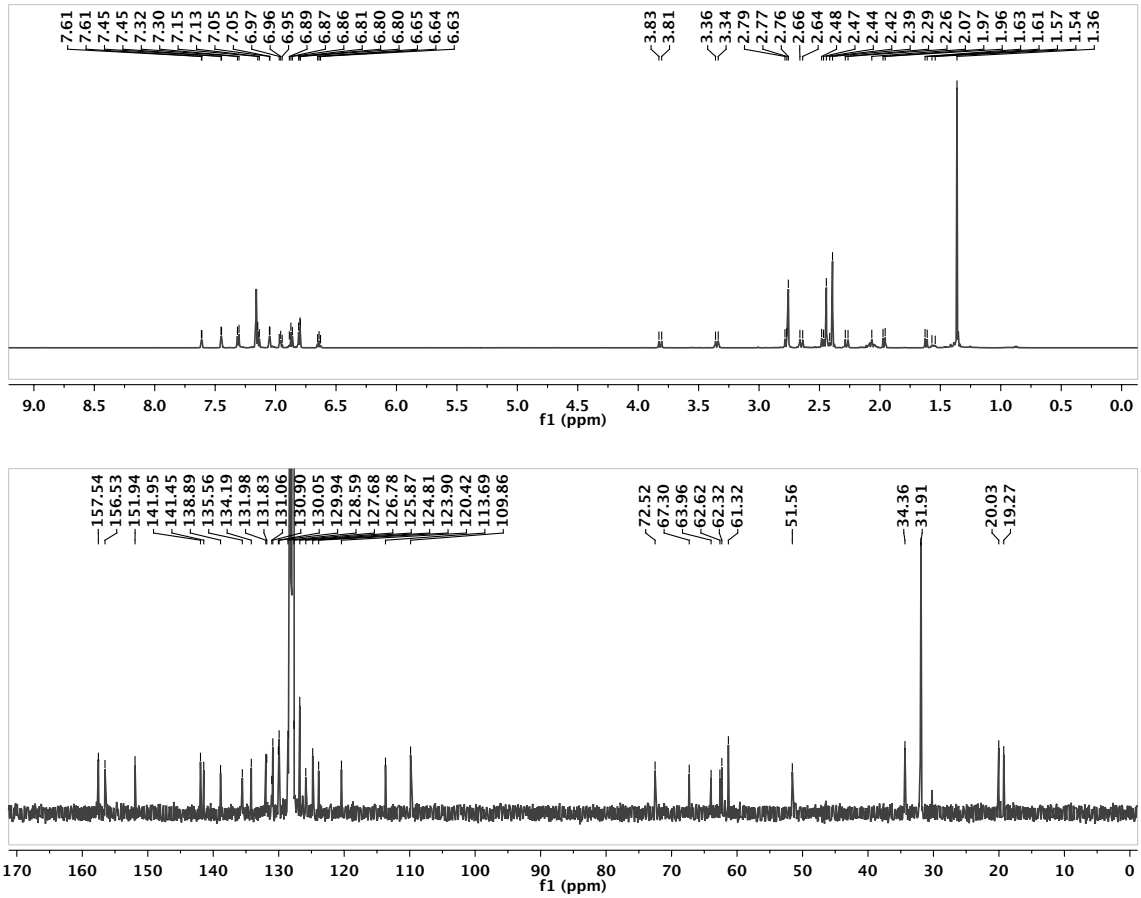

Figure C.92. ^{1}H (above) and ^{13}C (below) NMR spectra of **53b-OMe** in C_6D_6.

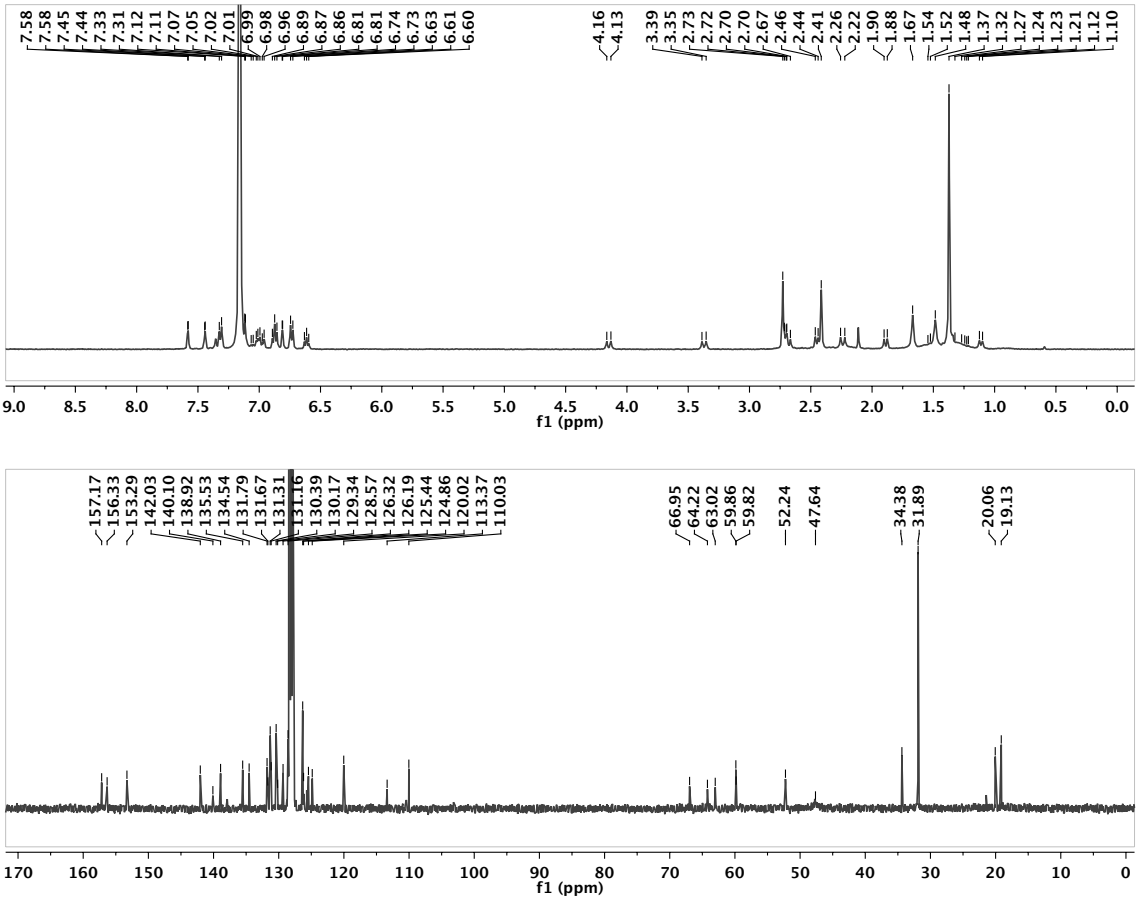

Figure C.93. ^{1}H (above) and ^{13}C (below) NMR spectra of **53b-NMe$_2$** in C_6D_6.

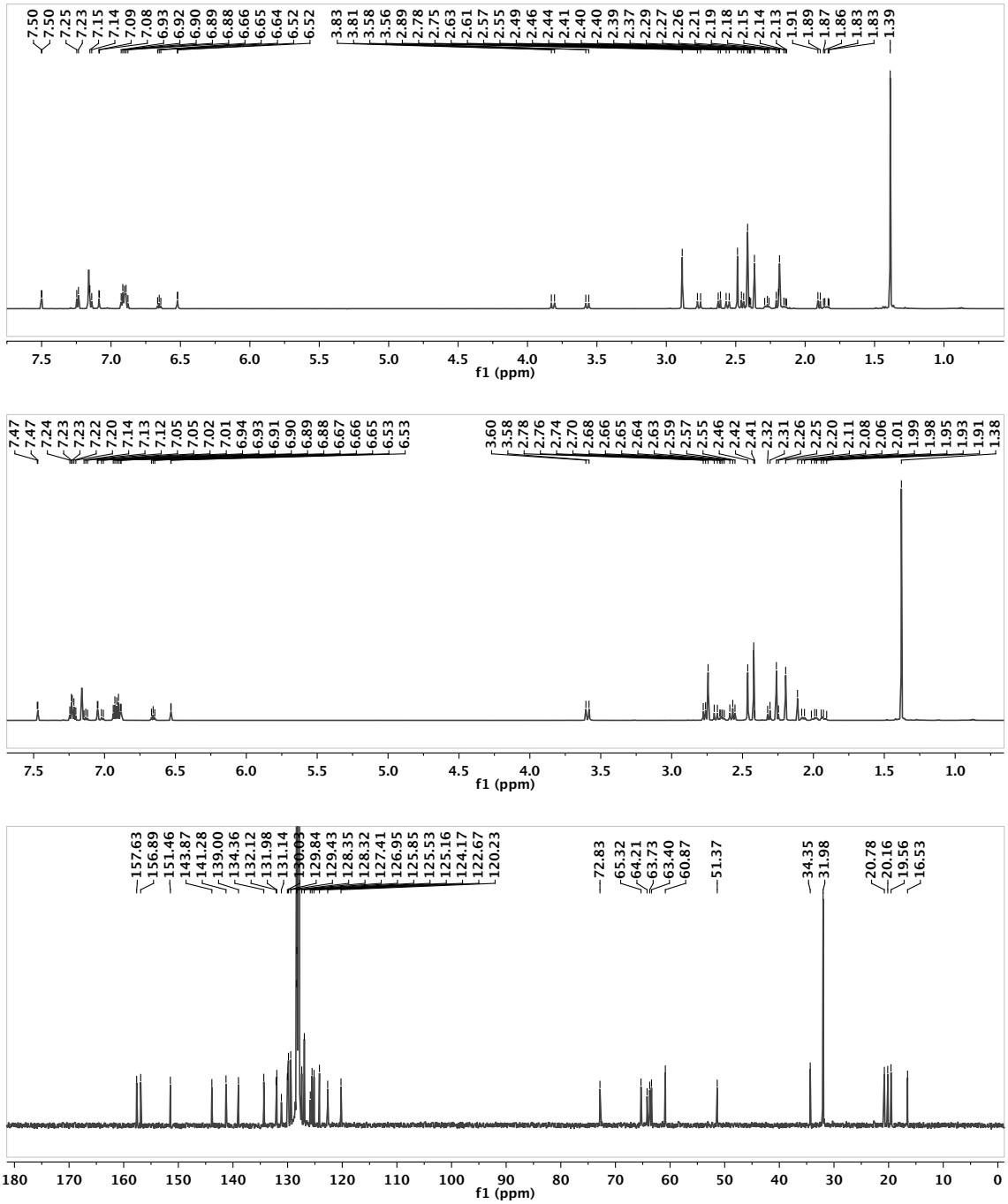

Figure C.94. ^{1}H NMR spectra in $C_6D_6$of the *pseudo-*C_2 (top) and the *pseudo-*C_S (middle) metallation isomers of **53c-OMe.** ^{13}C spectrum in C_6D_6corresponding to the top ^{1}H NMR spectrum.

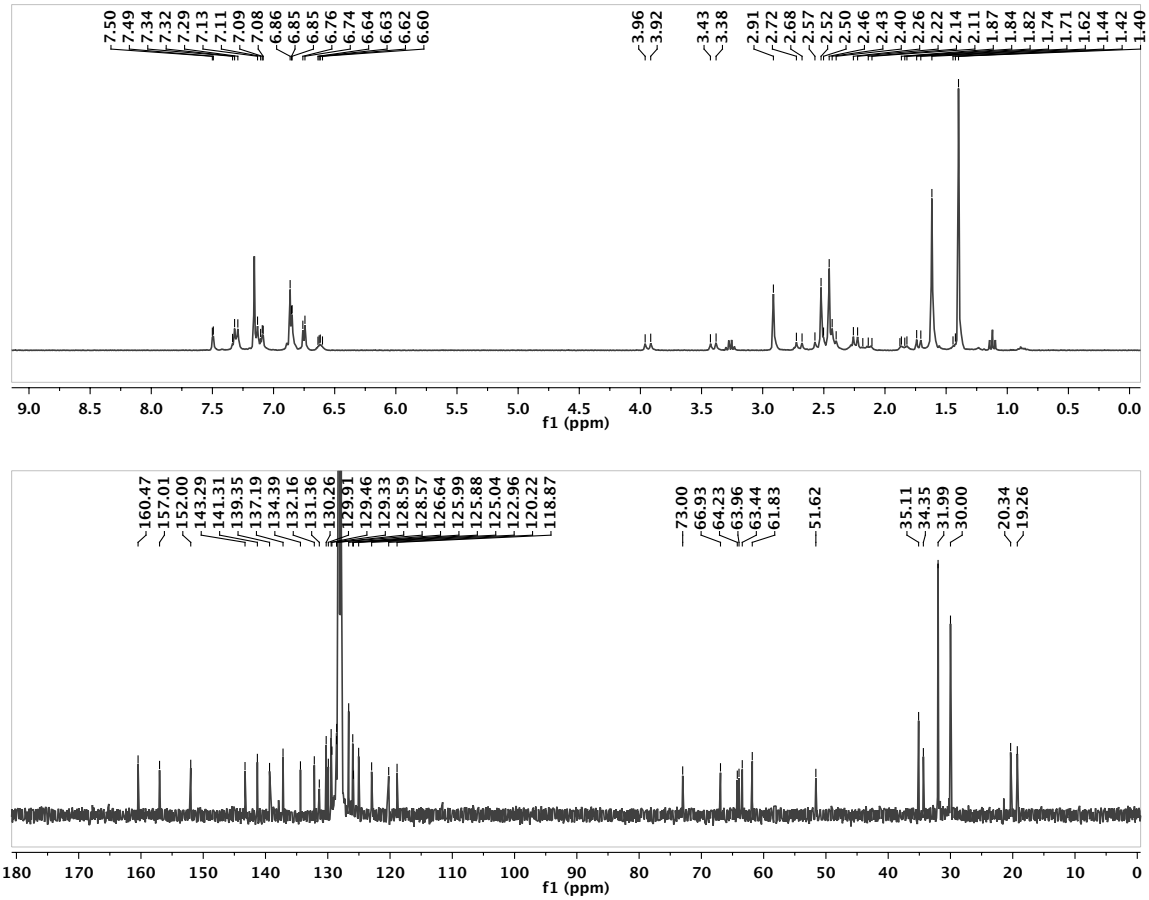

Figure C.95. ^{1}H (above) and ^{13}C (below) NMR spectra of **53d-OMe** in C_6D_6.

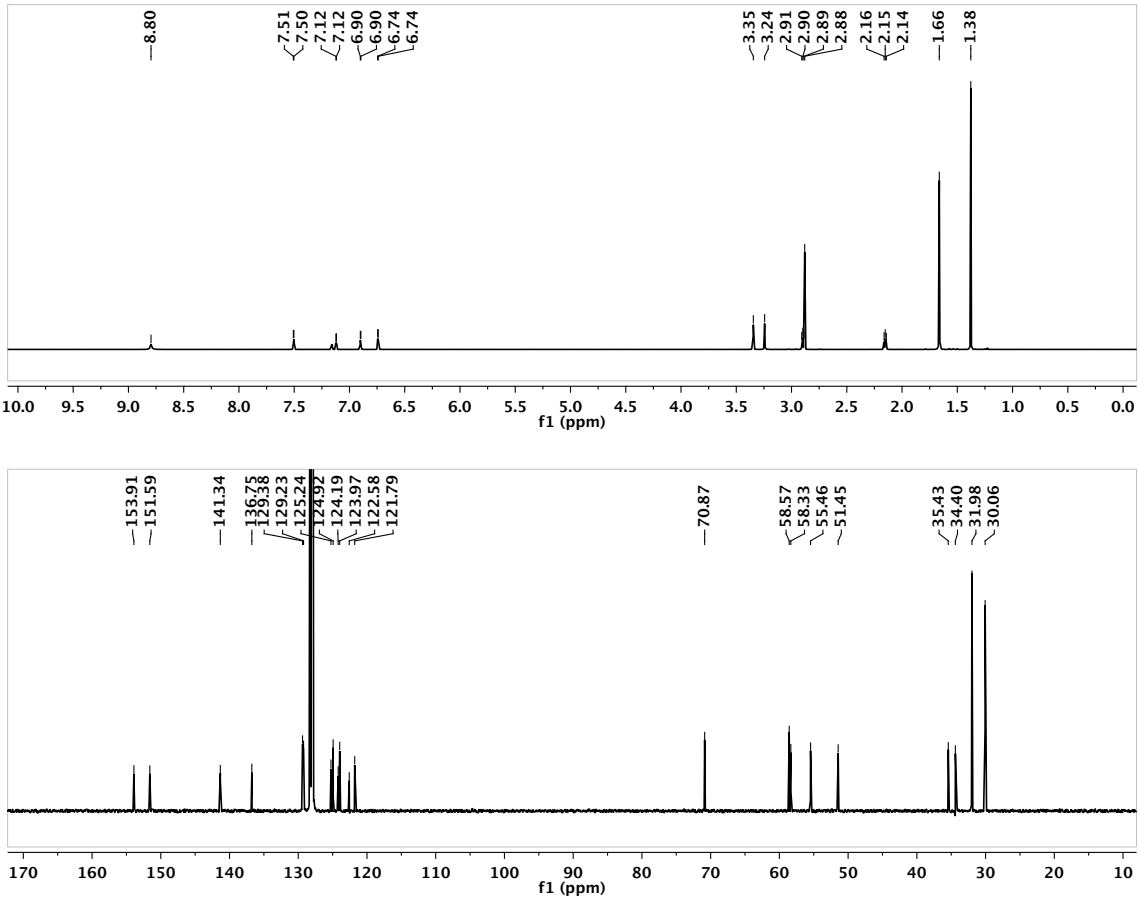

Figure C.96. ^{1}H (above) and ^{13}C (below) NMR spectra of **56-OMe** in C_6D_6.

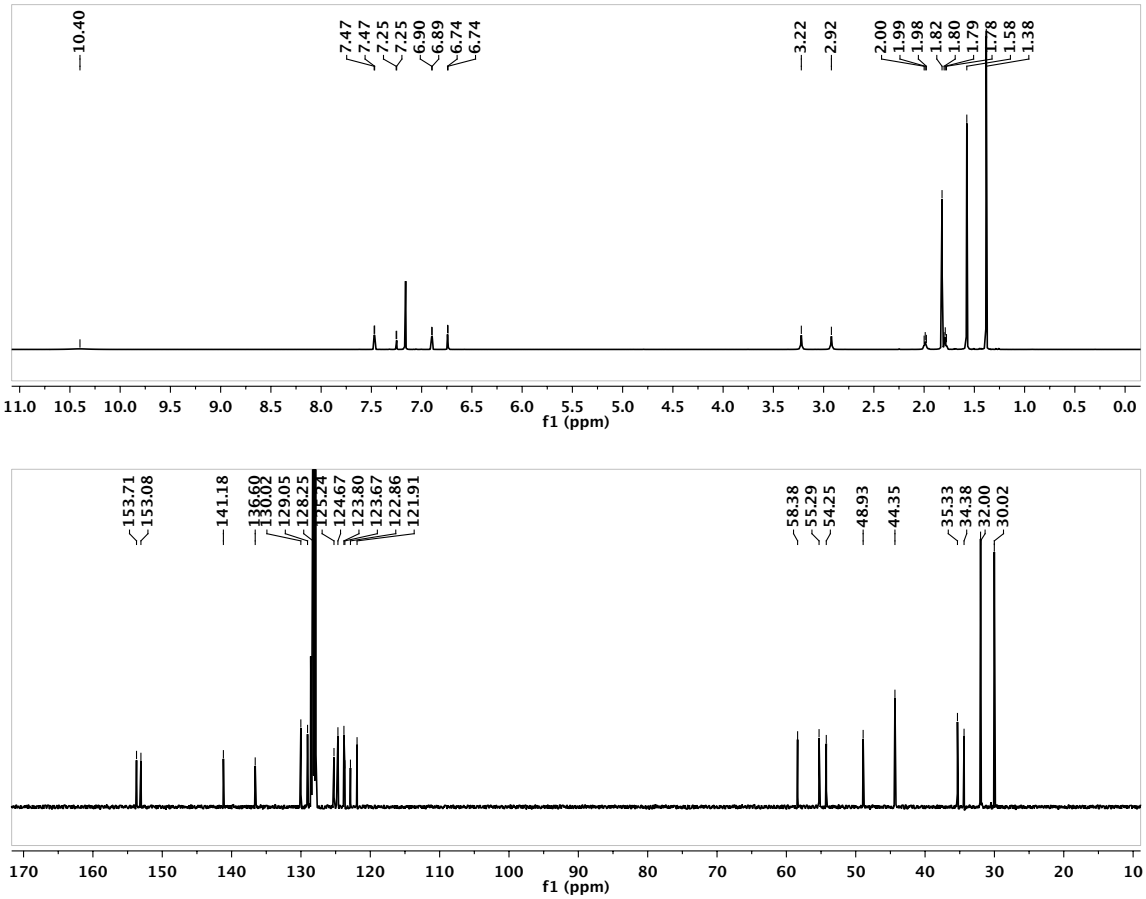

Figure C.97. ^{1}H (above) and ^{13}C (below) NMR spectra of **56-NMe$_2$** in C_6D_6.

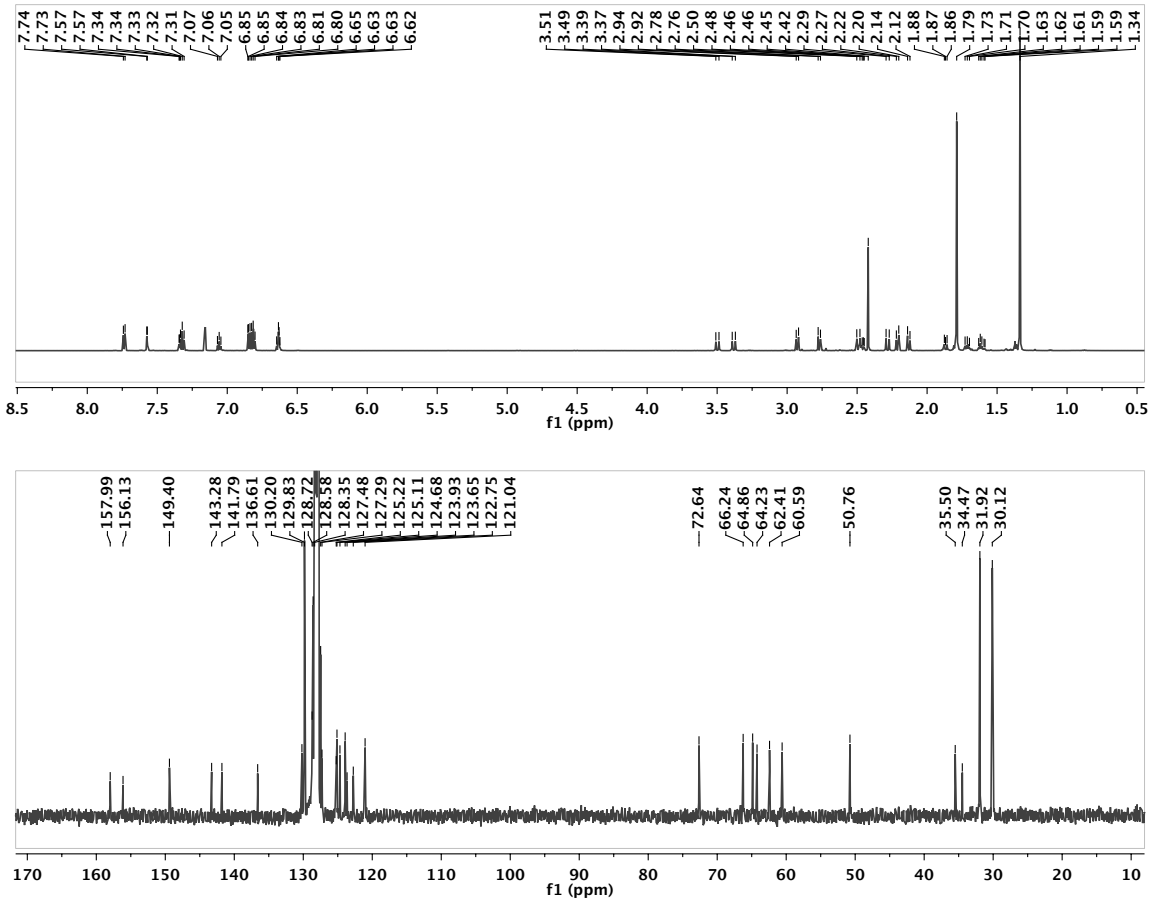

Figure C.98. ^{1}H (above) and ^{13}C (below) NMR spectra of **57-OMe** in C_6D_6.

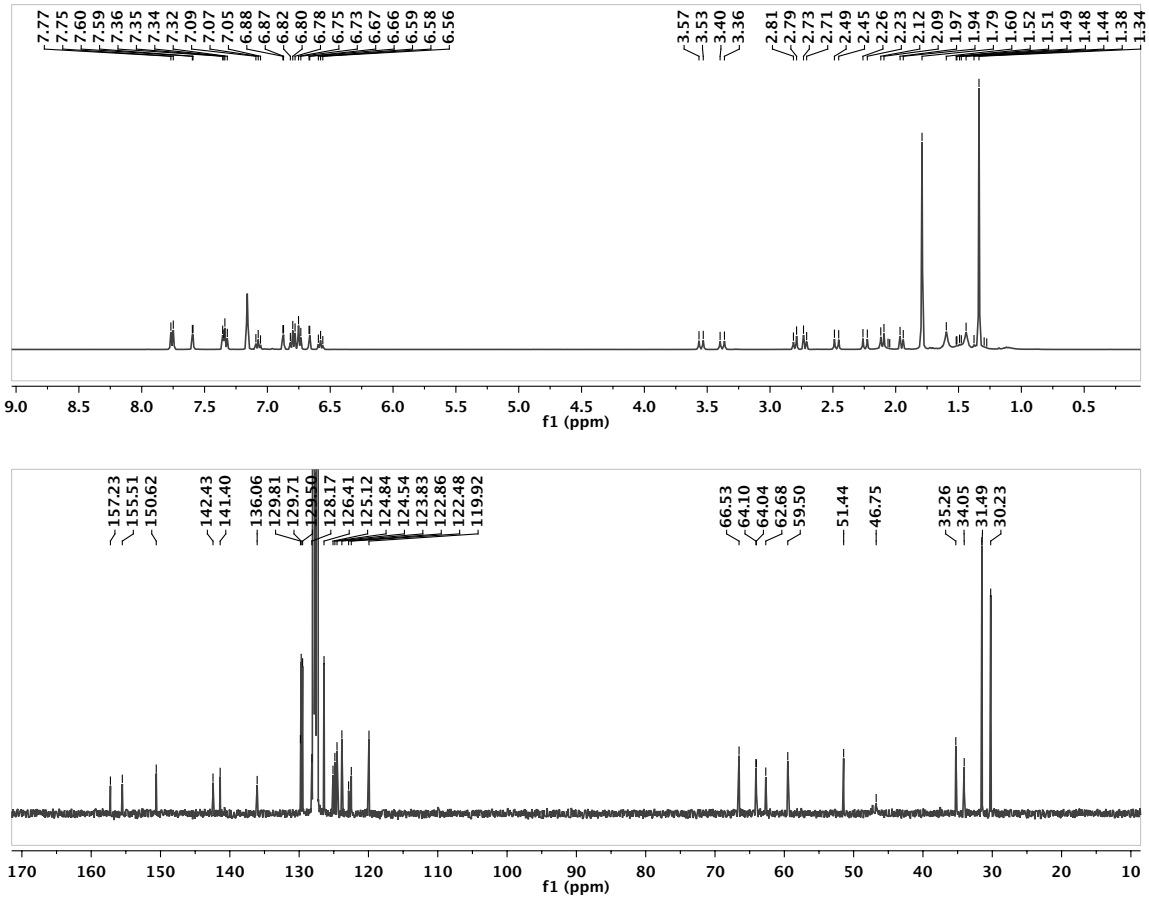

Figure C.99. ^{1}H (above) and ^{13}C (below) NMR spectra of **57-NMe$_2$** in C_6D_6.

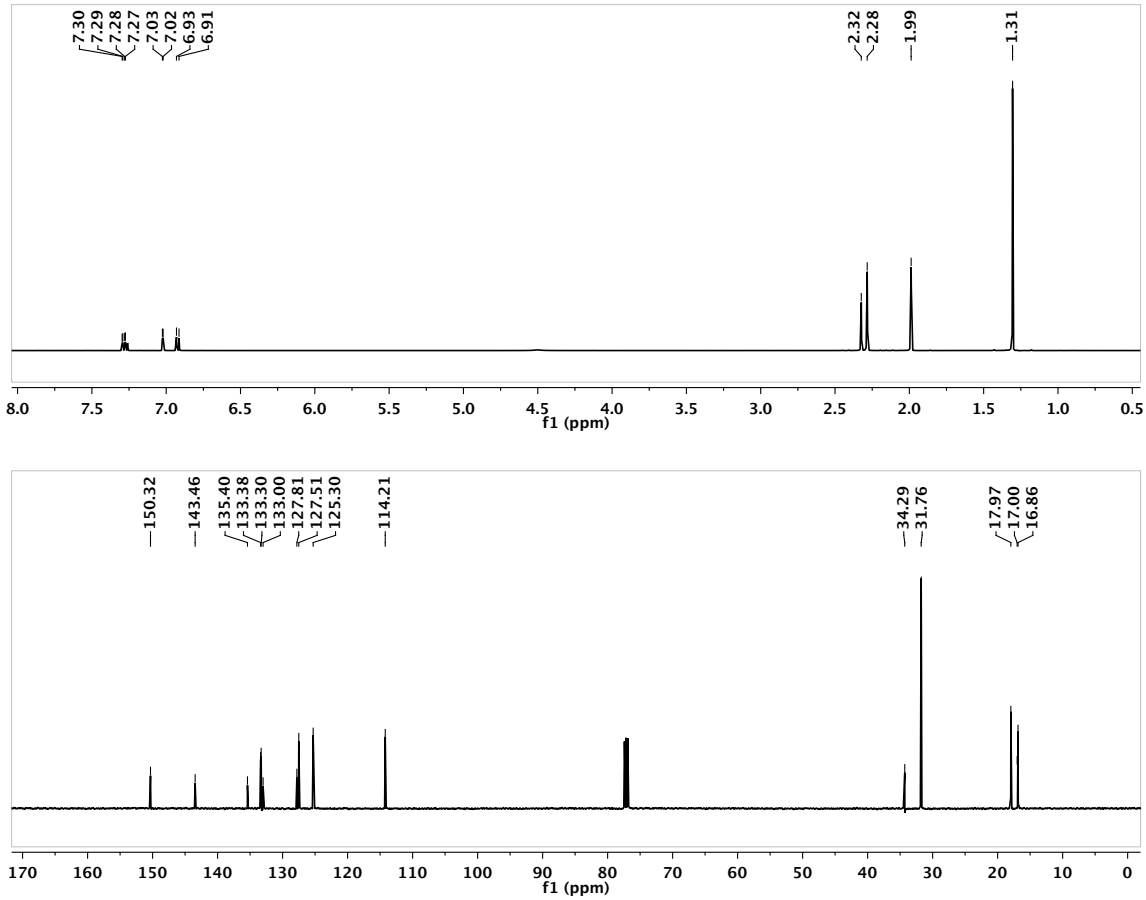

Figure C.100. ^{1}H (above) and ^{13}C (below) NMR spectra of **58** in $CDCl_3$.

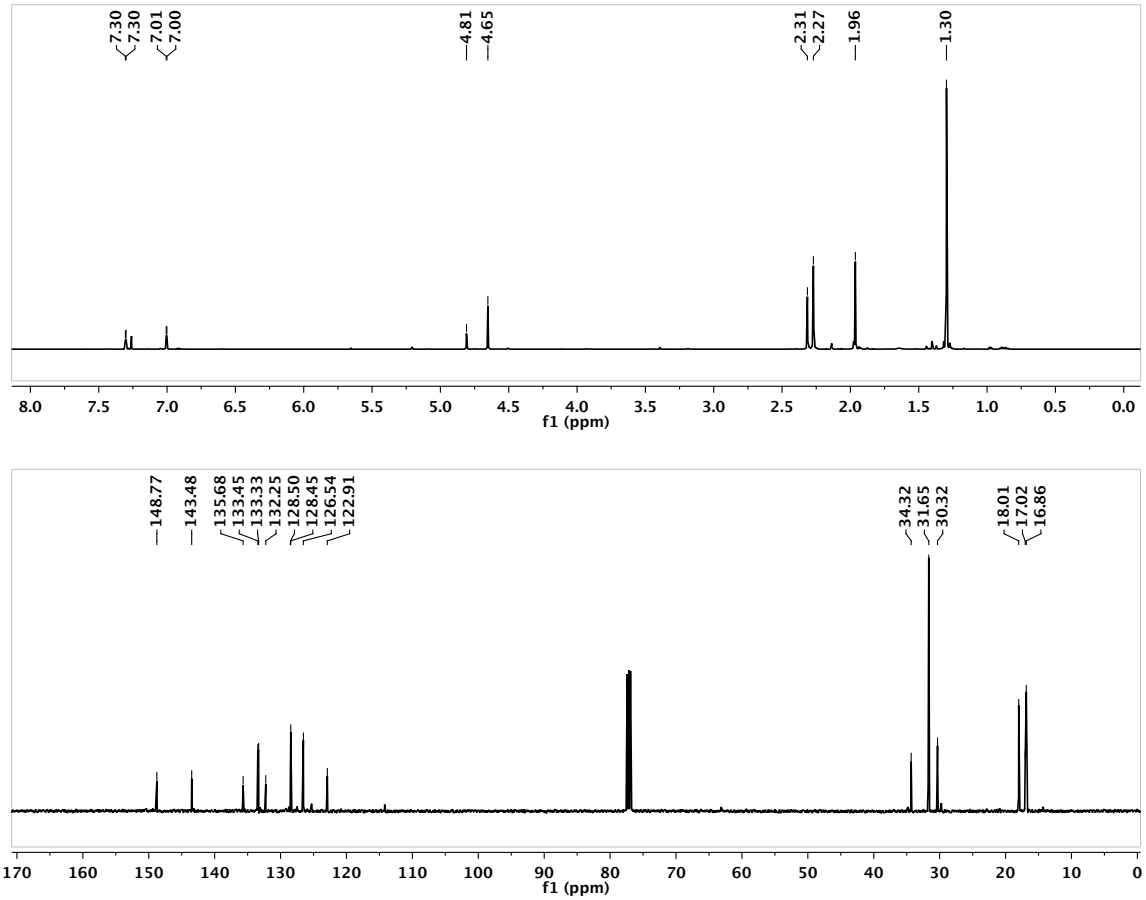

Figure C.101. ^{1}H (above) and ^{13}C (below) NMR spectra of **59** in $CDCl_3$.

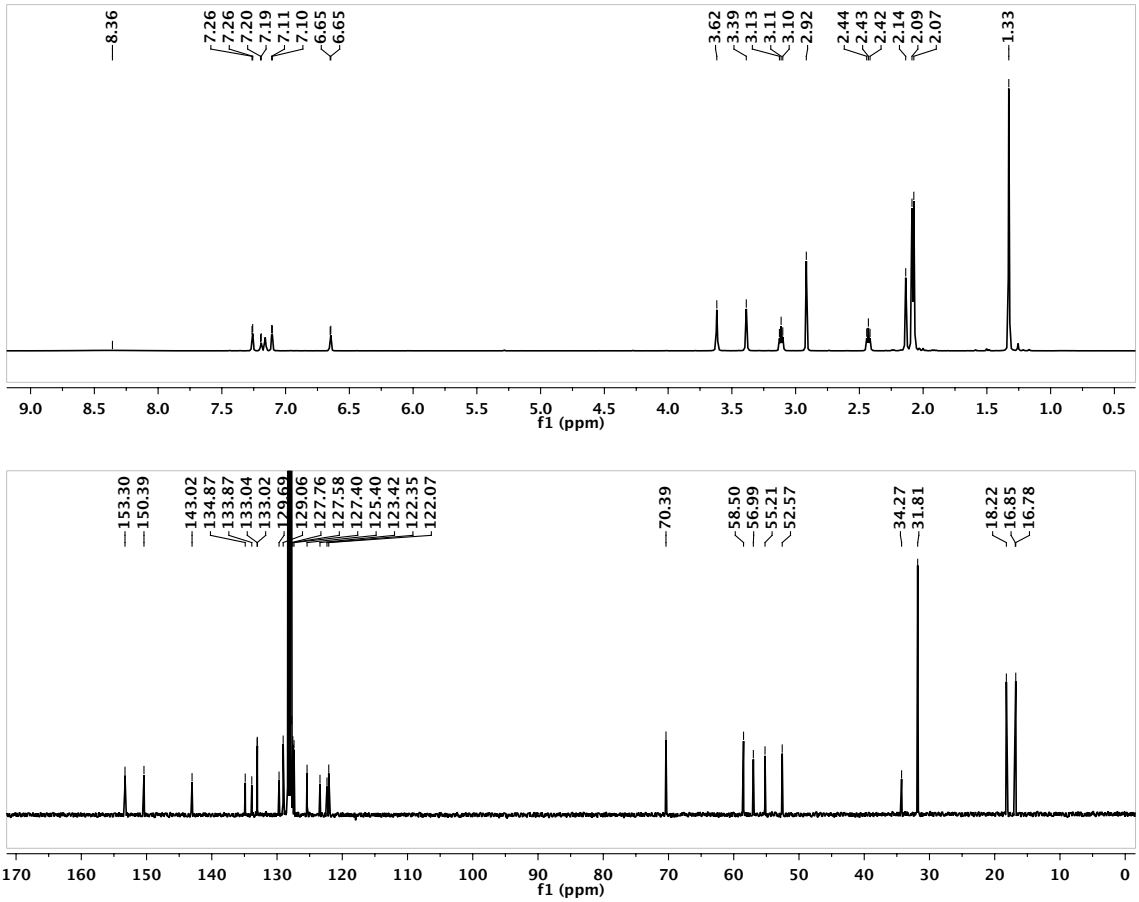

Figure C.102. ^{1}H (above) and ^{13}C (below) NMR spectra of **60-OMe** in C_6D_6.

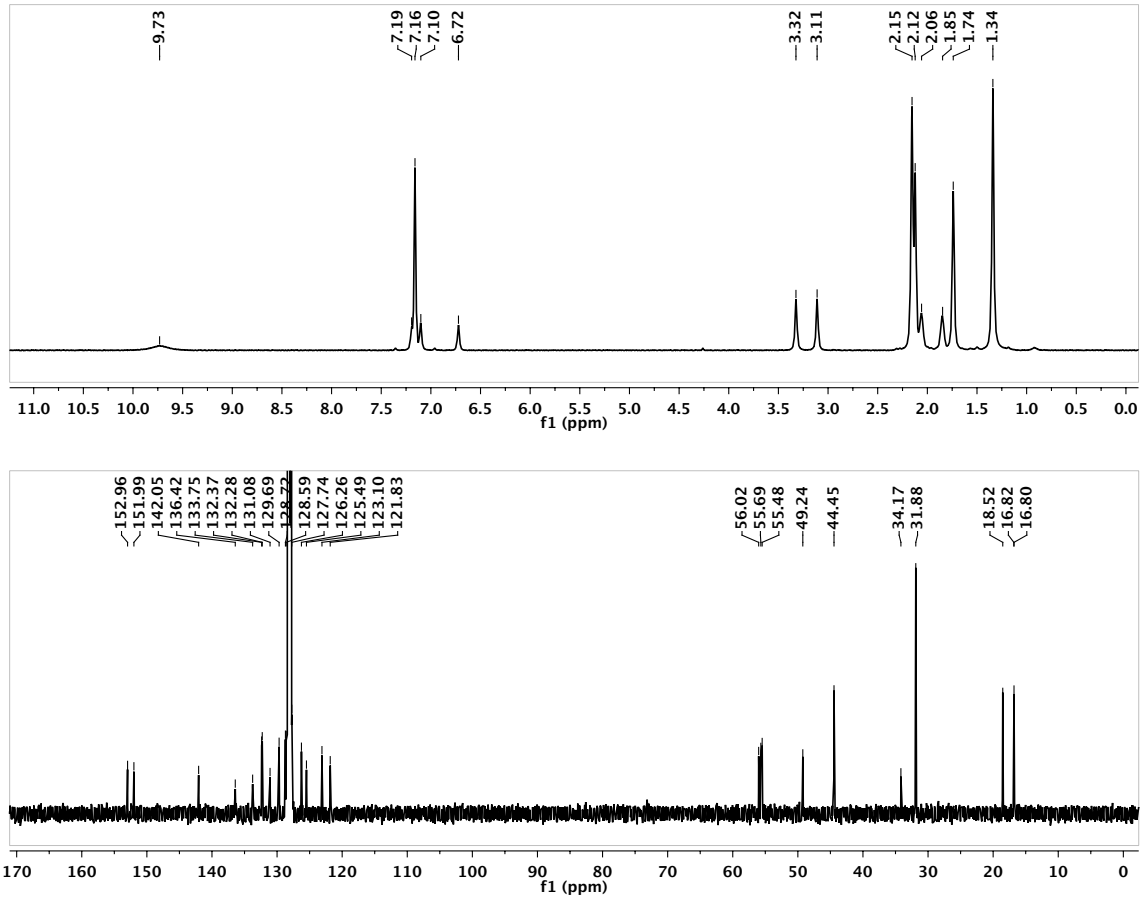

Figure C.103. ^{1}H (above) and ^{13}C (below) NMR spectra of **60-NMe$_3$** in C_6D_6.

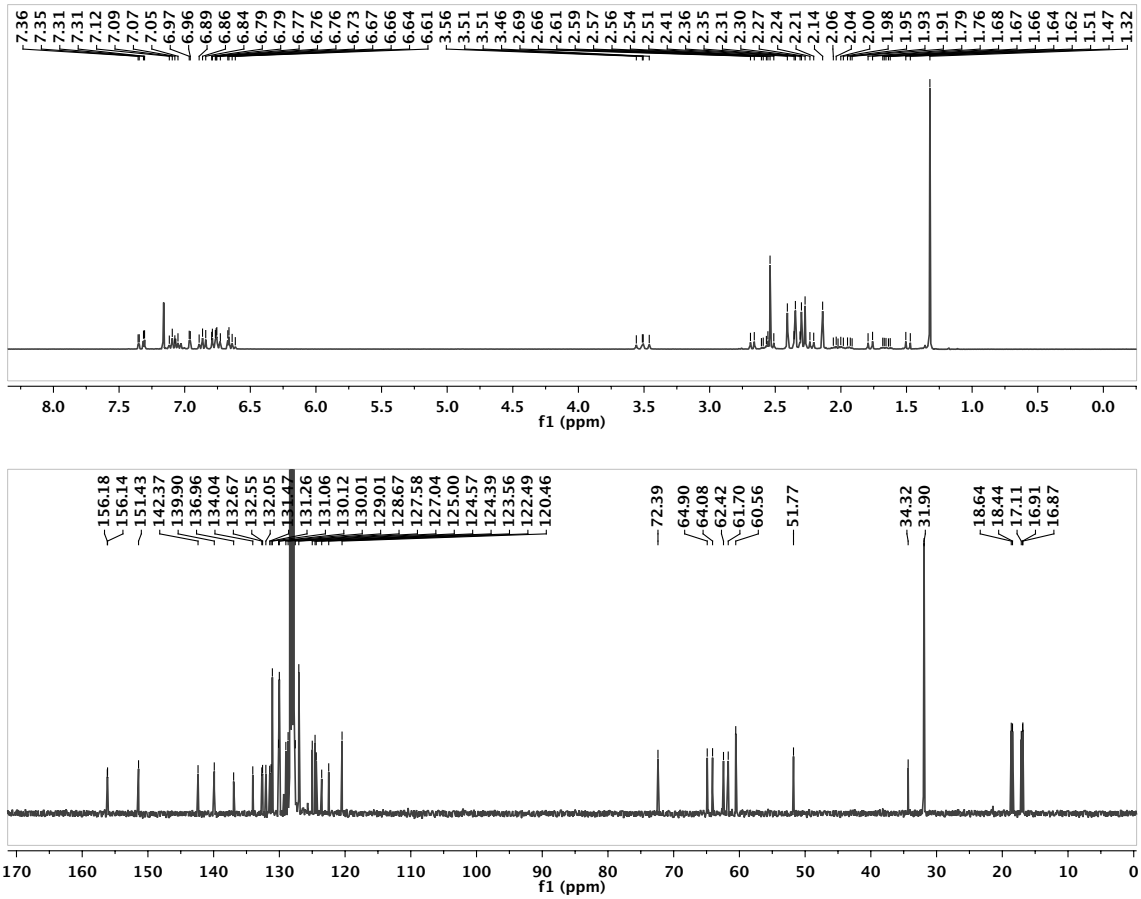

Figure C.104. ^{1}H (above) and ^{13}C (below) NMR spectra of **61-OMe** in C_6D_6.

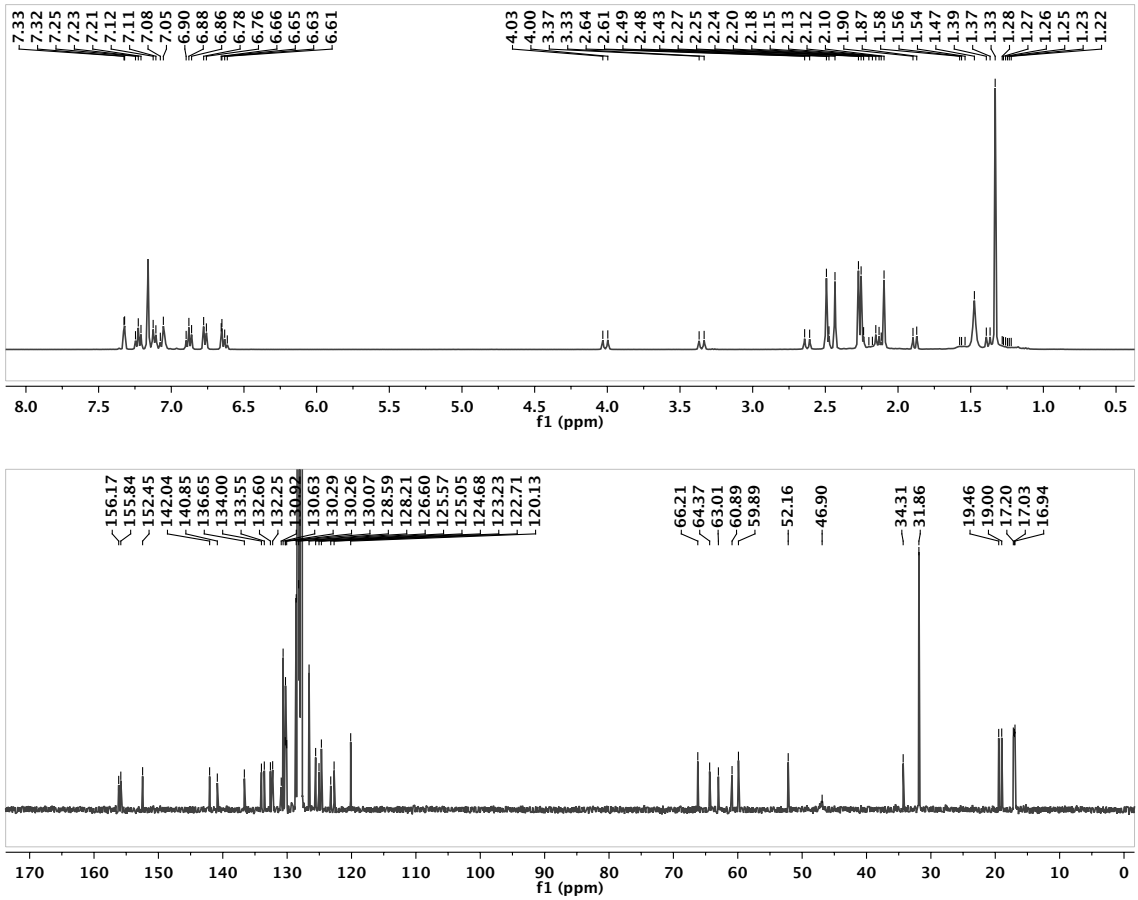

Figure C.105. ^{1}H (above) and ^{13}C (below) NMR spectra of **61-NMe$_3$** in C_6D_6.

APPENDIX A

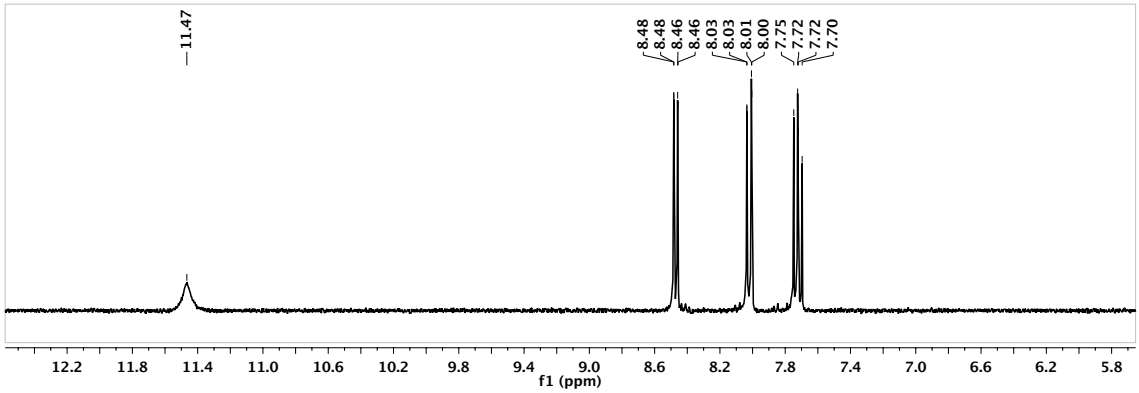

Figure C.106. ^{1}H NMR spectrum of **62** in $(CD_3)_2CO$.

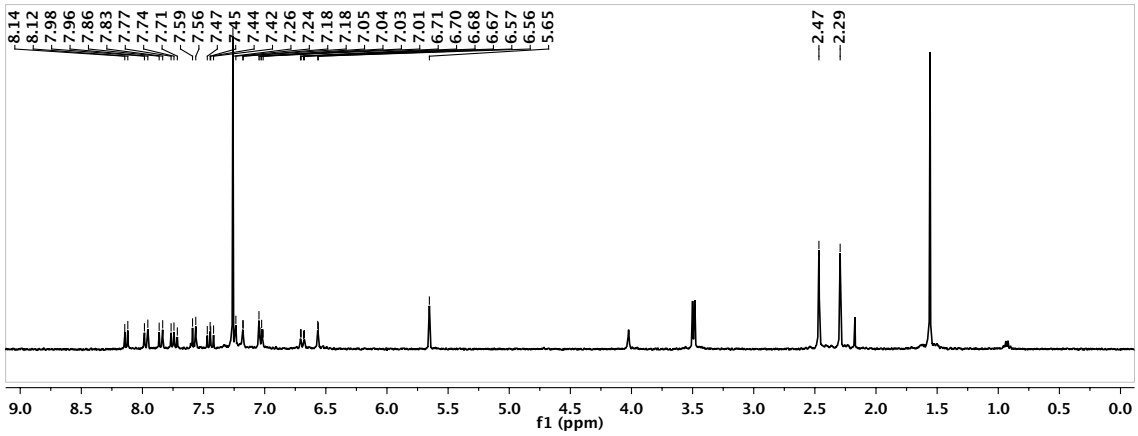

Figure C.107. ^{1}H NMR spectrum of **80** in $CDCl_3$.

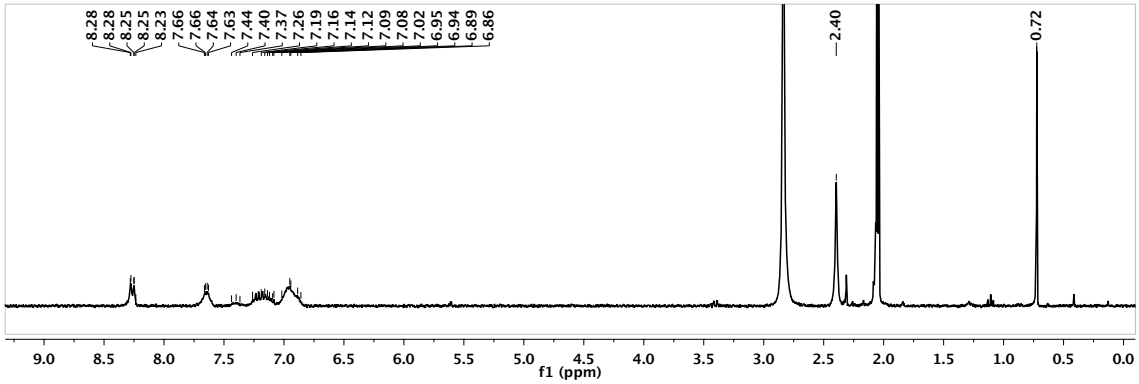

Figure C.108. ^{1}H NMR spectrum of **81** in $(CD_3)_2CO$.

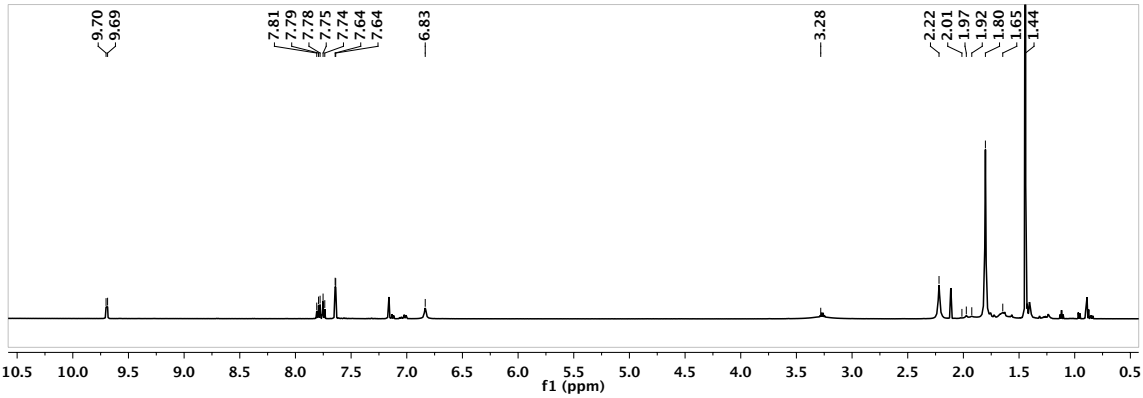

Figure C.109. ^{1}H NMR spectrum of **83** in C_6D_6.

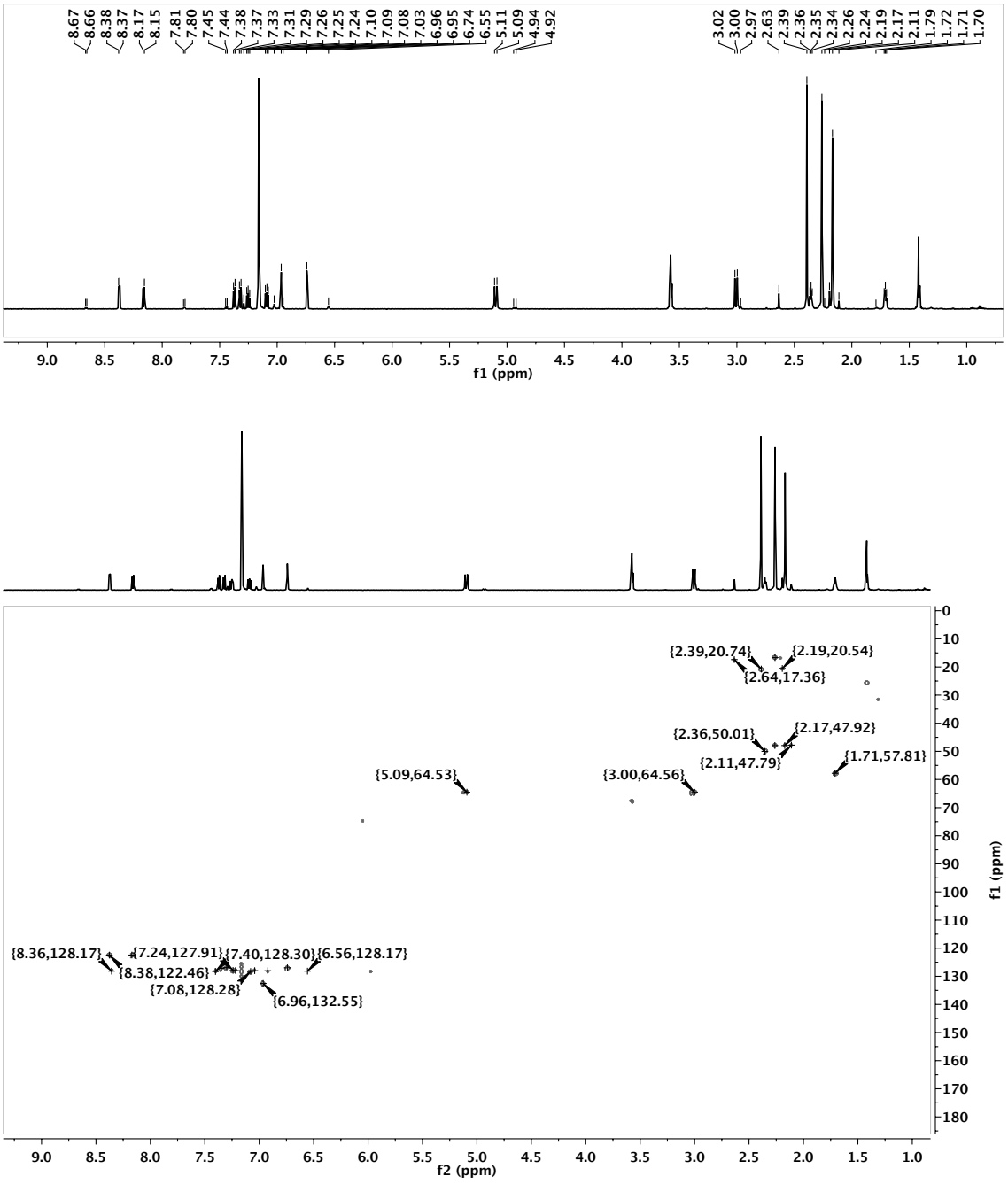

Figure C.110. ^{1}H (above) and ^{1}H-^{13}C HSQCAD (below) NMR spectra of **82** in C_6D_6.

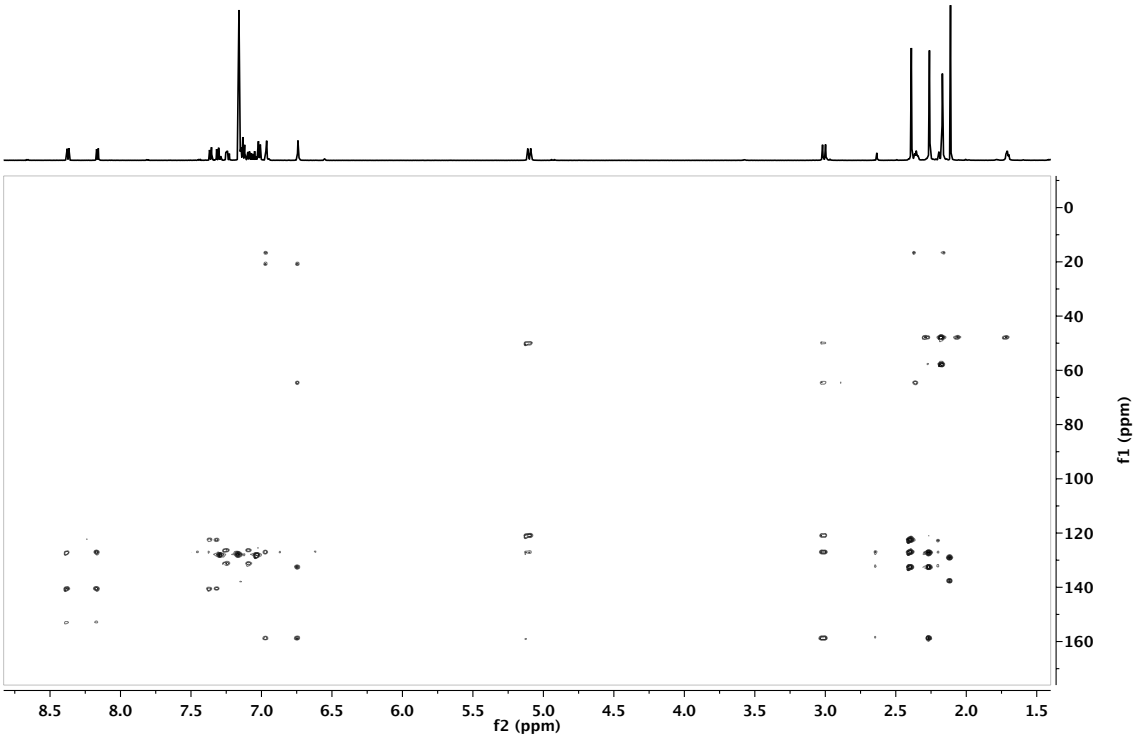

Figure C.111. ^{1}H-^{13}C gHMBCAD NMR spectrum of **82** in CD_2Cl_2.

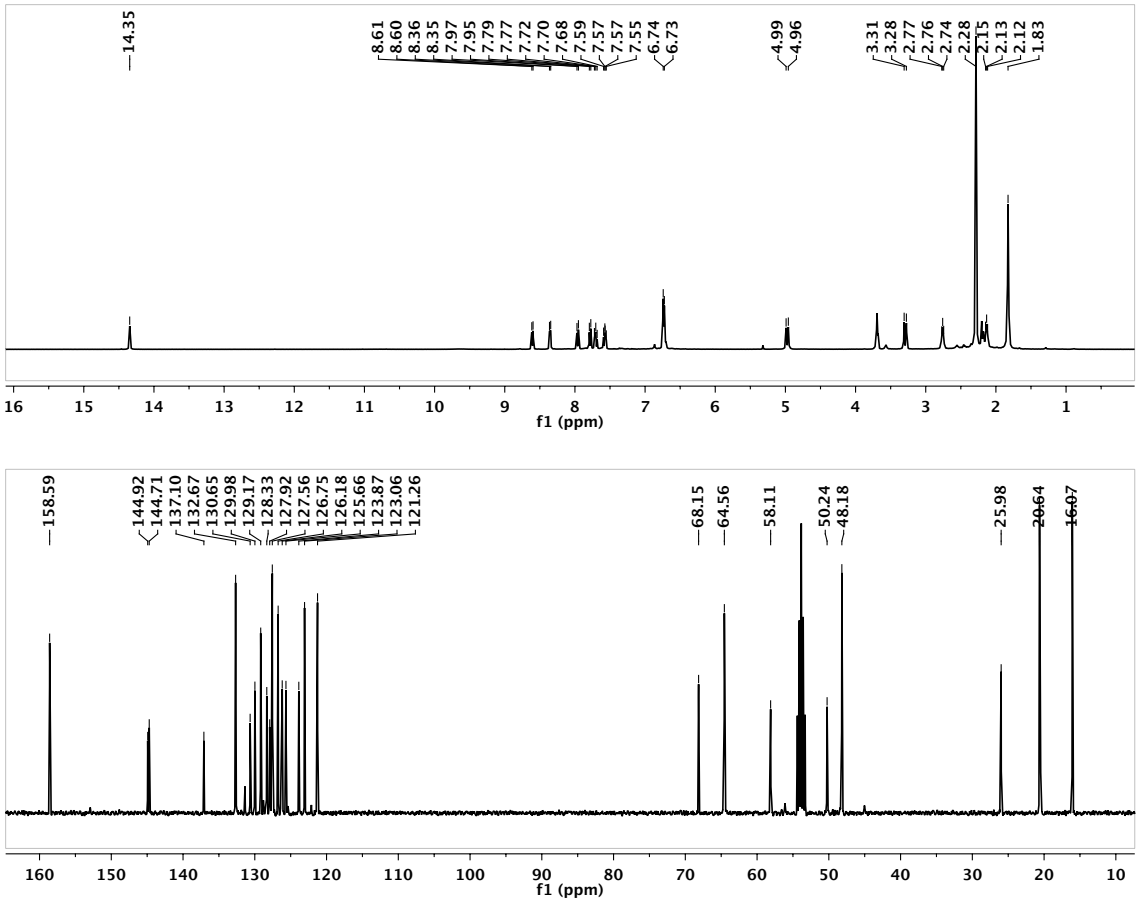

Figure C.112. ^{1}H (above) and ^{13}C (below) NMR spectra of **85** in CD_2Cl_2.

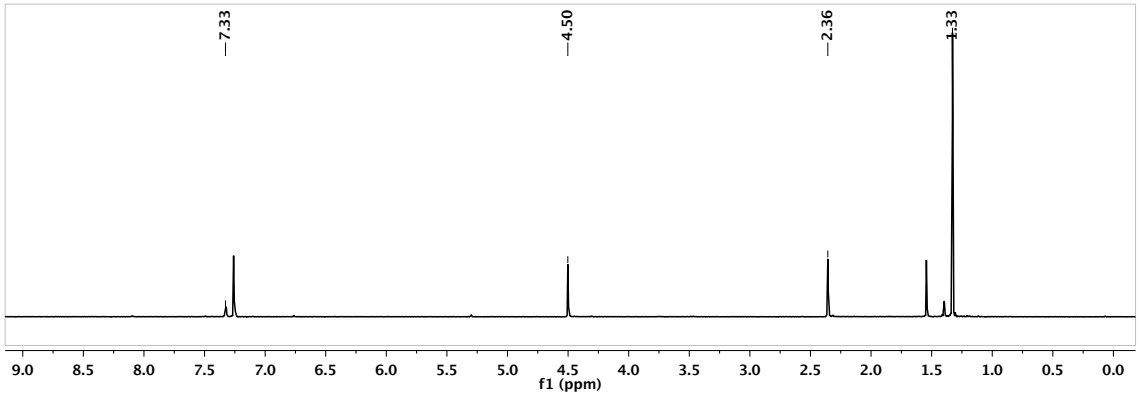

Figure C.113. ^{1}H NMR spectrum of **87** in $CDCl_3$.

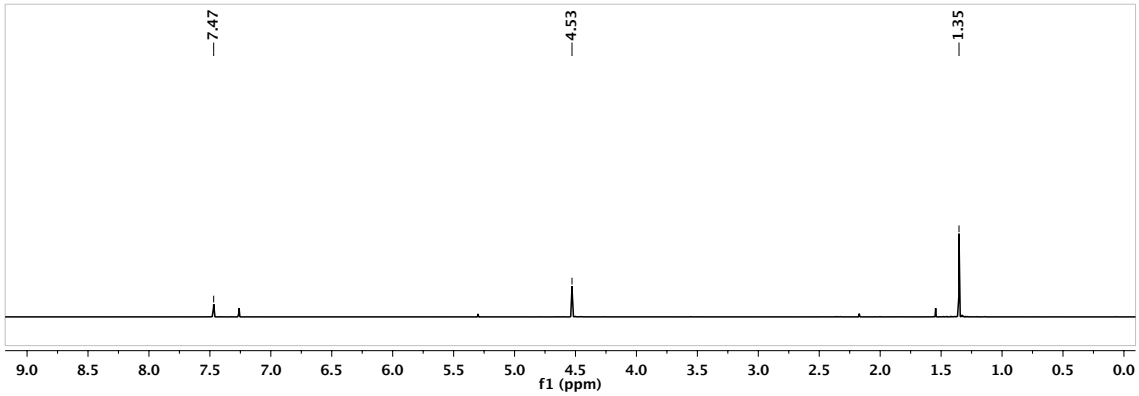

Figure C.114. ^{1}H NMR spectrum of the dibromide analogue of **87** in $CDCl_3$.

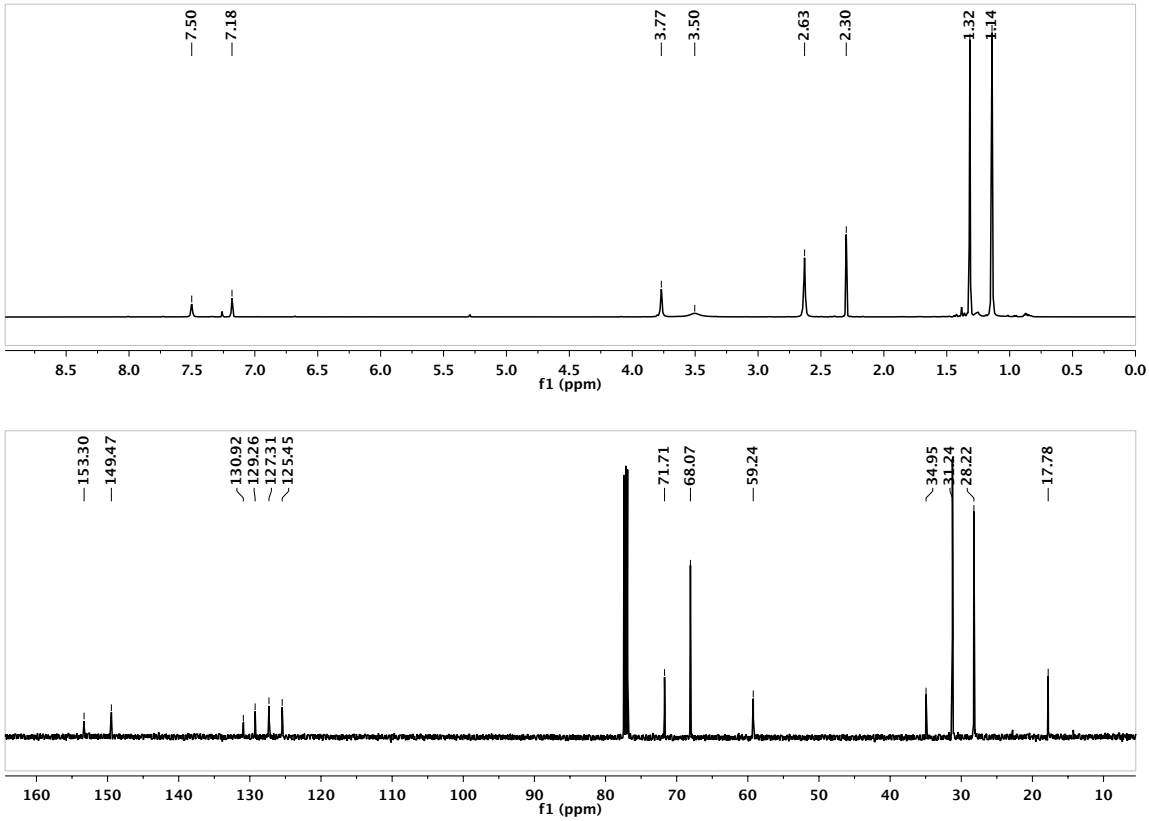

Figure C.115. ^{1}H (above) and ^{13}C (below) NMR spectra of **89** in $CDCl_3$.

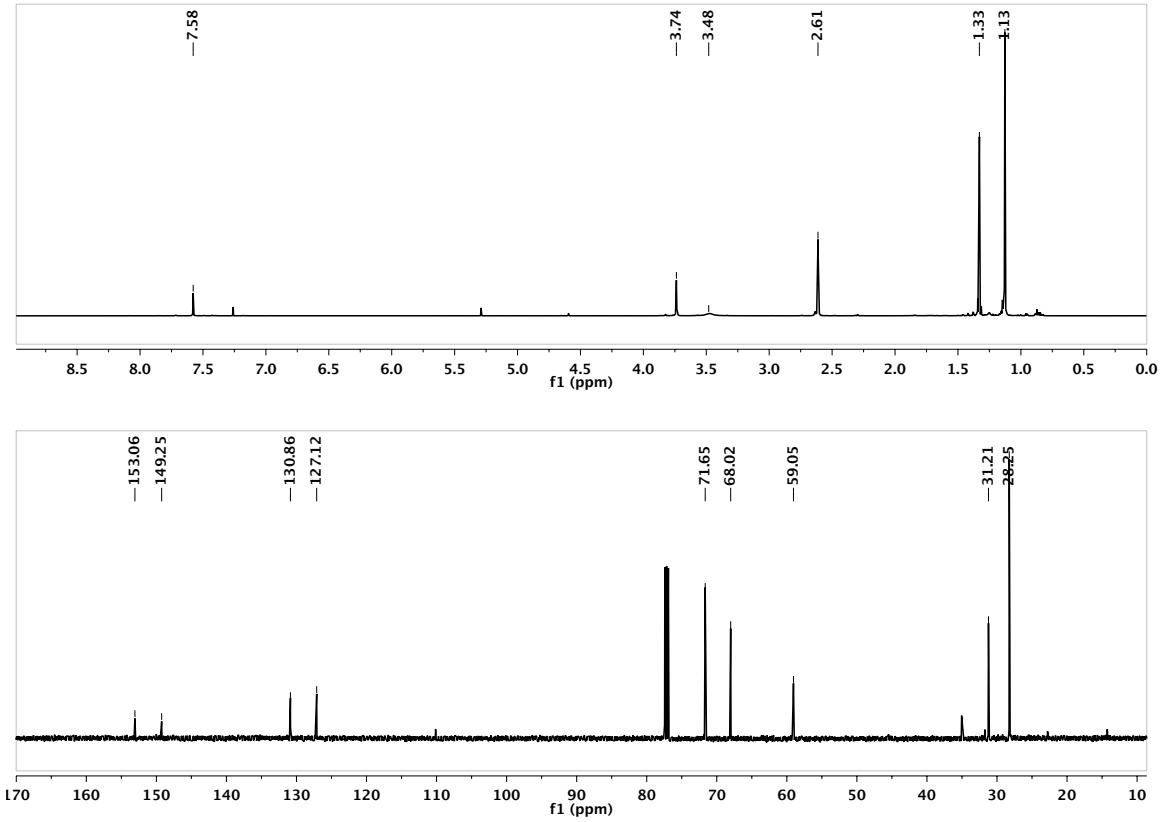

Figure C.116. ^{1}H (above) and ^{13}C (below) NMR spectra of the diubstituted analogue of **89** in $CDCl_3$.

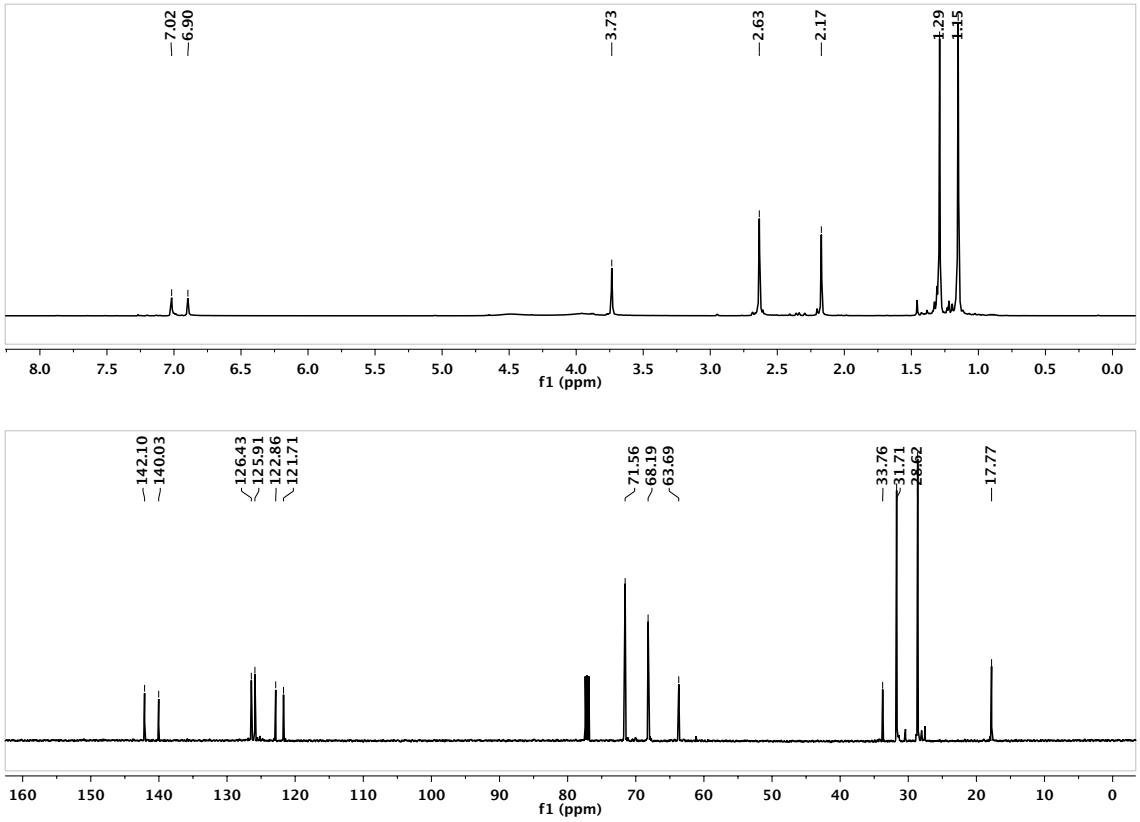

Figure C.117. ^{1}H (above) and ^{13}C (below) NMR spectra of **90** in $CDCl_3$.

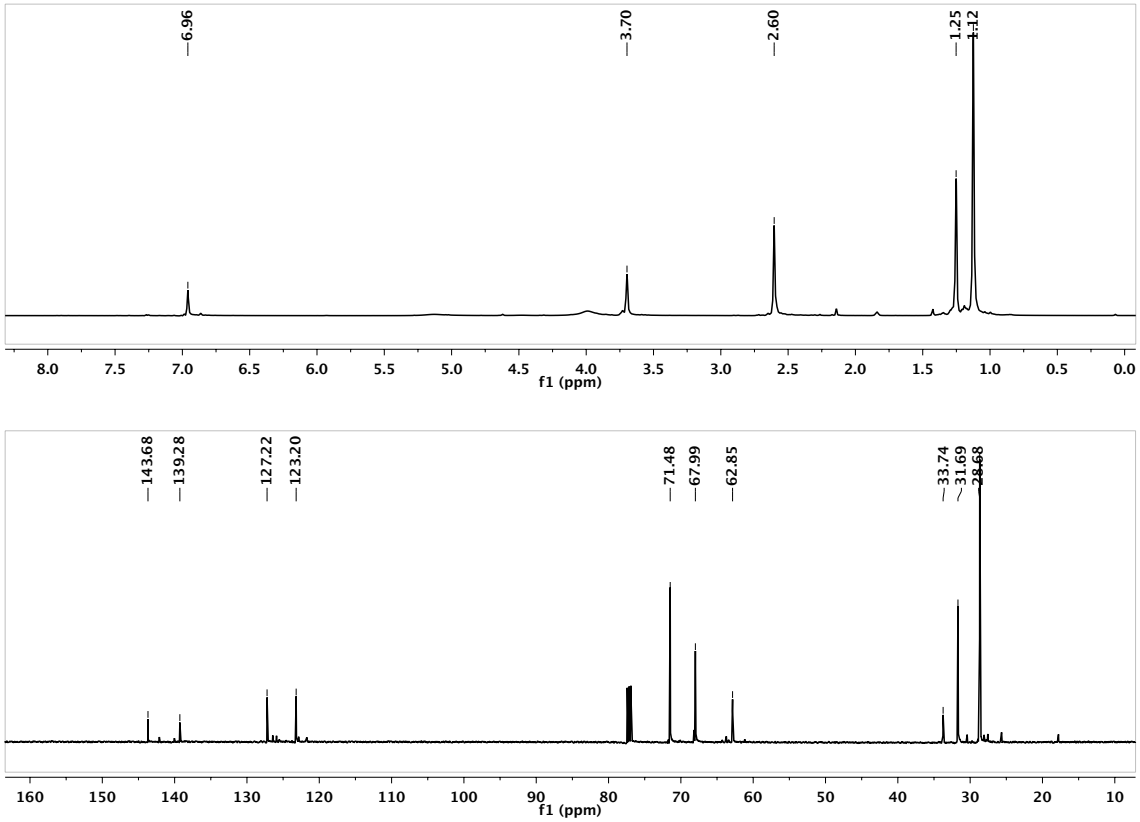

Figure C.118. ^{1}H (above) and ^{13}C (below) NMR spectra of the diubstituted analogue of **90** in $CDCl_3$.

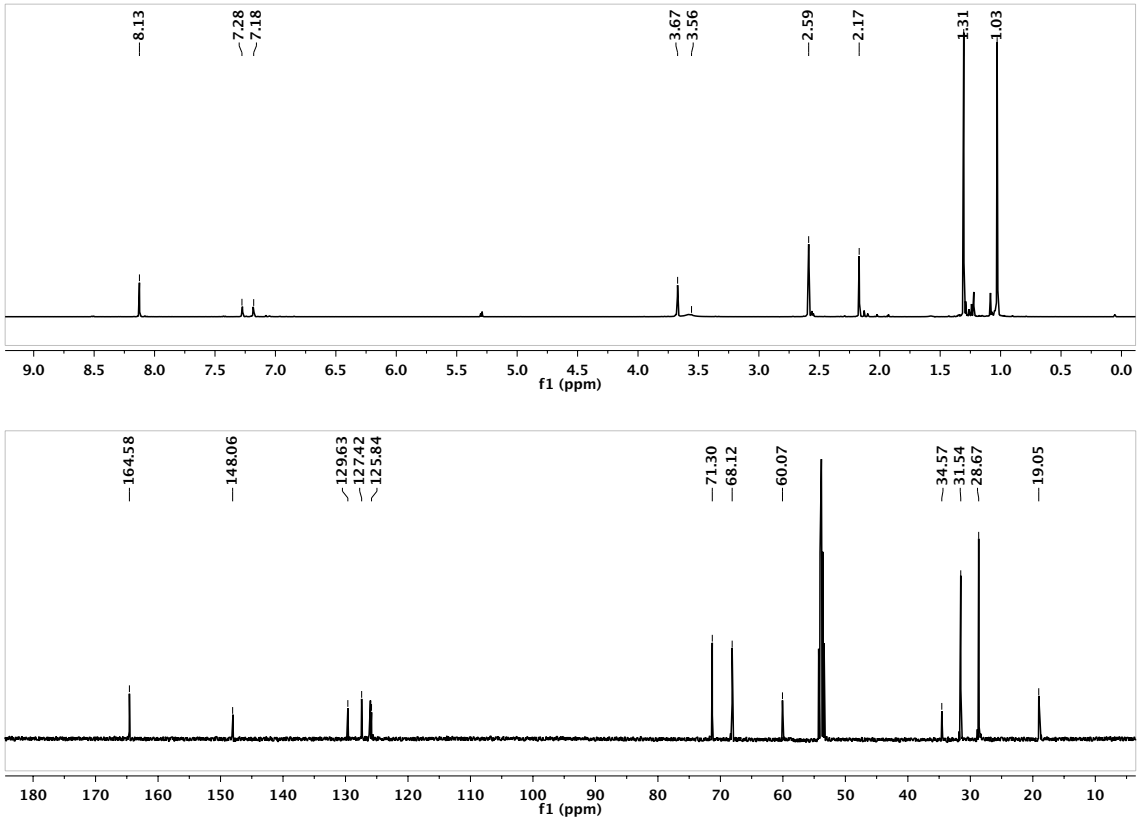

Figure C.119. ^{1}H (above) and ^{13}C (below) NMR spectra of **91** in $CDCl_3$.

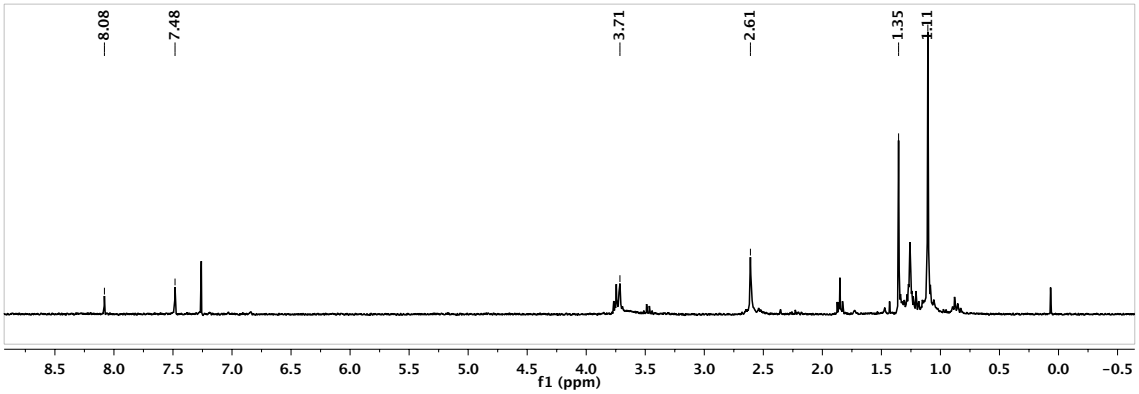

Figure C.120. ^{1}H NMR spectrum of the analogue of **91** with four aminediol moieties in $CDCl_3$.

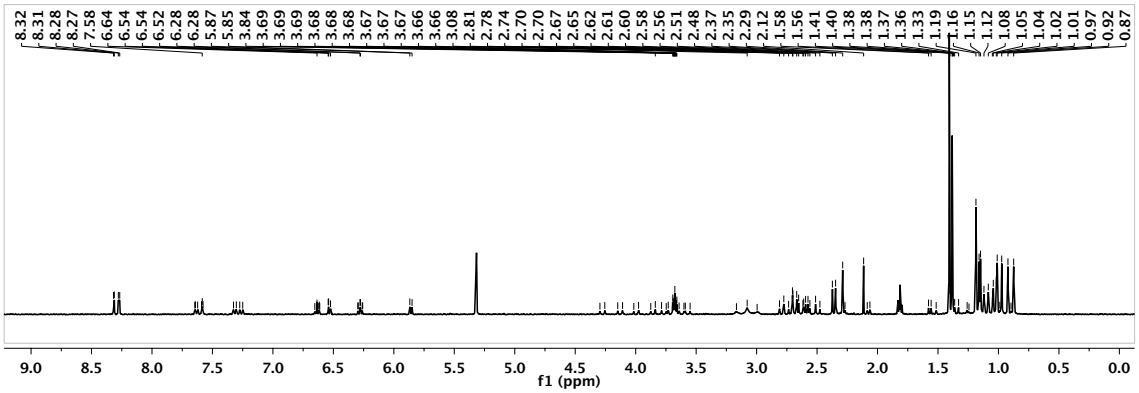

Figure C.121. ^{1}H NMR spectrum of **92**.

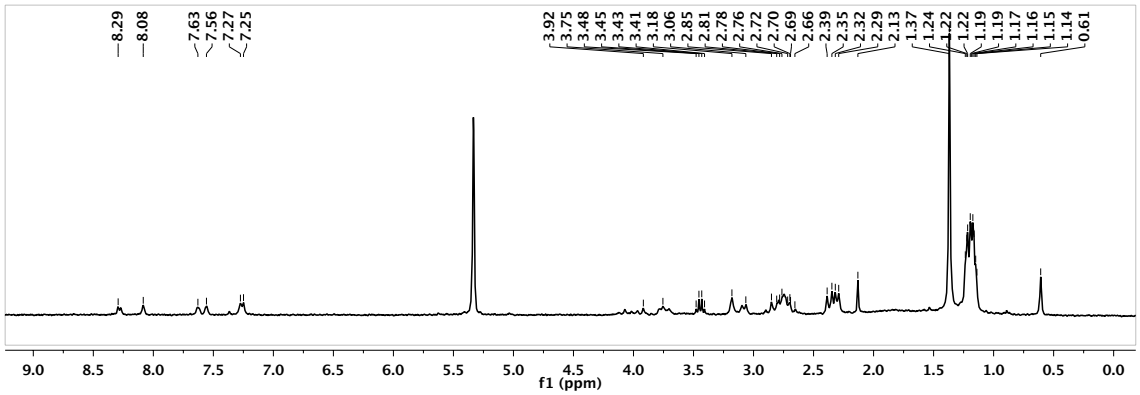

Figure C.122. ^{1}H NMR spectrum of **93** in CD_2Cl_2.

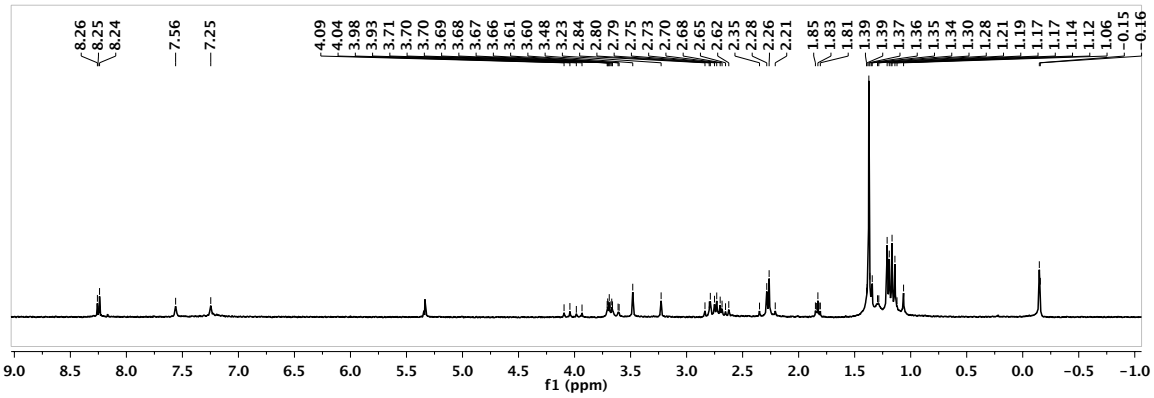

Figure C.123. ^{1}H NMR spectrum of **93** + $ZnMe_2$ in CD_2Cl_2.

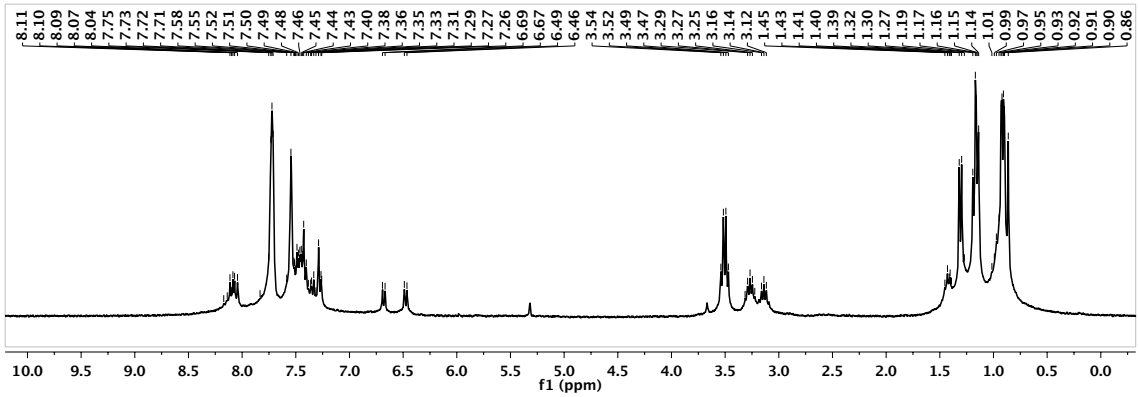

Figure C.124. ^{1}H NMR spectrum of **95** in CD_2Cl_2.

APPENDIX B

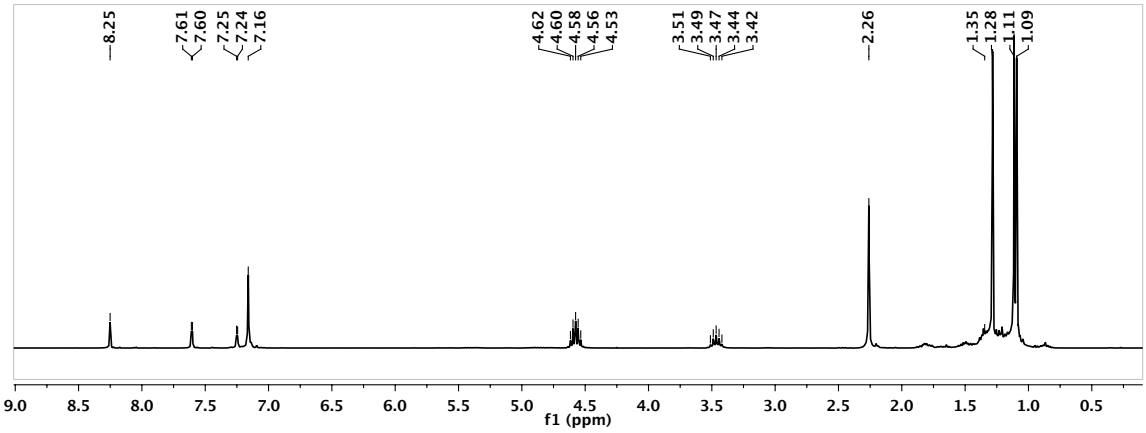

Figure C.125. ^{1}H NMR spectrum of **98-a** in C_6D_6.

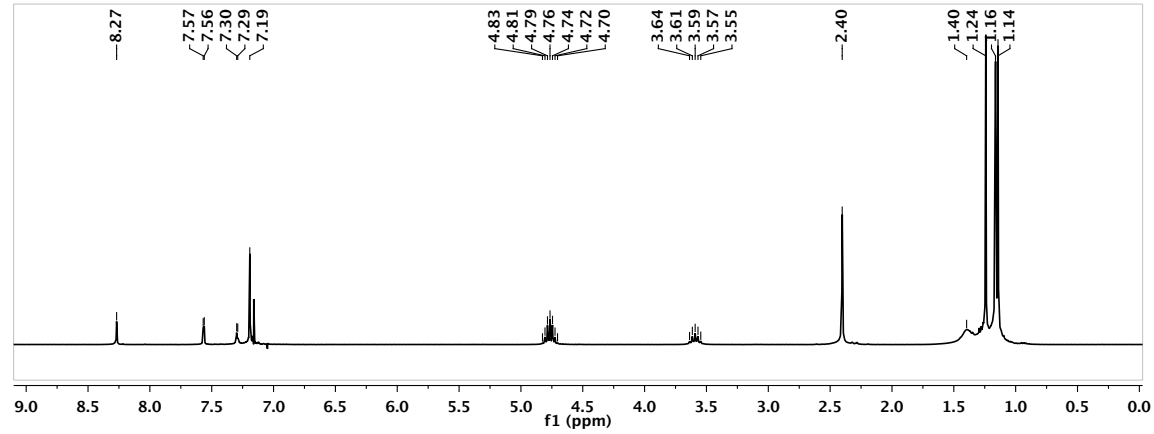

Figure C.126. ^{1}H NMR spectrum of **98-s** in C_6D_6.

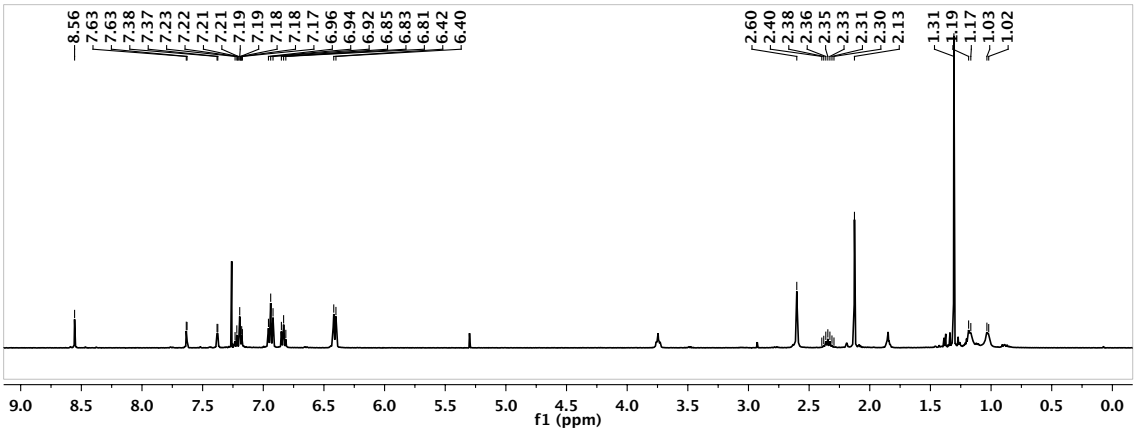

Figure C.127. ^{1}H NMR spectrum of **99-a** in $CDCl_3$.

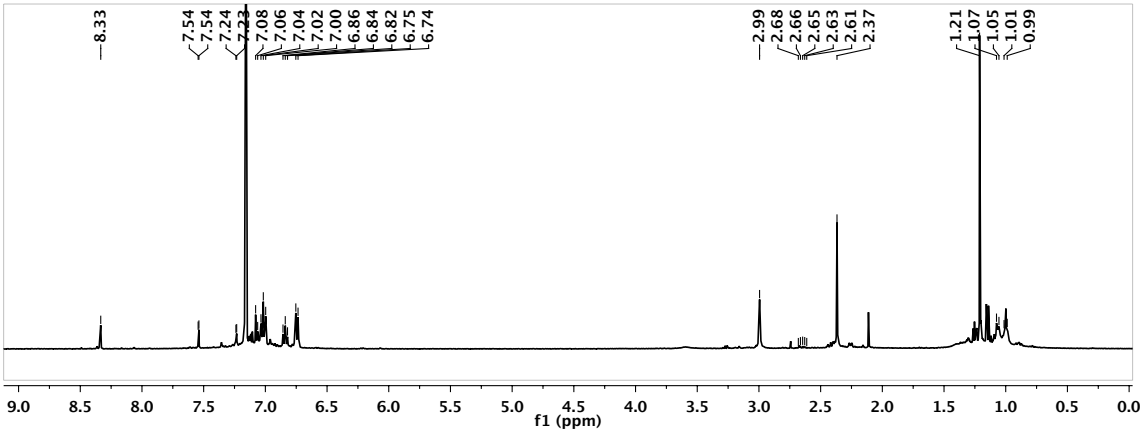

Figure C.128. ^{1}H NMR spectrum of **99-s** in C_6D_6.

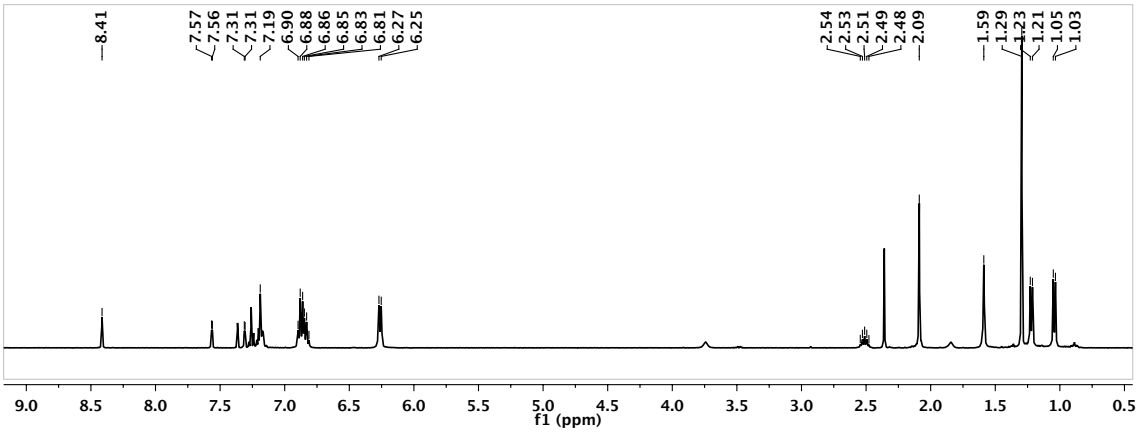

Figure C.129. ^{1}H NMR spectrum of **100-a** in $CDCl_3$.

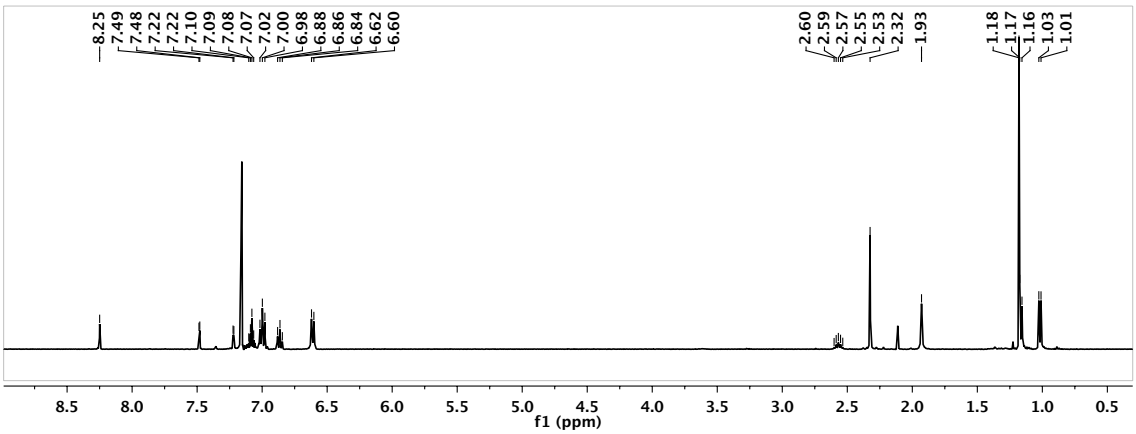

Figure C.130. ^{1}H NMR spectrum of **100-s** in C_6D_6.

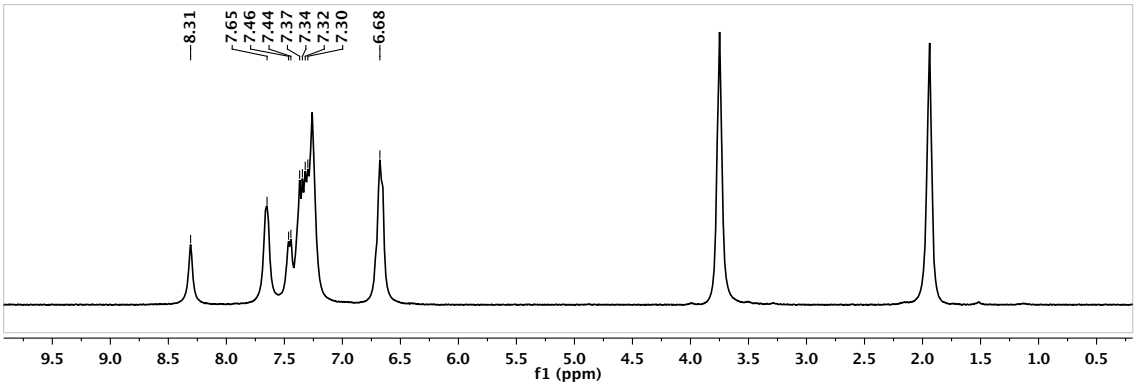

Figure C.131. ^{1}H NMR spectrum of **102** in $CDCl_3$.

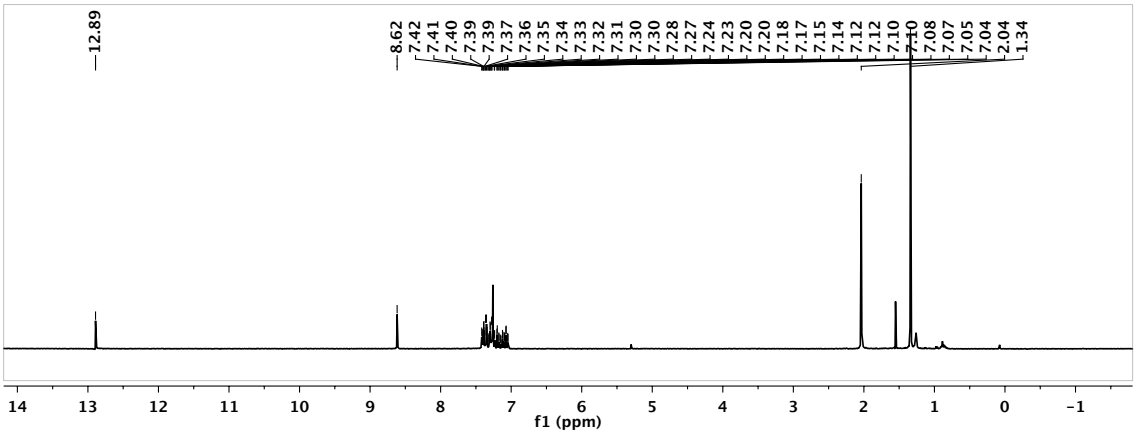

Figure C.132. ^{1}H NMR spectrum of **104-a** in $CDCl_3$.

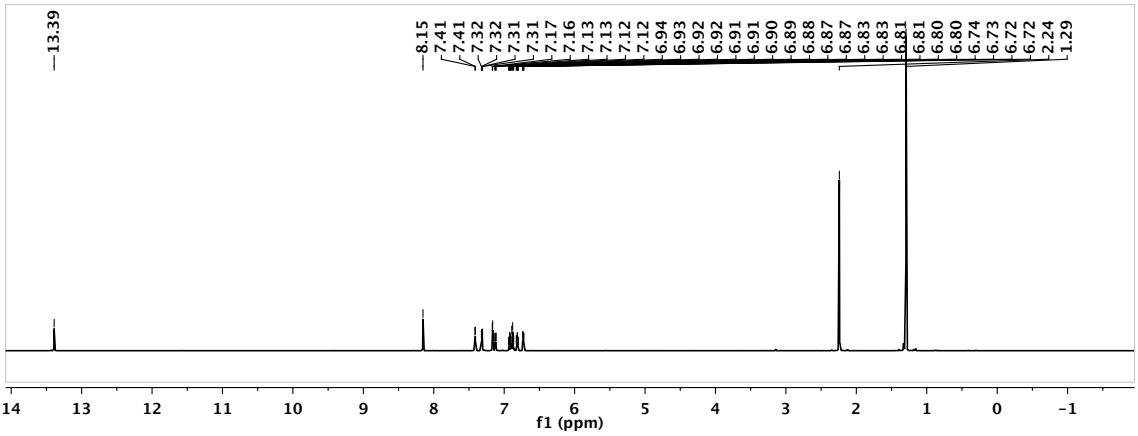

Figure C.133. ^{1}H NMR spectrum of **104-s** in C_6D_6.

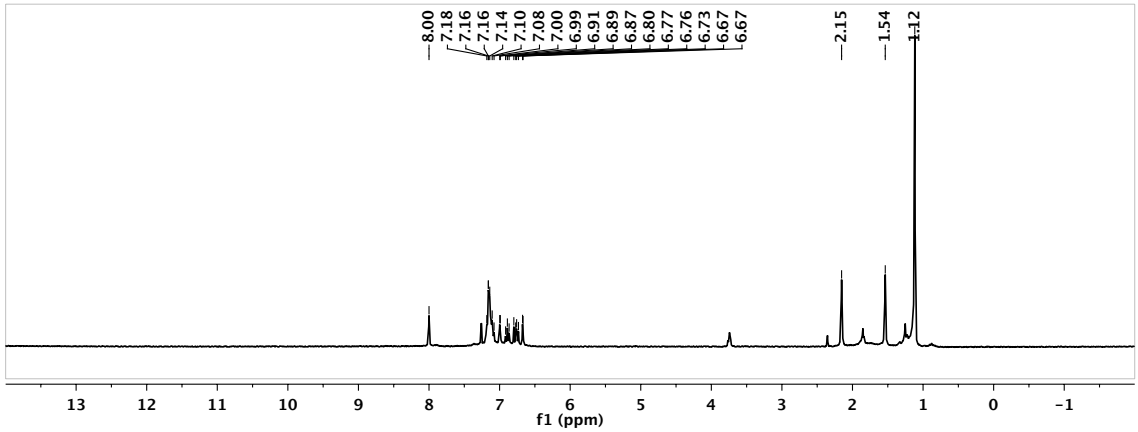

Figure C.134. ^{1}H NMR spectrum of **105-a** in $CDCl_3$.

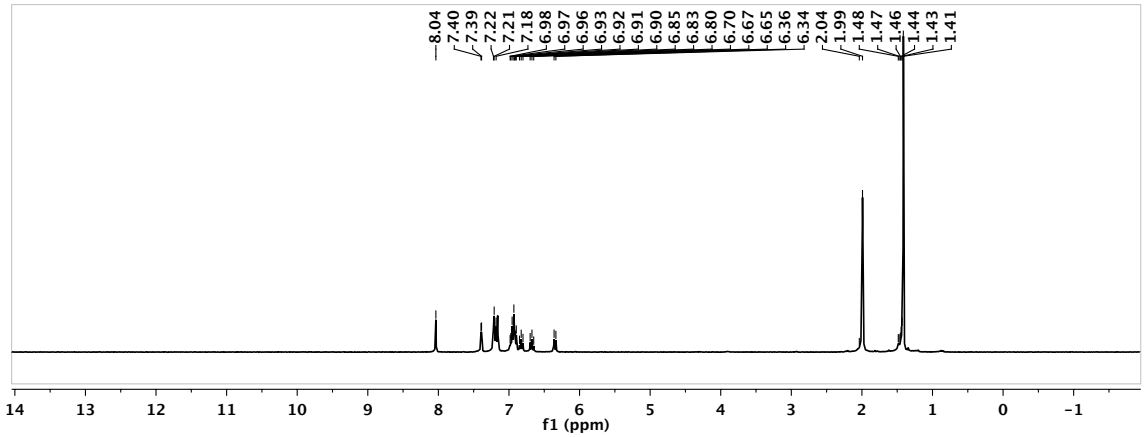

Figure C.135. ^{1}H NMR spectrum of **105-s** in C_6D_6.

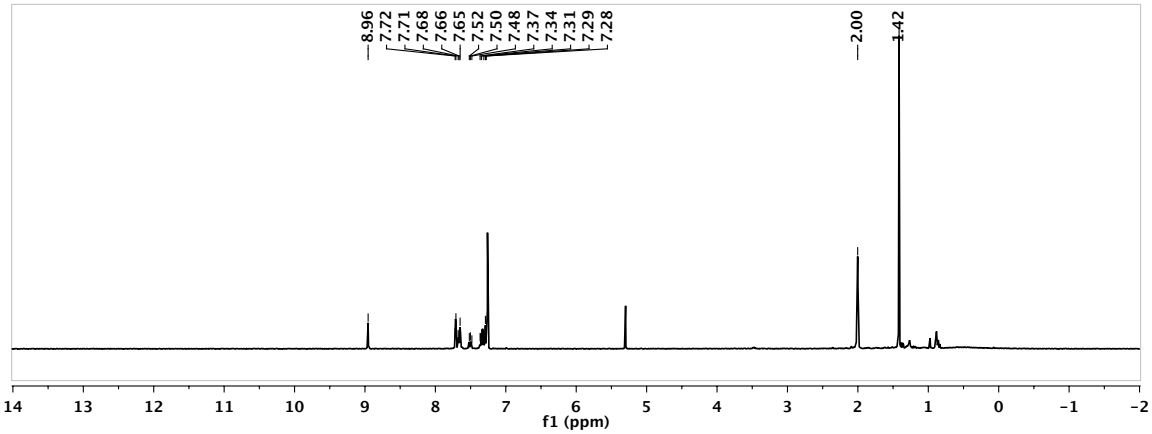

Figure C.136. ^{1}H NMR spectrum of **106-a** in $CDCl_3$.

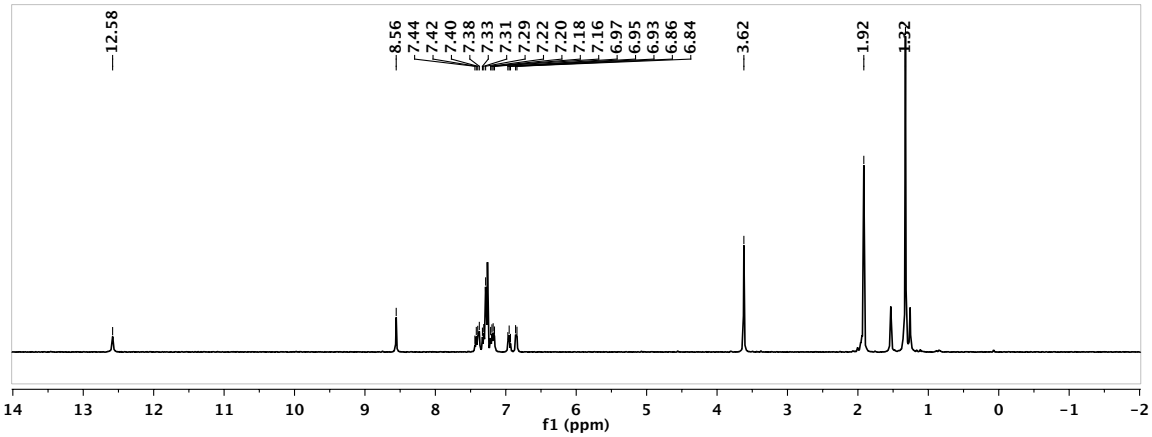

Figure C.137. ^{1}H NMR spectrum of **112-a** in $CDCl_3$.

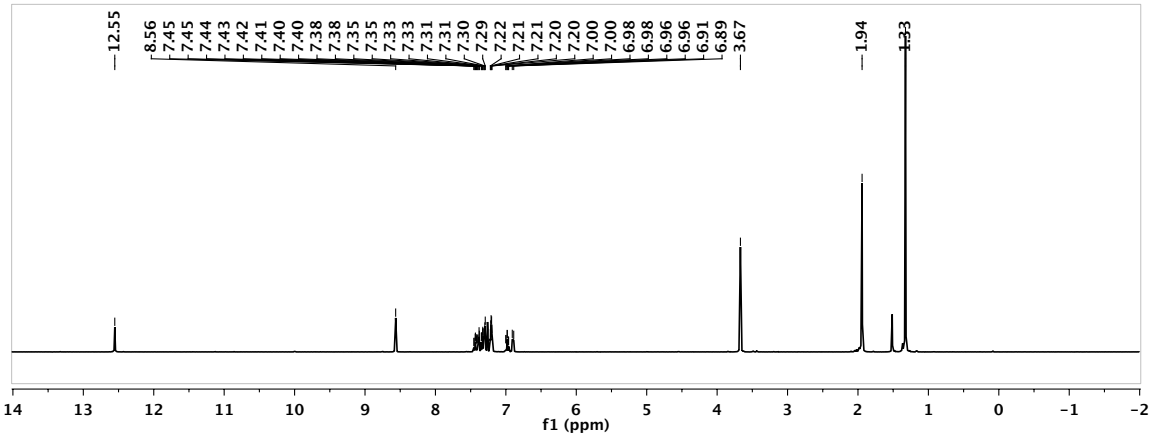

Figure C.138. ^{1}H NMR spectrum of **112-s** in $CDCl_3$.

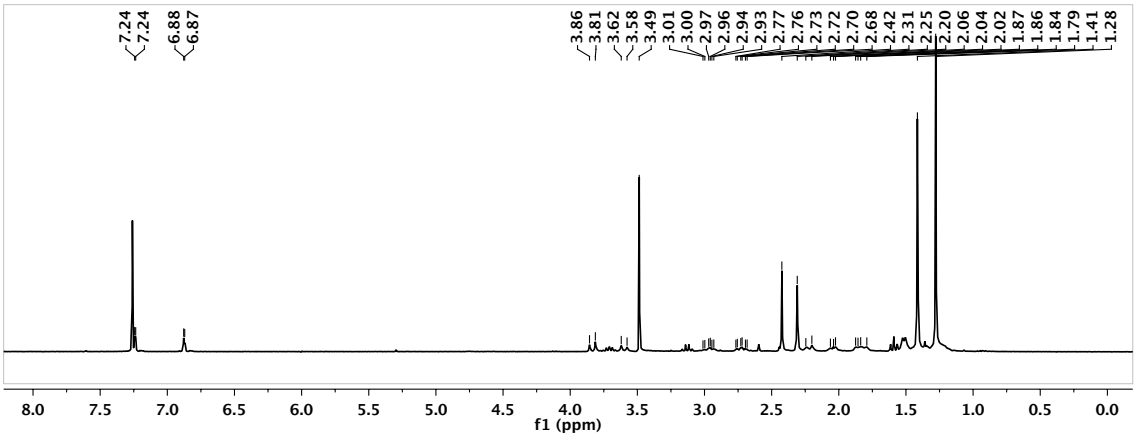

Figure C.139. ^{1}H NMR spectrum of **114** in $CDCl_3$.

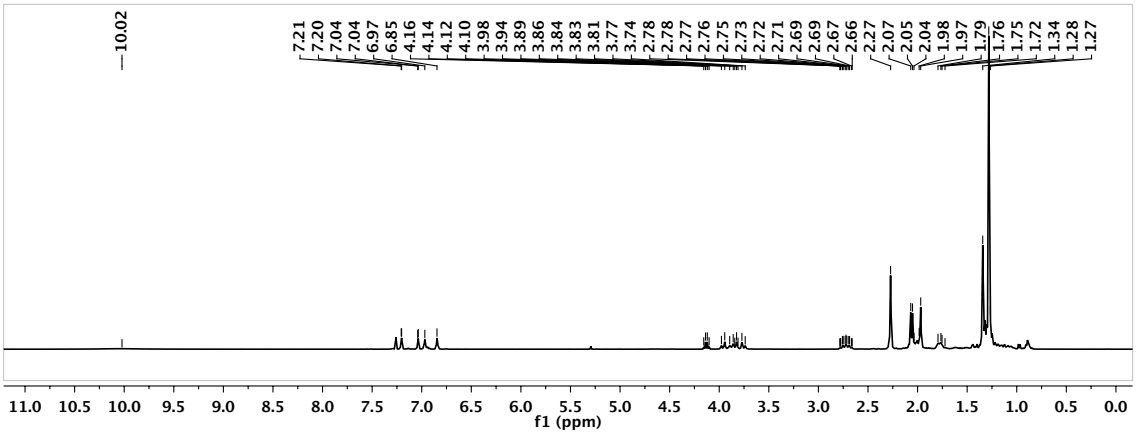

Figure C.140. ^{1}H NMR spectrum of **115-a** in $CDCl_3$.

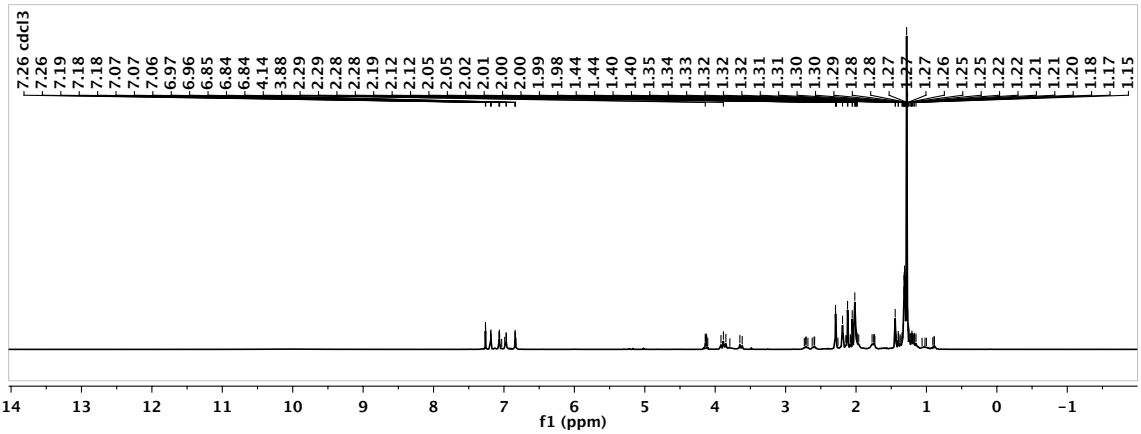

Figure C.141. ^{1}H NMR spectrum of **115-s** in $CDCl_3$.

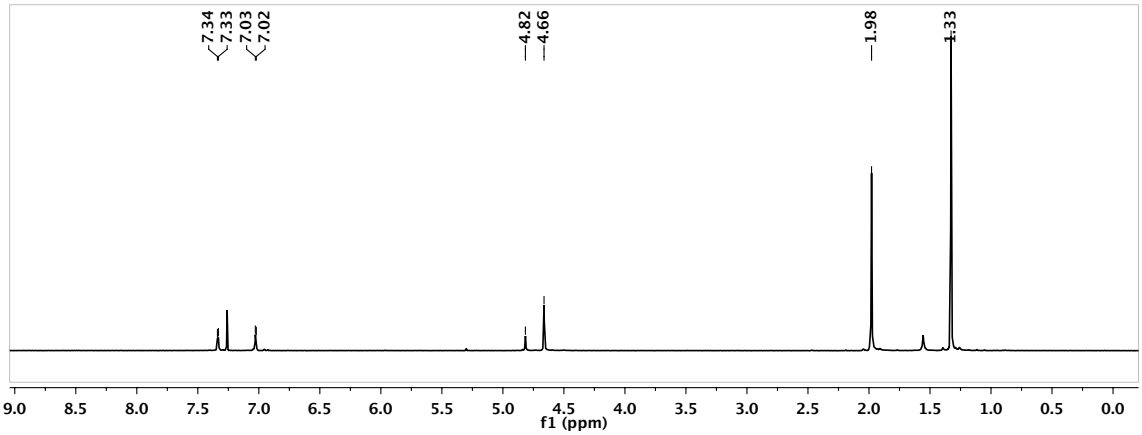

Figure C.142. ^{1}H NMR spectrum of **51-a** in $CDCl_3$.

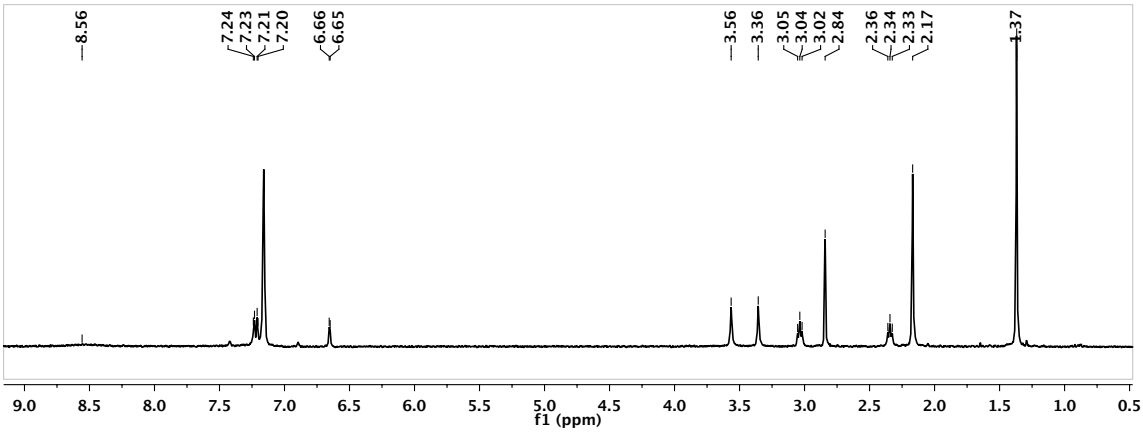

Figure C.143. ^{1}H NMR spectrum of **52a-OMe-a** in C_6D_6.

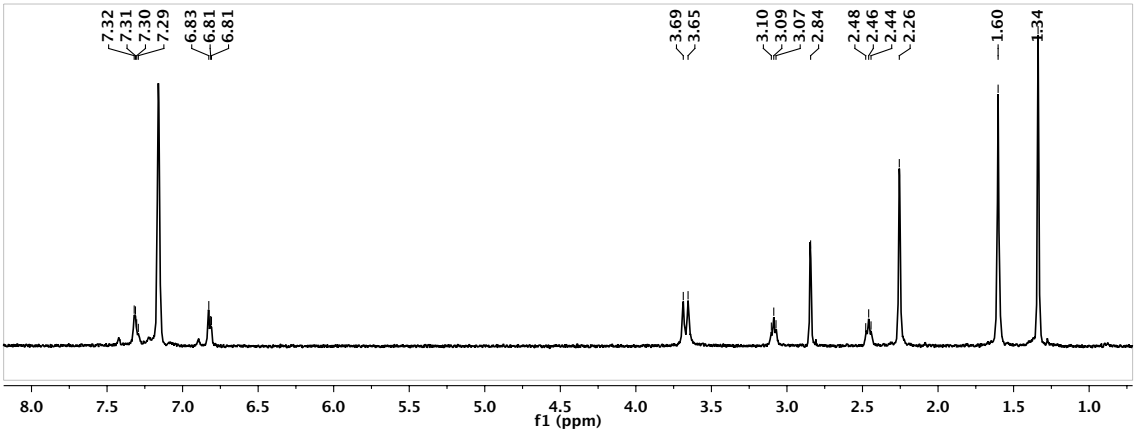

Figure C.144. ^{1}H NMR spectrum of **52d-OMe-a** in C_6D_6.

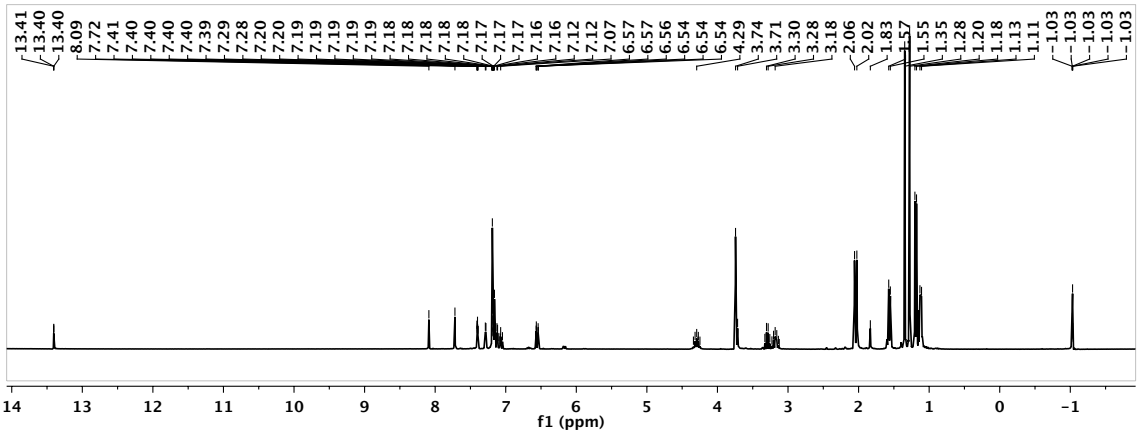

Figure C.145. ^{1}H NMR spectrum of **118** in $CDCl_3$.

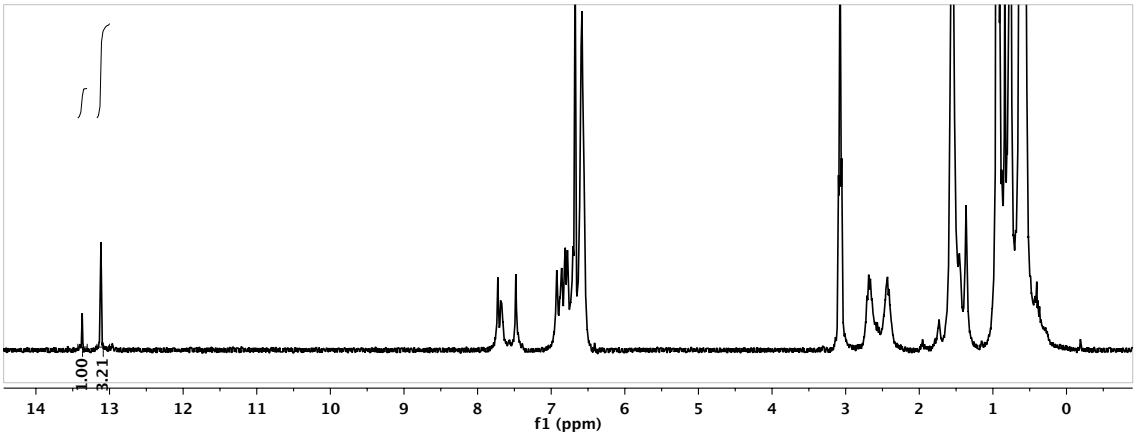

Figure C.146. ^{1}H NMR spectrum of **119** in C_6D_6.

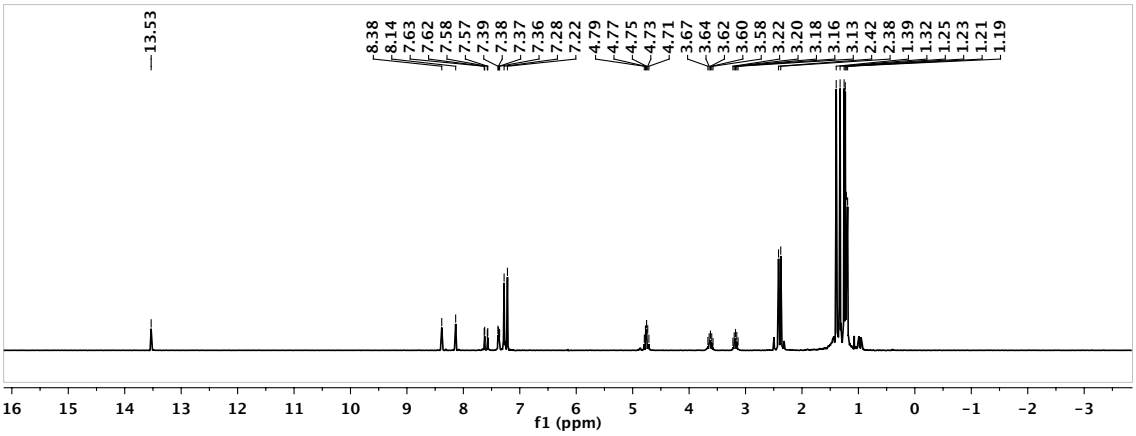

Figure C.147. ^{1}H NMR spectrum of **120** in C_6D_6.

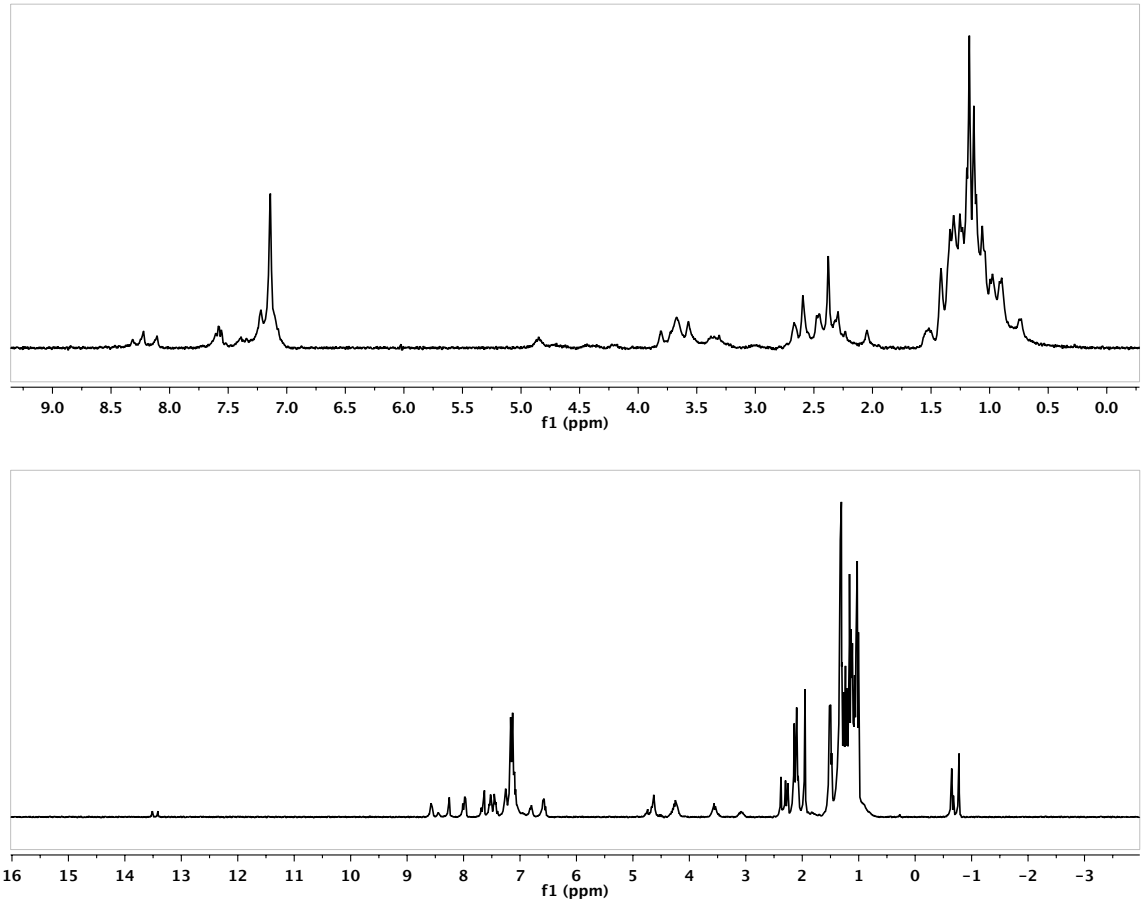

Figure C.148. ^{1}H NMR spectra in C_6D_6 of **120** + $TiCl_2(NMe)_2$ (above) and **120** + $NiMe_2$(tmeda).